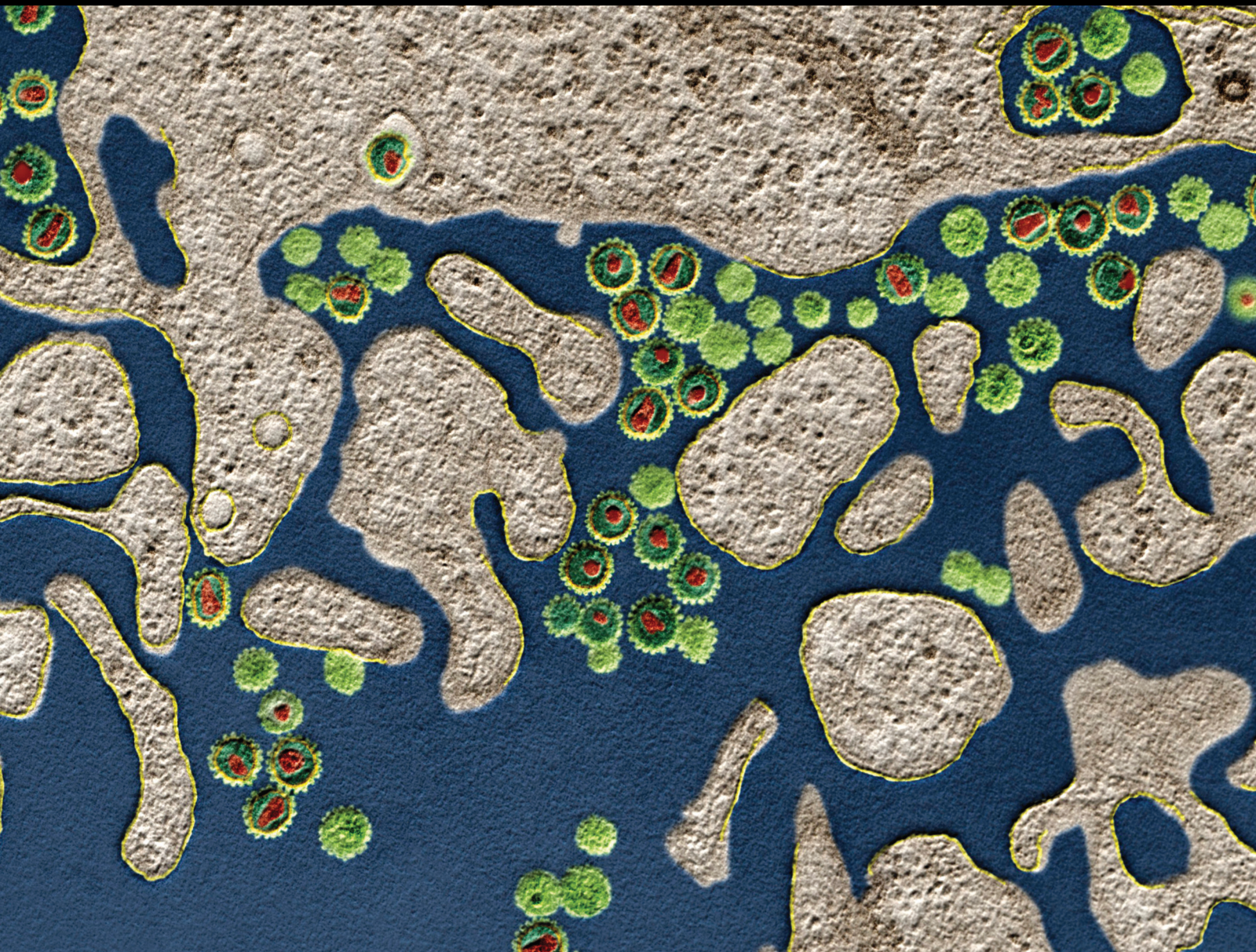


Peptide-Based Immunotherapeutics and Vaccines 2019

Lead Guest Editor: Pedro A. Reche

Guest Editors: Masha Fridkis Hareli, Yoshihiko Hoshino, and Darren R. Flower





**Peptide-Based Immunotherapeutics and
Vaccines 2019**

Journal of Immunology Research

**Peptide-Based Immunotherapeutics and
Vaccines 2019**

Lead Guest Editor: Pedro A. Reche

Guest Editors: Masha Fridkis Hareli, Yoshihiko
Hoshino, and Darren R. Flower



Copyright © 2020 Hindawi Limited. All rights reserved.

This is a special issue published in "Journal of Immunology Research." All articles are open access articles distributed under the Creative Commons Attribution License, which permits unrestricted use, distribution, and reproduction in any medium, provided the original work is properly cited.

Associate Editors

Douglas C. Hooper , USA
Senthamil R. Selvan , USA
Jacek Tabarkiewicz , Poland
Baohui Xu , USA

Academic Editors

Nitin Amdare , USA
Lalit Batra , USA
Kurt Blaser, Switzerland
Dimitrios P. Bogdanos , Greece
Srinivasa Reddy Bonam, USA
Carlo Cavaliere , Italy
Cinzia Ciccacci , Italy
Robert B. Clark, USA
Marco De Vincentiis , Italy
M. Victoria Delpino , Argentina
Roberta Antonia Diotti , Italy
Lihua Duan , China
Nejat K. Egilmez, USA
Theodoros Eleftheriadis , Greece
Eyad Elkord , United Kingdom
Weirong Fang, China
Elizabeth Soares Fernandes , Brazil
Steven E. Finkelstein, USA
JING GUO , USA
Luca Gattinoni , USA
Alvaro González , Spain
Manish Goyal , USA
Qingdong Guan , Canada
Theresa Hautz , Austria
Weicheng Hu , China
Giannicola Iannella , Italy
Juraj Ivanyi , United Kingdom
Ravirajsinh Jadeja , USA
Peirong Jiao , China
Youmin Kang , China
Sung Hwan Ki , Republic of Korea
Bogdan Kolarz , Poland
Vijay Kumar, USA
Esther Maria Lafuente , Spain
Natalie Lister, Australia

Daniele Maria-Ferreira, Saint Vincent and the Grenadines

Eiji Matsuura, Japan
Juliana Melgaço , Brazil
Cinzia Milito , Italy
Prasenjit Mitra , India
Chikao Morimoto, Japan
Paulina Niedźwiedzka-Rystwej , Poland
Enrique Ortega , Mexico
Felipe Passero, Brazil
Anup Singh Pathania , USA
Keshav Raj Paudel, Australia
Patrice Xavier Petit , France
Luis Alberto Ponce-Soto , Peru
Massimo Ralli , Italy
Pedro A. Reche , Spain
Eirini Rigopoulou , Greece
Ilaria Roato , Italy
Suyasha Roy , India
Francesca Santilli, Italy
Takami Sato , USA
Rahul Shivahare , USA
Arif Siddiqui , Saudi Arabia
Amar Singh, USA
Benoit Stijlemans , Belgium
Hiroshi Tanaka , Japan
Bufu Tang , China
Samanta Taurone, Italy
Mizue Terai, USA
Ban-Hock Toh, Australia
Shariq M. Usmani , USA
Ran Wang , China
Shengjun Wang , China
Paulina Wlasiuk, Poland
Zhipeng Xu , China
Xiao-Feng Yang , USA
Dunfang Zhang , China
Qiang Zhang, USA
Qianxia Zhang , USA
Bin Zhao , China
Jixin Zhong , USA
Lele Zhu , China

Contents

Design of Epitope-Based Peptide Vaccine against *Pseudomonas aeruginosa* Fructose Bisphosphate Aldolase Protein Using Immunoinformatics

Mustafa Elhag , Ruaa Mohamed Alaagib , Nagla Mohamed Ahmed , Mustafa Abubaker , Esraa Musa Haroun , Sahar Obi Abd Albagi , and Mohammed A. Hassan 
Research Article (11 pages), Article ID 9475058, Volume 2020 (2020)

DNA Vaccine Treatment in Dogs Experimentally Infected with *Trypanosoma cruzi*

Minerva Arce-Fonseca, Ana C. Carbajal-Hernández, Mónica Lozano-Camacho, Silvia del C. Carrillo-Sánchez, Francisco-Javier Roldán, Alberto Aranda-Fraustro, José Luis Rosales-Encina, and Olivia Rodríguez-Morales 
Research Article (18 pages), Article ID 9794575, Volume 2020 (2020)

Epitope-Based Peptide Vaccine against Glycoprotein G of Nipah *Henipavirus* Using Immunoinformatics Approaches

Arwa A. Mohammed , Shaza W. Shantier , Mujahed I. Mustafa, Hind K. Osman, Hashim E. Elmansi, Isam-Aldin A. Osman, Rawan A. Mohammed, Fatima A. Abdelrhman, Mihad E. Elnnewery, Einas M. Yousif, Marwa M. Mustafa, Nafisa M. Elfadol, Alaa I. Abdalla, Eiman Mahmoud, Ahmed A. Yagaub, Yassir A. Ahmed, and Mohamed A. Hassan
Research Article (12 pages), Article ID 2567957, Volume 2020 (2020)

Combined IMIG and Immune Ig Attenuate Allergic Responses in Beagle Dogs

R. M. Gorczynski , T. Maqbool, and G. Hoffmann
Research Article (10 pages), Article ID 2061609, Volume 2020 (2020)

Triggered Immune Response Induced by Antigenic Epitopes Covalently Linked with Immunoadjuvant-Pulsed Dendritic Cells as a Promising Cancer Vaccine

Chumeng Chen, Mohanad Aldarouish , Qilong Li, Xiangzhen Liu, Feng Han, Hui Liu, and Qijun Qian 
Research Article (10 pages), Article ID 3965061, Volume 2020 (2020)

Development and Validation of a *Bordetella pertussis* Whole-Genome Screening Strategy

Ricardo da Silva Antunes , Lorenzo G. Quiambao, Aaron Sutherland, Ferran Soldevila, Sandeep Kumar Dhanda , Sandra K. Armstrong, Timothy J. Brickman, Tod Merkel, Bjoern Peters, and Alessandro Sette
Research Article (11 pages), Article ID 8202067, Volume 2020 (2020)

Characterization of a Complex Mixture of Immunomodulator Peptides Obtained from Autologous Urine

Alberto Fragoso, Mérida Pedraza-Jiménez, Laura Espinoza-González, María Luisa Ceja-Mendoza, Hugo Sánchez-Mercado, Gloria Robles-Pérez, Julio Granados , and Emilio Medina-Rivero 
Research Article (7 pages), Article ID 3683782, Volume 2020 (2020)

West Nile Virus Vaccine Design by T Cell Epitope Selection: *In Silico* Analysis of Conservation, Functional Cross-Reactivity with the Human Genome, and Population Coverage

Frances M. Waller, Pedro A. Reche , and Darren R. Flower 
Research Article (7 pages), Article ID 7235742, Volume 2020 (2020)

Peptide-Based Vaccination Therapy for Rheumatic Diseases

Bin Wang, Shiju Chen, Qing Zheng, Yuan Liu , and Guixiu Shi 

Review Article (15 pages), Article ID 8060375, Volume 2020 (2020)

A Multiple Antigen Peptide Vaccine Containing CD4⁺ T Cell Epitopes Enhances Humoral Immunity against *Trichinella spiralis* Infection in Mice

Yuan Gu , Ximeng Sun , Jingjing Huang , Bin Zhan , and Xinping Zhu 

Research Article (14 pages), Article ID 2074803, Volume 2020 (2020)

Preliminary Evaluation of the Safety and Immunogenicity of an Antimalarial Vaccine Candidate Modified Peptide (IMPIPS) Mixture in a Murine Model

Jennifer Lambraño, Hernando Curtidor, Catalina Avendaño , Diana Díaz-Arévalo , Leonardo Roa ,

Magnolia Vanegas, Manuel E. Patarroyo, and Manuel A. Patarroyo 

Research Article (12 pages), Article ID 3832513, Volume 2019 (2019)

A Novel Adjuvant “Sublancin” Enhances Immune Response in Specific Pathogen-Free Broiler Chickens Inoculated with Newcastle Disease Vaccine

Yangke Liu, Jiang Zhang, Shuai Wang, Yong Guo, Tao He, and Rui Zhou 

Research Article (7 pages), Article ID 1016567, Volume 2019 (2019)

Immunoinformatics Approach for Multiepitope Vaccine Prediction from H, M, F, and N Proteins of Peste des Petits Ruminants Virus

Bothina B. M. Gaafar, Sumaia A. Ali , Khoubieb Ali Abd-elrahman, and Yassir A. Almofti 

Research Article (18 pages), Article ID 6124030, Volume 2019 (2019)

Enhancement of Macrophage Function by the Antimicrobial Peptide Sublancin Protects Mice from Methicillin-Resistant *Staphylococcus aureus*

Shuai Wang, Qianhong Ye, Ke Wang, Xiangfang Zeng, Shuo Huang, Haitao Yu, Qing Ge, Desheng Qi, and

Shiyan Qiao 

Research Article (13 pages), Article ID 3979352, Volume 2019 (2019)

Research Article

Design of Epitope-Based Peptide Vaccine against *Pseudomonas aeruginosa* Fructose Bisphosphate Aldolase Protein Using Immunoinformatics

Mustafa Elhag ¹, Ruaa Mohamed Alaagib ², Nagla Mohamed Ahmed ³,
Mustafa Abubaker ⁴, Esraa Musa Haroun ⁵, Sahar Obi Abd Albagi ³,
and Mohammed A. Hassan ⁶

¹Faculty of Medicine, University of Seychelles-American Institute of Medicine, Seychelles

²Department of Pharmacies, National Medical Supplies Fund, Sudan

³Faculty of Medical Laboratories Sciences, Al-Neelain University, Sudan

⁴Faculty of Medical Laboratory Sciences, Sudan University of Science and Technology, Sudan

⁵Faculty of Medical Pharmacology, Ahfad University for Women, Sudan

⁶Department of Bioinformatics, DETAGEN Genetics Diagnostic Center, Kayseri, Turkey

Correspondence should be addressed to Mustafa Elhag; mustafa@comxtreme.com

Received 10 September 2019; Revised 21 September 2020; Accepted 6 October 2020; Published 6 November 2020

Academic Editor: Enrique Ortega

Copyright © 2020 Mustafa Elhag et al. This is an open access article distributed under the Creative Commons Attribution License, which permits unrestricted use, distribution, and reproduction in any medium, provided the original work is properly cited.

Pseudomonas aeruginosa is a common pathogen that is responsible for serious hospital-acquired infections, ventilator-associated pneumonia, and various sepsis syndromes. Also, it is a multidrug-resistant pathogen recognized for its ubiquity and its intrinsically advanced antibiotic-resistant mechanisms. It usually affects immunocompromised individuals but can also infect immunocompetent individuals. There is no vaccine against it available till now. This study predicts an effective epitope-based vaccine against fructose bisphosphate aldolase (FBA) of *Pseudomonas aeruginosa* using immunoinformatics tools. The protein sequences were obtained from NCBI, and prediction tests were undertaken to analyze possible epitopes for B and T cells. Three B cell epitopes passed the antigenicity, accessibility, and hydrophilicity tests. Six MHC I epitopes were found to be promising, while four MHC II epitopes were found promising from the result set. Nineteen epitopes were shared between MHC I and II results. For the population coverage, the epitopes covered 95.62% worldwide excluding certain MHC II alleles. We recommend *in vivo* and *in vitro* studies to prove its effectiveness.

1. Introduction

Pseudomonas aeruginosa is a motile, nonfermenting, gram-negative opportunistic bacterium that is implicated in respiratory infections, urinary tract infections, gastrointestinal infections, keratitis, otitis media, and bacteremia in patients with compromised host defences (e.g., cancer, burn, HIV, and cystic fibrosis) [1]. Intensive care unit (ICU) hospitalized patients constitute one of the risk groups that are more susceptible to acquire pseudomonas infections as they may develop ventilator-associated pneumonia (VAP) and sepsis [2–4]. This organism is a ubiquitous and metabolically versa-

tile microbe that flourishes in many environments and possesses many virulence factors that contribute to its pathogenesis [1]. According to data from Centers for Disease Control, *P. aeruginosa* is responsible for millions of infections each year in the community, 10–15% of all healthcare-associated infections, with more than 300,000 cases annually in the EU, USA, and Japan [5]. It is a common nosocomial pathogen [6, 7] that causes infections with a high mortality rate [8, 9] which is attributable to the organism that possesses an intrinsic resistance to many antimicrobial agents [10] and the development of increased, multidrug resistance in healthcare settings [11–13], both of which

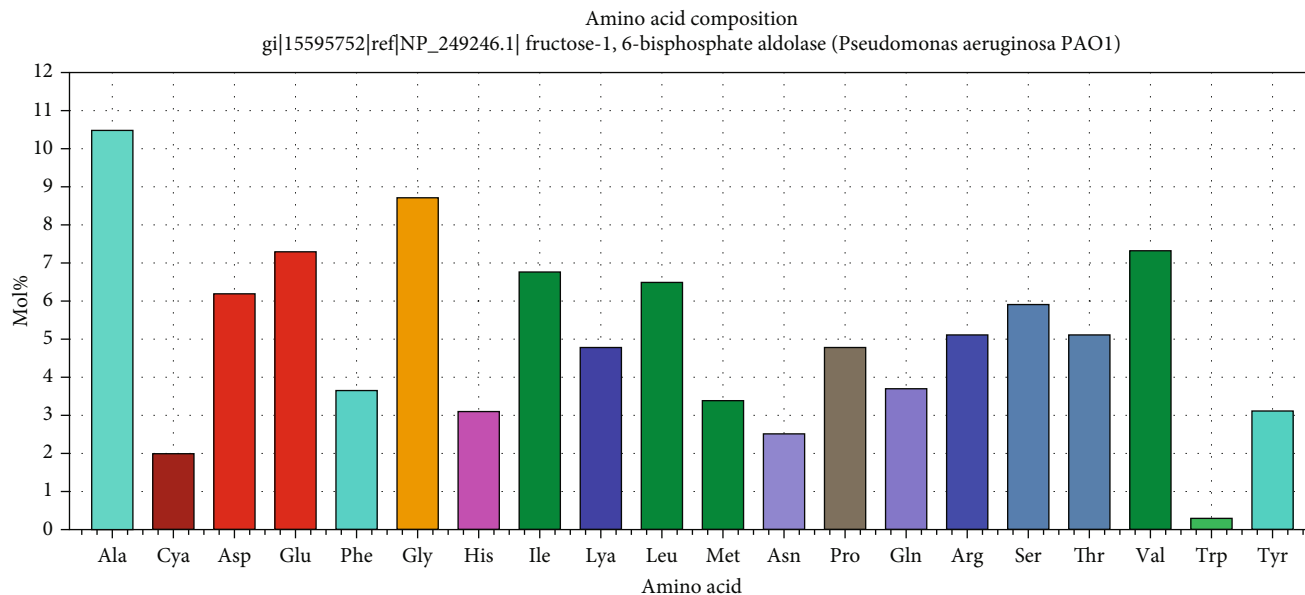


FIGURE 1: Amino acid composition for *Schistosoma mansoni* FBA using BioEdit software.

complicate antipseudomonal chemotherapy. As a result, it remains difficult to combat *P. aeruginosa* infections despite supportive treatments. Vaccines could be an alternative strategy to control *P. aeruginosa* infections and even reduce antibiotic resistance; however, no *P. aeruginosa* vaccine is currently available [14]. Döring and Pier represented that the serious obstacle to the development of a globally effective anti-*P. aeruginosa* vaccine is due to the antigenic variability of a microorganism that enables it to easily adapt to different growth conditions and escapes host immune recognition and to the high variability of the proteins among different *P. aeruginosa* strains and within the same strain, grown in diverse environmental conditions [15].

Contemporary, integrated genomics and proteomics approaches have been used to predict vaccine candidates against *P. aeruginosa* [16]. Although several vaccine formulations have been clinically tested, none has been licensed yet [15, 17]. The search for new targets or vaccine candidates is of high paramount. Bioinformatics-based approach is a novel platform to identify drug targets and vaccine candidates in human pathogens [18, 19]. Thus, the present study is aimed at designing an effective peptide vaccine against *P. aeruginosa* using computational approach through prediction of highly conserved T and B cell epitopes from the highly immunogenic protein fructose bisphosphate aldolase (FBA). This is the first study that predicts epitope-based vaccine from this moonlighting protein of *P. aeruginosa*. This technique has been successfully used by many authors to identify target vaccine candidates. These types of vaccines are easy to produce, specific, capable of keeping away any undesirable immune responses, reasonable, and safe when compared to the conventional vaccines such as killed and attenuated vaccines [20].

2. Materials and Methods

2.1. Protein Sequence Retrieval. A total of 20,201 strains of *Pseudomonas aeruginosa* FBA were retrieved in FASTA for-

TABLE 1: Molecular weight and amino acid frequency distribution of the protein.

Amino acid	Number	Mol%
Ala	37	10.45
Cys	4	1.13
Asp	22	6.21
Glu	26	7.34
Phe	13	3.67
Gly	31	8.76
His	11	3.11
Ile	24	6.78
Lys	17	4.8
Leu	23	6.5
Met	12	3.39
Asn	9	2.54
Pro	17	4.8
Gln	13	3.67
Arg	18	5.08
Ser	21	5.93
Thr	18	5.08
Val	26	7.34
Trp	1	0.28
Tyr	11	3.11

mat from the National Center for Biotechnology Information (NCBI) database (<https://ncbi.nlm.nih.gov>) on May 2019. The protein sequence had a length of 354 with the name fructose-1,6-bisphosphate aldolase.

2.2. Determination of Conserved Regions. The retrieved sequences of *Pseudomonas aeruginosa* FBA were subjected to multiple sequence alignment (MSA) using the ClustalW

TABLE 2: List of conserved peptides with their antigenicity, Emini surface accessibility, and Parker hydrophilicity scores (*peptides that successfully passed the three tests).

Peptide	Start	End	Length	Kolaskar & Tongaonkar antigenicity score (TH: 1.025)	Emini surface accessibility score (TH: 1)	Parker hydrophilicity prediction score (TH: 1.681)
RQMLDHAA	7	14	8	1.008	1.013	1.637
FNVNNLEQMRAIM	23	35	13	0.974	0.432	0.2
AADKTDSPVIVQASAGARK	37	55	19	1.031	0.776	3.3
ADKTDSPVI*	38	46	9	1.027	1.084	3.322
MHQDHGTSPDVCQ	80	92	13	1.035	0.868	3.785
SIQLGFSSVMMDGSL	94	108	15	1.03	0.082	0.38
EDGKTP	110	115	6	0.916	3.211	6.083
YNVRVTQQTVA	120	130	11	1.079	0.972	2.064
YNVRVTQQTV*	120	129	10	1.081	1.229	2.06
AHACGVSVEGELGCLGSLETGM	132	153	22	1.057	0.011	1.818
GEEDG	155	159	5	0.863	1.532	7.4
GAEGVLDHSQ	161	170	10	1.029	0.539	3.3
LTDPEE	172	177	6	0.965	2.317	3.95
DALAIAIGTSHGAY	188	201	14	1.044	0.109	1.179
THLVMHGSSVPQ	227	239	13	1.073	0.369	1.685
HGSSVPQ*	232	239	8	1.06	1.016	3.963
WLAI	241	245	5	1.102	0.134	-6.62
YGGEIKETYG	248	257	10	0.964	1.408	3.3
KVNIDTDLRLAST	273	285	13	1.018	0.843	1.985
AMRD	311	314	4	0.907	1.279	3.025
GTAGN	324	328	5	0.899	0.717	5.14
GEL	347	349	3	0.992	0.694	1.433

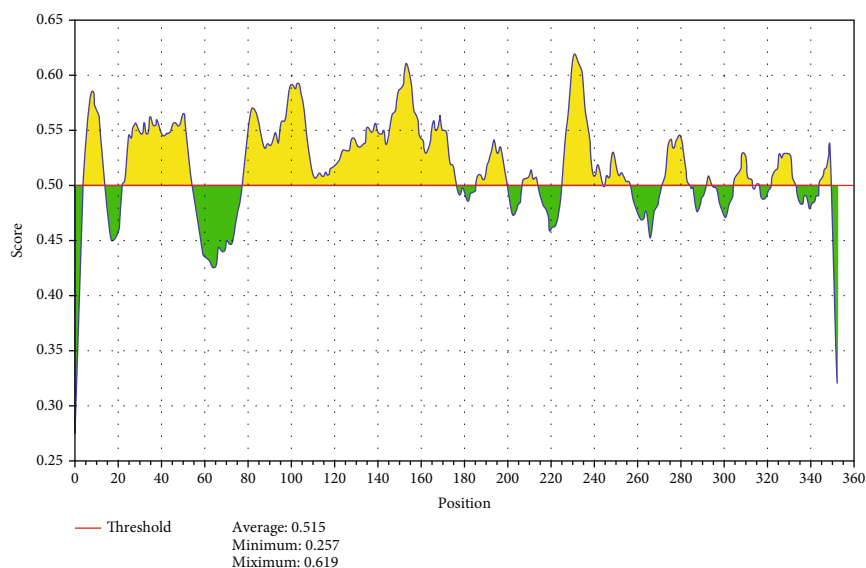


FIGURE 2: BepiPred linear epitope prediction; yellow areas above the threshold (red line) are proposed to be a part of B cell epitopes, and the green areas are not.

tool of BioEdit Sequence Alignment Editor Software version 7.2.5 to determine the conserved regions. Also, molecular weight and amino acid composition of the protein were obtained [21, 22].

2.3. *Sequenced-Based Method.* The reference sequence (NP_249246.1) of *Pseudomonas aeruginosa* FBA was submitted to different prediction tools at the Immune Epitope Database (IEDB) Analysis Resource (<http://www.iedb.org/>) to predict

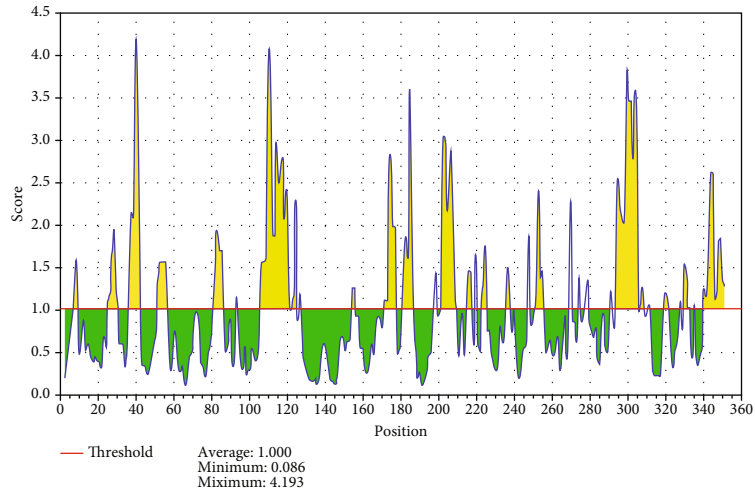


FIGURE 3: Emini surface accessibility prediction; yellow areas above the threshold (red line) are proposed to be a part of B cell epitopes, and the green areas are not.

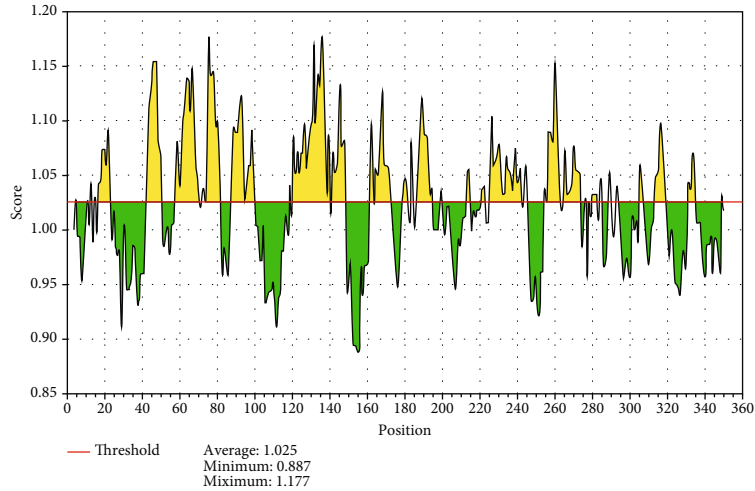


FIGURE 4: Kolaskar and Tongaonkar antigenicity prediction; yellow areas above the threshold (red line) are proposed to be a part of B cell epitopes, and green areas are not.

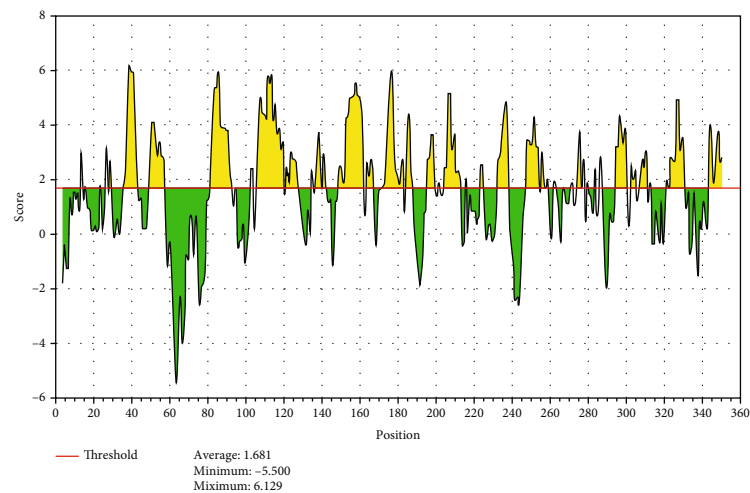


FIGURE 5: Parker hydrophilicity prediction; yellow areas above the threshold (red line) are proposed to be a part of B cell epitopes, and green areas are not.

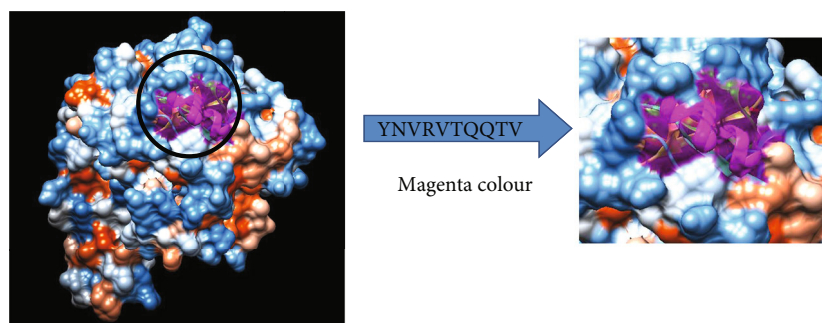


FIGURE 6: B cell epitopes proposed. The arrow shows the position of YNVRVTQQTV with Magenta colour in a structural level of fructose 1,6-bisphosphate aldolase. *The 3D structure was obtained using USCF Chimera software.

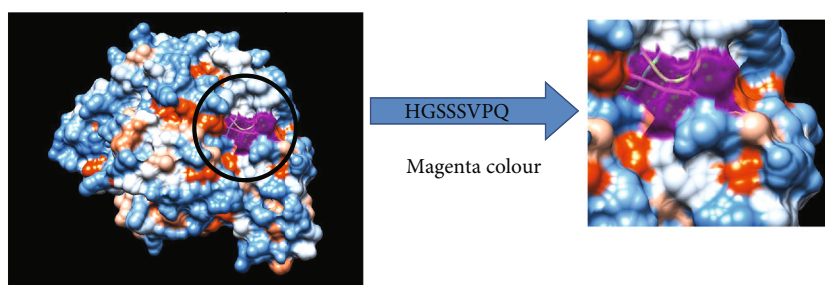


FIGURE 7: B cell epitopes proposed. The arrow shows the position of HGSSVPQ with Magenta colour in a structural level of fructose 1,6-bisphosphate aldolase. *The 3D structure was obtained using USCF Chimera software.

various B and T cell epitopes. Conserved epitopes would be considered candidate epitopes for B and T cell [23].

2.4. B Cell Epitope Prediction. B cell epitope is the portion of the vaccine that interacts with B lymphocytes which are a type of white blood cell of the lymphocyte subtype. Candidate epitopes were analyzed using several B cell prediction methods from the IEDB (<http://tools.iedb.org/bcell/>) to identify the surface accessibility, antigenicity, and hydrophilicity with the aid of random forest algorithm, a form of unsupervised learning. The BepiPred linear prediction 2 was used to predict linear B cell epitope with the default threshold value 0.533 (<http://tools.iedb.org/bcell/result/>). The Emini surface accessibility prediction tool was used to detect the surface accessibility with the default threshold value 1.00 (<http://tools.iedb.org/bcell/result/>). The Kolaskar and Tongaonkar antigenicity method was used to identify the antigenicity sites of a candidate epitope with the default threshold value 1.032 (<http://tools.iedb.org/bcell/result/>). The Parker hydrophilicity prediction tool was used to identify the hydrophilic, accessible, or mobile regions with the default threshold value 1.695 [24–28].

2.5. T Cell Epitope Prediction MHC Class I Binding. T cell epitope is the portion of the vaccine that interacts with T lymphocytes. Analysis of peptide binding to the MHC (major histocompatibility complex) class I molecule was assessed by the IEDB MHC I prediction tool (<http://tools.iedb.org/mhci/>) to predict cytotoxic T cell epitopes (also known as CD8+ cell). The presentation of peptide complex to T lymphocyte undergoes several steps. The Artificial Neural Network (ANN) 4.0 prediction method was used to predict the binding

affinity. Before the prediction, all human allele lengths were selected and set to 9 amino acids. The half-maximal inhibitory concentration (IC50) value required for all conserved epitopes to bind was a score less than 500 [29–35].

2.6. T Cell Epitope Prediction MHC Class II Binding. Prediction of T cell epitopes interacting with MHC class II was assessed by the IEDB MHC II prediction tool (<http://tools.iedb.org/mhcii/>) for helper T cell, which is known as CD4+ cell also. Human allele reference set was used to determine the interaction potentials of T cell epitopes and MHC class II allele (HLA DR, DP, and DQ). The NN-align method was used to predict the binding affinity. IC50 score values less than 100 were selected [36–39].

2.7. Population Coverage. The population coverage tool was selected to analyze the epitopes in the IEDB. This tool calculates the fraction of individuals predicted to respond to a given set of epitopes with known MHC restriction (<http://tools.iedb.org/population/iedbinput/>). The appropriate checkbox for calculation was checked based on MHC I, MHC II separately, and a combination of both [40].

2.8. Homology Modelling. The 3D structure was obtained using RaptorX (<http://raptorx.uchicago.edu/>), i.e., a protein structure prediction server developed by Peng and Xu's group, excelling at 3D structure prediction for protein sequences without close homologs in the Protein Data Bank (PDB). USCF Chimera (version 1.8) was the program used for visualization and analysis of molecular structure of the promising epitopes (<http://www.uscf.edu/chimera/>) [41, 42].

TABLE 3: The most promising T cell epitopes and their corresponding MHC I alleles.

Peptide	MHC I alleles
AADKTDSPV	HLA-C*05:01, HLA-C*03:03
AAIEEFPPI	HLA-A*02:06
AIGTSHGAY	HLA-A*30:02, HLA-B*15:01, HLA-A*29:02
ETYGVPEE	HLA-A*68:02
FNVNNLEQM	HLA-C*12:03
GEIKETYGV	HLA-B*40:02, HLA-B*40:01
GELGCLGSL	HLA-B*40:01, HLA-B*40:02
GTSHGAYKF	HLA-A*29:02, HLA-A*32:01, HLA-B*58
IAIGTSHGA	HLA-A*02:06
IEEFPPIV	HLA-B*40:01
IQLGFSSVM	HLA-B*15:01, HLA-A*02:06, HLA-B*15:02
ISLEGMFQR	HLA-A*31:01, HLA-A*68:01, HLA-A*11:01
IVQASAGAR	HLA-A*31:01, HLA-A*68:01
KPISLEGMF	HLA-B*35:01, HLA-B*07:02
KVNIDTDLR	HLA-A*31:01
LALAIQTSH	HLA-B*35:01, HLA-C*03:03
LVMHGSSSV	HLA-A*02:06, HLA-A*68:02, HLA-C*12:03, HLA-C*14:02, HLA-A*02:01
NVNNLEQMR	HLA-A*68:01
NVRVTQQTV	HLA-A*30:01
QMLDHAAEF	HLA-A*02:06, HLA-A*29:02, HLA-B*15:01, HLA-B*15:02, HLA-A*32:01
RKVNIDTDL	HLA-B*48:01
SIQLGFSSV	HLA-A*02:06
SLEGMFQRY	HLA-A*29:02, HLA-A*30:02
SPVIVQASA	HLA-B*07:02
VIVQASAGA	HLA-A*02:06
VPAFNVNLL	HLA-B*07:02
YGGEIKETY	HLA-C*12:03
YGVPEEIV	HLA-C*12:03

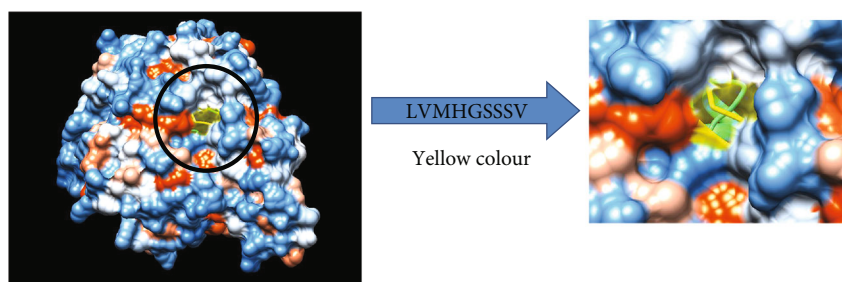


FIGURE 8: T cell epitopes proposed that interact with MHC I. The arrow shows the position of LVMHGSSSV with yellow colour in a structural level of fructose 1,6-bisphosphate aldolase. *The 3D structure was obtained using USCF Chimera software.

TABLE 4: The most promising T cell epitopes and their corresponding MHC II alleles.

Peptide	MHC II alleles
KVNIDTDLRLASTGA	HLA-DRB1*03:01, HLA-DRB1*11:01
GEIKETYGVPEEIV	HLA-DRB1*07:01, HLA-DRB1*13:02, HLA-DQA1*05:01/DQB1*02:01, HLA-DQA1*04:01/DQB1*04:02, HLA-DQA1*03:01/DQB1*03:02
GGEIKETYGVPEEIV	HLA-DRB1*07:01, HLA-DRB1*13:02, HLA-DQA1*04:01/DQB1*04:02, HLA-DQA1*03:01/DQB1*03:02
YGGEIKETYGVPEEIV	HLA-DRB1*07:01, HLA-DRB1*13:02

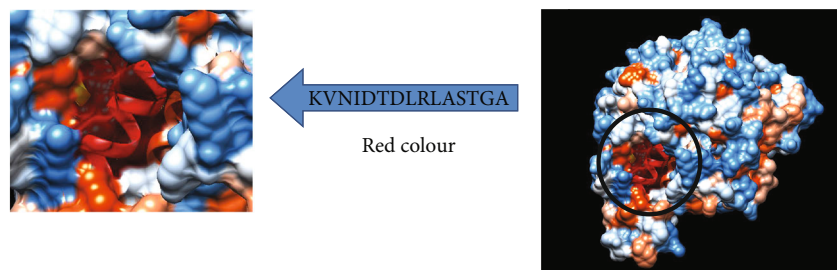


FIGURE 9: T cell epitopes proposed that interact with MHC II. The arrow shows the position of KVNIIDTLRLASTGA with red colour in a structural level of fructose 1,6-bisphosphate aldolase. *The 3D structure was obtained using USCF Chimera software.

TABLE 5: The population coverage of the whole world for the most promising epitopes of MHC I, MHC II, and MHC I and II combined.

Country	MHC I	MHC II	MHC I,II (combined)
World	88.75%	61.1%*	95.62%*

In the population coverage analysis of MHC II; 8 alleles were not included in the calculation; therefore, the above () percentages are for epitope sets excluding these alleles: HLA-DQA1*05:01/DQB1*03:01, HLA-DQA1*01:02/DQB1*06:02, HLA-DQA1*03:01/DQB1*03:02, HLA-DRB4*01:01, HLA-DRB5*01:01, HLA-DQA1*05:01/DQB1*02:01, HLA-DPA1*03:01/DPB1*04:02, HLA-DQA1*04:01/DQB1*04:02.

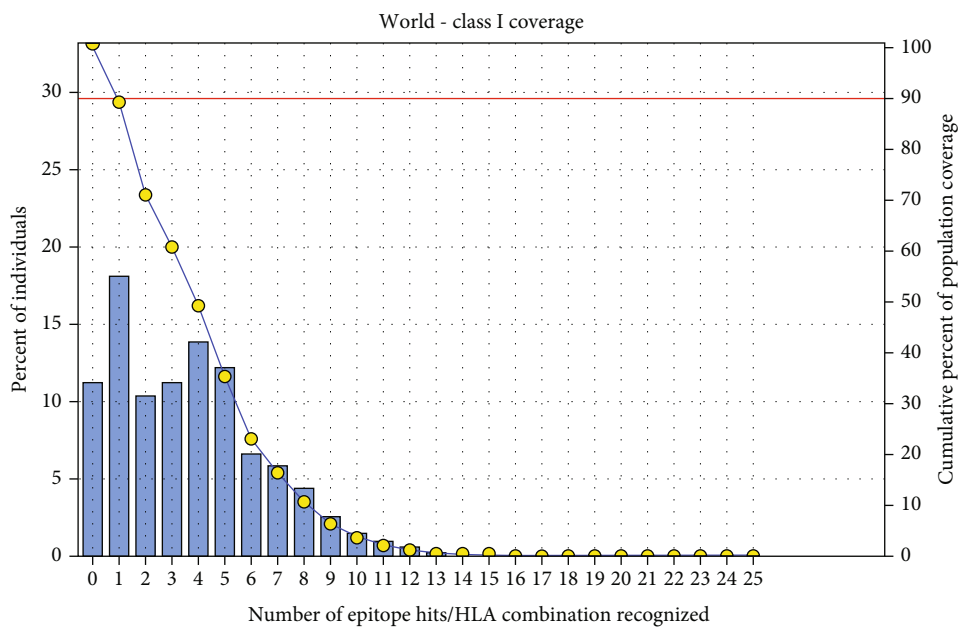


FIGURE 10: Population coverage for MHC class I epitopes.

3. Results

3.1. Amino Acid Composition. The amino acid composition for the reference sequence of *Pseudomonas aeruginosa* FBA is illustrated in Figure 1. Alanine and glycine were the most frequent amino acids (Table 1).

3.2. B Cell Epitope Prediction. The reference sequence of fructose 1,6-bisphosphate aldolase was subjected to BepiPred linear epitope prediction, Emini surface accessibility, Kolaskar and Tongaonkar antigenicity, and Parker hydrophilicity methods in the IEDB to test for various immunogenicity parameters (Table 2 and Figures 2–5). The tertiary structure of the proposed B cell epitopes is shown (Figures 6 and 7).

TABLE 6: Population coverage of the proposed peptide interaction with MHC class I.

Epitope	Coverage (%)	Total hits
LVMHGSSSV	60.41	7
QMLDHAAEF	31.70	8
ISLEGMFQR	25.64	3
KPISLEGMF	20.62	2
LAIAIGTSH	15.85	2

3.3. Prediction of Cytotoxic T Lymphocyte Epitopes and Interaction with MHC Class I. The reference fructose 1,6-bisphosphate aldolase sequence was analyzed using the (IEDB) MHC I binding prediction tool to predict T cell

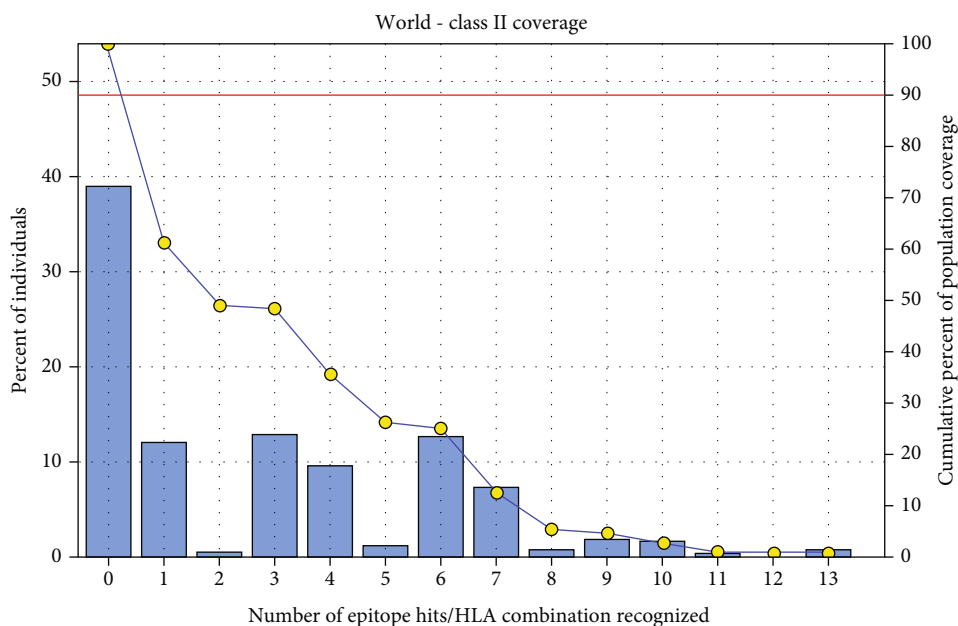


FIGURE 11: Population coverage for MHC class II epitopes.

epitopes which suggested interacting with different types of MHC class I alleles, based on Artificial Neural Network (ANN) with half-maximal inhibitory concentration (IC50) < 500 nm. 206 peptides were predicted to interact with different MHC I alleles.

The most promising epitopes and their corresponding MHC I alleles are shown in Table 3 along with the 3D structure of the proposed one (Figure 8).

3.4. Prediction of the T Cell Epitopes and Interaction with MHC Class II. The reference fructose 1,6-bisphosphate aldolase sequence was analyzed using the (IEDB) MHC II binding prediction tool based on NN-align with half-maximal inhibitory concentration (IC50) < 100 nm; there were 662 predicted epitopes found to interact with MHC II alleles. The most promising epitopes and their corresponding alleles are shown in (Table 4) along with the 3D structure of the proposed one (Figure 9)

3.5. Population Coverage Analysis. All promising MHC I and MHC II epitopes of fructose 1,6-bisphosphate aldolase were assessed for population coverage against the whole world (Table 5).

For MHC I, epitopes with the highest population coverage were LVMHGSSSV (60.41%) and QMLDHAAEF (31.7%) (Figure 10 and Table 6). For MHC class II, the epitopes that showed the highest population coverage were KVNIDTDLRLASTGA (27.37%) and GEIKETYGVPEEIV, GGEIKETYGVPEEI, and YGGEIKETYGVPEE (24.27%) (Figure 11 and Table 7). When combined together, the epitopes that showed the highest population coverage were LVMHGSSSV (60.41%), QMLDHAAEF (31.7%), and KVNIDTDLRLASTGA (27.37%) (Figure 12).

TABLE 7: Population coverage of proposed peptides interaction with MHC class II.

Epitope	Coverage (%)	Total hits
KVNIDTDLRLASTGA	27.37%	2
GEIKETYGVPEEIV	24.27%	5
GGEIKETYGVPEEI	24.27%	4
YGGEIKETYGVPEE	24.27%	2
GVRKVNIDTDLRLAS	23.90%	2

4. Discussion

Vaccination against *P. aeruginosa* is highly accredited due to the high mortality rates associated with the pathogen that spreads through healthcare areas. In addition, multidrug resistance of the pathogen demands the design of vaccine as an alternative [43]. In this study, immunoinformatics approaches were used to propose different peptides against FBA of *P. aeruginosa* for the first time. These peptides can be recognized by B cell and T cell to produce antibodies. Peptide vaccines overcome the side effects of conventional vaccines through easy production, effective stimulation of immune response, less allergy, and no potential infection possibilities [35]. Thus, the combination of humoral and cellular immunity is more promising at clearing bacterial infections than humoral or cellular immunity alone.

As B cells play a critical role in adaptive immunity, the reference sequence of *P. Aeruginosa* FBA was subjected to BepiPred linear epitope prediction 2 test to determine the binding to B cell, Emini surface accessibility test to test the surface accessibility, Kolaskar and Tongaonkar antigenicity test for antigenicity, and Parker hydrophilicity test for the hydrophilicity of the B cell epitope.

Out of the thirteen predicted epitopes using BepiPred 2 test, only three epitopes passed the other three tests

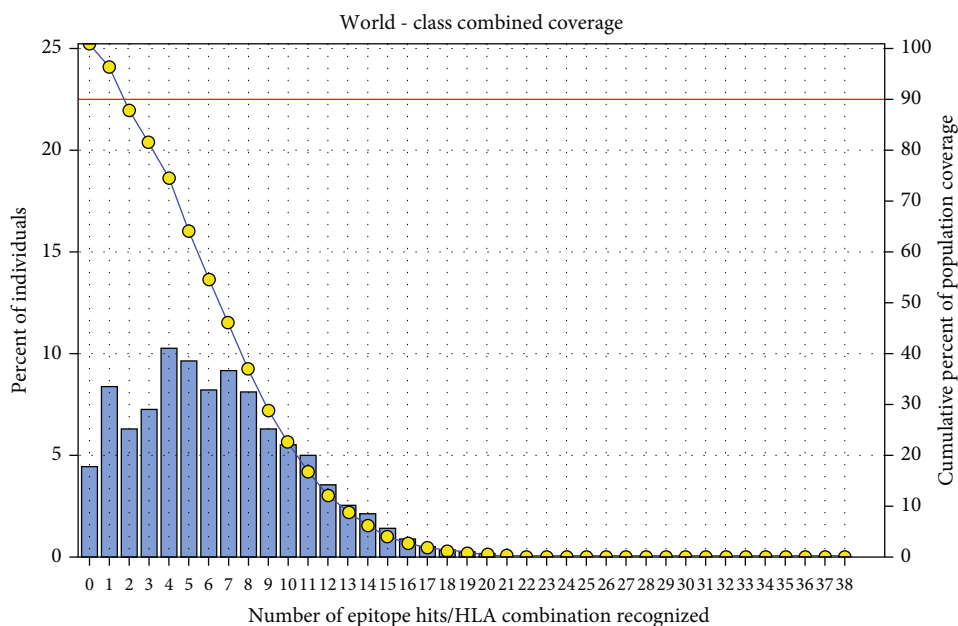


FIGURE 12: Population coverage for MHC class I and II epitopes combined.

(ADKTDSPVI, YNVRVTQQT, and HGSSVVPQ) after segmentation. BepiPred version 2 test was used because it implements random forest and therefore predicts large epitope segments.

The reference sequence was analyzed using the IEDB MHC I and II binding prediction tools to predict T cell epitopes. 28 epitopes were predicted to interact with MHC I alleles with half-maximal inhibitory concentration (IC_{50}) < 500. Six of them were most promising and had the affinity to bind to the highest number of MHC I alleles (LVMHGSSSV, QMLDHAAEF, AIGTSHGAY, GTSHGAYKF, IQLGFSSVM, and ISLEGMFQR). 19 predicted epitopes were interacted with MHC II alleles with IC_{50} < 100. Four of them were most promising and had the affinity to bind to the highest number of MHC II alleles (GEIKETYGVPVEEIV, GGEIKETYGVPVEEII, KVNIDTDLRLASTGA, and YGGEIKETYGVPVEE). Nineteen epitopes (NVNMLEQMR, IQLGFSSVM, AADKTDSPV, SIQLGFSSV, GEIKETYGV, AIGTSHGAY, VPAFNVNLL, KVNIDTDLR, LAIAIGTSH, IVQASAGAR, ETYGVPVEE, GTSHGAYKF, YGGEIKETY, VIVQASAGA, IAIGTSHGA, RKNIDTDL, FNVNLEQM, YGVPVEEIV, and SPVIV-QASA) appeared in both MHC I and II results.

The best epitope with the highest population coverage for MHC I was LVMHGSSSV (60.41%) with seven HLA hits, and the coverage of population set for the whole MHC I epitopes was 88.75%. Excluding certain alleles for MHC II, the best epitope was KVNIDTDLRLASTGA scoring 27.37% with two HLA hits, followed by GEIKETYGVPVEEIV scoring 24.27% with five HLA hits. The population coverage was 61.1% for all conserved MHC II epitopes. These epitopes have the ability to induce T cell immune response when interacting strongly with MHC I and MHC II alleles effectively generating cellular and humoral immune response against the invading pathogen. When combined, the epitope LVMHGSSSV had the highest population coverage percent 60.41% with seven HLA hits for both MHC I and MHC II.

Many studies had predicted peptide vaccines for different microorganisms such as rubella, Ebola, dengue, Zika, HPV, Lagos rabies virus, and mycetoma using immunoinformatics tools [44–51]. Limitations include the exclusion of certain HLA alleles for MHC II.

We hope that the world will benefit from these predicted epitopes in the formulation of the peptide-based vaccine and recommend further *in vivo* and *in vitro* studies to prove its effectiveness along with formulation of appropriate adjuvants. Finding another immunogenic target and analyzing the associated epitopes support the vaccine formula.

5. Conclusion

Vaccination is used to protect and minimize the possibility of infection leading to an increased life expectancy. The design of vaccines using immunoinformatics prediction methods is highly appreciated due to the significant reduction in cost, time, effort, and resources. Epitope-based vaccines are expected to be more immunogenic and less allergenic than traditional biochemical vaccines. We have illustrated different epitopes that have the ability to stimulate both B and T cells against fructose bisphosphate aldolase protein of *Pseudomonas aeruginosa* for the first time. Three B cell epitopes have successfully passed the required tests. Six MHC I epitopes were found to be most promising, while four were found from MHC II epitope result set. These epitopes covered 95.62% worldwide excluding certain MHC II alleles.

Data Availability

The data which support our findings in this study are available from the corresponding author upon reasonable request.

Conflicts of Interest

The authors declare that there is no conflict of interest.

Acknowledgments

Many thanks go to the National Center for Biotechnology Information (NCBI), BioEdit, Immune Epitope Database (IEDB) Analysis Resource, RaptorX server, and UCSF Chimera team.

References

- [1] K. N. Schurek, E. B. M. Breidenstein, and R. E. W. Hancock, "Pseudomonas aeruginosa: a persistent pathogen in cystic fibrosis and hospital-associated infections," *Antibiotic Discovery and Development*, pp. 679–715, 2012.
- [2] B. J. Williams, J. Dehnbostel, and T. S. Blackwell, "Pseudomonas aeruginosa: host defence in lung diseases," *Respirology*, vol. 15, no. 7, pp. 1037–1056, 2010.
- [3] S. L. Gellatly and R. E. W. Hancock, "Pseudomonas aeruginosa: new insights into pathogenesis and host defenses," *Pathogens and Disease*, vol. 67, no. 3, pp. 159–173, 2013.
- [4] J. Chastre and J.-Y. Fagon, "Ventilator-associated pneumonia," *American Journal of Respiratory and Critical Care Medicine*, vol. 165, no. 7, pp. 867–903, 2002.
- [5] H. W. Boucher, G. H. Talbot, J. S. Bradley et al., "Bad bugs, no drugs: no ESKAPE! An update from the Infectious Diseases Society of America," *Clinical Infectious Diseases*, vol. 48, no. 1, pp. 1–12, 2009.
- [6] R. N. Jones, M. G. Stilwell, P. R. Rhomborg, and H. S. Sader, "Antipseudomonal activity of piperacillin/tazobactam: more than a decade of experience from the SENTRY Antimicrobial Surveillance Program (1997–2007)," *Diagnostic Microbiology and Infectious Disease*, vol. 65, no. 3, pp. 331–334, 2009.
- [7] G. G. Zhanel, M. DeCorby, H. Adam et al., "Prevalence of antimicrobial-resistant pathogens in Canadian hospitals: results of the Canadian Ward Surveillance Study (CANWARD 2008)," *Antimicrobial Agents and Chemotherapy*, vol. 54, no. 11, pp. 4684–4693, 2010.
- [8] P. Mahar, A. A. Padiglione, H. Cleland, E. Paul, M. Hinrichs, and J. Wasiak, "Pseudomonas aeruginosa bacteraemia in burns patients: risk factors and outcomes," *Burns*, vol. 36, no. 8, pp. 1228–1233, 2010.
- [9] M.-L. Lambert, C. Suetens, A. Savey et al., "Clinical outcomes of health-care-associated infections and antimicrobial resistance in patients admitted to European intensive-care units: a cohort study," *The Lancet Infectious Diseases*, vol. 11, no. 1, pp. 30–38, 2011.
- [10] K. Poole, "Pseudomonas aeruginosa: resistance to the max," *Frontiers in Microbiology*, vol. 2, p. 65, 2011.
- [11] A. J. Kallen, A. I. Hidron, J. Patel, and A. Srinivasan, "Multi-drug resistance among gram-negative pathogens that caused healthcare-associated infections reported to the National Healthcare Safety Network, 2006–2008," *Infection Control & Hospital Epidemiology*, vol. 31, no. 5, pp. 528–531, 2010.
- [12] E. F. Keen III, B. J. Robinson, D. R. Hospenthal et al., "Prevalence of multidrug-resistant organisms recovered at a military burn center," *Burns*, vol. 36, no. 6, pp. 819–825, 2010.
- [13] E. B. Hirsch and V. H. Tam, "Impact of multidrug-resistant Pseudomonas aeruginosa infection on patient outcomes," *Expert Review of Pharmacoeconomics & Outcomes Research*, vol. 10, no. 4, pp. 441–451, 2014.
- [14] A. S. Ginsburg and K. P. Klugman, "Vaccination to reduce antimicrobial resistance," *The Lancet Global Health*, vol. 5, no. 12, pp. e1176–e1177, 2017.
- [15] G. Döring and G. B. Pier, "Vaccines and immunotherapy against Pseudomonas aeruginosa," *Vaccine*, vol. 26, no. 8, pp. 1011–1024, 2008.
- [16] M. I. Rashid, A. Naz, A. Ali, and S. Andleeb, "Prediction of vaccine candidates against Pseudomonas aeruginosa: an integrated genomics and proteomics approach," *Genomics*, vol. 109, no. 3–4, pp. 274–283, 2017.
- [17] A. Sharma, A. Krause, and S. Worgall, "Recent developments for Pseudomonas vaccines," *Human Vaccines*, vol. 7, no. 10, pp. 999–1011, 2014.
- [18] L. Florea, B. Halldorsson, O. Kohlbacher, R. Schwartz, S. Hoffman, and S. Istrail, "Epitope prediction algorithms for peptide-based vaccine design," in *Computational Systems Bioinformatics. CSB2003. Proceedings of the 2003 IEEE Bioinformatics Conference. CSB2003*.
- [19] K. Prabhavathy, P. Perumal, and N. SundaraBaalaji, *In silico identification of B- and T-cell epitopes on OMPLA and LsrC from Salmonella typhi for peptide-based subunit vaccine design*, NISCAIR-CSIR, India, 2011.
- [20] T. A. Ahmad, A. E. Eweida, and S. A. Sheweita, "B-cell epitope mapping for the design of vaccines and effective diagnostics," *Trials in Vaccinology*, vol. 5, pp. 71–83, 2016.
- [21] T. Hall, I. Biosciences, and C. Carlsbad, "BioEdit: an important software for molecular biology," *GERF Bulletin of Biosciences*, vol. 2, no. 1, pp. 60–61, 2011.
- [22] G. Zhang and B. Fang, "A uniform design-based back propagation neural network model for amino acid composition and optimal pH in G/11 xylanase," *Journal of Chemical Technology & Biotechnology*, vol. 81, no. 7, pp. 1185–1189, 2006.
- [23] R. Vita, S. Mahajan, J. A. Overton et al., "The immune epitope database (IEDB): 2018 update," *Nucleic Acids Research*, vol. 47, no. D1, pp. D339–D343, 2019.
- [24] T. A. Hall, "BioEdit: a user-friendly biological sequence alignment editor and analysis program for Windows 95/98/NT," in *Nucleic acids symposium series*, pp. c1979–c2000, Information Retrieval Ltd, London, 1999.
- [25] J. Larsen, O. Lund, and M. Nielsen, "Improved method for predicting linear B-cell epitopes," *Immunome Research*, vol. 2, no. 1, p. 2, 2006.
- [26] E. A. Emini, J. V. Hughes, D. S. Perlow, and J. Boger, "Induction of hepatitis a virus-neutralizing antibody by a virus-specific synthetic peptide," *Journal of Virology*, vol. 55, no. 3, pp. 836–839, 1985.
- [27] A. S. Kolaskar and P. C. Tongaonkar, "A semi-empirical method for prediction of antigenic determinants on protein antigens," *FEBS Letters*, vol. 276, no. 1–2, pp. 172–174, 1990.
- [28] J. M. R. Parker, D. Guo, and R. S. Hodges, "New hydrophilicity scale derived from high-performance liquid chromatography peptide retention data: correlation of predicted surface residues with antigenicity and X-ray-derived accessible sites," *Biochemistry*, vol. 25, no. 19, pp. 5425–5432, 2002.
- [29] M. Andreatta and M. Nielsen, "Gapped sequence alignment using artificial neural networks: application to the MHC class I system," *Bioinformatics*, vol. 32, no. 4, pp. 511–517, 2016.
- [30] S. Buus, S. L. Lauemøller, P. Worning et al., "Sensitive quantitative predictions of peptide-MHC binding by a 'Query by

- Committee' artificial neural network approach," *Tissue Antigens*, vol. 62, no. 5, pp. 378–384, 2003.
- [31] M. Nielsen, C. Lundegaard, P. Worning et al., "Reliable prediction of T-cell epitopes using neural networks with novel sequence representations," *Protein Science*, vol. 12, no. 5, pp. 1007–1017, 2003.
- [32] B. Peters and A. Sette, "Generating quantitative models describing the sequence specificity of biological processes with the stabilized matrix method," *BMC Bioinformatics*, vol. 6, no. 1, p. 132, 2005.
- [33] C. Lundegaard, K. Lamberth, M. Harndahl, S. Buus, O. Lund, and M. Nielsen, "NetMHC-3.0: accurate web accessible predictions of human, mouse and monkey MHC class I affinities for peptides of length 8–11," *Nucleic acids research*, vol. 36, supplement 2, pp. W509–W512, 2008.
- [34] M. Abdelbagi, T. Hassan, M. Shihabeldin et al., "Immunoinformatics prediction of peptide-based vaccine against African horse sickness virus," *Immunome Research*, vol. 13, no. 2, p. 2, 2017.
- [35] A. Patronov and I. Doytchinova, "T-cell epitope vaccine design by immunoinformatics," *Open Biology*, vol. 3, no. 1, p. 120139, 2013.
- [36] P. Wang, J. Sidney, C. Dow, B. Mothé, A. Sette, and B. Peters, "A systematic assessment of MHC class II peptide binding predictions and evaluation of a consensus approach," *PLoS Computational Biology*, vol. 4, no. 4, article e1000048, 2008.
- [37] P. Wang, J. Sidney, Y. Kim et al., "Peptide binding predictions for HLA DR, DP and DQ molecules," *BMC Bioinformatics*, vol. 11, no. 1, p. 568, 2010.
- [38] Y. Kim, J. Ponomarenko, Z. Zhu et al., "Immune epitope database analysis resource," *Nucleic Acids Research*, vol. 40, no. W1, pp. W525–W530, 2012.
- [39] M. Nielsen and O. Lund, "NN-align. An artificial neural network-based alignment algorithm for MHC class II peptide binding prediction," *BMC bioinformatics*, vol. 10, no. 1, p. 296, 2009.
- [40] H.-H. Bui, J. Sidney, K. Dinh, S. Southwood, M. J. Newman, and A. Sette, "Predicting population coverage of T-cell epitope-based diagnostics and vaccines," *BMC Bioinformatics*, vol. 7, no. 1, p. 153, 2006.
- [41] E. F. Pettersen, T. D. Goddard, C. C. Huang et al., "UCSF Chimera—a visualization system for exploratory research and analysis," *Journal of Computational Chemistry*, vol. 25, no. 13, pp. 1605–1612, 2004.
- [42] J. Peng and J. Xu, "RaptorX: exploiting structure information for protein alignment by statistical inference," *Proteins: Structure, Function, and Bioinformatics*, vol. 79, no. S10, pp. 161–171, 2011.
- [43] J. W. Costerton, P. S. Stewart, and E. P. Greenberg, "Bacterial biofilms: a common cause of persistent infections," *Science*, vol. 284, no. 5418, pp. 1318–1322, 1999.
- [44] A. A. Mohammed, A. M. H. ALnaby, S. M. Sabeel et al., "Epitope-based peptide vaccine against fructose-bisphosphate aldolase of *Madurella mycetomatis* Using immunoinformatics approaches," *Bioinformatics and Biology Insights*, vol. 12, article 117793221880970, 2018.
- [45] S. N. E. M. Elgenaid, E. M. Al Hajj, A. A. Ibrahim et al., "Prediction of multiple peptide based vaccine from E1, E2 and capsid proteins of rubella virus: an *in-silico* approach," *Immunome Research*, vol. 14, no. 1, p. 2, 2018.
- [46] S. M. Bolis, W. A. Omer, M. A. Abdelhamed et al., "Immunoinformatics prediction of epitope based peptide vaccine against *Madurella mycetomatis translationally controlled tumor protein*," *bioRxiv*, p. 441881, 2018.
- [47] A. A. Mohammed, O. Hashim, E. KAA, A. Hamdi, and M. A. Hassan, "Epitope-based peptide vaccine design against Mokola rabies virus glycoprotein G utilizing *in silico* approaches," *Immunome Research*, vol. 13, no. 3, p. 2, 2017.
- [48] S. O. A. Albagi, O. H. Ahmed, M. A. Gumaa, K. A. A. Elrahman, A. H. A. Haraz, and A. Mohammed, "Immunoinformatics-peptide driven vaccine and *in silico* modeling for Duvenhage rabies virus glycoprotein G," *Journal of Clinical & Cellular Immunology*, vol. 8, no. 4, p. 2, 2017.
- [49] A. H. A. Haraz, K. A. A. Elrahman, M. S. Ibrahim et al., "Multi epitope peptide vaccine prediction against Sudan Ebola virus using immuno-informatics approaches," *Advanced Techniques in Biology & Medicine*, vol. 5, no. 203, 2017.
- [50] M. M. O. Sahar Suliman Mohamed, S. M. Sami, H. A. Elgailany et al., "Immunoinformatics approach for designing epitope-based peptides vaccine of L1 major capsid protein against HPV type 16," *International Journal of Multidisciplinary and Current Research*, 2016.
- [51] M. M. B. Suluiman, M. M. Osman, A. A. E. F. Alla et al., "Highly conserved epitopes of Zika envelope glycoprotein may act as a novel peptide vaccine with high coverage: immunoinformatics approach," *Journal of Vaccines & Vaccination*, vol. 4, no. 3, pp. 46–60, 2016.

Research Article

DNA Vaccine Treatment in Dogs Experimentally Infected with *Trypanosoma cruzi*

Minerva Arce-Fonseca,¹ Ana C. Carbajal-Hernández,¹ Mónica Lozano-Camacho,¹ Silvia del C. Carrillo-Sánchez,¹ Francisco-Javier Roldán,² Alberto Aranda-Fraustro,³ José Luis Rosales-Encina,⁴ and Olivia Rodríguez-Morales¹

¹Department of Molecular Biology, Instituto Nacional de Cardiología “Ignacio Chávez”, Juan Badiano No. 1, Col. Sección XVI, Tlalpan, 14080 Mexico City, Mexico

²Department of Echocardiography, Instituto Nacional de Cardiología “Ignacio Chávez”, Juan Badiano No. 1, Col. Sección XVI, Tlalpan, 14080 Mexico City, Mexico

³Department of Pathology, Instituto Nacional de Cardiología “Ignacio Chávez”, Juan Badiano No. 1, Col. Sección XVI, Tlalpan, 14080 Mexico City, Mexico

⁴Department of Infectomics and Molecular Pathogenesis, Centro de Investigación y de Estudios Avanzados-IPN, Av. Instituto Politécnico Nacional 2508, Col. San Pedro Zacatenco, Gustavo A. Madero, 07360 Mexico City, Mexico

Correspondence should be addressed to Olivia Rodríguez-Morales; rm.olivia@gmail.com

Received 31 December 2019; Revised 8 March 2020; Accepted 6 April 2020; Published 5 May 2020

Guest Editor: Yoshihiko Hoshino

Copyright © 2020 Minerva Arce-Fonseca et al. This is an open access article distributed under the Creative Commons Attribution License, which permits unrestricted use, distribution, and reproduction in any medium, provided the original work is properly cited.

Chagas disease is a chronic and potentially lethal disorder caused by the parasite *Trypanosoma cruzi*, and an effective treatment has not been developed for chronic Chagas disease. The objective of this study was to determine the effectiveness of a therapeutic DNA vaccine containing *T. cruzi* genes in dogs with experimentally induced Chagas disease through clinical, pathological, and immunological analyses. Infection of Beagle dogs with the H8 *T. cruzi* strain was performed intraperitoneally with 3500 metacyclic trypomastigotes/kg body weight. Two weeks after infection, plasmid DNA immunotherapy was administered thrice at 15-day intervals. The clinical (physical and cabinet studies), immunological (antibody and cytokine profiles and lymphoproliferation), and macro- and microscopic pathological findings were described. A significant increase in IgG and cell proliferation was recorded after immunotherapy, and the highest stimulation index (3.02) was observed in dogs treated with the pBCSSP4 plasmid. The second treatment with both plasmids induced an increase in IL-1, and the third treatment with the pBCSSP4 plasmid induced an increase in IL-6. The pBCSP plasmid had a good Th1 response regulated by high levels of IFN-gamma and TNF-alpha, whereas the combination of the two plasmids did not have a synergistic effect. Electrocardiographic studies registered lower abnormalities and the lowest number of individuals with abnormalities in each group treated with the therapeutic vaccine. Echocardiograms showed that the pBCSSP4 plasmid immunotherapy preserved cardiac structure and function to a greater extent and prevented cardiomegaly. The two plasmids alone controlled the infection moderately by a reduction in the inflammatory infiltrates in heart tissue. The immunotherapy was able to reduce the magnitude of cardiac lesions and modulate the cellular immune response; the pBCSP treatment showed a clear Th1 response; and pBCSSP4 induced a balanced Th1/Th2 immune response that prevented severe cardiac involvement. The pBCSSP4 plasmid had a better effect on most of the parameters evaluated in this study; therefore, this plasmid can be considered an optional treatment against Chagas disease in naturally infected dogs.

1. Introduction

Chagas disease or American trypanosomiasis is a zoonotic disease caused by the hemoflagellated protozoan *Trypanosoma cruzi*. This parasite is transmitted to domestic and wild mammals through the metacyclic trypomastigote-contaminated feces of hematophagous hemipteran insects belonging to the Reduviidae family, Triatominae (triatomines) subfamily, and it is known in Mexico as the “kissing bug.” Chagas disease is endemic to the American continent, and approximately 6-7 million people are estimated to suffer from American trypanosomiasis. More than 10,000 people die each year as a result of the disease, which has an annual incidence of 30,000 cases [1]. The cardiac form is the most serious and frequent manifestation of chronic Chagas disease, and it develops in 20%-30% of individuals and typically leads to conduction system abnormalities, bradyarrhythmias and tachyarrhythmias, apical aneurysms, cardiac failure, thromboembolism, and sudden death [2].

According to the World Health Organization classification, the endemic countries can be divided into four groups (I, II, III, and IV). Mexico fits within group II for complying with the following characteristics: intradomiciliary transmission evidence with a clear association is observed between *T. cruzi* infection and electrocardiographic alterations as well as other pathologies attributable to Chagas disease, and formal control programs have not been established [3].

Among the parasite reservoirs, the dog is considered the most important domestic species in the *T. cruzi* infection dynamics because dogs are an important source of food for triatomine insects, and they can also ingest infected bugs. Therefore, the risk of transmission within human dwellings by infected dogs has been proven [4]. Several studies have reported seroreactive dogs to the parasite in some regions of Mexico and an important seroprevalence in Morelos, Estado de México, Puebla, Yucatán, Chiapas, Campeche, Jalisco, Sonora, and Nuevo León [5, 6].

Chagas disease treatment involves two aspects: the symptomatic or nonspecific and trypanocide or specific. Chronic Chagas cardiomyopathy is still a challenging disease whose current and emerging treatment includes drugs, implantable cardioverter-defibrillators, permanent pacemakers, transcatheter ablation, heart transplantation, resynchronization therapy, and cell therapy focusing mostly on management of heart failure and arrhythmias [7, 8]. The use of drugs that eliminate the parasite is indicated for the treatment of acute symptomatic disease, which is acquired by vector, congenital, or accidental routes. On the other hand, the effectiveness of the trypanocidal treatment in chronic cases of the disease is controversial [9].

In the acute phase, it is necessary to administer the drug as quickly as possible and the dose is varied according to the patient's age and weight. Nifurtimox and benznidazole are the only two drugs with adequate trypanocide activity whose effect is against blood and tissue forms. The effectiveness of conventional chemotherapy is very low. In early infected children, treatment is successful in 55.8% of cases; however, in the chronic phase, most patients are resistant to therapy with conventional drugs and carry a lifelong infection [10, 11].

The usefulness of these drugs in patients with Chagas disease in the asymptomatic or symptomatic chronic phases has not been established. In addition, it has been reported that a large proportion of subjects treated with benznidazole experience severe side effects, including digestive manifestations and hematological, skin, and neurological alterations [11]. Experimental toxicity studies with both drugs evidenced neurotoxicity, testicular damage, ovarian toxicity, and deleterious effects in the adrenal, colon, esophageal, and mammary tissue as well as significant mutagenic effects [12]. Despite recent efforts to discover new treatments for Chagas disease, such as drug combinations, drug repositioning, redosing schemes for current drugs, and identifying new drugs with specified target profiles or additive or synergistic interactions of compounds with different modes of actions, better safety and greater effectiveness of drug treatment is not yet available [13–15].

DNA vaccines are currently under research, and their potential use for both the prevention and the treatment of a variety of infectious diseases has been explored, including for Chagas disease [16–20]. The vast majority of our knowledge about immune mechanisms and protective response for *T. cruzi* infection comes from experimental animal models [21]. The use of a DNA vaccine as a treatment in Chagas disease has been partially successful in animal models as demonstrated by Dumonteil et al., who infected mice with *T. cruzi* and then treated them with DNA coding for parasite antigens and found less parasitemia, reduced cardiac tissue inflammation, and increased survival [20]. One of the most important advantages of using canine models in relation to other animal models is the advanced knowledge and similarity of the cardiac morphology and physiology of the heart conduction system with humans. Several clinical aspects of the disease similar to those verified in humans have been observed in dogs, thus leading to the possibility of performing electrocardiographic monitoring of the infected animal and verifying the correlations between these alterations and cardiac conduction system lesions and offering good interpretation of the results [21].

Vaccines against Chagas disease have been previously tested in dogs by our group [22–24] and by others [25–27]. The results, which focus mainly on the immune response and cardiac damage evaluated by histology, have been variable, although in all cases, the infection is not avoided and the degree of protection ranges from mild to moderate.

The aim of our study is to evaluate the therapeutic efficacy of the administration of plasmid DNA coding for the TcSPP4 and TcSP antigens of *T. cruzi* in dogs during the acute and chronic phases of Chagas disease through clinical, pathological, and immunological analyses of Beagle dogs infected with the H8 *T. cruzi* autochthonous Mexican strain.

2. Materials and Methods

2.1. Experimental Animals. Thirty male and female four-month-old Beagle puppies from healthy parents were subjected to a basic calendar of preventive medicine that included vaccination and deworming. All animals were tested for the absence of antibodies against *T. cruzi* using

TABLE 1: Study design for dogs experimentally infected with *T. cruzi* and treated with DNA vaccine containing the genes encoding a *trans*-sialidase protein (pBCSP), an amastigote-specific glycoprotein (pBCSSP4), or both as a mixture.

Group*	Group description (n)	Plasmid used as immunotherapy
Healthy	Control noninfected/nontreated (n = 5)	None
Infected/SS <i>mock</i> -treated	Positive control of infection with saline solution <i>mock</i> -treated (n = 5)	None
pBCSSP4	Infected and pBCSSP4 plasmid-treated (n = 5)	Construct derived from the pBK-CMV vector with <i>T. cruzi</i> amastigote-specific glycoprotein <i>TcSSP4</i> gene
pBCSP	Infected and pBCSP plasmid-treated (n = 5)	Construct derived from the pBK-CMV vector with <i>T. cruzi</i> <i>trans</i> -sialidase <i>TcSP</i> gene
Mixture	Infected and treated with both the pBCSSP4 and pBCSP plasmids (n = 5)	pBCSSP4 and pBCSP plasmids carrying both genes
pBK-CMV	Infected and empty cloning vector plasmid-treated (n = 5)	Empty vector control of the plasmid DNA

*The pBCSSP4, pBCSP, mixture, and pBK-CMV groups were treated thrice at 15-day intervals 15 days after the infection; SS was administered under this same scheme in the infected/SS *mock*-treated group.

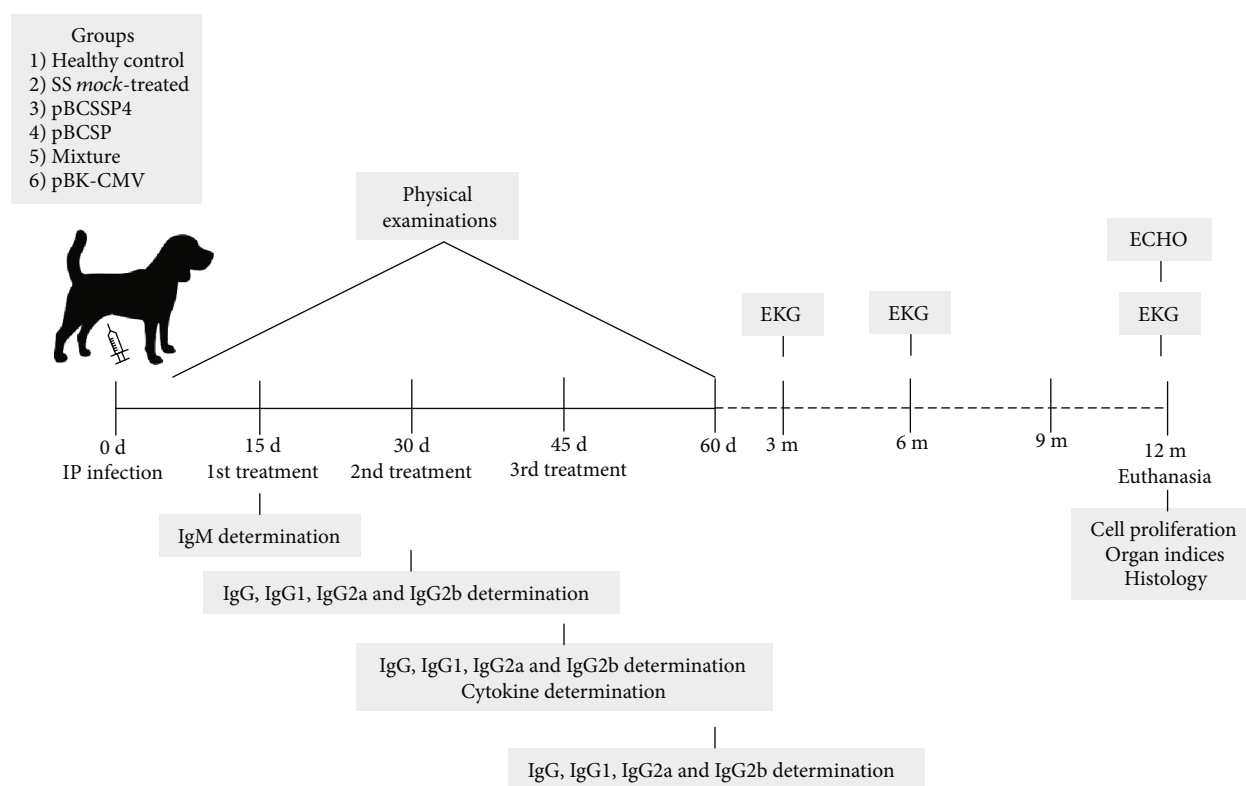


FIGURE 1: Schematic representation of the methodological design. Five groups of dogs were intraperitoneally infected with 3500 metacyclic trypomastigotes/kg body weight of the H8 *T. cruzi* strain to evaluate the effectiveness of the therapeutic DNA vaccine containing *T. cruzi* genes.

the enzyme-linked immunosorbent assay (ELISA). The dogs were separated in six experimental groups, which are detailed in Table 1. The healthy group included noninfected/untreated dogs as the control; the SS *mock*-treated group was used as the positive control of infection; the pBCSSP4 group included infected dogs treated with the pBCSSP4 plasmid; the pBCSP group included infected dogs treated with the pBCSP plasmid; the mixture group included infected dogs treated with the pBCSSP4 and pBCSP plasmids; and the pBK-CMV group included infected dogs treated with the

empty cloning vector plasmid. A representation of the experimental design is shown in Figure 1.

Animal handling followed the established guidelines of the International Guiding Principles for Biomedical Research involving Animals and the Norma Oficial Mexicana (NOM-062-ZOO 1999) Technical Specifications for the Care and Use of Laboratory Animals [28], and the experimental protocol was approved by the Research and Bioethics Committees of the Instituto Nacional de Cardiología, Ignacio Chávez (Registration number: 11-737).

2.2. Blood Samples. Blood extraction was performed directly from the cephalic vein. The dorsal area of the foreleg was constricted at the level of the elbow to raise the vein, and the puncture was started above the metacarpal joint using disposable 3 mL syringes with 21 G × 32 mm needles (PROTEC, Mexico). The sample was collected and immediately deposited in tubes without anticoagulant. Subsequently, the clot was removed and the serum was separated by centrifugation at 3500 rpm for 15 min. Sera were frozen at -20°C until use.

2.3. Diagnostic Serology for Chagas Disease. Before infecting the dogs, it was determined that they were not naturally infected with the parasite. After experimental infection, an enzyme-linked immunosorbent assay (ELISA) and indirect immunofluorescence (IIF) as a confirmatory test were used to determine IgM and IgG antibodies against *T. cruzi* as previously described [5, 29].

2.4. Physical Examinations. Physiological constants, inspections, auscultation, palpation, and percussion were performed during the general physical examinations in all animals. Parameters such as body weight, rectal temperature, body condition, mental state, heart rate, respiratory rate, heart auscultation, lung fields, lung field palm percussion, arterial pulse, mucous membranes, capillary refill time, lymph node palpation, dehydration percentage, head and face natural orifice examinations, cough reflex, swallowing reflex, and abdominal palpation were evaluated and registered [30].

2.5. Infection. Dogs were infected by intraperitoneal injection of 3500 metacyclic trypomastigotes of the H8 *T. cruzi* strain (MHOM/MX/1992/H8 Yucatán (*T. cruzi*)) [31]/kg body weight. The parasites were obtained from the urine and feces of triatomines and resuspended in saline solution (SS).

2.6. Plasmid Descriptions. Plasmids based on the pBK-CMV commercial plasmid vector (Stratagene (now Agilent Technologies), CA, USA) encoding the *T. cruzi* antigens TcSP and TcSSP4 have been described previously [22, 32, 33]. Briefly, pBK-CMV has 17 cloning sites flanked by the T3 and T7 promoters and contains the cytomegalovirus early promoter, which allows for eukaryotic expression and the polyadenylation sequence of the SV40 virus, thus providing the signal required for the termination of eukaryotic transcription and polyadenylation. This plasmid has a kanamycin resistance gene that allows for the selection of positive clones in bacteria. This plasmid was used for the construction of those carrying the *T. cruzi* genes, which will be used for immunotherapy against Chagas disease. pBK-CMV was also used as an empty vector control for the DNA treatment. The pBCSP plasmid is a construct derived from the pBK-CMV vector that possesses the gene coding for the TcSP protein of *T. cruzi*, an all stages-expressed *trans*-sialidase that adds sialic acid to the mucins of the surface cover for host-parasite interactions. pBCSSP4 is a construct derived from the pBK-CMV vector that possesses the gene coding for the TcSSP4 protein of *T. cruzi*, an acid glycoprotein that is expressed during the transformation of trypomastigotes into amastigotes.

2.7. Plasmid DNA Purification. Under aseptic conditions, the transformed *Escherichia coli* XL1-Blue strain carrying the pBCSSP4, pBCSP, and pBK-CMV plasmids was cultured in 500 mL of Luria Bertani broth with kanamycin by 16 h at 37°C/200 rpm incubation. Plasmid DNA was purified by alkaline lysis and ultrapurified using Qiagen (Hilden, Germany) columns. DNA used for immunotherapy was resuspended in lipopolysaccharide-free PBS (Gibco by Thermo Fisher, MA, USA), and its purity was estimated and quantified [34]. Aliquots of 0.5 mg dissolved in 0.5 mL of SS were generated and stored at -20°C until use.

2.8. Plasmid DNA Immunotherapy. At day 15 postinfection, the dogs were treated thrice at 15-day intervals by intramuscular injection of 500 µg of each recombinant plasmid (pBCSP or pBCSSP4) or a combination of 250 µg of each plasmid or vector DNA (pBK-CMV) in the semitendinosus and semimembranosus muscles of the pelvic members. The SS mock-treated control animals were injected with 500 µL of sterile SS on the same schedule as the treated dogs.

2.9. Antibodies Determination. Total IgM and IgG immunoglobulins as well as the IgG1, IgG2a, and IgG2b isotypes were evaluated 15 days postinfection (IgM) and 15 days after each treatment (total IgG, IgG1, IgG2a, and IgG2b) by the ELISA method using a whole protein extract of the *T. cruzi* INC-9 isolate as the antigen as described previously [5, 29]. Briefly, 96 MaxiSorp plates (Nunc by Thermo Fisher, MA, USA) were coated with the whole *T. cruzi* isolate extract (1 µg/mL) overnight at 4°C in 200 µL of NaCO₃/NaHCO₃ pH 9.6 (carbonate buffer). The plates were washed seven times with 215 µL PBS 1X-0.05% Tween-20 (PBS-T) and blocked with 200 µL 0.5% BSA in PBS-T (blocking buffer) for at least 30 min at 37°C. Serum samples were diluted in blocking buffer at a dilution of 1 : 200 in 200 µL/well and incubated (1 h, 37°C). Plates were then washed seven times, and 200 µL of peroxidase-conjugated anti-dog immunoglobulin G (IgG), IgG isotypes (IgG1, IgG2a, and IgG2b), or immunoglobulin M (IgM) secondary antibodies (Novus Biologicals, CO, USA) was added and incubated (1 h, 37°C). The conjugates were diluted in blocking buffer at 1 : 10,000. The plates were washed seven times, and 150 µL of peroxidase substrate OPD (*ortho*-phenylenediamine dihydrochloride, Sigma-Aldrich, MO, USA) in citrate buffer at pH 4.5-0.03% H₂O₂ was added. The reaction was stopped 10 min later by the addition of 50 µL of 5 N H₂SO₄. Absorbance values were determined at 495 nm in a Microplate Reader (Bio-Rad, CA, USA). All measurements were performed twice, and the data presented are the mean of the values for each dog.

2.10. Cytokine Quantification. The IL-1 alpha, IL-6, IL-12, IFN-gamma, and TNF-alpha levels in the sera of immune-treated dogs at 3, 8, 12, and 24 h after the last treatment dose were measured by ELISA using commercial kits (PeproTech, NJ, USA) in accordance with the manufacturer's instructions as follows. The capture antibody was diluted to 1.0 µg/mL with PBS, and 100 µL/well was added to the 96 MaxiSorp plates (Nunc) and incubated overnight at room temperature. The plates were washed four times with 215 µL PBS-T,

blocked with 200 μL of blocking buffer per well for 1 h at room temperature, and washed four times. The standard sample was prepared for each cytokine, and 100 μL /well was added; then, 100 μL of the immune-treated dog serum was added to each well and incubated 2 h at room temperature. The plates were washed four times, and then, 100 μL of the previously diluted detection antibody was added and incubated at room temperature for 1.5 h. The plates were washed, and then, 100 μL of previously diluted avidin was added and incubated 30 min at room temperature. The plates were washed again, and then, 100 μL of peroxidase substrate OPD (Sigma-Aldrich) in citrate buffer at pH 4.5-0.03% H_2O_2 was added. The plates were incubated 15 min at room temperature, and the reaction was stopped with 50 μL of 5 N H_2SO_4 per well. The reading was performed at 490 nm using a Microplate Reader (Bio-Rad, Model 550).

2.11. Cell Proliferation. At 10.5 months after the last treatment with the plasmid DNA (12 months postinfection), the proliferative response of spleen cells was studied *in vitro*. Splenocytes were obtained by necropsy, washed three times in Hank's solution (Sigma-Aldrich), and resuspended in Dulbecco's Modified Eagle Medium (DMEM, Gibco) supplemented with 1 mM nonessential amino acids, 10% fetal bovine serum, 2 mM L-glutamine, and 50 μM beta-mercaptoethanol at a concentration of 4×10^5 cells/mL. The viability percentage was obtained by exclusion with Trypan blue staining. The cells were cultured in 96-well flat bottom plates (Corning, NY, USA); and then, 100 μL of cell suspension and 10 $\mu\text{g}/\text{mL}$ antigen (whole protein extract of epimastigotes of *T. cruzi* INC-9 isolate) were added into each well. Concanavalin A (Sigma-Aldrich) was added at a concentration of 5 and 10 $\mu\text{g}/\text{mL}$ as a positive control. Each determination was performed in triplicate. The plates were incubated at 37°C in a 5% CO_2 for 120 h (or 72 h for Concanavalin A). At 16 h prior to the end of the incubation, 0.5 μCi of [^3H]-thymidine (Amersham, Buckinghamshire, UK) was added to each well. The lymphocytes were collected with a manual cell harvester (Nunc), and the amount of incorporated radioactive thymidine was measured using liquid scintillation spectroscopy (Beckman Coulter, CA, USA, model LS 5801). The stimulation of a specific cellular immune response is represented by the stimulation index (S.I.) by the average of the data obtained in triplicate and estimated as follows: mean counts per minute of stimulated cultures/mean counts per minute of nonstimulated cultures. S.I. values above 2.5 were considered positive [35].

2.12. Electrocardiography. To determine whether the treatment with recombinant DNA plasmids has any effect on the electrical conduction of the heart during the chronic stage of the disease, electrocardiographic recordings were performed for all animals at three, six, and 12 months after infection. The dogs were held by an attendant in right lateral recumbency, and no chemical restraint was employed; such manipulation was achieved via previous training through daily manipulation on examination tables to maintain the dogs at the desired position to carry out the study. Peripheral bipolar standard leads (I, II, and III), augmented unipolar

peripheral leads (aVR, aVL, and aVF), and special leads (unipolar precordial thoracic leads: CV_5RL , CV_6LL , CV_6LU , and V_{10}) were recorded (Schiller, FL, USA). For each tracing, the voltage was standardized at 1 mV/cm and the paper speed was 50 mm/s.

2.13. Echocardiography. Transthoracic echocardiography (Philips, Amsterdam, Netherlands, model IE33) with a 2-5-3.5 MHz probe was performed in all dogs during the chronic stage of infection (12 months after inoculation) to detect and compare morphological changes in the dogs' hearts. Most of the animals were positioned in dorsal and right or left lateral decubitus without any chemical restriction during the study, which was achieved via previous training through daily manipulation on examination tables to maintain the dogs in the desired position to carry out the study. Image acquisition was performed via a long parasternal axis and two- and four-chamber apical view in bidimensional mode. The end-diastolic and end-systolic diameters of the left ventricle were measured. The left ventricle (LV) septum walls, posterior wall, left atrium (LA), and aorta root (AR) were also recorded. The parameters of LV systolic function, i.e., fractional shortening (FS %), and left ventricular ejection fraction (LVEF %) were calculated from the end-diastolic and end-systolic volumes in the standard four-chamber long-axis two-dimension echo views and following the formula $[\text{end-diastolic volume} - \text{end-systolic volume}] / \text{end-diastolic volume} \times 100$. The LA size parameter was calculated from the ratio of LA and AR. The averages and standard deviations of all parameters were obtained for each group.

2.14. Euthanasia and Organ Indices. At 12 months postinfection, chronic chagasic dogs were euthanized according to the Norma Oficial Mexicana (NOM-033-SAG/ZOO-2014) Methods to Bring Death upon Domestic and Wild Animals [36] by direct intravenous injection of sodium pentobarbital (Barbital, Holland Animal Health, Mexico) at doses of 150 mg/kg into the cephalic vein. Prior to euthanasia, the animal weight was obtained (Bascule Inpros SA de CV, Mexico), and the heart, the spleen, and the popliteal lymph nodes were collected during necropsy and were weighed. Cardiomegaly, splenomegaly, and lymphadenopathy were evaluated by inspecting macroscopic alterations and determining the heart, spleen, and lymph node indices (organ weight/total body weight $\times 100$), respectively. The presence of cardiomegaly and splenomegaly was considered when the organ index was significantly higher than that observed in the organs from healthy noninfected animals [23, 37].

2.15. Histology. Longitudinal and transversal right ventricle (RV) and LV heart muscle tissues were obtained. Tissue sections were fixed in 10% buffered formalin for 24 h. Samples were dehydrated in absolute ethanol, rinsed in xylene, and embedded in paraffin. Noncontiguous sections at 5 μm thickness were cut and stained with hematoxylin and eosin and evaluated by light microscopy (Carl Zeiss, K7, Germany). Images were obtained through a BioDoc-It Imaging System image analyzer (UVP, LLC, USA). At least

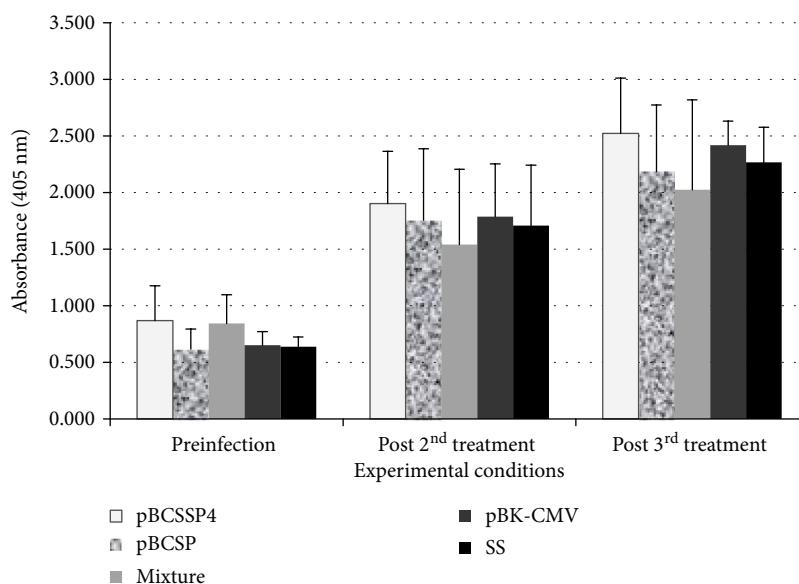


FIGURE 2: Total IgG titers in *T. cruzi*-infected dogs treated with plasmid DNA. ELISA was performed at different times to evaluate the serum levels (absorbance in optical density at 405 nm) of *T. cruzi* IgG-specific antibodies. Preinfection; post 2nd treatment: 45 days after infection and 15 days after the second immunotherapy; and post 3rd treatment: 60 days after infection and 15 days after the third immunotherapy. The values represent the average of triplicate assays \pm S.D. Significant differences ($*P \leq 0.05$) were not identified.

20 random microscopic fields (100 and 400x) were analyzed in each microscopic section using the open-source ImageJ software (NIH, USA). The severity of inflammation in the affected tissue was scored on a scale of 1 to 4. A score of 1 indicated one or less foci of inflammatory cells/field (400x); 2 indicated more than one focus of inflammatory cells/field; 3 indicated generalized coalescing foci of inflammation or disseminated inflammation with cell necrosis and retention of tissue integrity; and 4 indicated diffuse inflammation, tissue necrosis, interstitial edema, hemorrhage, and loss of tissue integrity.

2.16. Statistical Analysis. Continuous variables, such as body temperature, heart rate, antibody, or cytokine presence, and echocardiographic parameters were analyzed using the one-way or two-way ANOVA statistical test (SPSS software, version 17.0) followed by Tukey's analysis establishing a correlation between each experimental group and the control one. Nonparametric data, such as lymph node palpation, heart and spleen indices, and histological data, were analyzed by the Kruskal-Wallis test (SPSS software, version 17.0). In all cases, differences were considered significant at $P < 0.05$.

3. Results

3.1. Immunotherapy with Recombinant Plasmids Containing *T. cruzi* Genes Controlled Some Signs of Chagas Disease in Infected Dogs. The data from the physical examination were under the reference values or showed that all the dogs were healthy before the start of the project. The acute phase presentation of Chagas disease was characterized by fever, swelling of lymph nodes, pale mucous membranes, slow capillary refill time, anorexia, and slight weight loss, and it was observed in 100% of the infected/nontreated dogs from days 5 to 35-50 postinfection; however, in the immunotreated groups, only

25% of each group showed a mild fever and lymph node inflammation from days 22 to 30 postinfection (days 7 to 15 posttreatment).

3.2. *T. cruzi* Infection in Beagle Dogs Was Confirmed with Serological Diagnostic Tests. The ELISA serological test showed that all of the experimental animals were negative for the diagnosis of Chagas disease, which confirmed that the dogs were free of *T. cruzi* infection before any manipulation. Before the first immunotherapy, *T. cruzi* infection was demonstrated at day 15 postinfection by the detection of specific IgM anti-*T. cruzi* antibodies in all dogs (data not shown) and at 30 days postinfection by the detection of specific IgG anti-*T. cruzi* antibodies in all infected/nontreated groups by the ELISA method and IIF confirmatory test.

3.3. Immunotherapy Was Not Able to Differentially Modulate the Humoral Immune Response in Treated or Untreated Dogs Experimentally Infected by *T. cruzi*. To determine the effect of the therapeutic DNA vaccine on specific humoral responses against *T. cruzi* infection in chagasic dogs, antibodies were detected by ELISA. A significant increase in IgG was generated after 45 and 60 days postinfection in all groups (Figure 2) regardless of whether the dogs were vaccinated or not. In addition, a Th1- or Th2-polarized immune response was not observed after immunotherapy or infection based on the detection of IgG2a and IgG2b or IgG1, respectively; in other words, both subclasses remained at similar levels and there was no difference between them (data not shown).

3.4. pBCSSP4 Plasmid Was Able to Trigger a Balanced Response (Th1/Th2) by High IL-1 and IL-6 Production, While pBCSP Induced a Th1 Immune Response Profile by High IFN-Gamma, TNF-Alpha, and IL-1 Levels. To evaluate the

immunotherapy with the DNA vaccine on specific cellular immune responses against *T. cruzi* infection, the IL-1 alpha, IL-6, IL-12, IFN-gamma, and TNF-alpha cytokine levels were determined. Kinetics of the serum levels of these cytokines was quantified at 3, 8, 12, and 24 h after each treatment. The optimal time for all cytokines was at 3 h posttreatment because there were detectable levels of all cytokines at this time; therefore, only the analysis of the amounts of each cytokine obtained during the 3 h posttreatment is shown (Figure 3). According to the expected effect of the infection on cytokine production, it was possible to demonstrate that the infection itself induces a significant increase in the production of IL-12 in these dogs after 30 days of infection without treatment in comparison with the control group of healthy dogs (Figure 3(c)). As the infection progressed (at day 45 postinfection), the differences between these both groups were significant in all cytokines (Figure 3).

3.4.1. IL-1 Alpha. The separate administration of recombinant plasmids significantly stimulated the production of IL-1 alpha (Figure 3(a)) after the second treatment dose, and it was better than that of the pBCSP plasmid with an increase of approximately 10-fold. After the administration of the third treatment dose, the production of this cytokine was significantly increased by the pBCSP and pBK-CMV plasmids (Figure 3(a)) without exceeding the stimulation by the infection alone. None of the other treatments had a significant effect on stimulating the production of this cytokine at either time.

3.4.2. IL-6. The recombinant plasmids and the empty vector stimulated the production of IL-6 (Figure 3(b)) after the second dose of treatment. The mixture of both plasmids and the infection alone had no effect. With the third treatment (45 days after infection), the production of IL-6 in the group treated with *TcSSP4* gene was significantly increased by 4-fold above the SS *mock*-treated infected group while the *TcSP* gene, the mixture of both plasmids, and the pBK-CMV empty plasmid induced similar levels of this cytokine to those of the infected/SS *mock*-treated group (Figure 3(b)).

3.4.3. IL-12. The serum level of IL-12 (Figure 3(c)) increased with the second treatment of pBCSP plasmid and was as high as the infection alone, while the pBCSSP4 plasmid, the mixture of recombinant plasmids, and the empty vector did not have a significant effect. The empty vector showed similar values to those of the infected/SS *mock*-treated group in the third treatment, while the two genes separately and the mixture of genes had levels similar to those of the healthy control group, demonstrating that they did not stimulate IL-12 production any more than the infection alone. In fact, the levels were lower than those of the infected/SS *mock*-treated group.

3.4.4. IFN-Gamma. Significant IFN-gamma production (Figure 3(d)) was induced by both recombinant plasmids separately. The mixture of both plasmids and the empty vector and the infection alone had no effect at this time. With the third treatment, the pBCSP plasmid increased the levels of this cytokine by approximately 10-fold compared with those of the infected/SS *mock*-treated dogs. The mixture of

both plasmids also had a positive effect after the third treatment, although at a smaller proportion.

3.4.5. TNF-Alpha. After the second treatment, only the empty vector and the pBCSP plasmids increased the production of TNF-alpha (Figure 3(e)). With the third treatment, a significant increase was recorded in all groups compared with the control healthy group; however, those treated with the pBCSP plasmid had a 14-fold higher level of this cytokine than the infected/SS *mock*-treated group.

To summarize, immunotherapy with the pBCSSP4 plasmid was able to trigger a balanced response (Th1/Th2) by high IL-1 and IL-6 production while the treatment with the pBCSP plasmid induced a Th1 immune response profile based on the high IFN-gamma, TNF-alpha, and IL-1 levels.

3.5. Cell Proliferation Was Mostly Stimulated by the pBCSSP4 Recombinant Plasmid than by pBCSP. To evaluate the specific cellular immune response in infected dogs treated intramuscularly with *T. cruzi* genes, the lymphoproliferative response to stimulation with parasite antigens was studied. The lymphoproliferative responses were observed in the animals treated with both *T. cruzi* genes separately (Figure 4). The highest stimulation index (3.02) was observed in dogs treated with the pBCSSP4 plasmid, and proliferation of the splenocytes was also observed in the dogs that received the immunotherapy with the pBCSP plasmid (stimulation index 2.53). Proliferation occurred when the stimulation index is above 2.5 [35]. In the control groups and group treated with the mixture of the two recombinant plasmids, cell proliferation was not observed and the stimulation index values were below 2.5. The cultures stimulated with Con A showed a value of 8.65 ± 0.79 , thus demonstrating the viability of the cells in all experimental groups.

3.6. Electrocardiograms (EKG) of Dogs Immunotreated with Recombinant Plasmids Showed Few Nonserious Abnormalities. The DNA vaccines used as immunotherapy in the dogs infected with *T. cruzi* were moderately effective in preventing cardiac disturbances or delaying the onset associated with chronic chagasic cardiomyopathy evaluated by electrocardiography at three, six, and 12 months after infection (Table 2). In all groups, sinus arrhythmia was found at least once in the twelve months, and this condition was likely due to a physiological state associated with the physical restraint procedures related to respiration. The group treated with either the recombinant plasmids or the mixture had cardiac disturbances limited to only one alteration or in combination with two other abnormalities that did not represent a serious pathology at three months postinfection. In contrast, those animals that received treatment with pBK-CMV or SS showed a combination of four alterations, such as the mean electrical axis deviation (MEAD) of less than $+40^\circ$, QRS complex with a wide R wave, the absence of T waves in some recordings, and S-T segment elevation of 0.5 mV in II, III, aVF, and V_6LL in 60% of the animals. At six months postinfection, electrocardiographic abnormalities were only registered in 20% and 40% of the dogs in the groups treated with pBCSP and pBCSSP4, respectively. The EKG with the greatest

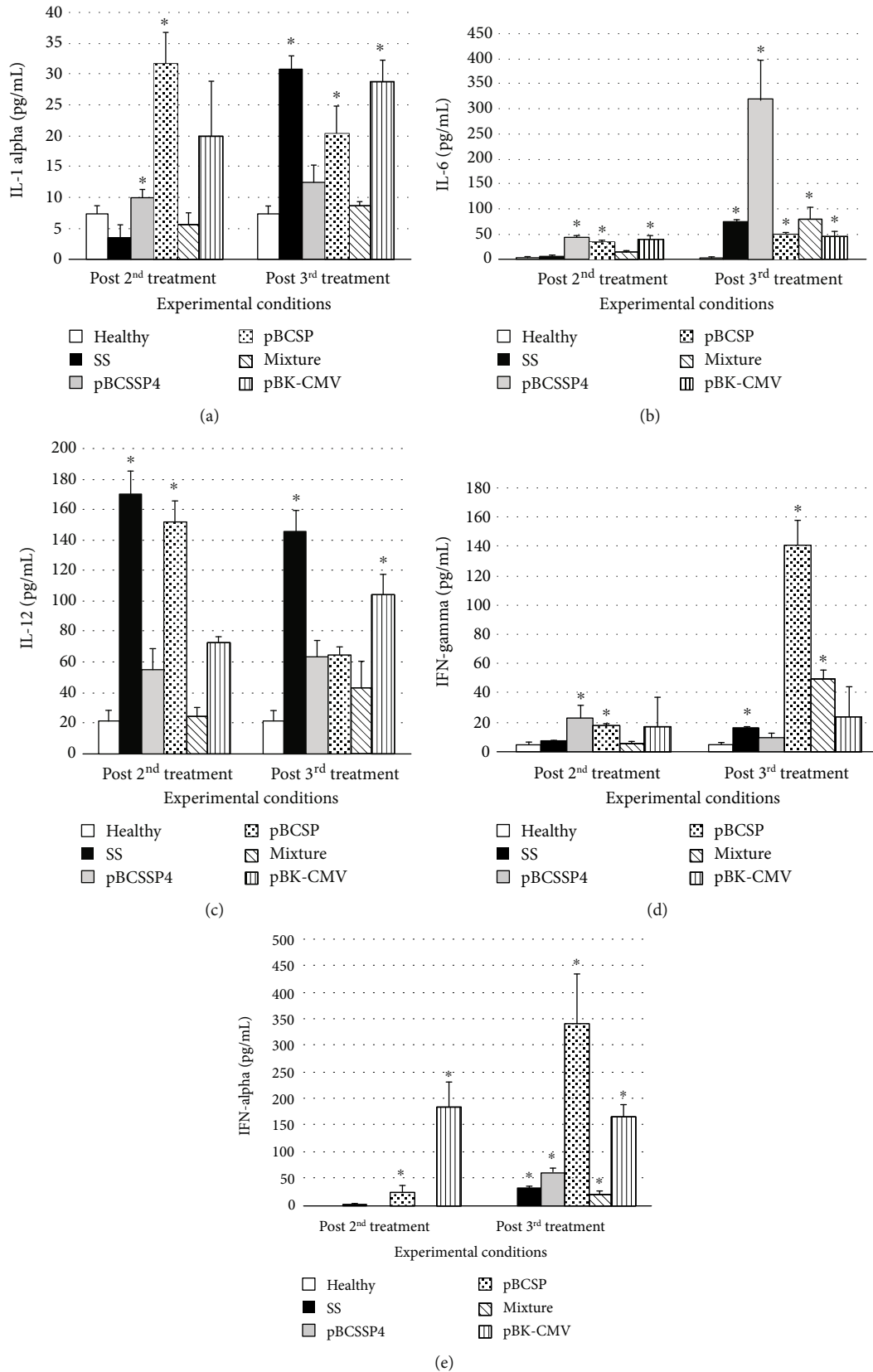


FIGURE 3: Serum level of cytokines in dogs infected with *T. cruzi* and treated with DNA vaccines. An ELISA was performed at 3 h after each treatment to evaluate the serum levels (absorbance in optical density at 405 nm) of each cytokine in dogs. (a) IL-1 alpha, (b) IL-6, (c) IL-12, (d) IFN-gamma, and (e) TNF-alpha. Post 2nd treatment: 30 days after infection; post 3rd treatment: 45 days after infection. The values represent the average of triplicate assays \pm S.D. (* $P \leq 0.05$).

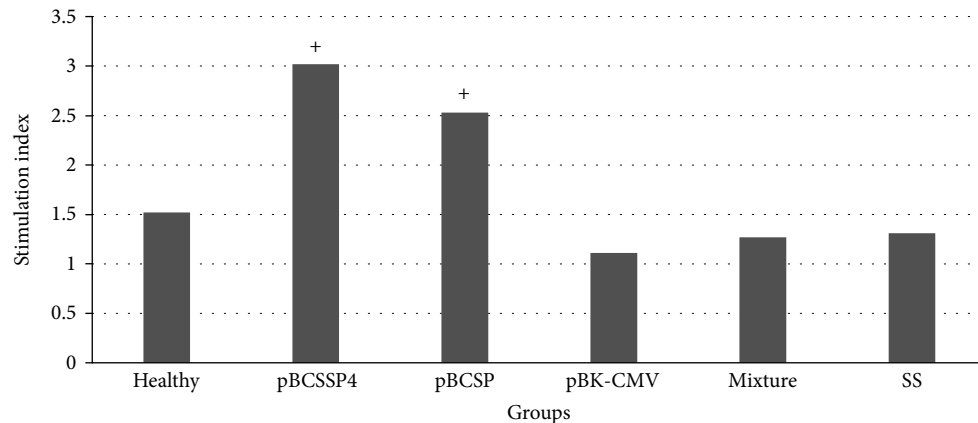


FIGURE 4: Lymphoproliferation of spleen cells of *T. cruzi*-infected dogs treated with plasmid DNA. The values represent the stimulation index and were considered positive (+) if they were equal to or above 2.5 [35].

number of abnormalities occurred in 80% of the individuals (4/5) in the empty plasmid or infected/SS *mock*-treated groups. By 10 months postinfection, an individual from the pBK-CMV group experienced sudden death; and in its last EKG, this dog had presented MEAD to the right; right bundle branch block (RBBB); ventricle enlargement, infarction, and ischemia; areas of myocardial infarction; adhesions between pericardium and pleura; and apical aneurysm of approximately 0.5 cm at necropsy. Finally, at 12 months postinfection, arrhythmia in combination with MEAD to the left, ventricle enlargement, ischemia, and microscopic intramural myocardial infarction were found in the pBK-CMV group, whereas both arrhythmia and ischemia in combination with MEAD to the left and/or to the right and ventricle enlargement were found in the SS *mock*-treated group.

3.7. Therapeutic DNA Vaccine with pBCSSP4 Showed a Better Protective Effect on Cardiac Function by Echocardiography. Each average value was compared with the reference values and the parameters from the dogs of the healthy group (Table 3). The diastolic and systolic diameters of the groups that received immunotherapy were not affected since the values were very similar to those of the healthy group, whereas significantly lower values were observed in the infected/SS *mock*-treated group. The shortening fraction of the LV was not affected by the infection or modified with immunotherapy, which indicates an efficient contractile force in all groups. The thickness values of the posterior wall and the septum in the dogs' hearts did not show significant differences with respect to the healthy group and were within the reference values except for the group treated with pBCSSP4, whose values resembled those of the infected/SS *mock*-treated group, suggesting hypertrophic cardiomyopathy. The pBCSP group had significantly lower LV ejection fraction values (43%) than the rest of the groups (49%-50%) and the healthy group (53%), which indicates significant myocardial injury probably due dilated heart disease caused by *T. cruzi* infection. This finding is supported by the ratio of the left atrial diameter and the diameter of the aortic root, which was 2.02, indicating a left atrial dilation in this group.

The echocardiographic study showed that the therapeutic vaccine with the pBCSSP4 recombinant plasmid had a better protective effect since the cardiac function was very similar to that of the healthy control group, while the pBCSP treatment showed structural and functional damage.

3.8. Immunotherapy with the pBCSSP4 Recombinant Plasmid Prevented Cardiomegaly. After euthanasia, the heart, spleen, and lymph node indices were calculated to determine whether cardiomegaly, splenomegaly, and lymphadenopathy had occurred, respectively. The H8 *T. cruzi* strain produced cardiomegaly in all infected dogs; however, the treatment with the pBCSSP4 recombinant plasmid prevented cardiomegaly in the chronic stage of Chagas disease by showing a similar heart index than the healthy group (Figure 5(a)). A significant splenomegaly was registered in the pBCSSP4 and mixture groups in the chronic phase of Chagas disease (Figure 5(b)). Neither immunotherapy nor chronic infection caused lymph node enlargement (data not shown).

3.9. Both Recombinant Plasmids Separately Showed Moderate Control of the *T. cruzi* Infection by Reducing Cardiac Inflammatory Infiltrates. No evidence of amastigote nests, fibrosis, or edema was observed in any of the analyzed tissue sections. The healthy control group did not show histological myocardial abnormalities (Figure 6(a)). Eosinophilic lymphoplasmacytic interstitial ventricular myocarditis was observed in all infected groups at varying severity, with the SS *mock*-treated group showing severe multifocal coalescent inflammation (score: 3.5 ± 0.5) (Figures 6(a, B) and 6(b)), with both the pBCSSP4 (Figure 6(a, C)) and pBCSP (Figure 6(a, D)) groups showing mild multifocal myocarditis (scores: 1 ± 0.4 and 2.2 ± 0.4 , respectively (Figure 6(b)), and with the pBCSP group also showing moderate myofibrillar degeneration. The group treated with the mixture of both plasmids (Figure 6(a, E)) and with the empty cloning vector (Figure 6(a, F)) showed inflammation foci similar to that found in those of the SS *mock*-treated group (scores: 3.2 ± 0.7 and 3.8 ± 0.4 , respectively) (Figure 6(b)). These findings suggest that the immunotherapy with both plasmids

TABLE 2: Abnormal electrocardiographic features in dogs experimentally infected with *T. cruzi* and treated with the DNA vaccine at 3, 6, and 12 months postinfection (mpi).

Group*	Suggested pathological conditions by EKG recordings [78, 79]	Affected dogs (dogs/ <i>n</i>) at 3 mpi	Affected dogs (dogs/ <i>n</i>) at 6 mpi	Affected dogs (dogs/ <i>n</i>) at 12 mpi
Inf/SS <i>mock</i> -treated	AV block+infarction	20% (1/5)		
	Ischemia	20% (1/5)		
	MEAD to the left+LBBB+infarction+ventricle enlargement	20% (1/5)		
	MEAD to the right+RBBB+infarction+ventricle enlargement		60% (3/5)	
	Arrhythmia+MEAD to the left+ventricle enlargement			20% (1/5)
pBCSSP4	Ischemia+MEAD to the right+ventricle enlargement			60% (3/5)
	AV block		20% (1/5)	
	LBBB	20% (1/5)		
	MEAD to the right+RBBB+infarction	20% (1/5)		
	MEAD to the left+LBBB+AV block	20% (1/5)		
pBCSP	LBBB+infarction+ischemia	40% (2/5)	20% (1/5)	
	RBBB+ischemia			40% (2/5)
	AV block	20% (1/5)		
	Infarction	20% (1/5)		
Mixture	Infarction+ischemia	20% (1/5)	20% (1/5)	
	Arrhythmia+AV block			20% (1/5)
	AV block+infarction+RBBB	20% (1/5)		
pBK-CMV	Ischemia	20% (1/5)	20% (1/5)	
	Arrhythmia+ischemia		20% (1/5)	
	AV block+ischemia		20% (1/5)	20% (1/5)
	Arrhythmia+ischemia		20% (1/5)	
	MEAD to the left+ventricle enlargement	40% (2/5)		
	MEAD to the left+LBBB+infarction+ventricle enlargement	20% (1/5)		
	Arrhythmia+MEAD to the right+ventricle enlargement+ischemia		20% (1/5)	
MEAD to the right+RBBB+ventricle enlargement+infarction+ischemia		40% (2/5)		
	Ventricle enlargement			20% (1/5)
	Arrhythmia+MEAD to the left+ventricle enlargement			20% (1/5)
	Arrhythmia+ventricle enlargement+ischemia+MIMI			20% (1/5)

*Group descriptions are shown in Table 1. mpi = months postinfection; Inf = infected; AV = atrioventricular; LBBB = left bundle branch block; RBBB = right bundle branch block; MEAD = mean electrical axis deviation; MIMI = microscopic intramural myocardial infarction.

separately moderately controlled the infection and consequently reduced the inflammatory infiltrate responsible for cardiomyopathy.

4. Discussion

DNA vaccines provide a new alternative for both the prevention and the treatment of a variety of infectious diseases, including Chagas disease [16]. In the development of vaccines against *Trypanosoma cruzi*, it has been suggested that to effectively control the parasite, a complete and complex

immune response involving lytic antibodies and cytotoxic T cells and the production of Th1 cytokines is required [38].

The control of parasitism of *T. cruzi* depends on both innate and acquired immune responses, which are triggered during early infection and considered critical for host survival, and they both involve the participation of macrophages, natural killer (NK) cells, and T and B lymphocytes and the production of Th1 proinflammatory cytokines, such as IFN-gamma, TNF-alpha, and IL-12 [39].

In the present study, the therapeutic efficacy of two plasmids, pBCSSP4 and pBCSP, was evaluated with regard

TABLE 3: Cardiovascular parameters based on echocardiography in dogs experimentally infected with *T. cruzi* and treated with the DNA vaccine containing genes encoding a *trans*-sialidase protein (pBCSP), an amastigote-specific glycoprotein (pBCSSP4), or both as a mixture.

Group*	Left ventricular (LV) diastolic diameter (mm)	Left ventricular (LV) systolic diameter (mm)	Fractional shortening (FS) (%)	Left ventricular ejection fraction (LVEF) (%)	Posterior wall (mm)	Septum (mm)	Left atrium (LA) diameter/aorta root (AR) diameter ratio
Healthy	30.25 ± 3.89	18.46 ± 2.07	42.12 ± 4.98	53.20 ± 3.83	5.86 ± 0.21	6.35 ± 0.21	1.73 ± 0.095
Inf/SS <i>mock</i> -treated	28.33 ± 3.32*	15.60 ± 1.57*	44.75 ± 3.97	50.31 ± 6.31	6.81 ± 0.40*	8.00 ± 1.19*	2.23 ± 0.19*
pBCSSP4	30.63 ± 4.88	20.00 ± 4.55	38.33 ± 5.90	50.15 ± 8.99	6.85 ± 0.84*	7.00 ± 0.94	1.92 ± 0.28
pBCSP	32.45 ± 5.89	20.00 ± 2.92	29.24 ± 3.36	43.25 ± 3.78*	5.65 ± 0.45	6.30 ± 0.78	2.02 ± 0.18*
Mixture	35.60 ± 2.74	23.85 ± 4.09	38.37 ± 9.36	49.75 ± 8.66	6.34 ± 0.92	7.08 ± 0.50	1.79 ± 0.40
pBK-CMV	30.18 ± 3.66	17.85 ± 1.57	38.05 ± 6.70	50.50 ± 6.10	6.40 ± 0.49	6.74 ± 0.71	1.78 ± 0.33

*Group descriptions are shown in Table 1. Inf = infected. All data are expressed as the means and standard deviations. *Significant difference ($P \leq 0.05$) between the treatment groups and the healthy dogs and/or with reference values [80].

to the modulation of the immune response from the plasmid DNA vaccines in a canine model. The effect of the treatment relative to the infected/SS *mock*-treated dogs was analyzed to evaluate both the humoral and cellular immune responses through antibody production, cytokine production, and cell proliferation. On the other hand, the analysis of the general physical state, electrocardiographic and echocardiographic studies, and macroscopic findings during necropsy evaluated the degree of protection provided by this immunotherapy.

Immunotherapy with these plasmids could provide a survival advantage by reducing the clinical signs of infection and ameliorating the cardiac damage of Chagas disease by avoiding disease progression as seen with other immunotherapeutic agents against various pathologies, such as allergies, herpes, cancer, viral diseases, mycosis, Chagas disease, and leishmaniasis [40–45]. For example, in dogs naturally infected with herpesvirus, early mucosal administration of liposome-TLR complexes generated a significant reduction in the clinical signs (e.g., conjunctivitis) of canine herpesvirus infection [43]. Fever and lymph node inflammation, which were the main clinical manifestations of the acute phase in Chagas disease in dogs [46–48], were ameliorated 7–15 days after immunotherapy in 25% of DNA-treated animals.

Vaccines based on transialidases and cruzipain as either DNA vaccines, recombinant proteins, or combinations as booster or in recombinant viral vectors have shown effective prophylactic and therapeutic effects against *T. cruzi* infection in mice [20, 46–50]. In the present study, we tested two plasmids that code for two different surface proteins of *T. cruzi*: TcSSP4, an amastigote-specific glycoprotein, and TcSP, a protein of the transialidase family present in all parasitic stages [51]. Other authors found that the production of IL-6 in endothelial cells and the increased expression of mRNA of TNF-alpha and IL-1 beta in infected cardiac myocytes were induced by a transialidase, suggesting that myocytes also respond to *T. cruzi* by the production of inflammatory cytokines [39]. Consistent with studies referenced by Machado et al. [39], our pBCSP plasmid stimulated the production of IL-1 alpha and IFN-gamma better than pBCSSP4, the mixture of both plasmids, and the infection itself. It would be very convenient to correlate the cardiomyocyte integrity of vaccinated and infected dogs with their levels of these cytokines

because cardiomegaly, a characteristic of Chagas disease, is attributable to local inflammatory processes related to the activation of nuclear factor kappa B (NF-kappa B) induced by Toll-like receptor 2 (TLR2) and IL-1 local production [52].

In our study, immunotherapy with the empty vector also induced similar levels of IL-12 relative to those produced by stimulation with *T. cruzi* infection and was also able to increase the levels of IFN-gamma and TNF-alpha and obtained a nonspecific response to the *T. cruzi* antigens that can be attributed to the immunomodulatory effect of the plasmid DNA as previously reported [53]. This finding is consistent with the study reported by Duan et al. [54], who immunized mice with the recombinant Sendai virus that expresses the ASP2 or UASP2 antigens of *T. cruzi* showing a protective response attributable to CD8+ T cells against *T. cruzi* infection, thus confirming the adjuvant effect of the viral vector on the activation of these cells.

CD4+ T cells play an important role in fighting pathogens via the secretion of IFN-gamma, which increases the production of nitric oxide, a substance that is toxic to intracellular parasites, and via the expression of major histocompatibility complex (MHC) class I molecules in infected cells, which allows for easier recognition by CD8+ T cells. CD8+ T cells also contribute to the elimination of intracellular pathogens by exhibiting cytotoxic activity against infected cell as well as by producing IFN-gamma after recognition of antigenic epitopes presented in combination with MHC class I molecules [54]. In this study, we found that treatment with both recombinant plasmids separately induced the expression of IFN-gamma in the acute stage of the disease, which is consistent with the findings reported by Zapata-Estrella et al. [55], who observed that immunotherapy with a plasmid encoding the TSA-1 antigen stimulated the immune system of infected mice and particularly activated IFN-gamma-producing CD4+ and CD8+ T cells in the acute and chronic phases of the experimental disease, suggesting a reorientation of the nonprotective immune response to a protective response throughout the treatment. Our recombinant plasmids used in the present study were also used in a prophylactic vaccination scheme for Chagas disease in canine models in previous studies [24], where the results indicated that vaccination with pBCSSP4 significantly increased the

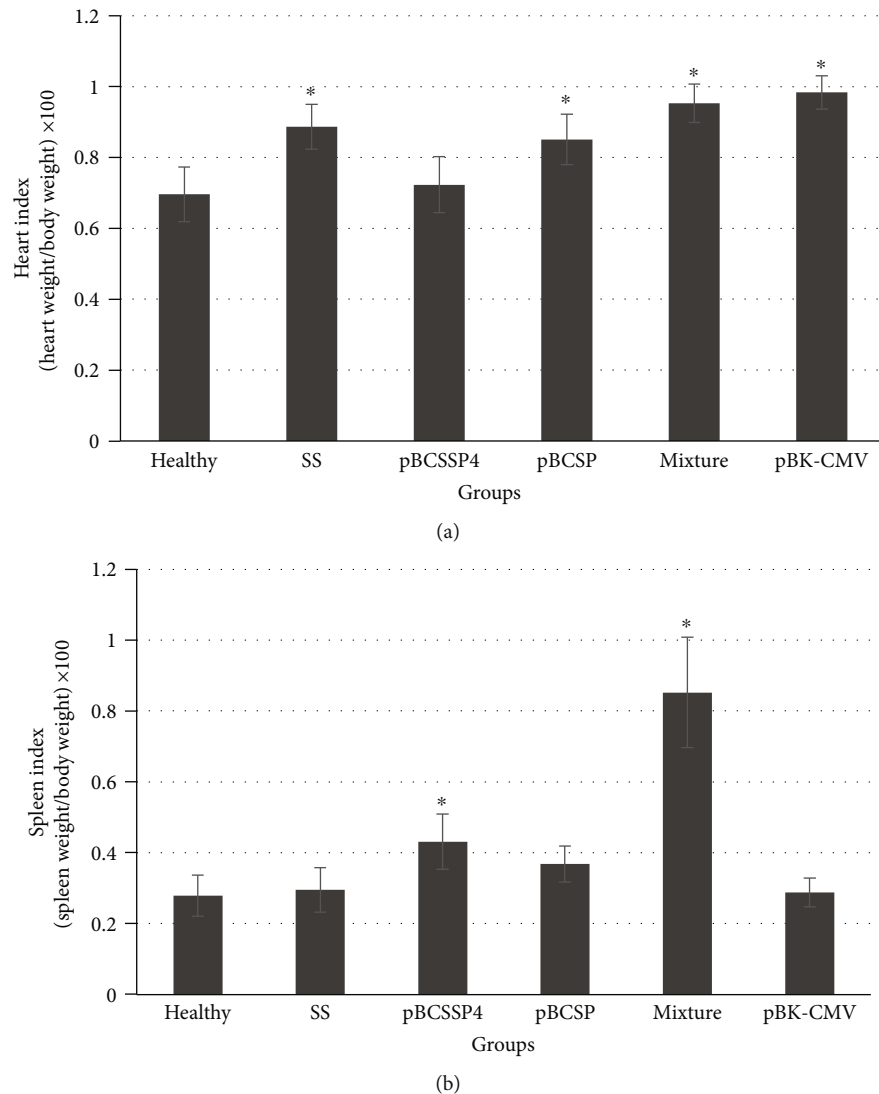


FIGURE 5: Cardiomegaly and splenomegaly during the chronic stage of infection with H8 *T. cruzi* strain in Beagle dogs treated with DNA vaccines. The enlargement of organs was calculated by the mean heart (a) and spleen (b) indices (\pm S.D.). Differences were considered significant at $*P \leq 0.05$ by the Kruskal-Wallis test among the healthy group versus the SS *mock*-treated, pBCSSP4, pBCSP, mixture, and pBK-CMV groups.

IFN-gamma and IL-10 levels at 9 months postinfection. In the present study, a therapeutic effect was evaluated with visible results at 45 days postinfection in the elevation of some evaluated cytokines, demonstrating that immunotherapeutic vaccines are able to redirect the immune response of infected hosts, which is consistent with Aufran et al. [56]. This elevation of IFN-gamma after the second treatment when plasmids pBCSP, pBCSSP4, and the empty vector were used and the increase of more than 10 times when immunotherapy was performed with the plasmid encoding the TcSP protein after the third treatment are partially consistent with Duan et al. [54], who showed that the main target cell of their vaccination strategy was infected cells since the best immune response vaccine antigen was the ASP2 protein, which is expressed exclusively on amastigotes, an intracellular proliferative parasitic form, and expressed at higher levels compared with that in trypomastigotes, which are found in the blood-

stream. The two antigens used in our study are expressed in the intracellular form of amastigotes.

Gupta and Garg used the multicomponent DNA vaccine TcVac2 and found that it stimulated a substantial response of CD8⁺ T cells associated with type 1 cytokines (IFN-gamma and TNF-alpha) that together resulted in acute parasitic load control. During the chronic stage, splenic activation of CD8⁺ T cells and these same cytokines decreased, with a predominance of IL-4/IL-10 in vaccinated mice. The role of Th1 cytokines in the immune control of *T. cruzi* has been addressed by these authors, who showed that overproduction of type 2 cytokines or blockage of type 1 cytokine production correlates with increased susceptibility to *T. cruzi* infection [57]. In our study, the concentrations of IL-4 or IL-10 were not determined; thus, we could not determine whether a certain level of susceptibility to *T. cruzi* infection could be established in infected and treated dogs due to polarization towards a certain

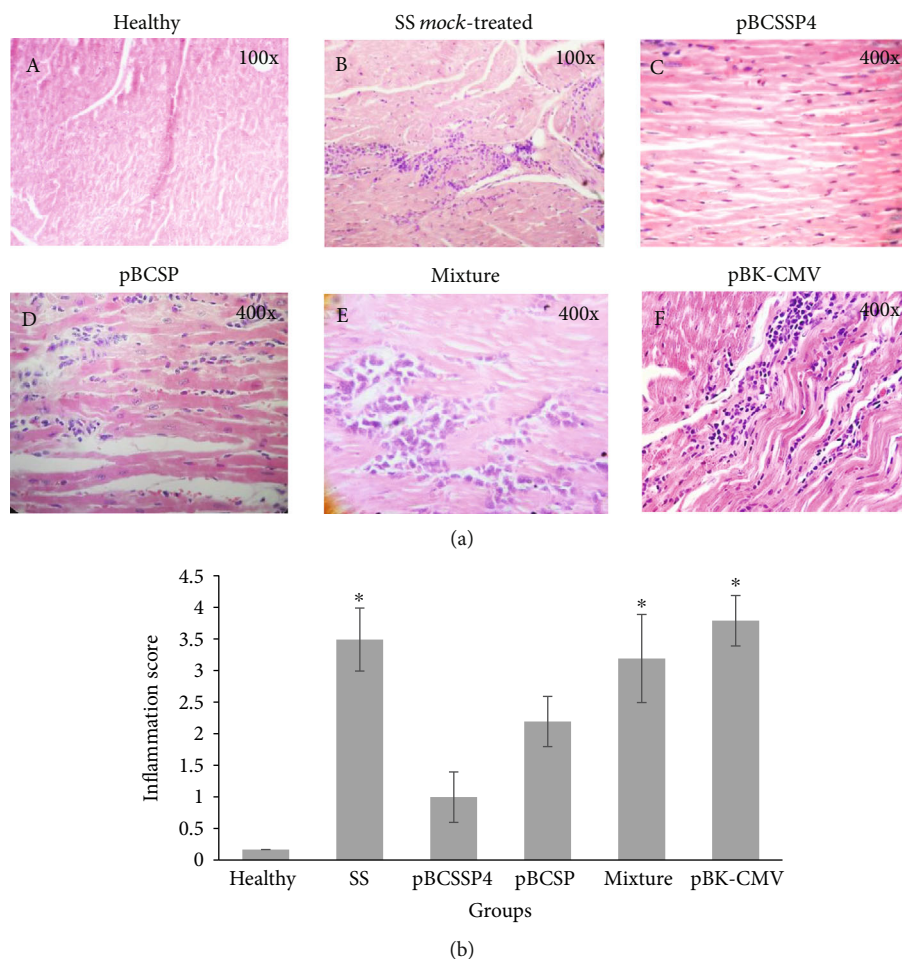


FIGURE 6: Histological ventricular myocardium findings of *T. cruzi*-infected dogs treated with DNA vaccines. (a) Representative micrographs of the heart tissue from all groups are shown. (A) Transverse section of the LV myocardium showing healthy tissue. (B) LV myocardial cross section of the SS *mock*-treated infected control group showing severe multifocal coalescent lymphoplasmacytic myocarditis (score: 4). (C) Longitudinal section of the LV myocardium of the pBCSSP4 plasmid-treated group showing mild multifocal interstitial lymphoplasmacytic myocarditis (score: 2). (D) Longitudinal section of the LV myocardium of the pBCSP plasmid-treated group showing mild multifocal interstitial lymphoplasmacytic myocarditis (score: 2) and moderate degeneration of muscle fibers. (E) RV myocardial longitudinal section of the plasmid mixture-treated group showing lymphocytic moderate multifocal coalescent myocarditis (score: 3). (F) Longitudinal section of the LV myocardium of the empty vector plasmid-treated group showing moderate to severe multifocal coalescent myocarditis (score: 4). Hematoxylin and eosin staining. (b) Inflammatory lesion (inflammatory cell infiltrates) scores. Data are expressed as the mean \pm S.D., and differences were considered significant when $*P \leq 0.05$ by the Kruskal-Wallis test for the healthy group versus the SS *mock*-treated, pBCSSP4, pBCSP, mixture, and pBK-CMV groups.

type of immune response. Such susceptibility was reported by other studies on the development of vaccines against the parasite of the genus *Leishmania*, where the Th1/Th2 paradigm was further studied with *L. major* in mice, and the results indicated that the activation of Th1 cells producing IFN-gamma could lead to protection while Th2 cells producing IL-4 could lead to susceptibility [58].

IL-12 production was stimulated both by the infection alone and by the second injection of pBCSP plasmid as immunotherapy in infected dogs, which indicates that this plasmid is a good candidate for prophylactic and therapeutic vaccination. These effects are consistent with that described by others, who affirmed that the persistence of the *Leishmania* parasite, another trypanosomatid protozoan, and the continuous production of IL-12 are important factors for the mainte-

nance of memory cells and long-term protective immunity [59, 60]. In contrast, immunotherapy with the plasmid pBCSSP4 induced a decrease of this cytokine in the acute stage of the infection, which is consistent with the findings reported by Ramos-Ligonio et al., who saw very low systemic and local (spleen) levels of IL-12 in immunized and infected mice when they used a recombinant SSP4 protein [61].

The elevated levels of IL-1 alpha and IL-6 produced by immunotherapy with the plasmid pBCSSP4 during the early acute stage of infection are also in accordance with Ramos-Ligonio et al., who demonstrated that the *T. cruzi* recombinant SSP4 protein is a humoral and cellular immune response modulator capable of inducing high levels of the IgG1, IgG2a, and IgG2b isotypes, the expression of inducible nitric oxide synthase, and the production of nitric oxide by macrophages

as well as mRNA expression for the IL-1 alpha, IL-6, IL-12, IFN-gamma, and TNF-alpha in control infected mice and IL-10 in immunized/infected mice [61]. The results in the present study also agree with other previous reports [32], where high levels of IL-6 and TNF-alpha at 3 h and 12 h post-immunization in the sera of mice vaccinated with adjuvant with the recombinant SSP4 protein, with the empty vector, and with the pBCSSP4 were detected, suggesting that animals immunized with this gene are able to develop a Th1 response.

Gao and Pereira reported that *T. cruzi* infection in animal models and humans produces a high level of IL-6 in serum and tissue, and it is induced during the ascending phase of parasitemia in the acute stage of Chagas disease [62]. In our study, this cytokine increased with the different treatments during the early phase of the acute infection and was four times higher at the end of the acute stage (after the third treatment) with the pBCSSP4 plasmid immunotherapy. Conversely, IL-6 levels decreased with the pBCSP plasmid. IL-6 is related to B cell proliferation; however, IgG levels did not show differential production among the experimental groups because B lymphocyte proliferation occurred by another route different from that induced by IL-6, such as by IL-4, IL-5, and IL-7 [63].

Transforming growth factor beta and IL-6 are cytokines that differ significantly between cardiac patients with different stages of chagasic heart disease progression. IL-6 is a key inflammatory factor whose secretion is activated by the C-reactive protein and has been implicated in the pathogenesis and clinical evolution of cardiovascular diseases. In patients with heart failure, high serum IL-6 concentrations have been detected, which correlates with left ventricular dysfunction severity [64]. In the same way, the increased IL-6 expression by cardiac tissue has been associated with the progression of heart failure [62, 64]. Other cytokines (TNF-alpha, IL-4, IL-17, IFN-gamma, CCL2, and IL-10) have shown differences between severe chagasic heart disease and the undetermined stage but not between the different stages of chagasic heart disease progression [64]. In this regard, a difference in IL-6 and IFN-gamma production patterns was seen when immunotherapy with the different plasmid DNA was performed, which could indicate different stages of progression of heart disease as demonstrated by electrocardiography and echocardiography as well as by macro- and microscopic findings from cardiac tissue at the time of euthanasia.

Compared to the main findings on EKG reported in the chronic phase of canine Chagas disease, such as right bundle branch block, left fascicular block, ventricular premature complex, ST-T segment changes, abnormal Q waves, low-voltage QRS complex, and electric axis deviation [9, 65, 66], it is possible to assert that immunotherapy does not prevent the presentation of these alterations since most of them were found in some individuals of the experimental groups; however, the reduction in the number of abnormalities and the number of individuals treated with the pBCSSP4 and pBCSP plasmids separately was evident. The alterations found in the EKG are consistent with those reported in other studies, where the most common findings in both dogs and humans are RBBB associated with left anterior-superior fascicular block followed by various degrees of atrioventricular block

[67, 68]. Respiratory sinus arrhythmia was the predominant rhythm during the assay period [68]. Sudden death was recorded in an individual who did not receive immunotherapy with recombinant plasmids which presented arrhythmia in combination with other alterations. This result is consistent with Quijano-Hernandez et al., who reported severe life-threatening cardiac arrhythmias in chagasic dogs [69].

The cardiac anatomophysiology results evaluated by echocardiography indicated that hypertrophic cardiomyopathy, characterized by the posterior wall and septum thickness [70], was the only alteration that pBCSSP4 immunotherapy was not able to prevent; however, the treatment was able to prevent other abnormalities that compromise not only the anatomy of the heart but also its functionality. Despite the presence of hypertrophic cardiomyopathy, fibrosis in myocardial tissue was not observed when performing the histological analysis, which is characteristic of many chronic diseases, including Chagas disease [70]. There were differences in the diastolic and systolic diameters when comparing the infected/SS *mock*-treated group and healthy group; and these results are not consistent with similar measurements performed by others who used young mongrel dogs infected with VL-10 strain of *T. cruzi* and did not find differences in the end-diastolic and end-systolic volumes when comparing infected and noninfected dogs [71]. On the other hand, diastolic and systolic diameters were in accordance with our previous study, in which the use of these recombinant plasmids used as a prophylactic treatment also had a protective effect based on similar parameter values found in both vaccinated and healthy control dogs with the exception of the empty vector (unpublished data).

A marked difference in the clinical and pathological conditions in the dogs infected with different *T. cruzi* strains has been described for decades. Cardiomegaly is the result of heart dysfunction in the chronic phase of Chagas disease [37, 72]. In this study, it was demonstrated that the pBCSSP4 plasmid used as therapeutic vaccine was able to prevent cardiomegaly in Beagle dogs infected with the H8 strain, and all experimental dogs that were not treated with this recombinant plasmid had a higher heart rate than the infected/SS *mock*-treated group, indicating the development of cardiomegaly. This pathological condition is in accordance with Guedes et al., who found that 20% of Beagle dogs infected with the Berenice-78 strain showed cardiomegaly, right ventricle flaccidity, inflammation, and fibrosis while 80% of the animals infected with the Y strain presented these alterations [37].

All animals showed normal popliteal node size and persistence of splenomegaly in the chronic phase of Chagas disease. These findings agree with the results reported by Guedes et al., who found similar lymphadenopathy and splenomegaly despite using different *T. cruzi* strains [73].

In this study, the therapeutic DNA vaccines carrying *T. cruzi* genes reduced multifocal myocarditis in a canine model of Chagas disease compared to unvaccinated dogs. These results are comparable to those reported in various immunoprotection studies using murine models. Using immunotherapy with the recombinant Tc24 protein reduced cardiac fibrosis by 50% [74]. In a study using a DNA vaccine

containing the cruzipain gene and a plasmid encoding the granulocyte-macrophage colony-stimulating factor with *T. cruzi*-infected mice, the effects on cardiac tissue included reduced inflammatory lymphocytic foci in muscle tissue, minimal perivascular infiltrate, scarcely infiltrated and dystrophic calcifications, and absence of interfiber infiltration [75]. In another study with chagasic mice using DNA immunization with the TcG2/TcG4 glutathione peroxidase genes and recombinant proteins as reinforcement, a relative decrease in the levels of inflammatory infiltrate in the myocardium (score: 0–2, average: 0.75) was reported [76]. All these examples are in accordance with the results obtained in the present study. It has been reported that chronic Chagas cardiomyopathy is characterized by inflammatory infiltrate and extensive reactive fibrosis [77]; therefore, the results of this study are encouraging and show that immunotherapy with recombinant DNA vaccines is moderately effective since it minimizes cardiac histological damage.

5. Conclusions

The studied therapeutic DNA vaccines were moderately effective in preventing cardiac complications associated with chronic chagasic cardiomyopathy or in delaying their occurrence as indicated by electrocardiography. *TcSSP4* and *TcSP* genes might be candidates for future study because they may represent a new therapeutic tool against Chagas disease, which has garnered considerable interest by researchers and physicians from several countries, not only in Latin America. Immunotherapy with *T. cruzi* genes limited the severity of heart damage in experimental chagasic dogs as evaluated by electrocardiography and macroscopic findings at necropsy.

The H8 strain of *T. cruzi* used in the experimental canine infection produced splenomegaly and cardiomegaly; however, treatment with both the *TcSP* and *TcSSP4* genes prevented splenic damage but not cardiac damage during chronic Chagas disease.

In addition, treatment with the pBCSSP4 plasmid had a partial protective effect in preventing cardiomegaly and microscopic damage in cardiac tissue since dogs in this group showed cardiac indexes similar to those of the control healthy dogs and microscopic lesions covered only subepicardial tissue. All these results support the promising novel therapeutic application of DNA using the *TcSSP4* and *TcSP* genes against Chagas disease.

Data Availability

The datasets generated and/or analyzed during the current study are available from the corresponding author on reasonable request.

Conflicts of Interest

The authors declare that they have no conflicts of interest.

Acknowledgments

This study was supported by an ICyTDF Grant ICyTDF/236/2010 to Minerva Arce-Fonseca. We wish to thank Dr. Ricardo Alejandro-Aguilar for providing metacyclic trypomastigote forms of the H8 *T. cruzi* strain.

References

- [1] Pan American Health Organization, World Health Organization, *Chagas in the Americas - fact sheet for health workers*, 2017, https://www.paho.org/hq/index.php?option=com_content&view=article&id=13568%3Achagas-in-the-americas-for-public-health-workers-2017&catid=6648%3Afact-sheets&Itemid=40721&lang=en.
- [2] A. Rassi Jr., A. Rassi, and J. A. Marin-Neto, "Chagas disease," *Lancet*, vol. 375, no. 9723, pp. 1388–1402, 2010.
- [3] A. Moncayo, "Chagas disease: epidemiology and prospects for interruption of transmission in the Americas," *World Health Statistics Quarterly*, vol. 45, no. 2-3, pp. 276–279, 1992.
- [4] R. E. Gurtler, M. C. Cecere, M. A. Lauricella, M. V. Cardinal, U. Kitron, and J. E. Cohen, "Domestic dogs and cats as sources of *Trypanosoma cruzi* infection in rural northwestern Argentina," *Parasitology*, vol. 134, no. 1, pp. 69–82, 2007.
- [5] M. Arce-Fonseca, S. C. Carrillo-Sánchez, R. M. Molina-Barrios et al., "Seropositivity for *Trypanosoma cruzi* in domestic dogs from Sonora, Mexico," *Infectious Diseases of Poverty*, vol. 6, no. 1, p. 120, 2017.
- [6] L. Galaviz-Silva, R. Mercado-Hernández, J. J. Zárate-Ramos, and Z. J. Molina-Garza, "Prevalence of *Trypanosoma cruzi* infection in dogs and small mammals in Nuevo León, Mexico," *Revista Argentina de Microbiología*, vol. 49, no. 3, pp. 216–223, 2017.
- [7] C. Muratore, "Current and emerging therapeutic options for the treatment of chronic chagasic cardiomyopathy," *Vascular Health and Risk Management*, vol. 2010, no. 6, pp. 593–601, 2010.
- [8] F. S. Machado, L. A. Jelicks, L. V. Kirchhoff et al., "Chagas heart disease: report on recent developments," *Cardiology in Review*, vol. 20, no. 2, pp. 53–65, 2012.
- [9] C. Bern, "Chagas' disease," *The New England Journal of Medicine*, vol. 373, no. 5, pp. 456–466, 2015.
- [10] R. Viotti, C. Vigliano, H. Armenti, and E. Segura, "Treatment of chronic Chagas' disease with benznidazole: clinical and serologic evolution of patients with long-term follow up," *American Heart Journal*, vol. 127, no. 1, pp. 151–162, 1994.
- [11] R. Viotti, C. Vigliano, B. Lococo et al., "Side effects of benznidazole as treatment in chronic Chagas disease: fears and realities," *Expert Review of Anti-Infective Therapy*, vol. 7, no. 2, pp. 157–163, 2009.
- [12] J. A. Castro, M. M. deMecca, and L. C. Bartel, "Toxic side effects of drugs used to treat Chagas' disease (American trypanosomiasis)," *Human and Experimental Toxicology*, vol. 25, no. 8, pp. 471–479, 2006.
- [13] J. A. Urbina and R. Docampo, "Specific chemotherapy of Chagas disease: controversies and advances," *Trends in Parasitology*, vol. 19, no. 11, pp. 495–501, 2003.
- [14] M. T. Bahia, L. F. Diniz, and V. C. F. Mosqueira, "Therapeutic approaches under investigation for treatment of Chagas disease," *Expert Opinion on Investigational Drugs*, vol. 23, no. 9, pp. 1225–1237, 2014.

- [15] E. Aguilera, J. Varela, E. Serna et al., "Looking for combination of benznidazole and Trypanosoma cruzi-triosephosphate isomerase inhibitors for Chagas disease treatment," *Memorias do Instituto Oswaldo Cruz*, vol. 113, no. 3, pp. 153–160, 2018.
- [16] E. Dumonteil, "DNA vaccines against protozoan parasites: Advances and challenges," *Journal of Biomedicine & Biotechnology*, vol. 2007, Article ID 090520, 11 pages, 2007.
- [17] M. Arce-Fonseca, M. Rios-Castro, S. Carrillo-Sánchez, M. Martínez-Cruz, and O. Rodríguez-Morales, "Prophylactic and therapeutic DNA vaccines against Chagas disease," *Parasites & Vectors*, vol. 8, no. 1, p. 121, 2015.
- [18] A. E. Bivona, N. Cerny, A. S. Alberti, S. I. Cazorla, and E. L. Malchiodi, "Attenuated Salmonella sp. as a DNA delivery system for Trypanosoma cruzi antigens," *Vaccine Design*, pp. 683–695, 2016.
- [19] M. N. Matos, A. Sánchez Alberti, C. Morales, S. I. Cazorla, and E. L. Malchiodi, "A prime-boost immunization with Tc52 N-terminal domain DNA and the recombinant protein expressed in Pichia pastoris protects against Trypanosoma cruzi infection," *Vaccine*, vol. 34, no. 28, pp. 3243–3251, 2016.
- [20] E. Dumonteil, J. Escobedo-Ortegon, N. Reyes-Rodriguez, A. Arjona-Torres, and M. J. Ramirez-Sierra, "Immunotherapy of Trypanosoma cruzi infection with DNA vaccines in mice," *Infection and Immunity*, vol. 72, no. 1, pp. 46–53, 2004.
- [21] M. de Lana, "Experimental studies of Chagas disease in animal models," in *In American Trypanosomiasis Chagas Disease One Hundred years of Research*, pp. 299–320, J. Telleria and M. Tibayreng, Ed., Elsevier, Netherlands, Amsterdam, 2017.
- [22] O. Rodríguez-Morales, M. Pérez-Leyva, M. A. Ballinas-Verdugo et al., "Plasmid DNA immunization with Trypanosoma cruzi genes induces cardiac and clinical protection against Chagas disease in the canine model," *Veterinary Research*, vol. 43, no. 1, p. 79, 2012.
- [23] O. Rodríguez-Morales, S. C. Carrillo-Sánchez, H. García-Mendoza et al., "Effect of the plasmid-DNA vaccination on macroscopic and microscopic damage caused by the experimental chronic Trypanosoma cruzi infection in the canine model," *BioMed Research International*, vol. 2013, Article ID 826570, 8 pages, 2013.
- [24] M. Arce-Fonseca, M. A. Ballinas-Verdugo, E. R. A. Zenteno et al., "Specific humoral and cellular immunity induced by Trypanosoma cruzi DNA immunization in a canine model," *Veterinary Research*, vol. 44, no. 1, p. 15, 2013.
- [25] I. A. Quijano-Hernández, A. Castro-Barcena, J. C. Vázquez-Chagoyán, M. E. Bolio-González, J. Ortega-López, and E. Dumonteil, "Preventive and therapeutic DNA vaccination partially protect dogs against an infectious challenge with Trypanosoma cruzi," *Vaccine*, vol. 31, no. 18, pp. 2246–2252, 2013.
- [26] J. E. Aparicio-Burgos, J. A. Zepeda-Escobar, R. M. de Oca-Jimenez et al., "Immune protection against Trypanosoma cruzi induced by TcVac4 in a canine model," *PLoS Neglected Tropical Diseases*, vol. 9, no. 4, p. e0003625, 2015.
- [27] B. Basso, V. Marini, D. Gauna, and M. Frias, "Vaccination of dogs with Trypanosoma rangeli induces antibodies against Trypanosoma cruzi in a rural area of Córdoba, Argentina," *Memórias do Instituto Oswaldo Cruz*, vol. 111, no. 4, pp. 271–274, 2016.
- [28] Norma Oficial Mexicana NOM-062-Z00-1999, *Especificaciones Técnicas para el Cuidado y Uso de Animales de Laboratorio*, Diario Oficial de la Federación, México, 1999.
- [29] O. Rodríguez-Morales, M. A. Ballinas-Verdugo, R. Alejandro-Aguilar, P. A. Reyes, and M. Arce-Fonseca, "Trypanosoma cruzi congenital transmission in dogs with Chagas disease. Experimental case report," *Vector Borne and Zoonotic Diseases*, vol. 11, no. 10, pp. 1365–1370, 2011.
- [30] O. V. Y. Tachika, *Manual de Prácticas de Medicina de perros y gatos*, Hospital de enseñanza UNAM-Banfield, FMVZ, México, 2008.
- [31] World Health Organization, "WHO technical report series control of Chagas disease," Second Report of the WHO Committee. Geneva 2002, <https://apps.who.int/iris/handle/10665/42443>.
- [32] M. Arce-Fonseca, A. Ramos-Ligonio, A. López-Monteón, B. Salgado-Jiménez, P. Talamás-Rohana, and J. L. Rosales-Encina, "A DNA vaccine encoding for TcSSP4 induces protection against acute and chronic infection in experimental Chagas disease," *International Journal of Biological Sciences*, vol. 7, no. 9, pp. 1230–1238, 2011.
- [33] B. Salgado-Jiménez, M. Arce-Fonseca, L. Baylón-Pacheco, P. Talamás-Rohana, and J. L. Rosales-Encina, "Differential immune response in mice immunized with the A, R or C domain from TcSP protein of Trypanosoma cruzi or with the coding DNAs," *Parasite Immunology*, vol. 35, no. 1, pp. 32–41, 2013.
- [34] T. Maniatis, E. F. Fritsch, and J. Sambrook, "Molecular Cloning," in *A Laboratory Manual. 2a. edición*, Cold Spring Harbor Laboratory Press, U. S. A., 1989.
- [35] S. Rafati, A. Nakhaee, T. Taheri et al., "Protective vaccination against experimental canine visceral leishmaniasis using a combination of DNA and protein immunization with cysteine proteinases type I and II of L. infantum," *Vaccine*, vol. 23, no. 28, pp. 3716–3725, 2005.
- [36] Norma Oficial Mexicana NOM-033-SAG/ZOO-2014, *Métodos para dar muerte a los animales domésticos y silvestres*, Diario Oficial de la Federación, Mexico, 2014.
- [37] P. M. Guedes, V. M. Veloso, M. V. Caliari et al., "Trypanosoma cruzi high infectivity in vitro is related to cardiac lesions during long-term infection in Beagle dogs," *Memorias do Instituto Oswaldo Cruz*, vol. 102, no. 2, pp. 141–147, 2007.
- [38] E. Dumonteil, "Vaccine development against Trypanosoma cruzi and Leishmania species in the post-genomic era," *Infection, Genetics and Evolution*, vol. 9, no. 6, pp. 1075–1082, 2009.
- [39] F. S. Machado, W. O. Dutra, L. Esper et al., "Current understanding of immunity to Trypanosoma cruzi infection and pathogenesis of Chagas disease," *Seminars in Immunopathology*, vol. 34, no. 6, pp. 753–770, 2012.
- [40] M. Dowst, A. Pavuk, R. Vilela, C. Vilela, and L. Mendoza, "An unusual case of cutaneous feline pythiosis," *Medical Mycology Case Reports*, vol. 26, pp. 57–60, 2019.
- [41] C. Han, W. Y. Chan, and P. B. Hill, "Prevalence of positive reactions in intradermal and IgE serological allergy tests in dogs from South Australia, and the subsequent outcome of allergen-specific immunotherapy," *Australian Veterinary Journal*, vol. 98, no. 1-2, pp. 17–25, 2020.
- [42] W. Hegazy-Hassan, J. A. Zepeda-Escobar, L. Ochoa-García et al., "TcVac1 vaccine delivery by intradermal electroporation enhances vaccine induced immune protection against Trypanosoma cruzi infection in mice," *Vaccine*, vol. 37, no. 2, pp. 248–257, 2019.
- [43] W. Wheat, L. Chow, A. Kuzmik et al., "Local immune and microbiological responses to mucosal administration of a

- Liposome-TLR agonist immunotherapeutic in dogs,” *BMC Veterinary Research*, vol. 15, no. 1, p. 330, 2019.
- [44] A. A. Gingrich, J. F. Modiano, and R. J. Canter, “Characterization and potential applications of dog natural killer cells in cancer immunotherapy,” *Journal of Clinical Medicine*, vol. 8, no. 11, p. 1802, 2019.
- [45] I. R. Pereira, G. Vilar-Pereira, V. Marques et al., “A human type 5 adenovirus-based *Trypanosoma cruzi* therapeutic vaccine re-programs immune response and reverses chronic cardiomyopathy,” *PLoS Pathogens*, vol. 11, no. 1, p. e1004594, 2015.
- [46] S. I. Cazorla, F. M. Frank, P. D. Becker, R. S. Corral, C. A. Guzman, and E. L. Malchiodi, “Prime-boost immunization with cruzipain co-administered with MALP-2 triggers a protective immune response able to decrease parasite burden and tissue injury in an experimental *Trypanosoma cruzi* infection model,” *Vaccine*, vol. 26, no. 16, pp. 1999–2009, 2008.
- [47] N. Garg and R. L. Tarleton, “Genetic immunization elicits antigen-specific protective immune responses and decreases disease severity in *Trypanosoma cruzi* infection,” *Infection and Immunity*, vol. 70, no. 10, pp. 5547–5555, 2002.
- [48] D. F. Hoft, C. S. Eickhoff, O. K. Giddings, J. R. C. Vasconcelos, and M. M. Rodrigues, “Trans-sialidase recombinant protein mixed with CpG motif-containing oligodeoxynucleotide induces protective mucosal and systemic *Trypanosoma cruzi* immunity involving CD8+ CTL and B cell-mediated cross-priming,” *Journal of Immunology*, vol. 179, no. 10, pp. 6889–6900, 2007.
- [49] Y. Miyahira, Y. Takashima, S. Kobayashi et al., “Immune responses against a single CD8+ -T-cell epitope induced by virus vector vaccination can successfully control *Trypanosoma cruzi* infection,” *Infection and Immunity*, vol. 73, no. 11, pp. 7356–7365, 2005.
- [50] G. Sanchez-Burgos, R. G. Mezquita-Vega, J. Escobedo-Ortegon et al., “Comparative evaluation of therapeutic DNA vaccines against *Trypanosoma cruzi* in mice,” *FEMS Immunology and Medical Microbiology*, vol. 50, no. 3, pp. 333–341, 2007.
- [51] N. W. Andrews, K. S. Hong, E. S. Robbins, and V. Nussenzweig, “Stage-specific surface antigens expressed during the morphogenesis of vertebrate forms of *Trypanosoma cruzi*,” *Experimental Parasitology*, vol. 64, no. 3, pp. 474–484, 1987.
- [52] E. Roggero, J. Wildmann, M. O. Passerini, A. del Rey, and H. O. Besedovsky, “Different peripheral neuroendocrine responses to *Trypanosoma cruzi* infection in mice lacking adaptive immunity,” *Annals of the New York Academy of Sciences*, vol. 1262, pp. 37–44, 2012.
- [53] D. M. Klinman, A. K. Yi, S. L. Beaucage, J. Conover, and A. M. Krieg, “CpG motifs present in bacteria DNA rapidly induce lymphocytes to secrete interleukin 6, interleukin 12, and interferon gamma,” *Proceedings of the National Academy of Sciences*, vol. 93, no. 7, pp. 2879–2883, 1996.
- [54] X. Duan, Y. Yonemitsu, B. Chou et al., “Efficient protective immunity against *Trypanosoma cruzi* infection after nasal vaccination with recombinant Sendai virus vector expressing amastigote surface protein-2,” *Vaccine*, vol. 27, no. 44, pp. 6154–6159, 2009.
- [55] H. Zapata-Estrella, C. Hummel-Newell, G. Sanchez-Burgos et al., “Control of *Trypanosoma cruzi* infection and changes in T cell populations induced by a therapeutic DNA vaccine in mice,” *Immunology Letters*, vol. 103, no. 2, pp. 186–191, 2006.
- [56] B. Autran, G. Carcelain, B. Combadiere, and P. Debre, “Therapeutic vaccines for chronic infections,” *Science*, vol. 305, no. 5681, pp. 205–208, 2004.
- [57] S. Gupta and N. J. Garg, “Prophylactic efficacy of TcVac2 against *Trypanosoma cruzi* in mice,” *Plos Neglected Tropical Diseases*, vol. 4, no. 8, p. e797, 2010.
- [58] S. L. Reiner and R. M. Locksley, “The regulation of immunity to *Leishmania major*,” *Annual Review of Immunology*, vol. 13, pp. 151–177, 1995.
- [59] I. Okwor and J. Uzonna, “Persistent parasites and immunologic memory in cutaneous leishmaniasis: implications for vaccine designs and vaccination strategies,” *Immunologic Research*, vol. 41, no. 2, pp. 123–136, 2008.
- [60] N. Pakpour, C. Zaph, and P. Scott, “The Central Memory CD4 +T Cell Population Generated during *Leishmania major* Infection Requires IL-12 to Produce IFN- γ ,” *The Journal of Immunology*, vol. 180, no. 12, pp. 8299–8305, 2008.
- [61] A. Ramos-Ligonio, A. López-Monteón, P. Talamás-Rohana, and J. L. Rosales-Encina, “Recombinant SSP4 protein from *Trypanosoma cruzi* amastigotes regulates nitric oxide production by macrophages,” *Parasite Immunology*, vol. 26, no. 10, pp. 409–418, 2004.
- [62] W. Gao and M. A. Pereira, “Interleukin-6 is required for parasite specific response and host resistance to *Trypanosoma cruzi*,” *International Journal of Parasitology*, vol. 32, no. 2, pp. 167–170, 2002.
- [63] X. Filella, R. Molina, and A. M. Ballesta, “Estructura y función de las citocinas,” *Medicina Integral*, vol. 39, no. 2, pp. 63–71, 2002.
- [64] L. López, K. Arai, E. Giménez et al., “Las concentraciones séricas de interleucina-6 y proteína C reactiva se incrementan a medida que la enfermedad de Chagas evoluciona hacia el deterioro de la función cardíaca,” *Revista Española de Cardiología*, vol. 59, no. 1, pp. 50–56, 2006.
- [65] M. de Lana, E. Chiari, and W. L. Tafuri, “Experimental Chagas’ disease in dogs,” *Memorias do Instituto Oswaldo Cruz*, vol. 87, no. 1, pp. 59–71, 1992.
- [66] A. Rassi Jr., A. Rassi, and J. M. de Rezende, “American Trypanosomiasis (Chagas Disease),” *Infectious Disease Clinics of North America*, vol. 26, no. 2, pp. 275–291, 2012.
- [67] C. A. Pastore, N. Samesima, H. G. P. Filho et al., “Rare Association: Chagas’ Disease and Hypertrophic Cardiomyopathy,” *Annals of Noninvasive Electrocardiology*, vol. 20, no. 5, pp. 498–501, 2015.
- [68] J. P. d. E. Pascon, G. B. Pereira Neto, M. G. Sousa, D. P. Júnior, and A. A. Camacho, “Clinical characterization of chronic chagasic cardiomyopathy in dogs,” *Pesquisa Veterinária Brasileira*, vol. 30, no. 2, pp. 115–120, 2010.
- [69] I. A. Quijano-Hernandez, M. E. Bolio-González, J. C. Rodríguez-Buenfil, M. J. Ramirez-Sierra, and E. Dumontel, “Therapeutic DNA vaccine against *Trypanosoma cruzi* infection in dogs,” *Annals of the New York Academy of Sciences*, vol. 1149, pp. 343–346, 2008.
- [70] T. R. Eijgenraam, H. H. W. Silljé, and R. A. de Boer, “Current understanding of fibrosis in genetic cardiomyopathies,” *Trends in Cardiovascular Medicine*, 2019.
- [71] E. B. Carvalho, I. P. R. Ramos, A. F. S. Nascimento et al., “Echocardiographic Measurements in a Preclinical Model of Chronic Chagasic Cardiomyopathy in Dogs: Validation and Reproducibility,” *Frontiers in Cellular and Infection Microbiology*, vol. 9, no. 332, 2019.

- [72] S. C. Barr, "Canine Chagas' Disease (American Trypanosomiasis) in North America," *The Veterinary Clinics of North America. Small Animal Practice*, vol. 39, no. 6, pp. 1055–1064, 2009.
- [73] P. M. M. Guedes, V. M. Veloso, L. C. C. Afonso et al., "Development of chronic cardiomyopathy in canine Chagas disease correlates with high IFN- γ , TNF- α , and low IL-10 production during the acute infection phase," *Veterinary Immunology and Immunopathology*, vol. 130, no. 1-2, pp. 43–52, 2009.
- [74] M. A. Barry, L. Versteeg, Q. Wang et al., "A therapeutic vaccine prototype induces protective immunity and reduces cardiac fibrosis in a mouse model of chronic *Trypanosoma cruzi* infection," *PLoS Neglected Tropical Diseases*, vol. 13, no. 5, p. e0007413, 2019.
- [75] N. Cerny, A. Sánchez Alberti, A. E. Bivona et al., "Coadministration of cruzipain and GM-CSF DNAs, a new immunotherapeutic vaccine against *Trypanosoma cruzi* infection," *Human Vaccines & Immunotherapeutics*, vol. 12, no. 2, pp. 438–450, 2016.
- [76] S. Gupta, C. Smith, S. Auclair, A. D. J. Delgadillo, and N. J. Garg, "Therapeutic efficacy of a subunit vaccine in controlling chronic *Trypanosoma cruzi* infection and Chagas disease is enhanced by glutathione peroxidase over-expression," *PLoS One*, vol. 10, no. 6, p. e0130562, 2015.
- [77] J. A. Marin-Neto, E. Cunha-Neto, B. C. Maciel, and M. V. Simoes, "Pathogenesis of chronic Chagas heart disease," *Circulation*, vol. 115, no. 9, pp. 1109–1123, 2007.
- [78] L. P. Tilley, *Essentials of Canine and Feline Electrocardiography: Interpretation and Treatment*, Lippincott Williams & Wilkins, Baltimore, USA, 1992.
- [79] L. P. Tilley and N. Burtnick, *ECG Electrocardiography for the Small Animal Practitioner*, Ed. Teton New Media, USA, 1999.
- [80] J. A. Boon, *Two Dimensional and M-Mode Echocardiography for the Small Animal Practitioner*, NewMedia, Jackson, WY, USA, 2002.

Research Article

Epitope-Based Peptide Vaccine against Glycoprotein G of Nipah *Henipavirus* Using Immunoinformatics Approaches

Arwa A. Mohammed ^{1,2} Shaza W. Shantier ^{1,3} Mujahed I. Mustafa,¹ Hind K. Osman,^{1,4} Hashim E. Elmansi,¹ Isam-Aldin A. Osman,^{1,5} Rawan A. Mohammed,⁶ Fatima A. Abdelrhman,^{1,7} Mihad E. Elnnewery,^{1,8} Einas M. Yousif,¹ Marwa M. Mustafa,¹ Nafisa M. Elfadol,¹ Alaa I. Abdalla,^{1,9} Eiman Mahmoud,^{1,10} Ahmed A. Yagoub,^{1,8} Yassir A. Ahmed,⁶ and Mohamed A. Hassan^{1,11}

¹Department of Biotechnology, Africa City of Technology, Sudan

²Department of Pharmacy, Sudan Medical Council, Khartoum, Sudan

³Department of Pharmaceutical Chemistry, Faculty of Pharmacy, University of Khartoum, Sudan

⁴Department of Pharmaceutics, Faculty of Pharmacy, University of Khartoum, Sudan

⁵Department of Molecular Biology, Institute of Endemic Diseases, University of Khartoum, Sudan

⁶Department of Bioinformatics, Faculty of Information and Science Technology, Multimedia University, Malaysia

⁷Department of Biochemistry, Faculty of Science, Bahri University, Sudan

⁸Department of Clinical Chemistry, Faculty of Medical Laboratory Sciences, Omdurman Islamic University, Sudan

⁹Department of Microbiology, Faculty of Medical Laboratory Sciences, Omdurman Islamic University, Sudan

¹⁰Department of Immunology, Faculty of Medicine, Alfhad University for Women, Sudan

¹¹Department of Bioinformatics, DETAGEN Genetics Diagnostic Center, Kayseri, Turkey

Correspondence should be addressed to Arwa A. Mohammed; drarwaahmed16@gmail.com

Received 5 November 2019; Revised 13 February 2020; Accepted 23 March 2020; Published 22 April 2020

Academic Editor: Darren R. Flower

Copyright © 2020 Arwa A. Mohammed et al. This is an open access article distributed under the Creative Commons Attribution License, which permits unrestricted use, distribution, and reproduction in any medium, provided the original work is properly cited.

Background. Nipah belongs to the genus *Henipavirus* and the *Paramyxoviridae* family. It is an endemic most commonly found at South Asia and has first emerged in Malaysia in 1998. Bats are found to be the main reservoir for this virus, causing disease in both humans and animals. The last outbreak has occurred in May 2018 in Kerala. It is characterized by high pathogenicity and fatality rates which varies from 40% to 70% depending on the severity of the disease and on the availability of adequate healthcare facilities. Currently, there are no antiviral drugs available for NiV disease and the treatment is just supportive. Clinical presentations for this virus range from asymptomatic infection to fatal encephalitis. **Objective.** This study is aimed at predicting an effective epitope-based vaccine against glycoprotein G of Nipah henipavirus, using immunoinformatics approaches. **Methods and Materials.** Glycoprotein G of the Nipah virus sequence was retrieved from NCBI. Different prediction tools were used to analyze the epitopes, namely, BepiPred-2.0: Sequential B Cell Epitope Predictor for B cell and T cell MHC classes II and I. Then, the proposed peptides were docked using Autodock 4.0 software program. **Results and Conclusions.** The two peptides TVYHCSAVY and FLIDRINWI have showed a very strong binding affinity to MHC class I and MHC class II alleles. Furthermore, considering the conservancy, the affinity, and the population coverage, the peptide FLIDRINWIT is highly suitable to be utilized to formulate a new vaccine against glycoprotein G of Nipah henipavirus. An in vivo study for the proposed peptides is also highly recommended.

1. Introduction

Nipah virus (NiV) is an RNA virus that belongs to the genus *Henipavirus* within the family *Paramyxoviridae* and has first emerged in Malaysia in 1998, gaining its name from a village called Sungai Nipah where it was isolated from the cerebrospinal fluid (CSF) of one of the patients [1–4]. NiV is transmitted zoonotically (from bats to humans, or from bats to pigs, and then to humans) as well as human-to-human routes. Its clinical presentation varies from asymptomatic (subclinical) infection to acute respiratory illnesses and fatal encephalitis in most of the patients who has been in direct contact with infected pigs. It has also been found that the virus causes central nervous system illnesses in pigs and respiratory illnesses in horses resulting in a significant economic loss for farmers [1, 5–9]. Large fruit bats of the genus *Pteropus* seem to act as a natural reservoir of NiV based on the isolation of Hendra virus which has showed the presence of neutralizing antibodies to the Hendra virus on the bats [10, 11]. Although, there are no more cases of NiV in Malaysia, several outbreaks have been frequently occurring in India, Bangladesh, Thailand, and Cambodia [12]. The case fatality rate ranges from 50% to 100%, making it one of the deadliest viruses known to infect humans [3, 13, 14].

Laboratory diagnosis of Nipah virus infection is made using reverse transcriptase polymerase chain reaction (RT-PCR) from throat swabs, cerebrospinal fluid, urine, and blood analysis during acute and convalescent stages of the disease. IgG and IgM antibody detection can be done after recovery to confirm Nipah virus infection. Immunohistochemistry on tissues collected during an autopsy can also confirm the disease [15, 16]. Currently, there are no effective treatments for the Nipah virus infection. Therefore, a few precautions should be followed such as practicing standard infection control, barrier nursing to avoid the spread of the infection from person to person, and the isolation of those suspected to have the infection [7, 8, 17]. Recent computational approaches have provided further information about viruses, including the study conducted by Badawi M et al. on Zika virus, where the envelope glycoprotein was obtained using protein databases. The most immunogenic epitope for the T and B cells involved in cell-mediated immunity was previously analyzed [18]. The main focus of the analysis was the MHC class I potential peptides using *in silico* analysis techniques [19, 20]. In this study, the same techniques were applied to keep MHC classes I and II along with the world population coverage as our main focus. Furthermore, in this study, we aimed to design an epitope-based peptide vaccine against Nipah virus using peptides of its glycoprotein G as an immunogenic part to stimulate a protective immune response [3].

Nipah virus invades host cells by the fusion of the host cell membranes at an optimal physiological pH for cleavage without requiring viral endocytosis. Cell-cell fusion is a pathological lineament of Nipah virus infections, resulting in a cell-to-cell spread, inflammation, and destruction of endothelial cells and neurons [21]. Both Nipah virus entry and cell-cell fusion require concerted efforts of the attachment of glycoprotein G and fusion (F) glycoprotein. Upon receptor

binding, Nipah virus glycoprotein G triggers a conformational cascade in Nipah virus glycoprotein F that executes a viral and/or a cell membrane fusion [22]. Due to the potency of glycoprotein G over F, we have considered this incident to be the target of this study. There are a lot of challenges regarding the development of peptide-based vaccines, and therefore, we have decided to study and propose a new vaccine against the Nipah virus, since they make a helpful alternative strategy that relies on the usage of short peptide fragments to induce immune responses [23–26]. Antigenic epitopes from single proteins may not be really necessary, whereas some of these epitopes may even be detrimental to the induction of protective immunity. This logic has created an interest in peptide vaccines and especially those containing only epitopes that are capable of inducing desirable T cell- and B cell-mediated immune responses. Less than 20 amino acid sequences make up the peptides used in such vaccines, which are then synthesized to form an immunogenic peptide molecule. These molecules represent a specific epitope of an antigen. These vaccines are also capable of inducing immunity against different strains of a specific pathogen by forming noncontiguous and immunodominant epitopes that are usually conserved in the strains of the pathogen [27].

The production of peptide vaccines is extremely safe and cost-effective, especially when they are compared to conventional vaccines. Traditional vaccines that prevent emerging infectious diseases (EIDs) are very difficult to produce because they require the need to culture pathogenic viruses *in vitro*. However, epitope-based peptide vaccines do not require any means of *in vitro* culturing which makes them biologically safe, allowing a large scale of bioprocessing to be carried out rapidly and economically. Finally, their selectivity allows a precise activation of the immunological responses by means of selecting immunodominant and conserved epitopes [25, 28]. The complexity of an epitope-based peptide vaccines' design depends largely on the properties of its carrier molecules' reactogenicity as well as its allergenicity [29, 30]. When it comes to the selection of epitopes, it is based on the analysis of the B cells, cytotoxic T cells, and the induction of the helper T cells. Then, it is important to identify the epitopes capable of activating T cells vital for stimulating a protective immunity. One of the issues concerning peptide vaccines representing T cells in a human population and that are highly MHC-heterogeneous is to identify the highly conserved immunodominant epitopes that are considered to be among a broad spectrum of vaccines due to their ability to work against multiple serovars of pathogens [30]. In this study, we have used a variety of bioinformatics tools for the prediction of epitopes along with the population coverage and epitope selection algorithms, including the translocation of peptides into MHC class I and MHC class II.

2. Materials and Methods

2.1. Sequence Retrieval. The amino acid sequences of glycoprotein G (Glycoside hydrolase family) for a total of 21 strains of Nipah virus were retrieved from the NCBI database (<https://www.ncbi.nlm.nih.gov/protein>) [31] in a FASTA

format on July 2018. Different prediction tools of Immune Epitope Database (IEDB) Analysis Resource (<http://www.iedb.org/>) [32] were then used to analyze the candidate epitopes.

2.2. Conservation Region and Physicochemical Properties. Conservation regions were determined using multiple sequence alignments with the help of Clustal-W in the BioEdit software version 7.2.5 [33]. Epitope conservancy prediction for individual epitopes was then calculated using the IEDB Analysis Resource. Conservancy can be defined as the portion of a protein sequence that restrains in which an epitope is measured at or which that is exceeding a specific level of identity [34]. The physicochemical properties of the retrieved sequence, molecular weight, and amino acid composition were also determined by using BioEdit software.

2.3. B Cell Epitope Prediction Tools. Candidate epitopes were analyzed using several B cell prediction methods to determine their antigenicity, flexibility, hydrophilicity, and surface accessibility. The predicted linear epitopes were obtained from the Immune Epitope Database (<http://tools.iedb.org/bcell/result/>) [35] using a BepiPred test with a threshold value of 0.149 and a window size of 6.0. Moreover, surface accessible epitopes were predicated with a threshold value of 1.0 and a window size of 6.0 using the Emini surface accessibility prediction tool [35]. Kolaskar and Tongaonkar antigenicity methods (<http://tools.iedb.org/bcell/result/>) were also proposed to determine the sites of antigenic epitopes with a default threshold value of 1.030 and a window size 6.0 [36].

2.4. T Cell Epitope Prediction Tools

2.4.1. Peptide Binding to MHC Class I Molecules. The binding peptide was assessed by the IEDB MHC I prediction tool at <http://tools.iedb.org/mhcI>. This tool employs different methods to determine the ability of the submitted sequence to bind to a specific MHC class I molecule. The artificial neural network (ANN) method was used to calculate IC₅₀ values of the peptide binding to MHC class I molecules. For both frequent and nonfrequent alleles, the peptide length was set to 9 amino acids prior to the prediction. The alleles having a binding affinity of IC₅₀ that are equal to or less than 500 nM were considered for further analysis [37].

2.4.2. Peptide Binding to MHC Class II Molecules. To predict the peptide binding to MHC class II molecules, the MHC II prediction tool <http://tools.iedb.org/mhcII> provided by the Immune Epitope Database (IEDB) Analysis Resource consisting of human allele references sets was used [38]. The artificial neural network prediction method was chosen to identify the binding affinity of MHC II grooves and MHC II binding core epitopes. All epitopes that bind to many alleles at a score equal to or less than 1000, half-maximal inhibitory concentration (IC₅₀), were selected for further analysis.

2.5. Population Coverage. The population coverage of each epitope was calculated by the IEDB population coverage tool at (http://tools.iedb.org/tools/population/iedb_input). This tool was used in order to determine the fraction of individuals predicted to respond to a given set of epitopes, with known MHC restrictions [39]. For every single population coverage, the tool computed the following information: (1) predicted population coverage, (2) HLA combinations recognized by the population, and (3) HLA combinations recognized by 90% of the population (PC90). All the epitopes and their MHC I and MHC II molecules were assessed against the population coverage area selected before submission.

2.6. Homology Modeling. The 3D structure of glycoprotein G of Nipah virus was predicted using the RaptorX web portal (<http://raptorx.uchicago.edu/>), where the reference sequence was submitted in a FASTA format on 14/9/2018 and the structure was received on 15/9/2018 [40]. This structure was then treated with UCSF Chimera 1.10.2 to visualize the position of the proposed peptides [41].

2.7. In Silico Molecular Docking

2.7.1. Ligand Preparation. In order to estimate the binding affinities between the epitopes and molecular structures of MHC I and MHC II, we have carried out an in silico molecular docking. Sequences of proposed epitopes were then selected from the Nipah virus reference sequence using Chimera 1.10 and saved as a (pdb) file. The obtained files were then optimized and energy minimized. The HLA-A*02:01 was selected as the macromolecule for docking. Its crystal structure (4UQ3) was downloaded from the RCSB Protein Data Bank (<http://www.rcsb.org/pdb/home/home.do>), which was in a complex with an azobenzene-containing peptide [42].

All water molecules and heteroatoms in the retrieved target file 4UQ3 were then removed. The target structure was further optimized and energy minimized using Swiss PDB viewer V.4.1.0 software [43].

Molecular docking was performed using AutoDock 4.0 software, based on the Lamarckian genetic algorithm, which combines energy evaluation through grids of affinity potential to find the suitable binding position for a ligand on a given protein [44, 45]. Polar hydrogen atoms were added to the protein targets, and Kollman united atomic charges were computed. The targets' grid map was calculated and set to 60 × 60 × 60 points with a grid spacing of 0.375 Å. The grid box was then allocated properly in the target to include the active residue in the center. The genetic algorithm and its run were set to 100 as the docking algorithms were set on default. Finally, results were retrieved as binding energies and poses that showed the lowest binding energies in which they were visualized using UCSF Chimera.

3. Results

3.1. Nipah Virus Glycoprotein G Physical and Chemical Parameters. The physicochemical properties of the Nipah virus glycoprotein G protein was assessed using BioEdit

TABLE 1: Number and Mol% of amino acids that constituted *Nipah virus glycoprotein G* using BioEdit software version 7.2.5.

Amino acid	Number	Mol%	Amino acid	Number	Mol%
Ala A	23	3.82	Met M	11	1.83
Cys C	17	2.82	Asn N	45	7.48
Asp D	27	4.49	Pro P	36	5.98
Glu E	26	4.32	Gln Q	25	4.15
Phe F	21	3.49	Arg R	22	3.65
Gly G	40	6.64	Ser S	51	8.47
His H	5	0.83	Thr T	37	6.15
Ile I	55	9.14	Val V	41	6.81
Lys K	39	6.48	Trp W	7	1.16
Leu L	49	8.14	Tyr Y	25	4.15

software version 7.0.9.0. The protein length was found to be 602 amino acids, and the molecular weight was at 67035.54 Daltons. The amino acids that form the Nipah virus glycoprotein G protein are shown in Table 1 along with their numbers and molar percentages in (Mol%).

3.2. B Cell Epitope Prediction. The ref sequence of the Nipah virus glycoprotein G was subjected to a Bepipred linear epitope prediction. Emini surface accessibility and Kolaskar and Tongaonkar antigenicity methods in IEDB were used to determine bindings to the B cell and in testing its surface and immunogenicity. The results are shown in Figures 1–3.

3.3. Prediction of T Helper Cell Epitopes and Interaction with MHC Class I Alleles. The Nipah virus glycoprotein G sequence was analyzed using the IEDB MHC class I binding prediction tool based on ANN-align with half-maximal inhibitory concentration (IC_{50}) ≤ 500 ; the least most promising epitopes that had a binding affinity with the class I alleles along with their positions in the Nipah virus glycoprotein G are shown in Table 2.

3.4. Prediction of T Helper Cell Epitopes and Interaction with MHC Class II Alleles. The Nipah virus glycoprotein G sequence was analyzed using the IEDB MHC class II binding prediction tool based on NN-align with half-maximal inhibitory concentration (IC_{50}) ≤ 1000 . The list of the epitopes and their correspondent bindings to MHC class II alleles, along with their positions in the Nipah virus glycoprotein G, while the list of the most promising epitopes that had a strong binding affinity to MHC class II alleles and depending on the number of their binding alleles is shown in Table 3.

3.5. Population Coverage. A population coverage test was performed to detect all the epitopes that bind to MHC class I alleles and MHC class II alleles available in the database in relation to the world, South Asia, Southeast Asia, Sudan, and North Africa.

3.6. 3D Structure

3.7. Molecular Docking

4. Discussion

Traditional vaccination approaches depend on the total amount of pathogens that are either live—constricted or inactivated. Among the significant issues, these vaccines have brought along pivotal security concerns. In light of the fact that they are being utilized for vaccination, this may have caused them to become actuated and may also cause contamination. Additionally, due to the varied hereditary pathogen strains found in the world, vaccines are probably going to lose their viability in various areas or even in certain populations.

However, novel vaccine approaches such as DNA- and epitope-based immunizations may possibly conquer obstructions for this type of immunization approaches, making them increasingly successful, explicit, and long-lasting in vulnerable reactions with insignificant structures and without any undesired impacts [46]. Moreover, many peptide-based vaccines have been effectively proposed through utilizing in silico approaches against *Madurella mycetomatis*, Mokola rabies virus, Lagos rabies virus, and others [47–52]. Such investigations, in regard to those viruses, have built up immunoinformatics in the computational analysis field.

In our present work, potential peptides were suggested to design an epitope-based vaccine for Nipah virus, using the latest amino acid sequences of glycoprotein G (glycoside hydrolase family) for a total of 21 strains of Nipah virus that were retrieved from the NCBI database (<https://www.ncbi.nlm.nih.gov/protein>) [31] on July 2018 after the last outbreak at the end of May 2018 in Kerala-India according to the WHO report [53]. Figure 4 summarizes the method of the present work.

Various literatures were surveyed to define the antigenic part of the virus. Glycoprotein G was found to be on the outer surface of the virus which was chosen as our target. Initially, we have evaluated the binding affinity of the virus to MHC alleles. This was done by submitting the protein reference sequence to IEDB MHC, a binding prediction tool, based on the ANN align method with $I_{C_{50}} \leq 500$ [37] for MHC class I molecules. 191 peptides were found to bind to MHC class I with different affinities. It is well known that a better immune response depends on whether or not the recognition of epitopes by HLA molecules with significant affinity is successful. Therefore, a peptide recognized by its highest number of HLA alleles has the best potential to induce a strong immune response, leading us to take into account the only three peptides found with a 100% conservancy. The conserved peptide FLIDRINWI was found to interact with 8 alleles (HLA-A*02:01, HLA-A*02:03, HLA-A*02:06, HLA-A*68:02, HLA-C*03:03, HLA-C*06:02, HLA-C*07:01, and HLA-C*12:03), while FSWDTMIKF with 8 alleles (HLA-A*02:06, HLA-A*29:02, HLA-B*35:01, HLA-B*46:01, HLA-B*53:01, HLA-B*57:01, HLA-B*58:01, and HLA-C*12:03) and TVYHCSAVY with 11 alleles (HLA-A*03:01, HLA-A*11:01, HLA-A*26:01, HLA-A*29:02, HLA-A*30:02, HLA-A*68:01, HLA-B*15:01, HLA-B*15:02, HLA-B*35:01, HLA-C*12:03, and HLA-C*14:02).

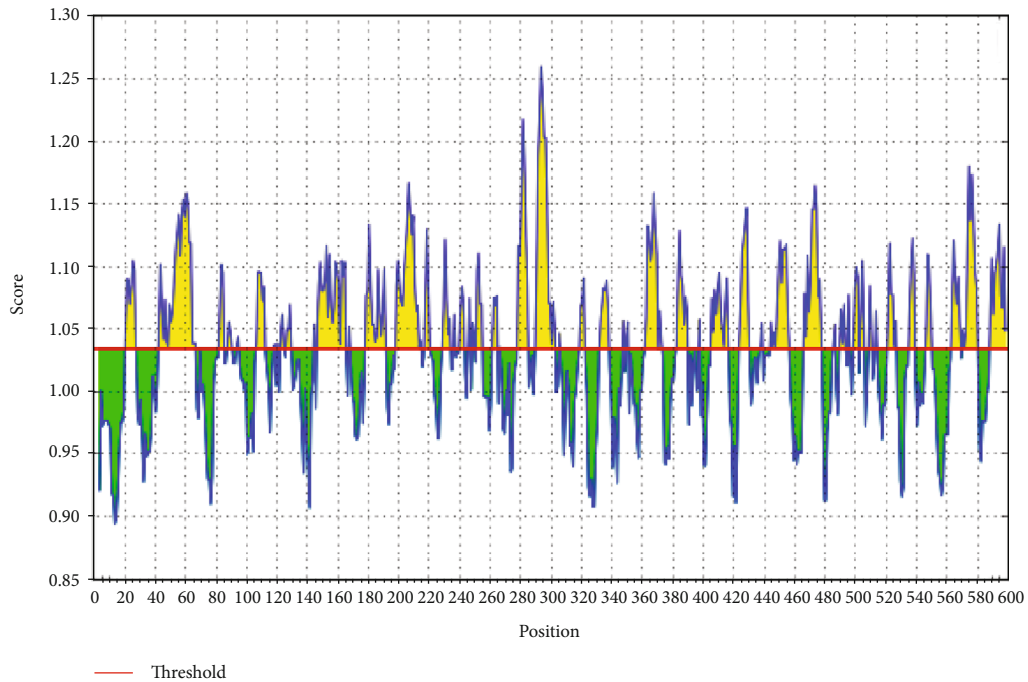


FIGURE 1: BepiPred linear prediction. Areas above the red line (threshold) are epitopes suggested to be binding to the B cells while the green areas are not.

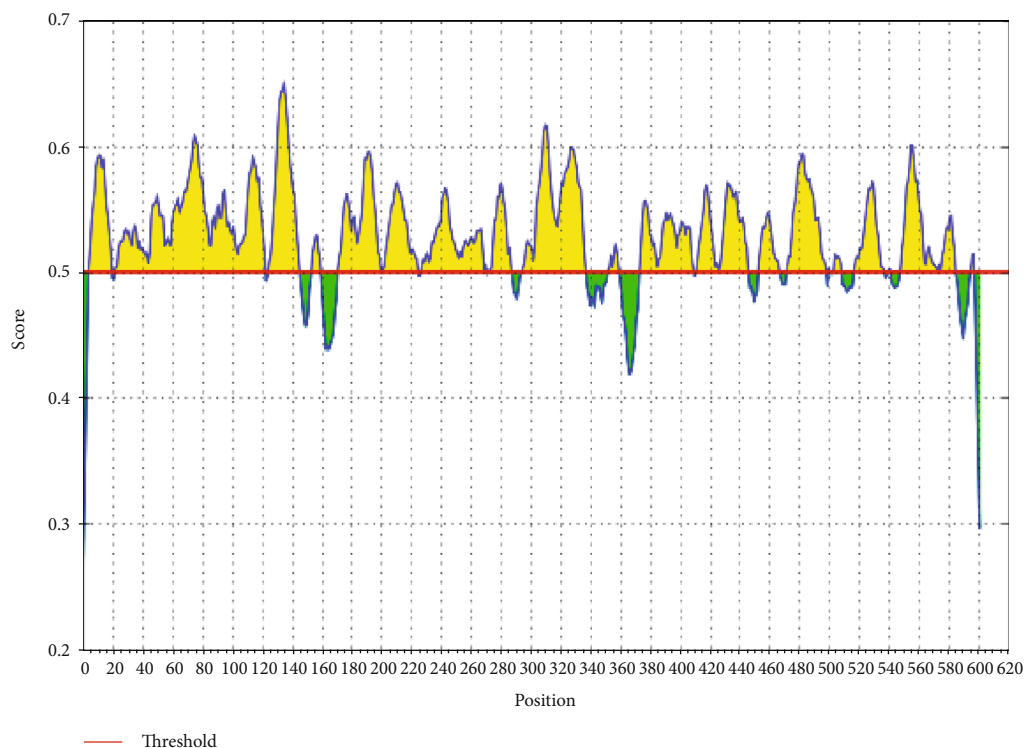


FIGURE 2: Emini surface accessibility prediction. Areas above the red line (threshold) are epitopes suggested to be binding to the B cells while the green areas are not.

The reference sequence of Nipah virus glycoprotein G was reanalyzed using the IEDB MHC II binding prediction tool based on NN-align with half-maximal inhibitory concentration ($IC_{50} \leq 1000$) [38]. The analysis resulted in

the prediction of 398 peptides from which FSWDTMIKF, FLIDRINWI, and ILSAFNTVI were potentially proposed according to their high number of binding alleles (15, 12, and 15 alleles, respectively). Additionally, the sequence of

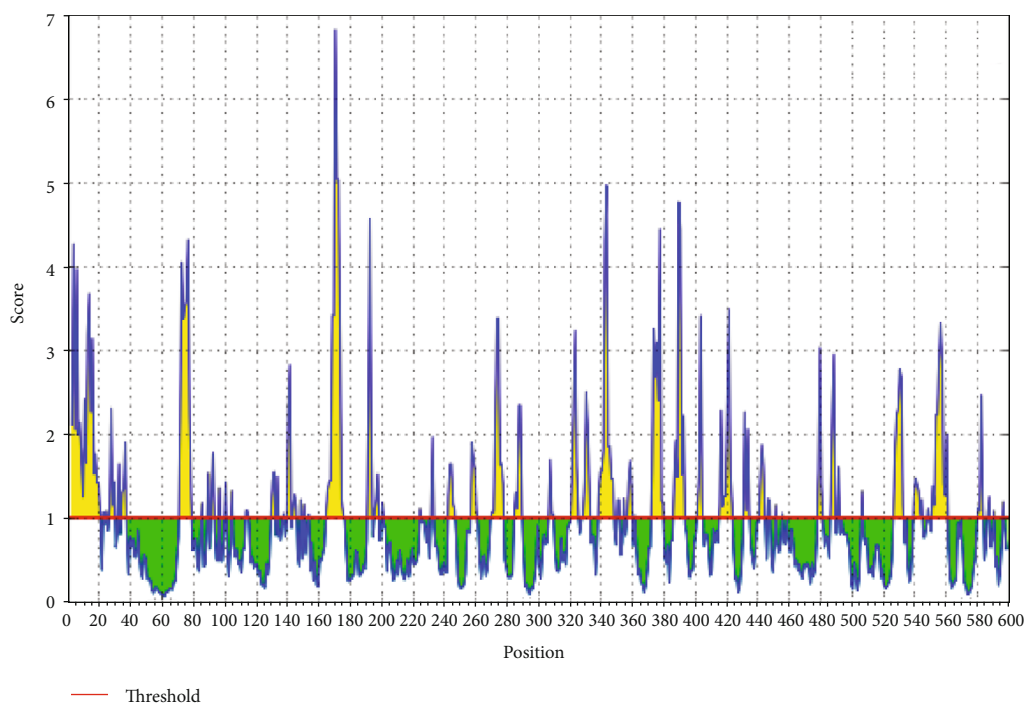


FIGURE 3: Kolaskar and Tongaonkar antigenicity prediction. Areas above the red line (threshold) are epitopes suggested to be binding to the B cells while the green areas are not.

Nipah virus glycoprotein G was subjected to BepiPred linear epitope prediction, Emini surface accessibility, and Kolaskar and Tongaonkar antigenicity methods in IEDB. Unfortunately, the peptides with the strongest binding affinities, utilizing the three mentioned tests, were absent.

Population coverage results for the total peptides found and the proposed peptides binding to MHC classes I and II alleles are summarized in Tables 4 and 5. Obtained results from the bindings to MHC I alleles revealed a 99.84% projected population coverage in the world, 98.55% in Southeast Asia, 98.40% in South Asia, 99.23% in North Africa, and 99.36% in Sudan while the population coverage results for the total number of peptides binding to MHC II alleles showed only a 56.84% projected population coverage in the world, 48.63% in Southeast Asia, 56.00% in South Asia, 62.37% in North Africa, and 55.75% in Sudan.

The selected peptides were further subjected to both MHC I- and MHC II-based population coverage analysis in the whole world, Southeast Asia, South Asia, North Africa, and Sudan as shown in Table 5. Among the six primarily selected epitopes, the obtained results showed a very strong potential in proposing the epitope FLIDRINWI as a vaccine candidate compared to the rest, taking into consideration its overall epitope conservancy, population coverage, and its affinity for the highest number of HLA molecules. Furthermore, *in silico* docking was carried out to measure the binding efficacy between the proposed peptides and HLA-A*02:01, in which it has been specifically chosen in relation to their contribution to several immunological and pathological diseases [54–56], although numerous investigations have shown a relationship between HLA alleles and disease susceptibility, which defines defensive HLA allelic associations

that possibly permit a recognizable proof that pathogen epitopes are limited by particular HLA alleles. These epitopes may then be fused into a vaccine design in the expectation that the immunization will be reproduced naturally [55, 56].

Calculations of the root mean square deviation (RMSD) between coordinates of the atoms and formation of clusters based on RMSD values have computed the resemblance of the docked structures. The most favorable docking is considered to be the conformation of the lowest binding energy. The least energy predictions of the peptide FLIDRINWI (-6.95 Kcal/mol) and the 3D structure of the allele and its peptide are shown in Figure 5. Furthermore, the monoisotopic mass, sum formula, and molecular weight of the three highly proposed peptides are shown in Table 6.

As a result of these interesting outcomes, formulating a vaccine using the suggested peptide is highly promising and encouraging to be highly proposed as a universal epitope-based peptide vaccine against Nipah virus.

5. Conclusions

The present study proposed a very promising epitope-based peptide vaccine against glycoprotein G of Nipah virus. It is expected to be highly antigenic with a minimum allergic effect. The proposed peptide FLIDRINWI has a strong binding affinity to both MHC class I and MHC class II alleles. Moreover, it shows an exceptional population coverage result for both MHC class I and MHC class II alleles in the whole world, Southeast Asia, South Asia, North Africa, and Sudan.

Despite having to validate the findings of the current study, an *in vivo* assessment of the most promising peptides,

TABLE 2: Most potential T cell epitopes interacting with MHC class I alleles, their positions, IC50, rank, and conservancy.

Peptide	Start	End	Allele	IC50	Rank	Conservancy
FAYSHLERI	229	237	HLA-A*02:01	376.44	2.5	76.19
	229	237	HLA-A*02:03	19.03	0.37	
	229	237	HLA-A*02:06	23.3	0.28	
	229	237	HLA-A*68:02	104.31	0.63	
	229	237	HLA-B*51:01	133.03	0.02	
	229	237	HLA-B*53:01	222.39	0.21	
	229	237	HLA-C*03:03	57.38	0.22	
	229	237	HLA-C*06:02	112.27	0.05	
	229	237	HLA-C*07:01	151.15	0.05	
	229	237	HLA-C*12:03	13.37	0.03	
229	237	HLA-C*15:02	207.16	0.12		
FLIDRINWI	512	520	HLA-A*02:01	3.65	0.02	100
	512	520	HLA-A*02:03	2.32	0.02	
	512	520	HLA-A*02:06	4.71	0.04	
	512	520	HLA-A*68:02	488.4	1.8	
	512	520	HLA-C*03:03	366.48	0.63	
	512	520	HLA-C*06:02	163.19	0.07	
	512	520	HLA-C*07:01	416.5	0.12	
512	520	HLA-C*12:03	55.27	0.13		
FSWDTMIKF	458	466	HLA-A*02:06	131.35	1.3	100
	458	466	HLA-A*29:02	328.77	1.2	
	458	466	HLA-B*35:01	70.16	0.24	
	458	466	HLA-B*46:01	470.72	0.09	
	458	466	HLA-B*53:01	95.8	0.12	
	458	466	HLA-B*57:01	380.38	0.93	
	458	466	HLA-B*58:01	313.77	0.77	
458	466	HLA-C*12:03	35.09	0.09		
KLISYTLPV	201	209	HLA-A*02:01	2.36	0.02	100
	201	209	HLA-A*02:03	2.4	0.02	
	201	209	HLA-A*02:06	3.77	0.02	
	201	209	HLA-A*30:01	146.34	0.44	
	201	209	HLA-A*32:01	21.39	0.04	
	201	209	HLA-B*15:01	303.74	1.3	
	201	209	HLA-C*14:02	187.05	0.28	
201	209	HLA-C*15:02	364.98	0.2		
TVYHCSAVY	278	286	HLA-A*03:01	84.04	0.35	100
	278	286	HLA-A*11:01	263.53	1.6	
	278	286	HLA-A*26:01	363.08	0.19	
	278	286	HLA-A*29:02	10.13	0.08	
	278	286	HLA-A*30:02	32.49	0.07	
	278	286	HLA-A*68:01	310.51	1.7	
	278	286	HLA-B*15:01	71.72	0.41	
	278	286	HLA-B*15:02	353.64	0.13	
	278	286	HLA-B*35:01	27.98	0.12	
	278	286	HLA-C*12:03	45.95	0.11	
278	286	HLA-C*14:02	103.08	0.18		

TABLE 3: The most potential T cell epitopes (core sequence) and the number of their binding alleles.

Core sequence	Alleles	Number of alleles
FLIDRINWI	HLA-DPA1*01/DPB1*04:01	12
	HLA-DPA1*01:03/DPB1*02:01	
	HLA-DPA1*02:01/DPB1*01:01	
	HLA-DPA1*02:01/DPB1*05:01	
	HLA-DPA1*03:01/DPB1*04:02	
	HLA-DQA1*01:01/DQB1*05:01	
	HLA-DQA1*05:01/DQB1*02:01	
	HLA-DRB1*01:01	
	HLA-DRB1*03:01	
	HLA-DRB1*04:01	
	HLA-DRB1*04:04	
HLA-DRB1*04:05		
FAYSHLERI	HLA-DPA1*01:03/DPB1*02:01	13
	HLA-DPA1*02:01/DPB1*01:01	
	HLA-DPA1*02:01/DPB1*05:01	
	HLA-DPA1*03:01/DPB1*04:02	
	HLA-DQA1*05:01/DQB1*02:01	
	HLA-DQA1*05:01/DQB1*03:01	
	HLA-DRB1*01:01	
	HLA-DRB1*04:04	
	HLA-DRB1*04:05	
	HLA-DRB1*07:01	
	HLA-DRB1*09:01	
HLA-DRB3*01:01		
HLA-DRB5*01:01		
FIEISDQRL	HLA-DPA1*01:03/DPB1*02:01	17
	HLA-DPA1*02:01/DPB1*01:01	
	HLA-DPA1*03:01/DPB1*04:02	
	HLA-DQA1*05:01/DQB1*02:01	
	HLA-DRB1*01:01	
	HLA-DRB1*04:05	
	HLA-DRB1*07:01	
	HLA-DRB1*08:02	
	HLA-DRB1*13:02	
	HLA-DRB1*15:01	
	HLA-DRB4*01:01	
	HLA-DRB5*01:01	
	HLA-DRB1*04:01	
	HLA-DRB1*07:01	
HLA-DRB1*09:01		
HLA-DRB1*11:01		
HLA-DRB1*13:02		
ILSAFNTVI	HLA-DPA1*03:01/DPB1*04:02	13
	HLA-DQA1*05:01/DQB1*03:01	
	HLA-DRB1*01:01	
	HLA-DRB1*04:05	

TABLE 3: Continued.

Core sequence	Alleles	Number of alleles
	HLA-DRB1*07:01 HLA-DRB1*08:02 HLA-DRB1*09:01 HLA-DRB1*11:01 HLA-DRB1*13:02 HLA-DRB1*15:01 HLA-DRB4*01:01 HLA-DRB5*01:01	
TVYHCSAVY	HLA-DQA1*05:01/DQB1*03:01 HLA-DRB1*07:01 HLA-DRB1*13:02 HLA-DRB1*15:01	4

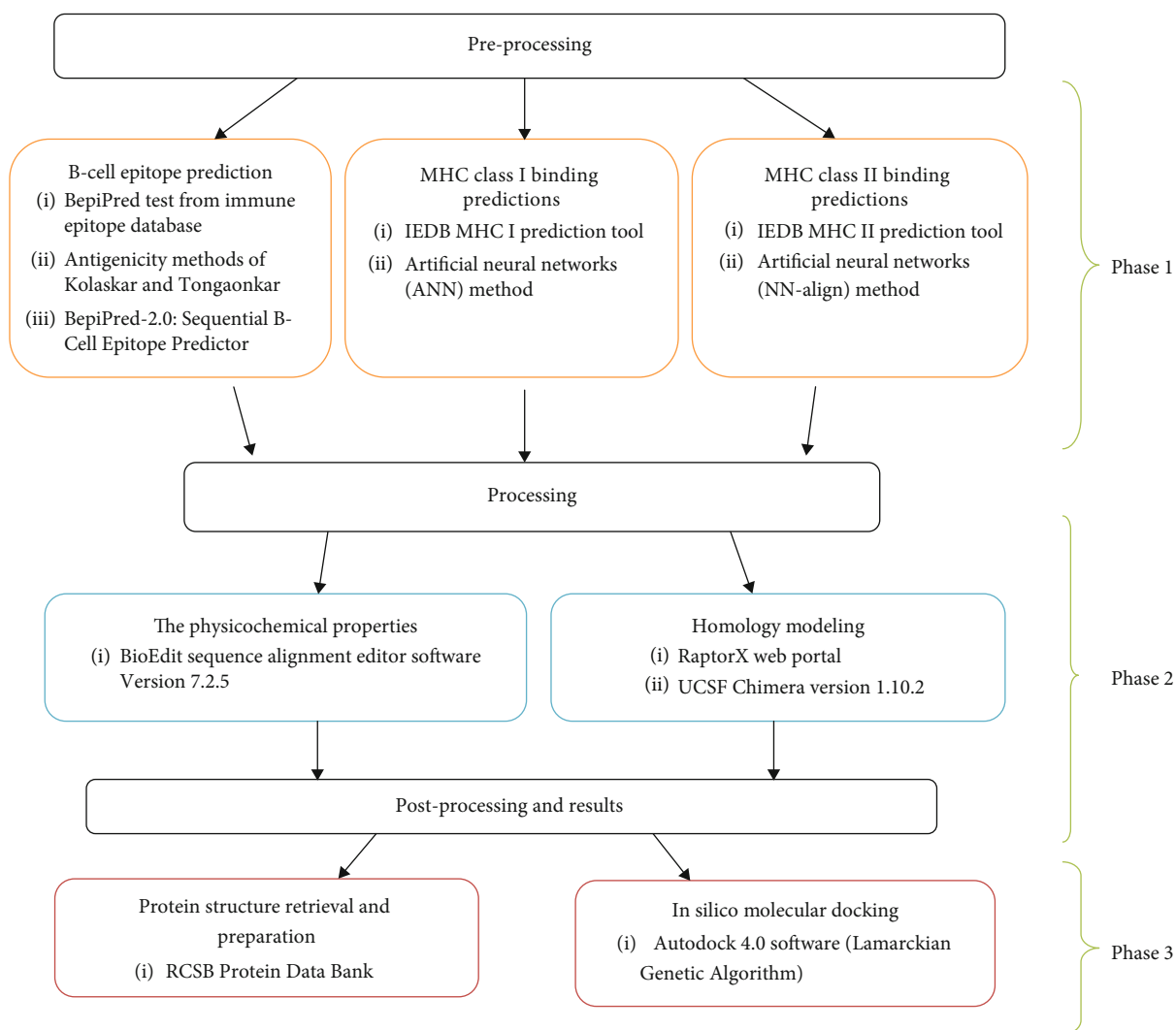


FIGURE 4: The three phases of Materials and Methods.

TABLE 4: A population coverage for all epitopes that bind to MHC classes I and II alleles from different parts of the world.

MHC classes	Population	World	South Asia	Southeast Asia	Sudan	North Africa
Class I	Coverage ^a	99.84%	98.40%	98.55%	99.36%	99.23%
	Average_hit ^b	36.62	30.60	28.42	34.02	32.43
	PC90 ^c	16.87	9.29	8.61	13.40	12.95
Class II	Coverage ^a	56.84%	56.0%	48.63%	55.75%	62.37%
	Average_hit ^b	54.88	50.50	36.27	36.89	50.09
	PC90 ^c	-24.24	-10.09	1.65	4.60	-3.31

^aProjected population coverage; ^baverage number of epitope hits/HLA combinations recognized by the population; ^cminimum number of epitope hits/HLA combinations recognized by 90% of the population.

TABLE 5: Population coverage of the three highly proposed peptides in MHC classes I and II in five different parts of the world.

Peptide	Population coverage %/area														
	World			Southeast Asia			South Asia			North Africa			Sudan		
	MHC I	MHC II	MHC I & II	MHC I	MHC II	MHC I & II	MHC I	MHC II	MHC I & II	MHC I	MHC II	MHC I & II	MHC I	MHC II	MHC I & II
FLIDRINWI	70.4%	43.7%	83.3%	44.5%	19.8%	55.5%	51.4%	29.8%	65.9%	71.0%	33.8%	80.8%	85.4%	30.7%	89.9%
FAYSHLERI	74.9%	40.2%	85.0%	50.6%	31.8%	66.3%	60.9%	40.5%	76.7%	77.5%	35.5%	85.5%	89.2%	19.5%	91.3%
TVYHCSAVY	61.3%	40.1%	76.8%	54.5%	18.4%	62.9%	63.7%	45.0%	80.0%	50.4%	43.5%	72.0%	50.2%	20.9%	60.6%

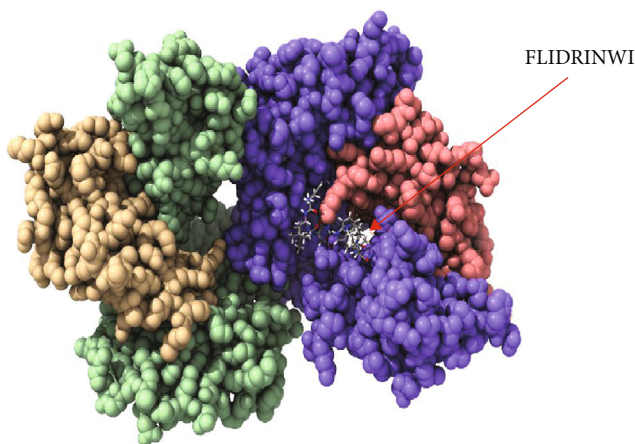


FIGURE 5: Molecular docking of FLIDRINWI peptide of Nipah virus docked in HLA-A*02:01 and visualized by UCSF Chimera X version 0.1.0.

TABLE 6: Monoisotopic mass, sum formula, and molecular weight of the three highly proposed peptides.

Sequence (N:H/C:OH)	Sum formula	Monoisot. mass	Mol. weight
FLIDRINWI	C ₅₈ H ₈₈ N ₁₄ O ₁₃	1188.66551	1189.40532
TVYHCSAVY	C ₄₇ H ₆₇ N ₁₁ O ₁₄ S	1041.45896	1042.16518
FAYSHLERI	C ₅₃ H ₇₈ N ₁₄ O ₁₄	1134.58218	1135.27182

namely, FLIDRINWI, TVYHCSAVY, and FAYSHLERI, is highly recommended and will serve as the ground data for such work as shown in Figures 5–9.

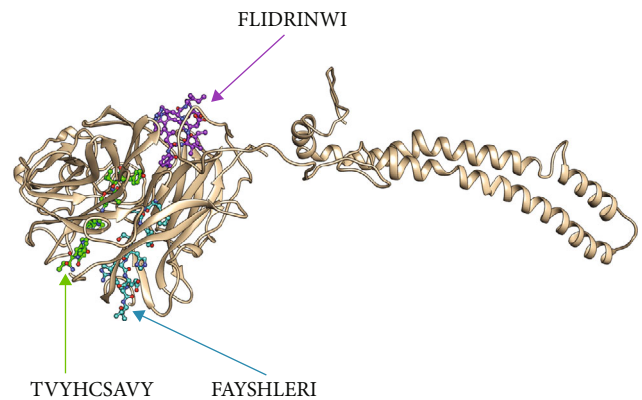


FIGURE 6: The four potential peptides bound to MHC class I and MHC class II visualized by Chimera X version 0.1.0.

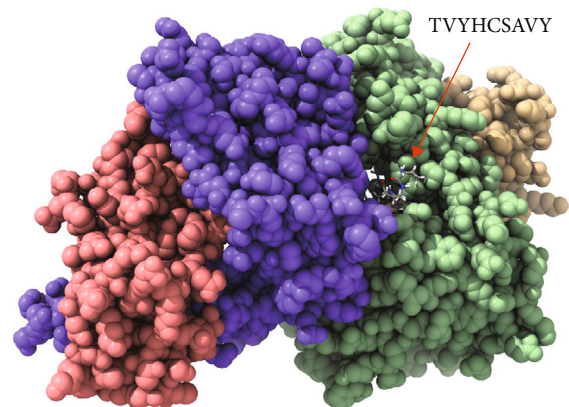


FIGURE 7: Molecular docking of TVYHCSAVY peptide of Nipah virus docked in HLA-A*02:01 and visualized by UCSF Chimera X version 0.1.0.

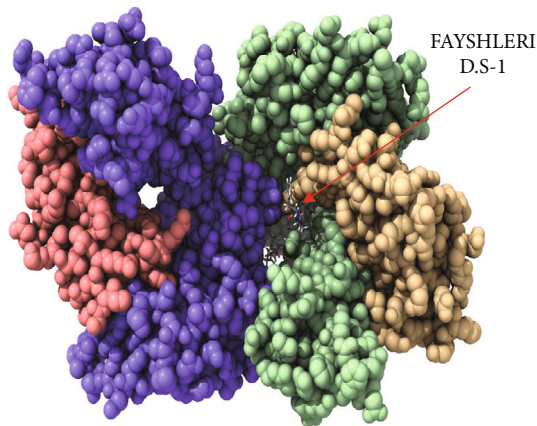


FIGURE 8: Molecular docking of FAYSHLERI peptide of Nipah virus docked in HLA-A*02:01 and visualized by UCSF Chimera X version 0.1.0. *D.S: Docking Side No.1.

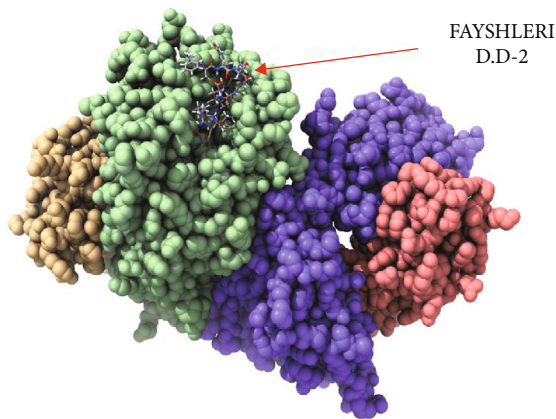


FIGURE 9: Molecular docking of FAYSHLERI peptide of Nipah virus docked in HLA-A*02:01 and visualized by UCSF Chimera X version 0.1.0. *D.S: Docking Side No.2.

Data Availability

The data used to support the findings of this study are available from the corresponding author upon request.

Conflicts of Interest

The authors declare that they have no competing interests.

References

- [1] V. K. Chattu, R. Kumar, S. Kumary, F. Kajal, and J. K. David, "Nipah virus epidemic in southern India and emphasizing "One Health" approach to ensure global health security," *Journal of Family Medicine and Primary Care*, vol. 7, no. 2, pp. 275–283, 2018.
- [2] Centers for Disease Control and Prevention (CDC), "Outbreak of Hendra-like virus—Malaysia and Singapore, 1998–1999," *Morbidity and Mortality Weekly Report*, vol. 48, no. 13, pp. 265–269, 1999.
- [3] C. C. Broder, K. Xu, D. B. Nikolov et al., "A treatment for and vaccine against the deadly Hendra and Nipah viruses," *Antiviral Research*, vol. 100, no. 1, pp. 8–13, 2013.
- [4] A. C. Breed, J. Meers, I. Sendow et al., "The distribution of henipaviruses in Southeast Asia and Australasia: is Wallace's line a barrier to Nipah virus?," *PLoS One*, vol. 8, no. 4, article e61316, 2013.
- [5] H. M. Weingartl, Y. Berhane, J. L. Caswell et al., "Recombinant nipah virus vaccines protect pigs against challenge," *Journal of Virology*, vol. 80, no. 16, pp. 7929–7938, 2006.
- [6] H. E. Field, "Bats and emerging zoonoses: henipaviruses and SARS," *Zoonoses and Public Health*, vol. 56, no. 6-7, pp. 278–284, 2009.
- [7] S. P. Luby, M. J. Hossain, E. S. Gurley et al., "Recurrent zoonotic transmission of Nipah virus into humans, Bangladesh, 2001–2007," *Emerging Infectious Diseases*, vol. 15, no. 8, pp. 1229–1235, 2009.
- [8] B. A. Clayton, "Nipah virus: transmission of a zoonotic paramyxovirus," *Current Opinion in Virology*, vol. 22, pp. 97–104, 2017.
- [9] K. B. Chua, "Epidemiology, surveillance, and control of Nipah virus infections in Malaysia," *The Malaysian Journal of Pathology*, vol. 32, no. 2, pp. 69–73, 2010.
- [10] S. A. Rahman, L. Hassan, J. H. Epstein et al., "Risk factors for Nipah virus infection among pteropid bats, Peninsular Malaysia," *Emerging Infectious Diseases*, vol. 19, no. 1, pp. 51–60, 2013.
- [11] K. Halpin, A. D. Hyatt, R. Fogarty et al., "Pteropid bats are confirmed as the reservoir hosts of henipaviruses: a comprehensive experimental study of virus transmission," *The American Journal of Tropical Medicine and Hygiene*, vol. 85, no. 5, pp. 946–951, 2011.
- [12] Z. Majid and W. S. Majid, "NIPAH virus: a new threat to South Asia," *Tropical Doctor*, vol. 48, no. 4, p. 376, 2018.
- [13] S. P. Luby, "The pandemic potential of Nipah virus," *Antiviral Research*, vol. 100, no. 1, pp. 38–43, 2013.
- [14] K. Ramphul, S. G. Mejias, V. C. Agumadu, S. Sombans, R. Sonaye, and P. Lohana, "The killer virus called Nipah: a review," *Cureus*, vol. 10, no. 8, article e3168, 2018.
- [15] K. J. Goh, C. T. Tan, N. K. Chew et al., "Clinical features of Nipah virus encephalitis among pig farmers in Malaysia," *The New England Journal of Medicine*, vol. 342, no. 17, pp. 1229–1235, 2000.
- [16] Y. Berhane, J. D. Berry, C. Ranadheera et al., "Production and characterization of monoclonal antibodies against binary ethylenimine inactivated Nipah virus," *Journal of Virological Methods*, vol. 132, no. 1-2, pp. 59–68, 2006.
- [17] H. Donaldson and D. Lucey, "Enhancing preparation for large Nipah outbreaks beyond Bangladesh: preventing a tragedy like Ebola in West Africa," *International Journal of Infectious Diseases*, vol. 72, pp. 69–72, 2018.
- [18] M. M. Badawi, M. M. Osman, A. A. F. Alla et al., "Highly conserved epitopes of ZIKA envelope glycoprotein may act as a novel peptide vaccine with high coverage: immunoinformatics approach," *American Journal of Biomedical Research*, vol. 4, no. 3, pp. 46–60, 2016.
- [19] A. Kazi, C. Chuah, A. B. A. Majeed, C. H. Leow, B. H. Lim, and C. Y. Leow, "Current progress of immunoinformatics approach harnessed for cellular- and antibody-dependent vaccine design," *Pathogens and Global Health*, vol. 112, no. 3, pp. 123–131, 2018.
- [20] S. Khalili, A. Jahangiri, H. Bornha, K. Ahmadi Zanoos, and J. Amani, "Computational vaccinology and epitope vaccine design by immunoinformatics," *Acta Microbiologica et Immunologica*, vol. 61, no. 3, pp. 285–307, 2014.

- [21] K. T. Wong, W.-J. Shieh, S. Kumar et al., "Nipah virus infection: pathology and pathogenesis of an emerging paramyxoviral zoonosis," *The American Journal of Pathology*, vol. 161, no. 6, pp. 2153–2167, 2002.
- [22] Q. Liu, B. Bradel-Tretheway, A. I. Monreal et al., "Nipah virus attachment glycoprotein stalk C-terminal region links receptor binding to fusion triggering," *Journal of Virology*, vol. 89, pp. 1838–1850, 2015.
- [23] J. Oscherwitz, "The promise and challenge of epitope-focused vaccines," *Human Vaccines & Immunotherapeutics*, vol. 12, no. 8, pp. 2113–2116, 2016.
- [24] A. Nandy and S. C. Basak, "A brief review of computer-assisted approaches to rational design of peptide vaccines," *International Journal of Molecular Sciences*, vol. 17, no. 5, p. 666, 2016.
- [25] M. Skwarczynski and I. Toth, "Peptide-based synthetic vaccines," *Chemical Science*, vol. 7, no. 2, pp. 842–854, 2016.
- [26] M. T. Ali, M. M. Morshed, and F. Hassan, "A computational approach for designing a universal epitope-based peptide vaccine against Nipah virus," *Interdisciplinary Sciences, Computational Life Sciences*, vol. 7, no. 2, article 23, pp. 177–185, 2015.
- [27] D. L. Woodland, "A focus on vaccine development," *Viral Immunology*, vol. 28, no. 6, p. 303, 2015.
- [28] P. M. Moyle, "Progress in vaccine development," *Current protocols in microbiology*, vol. 36, pp. 18.1.1–18.1.26, 2015.
- [29] P. Oyarzun, J. J. Ellis, F. F. Gonzalez-Galarza et al., "A bioinformatics tool for epitope-based vaccine design that accounts for human ethnic diversity: application to emerging infectious diseases," *Vaccine*, vol. 33, no. 10, pp. 1267–1273, 2015.
- [30] W. Li, M. D. Joshi, S. Singhanian, K. H. Ramsey, and A. K. Murthy, "Peptide vaccine: progress and challenges," *Vaccine*, vol. 2, no. 3, pp. 515–536, 2014.
- [31] "NCBI protein sequence database," 2018, <https://www.ncbi.nlm.nih.gov/protein>.
- [32] R. Vita, J. A. Overton, J. A. Greenbaum et al., "The immune epitope database (IEDB) 3.0," *Nucleic Acids Research*, vol. 43, no. D1, pp. D405–D412, 2015.
- [33] O. O. Oni, A. A. Owoade, and C. A. O. Adeyefa, "Design and evaluation of primer pairs for efficient detection of avian rotavirus," *Tropical Animal Health and Production*, vol. 50, no. 2, pp. 267–273, 2018.
- [34] H. H. Bui, J. Sidney, W. Li, N. Fusseder, and A. Sette, "Development of an epitope conservancy analysis tool to facilitate the design of epitope-based diagnostics and vaccines," *BMC Bioinformatics*, vol. 8, no. 1, p. 361, 2007.
- [35] J. E. Larsen, O. Lund, and M. Nielsen, "Improved method for predicting linear B-cell epitopes," *Immunome Research*, vol. 2, no. 1, p. 2, 2006.
- [36] A. S. Kolaskar and P. C. Tongaonkar, "A semi-empirical method for prediction of antigenic determinants on protein antigens," *FEBS Letters*, vol. 276, no. 1–2, pp. 172–174, 1990.
- [37] Y. Kim, J. Ponomarenko, Z. Zhu et al., "Immune epitope database analysis resource," *Nucleic Acids Research*, vol. 40, no. W1, pp. W525–W530, 2012.
- [38] Q. Zhang, P. Wang, Y. Kim et al., "Immune epitope database analysis resource (IEDB-AR)," *Nucleic Acids Research*, vol. 36, Supplement 2, pp. W513–W518, 2008.
- [39] H. H. Bui, J. Sidney, K. Dinh, S. Southwood, M. J. Newman, and A. Sette, "Predicting population coverage of T-cell epitope-based diagnostics and vaccines," *BMC Bioinformatics*, vol. 7, no. 1, p. 153, 2006.
- [40] S. Wang, W. Li, S. Liu, and J. Xu, "RaptorX-Property: a web server for protein structure property prediction," *Nucleic Acids Research*, vol. 44, no. W1, pp. W430–W435, 2016.
- [41] E. F. Pettersen, T. D. Goddard, C. C. Huang et al., "UCSF Chimera—a visualization system for exploratory research and analysis," *Journal of Computational Chemistry*, vol. 25, no. 13, pp. 1605–1612, 2004.
- [42] J. A. Choo, S. Y. Thong, J. Yap et al., "Bioorthogonal cleavage and exchange of major histocompatibility complex ligands by employing azobenzene-containing peptides," *Angewandte Chemie (International ed in English)*, vol. 53, no. 49, pp. 13390–13394, 2014.
- [43] N. Guex and M. C. Peitsch, "SWISS-MODEL and the Swiss-PdbViewer: an environment for comparative protein modeling," *Electrophoresis*, vol. 18, no. 15, pp. 2714–2723, 1997.
- [44] G. M. Morris, R. Huey, W. Lindstrom et al., "AutoDock4 and AutoDockTools4: automated docking with selective receptor flexibility," *Journal of Computational Chemistry*, vol. 30, no. 16, pp. 2785–2791, 2009.
- [45] G. M. Morris, D. S. Goodsell, R. S. Halliday et al., "Automated docking using a Lamarckian genetic algorithm and an empirical binding free energy function," *Journal of Computational Chemistry*, vol. 19, no. 14, pp. 1639–1662, 1998.
- [46] R. Arnon, "A novel approach to vaccine design—epitope-based vaccines," *The FEBS Journal*, vol. 273, pp. 33–34, 2006.
- [47] A. A. Mohammed, A. M. H. AlNaby, S. M. Sabeel et al., "Epitope-based peptide vaccine against fructose-bisphosphate aldolase of *Madurella mycetomatis* Using immunoinformatics approaches," *Bioinformatics and Biology Insights*, vol. 12, 2018.
- [48] A. A. Mohammed, O. Hashim, K. A. A. Elrahman, A. Hamdi, and M. A. Hassan, "Epitope-based peptide vaccine design against Mokola rabies virus glycoprotein G utilizing in silico approaches," *Immunome Research*, vol. 13, no. 3, 2017.
- [49] O. H. Ahmed, A. Abdelhalim, S. Obi, K. A. Abd elrahman, A. Hamdi, and M. A. Hassan, "Immunoinformatic approach for epitope-based peptide vaccine against Lagos rabies virus glycoprotein G," *Immunome Research*, vol. 13, no. 3, 2017.
- [50] S. Idrees and U. A. Ashfaq, "Structural analysis and epitope prediction of HCV E1 protein isolated in Pakistan: an in-silico approach," *Virology Journal*, vol. 10, no. 1, article 113, 2013.
- [51] M. A. Hasan, M. Hossain, and M. J. Alam, "A computational assay to design an epitope-based peptide vaccine against Saint Louis encephalitis virus," *Bioinformatics and Biology Insights*, vol. 7, pp. 347–355, 2013.
- [52] I. Sharmin, "A highly conserved WDYPKCDRA epitope in the RNA directed RNA polymerase of human coronaviruses can be used as epitope-based universal vaccine design," *BMC Bioinformatics*, vol. 15, no. 1, article 161, 2014.
- [53] <https://www.who.int/csr/don/07-august-2018-nipah-virus-india/en/>.
- [54] P. R. Burton, M. D. Tobin, and J. L. Hopper, "Key concepts in genetic epidemiology," *The Lancet*, vol. 366, no. 9489, pp. 941–951, 2005.
- [55] F. Calafell and N. Malats, "Basic molecular genetics for epidemiologists," *Journal of Epidemiology & Community Health*, vol. 57, no. 6, pp. 398–400, 2003.
- [56] M. P. Davenport and A. V. Hill, "Reverse immunogenetics: from HLA-disease associations to vaccine candidates," *Molecular Medicine Today*, vol. 2, no. 1, pp. 38–45, 1996.

Research Article

Combined IMIG and Immune Ig Attenuate Allergic Responses in Beagle Dogs

R. M. Gorczynski ^{1,2}, T. Maqbool,³ and G. Hoffmann²

¹University of Toronto, ON, Canada

²Network Immunology, Vancouver, BC, Canada

³Cedarlane Labs, Burlington, ON, Canada

Correspondence should be addressed to R. M. Gorczynski; reg.gorczynski@utoronto.ca

Received 7 January 2020; Revised 29 February 2020; Accepted 13 March 2020; Published 21 April 2020

Guest Editor: Masha Fridkis-Hareli

Copyright © 2020 R. M. Gorczynski et al. This is an open access article distributed under the Creative Commons Attribution License, which permits unrestricted use, distribution, and reproduction in any medium, provided the original work is properly cited.

Background. We previously reported attenuation of serum OVA-specific IgE levels and of lymphocyte-derived IL-4, both nominal markers of allergic immunity, following injection of a combination of homologous (mouse) polyclonal anti-idiotypic immunoglobulin (Ig) and immune Ig in BALB/c mice. We predicted this might generalize to other species and using heterologous mixtures of Igs. This was assessed in mice using OVA sensitization in the presence of human Igs as a source of both anti-idiotypic Ig and immune Ig and in dogs with peanut butter-induced allergic responses. **Methods.** Eight-week-old BALB/c mice received OVA immunization and 5 weekly injections of immune Ig or anti-idiotypic Ig from either homologous (mouse) or heterologous (human) sources. Five-month-old Beagles received weekly topical exposure (on the abdomen) to peanut butter and treatment with pooled dog Ig and dog antirabies immune Ig, or a combination of human IMIG and human anti-Tet. All mice/dogs thereafter received a final allergen challenge, and serum IgG, IgE, and allergen-induced IL-2/IL-4 and IL-31 production in 72 hr cultures was measured. **Results.** In mice attenuation of OVA-induced allergy (IgE-specific Ig and OVA-induced IL-4) was seen using both mouse and human Ig mixtures, without effect on OVA serum IgG or OVA-induced IL-2. Attenuation of concanavalin A- (ConA-) induced IL-4:IL-2 production and of peanut butter-induced IL-4 and IL-31 was seen in dogs receiving combinations of both heterologous and homologous immune Igs and anti-idiotypic Igs, with no decline in IL-2 production. Allergen-specific IgE/IgG was not detectable in dog serum, but there was a trend to lower total serum IgE levels (and decreased IgE:IgG ratios). **Conclusion.** Homologous and heterologous combinations of polyclonal IMIG and immune Ig attenuate allergic responses in mice and dogs. This treatment protocol represents a novel approach which can be adapted for allergic desensitization in veterinary and human use.

1. Introduction

Allergic rhinitis, asthma, and atopic eczema are among the commonest causes of chronic ill health, with a combined prevalence of 10-20% [1-3]. All such diseases are increasing in prevalence, with considerable burden to total health care costs. While the tendency to develop allergic reactions is lifelong, the actual manifestations of disease change over time. As an example, children often develop eczema early, followed by allergic rhinitis and asthma. All allergic diseases

impact quality of life and, in more extreme cases, morbidity and even mortality.

Currently, treatment for these diseases follows several major guiding principles [1], including allergen avoidance, drug therapy (including oral and topical potent anti-inflammatory medications (steroids), antihistamines, and in severe cases with anaphylaxis, adrenalin), and finally, where the allergen is identifiable, desensitization therapy [4]. The latter uses controlled exposure to escalating doses of purified allergen to alter the body's reaction to allergen exposure.

In general, desensitization therapy treatment is given long term and often still in association with conventional allergy-relieving medications. There remains an unmet need to develop novel therapies.

Given concerns regarding extrapolation of allergy studies from mouse to man [5], there has been a growing interest in the analysis of allergic reactivity in other animal species. Humans and their most important domestic animals, namely, cats and dogs, have a similar IgE receptor repertoire and expression pattern, with essentially similar cell types known to be implicated in the triggering and/or regulation of allergic responses, including mast cells, eosinophils, and regulatory T cells. Such animals have thus been favoured for preclinical research studies.

Skin, respiratory, and food allergies are not uncommon in dogs, and the immune mechanisms involved are more like humans than in rodents [5, 6], making them a favoured species for study [7–11]. Dust mite allergens are thought to be highly relevant to canine allergic responses [12], although skin reactivity and dust mite-specific serum IgE have also been detected in several dogs without clinical signs of allergy, suggesting that sensitization can occur without necessarily inducing clinically significant reactivity [13]. Dogs develop atopic dermatitis as a result of sensitization to storage mites [14] and plant-derived allergens [15], as well as to flea allergens [16]—though less so to other insects—and even moulds [17]. In all cases, IgE responses to several identified protein allergens have been documented. Induction of IL-31 is a prominent factor in the development of atopic dermatitis in dogs [18].

We reported on the use of a combined injection of polyclonal anti-idiotypic antibodies, along with polyclonal immune antibodies, on resetting immune regulatory networks in rodents [19]. This treatment regulated many immune reactivities, with decreased inflammatory cytokines in inflammatory colitis, decreased skin graft rejection in a transplant model, and decreased IgE and IL-4 sensitization in a rodent allergy model (to ovalbumin (OVA)). The antigen-specific regulation seen was independent of the specific antigens used to prepare the polyclonal immune Ig. One mechanism responsible for these effects involved perturbation of regulatory T cell networks, consistent with other data favouring a role for Tregs in control of allergic reactivity [20]. We have used the Beagle model described earlier [7] to assess whether a mixture of homologous antibodies (pooled dog Ig as a source of anti-idiotypic; pooled dog rabies immune globulin as a source of immune Ig) would attenuate allergic responses in dogs. In this model, application of peanut butter paste caused enhanced serum IgE and when animals were then challenged orally, pruritic dermatitis, eosinophilic dermatitis, and IgE-positive cells in skin were seen in atopic dogs [7]. We asked whether the treatment protocol used to attenuate allergic responses in mice decreased allergen-induced IL-4 and IL-31 production in sensitized dogs, without diminishing an IL-2 (nonatopic) response in the same animals. We also explored whether heterologous serum Ig mixtures (pooled polyclonal human Ig and pooled polyclonal human anti-tetanus Ig) would lead to similar allergic desensitization.

2. Materials and Methods

2.1. Preliminary Studies in Mice

2.1.1. Mice and Ethics Review. All mice were bred at Cedarlane labs from Jax founder stock. All studies were approved by a local institutional review board, certified by the Canadian Council on Animal Care. Animals were maintained under SPF conditions throughout the study.

Immunization of BALB/c mice to produce IgE against OVA was described elsewhere [19]. Eight mice per group received 10 μ g OVA emulsified in alum at day 0 and day 10. One control group received no OVA immunization. All but one OVA-immunized group and the no OVA control received ongoing exposure to egg white solution in the drinking water for 10 d until sacrifice—the other control group received OVA immunization only (no EWS). Beginning on day 7, groups of mice given OVA and EWS received 5 weekly 10 μ g intramuscular (IM) injections of pooled polyclonal BL/6 anti-C3H immune Ig, polyclonal C3H anti-anti-C3H Ig (C3H anti-BL/6 absorbed with BL/6: anti-idiotypic Ig), or a combination of these latter 2 Ig preparations (estimated \sim 0.5 mg/kg/dose). At 42 d, all mice received a booster injection of OVA in alum, with sacrifice 7 d later. In a separate study, mice received OVA stimulation in the same fashion, but the Ig preparations used for treatment were heterologous in nature (pooled human IVIG, given intramuscularly, hence IMIG) and pooled human anti-Tet immune Ig (both purchased from Grifols, USA). In trial studies, we have found that optimal dosing for this heterologous Ig used as anti-idiotypic (IMIG) was \sim 3x higher than the purified mouse polyclonal C3H anti-anti-C3H Ig, and accordingly, IMIG was used at a dose of \sim 1.5 mg/kg/dose. It should be noted that in separate studies (not shown), we have assessed different routes of delivery of immunomodulatory Igs, including intravenous (iv), intraperitoneal (ip), and subcutaneous (sq), without significant variation in efficacy, although anti-idiotypic and immune Igs must be given by separate routes for optimal effects.

Serum was obtained from mice at sacrifice by cardiac puncture [19]. At the same time, single-cell splenocyte preparations from individual animals were resuspended after washing (800g \times 5 min at 4°C) in RPMI with 10% fetal calf serum (RPMI₁₀). 5×10^6 splenocytes from individual animals were incubated in duplicate in vitro in 2 ml RPMI₁₀ with 0.1 mg/ml OVA for 72 hr, and culture supernatants assayed by ELISA for IL-2 and IL-4 production.

OVA-specific IgE or IgG was measured in all serum samples by ELISA using plates coated with 100 ng/well of OVA and developed with HRP-anti-mouse IgE or HRP anti-IgG, followed by appropriate substrate.

2.2. Dogs. Beagle dogs, aged 5 months at initiation of use, were purchased by CARE research (Fort Collins, Colorado) and housed in their facility, under supervision by approved veterinary services, and in accordance with a registered animal protocol committee. Animals were fed approved dog chow ad libitum, with daily exercise. Weights were followed 3x/week, with veterinary inspections weekly. Dogs were released for companion pets at the termination of the study.

There were no significant differences in weights pre-/post-treatment for any of the groups of dogs used in the study.

2.2.1. Ig Preparations for Injection. Pooled human IVIG and anti-Tet Ig were purchased from Grifols, USA. Pooled Beagle serum was purchased from BioIVT (Westbury, NY), and Ig was isolated following ammonium sulphate precipitation. Polyclonal dog rabies immune Ig was pooled from the serum (3 ml/animal) obtained, with the owner's consent, from 12 outbred dogs, 8-24 months of age, boosted with rabies vaccine 4 weeks before.

Groups of 5 Beagle dogs received IM gluteal injections in 0.5 ml sterile PBS of 12 mg/dose of pooled polyclonal Ig (dog IMIG-group 2, or human IMIG-group 3) and 4 mg IM in the opposite limb of 0.5 ml sterile PBS of polyclonal immune Ig (dog antirabies-group 2 or human anti-Tet-group 3). Control dogs (group 1) received only dog IMIG (total Ig used 16 mg/dose). Animals received weekly injections $\times 5$ weeks, followed by 3 further injections at 2-week intervals. Beginning on the first day of injection, all animals received ~ 15 gm peanut butter paste weekly smeared on their abdomens. A collar was applied for ~ 6 -8 hours after peanut butter application to prevent dogs from removing the peanut butter. Five days following the last IM injection, all animals received an oral challenge with peanut butter (~ 15 gm). Photographic images of the abdomen were taken daily for 3 days after oral challenge. Samples of heparinized blood (4 ml/dog) were harvested at the outset of the study, 3 days after oral challenge, and flown (FEDEX) at room temperature to Cedarlane Labs, Ontario, Canada, for analysis. All samples were received and harvested for serum/PBMCs for culture, within 24 hr of collection. All individuals at CARE were blinded to which treatment contained which individual dogs. During the study, 3 dogs (1 in each group) developed, at different times in the study, a minor skin irritation at the site of injection. In each case, the dogs were monitored by a CARE veterinarian, and the irritation resolved without treatment within 7-10 days, with no recurrence.

2.3. Dog Serum IgG and IgE Assays and IL-4, IL-2, and IL-31 Cytokine Assays. PBL harvested in heparinized tubes was diluted 1:1 with PBS, layered over 4 ml Ficoll/Hypaque, and centrifuged for 20 min at 1600 rpm at room temperature (rt). The diluted serum (1:1) overlaying the cell interface was collected with a Pasteur pipette, and the cells (PBMCs) were diluted into 10 ml RPMI with 5% fetal calf serum+5% dog serum (both sera heat inactivated 30 min at 56°C: hereafter RPMI_{sera}). This sample was centrifuged at 1600 rpm for 10 min at rt. The cell pellet was resuspended in 2 ml RPMI_{sera}, and cells were diluted in RPMI_{sera} to a concentration of 2.5×10^6 /ml. Serum samples were stored at -80°C for later Ig analysis (ELISA). 1.5×10^6 PBMCs were stimulated in duplicate in 1.5 ml RPMI_{sera} in 24-well culture plates with either 5 μ g/ml ConA (time zero and end of study) or with 20 μ l of DMSO extract of peanut butter (1 gm in 10 ml DMSO: final concentration in culture ~ 2 mg/ml); control samples were incubated with 1.5 ml RPMI_{sera} and 20 μ l DMS only. Supernatants were harvested from culture at 72 hr for IL-2/IL-4 detection by ELISA.

IgG and IgE concentrations in all sera were determined by ELISA as follows. Goat anti-dog IgG was purchased from Thermo Scientific, Fisher, Canada (Cat # 18763). Goat anti-dog IgE was from Bio-Rad, Canada (Cat # AHP946). Donkey anti-goat HRP was obtained from R&D Systems Canada. High-binding ELISA plates were from SARSTEDT (Cat # 82.1581.200) and ELISA substrate solution from Thermo Scientific (Cat #34028). 100 μ l aliquots of the experimental sera were diluted 1:100, 1:1000, and 1:10,000 and added in quadruplicate to microtiter plates in 100 μ l. All microtiter plates were coated overnight (37°C), along with duplicate control wells containing known concentrations of standard amounts of dog IgG or dog IgE (both purchased from R&D Systems). Thereafter, a routine ELISA was performed using steps including addition of anti-dog IgG or anti-dog IgE, followed by donkey anti-goat HRP and later addition of a substrate, with ultimate reading in an ELISA plate reader. IgG and IgE levels in test sera were determined from a standard curve using purified IgG and IgE.

IL-2 and IL-4 levels in ConA-activated or peanut butter-stimulated PBMCs were determined using commercial kits provided by R&D (Duo Set IL-2: Cat # 1815; Duo Set IL-4: Cat # DY754), along with auxiliary reagent kits (R&D Cat # DY 008). IL-31 was similarly assayed using a commercial kit with reagents/standards, from NeoScientific (Cat #C10041).

2.4. Statistics. All data from mouse experiments reported below are summed over at least two studies, with a minimum of 16 mice in all groups for all experiments. In general, for studies with multiple groups, a multivariate analysis of variance (MANOVA) test was first applied to assess for any significant differences between groups, and subsequently, where indicated, paired *t*-tests were used to compare individual groups with the documented control.

Dog studies were performed using the 3 groups described. Five animals/group were randomly assigned to the different treatments. Comparisons between groups were by MANOVA.

3. Results

3.1. OVA-Specific IgE, but Not IgG, Is Attenuated in OVA-Primed Mice by Combined Treatment with Pooled Anti-idiotype and Immune Ig, Even with a Heterologous Source of Igs. Our first studies repeated the findings previously reported [19]. BALB/c mice were immunized with OVA in alum and given EWS in the drinking supply as a source of persistent allergen exposure. Groups of mice also received 5 weekly IM injections of anti-idiotype and/or immune Igs as indicated in Materials and Methods. Following a final boost with OVA after these 5 Ig injections, mice were sacrificed 7 d after OVA, and serum IgG/IgE to OVA was detected by ELISA, with IL-2 and IL-4 levels detected at 72 hr from OVA-stimulated splenocytes. Data pooled from two such studies, using 8 mice/group, are shown in Figures 1 and 2.

Comparison of Figures 1(a) and 1(b) shows clearly that mice exposed to EWS following OVA immunization developed a greater IgG and IgE response than mice given OVA immunization only. Mice exposed to EWS alone (no

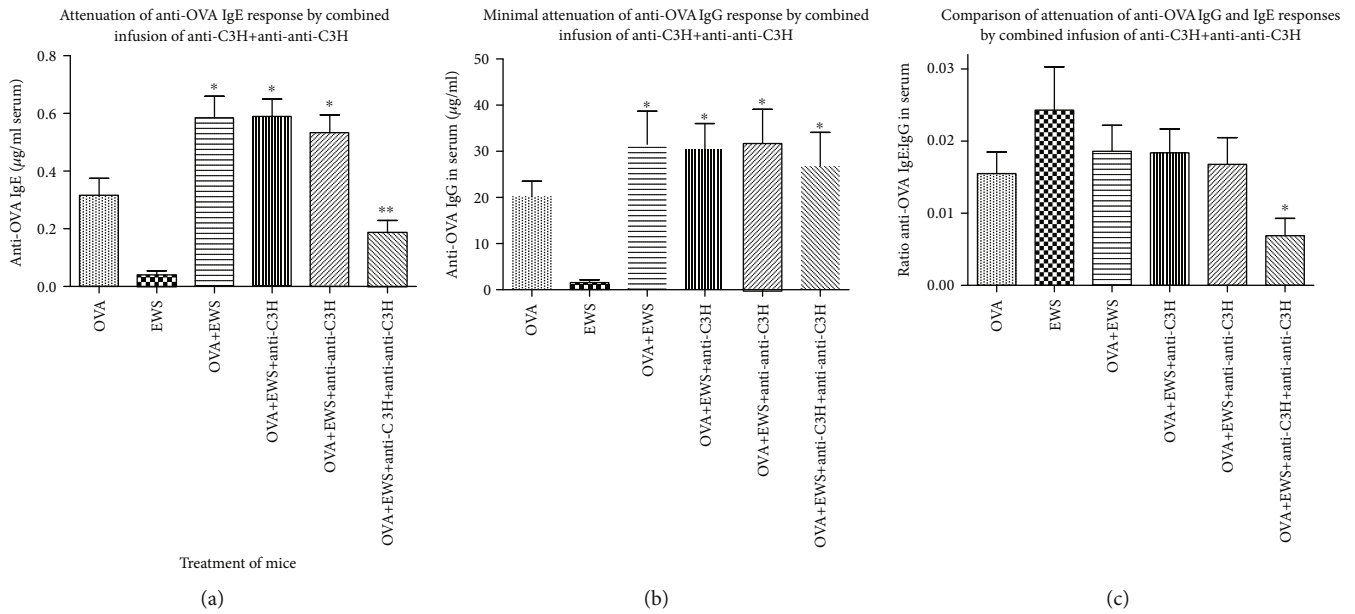


FIGURE 1: OVA-specific IgE ((a) mean \pm SD) and IgG (b) in mice immunized with OVA and immune or anti-idiotype sera (or both). OVA-immunized mice except for the control group (far left) drank EWS. (c) The ratio of $*p < 0.05$ compared with OVA only; $**p < 0.05$ compared with OVA+EWS.

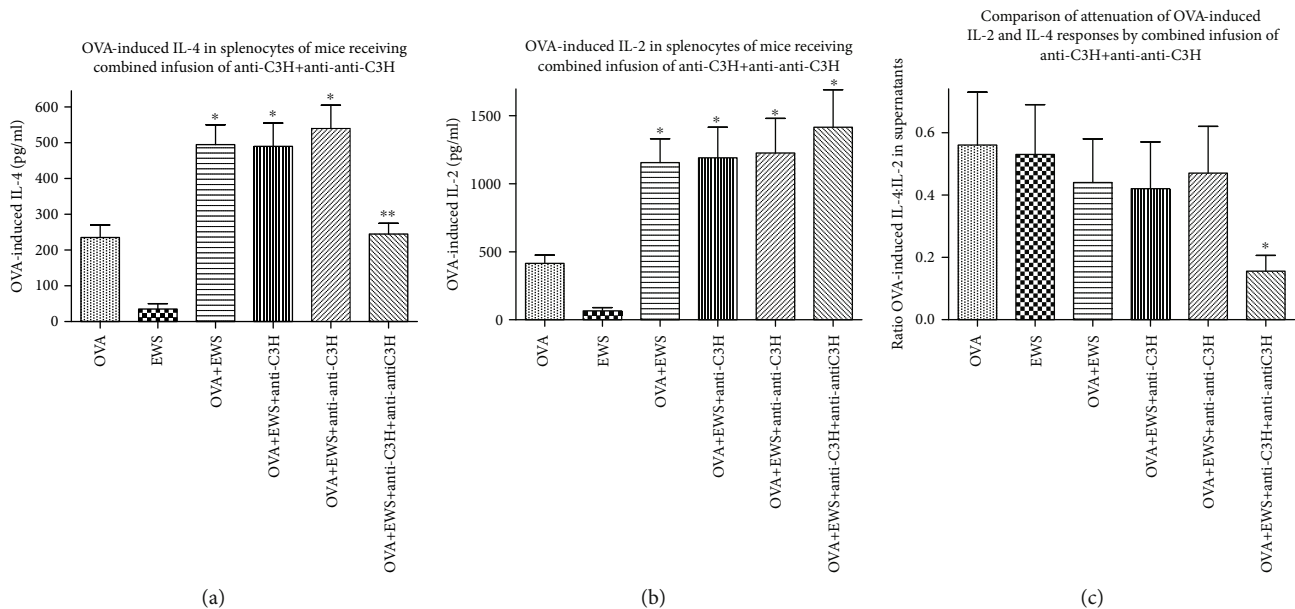


FIGURE 2: OVA-induced IL-4 production ((a) mean \pm SD) or IL-2 production (b) at 72 hr in OVA-stimulated splenocytes from mice of Figure 1. Data in (c) show changes in the induced IL-4:IL-2 ratios in supernatants harvested from OVA-stimulated cells of the different groups. $*p < 0.05$ compared with OVA only; $**p < 0.05$ compared with OVA+EWS.

OVA immunization) produced little OVA-specific Ig. Treatment of mice with the combined Ig preparations, but not either Ig preparation alone, led to the attenuation of the IgE response (Figure 1(a)), but not the IgG response (Figure 1(b)). The effect produced by the combined Ig preparations is emphasized by comparison of the OVA-specific IgE:IgG ratios in all groups (Figure 1(c))—attenuation occurred only in the group receiving combined Ig treatment.

OVA-induced IL-4 and IL-2 production looked like the IgE/IgG levels in all groups. Treatment with the combined Ig preparations led to the attenuation of IL-4 levels after OVA stimulation (Figure 2(a)), but not IL-2 levels (Figure 2(b)), an effect emphasized by assessment of IL-4:IL-2 ratios in these groups (Figure 2(c)).

We had predicted that in vertebrates with a shared ancestral immune system, even heterologous Igs (immune+anti-

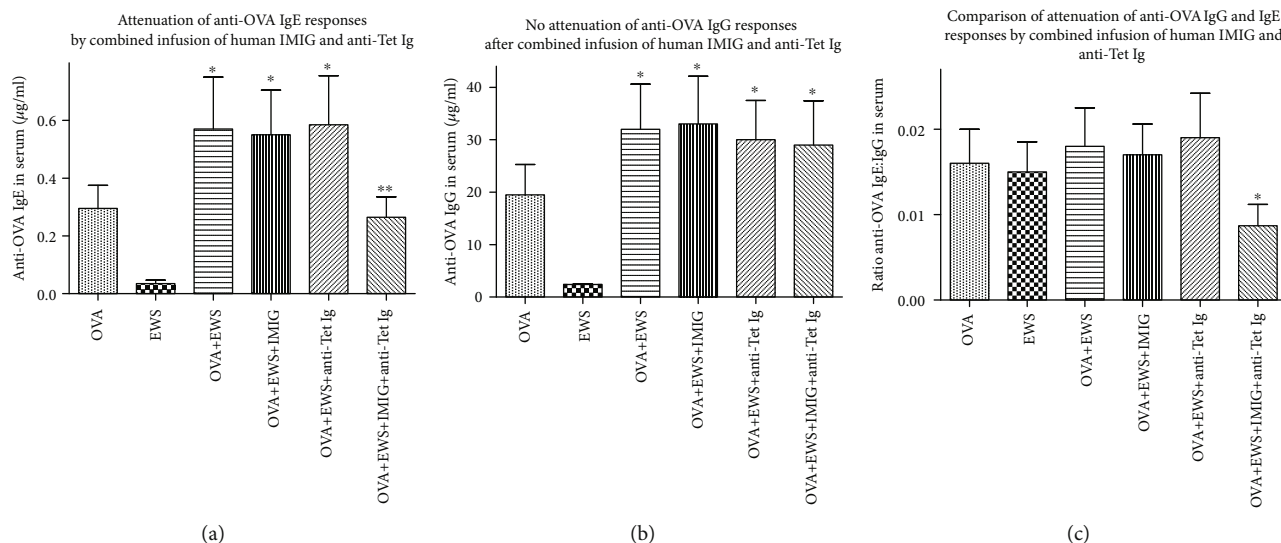


FIGURE 3: As for Figure 1, except that in this case all mice received heterologous Ig treatments (human-derived IMiG and/or pooled human immune anti-Tet Ig) not homologous immune or anti-idiotype Igs. * $p < 0.05$ compared with OVA only mice; ** $p < 0.05$ compared with the OVA+EWS group.

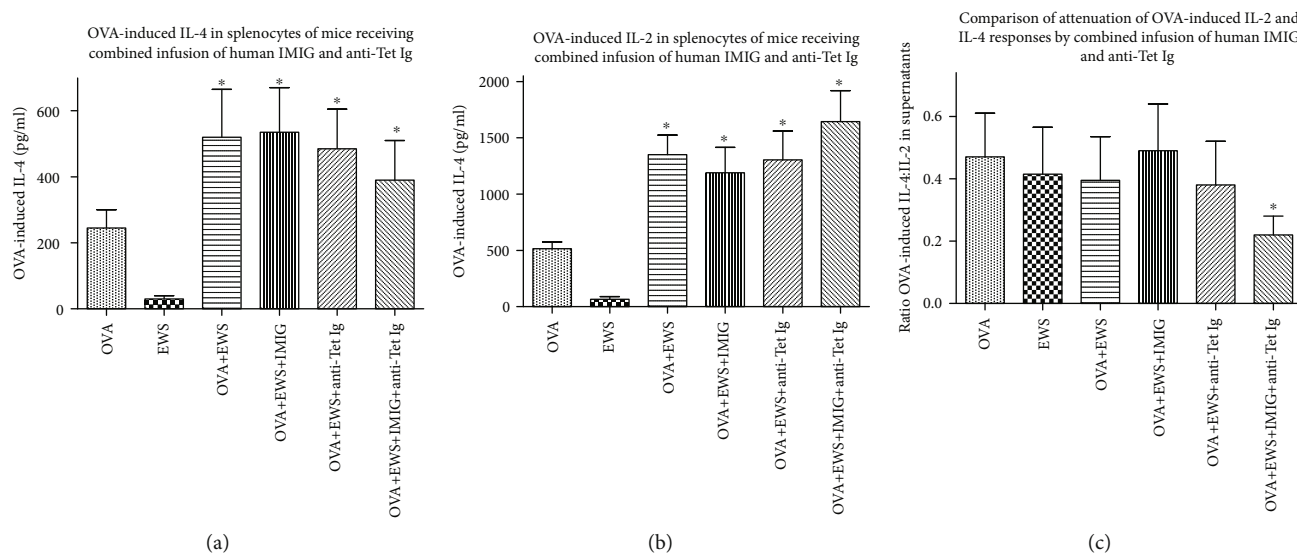


FIGURE 4: Attenuation of OVA-induced IL-4 production (a) but not IL-2 production (b) at 72 hr in OVA-stimulated splenocytes from mice in Figure 3. Data in (c) show changes in the calculated induced IL-4:IL-2 ratios in supernatants harvested from OVA-stimulated cells of the different groups. All data show mean \pm SD of triplicate cultures using splenocytes harvested from 8 mice/group.

idiotype) might produce the same effects as mixtures of homologous Igs [19, 21, 22]. Accordingly, OVA-immunized mice were treated with polyclonal immune human Ig (anti-Tet Ig) and/or polyclonal human anti-idiotype Ig (using IViG as a source of this [22, 23]—since delivery was intramuscular, this is henceforth referred to as IMiG). Data in Figures 3 and 4 are pooled from 2 such studies.

Comparison of Figures 1–4 shows that the effects seen using homologous (mouse) combinations of immune Ig and anti-idiotype Ig were recapitulated using heterologous (human) reagents as the antibody source.

3.2. Effect of Combinations of Immune Ig and Anti-idiotype Ig on Peanut Butter-Induced Sensitization in Beagle Dogs. Groups of 5/group 8 kg Beagle dogs receiving topical exposure to peanut butter were given 5 weekly injections of dog immunoglobulins (pooled IMiG and antirabies immune Ig) or human immunoglobulins (pooled IMiG or anti-Tet immune Ig) as described in Materials and Methods. After one final oral challenge with peanut butter, serum and PBMCs were harvested and total dog serum IgE and IgG levels were determined by ELISA (Figure 5)—for technical reasons, we were unable to detect the presence of peanut

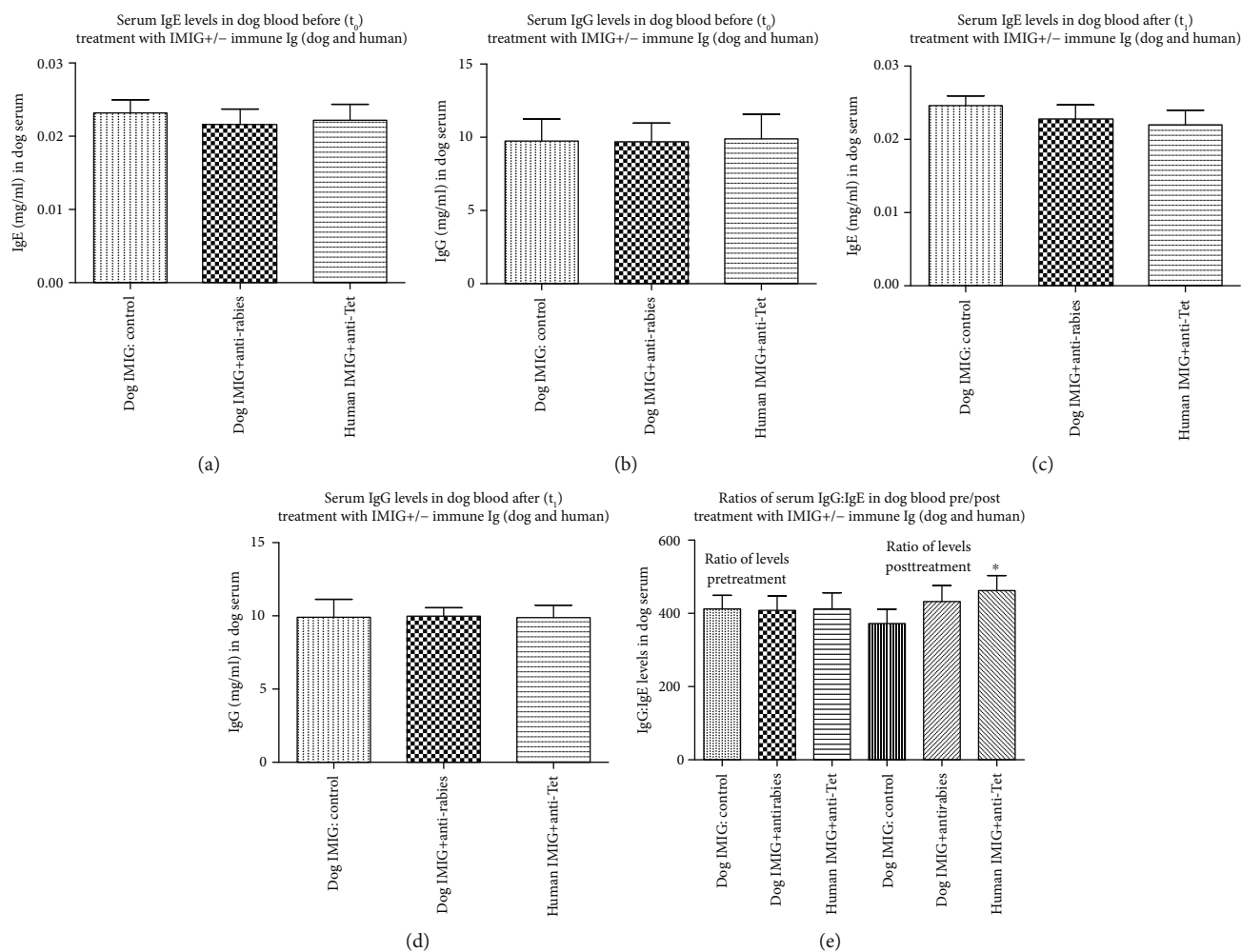


FIGURE 5: Serum IgE and IgG (mean \pm SD) in dogs exposed to be peanut butter and treated with dog IMIG/dog immune Ig, or human IMIG/human immune Ig. Controls received only dog IMIG injection. Levels are shown at pretreatment (a, b) and posttreatment (c, d). (e) The ratio of IgG : IgE in all groups. * $p < 0.05$ compared with posttreatment IMIG controls.

butter specific dog IgE or IgG. In addition, we measured ConA-induced IL-2 and IL-4 levels assayed from PBMC cultures of both pre- and posttreatment dog samples stimulated (see Materials and Methods) with 5 μ g/ml ConA (Figure 6). Peanut butter-induced IL-2, IL-4, and IL-31 levels were measurable only on posttreatment dog samples, using PBMCs stimulated with 2 mg/ml (estimated) DMSO peanut butter extract.

In Figure 7, no IL-2/IL-4/IL-31 production was seen in these samples after culture with DMSO vehicle alone.

Firstly, there were no significant differences in overall IgE or IgG levels in any groups before/after treatment (Figures 5(a)–5(d)). There was a trend to an increased IgG to IgE ratio after peanut butter sensitization in dogs treated with the combined dog or human Igs, which reached significance for the group treated with human Igs (Figure 5(e)), implying a relative decrease in IgE levels (to IgG) in this group. We suspect purely for technical reasons we were unable to detect any dog-specific IgE or IgG levels in any groups after sensitization. A generalized decrease in allergic reactivity in the groups treated with combined Ig infusions was suggested by analysis of IL-2 and IL-4 release in

response to ConA in various groups. While there was no significant difference in IL-2 production in the various groups before or after treatment, with a generalized trend to increased IL-2 production in all groups after prolonged peanut butter exposure (Figure 6(b) vs. Figure 6(a)), there was a trend to decreased IL-4 production after treatment with combined dog or human Igs (Figure 6(d)), which again reached significance for the group treated with human Ig. Comparison of IL-2:IL-4 ratios in all groups before/after treatment (Figure 6(e)) confirmed a relative decrease in IL-4 production in sensitized groups treated with either dog or human Igs. Finally, analysis of allergen-induced IL-2, IL-4, and IL-31 production in sensitized dogs showed significant differences only in IL-4/IL-31 production (not IL-2 levels) in dogs treated with dog or human Igs (Figure 7(a)), which again translated to a highly significant increase in IL-2:IL-4 and IL-2:IL-31 ratios in the same groups (Figure 7(b)).

4. Discussion

Exploration of novel therapies for treatment of allergic diseases has highlighted measures which decrease IgE levels

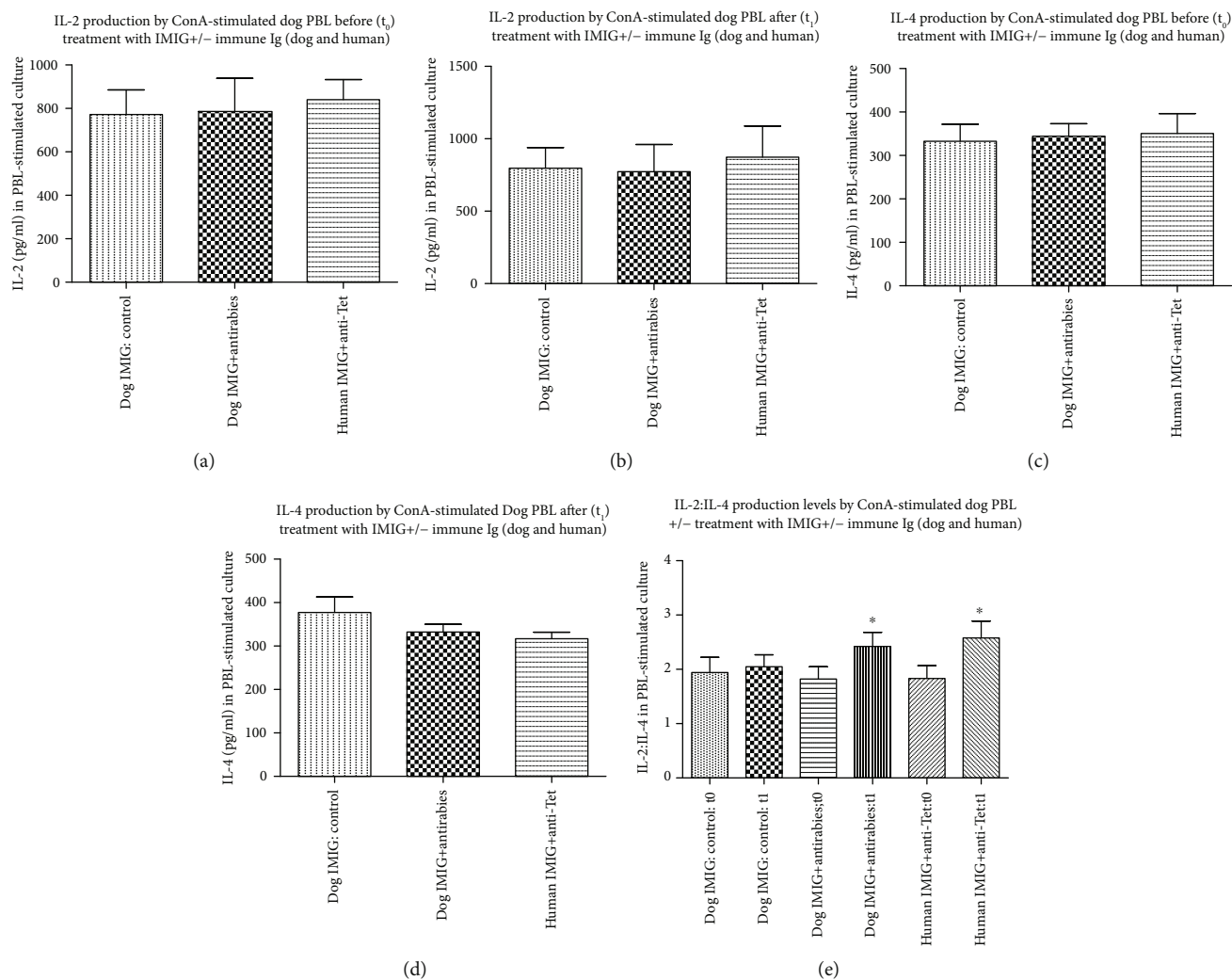


FIGURE 6: Levels of ConA-induced IL-2 and IL-4 (mean \pm SD) in 72 hr cultures of PBMCs from groups dogs from Figure 5. PBMCs were cultured at pretreatment (a, c) and posttreatment (b, d). (e) The ratio of IL-2:IL-4 in all groups. * $p < 0.05$ compared with equivalent IMiG controls.

and target cytokines (e.g., IL-4, IL-5, and IL-31) thought to be implicated in control of those levels and other cell populations (eosinophils/basophils) implicated in allergic disease [18, 24–30]. We reported on the use of a novel therapy aimed at manipulating self-reactive immune regulatory networks through deliberate perturbation of idiotype:anti-idiotype interactions, as a potential mechanism to attenuate several pathological immune reactions in rodents, including allergic sensitization to ovalbumin [19]. To date, no investigations of the effects of these treatments in larger animals or humans have been performed.

We hypothesized that attenuation of mouse allergic responses to ovalbumin following repeated injection with immune Ig and anti-anti-self Ig (Figures 1 and 2) was best understood in terms of an effect mediated by a resetting of both B cell and T regulatory (Treg) cell immune networks in mice receiving combined immune Ig and anti-idiotype Ig [19, 22]. We have shown furthermore that in rodents, the mechanism(s) implicated in the attenuation of allergic

responses after such treatment critically involves augmentation of Treg activity induced by combinations of immune Ig and anti-idiotype Ig [22, 31]. We had predicted that in vertebrates with a shared ancestral immune system, even heterologous Igs (immune+anti-idiotype) would produce the same effects [21, 22]. Testing this hypothesis initially in a mouse model using BALB/c mice sensitized with ovalbumin showed that attenuation of allergic responses was seen in mice receiving commercial immune Ig and anti-idiotype Ig of human origin, see Figures 3 and 4. These important observations justified a pilot preclinical trial of this same therapy in a dog model (Beagles) of atopic dermatitis, the most common allergic skin disease in dogs [5–10].

Dogs sensitized to peanut butter [7] showed evidence for a generalized relative decrease in serum IgE:IgG levels following combined treatment with the two Ig preparations, along with a similar attenuation of the IL-4:IL-2 ratio from ConA-stimulated PBMCs (Figures 5 and 6). More dramatically, allergen-induced IL-4 and IL-31 production

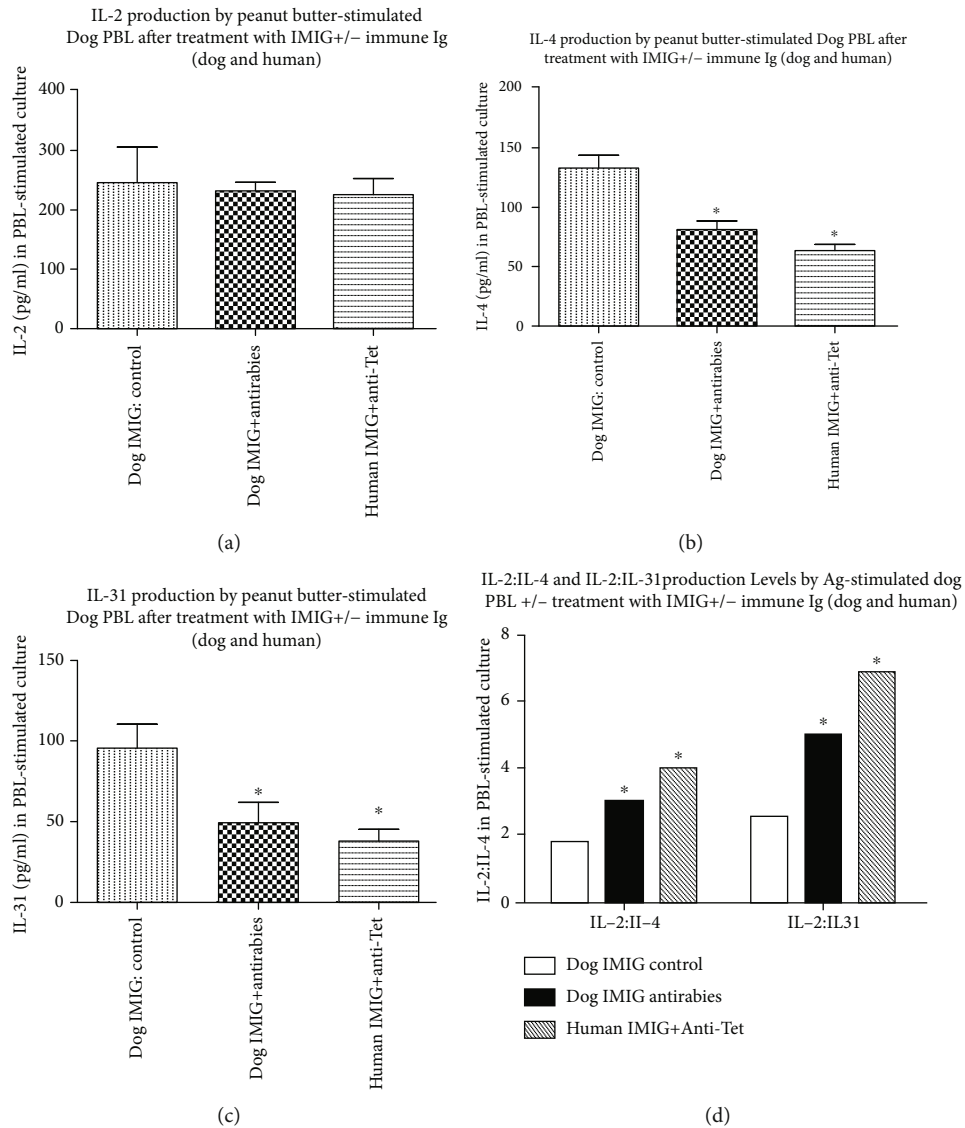


FIGURE 7: Peanut butter-induced IL-2, IL-4, and IL-31 (a-c) in stimulated PBMCs from Figures 5 and 6. No IL-2/IL-4/IL-31 production was detected from stimulated PBMCs from dogs pretreated with peanut butter or from posttreatment PBMCs stimulated with DMSO vehicle only (not shown). (d) The ratio of IL-2:IL-4 and IL-2:IL-31, respectively, in all groups. * $p < 0.05$ compared with equivalent IMIG controls.

and IL-4:IL-2 and IL-31:IL-2 levels were decreased in treated animals (Figure 7). The attenuation of IL-31 production following this treatment is particularly interesting given the evidence that IL-31 is a key cytokine implicated in itching in allergic dogs and that mAb directed to IL-31 has been licenced for use in the treatment of allergic dermatitis [18], while vaccination against IL-31 has also been proposed as a novel therapy in such animals [30]. Somewhat surprisingly, the effects we saw on the attenuation of IL-4/IL-31 production were most pronounced using combinations of human immune Ig and anti-idiotypic Ig (commercial anti-Tet and IMIG) rather than combinations of dog reagents (antirabies IgG and pooled IMIG). We suspect this may simply reflect an unexplored dose-response effect, which is already under investigation. It is important to note that we were unable to detect any

allergen-specific IgE or IgG in peanut butter-sensitized dogs, although this failure is hypothesized to be more technical than real, particularly given evidence for allergen-induced IL-2 and IL-4 in the same animals (Figure 7). We are in the process of assessing responses in dogs treated with a purified allergen (dust mite) to clarify this issue further. Our data are consistent with the notion that the attenuation of allergen-induced IL-4/IL-31 responses by the therapy used is instrumental in the effects seen, as suggested elsewhere [18, 19, 26, 28, 30].

In summary, we have extended our previous studies which reported on a novel therapy which could attenuate allergic immunity in rodents, to show that the same approach is efficacious in suppressing such immunity in large animals (dogs), a result which has important implications for the veterinary community.

Data Availability

Data and materials (where available) included in this study will be made freely available.

Ethical Approval

All mouse and dog studies were performed after approval by a local animal care committee, as documented in Materials and Methods.

Conflicts of Interest

G Hoffmann and RM Gorczynski declare purchase of shares in NI Inc. G Hoffmann is a member of the Research Advisory Board of NI Inc. T Maqbool has no competing interests. None of the authors is a paid employee of NI Inc., and no one received any remuneration for work performed in this study.

Authors' Contributions

RMG designed and carried out thesis experiment and drafted the initial and final version of the manuscript. GWH assisted in experimental design and data analysis. TM assisted in all studies in mice and data collection/analysis. All authors have read the manuscript, are fully conversant with the data below, and agree to publication in its present form.

Acknowledgments

The authors and NI acknowledge the additional technical assistance of Moyo Williams and Asmahan Haddad at Cedarlane Labs for the ELISA studies reported and Christopher Gorczynski (ACCESSIFLY) for the data analysis, the management at Cedarlane (Eddie Johnson and John Course) for their support throughout the pursuit of this research, and the assistance of CARE (Fort Collins, Colorado) for performing all of the dog studies described. All research costs, supplies, reagents, animals, and laboratory overheads were financed by Network Immunology Inc. (NI Inc., BC, Canada).

References

- [1] L. M. Wheatley and A. Togias, "Clinical practice. Allergic rhinitis," *The New England Journal of Medicine*, vol. 372, no. 5, pp. 456–463, 2015.
- [2] S. F. Thomsen, "Atopic dermatitis: natural history, diagnosis, and treatment," *ISRN Allergy*, vol. 2014, Article ID 354250, 7 pages, 2014.
- [3] C. Anandan, U. Nurmatov, O. C. van Schayck, and A. Sheikh, "Is the prevalence of asthma declining? Systematic review of epidemiological studies," *Allergy*, vol. 65, no. 2, pp. 152–167, 2010.
- [4] G. W. Canonica, J. Bousquet, T. Casale et al., "Sub-lingual immunotherapy: World Allergy Organization position paper 2009," *Allergy*, vol. 64, pp. 1–59.
- [5] E. Jensen-Jarolim, I. Pali-Schöll, and F. Roth-Walter, "Outstanding animal studies in allergy I. From asthma to food allergy and anaphylaxis," *Current Opinion in Allergy and Clinical Immunology*, vol. 17, no. 3, pp. 169–179, 2017.
- [6] E. Jensen-Jarolim, L. Einhorn, I. Herrmann, J. G. Thalhammer, and L. Panakova, "Pollen allergies in humans and their dogs, cats and horses: differences and similarities," *Clinical and Translational Allergy*, vol. 5, no. 1, article 15, 2015.
- [7] R. Marsella, "Experimental model for peanut allergy by epicutaneous sensitization in atopic beagle dogs," *Experimental Dermatology*, vol. 24, no. 9, pp. 711–712, 2015.
- [8] E. Maina, M. Pelst, M. Hesta, and E. Cox, "Food-specific sublingual immunotherapy is well tolerated and safe in healthy dogs: a blind, randomized, placebo-controlled study," *BMC Veterinary Research*, vol. 13, article 25, 2017.
- [9] R. S. Mueller, T. Olivry, and P. Prelaud, "Critically appraised topic on adverse food reactions of companion animals (2): common food allergen sources in dogs and cats," *BMC Veterinary Research*, vol. 12, no. 1, article 9, 2016.
- [10] T. Olivry and R. S. Mueller, "Critically appraised topic on adverse food reactions of companion animals (3): prevalence of cutaneous adverse food reactions in dogs and cats," *BMC Veterinary Research*, vol. 13, article 51, 2017.
- [11] I. Furdos, J. Fazekas, J. Singer, and E. Jensen-Jarolim, "Translating clinical trials from human to veterinary oncology and back," *Journal of Translational Medicine*, vol. 13, no. 1, article 265, 2015.
- [12] A. P. Jackson, A. P. Foster, B. J. Hart, C. R. Helps, and S. E. Shaw, "Prevalence of house dust mites and dermatophagoides group 1 antigens collected from bedding, skin and hair coat of dogs in south-west England," *Veterinary Dermatology*, vol. 16, no. 1, pp. 32–38, 2005.
- [13] T. M. Lian and R. E. Halliwell, "Allergen-specific IgE and IgGd antibodies in atopic and normal dogs," *Veterinary Immunology and Immunopathology*, vol. 66, no. 3-4, pp. 203–223, 1998.
- [14] R. Marsella and M. N. Saridomichelakis, "Environmental and oral challenge with storage mites in beagles experimentally sensitized to *Dermatophagoides farinae*," *Veterinary Dermatology*, vol. 21, no. 1, pp. 105–111, 2010.
- [15] R. S. Mueller, S. V. Bettenay, and L. Tideman, "Aeroallergens in canine atopic dermatitis in southeastern Australia based on 1000 intradermal skin tests," *Australian Veterinary Journal*, vol. 78, no. 6, pp. 392–399, 2000.
- [16] E. L. Willis, G. A. Kunkle, R. E. Esch, T. J. Grier, and P. S. Kubilis, "Intradermal reactivity to various insect and arachnid allergens among dogs from the southeastern United States," *Journal of the American Veterinary Medical Association*, vol. 209, no. 8, pp. 1431–1434, 1996.
- [17] P. B. Hill and D. J. DeBoer, "The ACVD task force on canine atopic dermatitis (IV): environmental allergens," *Veterinary Immunology and Immunopathology*, vol. 81, no. 3-4, pp. 169–186, 2001.
- [18] M. Furue, K. Yamamura, M. Kido-Nakahara, T. Nakahara, and Y. Fukui, "Emerging role of interleukin-31 and interleukin-31 receptor in pruritus in atopic dermatitis," *Allergy*, vol. 73, no. 1, pp. 29–36, 2018.
- [19] R. M. Gorczynski and G. W. Hoffmann, "Toward a new kind of vaccine: a logical extension of the symmetrical immune network theory," *Interactive Journal of Medical Research*, vol. 6, no. 2, article e8, 2017.
- [20] T. H. Schreiber, D. Wolf, M. S. Tsai et al., "Therapeutic Treg expansion in mice by TNFRSF25 prevents allergic lung inflammation," *The Journal of Clinical Investigation*, vol. 120, no. 10, pp. 3629–3640, 2010.

- [21] G. W. Hoffmann, *Immune Network Theory*, 2008, <https://www.physics.ubc.ca/~hoffmann/ni.html>.
- [22] R. M. Gorczynski, T. Maqbool, and G. Hoffmann, "Mechanism(s) of prolonged attenuation of allergic responses after modulation of idiotypic regulatory network," *Allergy, Asthma & Clinical Immunology*, vol. 15, article 79, 2019.
- [23] D. Mimouni, M. Blank, and A. S. Payne, "Efficacy of intravenous immunoglobulin (IVIG) affinity-purified anti-desmoglein anti-idiotypic antibodies in the treatment of an experimental model of pemphigus vulgaris," *Clinical & Experimental Immunology*, vol. 162, no. 3, pp. 543–549, 2010.
- [24] N. Patel and L. C. Strowd, "The future of atopic dermatitis treatment," *Advances in Experimental Medicine and Biology*, vol. 1027, pp. 185–210, 2017.
- [25] S. F. Weinstein, R. Katial, S. Jayawardena et al., "Efficacy and safety of dupilumab in perennial allergic rhinitis and comorbid asthma," *The Journal of Allergy and Clinical Immunology*, vol. 142, no. 1, pp. 171–177.e1, 2018.
- [26] I. H. Iftikhar, M. Schimmel, W. Bender, C. Swenson, and D. Amrol, "Comparative efficacy of anti IL-4, IL-5 and IL-13 drugs for treatment of eosinophilic asthma: a network meta-analysis," *Lung*, vol. 196, no. 5, pp. 517–530, 2018.
- [27] K. Ohta, H. Nagase, M. Suzukawa, and S. Ohta, "Antibody therapy for the management of severe asthma with eosinophilic inflammation," *International Immunology*, vol. 29, no. 7, pp. 337–343, 2017.
- [28] H. Nakajima-Adachi, K. Shibahara, Y. Fujimura et al., "Critical role of intestinal interleukin-4 modulating regulatory T cells for desensitization, tolerance, and inflammation of food allergy," *PLoS One*, vol. 12, no. 2, article e0172795, 2017.
- [29] F. Tabatabaian, D. K. Ledford, and T. B. Casale, "Biologic and new therapies in asthma," *Immunology and Allergy Clinics of North America*, vol. 37, no. 2, pp. 329–343, 2017.
- [30] M. F. Bachmann, A. Zeltins, G. Kalnins et al., "Vaccination against IL-31 for the treatment of atopic dermatitis in dogs," *The Journal of Allergy and Clinical Immunology*, vol. 142, no. 1, pp. 279–281.e1, 2017.
- [31] R. M. Gorczynski and G. W. Hoffmann, "A novel mechanism for induction of Tregs to control allergic disease," *Internal Medicine Review*, vol. 5, no. 8, 2019.

Research Article

Triggered Immune Response Induced by Antigenic Epitopes Covalently Linked with Immunoadjuvant-Pulsed Dendritic Cells as a Promising Cancer Vaccine

Chumeng Chen,¹ Mohanad Aldarouish ,^{2,3,4} Qilong Li,^{2,3} Xiangzhen Liu,^{2,3} Feng Han,⁴ Hui Liu,⁴ and Qijun Qian ^{1,2,3,4}

¹Xinyuan Institute of Medicine and Biotechnology, College of Life Sciences and Medicine, Zhejiang Sci-Tech University, Hangzhou 310018, China

²Shanghai Cell Therapy Research Institute, Shanghai 201805, China

³Shanghai Research and Development Center, Shanghai Cell Therapy Group, Shanghai 201805, China

⁴Immune Cell Division, Shanghai Cell Therapy Group, Shanghai 201805, China

Correspondence should be addressed to Mohanad Aldarouish; imm_moh@yahoo.com and Qijun Qian; qian@shcell.org

Received 21 December 2019; Revised 3 March 2020; Accepted 11 March 2020; Published 4 April 2020

Academic Editor: Pedro A. Reche

Copyright © 2020 Chumeng Chen et al. This is an open access article distributed under the Creative Commons Attribution License, which permits unrestricted use, distribution, and reproduction in any medium, provided the original work is properly cited.

The success of peptide-based dendritic cell (DC) cancer vaccines mainly depends on the utilized peptides and selection of an appropriate adjuvant. Herein, we aimed to evoke a broad immune response against multiple epitopes concurrently in the presence of immunoadjuvant. Three synthetic HLA-A*0201-restricted peptides were separately linked with HMGB1-derived peptide (SAFFLFCSE, denoted as HB₁₀₀₋₁₀₈) as immunoadjuvant via double arginine (RR) linker and loaded onto human monocyte-derived DCs. Peptide uptake was detected by immunofluorescence microscopy and flow cytometry. The maturation and activation status of pulsed DCs were monitored by detection of the expression of specific markers and released cytokines. The ability of peptide-pulsed DCs to activate allogeneic T cells has been assessed by a degranulation assay and detection of secreted cytokines. The lytic activity of effector T cells against cancer cells in vitro was analyzed by a lactate dehydrogenase (LDH) assay. Results revealed that DCs efficiently take up peptides+HB₁₀₀₋₁₀₈ and expressed higher levels of surface markers (HLA-ABC, HLA-DR, CD80, CD86, CD83, CD40, and CCR7) and proinflammatory cytokines (IL-6, IFN- γ , TNF- α , and IL-12) than control DCs, free peptide-pulsed DCs, and free HB₁₀₀₋₁₀₈-pulsed DC groups. Moreover, peptides+HB₁₀₀₋₁₀₈/pulsed DCs were capable of activating allogeneic T cells and enhance their lytic activity against a pancreatic cancer cell line (PANC-1) in vitro. These findings suggest that antigenic peptides covalently linked with HB₁₀₀₋₁₀₈/pulsed DCs could be a promising strategy to improve the current DC-based cancer vaccines.

1. Introduction

The unique characteristics of dendritic cells (DCs) as the most potent antigen-presenting cells (APCs) lead them to be considered as a promising tool for cancer immunotherapy [1]. In the last few years, there has been a growing interest in peptide-, RNA-, and DNA-based DC vaccines as an effective approach for cancer immunotherapy due to its promising results in achieving significance and durable treatment responses with mild adverse events [2, 3]. Peptide-based vaccines provide several advantages in comparison to other

types of cancer vaccines. They are easily synthesized, stable in many storage conditions, and safe, and they could enhance an effective CD4 and CD8 immune response. However, the success of the peptide-based vaccine strategy mainly depends on the utilized peptides and selection of an appropriate adjuvant [4].

High mobility group box 1 (HMGB1) is highly conserved protein in mammals that translocates to the nucleus to regulate the gene expression and released during cell injury and inflammation [5]. HMGB1 is composed of two DNA-binding motifs, box A and box B, in addition to C tail

[6]. It has been found that HP91, a short peptide corresponding to amino acids 91–108 in the B box, has the ability to enhance the maturation and activation of DCs, induce the secretion of proinflammatory cytokines such as IL-6 and IL-12, and trigger the polarization of Th1 cells [7–9]. Saenz and his group demonstrated that HP91 could function as adjuvant *in vivo* through potentiating cellular and humoral immune responses [10]. Further studies showed that the region of HP91 which is responsible for its immunostimulatory function is located in the C-terminal, a peptide corresponding to amino acids 100–108 of HMGB1 [10, 11]. In this study, we denoted this short peptide as HB₁₀₀₋₁₀₈.

It is well known that no single antigenic peptide might be adequate to achieve an efficient antitumor immune response. Thus, multiple epitopes are required to elicit a broad immune response [12]. Consequently, combining multiple tumor-associated antigens (TAA) could be a preferable strategy to elicit strong antitumor immunity.

A large number of studies confirmed that the following tumor-associated antigens, survivin, human epidermal growth factor receptor 2 (Her2), and carcinoembryonic antigen (CEA), are overexpressed in a variety of tumors, by which survivin is overexpressed in the lung, breast, pancreatic, and melanoma [13–16]; Her2 is overexpressed in the breast, stomach, ovary, uterine serous endometrial carcinoma, colon, pancreatic, bladder, lung, uterine cervix, head and neck, and esophagus cancer [17, 18]; and CEA is overexpressed in gastric, colorectal, breast, ovarian, lung, and pancreatic cancer [19].

In this study, human monocyte-derived DCs (moDCs) were pulsed with three antigenic peptides, survivin, Her2, and CEA, which are covalently linked with HB₁₀₀₋₁₀₈ via protease-sensitive linker (double arginine (RR)). Results revealed that peptides covalently linked with HB₁₀₀₋₁₀₈ (denoted as peptides+HB₁₀₀₋₁₀₈) were efficiently taken up by immature DCs and significantly induced their maturation and activation compared with free peptides without HB₁₀₀₋₁₀₈ (denoted as peptides-HB₁₀₀₋₁₀₈). Moreover, peptides+HB₁₀₀₋₁₀₈/pulsed DCs greatly induced the activation and lytic activity of allogeneic T cells by which they exhibited a potent cytotoxicity against tumor cells *in vitro*.

2. Materials and Methods

2.1. DC Generation. Monocyte-derived DCs were generated from peripheral blood monocyte (PBMC) by standard Ficoll density centrifugation (GE Healthcare, Uppsala, Sweden) to isolate PBMCs from patient leukapheresis samples. PBMCs were plated in serum-free AIM-V media (Life Technologies, Grand Island, NY) and allowed to adhere to 0.22 μ m filter-capped culture flasks (TPP, Germany). After 2 hours, the nonadherent cells were removed, and adherent monocytes were subsequently cultured for 6 days in AIM-V containing 50 ng/ml rhIL-4 (R&D Systems, Minneapolis, MN) and 100 ng/ml rhGM-CSF (Sanofi, Bridgewater, NJ). On day 3, half of the medium was replaced with fresh medium containing GM-CSF and IL-4. In some experiments, a maturation cocktail containing 100 IU/ml IFN- γ , 30 μ g/ml poly(I:C), and 5 μ g/ml R848 was used to mature the generated DCs.

2.2. Synthetic Peptides. The following synthetic HLA-A*0201-restricted peptides, survivin (LTLGEFLKL), Her2 (RLQETELV), CEA (YLSGANLNL), and HB₁₀₀₋₁₀₈ (SAFFLFCSE), were synthesized with purity greater than 95%. Following their synthesis, the first three peptides were linked with HB₁₀₀₋₁₀₈ via a protease-sensitive linker (double arginine (RR) residue sequence). It is expected that once DCs internalize a peptide-RR-HB₁₀₀₋₁₀₈ construct, the intracellular proteases would cleave at the RR site and separate peptide from HB₁₀₀₋₁₀₈ and thus could enhance the processing and presentation of engulfed peptides [20]. Peptides were purchased from Shanghai Top-peptide Bio Co., Ltd. (Shanghai, China). To examine their phagocytosis by DCs, peptides \pm HB₁₀₀₋₁₀₈ were labeled with FITC fluorochrome at their N-terminus. All peptides were dissolved in PBS.

2.3. Peptide Uptake Assay. Immature moDCs, generated as described above, were seeded in a 24-well plate and pulsed separately with synthetic peptides \pm HB₁₀₀₋₁₀₈-coupled FITC (40 μ g/ml for each peptide) for 1 hour at 37°C, 5% CO₂. After a triple wash with PBS, cells were examined by fluorescent microscopy and the uptake was quantified by FACS analysis. To quench the extracellular FITC signal, 50 μ g/ml of trypan blue was added to the cell suspension prior to flow cytometry analysis. Unpulsed DCs were used as the negative control. Cells that were found positive for FITC were considered as cells that had successfully engulfed peptides.

2.4. Flow Cytometry. The purity of generated DCs was assessed as CD14⁺CD11C⁺ by staining 1×10^6 cells with anti-CD11C-APC and anti-CD14-FITC (BD Biosciences, San Diego, CA, USA).

Immature moDCs were resuspended to 1×10^6 cells/ml and loaded with peptides \pm HB₁₀₀₋₁₀₈ (40 μ g/ml for each peptide) or 40 μ g/ml of free HB₁₀₀₋₁₀₈ at 37°C, 5% CO₂. After one hour, pulsed DCs were washed and cultured overnight. The following monoclonal antibodies (mAbs) were used to characterize the maturation and activation status of DCs: anti-HLA-ABC-PE, anti-HLA-DR-PE/Cy7, anti-CD80-PE, anti-CD86-APC, anti-CD83-APC, anti-CD40-Alexa Fluor 700, and anti-CCR7-PE/Cy7 (BioLegend, San Diego, CA, USA). Isotype-matched fluorescent antibodies were used as negative controls. Cells were incubated with antibodies at 4°C for 30 minutes. After washing, samples were detected by a FACSCalibur analyzer (BD Biosciences, San Jose, CA, USA). The data were analyzed by FlowJo software (TreeStar).

2.5. Enzyme-Linked Immunosorbent Assay (ELISA). Immature moDCs were resuspended to 1×10^6 cells/ml and loaded with peptides \pm HB₁₀₀₋₁₀₈ (40 μ g/ml for each peptide) or only 40 μ g/ml of free HB₁₀₀₋₁₀₈ at 37°C, 5% CO₂. After one hour, pulsed DCs were washed and cultured for 48 hours. The secreted IL-12 was detected by a IL-12 ELISA kit (Sino Biological, China) according to the manufacturer's protocol. The optical density (OD) of samples was assessed at 550 nm using a microtiter plate spectrophotometer (Beckman Coulter detection platform, USA).

2.6. Degranulation Assay and Cytokine Detection. Peptides \pm HB₁₀₀₋₁₀₈/pulsed DCs were cultured in the presence of a

maturation cocktail (100 IU/ml IFN- γ , 30 μ g/ml poly(I:C), and 5 μ g/ml R848) for 24 hours. Cells were washed extensively and seeded with responder allogeneic T cells at a DC : T cell ratio of 1 : 10 for 18 hours. Supernatants were collected at the end of culture, and cytokine production was detected using a cytometric bead array (CBA) kit (BD Biosciences), following the manufacturer's instructions.

For the CD107a degranulation assay, allogeneic T cells were stimulated with empty DCs or peptides \pm HB₁₀₀₋₁₀₈/pulsed DCs (at a DC : T cell ratio of 1 : 10) in the presence of GolgiStop (monensin, BD) and anti-CD107a-APC mAb (BD Pharmingen). After incubation for 12 hours at 37°C, cells were collected and stained with anti-CD8-PE mAb (BD Pharmingen) and analyzed by flow cytometry.

2.7. Cancer Cells. The human pancreatic cancer PANC-1 cell line (ATCC® CRL-1469™) was cultured in DMEM supplemented with 10% FBS and penicillin/streptomycin at 37°C in a humidified 5% CO₂ atmosphere.

2.8. Cytotoxicity Assays. Peptides \pm HB₁₀₀₋₁₀₈-pulsed DCs were matured in the presence of a maturation cocktail, followed by coculturing with allogeneic T cells at DC : T cell ratios of 1 : 10 for 24 hours. Then, T cells were collected as effector cells, and Panc-1 cells were used as the target cells. Effector cells included the negative control group (T cells without preculturing with DCs), empty DC group (T cells stimulated with nonpulsed DCs), peptides-HB₁₀₀₋₁₀₈ group (T cells stimulated with free peptides/pulsed DCs), and peptides+HB₁₀₀₋₁₀₈ group (T cells stimulated with peptides covalently linked with HB₁₀₀₋₁₀₈/pulsed DCs). Effector cells and target cells (PANC-1 cancer cell line) were incubated at ratios of 5 : 1 for 4 h at 37°C in 96-well plates. The activity of T cells against the target tumor cells was measured by an LDH cytotoxicity assay kit (Beyotime, China) following the manufacturer's instructions. The cytotoxicity of the T cells was calculated as a percentage of specific lysis using the following formula: %specific lysis = (effector/target release – spontaneous release)/(maximal release – spontaneous release) \times 100%. Data are presented as the means \pm standard deviation.

2.9. Statistical Analysis. Statistical analyses were carried out using GraphPad Prism 5.0 (GraphPad Software, San Diego, CA). The mean \pm SD was determined for each treatment group in the individual experiments. Differences among groups were analyzed using Student's *t*-test, and *P* < 0.05 was considered statistically significant.

3. Results

3.1. Immature moDCs Efficiently Take Up Peptides Covalently Linked with HB₁₀₀₋₁₀₈. In this study, three antigenic synthetic peptides (survivin, Her2, and CEA) were covalently linked with HB₁₀₀₋₁₀₈ (as immunoadjuvant) via double arginine (RR) residues as a protease-sensitive linker (Figure 1(a)). To detect whether the covalent linking of synthetic peptides with HB₁₀₀₋₁₀₈ via RR linker could accelerate their acquisition by DCs, cells were incubated with survivin \pm HB₁₀₀₋₁₀₈, Her2 \pm HB₁₀₀₋₁₀₈, or CEA \pm HB₁₀₀₋₁₀₈ in culture medium for

1 hour at 37°C. All peptides were conjugated with FITC. Flow cytometry results showed that DCs more efficiently take up peptides covalently linked with HB₁₀₀₋₁₀₈ than single free peptides (Figure 1(b)). The high efficiency of DCs to engulf peptides+HB₁₀₀₋₁₀₈ was also confirmed by immunofluorescence microscopy (Figure 1(c)). These findings indicate that HB₁₀₀₋₁₀₈ could play an important role in the acceleration of peptide phagocytosis by immature DCs.

3.2. Maturation and Activation of DCs Were Induced by Peptides Covalently Linked with HB₁₀₀₋₁₀₈. To determine the optimum concentration of peptides covalently linked with HB₁₀₀₋₁₀₈ that promote the highest level of DC maturation and activation, cells were loaded with different concentrations of peptides+HB₁₀₀₋₁₀₈ (0, 20, 40, and 60 μ g/ml for each peptide) for 1 hour. Then, cells were collected, washed, and cultured overnight followed by detection of surface markers by flow cytometry. Data revealed that peptides+HB₁₀₀₋₁₀₈ induced the expression levels of HLA-ABC, HLA-DR, CD80, CD83, CD40, and CCR7 in a dose-dependent manner without a significant difference between 40 and 60 μ g/ml (Supplementary Figure 1). Based on these findings, 40 μ g/ml of peptides+HB₁₀₀₋₁₀₈ was used as a preferable concentration in the next experiments.

To detect whether peptides+HB₁₀₀₋₁₀₈ could induce the maturation and activation of DCs, immature DCs were divided into four groups: group (1) cells left untreated; group (2) cells incubated with free peptides: survivin, Her2, and CEA; group (3) cells incubated with survivin+HB₁₀₀₋₁₀₈, Her2+HB₁₀₀₋₁₀₈, and CEA+HB₁₀₀₋₁₀₈; and group (4) cells incubated with free HB₁₀₀₋₁₀₈. After 1 hour, cells were collected, washed, and cultured overnight followed by detection of surface markers by flow cytometry. Results showed that peptides+HB₁₀₀₋₁₀₈/pulsed DCs exhibited remarkably increased expression of HLA-ABC, HLA-DR, CD80, CD86, CD83, CD40, and CCR7 compared to the other three groups. Importantly, free HB₁₀₀₋₁₀₈ failed to upregulate the expression of those markers on pulsed DCs (except HLA-DR and CD86) compared with the control and peptides-HB₁₀₀₋₁₀₈/pulsed DC groups (Figure 2). These data suggest that coupling of antigenic peptides with HB₁₀₀₋₁₀₈ could serve as an efficient strategy to enhance the maturation and activation of DCs.

3.3. Peptides Covalently Linked with HB₁₀₀₋₁₀₈/Pulsed DCs Secreted Abundant Levels of Proinflammatory Cytokines. To investigate the ability of peptides covalently linked with HB₁₀₀₋₁₀₈ to enhance the secretion of proinflammatory cytokines by DCs, cells were divided into four groups and treated as mentioned in the previous section. After 1 hour of incubation, cells were collected, washed, and cultured for 48 hours to detect IL-12 by ELISA and for 24 hours to detect other cytokines. Supernatants were collected, and the level of IL-12 was detected by a CBA kit using flow cytometry. Data revealed that peptides+HB₁₀₀₋₁₀₈/pulsed DCs secreted abundant levels of IL-6 (Figure 3(a)), IFN- γ (Figure 3(b)), TNF- α (Figure 3(c)), and IL-12 (Figure 3(d)) compared to the other three groups. Consistent with the results of surface markers, the levels of those cytokines were comparable between the

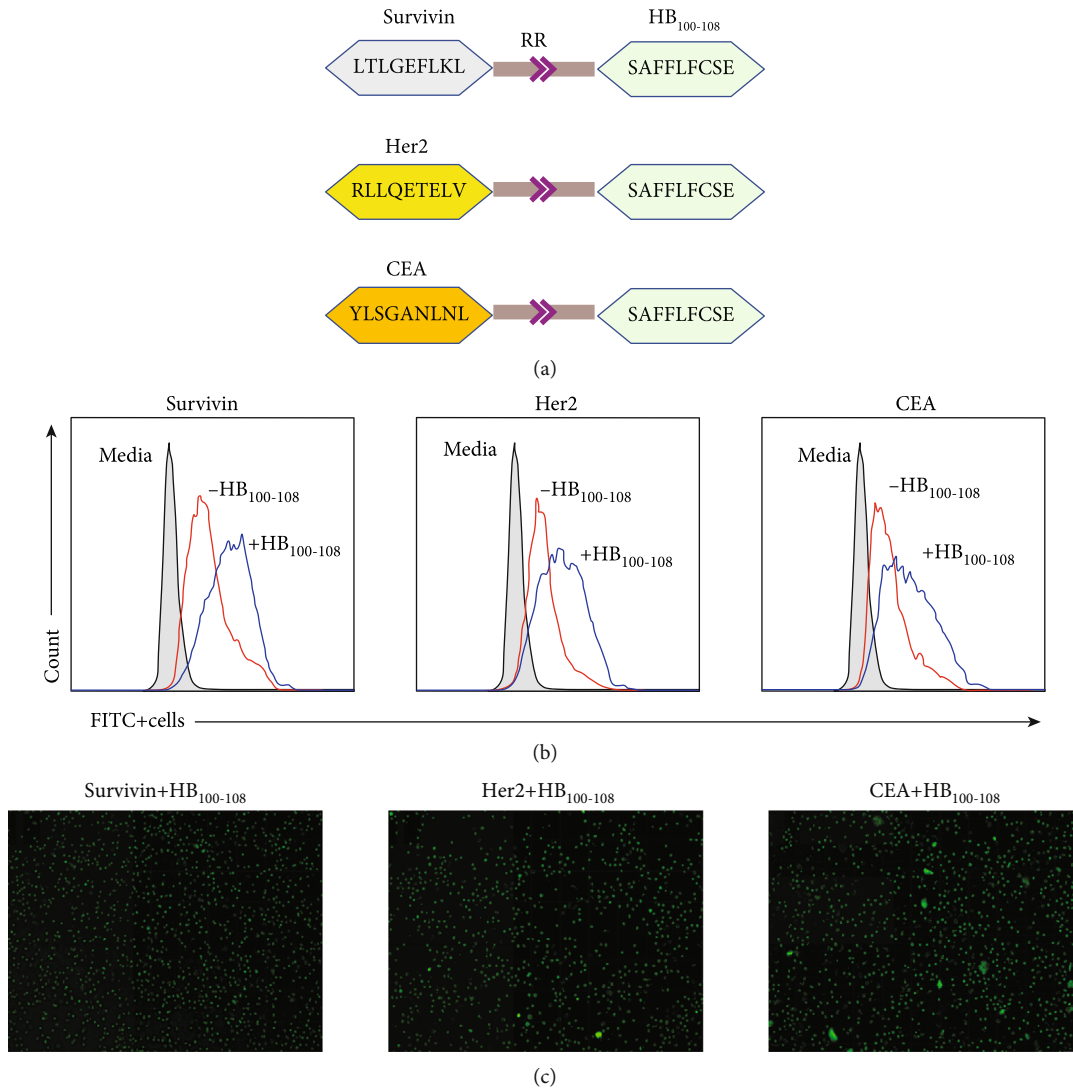


FIGURE 1: Immature DCs efficiently phagocytized antigenic peptides that are covalently linked with HB₁₀₀₋₁₀₈. (a) A schematic diagram illustrates the synthetic peptides used in this study. Three HLA-A*0201-restricted peptides (survivin, Her2, and CEA) were covalently linked with HB₁₀₀₋₁₀₈ via double arginine (RR) residues as a protease-sensitive linker. (b) Immature moDCs were pulsed with 40 $\mu\text{g}/\text{ml}$ of FITC fluorochrome-conjugated peptides \pm HB₁₀₀₋₁₀₈ for 1 hour at 37°C. After a triple wash with PBS, the uptake was quantified by FACS analysis. To quench the extracellular FITC signal, 50 $\mu\text{g}/\text{ml}$ of trypan blue was added to the cell suspension prior to flow cytometry analysis. Unpulsed DCs were used as the negative control. (c) Immunofluorescence microscopy images showing the uptake of FITC-peptides+HB₁₀₀₋₁₀₈ by immature moDCs.

control DCs, peptides-HB₁₀₀₋₁₀₈, and HB₁₀₀₋₁₀₈ groups. These results demonstrate that peptides+HB₁₀₀₋₁₀₈ have a considerable potential to promote DCs to secrete proinflammatory cytokines, by which they are important in skewing of T cell responses.

3.4. Peptides Linked with HB₁₀₀₋₁₀₈/Pulsed DCs Elicited Allogeneic T Cells to Produce Several Cytokines and Induced the Lytic Activity of CD8⁺ T Cells. To investigate the lytic activity of CD8⁺ T cells, allogeneic T cells were cocultured with empty DCs or peptides \pm HB₁₀₀₋₁₀₈/pulsed DCs for 12 hours in the presence of anti-CD107a-APC mAb; then, cells were stained with anti-CD8-PE mAb and analyzed by flow cytometry. As shown in Figure 4(a), only peptides+HB₁₀₀₋₁₀₈/pulsed DCs were able to induce a robust degranulation

of CD8⁺ T cells, as identified by the expression of surface marker CD107a, indicating that those T cells could secrete cytotoxic effector molecules upon encountering DC-loaded peptides+HB₁₀₀₋₁₀₈, whereas empty DCs and DC-loaded peptides-HB₁₀₀₋₁₀₈ failed to enhance the degranulation of CD8⁺ T cells.

To evaluate the effect of DC-loaded peptides on the cytokine secretion by T lymphocytes, allogeneic T cells were cultured alone as a negative control (group 1) or cocultured with empty DCs (group 2), peptides-HB₁₀₀₋₁₀₈/pulsed DCs (group 3), or peptides+HB₁₀₀₋₁₀₈/pulsed DCs (group 4) at DC : T cell ratios of 1 : 10. 18 hours later, secreted cytokines were detected in the supernatant by the CBA kit. Data showed that the levels of secreted IL-4, IL-6, TNF- α , and IFN- γ in group 4 (peptides+HB₁₀₀₋₁₀₈/pulsed DCs/T cells) were

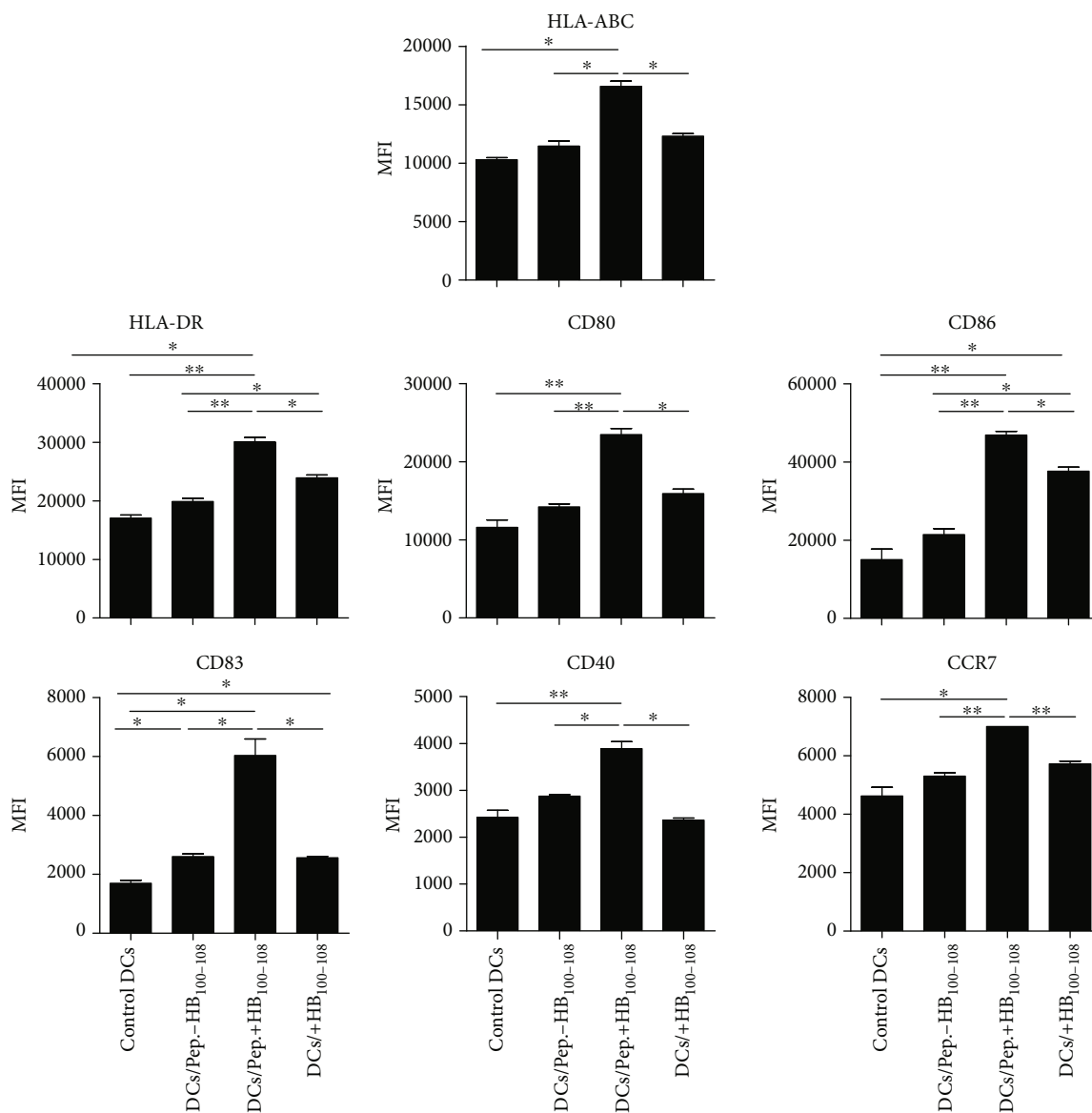


FIGURE 2: Peptides+HB₁₀₀₋₁₀₈ enhanced the maturation and activation of immature DCs. Immature moDCs were left untreated or pulsed with peptides±HB₁₀₀₋₁₀₈ or free HB₁₀₀₋₁₀₈ (each with 40 μg/ml) for 1 hour at 37°C. Then, cells were washed and cultured overnight. The expression of HLA-ABC, HLA-DR, CD80, CD86, CD83, CD40, and CCR7 was measured by flow cytometry. Results represent the mean ± SEM of three independent experiments.

significantly higher than those of the other three groups. Importantly, the levels of secreted IL-10 in group 4 were obviously lower than those in group 2 (empty DCs/T cells) and group 3 (peptides-HB₁₀₀₋₁₀₈/pulsed DCs/T cells) (Figure 4(b)). Collectively, these results suggest that peptides covalently linked with HB₁₀₀₋₁₀₈/pulsed DCs are potent to promote the lytic activity of T cells, as well as enhance the secretion of type 1 and type 2 cytokines and diminish the secretion of the inhibitory cytokine IL-10.

3.5. Peptides Linked with HB₁₀₀₋₁₀₈/Pulsed DCs Induced the Cytolytic Activity of T Cells against PANC-1 Cell Line In Vitro. It has been documented that pancreatic tumor cells expressed high levels of survivin, Her2, and CEA antigenic peptides [21]. To test whether the peptides±HB₁₀₀₋₁₀₈/pulsed

DCs could induce the cytolytic activity of T cells against tumor cells in vitro, allogeneic T cells were firstly cocultured with empty DCs (group 2), peptides-HB₁₀₀₋₁₀₈/pulsed DCs (group 3), or peptides+HB₁₀₀₋₁₀₈/pulsed DCs (group 4). Untreated T cells served as the negative control (group 1). After 24 hours, T cells were collected as effector cells and cocultured with PANC-1 cancer cells as target cells at a ratio of 5 : 1 (*E* : *T*). The activity of T cells against the target tumor cells was measured by the LDH cytotoxicity assays kit. As demonstrated in Figure 5, the percentage of tumor lysis in the peptides/HB₁₀₀₋₁₀₈ group was higher than that in the negative control and empty DC groups. More importantly, T cells in the peptides+HB₁₀₀₋₁₀₈ group significantly induced the lysis of tumor cells in comparison with the other three groups, indicating that peptides+HB₁₀₀₋₁₀₈/pulsed DCs could

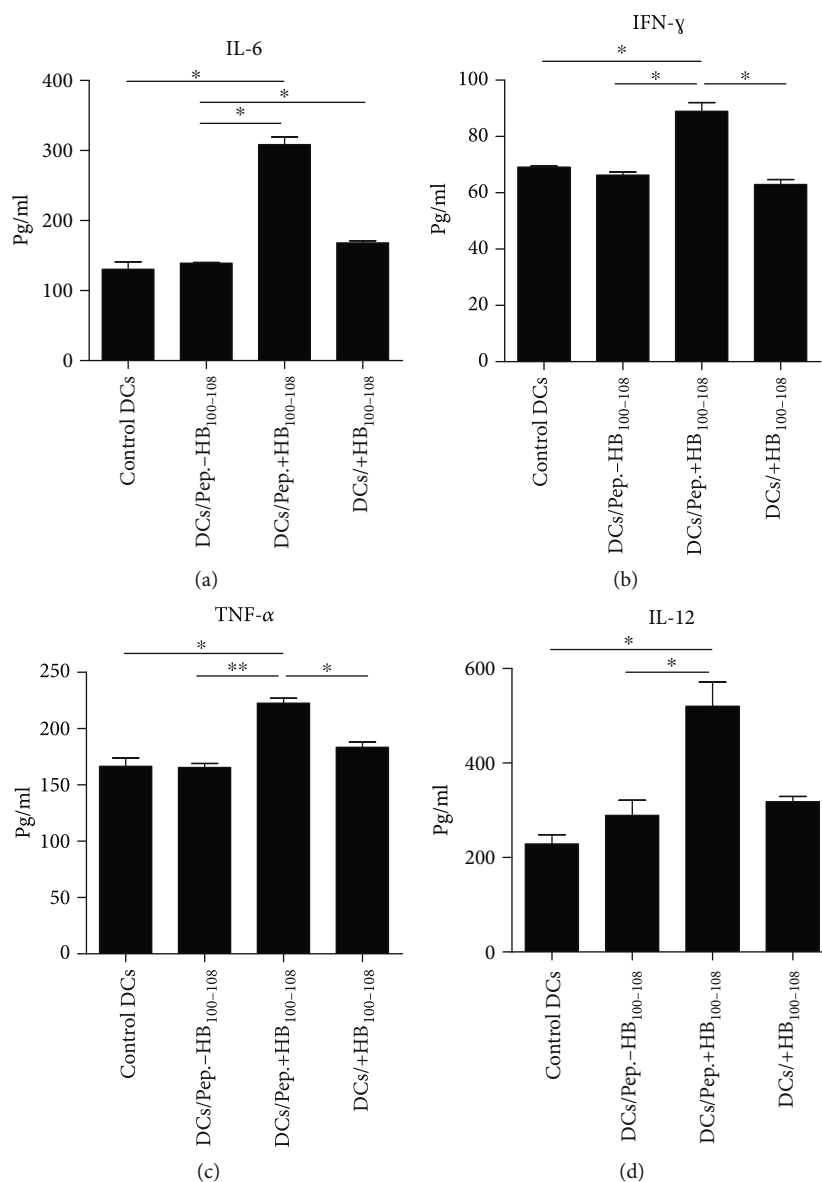


FIGURE 3: Peptides+HB₁₀₀₋₁₀₈/pulsed DCs secreted abundant levels of proinflammatory cytokines. Immature moDCs were left untreated or pulsed with peptides±HB₁₀₀₋₁₀₈ or free HB₁₀₀₋₁₀₈ (each with 40 μg/ml) for 1 hour at 37°C. Then, cells were washed and cultured for 24 hours, followed by detection of the secreted IL-6 (a), IFN-γ (b), and TNF-α (c) in the culture media by a cytometric bead array (CBA) kit. (d) IL-12 was detected by ELISA after 48 hours. Results represent the mean ± SEM of three independent experiments.

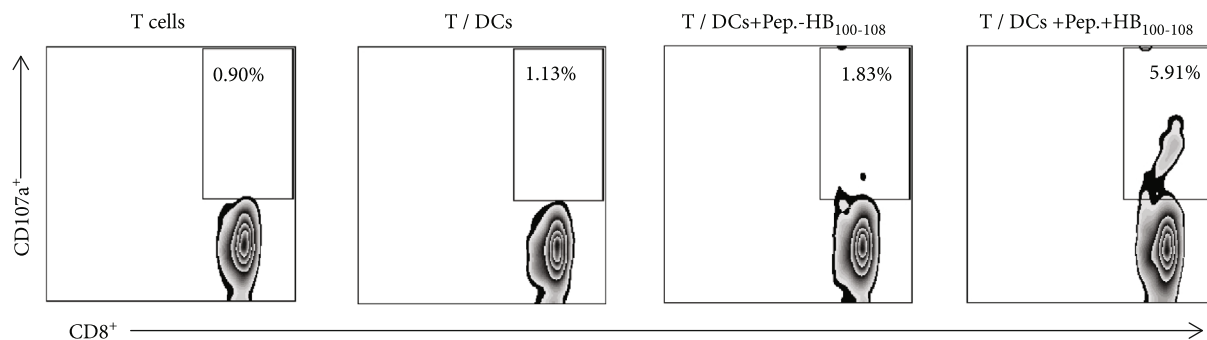
stimulate high cytolytic activity of the T cells against PANC-1 *in vitro*.

4. Discussion

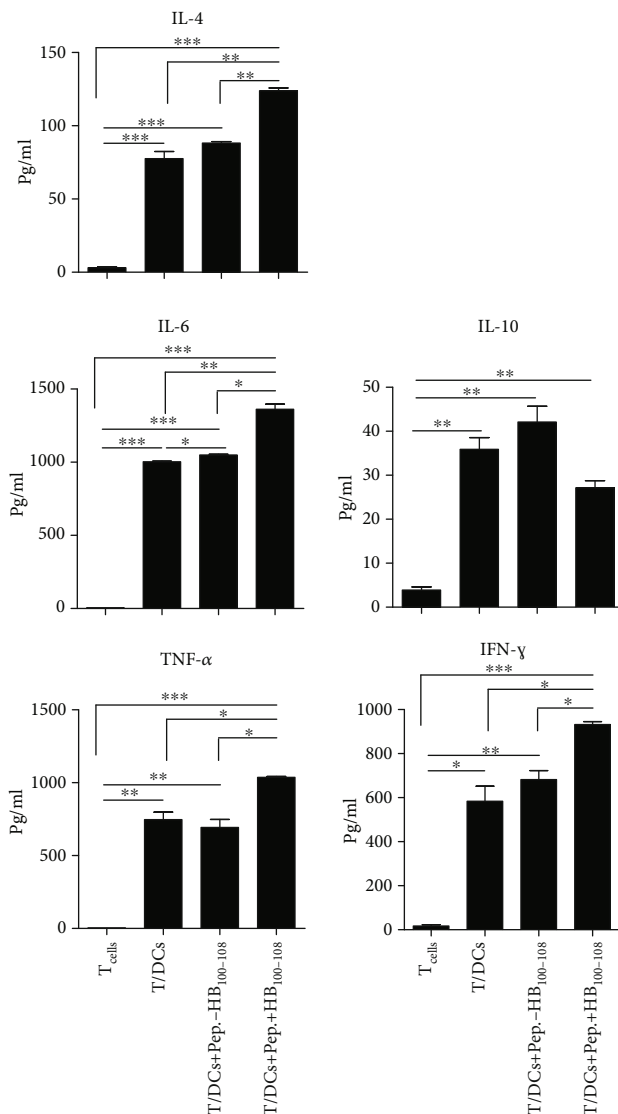
Immunotherapy based on peptides possesses numerous advantages including easy synthesis, low molecular weight, low toxicity, and the specific targeting of cancer cells. However, peptide-based anti-cancer vaccines encountered several limitations in the clinical setting due to several reasons including the following: (1) there is lack of CD4⁺ T cell help, (2) peptides are prone to degradation, (3) they may induce tolerance, (4) they induce low magnitude or transient

immune response, and (5) there is dysfunction of DCs upon cancer [4, 22].

In the recent years, there has been a growing interest in cancer DC-based vaccines due to their promising results in achieving meaningful treatment responses with safety profile [23]. It has been documented that compared with synthetic short peptides (SSPs), the synthetic long peptides (SLPs) are efficiently processed and crosspresented by DCs *in vivo*, resulting in the priming of both CD4⁺ and CD8⁺ T cell responses [24, 25]. Several studies indicated that the direct vaccination with short peptides may lead to tolerance and anergy and promote the growth of tumor cells [26, 27]. In contrast, *ex vivo*-differentiated DCs loaded with short peptides could elicit potent antitumor immune response



(a)



(b)

FIGURE 4: Peptides+HB₁₀₀₋₁₀₈/pulsed DCs induced the degranulation of CD8⁺ T cells and enhanced allogeneic T cells to secrete inflammatory cytokines. Immature moDCs were left untreated or pulsed with peptides±HB₁₀₀₋₁₀₈ (each with 40 μg/ml). Cells were washed and matured in the presence of a maturation cocktail for 24 hours. (a) Allogeneic T cells were stimulated with empty DCs or peptides±HB₁₀₀₋₁₀₈/pulsed DCs at T : DC cell ratio of 5 : 1 in the presence of GolgiStop and anti-CD107a-APC mAb. After incubation for 12 hours at 37°C, cells were collected and stained with anti-CD8-PE mAb and analyzed by flow cytometry. (b) Empty DCs or peptides±HB₁₀₀₋₁₀₈/pulsed DCs were cocultured with responder allogeneic T cells at a DC : T cell ratio of 1 : 5 for 18 hours. Supernatants were collected at the end of culture, and cytokine production was detected using a cytometric bead array (CBA) kit. Results represent the mean ± SEM of three independent experiments.

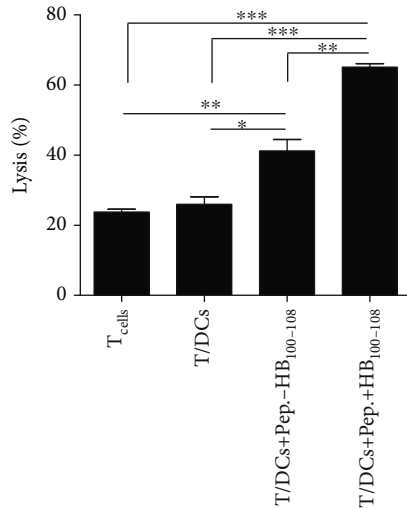


FIGURE 5: T cells stimulated by peptides+HB₁₀₀₋₁₀₈/pulsed DCs exert considerable lysis of the PANC-1 cell line in vitro. After stimulation with empty DCs or peptides±HB₁₀₀₋₁₀₈/pulsed DCs for 24 hours or no stimulation, allogeneic T cells were collected as the effector cells and the PANC-1 cancer cell line was used as target cells. The target cells were cocultured with the effector cells at a $T : E$ ratio of 1:5. The cytolytic activity was assessed by measurement of lactate dehydrogenase (LDH) release. This experiment has been performed in triplicate and repeated three times with similar results.

in vitro and in vivo [28, 29]. Thus, DCs appear to be a powerful carrier for the peptide-based vaccines.

As mentioned previously, the success of peptide-based vaccines mainly depends on the utilized peptides and selection of an appropriate adjuvant. Herein, it has been found that the covalent linking of adjuvant to tumor-associated antigens (TAAs) could result in the maturation and activation of DCs in vitro and induced a potent antitumor immune response in vivo compared to TAAs which they physically mixed with adjuvant [30, 31].

It is well known that Toll-like receptor (TLR) ligands have a potent activity to enhance the maturation of DCs and promote them to express proinflammatory cytokines and costimulatory molecules [32]. Later studies demonstrated that TLR ligands can efficiently increase the capacity of antigen crosspresentation in DCs [33]. HMGB1 protein has been shown to activate immune cells and induce signalling via interacting with different TLRs [34]. Thus, the addition of HMGB1 protein or its derivative peptides to the peptide-based subunit vaccines could be a promising strategy to enhance crosspresentation and crosspriming in DCs.

In this study, three antigenic synthetic peptides, which are overexpressed in several cancer types, were covalently linked with HMGB1-derived peptide (HB₁₀₀₋₁₀₈) as immunoadjuvant via double R linker and loaded into immature DCs. This design includes three main advantages: (1) long synthetic peptides, (2) the covalent linking of immunoadjuvant, and (3) RR linker, which is cleaved by the protease of DCs, and thus could facilitate and enhance the processing and presentation of loaded peptides.

It is well established that only mature DCs can costimulate and activate naïve T cells and thus requiring the recognition of peptide-MHC complexes by T cell receptor and interactions between costimulatory molecules (CD40, CD80, and CD86) on the DCs and CD28 receptors on target T cells [35]. Our data showed that peptides+HB₁₀₀₋₁₀₈ (but not peptides-HB₁₀₀₋₁₀₈ or free HB₁₀₀₋₁₀₈)/pulsed DCs exhibited high levels of several surface molecules (HLA-DR, HLA-ABC, CD83, CD80, CD86, and CD40), indicating that peptides+HB₁₀₀₋₁₀₈ could efficiently trigger the maturation and activation of immature DCs. Furthermore, peptides+HB₁₀₀₋₁₀₈/pulsed DCs expressed a high level of CCR7, which plays an important role in the migration of DCs to lymph nodes where they activate naïve T cells and elicit specific immune response [36].

It is well known that the secretion of inflammatory cytokines by DC-loaded antigen plays a crucial role in the induction of antigen-specific antitumor immune responses [37]. In this study, peptides+HB₁₀₀₋₁₀₈ (but not peptides-HB₁₀₀₋₁₀₈ or free HB₁₀₀₋₁₀₈)/pulsed DCs secreted high levels of IL-6, TNF- α , IFN- γ , and IL-12p70 and low levels of IL-10. The high level and low level of IL-12p70 and IL-10, respectively, indicate that peptides+HB₁₀₀₋₁₀₈/pulsed DCs could induce the differentiation of T cells toward Th2 phenotype [38].

These findings are consistent with previous studies indicating that the free HMGB1-derived peptide has almost no effect on the maturation and activation of DCs [31]. They are also consistent with results of studies showing that the adjuvant covalently linked to the short peptides could stimulate higher epitope recognition than the physically mixed formulation of the same molecules [39, 40]. To achieve maximum immunostimulatory effect, immunoadjuvant should be in close proximity with antigen [41]. Our data revealed that peptides+HB₁₀₀₋₁₀₈, but not free HB₁₀₀₋₁₀₈, effectively enhanced the maturation and activation of DCs after rapid phagocytosis. The potential reason is that linking epitopes with HB₁₀₀₋₁₀₈ might promote the peptide multimerization and lead to an efficient binding to the receptor of DCs via cross-linking [10]. It is important to mention that in case of direct vaccination, rather than ex vivo DC loading, peptides+HB₁₀₀₋₁₀₈ will be taken up and presented by the same APCs by which can prevent the nonspecific DC stimulation. In conclusion, HB₁₀₀₋₁₀₈ might exhibit a synergistic effect when covalently linked with antigenic peptides and thus could lead to maximizing the antitumor immune response.

Several studies indicated that the efficient DC vaccine should finally activate antigen-specific T cell responses. Thus, the ability of cytokine secretion is critical to confirm the activation status of T cells upon encountering the presented antigen by DCs [42]. In the present study, we found that the expression of IL-4, IL-6, TNF- α , and IFN- γ but not IL-10 dramatically increased after T cell interaction with peptides+HB₁₀₀₋₁₀₈/pulsed DCs, indicating that this vaccine design has the ability to activate allogeneic T cells against tumor antigen.

The ultimate goal of cancer vaccine is to drive the activated T cells toward the tumor site and selectively kill cancer cells. In this study, T cells which were activated by (survivin, Her2, and CEA)+HB₁₀₀₋₁₀₈/pulsed DCs showed a

significantly high cytolytic activity against the PANC-1 cell line in vitro. This suggests that T cell stimulated by peptides+HB₁₀₀₋₁₀₈-pulsed DCs could exert significant antigen-specific lysis on pancreatic cancer cells which express survivin, Her2, and CEA peptides.

In conclusion, our findings provide evidence that the covalently linked antigenic peptides with immunoadjuvant HB₁₀₀₋₁₀₈ are efficiently phagocytized by DCs and induce their full maturation and activation. Those activated DCs have the ability to activate allogeneic T cells and enhance their cytolytic activity against cancer cells. This work suggests a potent strategy to improve DC-based peptide immunotherapy and supports further studies to test the efficacy of this vaccine in clinical trials.

Data Availability

The relevant data used to support the findings of this study are included within the article.

Ethical Approval

This study was approved by the Medical Ethics Committee of Shanghai Cell Therapy Research Institute and carried out in accordance with the 1964 Declaration of Helsinki and its later amendments or comparable ethical standards.

Conflicts of Interest

All authors declare that there is no conflict of interests regarding the publication of this paper.

Authors' Contributions

Chumeng Chen and Mohanad Aldarouish contributed equally to this work.

Acknowledgments

This work was supported by the Natural Science Foundation of Shanghai No. 19ZR1454200.

Supplementary Materials

Supplementary Figure 1: determination of the optimum concentration of peptides+HB₁₀₀₋₁₀₈ that promote the highest level of DC maturation and activation. (*Supplementary Materials*)

References

- [1] T. A. Patente, M. P. Pinho, A. A. Oliveira, G. C. M. Evangelista, P. C. Bergami-Santos, and J. A. M. Barbuto, "Human dendritic cells: their heterogeneity and clinical application potential in cancer immunotherapy," *Frontiers in Immunology*, vol. 9, p. 3176, 2019.
- [2] J. Chen, H. Y. Li, D. Wang, J. J. Zhao, and X. Z. Guo, "Human dendritic cells transfected with amplified MUC1 mRNA stimulate cytotoxic T lymphocyte responses against pancreatic cancer in vitro," *Journal of Gastroenterology and Hepatology*, vol. 26, no. 10, pp. 1509–1518, 2011.
- [3] B. Mastelic-Gavillet, K. Balint, C. Boudousquie, P. O. Gannon, and L. E. Kandalaft, "Personalized dendritic cell vaccines—recent breakthroughs and encouraging clinical results," *Frontiers in Immunology*, vol. 10, p. 766, 2019.
- [4] C. L. Slingluff Jr., "The present and future of peptide vaccines for cancer: single or multiple, long or short, alone or in combination?," *The Cancer Journal*, vol. 17, no. 5, pp. 343–350, 2011.
- [5] Y. Ye, Z. Zeng, T. Jin, H. Zhang, X. Xiong, and L. Gu, "The role of high mobility group box 1 in ischemic stroke," *Frontiers in Cellular Neuroscience*, vol. 13, p. 127, 2019.
- [6] H. Yang, H. Wang, S. S. Chavan, and U. Andersson, "High mobility group box protein 1 (HMGB1): the prototypical endogenous danger molecule," *Molecular Medicine*, vol. 21, Supplement 1, pp. S6–S12, 2015.
- [7] I. E. Dumitriu, P. Baruah, M. E. Bianchi, A. A. Manfredi, and P. Rovere-Querini, "Requirement of HMGB1 and RAGE for the maturation of human plasmacytoid dendritic cells," *European Journal of Immunology*, vol. 35, no. 7, pp. 2184–2190, 2005.
- [8] D. Messmer, H. Yang, G. Telusma et al., "High mobility group box protein 1: an endogenous signal for dendritic cell maturation and Th1 polarization," *Journal of Immunology*, vol. 173, no. 1, pp. 307–313, 2004.
- [9] G. Telusma, S. Datta, I. Mihajlov et al., "Dendritic cell activating peptides induce distinct cytokine profiles," *International Immunology*, vol. 18, no. 11, pp. 1563–1573, 2006.
- [10] R. Saenz, C. S. Souza, C. T. Huang, M. Larsson, S. Esener, and D. Messmer, "HMGB1-derived peptide acts as adjuvant inducing immune responses to peptide and protein antigen," *Vaccine*, vol. 28, no. 47, pp. 7556–7562, 2010.
- [11] R. Saenz, B. Messmer, D. Futalan et al., "Activity of the HMGB1-derived immunostimulatory peptide Hp91 resides in the helical C-terminal portion and is enhanced by dimerization," *Molecular Immunology*, vol. 57, no. 2, pp. 191–199, 2014.
- [12] L. M. F. de Oliveira, M. G. Morale, A. A. M. Chaves et al., "Design, immune responses and anti-tumor potential of an HPV16 E6E7 multi-epitope vaccine," *PLoS One*, vol. 10, no. 9, article e0138686, 2015.
- [13] M. Monzo, R. Rosell, E. Felip et al., "A novel anti-apoptosis gene: re-expression of survivin messenger RNA as a prognosis marker in non-small-cell lung cancers," *Journal of Clinical Oncology*, vol. 17, no. 7, pp. 2100–2104, 1999.
- [14] K. Tanaka, S. Iwamoto, G. Gon, T. Nohara, M. Iwamoto, and N. Tanigawa, "Expression of survivin and its relationship to loss of apoptosis in breast carcinomas," *Clinical Cancer Research*, vol. 6, no. 1, pp. 127–134, 2000.
- [15] K. Satoh, K. Kaneko, M. Hirota, A. Masamune, A. Satoh, and T. Shimosegawa, "Tumor necrosis factor-related apoptosis-inducing ligand and its receptor expression and the pathway of apoptosis in human pancreatic cancer," *Pancreas*, vol. 23, no. 3, pp. 251–258, 2001.
- [16] D. Grossman, J. M. McNiff, F. Li, and D. C. Altieri, "Expression and targeting of the apoptosis inhibitor, survivin, in human melanoma," *Journal of Investigative Dermatology*, vol. 113, no. 6, pp. 1076–1081, 1999.
- [17] N. Iqbal and N. Iqbal, "Human epidermal growth factor receptor 2 (HER2) in cancers: overexpression and therapeutic implications," *Molecular Biology International*, vol. 2014, Article ID 852748, 9 pages, 2014.

- [18] U. Reichelt, P. Duesedau, M. C. Tsourlakis et al., "Frequent homogeneous HER-2 amplification in primary and metastatic adenocarcinoma of the esophagus," *Modern Pathology*, vol. 20, no. 1, pp. 120–129, 2007.
- [19] J. A. Hensel, V. Khattar, R. Ashton, and S. Ponnazhagan, "Recombinant AAV-CEA tumor vaccine in combination with an immune adjuvant breaks tolerance and provides protective immunity," *Molecular Therapy Oncolytics*, vol. 12, pp. 41–48, 2019.
- [20] J. T. Ulrich, W. Cieplak, N. J. Paczkowski, S. M. Taylor, and S. D. Sanderson, "Induction of an antigen-specific CTL response by a conformationally biased agonist of human C5a anaphylatoxin as a molecular adjuvant," *The Journal of Immunology*, vol. 164, no. 10, pp. 5492–5498, 2000.
- [21] L. F. Dodson, W. G. Hawkins, and P. Goedegebuure, "Potential targets for pancreatic cancer immunotherapeutics," *Immunotherapy*, vol. 3, no. 4, pp. 517–537, 2011.
- [22] W. Li, M. Joshi, S. Singhanian, K. Ramsey, and A. Murthy, "Peptide vaccine: progress and challenges," *Vaccine*, vol. 2, no. 3, pp. 515–536, 2014.
- [23] A. Huber, F. Dammeijer, J. G. J. V. Aerts, and H. Vroman, "Current state of dendritic cell-based immunotherapy: opportunities for in vitro antigen loading of different DC subsets?," *Frontiers in Immunology*, vol. 9, p. 2804, 2018.
- [24] R. A. Rosalia, E. D. Quakkelaar, A. Redeker et al., "Dendritic cells process synthetic long peptides better than whole protein, improving antigen presentation and T-cell activation," *European Journal of Immunology*, vol. 43, no. 10, pp. 2554–2565, 2013.
- [25] H. Zhang, H. Hong, D. Li et al., "Comparing pooled peptides with intact protein for accessing cross-presentation pathways for protective CD8⁺ and CD4⁺ T cells," *The Journal of Biological Chemistry*, vol. 284, no. 14, pp. 9184–9191, 2009.
- [26] R. E. Toes, R. J. Blom, R. Offringa, W. M. Kast, and C. J. Melief, "Enhanced tumor outgrowth after peptide vaccination. Functional deletion of tumor-specific CTL induced by peptide vaccination can lead to the inability to reject tumors," *Journal of Immunology*, vol. 156, pp. 3911–3918, 1996.
- [27] R. E. Toes, R. Offringa, R. J. Blom, C. J. Melief, and W. M. Kast, "Peptide vaccination can lead to enhanced tumor growth through specific T-cell tolerance induction," *Proceedings of the National Academy of Sciences of the United States of America*, vol. 93, no. 15, pp. 7855–7860, 1996.
- [28] Y. J. Choi, S. J. Park, Y. S. Park, H. S. Park, K. M. Yang, and K. Heo, "EpCAM peptide-primed dendritic cell vaccination confers significant anti-tumor immunity in hepatocellular carcinoma cells," *PLoS One*, vol. 13, no. 1, article e0190638, 2018.
- [29] W. J. Lesterhuis, I. J. de Vries, G. Schreiber et al., "Immunogenicity of dendritic cells pulsed with CEA peptide or transfected with CEA mRNA for vaccination of colorectal cancer patients," *Anticancer Research*, vol. 30, no. 12, pp. 5091–5097, 2010.
- [30] J. Zhao, N. Pan, F. Huang et al., "Vx3-functionalized alumina nanoparticles assisted enrichment of ubiquitinated proteins from cancer cells for enhanced cancer immunotherapy," *Bioconjugate Chemistry*, vol. 29, no. 3, pp. 786–794, 2018.
- [31] S. Dong, T. Xu, P. Wang, P. Zhao, and M. Chen, "Engineering of a self-adjuvanted iTEP-delivered CTL vaccine," *Acta Pharmacologica Sinica*, vol. 38, no. 6, pp. 914–923, 2017.
- [32] P. Blanco, A. K. Palucka, V. Pascual, and J. Banchereau, "Dendritic cells and cytokines in human inflammatory and autoimmune diseases," *Cytokine & Growth Factor Reviews*, vol. 19, no. 1, pp. 41–52, 2008.
- [33] N. I. Ho, L. G. M. Huis in 't Veld, T. K. Raaijmakers, and G. J. Adema, "Adjuvants enhancing cross-presentation by dendritic cells: the key to more effective vaccines?," *Frontiers in Immunology*, vol. 9, p. 2874, 2018.
- [34] W. L. Anggayasti, R. L. Mancera, S. Bottomley, and E. Helmerhorst, "The self-association of HMGB1 and its possible role in the binding to DNA and cell membrane receptors," *FEBS Letters*, vol. 591, no. 2, pp. 282–294, 2017.
- [35] T. Liechtenstein, I. Dufait, A. Lanna, K. Breckpot, and D. Escors, "Modulating co-stimulation during antigen presentation to enhance cancer immunotherapy," *Immunology, Endocrine & Metabolic Agents in Medicinal Chemistry*, vol. 12, no. 3, pp. 224–235, 2012.
- [36] D. R. Saban, "The chemokine receptor CCR7 expressed by dendritic cells: a key player in corneal and ocular surface inflammation," *The Ocular Surface*, vol. 12, no. 2, pp. 87–99, 2014.
- [37] A. Gardner and B. Ruffell, "Dendritic cells and cancer immunity," *Trends in Immunology*, vol. 37, no. 12, pp. 855–865, 2016.
- [38] Y. Wang, X. Xiong, D. Wu, X. Wang, and B. Wen, "Efficient activation of T cells by human monocyte-derived dendritic cells (HMDCs) pulsed with *Coxiella burnetii* outer membrane protein Com1 but not by HspB-pulsed HMDCs," *BMC Immunology*, vol. 12, no. 1, p. 52, 2011.
- [39] P. Daftarian, R. Sharan, W. Haq et al., "Novel conjugates of epitope fusion peptides with CpG-ODN display enhanced immunogenicity and HIV recognition," *Vaccine*, vol. 23, no. 26, pp. 3453–3468, 2005.
- [40] R. L. Coffman, A. Sher, and R. A. Seder, "Vaccine adjuvants: putting innate immunity to work," *Immunity*, vol. 33, no. 4, pp. 492–503, 2010.
- [41] C. Bode, G. Zhao, F. Steinhagen, T. Kinjo, and D. M. Klinman, "CpG DNA as a vaccine adjuvant," *Expert Review of Vaccines*, vol. 10, no. 4, pp. 499–511, 2011.
- [42] O. Millán, L. Rafael-Valdivia, E. Torrademé et al., "Intracellular IFN- γ and IL-2 expression monitoring as surrogate markers of the risk of acute rejection and personal drug response in de novo liver transplant recipients," *Cytokine*, vol. 61, no. 2, pp. 556–564, 2013.

Research Article

Development and Validation of a *Bordetella pertussis* Whole-Genome Screening Strategy

Ricardo da Silva Antunes ¹, Lorenzo G. Quiambao,¹ Aaron Sutherland,¹ Ferran Soldevila,¹ Sandeep Kumar Dhanda ¹, Sandra K. Armstrong,² Timothy J. Brickman,² Tod Merkel,³ Bjoern Peters,^{1,4} and Alessandro Sette^{1,4}

¹Division of Vaccine Discovery, La Jolla Institute for Immunology, La Jolla, San Diego, California, USA

²Department of Microbiology and Immunology, University of Minnesota Medical School, Minneapolis, Minnesota, USA

³Division of Bacterial, Parasitic and Allergenic Products, Center for Biologics Evaluation and Research, U.S. Food and Drug Administration, Silver Spring, Maryland, USA

⁴University of California San Diego School of Medicine, La Jolla, San Diego, California, USA

Correspondence should be addressed to Ricardo da Silva Antunes; rantunes@lji.org

Received 2 January 2020; Accepted 6 March 2020; Published 2 April 2020

Academic Editor: Pedro A. Reche

Copyright © 2020 Ricardo da Silva Antunes et al. This is an open access article distributed under the Creative Commons Attribution License, which permits unrestricted use, distribution, and reproduction in any medium, provided the original work is properly cited.

The immune response elicited by the protective whole-cell pertussis (wP) versus the less-protective acellular pertussis (aP) vaccine has been well characterized; however, important clinical problems remain unsolved, as the inability of the currently administered aP vaccine is resulting in the reemergence of clinical disease (i.e., whooping cough). Strong evidence has shown that original, childhood aP and wP priming vaccines provide a long-lasting imprint on the CD4⁺ T cells that impacts protective immunity. However, aP vaccination might prevent disease but not infection, which might also affect the breadth of responses to *Bordetella pertussis* (BP) antigens. Thus, characterizing and defining novel targets associated with T cell reactivity are of considerable interest. Here, we compare the T cell reactivity of original aP and wP priming for different antigens contained or not contained in the aP vaccine and define the basis of a full-scale genomic map of memory T cell reactivity to BP antigens in humans. Our data show that the original priming after birth with aP vaccines has higher T cell reactivity than originally expected against a variety of BP antigens and that the genome-wide mapping of BP using an ex vivo screening methodology is feasible, unbiased, and reproducible. This could provide invaluable knowledge towards the direction of a new and improved pertussis vaccine design.

1. Introduction

Several studies and epidemiological evidence suggest that the immunity induced by *Bordetella pertussis* (BP) acellular vaccines (aP) wanes more rapidly as compared to the immunity elicited by vaccines based on whole BP cells (wP) [1–8]. In previous studies [9, 10], we have investigated potential immune correlates of this waning immunity, by dissecting immune responses in young adults, originally primed with either aP or wP vaccines. These studies were enabled by the definition of the T cell epitopes contained in the BP antigens contained in the aP vaccines (pertussis toxin, PtTox; two serotypes of fimbriae, Fim2/3; filamentous hemagglutinin,

FHA; and pertactin, PRN), which was achieved following the systematic analysis of responses following the expansion of antigen-specific T cells in short-term in vitro culture [9], and the development of the activation-induced marker (AIM) assays, which allowed measurement of responses directly ex vivo without any further manipulation [11, 12].

When immune responses to aP boosters in individuals who received their initial doses with either wP or aP vaccines were compared, BP-specific memory CD4⁺ T cell responses were associated with Th1/Th17 versus Th2 differential polarization as a function of childhood vaccination [10]. Strikingly, after aP booster, donors originally primed with aP were associated with lower responses ex vivo and lower

in vitro proliferation. These observations led to the hypothesis that lower proliferative capacity of aP might be linked to a regulatory cell population, since no difference between cohorts was noted when purified T cell subpopulations were assayed.

As mentioned above, the available data demonstrates that the BP wP vaccine is effective and prevents infection, but the total breadth of responses is not known. Based on these observations, it could be expected that broad responses are elicited upon vaccination, directed against a variety of different BP antigens. These responses could be possibly blunted over time with repeated aP boosters. The data present in the literature also demonstrate that the aP vaccine despite waning over time is also effective in initial protection against whooping cough [3, 13–15], but by comparison to the wP vaccine, it could be expected that this vaccine would elicit a narrow response directed mostly against the four vaccine antigens. As a result, little or no response against non-aP vaccine BP antigens would be detected. Several lines of evidence argue against this simplistic view, which are related to the possible interplay between vaccination and natural BP exposure/infection [16]. Specifically, recent data from both baboon and mouse models [15, 17–21] suggests that aP vaccination might prevent disease but not infection or in particular nasopharyngeal subclinical colonization. This might paradoxically result in broad responses in aP and is of greater magnitude than wP because of heavier and more frequent exposure.

To specifically address this, we set out to study T cell responses from BP antigens not contained in the aP vaccine, as function of either aP or wP priming vaccination, as well as to address the feasibility of using a large-scale ex vivo methodology for T cell epitope identification specific for BP.

2. Materials and Methods

2.1. Study Subjects. We recruited 31 healthy adults from San Diego, USA (Supplementary Table 1). All participants provided a written informed consent for participation, and clinical medical history was collected and evaluated by the clinical coordinators through questionnaires, recording dates and numbers of vaccination, including the information that no boost was administered in at least the previous four years prior to this study. All donors were from the San Diego area and originally vaccinated with either DTwP or DTaP priming vaccines in infancy (three doses at 2, 4, and 6 months and then two doses between 15-18 months and 4-6 years) and followed the recommended vaccination regimen (which is also necessary for enrollment in the California school system), which entails immunization with the acellular booster vaccine Tdap at 11-12 years and then every 10 years and during pregnancy. The pertussis (P) compounds in these vaccines (“w” for whole-cell, also wP for short, and “a” for acellular, also aP for short) are coadministered with diphtheria toxoid (D) and tetanus toxoid (T). Also, the capital and lowercase letters denote higher or lower proportions of the overall components between vaccines. Individuals who had been diagnosed with BP infection at any given time in their life were excluded. In all groups, male and female subjects were included equally.

2.2. Study Approval. This study was performed with approvals from the Institutional Review Board at La Jolla Institute for Immunology (protocols: VD-101-0513 and VD-059-0813). All participants provided a written informed consent for participation, and clinical medical history was collected and evaluated.

2.3. Peptides. Peptide selection was derived either from *Bordetella pertussis* (BP) whole-genome predictions from the Tohama I strain or from experimentally validated antigens included in the aP vaccines (FHA, Fim2/3, PRN, and PtTox). Experimentally validated peptides were selected from a total of 785 peptides tested from the BP strain Tohama I, encompassing 16-mers overlapping by eight residues of the full-length coverage of all antigens. The top epitopes recognized by >5% donors corresponding to 132 peptides were chosen, and the megapool (MG) of all combined peptides is described as PT (MG) hereafter [9, 10]. BP genome-wide identification was performed by scanning for the presence of predicted HLA class II promiscuous binding peptides. MHC-peptide binding predictions were performed using publicly available tools hosted by the Immune Epitope Database (IEDB) Analysis Resource [22]. Specifically, the prediction of peptides was established by the 7-allele HLA class II restricted method and by using peptides 15 residues in length and overlapping by 10 residues [23, 24]. Additional filtering using an epitope cluster analysis tool [25] was performed. Briefly, the peptides from each ORF were created in an overlapping fashion, which due to a shared 9-amino acid core prediction base often had similar binding affinities (percentile score). A modified algorithm from IEDB clustering tool to remove redundant peptides sharing a stretch of 9-amino acids in 15-mers was performed. In case of peptides sharing a core, the peptides with highest binding affinities were picked. At least 2 peptides per open reading frame (ORF) were selected. The selected peptides were pooled together and underwent sequential lyophilization as described elsewhere [10] and arranged in “megapools” (MGs) of approximately 200 peptides each further divided into groups of 8 “mesopools” (MSs) of 24 individual peptides. For BP adenylate cyclase toxin (ACT), the full length of the antigen was covered and the top 20% predicted epitopes were selected to originate a 54 peptide ACT MGs. All individual peptides (Supplementary Table 2) were synthesized by Mimotopes (Victoria, Australia) and resuspended to a final concentration of 1 mg/mL in DMSO.

2.4. PBMC Isolation. Peripheral blood mononuclear cells (PBMCs) were isolated from whole blood or leukapheresis by density gradient centrifugation according to the manufacturer’s instructions (Ficoll-Paque Plus, Amersham Biosciences, Uppsala, Sweden) as previously described [26]. The cells were cryopreserved in liquid nitrogen and suspended in fetal bovine serum (FBS) containing 10% (vol/vol) dimethyl sulfoxide (DMSO).

2.5. *Bordetella pertussis* Lysate Production. BP lysates were prepared from iron-starved bacteria (to simulate growth conditions in the natural mammalian host environment)

[27–29], provided by Drs. Sandra Armstrong and Timothy Brickman (University of Minnesota Medical School, USA). Specifically, the bacteria were cultured in the iron-deficient chemically defined Stainer-Scholte medium [30, 31]. The bacterial cells were harvested at mid- to late-exponential growth phase and suspended in phosphate-buffered saline. The lysate was generated by mechanical shearing at low temperature (French press), frozen in liquid nitrogen, and then shipped to the La Jolla Institute for Immunology (CA, USA). Growth was monitored by optical density readings, and the iron starvation status of the bacteria was confirmed using siderophore detection assays [32, 33] and SDS-PAGE analysis of proteins.

2.6. AIM Assay. The activation-induced marker (AIM) assay was previously described [12]. This assay detects cells that are activated as a result of antigen-specific stimulation by staining antigen-experienced CD4⁺ T cells for TCR-dependent upregulation of OX40 and CD25 (AIM25) and/or PD-L1 (AIMPD) after an optimal time of 18–24 h of culture. Briefly, cryopreserved PBMCs were thawed, and 1×10^6 cells/condition were immediately cultured together with PT and ACT peptide pools (2 $\mu\text{g}/\text{mL}$), selected MS (1 $\mu\text{g}/\text{mL}$), individual peptides (10 $\mu\text{g}/\text{mL}$), or PHA (10 $\mu\text{g}/\text{mL}$; Roche) and DMSO as positive and negative controls, respectively, in 5% human serum (Gemini Bio-Products) for 24 h. To determine the memory phenotype of responding T cells, staining for CD45RA and CCR7 markers was performed and subpopulations were defined as follows: naive T cells (T_n): CD45RA⁺CCR7⁺; effector memory RA T cells (T_{em}): CD45RA⁺CCR7⁻; T central memory (T_{cm}): CD45RA⁻CCR7⁺; and T effector memory (T_{em}): CD45RA⁻CCR7⁻. The samples were acquired using a BD LSR II flow cytometer (BD Biosciences) and analyzed using the FlowJo X software. Specific signals were all subtracted to the DMSO control displayed as % of CD4 T cells and normalized and displayed as the number of cells per 1×10^6 CD4 T cells. All flow cytometry mAb reagents for surface staining are listed in Supplementary Table 3.

2.7. ELISpot and FluoroSpot Assays. Culturing of PBMCs for in vitro expansion was performed by incubating in RPMI (Omega Scientific) supplemented with 5% human AB serum, GlutaMAX (Gibco), and penicillin/streptomycin (Omega Scientific) at 2×10^6 per mL in the presence of BP lysates at 10 $\mu\text{g}/\text{mL}$. Every 3 days, 10 U/mL IL-2 in RPMI medium was added to the cultures. After 14 days in culture with the BP lysate, the expanded T cells were tested for the recognition of the epitope pools or individual peptides as described above. As readout, the standard IFN γ /IL-5 and IL-17/IL-9 cytokine combination for ELISpot assay or IFN γ /IL-5/IL-13 cytokine combination for FluoroSpot assay was performed as described [9, 34]. For ex vivo determinations, the same combination of cytokines was used after 20 h incubation with lysate (10 $\mu\text{g}/\text{mL}$), epitope pools (2 $\mu\text{g}/\text{mL}$), or individual peptides (10 $\mu\text{g}/\text{mL}$) besides PHA (2 $\mu\text{g}/\text{mL}$) and DMSO as positive and negative controls, respectively. Consistent with these previous studies in order to be considered positive, a response in both in vitro or ex vivo modalities had to match

all three different criteria: (1) eliciting at least 20 spot-forming cells (SFC) per 10^6 PBMCs; (2) $p \leq 0.05$ by Student's *t*-test or by the Poisson distribution test; and (3) stimulation index (SI) ≥ 2 .

2.8. Statistical Analysis. Comparisons between groups were made using the nonparametric two-tailed, unpaired Mann-Whitney *U* or Spearman's rank correlation coefficient tests. Prism 8.0.1 (GraphPad) was used for all these calculations. All figure data in which error bars are shown are presented as median \pm interquartile range when each dot represents an individual donor or as mean \pm SEM when each dot represents a technical replicate. A *p* value < 0.05 was considered statistically significant.

3. Results and Discussion

3.1. Original aP and wP Primes Are Associated with High T Cell Reactivity for All Antigens Contained and Not Contained in aP Vaccine. There are emerging proofs of BP subclinical colonization in vaccinated individuals, including indirect evidences of asymptomatic transmission [35–38], as observed in animal models [19, 21], which could affect T cell responses against BP antigens to a greater extent than originally expected.

To address this issue, we examined memory CD4 responses to a previously defined peptide pool of BP epitopes encompassing the 4 antigens (FHA, Fim2/3, PRN, and PtTox) contained in the aP vaccine [10] in a set of PBMCs derived from 31 donors either originally vaccinated with aP ($n = 16$) or originally vaccinated with wP ($n = 15$). We used two assay formats, one is an ex vivo AIM assay that measures the antigen-specific upregulation of OX40 and CD25 markers and the other is a lysate expansion followed by an ELISpot assay. Using the lysate expansion, we found that responses in the two groups were equivalent (with a small trend towards higher response in the aP group) (Figure 1(a), top). In the same experiments, we also measured responses against a pool of BP epitopes from the adenylate cyclase toxin (ACT) antigen, a virulence factor that is not contained in the aP vaccine [39]. Interestingly, we found that aP donors also exhibited equivalent memory T cell reactivity against the ACT antigen (Figure 1(a), bottom). Importantly, the same results were corroborated when assaying responses in a different subset of donors and using the ex vivo AIM modality (Figure 1(b)). Finally, responses against the set of antigens present in the aP vaccine showed differential polarization as a function of the original priming vaccination consistent with literature [9, 10, 40, 41], but surprisingly, responses against ACT did not (Figure 1(c)). Overall, aP-vaccinated subjects are associated with immune responses against a variety of BP antigens, including antigens not present in the aP vaccine, consistent with the notion that aP prevents disease but not colonization/exposure, and this result is apparent using two different assay modalities.

3.2. A Genome-Wide Reactivity Screen of T Cell Reactivity to BP with Different Assay Modalities Considered. The data

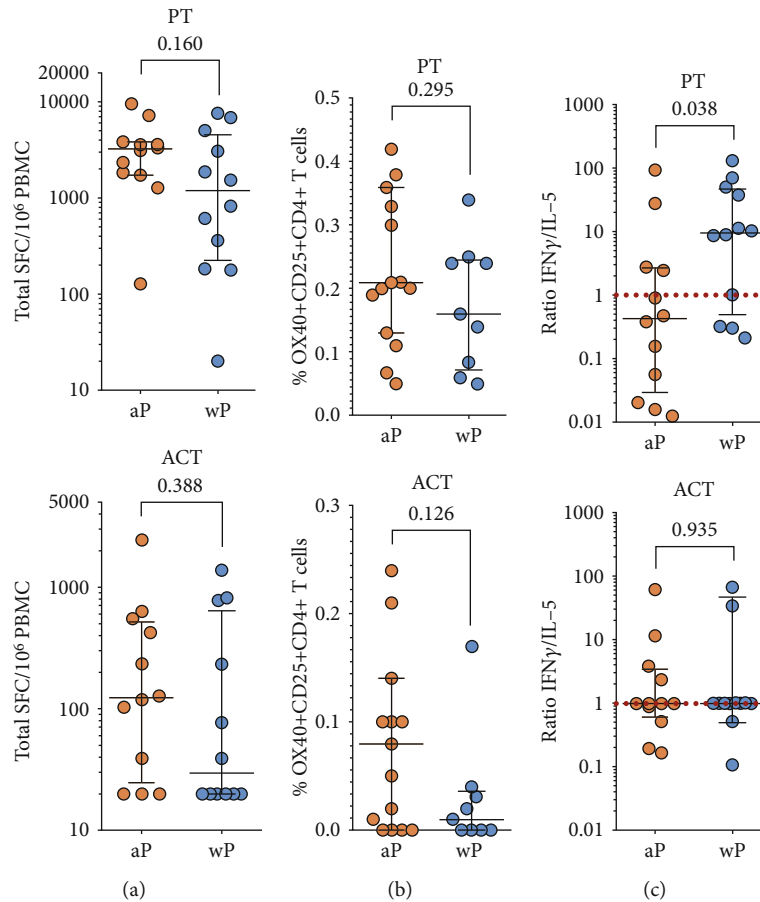


FIGURE 1: Original childhood aP priming is associated with high reactivity to pertussis antigens. (a) Cytokine production was measured by ELISpot following in vitro restimulation with BP lysate. Magnitude of responses expressed by spot-forming cells (SFC) is shown for the sum of T cell responses (IFN γ , IL-5, IL-17, and IL-9) for all aP antigens (PT) or ACT between wP- and aP-primed donors ($n = 12$ for aP and $n = 12$ for wP cohorts). (b) % of BP-specific CD4⁺ memory T cells for PT or ACT antigens by AIM assay for donors originally primed with wP or aP vaccine ($n = 15$ for aP and $n = 9$ for wP cohorts). (c) Differential polarization of T cell responses for PT but not ACT. Each data point represents the ratio of IFN γ /IL-5 SFCs from each donor ($n = 12$ for aP and $n = 12$ for wP cohorts). Data are expressed as median \pm interquartile range for each cohort with the Mann-Whitney U test comparison value.

discussed in the previous section suggests that the definition of a full-scale genomic map of memory T cell reactivity to BP antigens in humans should be both feasible and of considerable interest [42]. Indeed, a similar genome-wide mapping of T cell responses to *Mycobacterium tuberculosis* antigens has been recently accomplished [43].

To explore the feasibility of a similar screen in the case of BP antigens, bioinformatic epitope predictions [42, 44] for the whole BP genome indicated the synthesis of approximately 25,000 peptides, spanning over 3300 BP putative ORFs. Here, we wanted to specifically test the practicality of a potential large-scale screening strategy, by testing a selected set of these 25,000 peptides, which would be initially arranged in approximately 130 “megapools” (MGs) of approximately 200 peptides each. Additionally, we envisioned that each MG would be further divided into 8 “mesopools” (MSs) of about 24 individual peptides. These various pools and peptides would be tested using PBMCs derived from apheresis from 20 young adults originally vaccinated with either wP or aP vaccines.

Below, we report the results of a pilot study using the selected wP and aP donors to define the screening methodology. We tested 8 MSs containing peptides that have been mapped in the whole BP genome to include the 4 antigens contained in the aP vaccine (PRN, PtTox, Fim2/3, and FHA), but also novel ORFs, not yet assayed for T cell reactivity (Supplementary Table 2). As a positive control, we tested the previously described PT MG [10], produced with the previously identified vaccine-reactive epitopes and containing 132 peptides. The purpose of the experiments was to specifically compare the results obtained with different screening modalities, including the ex vivo ELISpot/FluoroSpot [43], the 14-day restimulation ELISpot/FluoroSpot [9], and the ex vivo AIM assay [12] (Figure 2).

3.3. In Vitro Lysate Stimulation Allows Identification of BP-Specific Responses. In the first series of experiments, we evaluated the FluoroSpot assay platform ex vivo. When we tested IFN γ , IL-5, IL-13, IL-17, IL-9, and TNF- α production in response to the 8 MSs, no positive responses were detected.

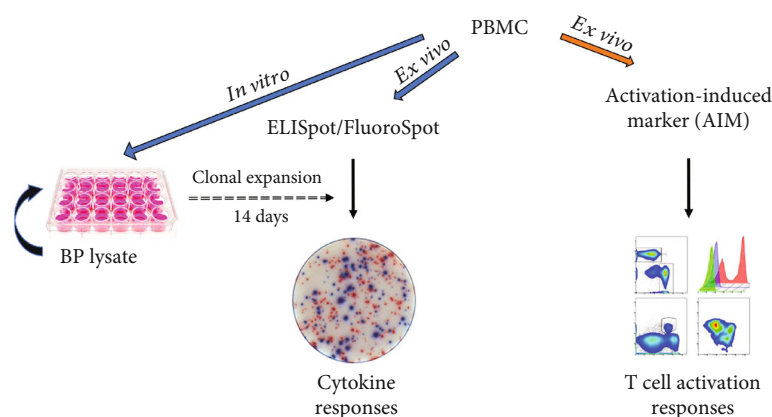


FIGURE 2: Approaches for genome-wide screening and measurement of T cell reactivity. Schematic design for the screening of BP whole genome using different assay modalities (AIM versus ELISpot/FluoroSpot) and strategies (in vitro versus ex vivo) to capture T cell-specific responses.

The PT MG composed of known epitopes and used as a positive control also did not elicit any detectable responses (not shown). These results show that, in the case of BP, direct ex vivo screening is not feasible with the FluoroSpot platform as reported for mycobacterial tuberculosis [43].

As an alternative, and similar to the assay shown in Figure 1(a), we considered an in vitro restimulation step, to expand antigen-specific T cells. In fact, this assay modality has been successfully utilized in numerous studies where allergen extracts were employed to expand allergen-specific T cells [45–48]. In this context, we wanted to determine whether a BP lysate could be also utilized to expand BP-specific T cells and measure BP-specific responses. Accordingly, we produced a lysate prepared from iron-starved BP cultures. PBMCs were stimulated in vitro for 14 days with 10 $\mu\text{g}/\text{mL}$ of the lysate, and the expanded T cells were tested in a 24 h FluoroSpot assay, where the number of cells secreting the various cytokines was recorded. The results of a pilot study utilizing PBMCs from 12 aP and 12 wP donors, respectively, are shown in Figure 3, demonstrate that the BP lysate can be used to expand cells for subsequent use in the 14-day restimulation FluoroSpot assay.

3.4. In Vitro Lysate Stimulation Allows Identification of Novel BP Antigens and Epitopes. In the next series of experiments, with the method established above, we assayed in vitro cultures from two independent donors, and after the 14-day lysate expansion, the 8 MSs were tested in the FluoroSpot assay for the most abundant cytokine production (i.e., IFN γ , IL-5, and IL-13). The MS encompassing peptides from known and novel antigens were all associated with positive signals in the restimulation FluoroSpot assay as well as the positive control (not shown). Representative data are shown for one of the two donors and one of the MSs, where the signal was deconvoluted to map the individual peptides recognized by the responding T cells (Figure 4).

The results indicate that deconvolution of positive MS reidentified the known antigens; in the case of the representative data shown, a vigorous pertactin response was observed. Most importantly, the results indicate that the

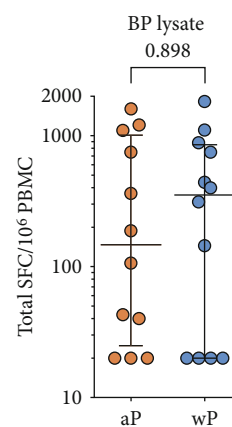


FIGURE 3: BP lysates can be used to expand cells for assessing BP antigen reactivity. The magnitude of responses expressed by spot-forming cells (SFC) is shown for the sum of T cell responses (IFN γ , IL-5, IL-17, and IL-9) for lysate restimulation after 14 days of expansion with BP lysate ($n = 12$ for aP and $n = 12$ for wP cohorts). Data are expressed as median \pm interquartile range for each cohort with the Mann–Whitney U test comparison value.

approach also identifies epitopes from *novel* antigens endowed with high immunoreactivity. Specifically, strong responses were noted for peptide epitopes derived from DD-transpeptidase antigen, a bacterial enzyme involved in cell wall biosynthesis [49]. Further analysis indicated that the MS responses observed were associated with the expected polarization pattern (Th2 for aP, Th1/Th17 for wP) when performing parallel intracellular staining assays (not shown). In conclusion, these results indicate that the in vitro restimulation combined with a FluoroSpot assay is a suitable methodology for the large-scale BP screen.

3.5. Ex Vivo AIM Assay Reproducibly Identifies Candidates for Deconvolution. In the next series of experiments, we evaluated the feasibility of a screening modality utilizing an ex vivo AIM assay [10–12] similar to the approach used in Figure 1(b). The results of AIM assays where PBMC from a representative donor out of 6 donors were stimulated with

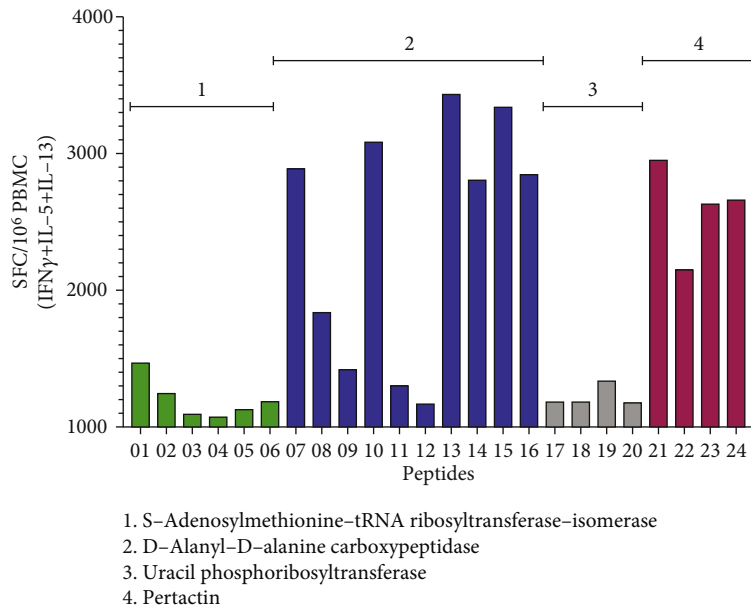


FIGURE 4: Deconvolution of positive MS reidentifies known antigens and identifies epitopes from novel antigens. Cytokine production was measured by FluoroSpot after 14 days of in vitro restimulation with BP lysate. The magnitude of responses expressed by spot-forming cells (SFC) is shown for the sum of T cell responses (IFN γ , IL-5, and IL-13) of a representative donor for all individual peptides ($n = 24$) from a positive mesopool containing the known pertactin antigen. The name of the all the antigens encompassing the group of peptides is shown.

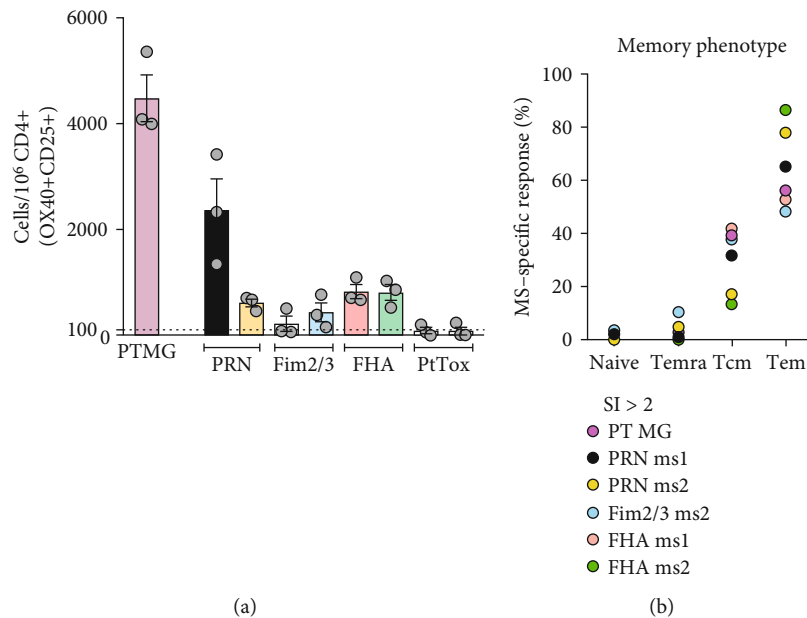
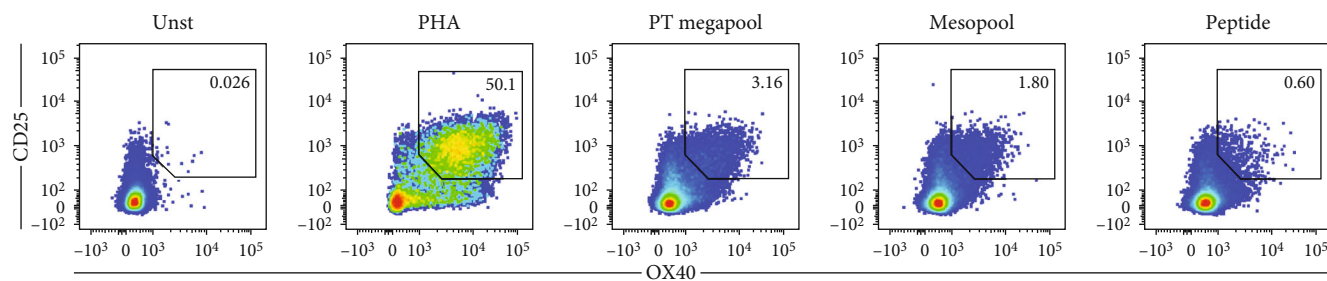


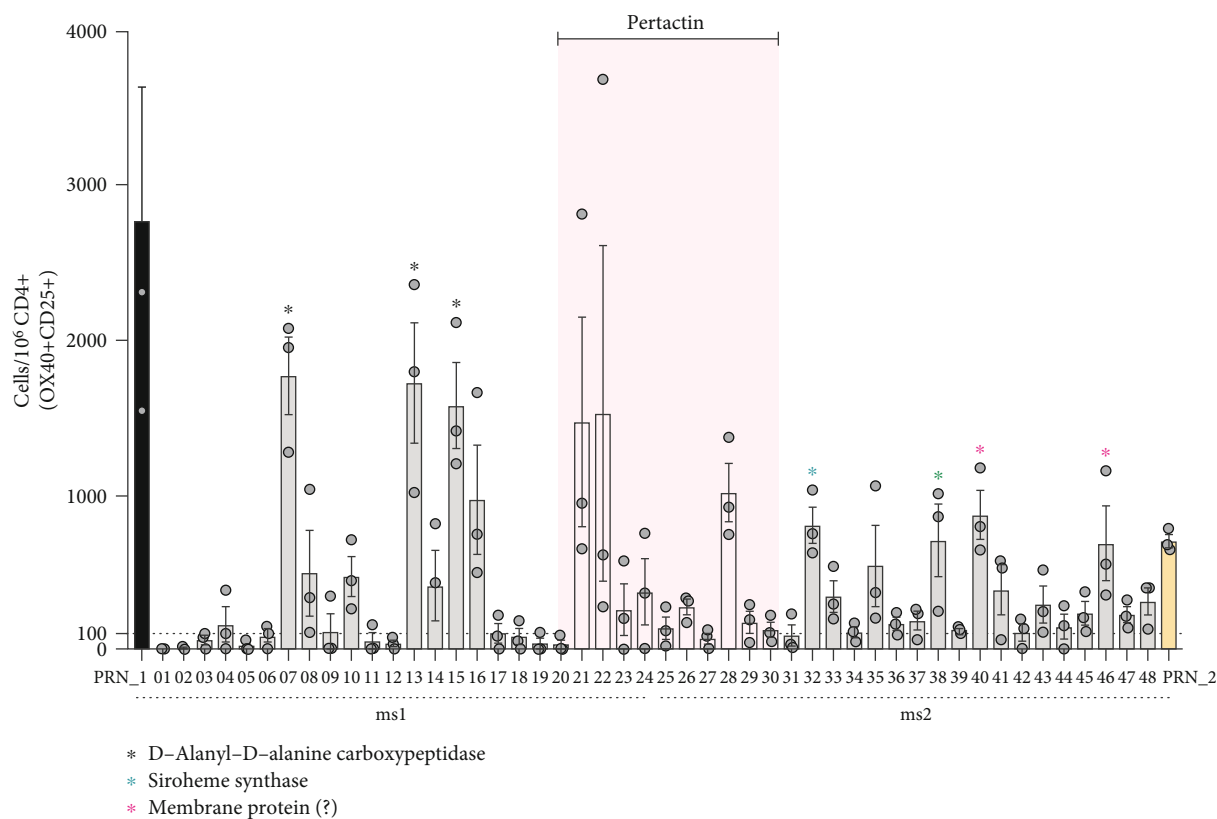
FIGURE 5: Ex vivo AIM assay pool screening on different days reproducibly identifies candidates for deconvolution. (a) % of BP-specific CD4+ T cells for the pool of aP antigens (PT) or for the 8 MSs containing peptides from the 4 individual aP antigens was measured by the AIM assay. Peptides from the 4 individual antigens are aligned by ORF position but flanked by peptides from other antigens and unequally distributed over 2 adjacent and unique MSs each. Individual circles represent an independent technical replicate of the same donor performed on a different day. A representative donor is shown. Data are expressed as mean \pm SEM. Dotted line indicates positive response threshold of 100 cells set to identify MS candidates for deconvolution. (b) Memory subset composition of PT MG- and MS-specific responses ($SI > 2$) is shown as % of total CD4+ T cells gated in AIM-positive cells (Tn: CD45RA+CCR7+, Temra: CD45RA+CCR7-, Tcm: CD45RA-CCR7+, and Tem: CD45RA-CCR7-). The average data for each positive mesopool are shown ($n = 5$).

the eight MSs are shown in Figure 5(a). The results show data obtained in three completely independent experiments on different days. The results between different days were highly

correlated with high significance ($p < 0.0001$) when performing a multiple linear regression analysis, regardless of whether the absolute positive cells/ 10^6 cells or SI (signal to



(a)



(b)

FIGURE 6: Ex vivo AIM assay can reproducibly detect signals down to the peptide level. (a) Representative flow cytometry plots of CD25 +OX40+ upregulation by CD4+ T cells in cells left unstimulated (Unst) or stimulated with pools of peptides (PT-megapool ($n = 132$ peptides) or mesopool ($n = 24$ peptides)) or individual peptides as well as PHA as a positive control. (b) % of BP-specific CD4+ memory T cells for each individual peptide ($n = 48$) deconvoluted from 2 contiguous positive MSs (PRN_1 (ms1, $n = 24$) and PRN_2 (ms2, $n = 24$)) containing among others, peptides ($n = 10$) from the known antigen pertactin (PRN; pink area) as measured by AIM assay. Each dot represents an independent technical replicate of the same donor performed on a different day. A representative donor is shown. Data are expressed as mean \pm SEM. The names of the all the antigens encompassing the group of peptides whose responses were significant are shown.

noise ratios) were considered. Based on these results, a threshold of 100 cells and SI of 2 were provisionally set to identify MS candidates for deconvolution.

Parallel experiments investigated the memory phenotype of the responding cells, defined on the basis of the expression of the CD45RA and CCR7 markers as described in more detail in Materials and Methods. As expected and in a similar fashion to PT MG composed of known epitopes, the BP-specific T cells detected in the reactive MS (SI > 2) were mostly derived from the effector memory (Tem) and central memory (Tcm) subsets (Figure 5(b)).

Finally, we investigated whether the two positive MSs containing the pertactin antigen could be further deconvoluted, down to the level of individual peptides. The results shown in Figure 6 show that this is indeed the case. The deconvolution identified peptides from the known aP antigen pertactin and in addition identified epitopes from novel antigens. Specifically, strong responses were noted for peptide epitopes derived from the D-alanyl-D-alanine transpeptidase and siroheme synthase antigens, both enzymes associated with BP biosynthetic processes. The graph shows the results from three independent assays performed on

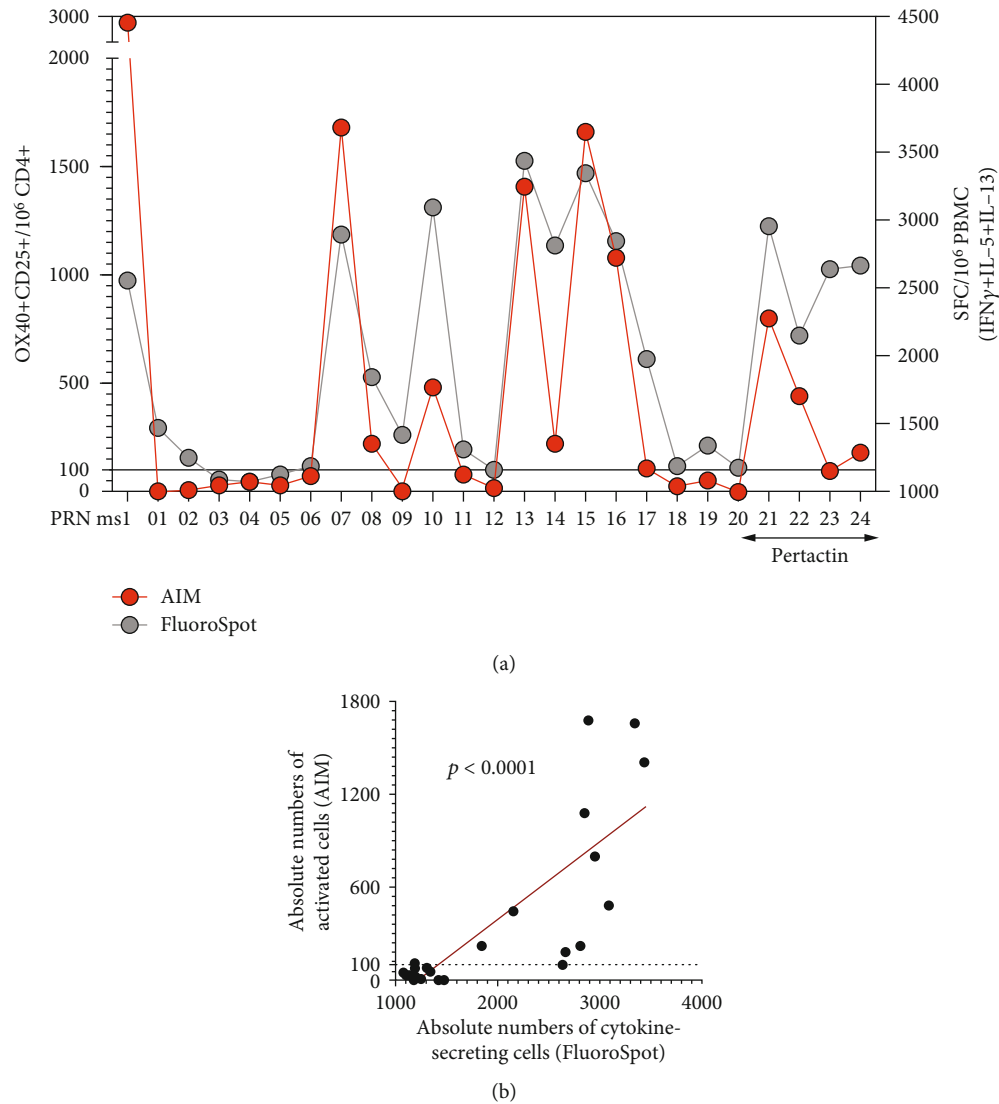


FIGURE 7: Correlation of results of the ex vivo AIM assay and 14 days restimulation assays. (a) The data show the overlay of the average of the individual peptide response as captured by either AIM or FluoroSpot assays for a selected mesopool deconvolution from a representative donor. (b) The best fit of the peptide data set is represented by a linear regression line (red) and the p value expresses Spearman's rank correlation coefficient test.

different days and indicates that the assay results are associated with minimal day-to-day variability and high correlation ($p < 0.0001$). Further experiments also revealed a good correlation between the results of the ex vivo AIM assay and cytokine production by the Ag-reactive T cell enrichment (ARTE) assay ([50]; not shown) suggesting that peptide stimulation captures activated cells that are actively producing cytokines. In conclusion, these results indicate that the ex vivo AIM assay is also a suitable methodology for the large-scale BP screen.

3.6. Ex Vivo and In Vitro Assays Are Highly Correlated. The results presented above indicate that both the in vitro restimulation/FluoroSpot and the ex vivo AIM assays are suitable methodologies for the large-scale BP screen. Given that both assays are suitable, we next addressed the question of whether the two different assay platforms would also lead to the identification of similar epitopes. When compared, it was found

(Figure 7) that the two results obtained in the in vitro restimulation/FluoroSpot and the ex vivo AIM assays were highly correlated ($p < 0.0001$). In general, the correlation between the two assays is high. However, it is also noted that in some instances (Figure 7(a)), peptides 10, 14, 23, and 24 are associated with high activity in the FluoroSpot assay and relatively low AIM signal. It is not clear whether this is simply within experimental error or corresponds to a true reproducible phenomenon. In any case, it is noted that in the vast majority of instances, the peptides associated with high FluoroSpot activity are still positive for the specified AIM assay threshold. Since our concern is to identify an assay to be used as primary screen, those peptides would still be identified as positive and characterized in more detail in secondary assays, regardless whether the FluoroSpot or AIM would be used as a primary screen. Overall, based on these results, it appears that the two platforms are equivalent and potentially interchangeable.

4. Conclusions

The results of this study demonstrate that both the in vitro restimulation/FluoroSpot and the ex vivo AIM assays are suitable methodologies for the large-scale BP screen. In general, both assay platforms yield reproducible results when the assays are repeated in independent experiments performed on different days, and these findings have been verified utilizing different independent donors. Based on the results, we tentatively set a threshold of 100 cells and SI of 2 to identify positive MS candidates for deconvolution.

Surprisingly, our results indicate that aP donors also exhibited equivalent memory T cell reactivity against the ACT antigen, which is not found in the aP vaccines. Higher levels of antibody against ACT have also been observed in the plasma of aP-primed donors (unpublished observations). Thus, aP-vaccinated subjects are associated with immune responses against a variety of BP antigens not just present in the aP vaccine, which is consistent with the notion that aP prevents disease but not BP colonization/exposure [18, 19, 21].

Because both assay platforms appear to yield equivalent results, the question arises related to which of the two might be preferable. The ex vivo AIM platform is more laborious on the assay day (but this step can be at least partially automated), while the in vitro restimulation step, by definition, has a longer time to completion and requires more steps. The ex vivo AIM assay has three important advantages, as (1) it is not dependent on the responding cell to secrete any particular cytokine, (2) it introduces minimal physiological perturbations, as compared to a 2-week culture period, and (3) it allows mapping of subcellular populations and further phenotypic characterization [42].

Finally, in terms of biological relevance, both assay platforms correctly reidentify known antigens such as pertactin as an important source of BP epitopes and in addition identify novel epitopes derived from novel antigens such as D-alanyl-D-alanine transpeptidase and siroheme synthase. These results further support the interest and feasibility of performing a whole-genome-wide screen of BP T cell antigens. Both the in vitro restimulation/FluoroSpot and the ex vivo AIM assays results are associated with the expected polarization patterns, further underlining the biological relevance of the observations. In an age of increasingly reported cases and outbreaks of whooping cough throughout the globe, along with imperfect protection provided by currently administered aP vaccines, the identification of novel antigens associated with BP virulence and persistence is warranted and crucial for better control and prevention of both transmission and disease.

Data Availability

All The data used to support the findings of this study are included within the article or included within the supplementary information associated with this manuscript.

Conflicts of Interest

The authors have declared that no conflict of interest exists.

Acknowledgments

Research reported in this publication was supported by the National Institute of Allergy and Infectious Diseases of the National Institutes of Health under Award Numbers U01 AI141995, U19 AI142742, and 75N93019C00066. The content is solely the responsibility of the authors and does not necessarily represent the official views of the National Institutes of Health. We are grateful to all donors that participated in the study and the clinical studies group staff, particularly Shariza Bautista, Brittany Schwan, and Gina Levi, for all the invaluable help.

Supplementary Materials

Supplementary Table 1: characteristics of the donor population. Supplementary Table 2: list of individual peptides of each megapool. Supplementary Table 3: list of antibodies used in the study. (*Supplementary Materials*)

References

- [1] D. A. Diavatopoulos and K. M. Edwards, "What is wrong with pertussis vaccine immunity? Why immunological memory to pertussis is failing," *Cold Spring Harbor Perspectives in Biology*, vol. 9, no. 12, 2017.
- [2] M. D. de Cellès, F. M. G. Magpantay, A. A. King, and P. Rohani, "The impact of past vaccination coverage and immunity on pertussis resurgence," *Science Translational Medicine*, vol. 10, no. 434, 2018.
- [3] M. Domenech de Celles, P. Rohani, and A. A. King, "Duration of immunity and effectiveness of diphtheria-tetanus-acellular pertussis vaccines in children," *JAMA Pediatrics*, vol. 173, no. 6, pp. 588–594, 2019.
- [4] N. P. Klein, J. Bartlett, A. Rowhani-Rahbar, B. Fireman, and R. Baxter, "Waning protection after fifth dose of acellular pertussis vaccine in children," *The New England Journal of Medicine*, vol. 367, no. 11, pp. 1012–1019, 2012.
- [5] M. Saadatian-Elahi, S. Plotkin, K. H. G. Mills et al., "Pertussis: biology, epidemiology and prevention," *Vaccine*, vol. 34, no. 48, pp. 5819–5826, 2016.
- [6] K. L. Sealey, T. Belcher, and A. Preston, "*Bordetella pertussis* epidemiology and evolution in the light of pertussis resurgence," *Infection, Genetics and Evolution*, vol. 40, pp. 136–143, 2016.
- [7] S. van der Lee, L. H. Hendriks, E. A. M. Sanders, G. A. M. Berbers, and A. M. Buisman, "Whole-cell or acellular pertussis primary immunizations in infancy determines adolescent cellular immune profiles," *Frontiers in Immunology*, vol. 9, 2018.
- [8] O. Zerbo, J. Bartlett, K. Goddard, B. Fireman, E. Lewis, and N. P. Klein, "Acellular pertussis vaccine effectiveness over time," *Pediatrics*, vol. 144, no. 1, 2019.
- [9] T. Bancroft, M. B. C. Dillon, R. da Silva Antunes et al., "Th1 versus Th2 T cell polarization by whole-cell and acellular childhood pertussis vaccines persists upon re-immunization

- in adolescence and adulthood," *Cellular Immunology*, vol. 304-305, pp. 35-43, 2016.
- [10] R. da Silva Antunes, M. Babor, C. Carpenter et al., "Th1/Th17 polarization persists following whole-cell pertussis vaccination despite repeated acellular boosters," *The Journal of Clinical Investigation*, vol. 128, no. 9, pp. 3853-3865, 2018.
- [11] R. da Silva Antunes, S. Paul, J. Sidney et al., "Definition of human epitopes recognized in tetanus toxoid and development of an assay strategy to detect ex vivo tetanus CD4+ T cell responses," *PloS one*, vol. 12, no. 1, 2017.
- [12] J. M. Dan, C. S. Lindestam Arlehamn, D. Weiskopf et al., "A cytokine-independent approach to identify antigen-specific human germinal center T follicular helper cells and rare antigen-specific CD4+ T cells in blood," *Journal of Immunology*, vol. 197, no. 3, pp. 983-993, 2016.
- [13] C. M. Ausiello and A. Cassone, "Acellular pertussis vaccines and pertussis resurgence: revise or replace?," *MBio*, vol. 5, no. 3, 2014.
- [14] S. Esposito, P. Stefanelli, N. K. Fry et al., "Pertussis prevention: reasons for resurgence, and differences in the current acellular pertussis vaccines," *Frontiers in Immunology*, vol. 10, 2019.
- [15] P. Kapil and T. J. Merkel, "Pertussis vaccines and protective immunity," *Current Opinion in Immunology*, vol. 59, pp. 72-78, 2019.
- [16] I. F. Miller and C. J. Metcalf, "Vaccine-driven virulence evolution: consequences of unbalanced reductions in mortality and transmission and implications for pertussis vaccines," *Journal of The Royal Society Interface*, vol. 16, no. 161, 2019.
- [17] A. C. Allen, M. M. Wilk, A. Misiak, L. Borkner, D. Murphy, and K. H. G. Mills, "Sustained protective immunity against *Bordetella pertussis* nasal colonization by intranasal immunization with a vaccine-adjuvant combination that induces IL-17-secreting T_{RM} cells," *Mucosal Immunology*, vol. 11, no. 6, pp. 1763-1776, 2018.
- [18] L. Solans and C. Locht, "The role of mucosal immunity in pertussis," *Frontiers in Immunology*, vol. 9, 2019.
- [19] J. M. Warfel, L. I. Zimmerman, and T. J. Merkel, "Acellular pertussis vaccines protect against disease but fail to prevent infection and transmission in a nonhuman primate model," *Proceedings of the National Academy of Sciences of the United States of America*, vol. 111, no. 2, pp. 787-792, 2014.
- [20] J. M. Warfel, L. I. Zimmerman, and T. J. Merkel, "Comparison of three whole-cell pertussis vaccines in the baboon model of pertussis," *Clinical and Vaccine Immunology*, vol. 23, no. 1, pp. 47-54, 2016.
- [21] M. M. Wilk, L. Borkner, A. Misiak, L. Curham, A. C. Allen, and K. H. G. Mills, "Immunization with whole cell but not acellular pertussis vaccines primes CD4 TRM cells that sustain protective immunity against nasal colonization with *Bordetella pertussis*," *Emerging Microbes & Infections*, vol. 8, no. 1, pp. 169-185, 2019.
- [22] S. K. Dhanda, S. Mahajan, S. Paul et al., "IEDB-AR: immune epitope database-analysis resource in 2019," *Nucleic Acids Research*, vol. 47, no. W1, pp. W502-W506, 2019.
- [23] S. K. Dhanda, E. Karosiene, L. Edwards et al., "Predicting HLA CD4 immunogenicity in human populations," *Frontiers in Immunology*, vol. 9, 2018.
- [24] S. Paul, C. S. Lindestam Arlehamn, T. J. Scriba et al., "Development and validation of a broad scheme for prediction of HLA class II restricted T cell epitopes," *Journal of Immunological Methods*, vol. 422, pp. 28-34, 2015.
- [25] S. K. Dhanda, K. Vaughan, V. Schulten et al., "Development of a novel clustering tool for linear peptide sequences," *Immunology*, vol. 155, no. 3, pp. 331-345, 2018.
- [26] A. Boyum, "Isolation of mononuclear cells and granulocytes from human blood. Isolation of mononuclear cells by one centrifugation, and of granulocytes by combining centrifugation and sedimentation at 1 g," *Scandinavian Journal of Clinical and Laboratory Investigation. Supplementum*, vol. 97, pp. 77-89, 1968.
- [27] J. J. Bullen, "The significance of iron in infection," *Reviews of Infectious Diseases*, vol. 3, no. 6, pp. 1127-1138, 1981.
- [28] T. Ganz and E. Nemeth, "Iron homeostasis and its disorders in mice and men: potential lessons for rhinos," *Journal of Zoo and Wildlife Medicine*, vol. 43, no. 3s, pp. S19-S26, 2012.
- [29] E. D. Weinberg, "Iron and infection," *Microbiological Reviews*, vol. 42, no. 1, pp. 45-66, 1978.
- [30] S. K. Armstrong and M. O. Clements, "Isolation and characterization of *Bordetella bronchiseptica* mutants deficient in siderophore activity," *Journal of Bacteriology*, vol. 175, no. 4, pp. 1144-1152, 1993.
- [31] D. W. Stainer and M. J. Scholte, "A simple chemically defined medium for the production of phase I *Bordetella pertussis*," *Journal of General Microbiology*, vol. 63, no. 2, pp. 211-220, 1970.
- [32] T. J. Brickman and S. K. Armstrong, "The ornithine decarboxylase gene *odc* is required for alcaligin siderophore biosynthesis in *Bordetella* spp.: putrescine is a precursor of alcaligin," *Journal of bacteriology*, vol. 178, no. 1, pp. 54-60, 1996.
- [33] B. Schwyn and J. B. Neilands, "Universal chemical assay for the detection and determination of siderophores," *Analytical Biochemistry*, vol. 160, no. 1, pp. 47-56, 1987.
- [34] G. Birrueta, A. Frazier, A. Pomés et al., "Variability in German cockroach extract composition greatly impacts T cell potency in cockroach-allergic donors," *Frontiers in Immunology*, vol. 10, 2019.
- [35] B. M. Althouse and S. V. Scarpino, "Asymptomatic transmission and the resurgence of *Bordetella pertussis*," *BMC Medicine*, vol. 13, no. 1, 2015.
- [36] C. Gill, P. Rohani, and D. M. Thea, "The relationship between mucosal immunity, nasopharyngeal carriage, asymptomatic transmission and the resurgence of *Bordetella pertussis*," *F1000Res*, vol. 6, p. 1568, 2017.
- [37] R. Palazzo, M. Carollo, G. Fedele et al., "Evidence of increased circulation of *Bordetella pertussis* in the Italian adult population from seroprevalence data (2012-2013)," *Journal of Medical Microbiology*, vol. 65, no. 7, pp. 649-657, 2016.
- [38] Q. Zhang, Z. Yin, Y. Li et al., "Prevalence of asymptomatic *Bordetella pertussis* and *Bordetella parapertussis* infections among school children in China as determined by pooled real-time PCR: a cross-sectional study," *Scandinavian Journal of Infectious Diseases*, vol. 46, no. 4, pp. 280-287, 2014.
- [39] N. H. Carbonetti, "Pertussis toxin and adenylate cyclase toxin: key virulence factors of *Bordetella pertussis* and cell biology tools," *Future Microbiology*, vol. 5, no. 3, pp. 455-469, 2010.
- [40] C. M. Ausiello, F. Urbani, A. la Sala, R. Lande, and A. Cassone, "Vaccine- and antigen-dependent type 1 and type 2 cytokine induction after primary vaccination of infants with whole-cell or acellular pertussis vaccines," *Infection and Immunity*, vol. 65, no. 6, pp. 2168-2174, 1997.
- [41] E. J. Ryan, L. Nilsson, N. I. M. Kjellman, L. Gothefors, and K. H. G. Mills, "Booster immunization of children with an

- acellular pertussis vaccine enhances Th2 cytokine production and serum IgE responses against pertussis toxin but not against common allergens,” *Clinical and Experimental Immunology*, vol. 121, no. 2, pp. 193–200, 2000.
- [42] Y. Tian, R. da Silva Antunes, J. Sidney et al., “A review on T cell epitopes identified using prediction and cell-mediated immune models for mycobacterium tuberculosis and *Bordetella pertussis*,” *Frontiers in Immunology*, vol. 9, 2018.
- [43] C. S. Lindestam Arlehamn, A. Gerasimova, F. Mele et al., “Memory T cells in latent Mycobacterium tuberculosis infection are directed against three antigenic islands and largely contained in a CXCR3+CCR6+ Th1 subset,” *PLoS Pathog*, vol. 9, no. 1, 2013.
- [44] K. Vaughan, E. Seymour, B. Peters, and A. Sette, “Substantial gaps in knowledge of *Bordetella pertussis* antibody and T cell epitopes relevant for natural immunity and vaccine efficacy,” *Human Immunology*, vol. 75, no. 5, pp. 440–451, 2014.
- [45] G. Birrueta, V. Tripple, J. Pham et al., “Peanut-specific T cell responses in patients with different clinical reactivity,” *PloS one*, vol. 13, no. 10, 2018.
- [46] R. da Silva Antunes, J. Pham, C. McMurtrey et al., “Urinary peptides as a novel source of T cell allergen epitopes,” *Frontiers in Immunology*, vol. 9, 2018.
- [47] C. Oseroff, J. Sidney, R. Vita et al., “T cell responses to known allergen proteins are differently polarized and account for a variable fraction of total response to allergen extracts,” *Journal of Immunology*, vol. 189, no. 4, pp. 1800–1811, 2012.
- [48] V. Schulten, J. A. Greenbaum, M. Hauser et al., “Previously undescribed grass pollen antigens are the major inducers of T helper 2 cytokine-producing T cells in allergic individuals,” *Proceedings of the National Academy of Sciences of the United States of America*, vol. 110, no. 9, pp. 3459–3464, 2013.
- [49] R. R. Yocum, D. J. Waxman, J. R. Rasmussen, and J. L. Strominger, “Mechanism of penicillin action: penicillin and substrate bind covalently to the same active site serine in two bacterial D-alanine carboxypeptidases,” *Proceedings of the National Academy of Sciences*, vol. 76, no. 6, pp. 2730–2734, 1979.
- [50] P. Bacher, C. Schink, J. Teutschbein et al., “Antigen-reactive T cell enrichment for direct, high-resolution analysis of the human naive and memory Th cell repertoire,” *Journal of Immunology*, vol. 190, no. 8, pp. 3967–3976, 2013.

Research Article

Characterization of a Complex Mixture of Immunomodulator Peptides Obtained from Autologous Urine

Alberto Frago,¹ **Mérida Pedraza-Jiménez**,¹ **Laura Espinoza-González**,¹
María Luisa Ceja-Mendoza,¹ **Hugo Sánchez-Mercado**,¹ **Gloria Robles-Pérez**,¹
Julio Granados ^{1,2} and **Emilio Medina-Rivero** ³

¹*Instituto de Alergias y Autoinmunidad Dr. Maximiliano Ruiz Castañeda A.C., Luisa Isabel Campos #16, col. Revolución, Acambay, Edo. de México 50300, Mexico*

²*Departamento de Trasplantes, Instituto Nacional de Ciencias Médicas y Nutrición Salvador Zubirán, Ciudad de México, Mexico*

³*Unidad de Desarrollo e Investigación en Bioprocesos (UDIBI), Escuela Nacional de Ciencias Biológicas, Instituto Politécnico Nacional, Ciudad de México 11340, Mexico*

Correspondence should be addressed to Julio Granados; julgrate@yahoo.com
and Emilio Medina-Rivero; emilio.medina@udibi.com.mx

Received 16 October 2019; Revised 1 February 2020; Accepted 2 March 2020; Published 2 April 2020

Guest Editor: Yoshihiko Hoshino

Copyright © 2020 Alberto Frago et al. This is an open access article distributed under the Creative Commons Attribution License, which permits unrestricted use, distribution, and reproduction in any medium, provided the original work is properly cited.

A complex mixture of peptides plays a key role in the regulation of the immune system; different sources as raw materials mainly from animals and vegetables have been reported to provide these extracts. The batch-to-batch product consistency depends on in-process controls established. However, when an immunomodulator is a customized product obtained from the same volunteer who will receive the product to personalize the treatment, the criteria to establish the consistency between volunteers are different. In this sense, it is expected to have the same molecular weight range although the profile of peptide abundance is different. Here, we characterized the peptide profile of three extracts of an immunomodulator obtained from the urine of different volunteers suffering from three different diseases (i.e., allergic rhinitis, rheumatoid arthritis, and chronic rhinopharyngitis), using size exclusion chromatography (SEC) and mass spectrometry (MS). The peptides contained in the immunomodulators were stable after six months, stored in a refrigerator. Our results showed a chromatographic profile with the same range of low molecular weight (less than 17 kDa) in all analyzed samples by SEC; these results were also confirmed by MS showing an exact mass spectrum from 3 to 13 kDa. The fact that the peptide profiles were conserved during a six-month period at refrigeration conditions (2 to 8°C) maintaining the quality and stability of the immunomodulator supports the notion that it might be an alternative in the treatment of chronic hypersensitivity disorders.

1. Introduction

Biological extracts containing a complex mixture of peptides represent an alternative for the treatment of chronic-degenerative diseases. This peptide distribution promotes the modulation of the immune response by a different mechanism of action still not fully understood, yet they have shown therapeutic properties and therefore represent an improvement in certain diseases [1, 2]. For this reason, it is essential to demonstrate consistency in the physicochemical properties of the product in order to obtain the expected

response. Previous studies on similar products containing peptide distribution such as transfer factor (Transferon®) or collagen hydrolysate (Colagenart®) showed a high reproducibility in the physicochemical properties among batches. Transferon® is used as a drug product for the treatment of chronic-degenerative diseases, while Colagenart® is prescribed as a dietary supplement, which have been used as a viable alternative to preserve joint and skin health [3–5].

Nowadays, personalized medicine, also known as individualized medicine or precision medicine, is becoming an innovative treatment in critical areas such as oncology. This

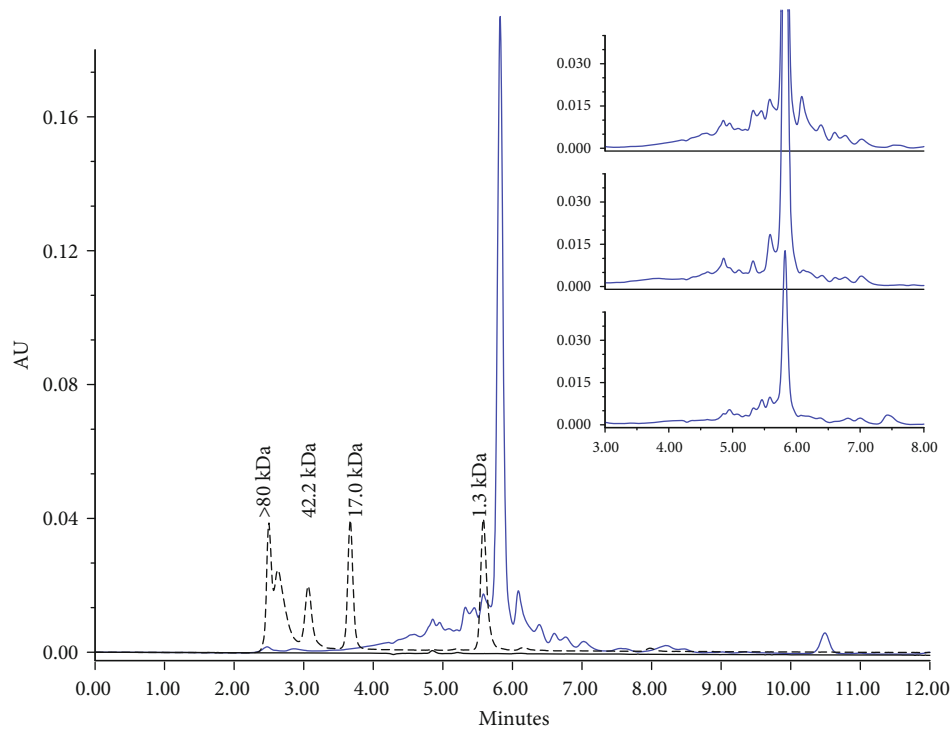


FIGURE 1: Peptide mass distribution of the immunomodulator by size exclusion chromatography. The main figure shows the characteristic chromatographic profile of the immunomodulator (blue line), the molecular weight marker (dotted line), and matrix (black line). At the right side, it shows the consistency in the mass distribution of three immunomodulators obtained from different volunteers.

approach, based on vaccination, consists on reinjecting a sample from the patient's own immunomodulator, after sample processing, to obtain a fraction of them that contains the peptide distribution which will be presented as own antigens to boost the immune response and serve as an immunomodulator and, therefore, might also be useful in people suffering from autoimmune diseases or in certain innate or adaptive immunodeficiencies [6–12].

This complex mixture of peptides, for reinjecting, is extracted mainly from blood cells or tissues (e.g., solid tumors) [13] and then extracted by standard separation bioprocesses such as precipitation, filtration, or chromatography, followed by formulation, sterile filtration, and the filling of the vials.

Peptides obtained from urine have been used for the treatment of patients with various forms of hypersensitivity (allergies of the skin and mucous membranes) like asthma and various forms of arthritis, for the last 40 years, showing a remarkable clinical improvement within the first weeks of treatment that last for months or even years particularly in patients with early diagnosis [7, 8]. Since the scientist Ruiz Castañeda developed the process to obtain peptides from urine, it allowed to invent the immunomodulator administered by injection or via oral for the treatment of various pathologies, such as autoimmune and allergic diseases. It was possible due to the experience accumulated in medicine, immunology, and bacteriology, which was obtained during his stay in the National School of Medicine, University of Paris, Pasteur Institute, and Harvard [14].

Since 1940, endogenous intradermal injection of the peptides extracted from autologous urine has been used for the

treatment of chronic immunologic disorders; according to a repeated dose scheme during 6 months, the results have been proven to be safe (no adverse effects have been reported) and effective mainly in the treatment of allergies of the skin and mucosa, reactive arthritis, and psoriasis [14].

In this study, the distribution of a complex mixture of peptides extracted from human urine in 3 patients was characterized, one with allergic rhinitis, a second one with arthritis rheumatoid, and a third one with chronic rhinopharyngitis. All three patients used the formulation in weekly doses (once a week for six months). For peptide analysis, cutting-edge technology was employed and included size exclusion chromatography and mass spectrometry. Additionally, peptide stability (at $5 \pm 3^\circ\text{C}$) during a 6-month period was demonstrated.

2. Materials and Methods

2.1. Samples and Reagents. Three samples of immunomodulator obtained from patients with allergic rhinitis, rheumatoid arthritis, and chronic rhinopharyngitis were provided by Instituto de Alergias y Autoinmunidad Dr. Maximiliano Ruiz Castañeda A.C. (Mexico City, Mexico). The immunomodulators were obtained by a bioprocess containing several steps that include selective precipitation of low molecular peptides with organic solvents [14]. Sodium chloride, and monobasic, dibasic sodium phosphate, and sodium 3-(trimethylsilyl)tetrauteriopropionate (TSP) were obtained from J. T. Baker and (NY, USA) Sigma-Aldrich (MO, USA).

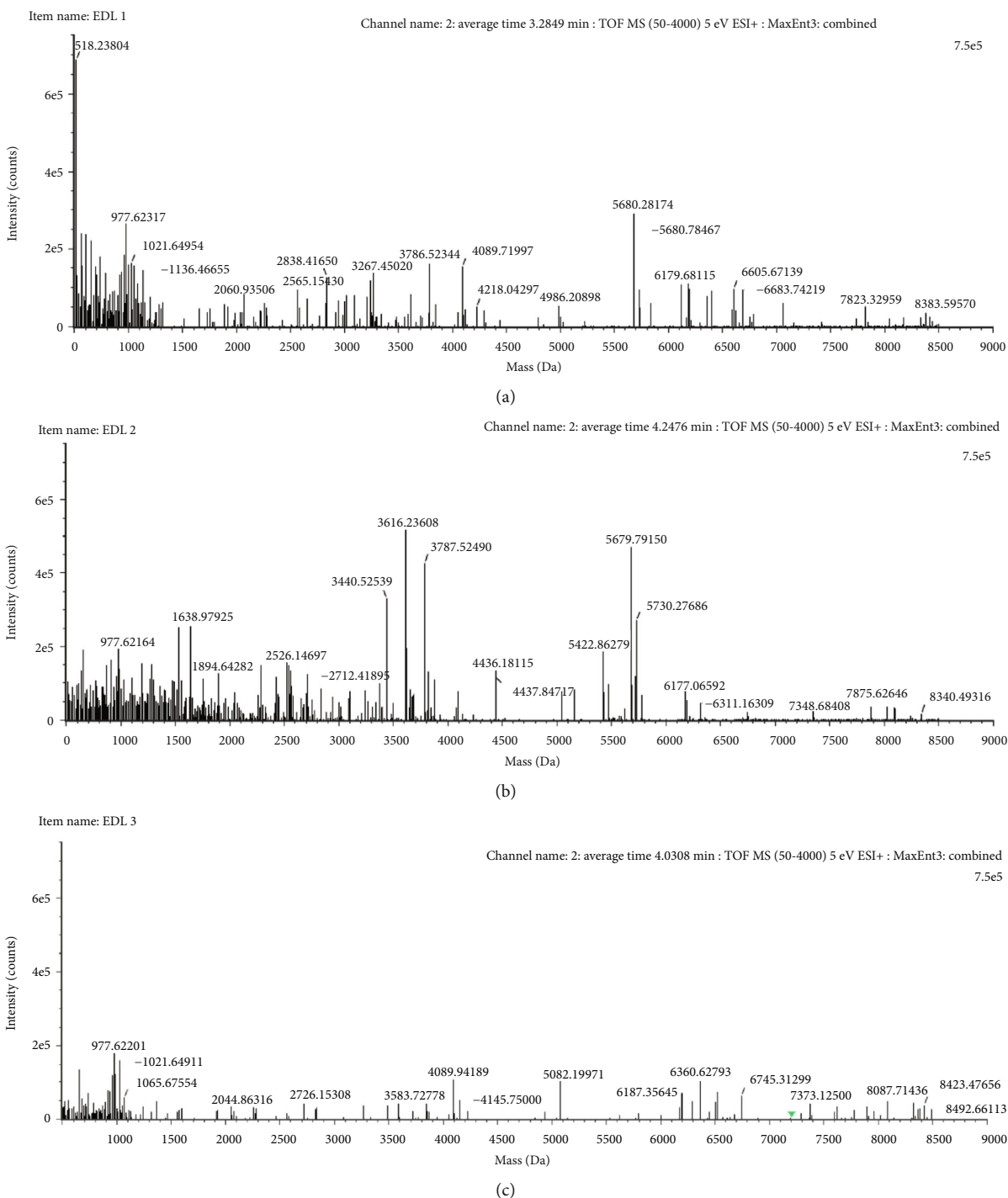


FIGURE 2: Immunomodulator exact mass distribution spectra obtained from (a) volunteer 1 with allergic rhinitis, (b) volunteer 2 with arthritis rheumatoid, and (c) volunteer 3 with chronic rhinopharyngitis. The horizontal and vertical axes show the mass in daltons and the intensity generated by ionized peptides, respectively.

Mass spectrometry grade water, formic acid, and acetonitrile were obtained from Sigma-Aldrich (MO, USA).

2.2. Methods

2.2.1. Size Exclusion Chromatography (SEC). A size exclusion chromatography analysis (SE-UPLC) was performed accord-

ing to Medina-Rivero et al. [3]. Briefly, 10 μL of each immunomodulator was injected in a Waters® BEH 125 SEC column (1.7 $\mu\text{m} \times 4.6 \times 150$ mm) using an Acquity UPLC Class-H system (Waters; MA, USA) with UV detection. A 50 mM phosphate-buffered solution (pH 6.8) was used as mobile phase. Data was acquired and processed with the Empower® software (Waters®).

TABLE 1: Design of the stability test of immunomodulator.

Test	Method	Time point for sample analysis (months)		
		0	3	6
Appearance	Visual	X	X	X
pH	Potentiometric	X	X	X
Total protein	UV	X	X	X
Mass distribution	SEC	X	X	X
Sterility	Microorganisms culture	X	ND	X

ND: not determined.

2.2.2. Mass Spectrometry (MS). MS analyses were performed according to our previous studies for the analysis of the quality attributes of complex molecules in order to demonstrate batch-to-batch consistency [4, 5]. In brief, peptide samples were separated and in-line desalted using a Waters® CSH C18 reverse phase column (1.7 μ m, 2.1 \times 150 mm) and a gradient from 0% to 25% of Acetonitrile with formic acid (0.1%) as a mobile phase. Analyte ions were obtained by electrospray ionization and analyzed using a quadrupole–time-of-flight (MS-Q-Tof) Vion® spectrometer coupled to an Acquity UPLC class H chromatograph (Waters®). Data was acquired and processed with the UNIFI® software (Waters).

2.2.3. Stability Test. A long-term stability test was performed in order to define the shelf life of the immunomodulator during a 6-month period under refrigeration conditions (5°C \pm 3°C). The samples were analyzed by appearance, pH, total protein by UV at 280 nm, SEC, and sterility every three months (0, 3, and 6 months).

3. Results and Discussion

The immunomodulators used for the treatment of chronic diseases were analyzed through SEC and MS, in order to demonstrate consistency and peptide distribution stability, unlike standard drugs which contain a single and well-defined compound as the active pharmaceutical ingredient (API) that complies with a quality specification. In biological products such as the immunomodulator peptide studied here, which is obtained from autologous urine, thus, differences in peptide sequences among patients are expected. Therefore, the consistency of the process is determined by the peptide polydispersity given by the molecular mass of distribution of the peptides and the total protein content along with other attributes such as appearance and safety testing.

3.1. Size Exclusion Analysis. Mixture peptide distribution obtained from the immunomodulator showed a peptide size range lower than 17.0 and 1.3 kDa, according to molecular weight markers. A main peak is showed in a retention time of 5.8 min, which corresponds to the formulation excipient (Figure 1). A robust process was designed to extract the immunomodulator from the same source in this case urine of a different volunteer for reinjecting treatment in order to obtain peptides in the expected size range as was showed in

the analysis of three independent samples studied by SEC (Figure 1). In these samples, the same range of size was observed but with a different relative abundance of peptide according to the chromatographic profile. The difference depends on the protein concentration, relative abundance, and type of peptides in the urine; it is well known that protein concentration could be increased in donors with some disease and even their urine could present different proteins to those that are normally found [15–17].

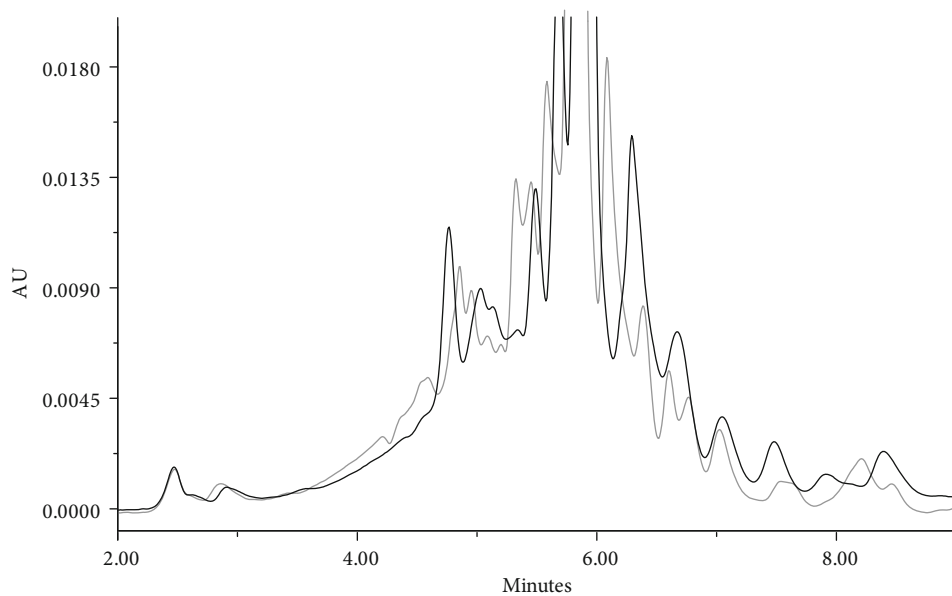
3.2. Mass Spectrometry Analysis. The mass spectrum criterium was based on the quantitative range of molecular mass of the peptides between 200 and 9000 Da. It confirms, orthogonally, the masses of SEC chromatographic profile. The results showed expected intrinsic differences in peptide abundance among samples. This intrinsic heterogeneity of peptides between volunteers is found in previous studies when screening peptides from urine in order to find diagnostic and prognostic makers, even to use them as therapy in the treatment for some disease [7, 8]. In all cases, the appearance of a high frequency of low molecular weight peptides lower than 2000 Da was found (Figure 2). The mass spectra of the samples from patients showed differences in the abundance of peptides (Figure 2). These mass spectra were obtained from deconvoluted m/z from reversed-phase chromatograms (Figure S1). This result demonstrated that the origin and abundance of peptides depend on the health status of the donor. Immunomodulators could have sequences of peptides that mimic the epitopes of several antigens that could explain why the immunomodulators could turn on or turn off the innate immune response as universal immunocorrectors. The personalized medicine, such as the present immunomodulator, could contain relevant peptides for the patient from which they were extracted. These peptides could induce a specific immune response that improves the condition of the patient.

3.3. Stability Test Analysis. The shelf life of the immunomodulator was performed during six months, analyzing every three months (Table 1). The results showed consistency in the critical quality attributes evaluated; in all cases, the expected results from each analysis were within the established specifications limits (Table 2). The results from this study allowed to establish shelf life stability of the product. The results by SEC in the independent samples showed the same molecular size distribution and similar chromatographic profile at started time and after six months of storage in refrigeration condition; the total area under the peaks is maintained, which suggests that the peptides are in solution without significant structural changes (Figure 3). Additionally, the size distribution profile remained was confirmed by MS after nine months at refrigeration (Figures S2). The immunomodulator obtained from a volunteer contains a high peptide heterogeneity in terms of size and sequence; even this heterogeneity is greater among volunteers, since it depends on the proteins that have been secreted in the urine. Therefore, the conservation of the peptide distribution is a stability-indicating analysis.

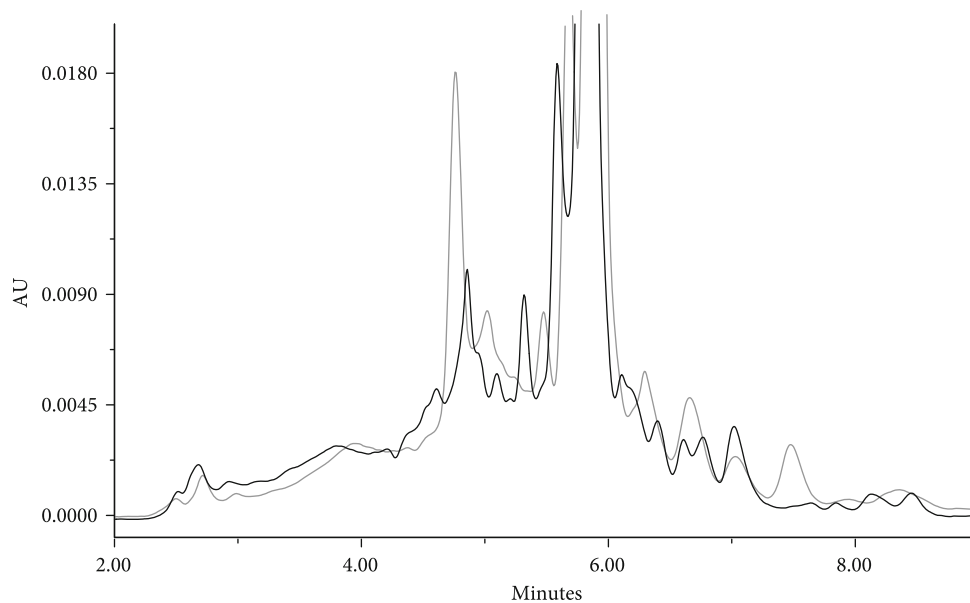
TABLE 2: Resume of stability test of the immunomodulator at $5 \pm 3^\circ\text{C}$.

Test	Specification	Results of the analyses in each time								
		V1	0 V2	V3	V1	3 V2	V3	V1	6 V2	V3
Appearance	Clear and colorless liquid	C	C	C	C	C	C	C	C	C
pH	5 to 7	6	6	6	7	7	7	7	7	7
Total protein	5.5 to 7.5 mg/mL	6.9	6.5	6.5	6.6	6.5	6.4	7.2	6.8	7.0
Mass distribution	Peptide distribution < 17.0 kDa	C	C	C	C	C	C	C	C	C
Sterility	Sterile	C	C	C	ND	ND	ND	C	C	C

ND: not determined; V: volunteer; C: comply.



(a)



(b)

FIGURE 3: Continued.

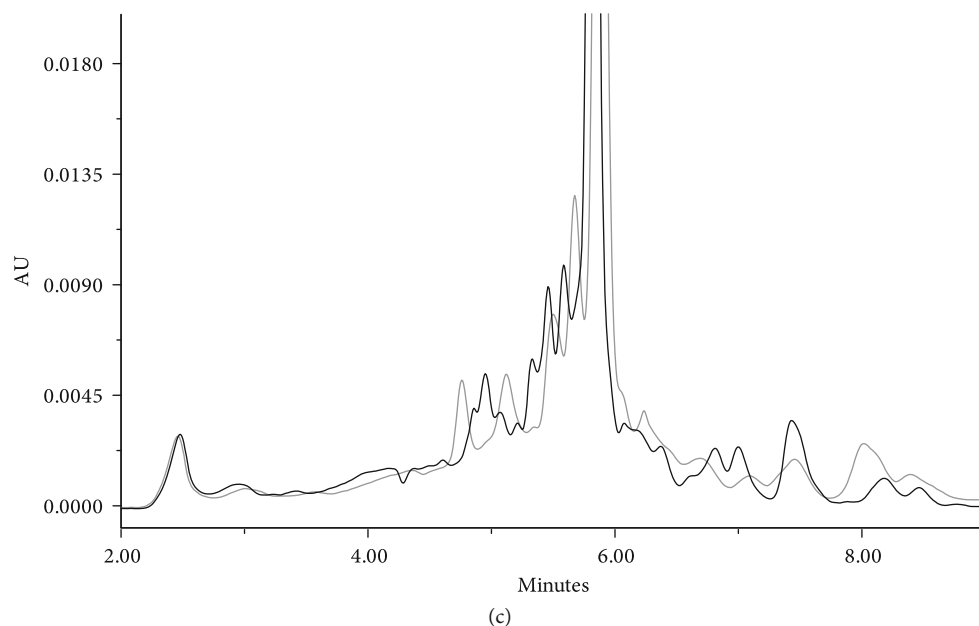


FIGURE 3: Size distribution profile of immunomodulator product by SEC during stability test at started time (gray line) and after six months (black line). The immunomodulator was produced from (a) volunteer 1, (b) volunteer 2, and (c) volunteer 3.

4. Conclusion

The consistency in the size distribution profile of complex mixture of peptides obtained by established process is reproducible among different volunteers; it is key to expect the desired response in the treatment of chronic immunological disorders such as allergies of the skin and mucosa, reactive arthritis, and psoriasis. In addition, the product showed to be stable, maintaining its critical quality attributes when it is stored between 5 and 8°C before its use. Therefore, this immunomodulator represents a viable alternative for the treatment of chronic immunological disorders.

Data Availability

No data were used to support this study.

Conflicts of Interest

Authors Fragoso, Pedraza-Jiménez, Espinoza-González, Ceja-Mendoza, Sánchez-Mercado, and Robles-Pérez are involved in the development and manufacturing of the immunomodulator. All other authors declare no competing interests.

Acknowledgments

We want to thank Dr. Ma Guadalupe Pérez Ruiz for believing, maintaining, and safeguarding the knowledge and research of Dr. M. Ruiz Castañeda and for preserving the institute that bears his name: Institute of Allergy and Autoimmunity Dr. M. Ruiz Castañeda. This work was supported by the Instituto de Alergias y Autoinmunidad Dr. Maximiliano Ruiz Castañeda A.C.

Supplementary Materials

Figure S1: reversed-phase base peak intensity profile of immunomodulators from volunteer 1 with allergic rhinitis (A), volunteer 2 with rheumatoid arthritis (B), volunteer 3 with chronic rhinopharyngitis (C), and matrix (D). Figure S2: exact mass distribution spectra of immunomodulators after storage at $5 \pm 3^\circ\text{C}$ for 9 months. (*Supplementary Materials*)

References

- [1] O. Corrales, L. Hernández, D. Prada et al., "CIGB-814, an altered peptide ligand derived from human heat-shock protein 60, decreases anti-cyclic citrullinated peptides antibodies in patients with rheumatoid arthritis," *Clinical Rheumatology*, vol. 38, no. 3, pp. 955–960, 2019.
- [2] B. J. Coventry, "Therapeutic vaccination immunomodulation: forming the basis of all cancer immunotherapy," *Therapeutic Advances in Vaccines and Immunotherapy*, vol. 7, 2019.
- [3] E. Medina-Rivero, G. Merchand-Reyes, L. Pavón et al., "Batch-to-batch reproducibility of Transferon™," *Journal of Pharmaceutical and Biomedical Analysis*, vol. 88, pp. 289–294, 2014.
- [4] C. A. López-Morales, S. Vázquez-Leyva, L. Vallejo-Castillo et al., "Determination of peptide profile consistency and safety of collagen hydrolysates as quality attributes," *Journal of Food Science*, vol. 84, no. 3, pp. 430–439, 2019.
- [5] S. Vázquez-Leyva, L. Vallejo-Castillo, C. A. López-Morales et al., "Identity profiling of complex mixtures of peptide products by structural and mass mobility orthogonal analysis," *Analytical Chemistry*, vol. 91, no. 22, pp. 14392–14400, 2019.
- [6] A. M. Gonzalez-Angulo, B. T. J. Hennessy, and G. B. Mills, "Future of personalized medicine in oncology: a systems biology approach," *Journal of Clinical Oncology*, vol. 28, no. 16, pp. 2777–2783, 2010.
- [7] D. M. Good, P. Züribig, À. Argilés et al., "Naturally occurring human urinary peptides for use in diagnosis of chronic kidney

- disease,” *Molecular & Cellular Proteomics*, vol. 9, no. 11, pp. 2424–2437, 2010.
- [8] F. Guangzhen, N. Liu, L. Chu, and M. Zhang, “Screening high abundance of peptide for making examination possible in human urine,” *Annals of Clinical & Laboratory Science*, vol. 45, pp. 264–269, 2015.
- [9] G. Acosta, M. Garcia, J. Vásquez, M. Hernández, and M. E. Elevated concentration of interleukine IL-10 and IL-2 in the urinary immunomodulator, M. R. Castañeda, Ed., 10th International Congress of Immunology, New Delhi, India, 1998.
- [10] M. C. Ruíz, “A simple test for detection of specific and unspecific immunological reactions in cancer,” *Archivos de Investigacion Medica*, vol. 11, no. 1, pp. 83–93, 1980.
- [11] N. J. Schork, “Personalized medicine: time for one-person trials,” *Nature*, vol. 520, no. 7549, pp. 609–611, 2015.
- [12] S. D. Martin, G. Coukos, R. A. Holt, and B. H. Nelson, “Targeting the undruggable: immunotherapy meets personalized oncology in the genomic era,” *Annals of Oncology*, vol. 26, no. 12, pp. 2367–2374, 2015.
- [13] V. Le Joncour and P. Laakkonen, “Seek & Destroy, use of targeting peptides for cancer detection and drug delivery,” *Bioorganic & Medicinal Chemistry*, vol. 26, no. 10, pp. 2797–2806, 2018.
- [14] O. B. Cano, *Doctor Maximiliano Ruiz Castañeda: Eminente Científico Mexicano*, Universidad Nacional Autónoma de México. Facultad de Medicina, 1st edition, 2019.
- [15] A. Thomas, C. Görgens, S. Guddat et al., “Simplifying and expanding the screening for peptides <2 kDa by direct urine injection, liquid chromatography, and ion mobility mass spectrometry,” *Journal of Separation Science*, vol. 39, no. 2, pp. 333–341, 2016.
- [16] E. Semenistaya, I. Zvereva, G. Krotov, and G. Rodchenkov, “Solid-phase extraction of small biologically active peptides on cartridges and microelution 96-well plates from human urine,” *Drug Testing and Analysis*, vol. 8, no. 9, pp. 940–949, 2016.
- [17] E. Nkuipou-Kenfack, A. Bhat, J. Klein et al., “Identification of ageing-associated naturally occurring peptides in human urine,” *Oncotarget*, vol. 6, no. 33, pp. 34106–34117, 2015.

Research Article

West Nile Virus Vaccine Design by T Cell Epitope Selection: *In Silico* Analysis of Conservation, Functional Cross-Reactivity with the Human Genome, and Population Coverage

Frances M. Waller,¹ Pedro A. Reche ², and Darren R. Flower ¹

¹*School of Life and Health Sciences, Aston University, Aston Triangle, Birmingham, UK B4 7ET*

²*Immunomedicine Group, Facultad de Medicina, Departamento de Inmunología & O2, Universidad Complutense de Madrid, Madrid, Spain*

Correspondence should be addressed to Pedro A. Reche; parecheg@med.ucm.es and Darren R. Flower; darrenflower@googlemail.com

Received 21 September 2019; Accepted 5 December 2019; Published 19 March 2020

Academic Editor: Bogdan Kolarz

Copyright © 2020 Frances M. Waller et al. This is an open access article distributed under the Creative Commons Attribution License, which permits unrestricted use, distribution, and reproduction in any medium, provided the original work is properly cited.

West Nile Virus (WNV) causes a debilitating and life-threatening neurological disease in humans. Since its emergence in Africa 50 years ago, new strains of WNV and an expanding geographical distribution have increased public health concerns. There are no licensed therapeutics against WNV, limiting effective infection control. Vaccines represent the most efficacious and efficient medical intervention known. Epitope-based vaccines against WNV remain significantly underexploited. Here, we use a selection protocol to identify a set of conserved prevalidated immunogenic T cell epitopes comprising a putative WNV vaccine. Experimentally validated immunogenic WNV epitopes and WNV sequences were retrieved from the IEDB and West Nile Virus Variation Database. Clustering and multiple sequence alignment identified a smaller subset of representative sequences. Protein variability analysis identified evolutionarily conserved sequences, which were used to select a diverse set of immunogenic candidate T cell epitopes. Cross-reactivity and human leukocyte antigen-binding affinities were assessed to eliminate unsuitable epitope candidates. Population protection coverage (PPC) quantified individual epitopes and epitope combinations against the world population. 3 CD8⁺ T cell epitopes (ITYTDVLRV, TLARGFPFV, and SYHDRRWCF) and 1 CD4⁺ epitope (VTVNPFVSVATANAKVLI) were selected as a putative WNV vaccine, with an estimated PPC of 97.14%.

1. Introduction

West Nile Virus (WNV) is a mosquito-borne Flavivirus that causes West Nile Fever (WNF) and West Nile neuroinvasive disease (WNND) in birds, humans, and horses [1]. Originating in the West Nile regions of Uganda in 1937, WNV has now become a prevalent human infection. Before mid-1990, the virus was confined to Africa and Europe, then spread to North America, the Middle East, and West Asia. Two and a half million cases were reported between 1999 and 2010, of which, 12,000 were WNND, resulting in over 1300 deaths. Thus, WNV has become a major global public health concern.

WNV infection manifests as one of three disease states: asymptomatic carrier, West Nile Fever (WNF), and West Nile neuroinvasive disease (WNND) [1]. After the initial mosquito bite, 3-14 days elapse before the first symptoms, with rapid progression thereafter. Asymptomatic carriers represent 75% of all cases, with 25% presenting with WNF or WNND [2]. WNF is a mild, self-limiting disease which presents as general fever, malaise, and muscle and gastrointestinal pain [3]. Overall mortality is ~4.2% but rises to 9.6% in WNND.

WNV is part of the Flavivirus genus, which comprises over 70 viruses and many human pathogens, including numerous mosquito-borne viruses [4]. WNV is transmitted

from an infected host via a mosquito bite, primarily by the *Culex* spp. and to a lesser extent the *Aedes* spp. [5]. Human and equine infections occur outside the natural transmission lifecycle sustained between mosquitos and birds [6]. Horses and humans are “dead-end” hosts, unable to reinfect mosquitos due to insufficient viremia [4].

The WNV genome comprises a single-stranded nonsegmented positive sense RNA of ~11,000 nucleotides [7]. It is transcribed into a single polyprotein, which is cleaved by viral proteases into ten mature viral proteins: three 5' structural segments (C, PrM, and E) and seven 3' nonstructural protein elements (NS1, NS2A, NS2B, NS3, NS4A, NS4B, and NS5). Phylogenetic analysis suggests that there are at least seven distinct WNV lineages [8]. While infection from other lineages is known, major human outbreaks arise solely from lineages 1, 2, and 5 [6].

There are no current FDA-approved WNV treatments. Reducing exposure to mosquitos is the main strategy, via mosquito nets, protective clothing, and insect repellent and by staying indoors [8]. In the absence of viable therapeutic interventions, effective vaccines could provide long-term protection against WNV. No commercial human WNV vaccines exist [9], but successful vaccines for closely related Flaviviruses—Japanese encephalitis virus, tick-borne virus, and Yellow Fever virus—suggest that an effective, well-tolerated WNV vaccine is feasible [10]. Adaptive immune responses promote viral clearance and control WNV infection [11]. Several novel vaccine candidates are currently in phase I and phase II clinical trials [12], yet WNV clinical trials face several challenges including late or sporadic presentation of symptoms, asymptomatic carriers, inconsistency of outbreaks, trial logistics, and comorbidities in the elderly [8].

The only trialed WNV inactivated vaccine comprised a minimally pathogenic Kunjin virus incubated with hydrogen peroxide [9]. PrM and E proteins of lineages 1 and 2 have been exploited as subunit vaccines. Lineages 1 and 2 can provide crossprotection against other lineages suggesting that a single universal vaccine is feasible [13]. Recent approaches have tried to induce neutralising antibodies by targeting highly immunogenic E antigens. Capitalising on the successful equine vaccine PreveNile [12], the most promising current human vaccine, ChimeriVax-WN02, uses the Yellow Fever 17D backbone to incorporate PrM and E genes [10]. Three gene mutations (L107F, A316V, and K440R) attenuated the virus [13].

PrM, E, NS3, and NS4B proteins are commonly targeted by CTLs [11]. Long-lasting immunity has been achieved in phase I subunit vaccine trials using adjuvants and DIII regions of the WNV E protein [4]. A DNA vaccine expressing the NY99 capsid protein generates a strong CD4+ immune response with a significant rise in IL-2 and IFN- γ levels [12]. Vaccines expressing domain II of the E protein have produced WNV-neutralising antibodies in phase I trials [9].

The lack of extant WNV vaccines prompts us to evaluate potential epitope ensemble vaccines as an alternative, exploiting our evolving approach to vaccine design. We have exemplified this by identifying putative vaccines against hepatitis C [14], influenza [15], malaria [16], Epstein-Barr virus [17], TB [18, 19], and dengue [20]. By focusing on highly

conserved immunogenic epitopes with a broad population coverage, we identified optimal selections of prevalidated epitopes of proven immunogenicity. To avoid undesired immunogenicity in designed vaccines, we extend our prior work here to filter out epitope cross-reactivity with the human genome.

2. Methods

2.1. Identification of West Nile Virus CD8+ and CD4+ T Cell Epitopes. Experimentally confirmed West Nile epitopes (ID: 11082) were retrieved from the Immune Database and Analysis Resource (IEDB) (<http://www.iedb.org/>). Epitopes were restricted to host “Humans,” “T cell Assays,” “Positive Assays,” and “Any MHC restrictions.” CD8+ and CD4+ data were collected separately.

2.2. Acquisition, Processing, and Alignment of the West Nile Virus Polyprotein. Complete West Nile Virus genome sequences for all human variants and lineages were obtained from the National Centre for Biotechnology Information (NCBI) West Nile Virus Variation Database Resource (URL: <https://www.ncbi.nlm.nih.gov/genome/viruses/variation/WestNile/>). Incomplete and duplicated sequences were removed. Sequences were clustered using CD-HIT (URL: http://weizhongli-lab.org/cdhit_suite/cgi-bin/index.cgi?cmd=cd-hit) to form a set of representative sequences. Identified cut-off was 0.99. The clustered sequences were multiply aligned using MUSCLE (URL: <http://www.ebi.ac.uk/Tools/msa/muscle/>) to form multiple sequence alignment (MSA).

2.3. Analysis of Epitope Sequence Variability. Conserved epitopes were identified by analysing conservation of the MSA, using the Protein Variability Server (PVS) [21] (URL: <http://imed.med.ucm.es/PVS/>). The first sequence in the alignment was used as a reference. Sequence variability was masked, and only fragments with a length greater or equal to 9 were selected. The Shannon entropy threshold was 0.5. CD8+ and CD4+ epitopes with at least 50% overlap were retained for subsequent analysis.

2.4. Analysis of Epitope Cross-Reactivity. CD8+ cross-reactivity was analysed using iCrossR (URL: <http://webclu.bio.wzw.tum.de/icrossr/>) after determining class I binding profiles, as below. The number of mismatches was set to “0, 1, 2, and 3” for each binding prediction. Epitopes with a cross-reactivity index (ICR) of 0.01 or greater were removed.

2.5. HLA Binding Profile Prediction and Calculation of Population Protection Coverage (PPC). Binding affinities of conserved CD8+ (<http://tools.iedb.org/mhci/>) and CD4+ (<http://tools.iedb.org/mhcii/>) T cell epitopes were predicted using IEDB. HLA I reference set was used for MHC I epitopes (Weiskopf, Angelo et al. 2013) and an HLA II reference set was used for MHC II epitopes (Greenbaum et al. [22]) Class I binding profiles present in the top one percentile rank were retained. For MHC Class II, epitopes less than 15 amino acids in length were eliminated and binding profiles in the top five percentile rank were obtained.

Conserved CD8+ epitopes were also analysed using EPI-SOPT (URL: <http://bio.med.ucm.es/episopt.html>) selecting all ethnic groups in the US population (Caucasian, Black, Hispanic, Asian, and native North American) and a PPC above 95%. Global PPC values for highly-conserved epitopes were calculated using IEDB (http://tools.iedb.org/tools/population/iedb_input). MHC I and MHC II epitopes were then ranked by PPC. Epitopes were combined within each class to calculate overall PPC values. To create a potential 'universal' vaccine candidate CD8+ and CD4+ epitopes were combined and PPC calculated using IEDB as above.

3. Results

Searching IEDB identified 165 linear CD4+ and CD8+ T cell epitopes presented to T cells during WNV infection: 53 HLA class I and 112 HLA class II epitopes. Epitope length ranged from 8 to 20 amino acids. Genomic sequences representing all strain variants of WNV were also retrieved from the NCBI West Nile Virus Variation Database. 126 unique protein sequences were retrieved. AJR27178, AJR27181, and AJR27181; AJW82677 and AKH144860; and AJW59216 and AJW59220 were found to be identical. Only unique sequences were retained. Sequence clustering using CD-HIT identified nonredundant sequences representative of all WNV sequences. All major human lineages were present; 5 sequences were generated with two representing lineage 2: AJW59217 (USA, 2002), AJR27898 (Italy, 2014), AHB37632 (Italy, 2013/08), AMZ00438 (India, 1988/02/12), and ALK02494 (Australia, 1991). AHB37632 was discarded due to sequence anomalies.

A multiple sequence alignment (MSA) was performed on the remaining 4 sequences. All four lineages were highly conserved: 3069 positions had identical amino acids (89.37%), and only 64 positions showed variable amino acids (1.87%). The remainder was either partially conserved (3.17%) or highly conserved (5.59%). Analysis with PVS showed that 122 of the 165 epitopes had $\geq 50\%$ sequence identity to the masked WNV reference sequence: 32 CD8+ 9mers, three 10mers, and one 11mer, with 19 epitopes showing 100% sequence identity; 86 CD4+ epitopes had $\geq 50\%$ sequence identity, with 19 of the 86 epitopes showing 100% sequence identity.

As therapeutic peptides can evoke autoimmune responses, conserved epitopes were screened computationally to detect undesirable cross-reactivity against human tissues. Cross-reactivity (CR) was computed using iCrossR for HLA-I 9mer epitopes only. The output for each mutation was averaged to calculate an overall cross-reactivity index (ICR).

Our results show that none of the epitopes have an ICR greater than 0.01; thus, it seems unlikely that self-antigen recognition and toxic effects would occur; when tested at the three mutation levels, many epitopes did exhibit CR. HLA-I binding profiles and PPC were calculated using EPISOPT and IEDB. All CTL 9mer epitopes were entered into EPISOPT to estimate the PCC for the five US ethnic groups (see Table 1). ITYTDVLRV had the largest number of binding alleles (10) and the highest PPC. EPISOPT analysis

showed that a PPC > 95% could be reached using HLA-I alleles alone.

Using three epitopes, the maximum PPC was 97.65%, with 24 distinct class I restrictions: TLARGFPFV, GPIRFVLAL, and ITYTDVLRV. 190 different combinations of four epitopes achieved a PPC > 95%. TLARGFPFV and ITYTDVLRV were present in most highly scoring epitope sets, with many epitopes absent from all candidate ensembles.

HLA-I binding profiles were also obtained using IEDB. Peptides in the top 1% rank were retained to ensure strong binding and sufficient immunogenicity. More HLA-A binding alleles (14) were seen than HLAB (9). The IEDB PPC tool predicted that the top EPISOPT ensemble had only an 84.68% PPC. To achieve a PPC of >95%, 6 epitopes are needed: TLARGFPFV, ITYTDVLRV, KSYETEYPK, SYHRRWCF, MPNGLIAQF, and GPIRFVLAL (see Table 2).

HLA-II binding profiles were estimated using IEDB, retaining epitopes in the top 5% rank. PPC calculation showed that individual epitopes had a relatively high PPC, with 8 having values over 50%. VTVNPFVSVATANAKVLI and GEFLDLRPATAWSLYAV had the highest value: 70.55%. ILVSLAAVVVNPSVKTVR and VTVNPFVSVATANAKVLI achieved a combined PPC of 81.81%. The addition of further epitopes had no effect. Many CD4+ epitopes had binding profiles that were subsets of other epitopes. These epitopes were removed, leaving a set of HLA-II alleles covering all epitopes (see Table 3). Many of the high-scoring epitopes also had overlapping binding profiles.

Both CD4+ and CD8+ T cells are important in viral clearance. CD8+ and CD4+ epitopes were combined to calculate a PPC, using the PPC tool on IEDB. By combining the top two epitopes from each HLA subset VTVNPFVSVATANAKVLI and ILVSLAAVVVNPSVKTVR, and ITYTDVLRV and TLARGFPFV, a PPC of 96.36% was achieved. A vaccine ensemble comprising ITYTDVLRV, TLARGFPFV, and SYHRRWCF and VTVNPFVSVATANAKVLI covered 97.14% of the world's populations. This increased to 99.52% when using 11 epitopes (see Table 4).

4. Discussion

West Nile Virus has been recognized as a reemerging global pathogen. Present in Africa for over 50 years, recent geographical transmission has raised its profile as a public health concern. There are no current effective treatments, and the cost-to-benefit ratio of the WNV development pipeline is poor. Vaccination is a key intervention. An efficacious WNV vaccine could significantly benefit the global population. Vaccines are available for closely related Flaviviruses and against equine WNV, resulting in a significant reduction in annual mortalities. Veterinary vaccine Equilis West Nile is an inactivated whole virus vaccine comprising a strain known as Yellow Fever-West Nile. The vaccine is given to horses over six months via 2 intramuscular injections, 3 to 5 weeks apart, with a single booster injection given a year later. In comparative evaluations, correlates of protection were seen in 89-94% of treated animals in different test groups. Most previous candidate WNV vaccines have relied on B cell-mediated immunity. Here, we attempt to identify

TABLE 1: HLA-I binding profiles and population protection coverage calculated by EPISOPT and IEDB for the five main ethnic groups.

(a) EPISOPT		
Peptide	HLA-I binding profile EPISOPT	PPC (%)
ITYTDLVRLY	A0301 A1101 A6801 B1502 B1516 B1517 B2702 B2709 B5502 C0702	44.66
TLARGFPFV	A0201 A0202 A0203 A0204 A0205 A0206 A6802	34.52
SLFGGMSWI	A0201 A0202 A0206 B1508	27.58
KSYETEYPK	A1101 A3101 A3301 A6801	14.86
LYRHKVVK	A0301 A1101 A3101 A3301 A6801 B1502	32.51
RVLSLIGLK	A0203 A0301 A1101 A3101	24.47
AVVVNPSVK	A0301 A1101	17.83
SYHRRWCF	A2402 C0702	22.05
RYLVKTESW	B1513 B5701 B5702	2.48
MPNGLIAQF	B0702 B1502 B1508 B3501 B3801 B5301 B5401 B5702 B5801	35.45
GPIRFVLAL	A0203 A0214 B0702 B0801 B3501 B5301 B5401 C0304	44.48
AEVEEHRTV	A2902 B4002	7.11
WMDSTKATRY	—	0
KGDTTTGVY	B1516 B5702 B5801	2.13
VVEKQSGLY	A1101	4.70
QTDNQLAVF	A0207 B3801 B5702 B5801	3.71
ALRGLPIRY	A0201 A0203 A0301 B1517	27.34
TEVMTAVGL	A2902 B39011 B3909 B4002 B4402	12.41
MTTEDMLEVW	—	0
RPAADGKTV	B0702 B5101 B5102 B5103 B5401 B5502	18.59
ILRNPGYAL	A0202 A0206 A0214 B0702 B1502 C0304	29.62
RVLEMVEDW	B1513 B5701 B5702 B5801	5.79
RSLFGGMSW	B5701	1.93
RAWNSGYEW	B5801	1.59
HTTKGAALM	B1510	0
SVGGVFTSV	A0201 A0202 A0203 A0206	28.88
VLNETTNWL	A0201	18.04
SLVNGVVRL	A0201 A0202 A0203 A0205 A0206 A0214 B1510 B1517 B3909	34.47
FVDVGVSAI	A0204 A0205 A0206 A0207 A0214 B3801 C0102	6.65
YRHKVVKVM	B1510 B2701 B3801 B39011 B3909	3.94
RRSRSLTV	B2703 B2704 B2705 B2706 B2709	2.39
ATWAENIQV	A0202 A0204 A0205 A0207 A0209 B1516	1.49

(b) IEDB

Peptide	HLA-I binding profile IEDB (top 1 percentile rank)	PPC (%)
ITYTDLVRLY	A0101 A0301 A3002 B5801 B5701 A2601 A1101	54.74
TLARGFPFV	A0206 A0203 A0201	41.35
SLFGGMSWI	A0203 A0201	39.84
KSYETEYPK	A1101 A0301 A3001 A3101	38.48
LYRHKVVK	A0301 A1101 A3101	35.36
RVLSLIGLK	A0301 A1101 A3001	34.14
AVVVNPSVK	A1101 A0301	30.92
SYHRRWCF	A2301 A2402	26.18
RYLVKTESW	A2301 A2402	26.18
MPNGLIAQF	B5301 B3501 B0702	22.88
GPIRFVLAL	B0702 B0801	22.61
AEVEEHRTV	B4403 B4001 B4402	20.88
WMDSTKATRY	A0101 A3002	19.55
KGDTTTGVY	A3002 A0101	19.55
VVEKQSGLY	A3002 A0101	19.55
QTDNQLAVF	A0101	17.34
ALRGLPIRY	A0301	16.81
TEVMTAVGL	B4001 B4403	13.83
MTTEDMLEVW	B5701 A6802 A0206 B5301 B5801	13.7
RPAADGKTV	B0702	12.78
ILRNPGYAL	B0702	12.78
RVLEMVEDW	B5701 B5801 A3201	11.53
RSLFGGMSW	B5701 B5801 A3201	11.53
RAWNSGYEW	B5701 B5801	7.26
HTTKGAALM	A2601	5.82
SVGGVFTSV	A6802 A0203	3.46
VLNETTNWL	A0203	0.97

highly conserved T cell epitopes that might form an epitope ensemble sufficiently immunogenic to protect against geographically diverse WNV strains.

Epitopes in adoptive immunotherapies may exhibit undesired side effects [23], such as CR when foreign peptide sequences resemble those of self-peptides sufficiently to initiate an unwanted autoimmune response. Addition of computational CR prediction to our design-by-selection protocol is a key advance over previous work [14–20] and should accelerate the early selection of safe vaccines. When using iCrossR [23], none of the epitopes were identified to elicit responses cross-reactive with human tissues. McMurtrey et al. [24] and Kaabinejadian et al. [25] identified epitopes presented by HLA-A*02:01 and HLA-A*11:01, and many were also selected by our approach, including RVL9, SVG9, TLA9, KYS9, AVV9, RLD10, ATW9, and SLT9. YTM9, SLF9, and KNM9 were eliminated as they lacked $\geq 50\%$ sequence identity to the viral reference.

No single epitope provided protection against WNV. A PPC > 95% was only possible when multiple epitopes were combined. A potent immune response needs both CD4+ and CD8+ T cell responses [26]. Combined epitopes generate

TABLE 2: Candidate epitope ensemble vaccines with >95% PPC, as calculated by EPISOPT and IEDB.

Ensemble	Method	Peptides	PPC
1	EPISOPT	TLARGFPFV ITYTDVLRV	GPIRFVLAL 99.00
2	EPISOPT	TLARGFPFV ITYTDVLRV	GPIRFVLAL MPNGLIAQF 99.00
3	EPISOPT	TLARGFPFV TEVMTAVGL MPNGLIAQF	ITYTDVLRV 99.23
4	EPISOPT	TLARGFPFV ITYTDVLRV	GPIRFVLAL 97.65
5	IEDB	TLARGFPFV KSYETEYPK MPNGLIAQF AEVEEHRTV MTTEDMLEVW RSLFGGMSW	ITYTDVLRV SYHRRWCF GPIRFVLAL 97.34
6	IEDB	TLARGFPFV KSYETEYPK MPNGLIAQF AEVEEHRTV MTTEDMLEVW	ITYTDVLRV SYHRRWCF GPIRFVLAL 96.81
7	IEDB	TLARGFPFV KSYETEYPK MPNGLIAQF AEVEEHRTV	ITYTDVLRV SYHRRWCF GPIRFVLAL 96.49
8	IEDB	TLARGFPFV KSYETEYPK MPNGLIAQF GPIRFVLAL	ITYTDVLRV SYHRRWCF 95.25

TABLE 3: Subset of epitopes that represent all HLA-II alleles by elimination of repetitive binding profiles.

Epitope	HLA-II binding profile top 5 percentile rank	PPC
VTVNPVSVATANAKVLI	HLA-DRB1*08:02, HLA-DRB1*04:01, HLA-DRB1*09:01, HLA-DRB1*11:01, HLA-DRB1*04:05, HLA-DRB1*01:01, HLA-DRB3*02:02, HLA-DRB5*01:01, HLA-DRB1*07:01, HLA-DRB1*13:02, HLA-DRB1*15:01, HLA-DQA1*01:02/DQB1*06:02	70.55
ILVSLAAVVVNPSVKTVR	HLA-DRB1*08:02, HLA-DRB1*01:01, HLA-DRB1*03:01, HLA-DRB1*04:01, HLA-DQA1* 01:02/DQB1*06:02, HLA-DRB1*12:01, HLA-DRB1*04:05, HLA-DRB1*15:01, HLA-DRB1*13:02, HLA-DQA1*05:01/DQB1*03:01, HLA-DRB1*11:01, HLA-DRB3*02:02	69.22
RVVFFVLLLLVAPAYS	HLA-DPA1*03:01/DPB1*04:02, HLA-DPA1*02:01/DPB1*01:01, HLA-DRB1*11:01, HLA-DPA1*01:03/DPB1*02:01, HLA-DPA1*01/DPB1*04:01, HLA-DRB1*12:01, HLA-DRB1* 08:02, HLA-DRB1*15:01, HLA-DRB1*04:01, HLA-DRB1*04:05, HLA-DPA1*02:01/DPB1*05:01, HLA-DRB1*01:01, HLA-DRB3*01:01, HLA-DRB5*01:01, HLA-DRB1*03:01, HLA-DQA1* 05:01/DQB1*02:01	65.33
SGNVVHSVNMSTQVLLGR	HLA-DRB1*03:01, HLA-DRB1*07:01, HLA-DRB1*04:05, HLA-DRB1*04:01, HLA-DRB1*11:01, HLA-DQA1*01:02/DQB1*06:02, HLA-DRB1*08:02, HLA-DRB1*13:02, HLA-DRB4*01:01, HLA-DRB1*04:01	59.32
VLSLIGLKRAMSLIDGK	HLA-DRB1*08:02, HLA-DRB1*11:01, HLA-DRB1*09:01, HLA-DRB5*01:01, HLA-DRB1*03:01, HLA-DPA1*02:01/DPB1*14:01, HLA-DRB4*01:01, HLA-DRB3*02:02, HLA-DRB1*15:01, HLA-DPA1*02:01/DPB1*01:01	49.41
LVQSYGWNIVTMKSGVDV	HLA-DRB1*07:01, HLA-DRB5*01:01, HLA-DQA1*01:01/DQB1*05:01, HLA-DRB1*15:01 HLA-DRB1*09:01, HLA-DQA1*04:01/DQB1*04:02, HLA-DQA1*03:01/DQB1*03:02,	34.78
GLLSYQAGAGVMVEGVF	HLA-DRB1*07:01, HLA-DQA1*01:02/DQB1*06:02, HLA-DQA1*05:01/DQB1*03:01, HLA-DRB1*01:01	34.02

TABLE 4: Final epitope combinations corresponding to candidate epitope ensemble vaccine and PPC.

Ensemble	HLA-I epitopes	HLA-II epitopes	PPC (%)
1	ITYTDVLRV TLARGPPFV	VTVNPFFSVATANAKVLI ILVSLAAVVVNPSVKTVR	96.36
2	ITYTDVLRV TLARGPPFV SYHRRWCF	VTVNPFFSVATANAKVLI	97.14
3	ITYTDVLRV TLARGPPFV KSYETEYPK	VTVNPFFSVATANAKVLI	95.23
4	ITYTDVLRV TLARGPPFV KSYETEYPK SYHRRWCF	VTVNPFFSVATANAKVLI ILVSLAAVVVNPSVKTVR	98.71
5	ITYTDVLRV TLARGPPFV KSYETEYPK SYHRRWCF MPNGLIAQF	VTVNPFFSVATANAKVLI ILVSLAAVVVNPSVKTVR	99.01
6	ITYTDVLRV TLARGPPFV KSYETEYPK SYHRRWCF MPNGLIAQF GPIRFVLAL AEVEEHRV MTTEDMLEVW RSLFGGMSW	VTVNPFFSVATANAKVLI ILVSLAAVVVNPSVKTVR	99.52

greater T cell responses than a single epitope, reinforcing the need for multiple conserved epitopes [27]. At least four epitopes were needed for a PPC > 95%. HLA class I 9mers (TLA9, SYH9, and ITY9) combined with one HLA-II epitope (VTV18n) gave a cumulative population coverage of 97.14%.

Virus replication introduces mutations which can eventually generate new strains or alter existing ones; yet, we found that 90% of the WNV sequence is conserved ($H < 0.5$). This lack of variability is an aid to vaccine design as conserved regions can be exploited as therapeutic targets, as newly emerging strains retain conserved amino acids. CD-HIT was used to remove redundant protein sequences. While remaining sequences represented the most common human WNV lineages (1a, 1b, 2, and 5), the less common lineages (3 and 4) were excluded. To generate a truly universal vaccine, crossprotection against all WNV lineages and strains should be investigated. Thus, a second-generation WNV vaccine may need inclusion of lineages 3 and 4.

All T cell epitopes included in our final vaccine combination were either located in the E protein (VTV18), NS2A (ITY9), NS3 (SYH9), or NS4B (TLA9). Finding highly conserved epitopes in the E protein, NS3, and NS4B is expected, since previous work has shown these proteins to be highly immunogenic and common targets for CTLs [11, 28]. Variability across the genome is uneven, with the structural proteins being the least variable [29].

The C region has the highest proportion of residue alterations (~23%) [30]. The E protein has been exploited in previous vaccine design: most current DNA vaccine candidates against Flaviviruses express the viral E and PrM proteins [31]. Sarri and coworkers identified HLA alleles responsible for susceptibility to WNV infection. They categorized HLA alleles to be either “protective,” increased “susceptibility,” or CNS-high risk [32]. None of the protective binding alleles suggested by Sarri et al. were identified here. This “protective” function of HLA alleles could be exploited in WNV vaccine development to provide protection for all ethnicities.

By considering functional cross-reactivity with human proteins, the work described here represents a step forward in our evolving approach to vaccine design. Work based on naive sequence similarity have not previously proved useful [33–35]. Here, it proved possible to combine 4 epitopes—3

CD8+ and 1 CD4+ T cell epitopes—to achieve a global PPC of 97.14%. Combined CTL and CD4+ are required for successful viral clearance. The ensemble identified is a viable starting point for further in vitro characterization or phase 0 trials, since we can assume that this epitope selection is likely both safe and immunogenic in the majority of most populations. This paper emphasises the application of computational cross-reactivity prediction to vaccine design, only allowing selection of epitopes without either structural or sequence similarity to the human genome. Overall, our work provides a promising starting point for the exploration of next-generation WNV vaccines.

Data Availability

Data is available from <http://www.iedb.com> and available from the authors.

Conflicts of Interest

The authors declare that they have no conflicts of interest.

Funding

This research was supported by grant BIO2014:54164-R to PAR.

Acknowledgments

We wish to thank Aston University for supporting this research.

References

- [1] T. M. Colpitts, M. J. Conway, R. R. Montgomery, and E. Fikrig, “West Nile virus: biology, transmission, and human infection,” *Clinical Microbiology Reviews*, vol. 25, no. 4, pp. 635–648, 2012.
- [2] I. J. Amanna and M. K. Slifka, “Current trends in West Nile virus vaccine development,” *Expert Review of Vaccines*, vol. 13, no. 5, pp. 589–608, 2014.
- [3] J. J. Sejvar, “The long-term outcomes of human West Nile virus infection,” *Clinical Infectious Diseases*, vol. 44, no. 12, pp. 1617–1624, 2007.

- [4] M. De Filette, S. Ulbert, M. Diamond, and N. N. Sanders, "Recent progress in West Nile virus diagnosis and vaccination," *Veterinary Research*, vol. 43, no. 1, p. 16, 2012.
- [5] A. T. Ciota and L. D. Kramer, "Vector-virus interactions and transmission dynamics of West Nile virus," *Viruses*, vol. 5, no. 12, pp. 3021–3047, 2013.
- [6] C. Chancey, A. Grinev, E. Volkova, and M. Rios, "The global ecology and epidemiology of West Nile virus," *BioMed Research International*, vol. 2015, Article ID 376230, 20 pages, 2015.
- [7] M. A. Brinton, "Replication cycle and molecular biology of the West Nile virus," *Viruses*, vol. 6, no. 1, pp. 13–53, 2013.
- [8] T. J. Gray and C. E. Webb, "A review of the epidemiological and clinical aspects of West Nile virus," *International Journal of General Medicine*, vol. 7, pp. 193–203, 2014.
- [9] S. Ulbert and S. E. Magnusson, "Technologies for the development of West Nile virus vaccines," *Future Microbiology*, vol. 9, no. 10, pp. 1221–1232, 2014.
- [10] K. L. Tyler, "Current developments in understanding of West Nile virus central nervous system disease," *Current Opinion in Neurology*, vol. 27, no. 3, pp. 342–348, 2014.
- [11] M. C. Lanteri, J. W. Heitman, R. E. Owen et al., "Comprehensive analysis of West Nile virus-specific T cell responses in humans," *The Journal of Infectious Diseases*, vol. 197, no. 9, pp. 1296–1306, 2008.
- [12] A. V. Iyer and K. G. Kousoulas, "A review of vaccine approaches for West Nile virus," *International Journal of Environmental Research and Public Health*, vol. 10, no. 9, pp. 4200–4223, 2013.
- [13] S. Brandler and F. Tangy, "Vaccines in development against West Nile virus," *Viruses*, vol. 5, no. 10, pp. 2384–2409, 2013.
- [14] M. Molerio-Abraham, E. M. Lafuente, D. R. Flower, and P. A. Reche, "Selection of conserved epitopes from hepatitis C virus for pan-population stimulation of T-cell responses," *Clinical & Developmental Immunology*, vol. 2013, article 601943, 10 pages, 2013.
- [15] Q. M. Sheikh, D. Gatherer, P. A. Reche, and D. R. Flower, "Towards the knowledge-based design of universal influenza epitope ensemble vaccines," *Bioinformatics*, vol. 32, no. 21, pp. 3233–3239, 2016.
- [16] S. A. Damfo, P. Reche, D. Gatherer, and D. R. Flower, "In silico design of knowledge-based *Plasmodium falciparum* epitope ensemble vaccines," *Journal of Molecular Graphics & Modelling*, vol. 78, pp. 195–205, 2017.
- [17] J. Alonso-Padilla, E. M. Lafuente, and P. A. Reche, "Computer-aided design of an epitope-based vaccine against Epstein-Barr virus," *Journal of Immunology Research*, vol. 2017, Article ID 9363750, 15 pages, 2017.
- [18] J. Mistry and D. R. Flower, "Designing epitope ensemble vaccines against TB by selection: prioritizing antigens using predicted immunogenicity," *Bioinformation*, vol. 13, no. 7, pp. 220–223, 2017.
- [19] P. Shah, J. Mistry, P. A. Reche, D. Gatherer, and D. R. Flower, "In silico design of mycobacterium tuberculosis epitope ensemble vaccines," *Molecular Immunology*, vol. 97, pp. 56–62, 2018.
- [20] D. Murphy, P. Reche, and D. R. Flower, "Selection-based design of in silico dengue epitope ensemble vaccines," *Chemical Biology & Drug Design*, vol. 93, no. 1, pp. 21–28, 2019.
- [21] M. Garcia-Boronat, C. M. Diez-Rivero, E. L. Reinherz, and P. A. Reche, "PVS: a web server for protein sequence variability analysis tuned to facilitate conserved epitope discovery," *Nucleic Acids Research*, vol. 36, Web Server, pp. W35–W41, 2008.
- [22] J. Greenbaum, J. Sidney, J. Chung, C. Brander, B. Peters, and A. Sette, "Functional classification of class II human leukocyte antigen (HLA) molecules reveals seven different supertypes and a surprising degree of repertoire sharing across supertypes," *Immunogenetics*, vol. 63, no. 6, pp. 325–335, 2011.
- [23] V. Jaravine, S. Raffeggerst, D. J. Schendel, and D. Frishman, "Assessment of cancer and virus antigens for cross-reactivity in human tissues," *Bioinformatics*, vol. 33, no. 1, pp. 104–111, 2017.
- [24] C. P. McMurtrey, A. Lelic, P. Piazza et al., "Epitope discovery in West Nile virus infection: identification and immune recognition of viral epitopes," *Proceedings of the National Academy of Sciences of the United States of America*, vol. 105, no. 8, pp. 2981–2986, 2008.
- [25] S. Kaabinejadian, C. P. McMurtrey, S. Kim et al., "Immunodominant West Nile virus T cell epitopes are fewer in number and fashionably late," *Journal of Immunology*, vol. 196, no. 10, pp. 4263–4273, 2016.
- [26] P. Oyarzun and B. Kobe, "Recombinant and epitope-based vaccines on the road to the market and implications for vaccine design and production," *Human Vaccines & Immunotherapeutics*, vol. 12, no. 3, pp. 763–767, 2016.
- [27] D. Fenoglio, A. Parodi, R. Lavieri et al., "Immunogenicity of GX301 cancer vaccine: four (telomerase peptides) are better than one," *Human Vaccines & Immunotherapeutics*, vol. 11, no. 4, pp. 838–850, 2015.
- [28] M. V. Larsen, A. Lelic, R. Parsons et al., "Identification of CD8⁺ T cell epitopes in the West Nile virus polyprotein by reverse-immunology using NetCTL," *PLoS One*, vol. 5, no. 9, article e12697, 2010.
- [29] C. M. Diez-Rivero and P. A. Reche, "CD8 T cell epitope distribution in viruses reveals patterns of protein biosynthesis," *PLoS One*, vol. 7, no. 8, article e43674, 2012.
- [30] Q. Y. Koo, A. M. Khan, K. O. Jung et al., "Conservation and variability of West Nile virus proteins," *PLoS One*, vol. 4, no. 4, article e5352, 2009.
- [31] A. Schneeweiss, S. Chabierski, M. Salomo et al., "A DNA vaccine encoding the E protein of West Nile virus is protective and can be boosted by recombinant domain DIII," *Vaccine*, vol. 29, no. 37, pp. 6352–6357, 2011.
- [32] C. A. Sarri, M. Markantoni, C. Stamatis et al., "Genetic contribution of MHC class II genes in susceptibility to West Nile virus infection," *PLoS One*, vol. 11, no. 11, article e0165952, 2016.
- [33] K. Ramakrishnan and D. R. Flower, "Discriminating antigen and non-antigen using proteome dissimilarity II: viral and fungal antigens," *Bioinformation*, vol. 5, no. 1, pp. 35–38, 2010.
- [34] K. Ramakrishnan and D. R. Flower, "Discriminating antigen and non-antigen using proteome dissimilarity III: tumour and parasite antigens," *Bioinformation*, vol. 5, no. 1, pp. 39–42, 2010.
- [35] K. Ramakrishnan and D. R. Flower, "Discriminating antigen and non-antigen using proteome dissimilarity: bacterial antigens," *Bioinformation*, vol. 4, no. 10, pp. 445–447, 2010.

Review Article

Peptide-Based Vaccination Therapy for Rheumatic Diseases

Bin Wang, Shiju Chen, Qing Zheng, Yuan Liu , and Guixiu Shi 

Department of Rheumatology and Clinical Immunology, The First Affiliated Hospital of Xiamen University, Xiamen 361003, China

Correspondence should be addressed to Yuan Liu; liuyuancuto@163.com and Guixiu Shi; gshi@xmu.edu.cn

Bin Wang and Shiju Chen contributed equally to this work.

Received 31 October 2019; Accepted 28 February 2020; Published 18 March 2020

Guest Editor: Masha Fridkis-Hareli

Copyright © 2020 Bin Wang et al. This is an open access article distributed under the Creative Commons Attribution License, which permits unrestricted use, distribution, and reproduction in any medium, provided the original work is properly cited.

Rheumatic diseases are extremely heterogeneous diseases with substantial risks of morbidity and mortality, and there is a pressing need in developing more safe and cost-effective treatment strategies. Peptide-based vaccination is a highly desirable strategy in treating noninfectious diseases, such as cancer and autoimmune diseases, and has gained increasing attentions. This review is aimed at providing a brief overview of the recent advances in peptide-based vaccination therapy for rheumatic diseases. Tremendous efforts have been made to develop effective peptide-based vaccinations against rheumatoid arthritis (RA) and systemic lupus erythematosus (SLE), while studies in other rheumatic diseases are still limited. Peptide-based active vaccination against pathogenic cytokines such as TNF- α and interferon- α (IFN- α) is shown to be promising in treating RA or SLE. Moreover, peptide-based tolerogenic vaccinations also have encouraging results in treating RA or SLE. However, most studies available now have been mainly based on animal models, while evidence from clinical studies is still lacking. The translation of these advances from experimental studies into clinical therapy remains impeded by some obstacles such as species difference in immunity, disease heterogeneity, and lack of safe delivery carriers or adjuvants. Nevertheless, advances in high-throughput technology, bioinformatics, and nanotechnology may help overcome these impediments and facilitate the successful development of peptide-based vaccination therapy for rheumatic diseases.

1. Introduction

Rheumatic diseases consist of more than 100 heterogeneous autoimmune disorders and can result in substantial morbidity and mortality [1]. The pathogenic mechanisms of most rheumatic diseases have not been clearly defined. Apart from the physical impairment, rheumatic diseases also have caused a heavy socioeconomic burden [2, 3]. The treatment of rheumatic diseases such as rheumatoid arthritis (RA), systemic lupus erythematosus (SLE), and Sjögren's syndrome (SjS) varies across patients with different clinical characteristics [4–6]. Current therapies for rheumatic diseases mainly include conventional synthetic disease-modifying antirheumatic drugs (DMARDs) and newly developed biologic therapies [4, 7]. The introduction of biologic therapies has revolutionized the treatment of many rheumatic diseases such as RA and ankylosing spondylitis (AS) in the past decade. However, a large part of patients with rheumatic diseases are still not well treated, which is possibly attributed to poor response to ther-

apeutic agents, delayed diagnosis, or poor medication adherence [4, 7, 8]. Additionally, biologic therapies such as tumor necrosis factor- α (TNF- α) antagonists (monoclonal antibodies or soluble receptors) can increase the risk of opportunistic infections such as tuberculosis [9]. Moreover, the clinical application of biological agents is still limited for their high costs especially in developing countries [10]. Therefore, there is a pressing need in the development of both more safe and cost-effective treatment strategies for rheumatic diseases.

As the greatest success in public health, the major goal of vaccination is to prevent infections such as influenza, tuberculosis, hepatitis, and malaria [11, 12]. Nevertheless, the roles of vaccinations in the treatment of noninfectious diseases such as cancer and allergic diseases have gained increasing attentions in recent years [13–17]. Among those distinct approaches of therapeutic vaccines, peptide-based vaccination is a highly desirable strategy and has gained increasing attentions [18, 19]. Peptide-based vaccines are aimed at precisely inducing immune response against antigens by key

TABLE 1: Comparison of those two peptide-based therapeutic vaccination strategies for rheumatic diseases.

Comparison items	Peptide-based active vaccination against pathogenic cytokines	Peptide-based tolerogenic vaccination
Sources of peptides	Pathogenic cytokines	Self-antigens, TCR repertoire
Therapeutic targets	Pathogenic cytokines	Autoimmune attacks against host cells or tissues caused by autoreactive lymphocytes
Main effects	Induce the production of neutralizing antibodies against pathogenic molecules	Induce immune tolerance to self-antigens by inhibiting autoreactive lymphocytes while promoting Tregs
Adjuvant	Need adjuvant	Not necessary
Relevant immune cells	Mainly B cells	Autoreactive T cells, Tregs, tolDCs, etc.
Evidence from clinical trials	Limited	Limited
Diseases	RA, SLE, and SjS	RA, SLE, and SjS

Tregs: regulatory T cells; tolDCs: tolerogenic dendritic cells; RA: rheumatoid arthritis; SLE: systemic lupus erythematosus; SjS: Sjögren's syndrome; VLP: virus-like particle; TCR: T cell receptor.

epitope peptides but not the entire antigen and thus have several advantages over traditional vaccines such as higher specificity, higher safety, lower costs, and less adverse events [19–21]. Studies in recent years have suggested that peptide-based vaccinations are promising in treating diseases such as cancer and allergic diseases, and some have shown impressive clinical benefits [22–24]. Besides, peptide-based vaccination has also been proposed as a promising immunotherapy for autoimmune diseases such as type 1 diabetes mellitus (T1DM) and multiple sclerosis (MS) [25–27]. Some studies also have reported encouraging findings on peptide-based immunotherapeutic vaccinations in rheumatic diseases [28–32]. This review is aimed at providing a brief overview of recent advances in peptide-based vaccinations in rheumatic diseases such as RA, SLE, and SjS.

2. Types of Peptide-Based Vaccination Therapy

The pathologic hallmark of rheumatic diseases is the breakdown of immune homeostasis and the loss of immune tolerance to self-antigens, which can trigger the formation of autoreactive T cells and B cells recognizing epitopes on autoantigens [33]. Both autoreactive immune cells and their secreted cytokines can result in harmful autoreactive immune attacks towards host cells and tissues, and thus, they are the two main targets for immunotherapy in rheumatic diseases. Distinct forms of peptide-based vaccinations have been studied for therapeutic or preventive strategies for diseases such as cancer, rheumatic diseases, and allergic disorders [34–38]. According to the therapeutic targets, peptide-based vaccinations used for rheumatic diseases can be classified into two main subtypes including peptide-based active vaccination against pathogenic cytokines and peptide-based tolerogenic vaccination. The former mainly targets pathogenic cytokines, while the latter mainly targets autoimmune attacks against host cells or tissues and is aimed at inducing immune tolerance by inhibiting autoreactive lymphocytes (Table 1).

2.1. Peptide-Based Active Vaccination against Pathogenic Cytokines. Pathogenic cytokines such as TNF- α , interferon- α (IFN- α), and interleukin-6 (IL-6) are critical mediators of autoimmune damages to host cells and tissues and

have long been regarded as therapeutic targets for rheumatic diseases [39]. Passive immunization aimed at neutralizing the pathogenic cytokines such as TNF- α and IL-6 with monoclonal antibodies (mAbs) or soluble receptors has been proven to be an effective therapy strategy of rheumatic diseases such as RA and AS [5]. However, passive immunization with mAbs targeting cytokines has several drawbacks such as risk of infections, antidrug antibodies, high cost, and low treatment response, which suggests the need of an alternative therapeutic approach to target those cytokines [40, 41]. Therapeutic active vaccination against pathogenic cytokines has been proposed to be a promising treatment strategy in treating rheumatic diseases and has gained increasing concerns in recent years [42–44]. Compared with passive immunization therapy, therapeutic active vaccination has several possible advantages such as lower costs, lower risk of infections, and less frequent administrations.

Active vaccination with the entire molecule or key peptides derived from targeted cytokines can elicit the activation of B cells and trigger the production of neutralizing antibodies against pathogenic cytokines, thus inhibiting the pathogenic effects of those cytokines [45]. Distinct forms of engineered immunogens have been used such as entire inactive molecule, key epitope peptides, modified peptides, or engineered DNA vaccine encoding pathogenic molecules. Moreover, vaccines containing multi-epitope peptides may also be considered, which may restore wider immune tolerance and achieve more benefits than a single peptide-based vaccination. Active immunization with entire pathogenic molecules or key peptides can both induce neutralizing antibodies against those pathogenic molecules, but the former have a higher risk of inducing nonneutralizing antibodies or cross-reactive antibodies against other host self-antigens. Therefore, peptide-based vaccinations are more promising to be used in clinical practice since they can induce peptide-specific antibodies and decrease the risk of cross-reactivity.

A widely studied therapeutic active vaccination is the active immunization against TNF- α , which has been proposed as a promising alternative strategy for TNF- α -targeting therapy. Previous studies have reported a successful

vaccination therapy using a compound named kinoid of human TNF- α (TNF-K) in the treatment of RA [46, 47]. TNF-K contains the entire inactivated human TNF- α and keyhole limpet hemocyanin (KLH) as a carrier protein. Though TNF-K is not a peptide-based vaccine, it has been proven to be a successful active vaccination against the pathogenic TNF- α in RA in both preclinical studies and clinical trials and has thus provided some indications for future studies exploring the feasibility of peptide-based anti-TNF- α active vaccination in treating rheumatic diseases [48, 49]. Moreover, numerous studies have explored distinct forms of peptide-based active vaccinations against TNF- α and also have provided encouraging findings in experimental studies using animal disease models.

Anticytokine active vaccination needs to overcome the natural tolerance of the immune system to self-proteins and thus induce high titers of effective neutralizing antibodies. However, a major shortcoming for peptide-based vaccines is the low immunization response caused by minimal antigenic epitopes, which is a major limitation during the development of an effective anticytokine active vaccination for rheumatic diseases. To ensure the immunization response or the efficacy of peptide-based vaccines, adjuvant or other molecules with adjuvant potency is especially necessary. Most previous studies using animal models used traditional adjuvants, while other studies used some carrier molecules to increase the immunogenicity of peptides such as virus-like particles (VLPs) [50–52]. VLPs can induce potent B cell responses effectively even in the absence of adjuvants and thus can be used in the molecular assembly system to induce strong B cell responses against most antigens [50]. Currently, there is a lack of both effective and safe adjuvants to ensure the use of peptide-based vaccinations in clinical trials, which is also a major obstacle in limiting the clinical use of peptide-based anticytokine active vaccination in treating rheumatic diseases. Considering the autoimmune reaction risk caused by some adjuvants [53], adequate adjuvants or carrier molecules with both high capability of inducing immune response and high safety are urgently needed for the clinical use of peptide-based vaccines. Advances in vaccine design technology such as the promising nanoparticle-carried vaccines may help overcome this limit.

2.2. Peptide-Based Tolerogenic Vaccinations. Rheumatic diseases are characterized by the breakdown of immune homeostasis and loss of immune tolerance to self-antigens, which further triggers the formation of autoreactive lymphocytes and autoimmune attacks to host tissues [54, 55]. Therefore, rebalancing immune homeostasis by inducing immune tolerance is a critical strategy in treating rheumatic diseases [33, 56]. Compared with conventional immune suppression therapy and biologic agents, immune tolerance induction therapy has the potential to inhibit autoimmune attacks while at the same time maintaining the ability to cope with danger signals, leading to a safe and efficacious therapy for rheumatic diseases [56]. Several strategies of inducing immune tolerance have been proposed as candidate treatments for rheumatic diseases such as stem cell therapy, tolerogenic dendritic cells (DCs) therapy, expansion of T regulatory cells (Tregs) by

low-dose IL-2, and tolerogenic vaccination therapy [57–59]. Among them, treating rheumatic diseases through peptide-based tolerogenic vaccination is of great interest and has gained increasing concerns in recent years [28, 60, 61].

It has been well defined that vaccination with an entire antigen or key tolerogenic peptides in the absence of adjuvant or costimulation signals has the potential to induce antigen-specific immune tolerance, which is a potentially effective approach in treating autoimmune diseases [62–64]. Therefore, modulation of the pathogenic immune response through antigen-specific tolerogenic vaccination has the potential to restore immune tolerance and ameliorate autoimmune attacks in rheumatic diseases [62, 65]. Most of those studies were based on animal models of autoimmune diseases, while relevant clinical studies are still limited. Several clinical trials had evaluated the safety and feasibility of peptide-based tolerogenic vaccination in patients with autoimmune diseases such as T1DM, RA, and MS, and some of them showed encouraging findings [66, 67]. Unlike the vaccines against infections which contain non-self-antigens and are aimed at inducing active immunization, tolerogenic vaccines contain self-antigens or key peptides and are aimed at inducing antigen-specific immune tolerance [28, 56]. Moreover, contrary to the capability of peptide-based anticytokine active vaccination in eliciting a strong immune response and inducing the activation of autoimmune B cells, peptide-based tolerogenic vaccinations are aimed at reestablishing immune tolerance to eliminate attacks.

The selection of epitope peptides for tolerogenic vaccinations is a critical essential step. Some antigen epitopes may mainly exert roles in the development of rheumatic diseases as immunogens to induce autoimmune response, while others may mainly act as tolerogens to induce immune tolerance [68–71]. Some antigens may have the capability of inducing either an immune response or immunologic tolerance under different exposure conditions and concomitant stimulators. Therefore, epitope peptides with the potential to induce immune tolerance under different exposure conditions are ideal targets for tolerogenic vaccinations. However, the ideal candidate epitope peptides for most rheumatic diseases are still largely elusive. Advances in vaccinomics and immunoinformatics may promote the identification of T and B cell epitopes by integrating useful information from multiple databases of different disciplines [72–75]. Moreover, both native and posttranslational modified epitopes have the possibility of exerting critical roles during the development of autoimmunity, both of which have the potential to be candidate therapeutic targets for tolerogenic vaccinations. Apart from epitope peptides from self-antigens, analog peptides of epitopes produced mainly by amino acid substitutions also have the potential to be candidate tolerogenic peptides [76]. There are also some tolerogenic peptides with therapeutic potential for rheumatic diseases, though they are not the peptides of certain antigens involved in the pathogenesis of diseases. hCDR1 is a tolerogenic peptide designed by the sequence of the heavy chain complementarity-determining region 1 (CDR1) of monoclonal anti-DNA antibodies and has been proven to be able to treat SLE by peptide-specific induction of Tregs [77–79].

Though the molecular mechanisms underlying the effects of peptide-based tolerogenic vaccinations in treating autoimmune diseases is still not clearly defined, their roles in mediating the anergy of autoactive T cell and promoting the expansion of Tregs have been considered to be major contributors [80, 81]. Tolerogenic peptides can be taken up by antigen-presenting cells (APCs) such as DCs, which further induce immune tolerance by inhibiting autoactive T cell or inducing Tregs. Recent studies reveal that central tolerance mediated by negative selection can prune but not completely eliminate autoreactive T cells, which leads to the incomplete negative selection and the existence of autoreactive T cells in the circulating system among healthy individuals [82–85]. The findings above further suggest the importance of peripheral tolerance in fighting against autoimmunity such as Treg-mediated suppression and the necessity of reestablishing immune tolerance by tolerogenic vaccinations in treating autoimmune diseases.

DCs are key immune cells which not only present antigens to adaptive immune cells such as T cells but also have a critical role in regulating immune tolerance [86]. Inadequate activation of DCs can cause autoimmunity by inducing the activation and differentiation of autoreactive T cells or B cells. However, the induction of tolerogenic DCs (tolDCs) with tolerogenic features and the ability of ameliorating autoimmunity have emerged as a promising therapy for autoimmune diseases [87]. tolDCs can produce anti-inflammatory cytokines and deviate T cells to regulatory or immunosuppressive phenotypes, thus inhibiting autoreactive T cells [88]. Currently, an alternative approach to induce antigen-specific immune tolerance is the induction of tolDCs towards self-antigens [33, 89]. tolDCs may present antigens to T cells but not give strong costimulatory signals owing to the low expression levels of costimulators, which can lead to the deletion or anergy of autoreactive T cells and induce Tregs. Antigen-boosted tolDCs have been proposed as a promising approach in treating autoimmune diseases [90]. Some clinical studies have been done to evaluate the safety and efficacy of autologous tolDCs loaded with autoantigens or key peptides in treating rheumatic diseases. Nevertheless, the adequate selection of epitope peptides from autoantigens for the induction of tolDCs is also critical for the efficacy of this intervention strategy [91].

With the rapid advances in nanotechnology, nanoparticle-carried vaccines have emerged as novel approaches to vaccine design, and their use in peptide-based tolerogenic vaccinations has gained increasing concerns in recent years [19, 92]. Nanoparticles coated with tolerogenic antigen peptides is a novel and promising strategy for inducing antigen-specific immune tolerance, which may promote the application of peptide-based vaccination in rheumatic diseases. Those nanoparticles can be taken up by APCs such as DCs, which further induce immune tolerance by mediating the anergy of autoactive T cell and promoting the expansion of Tregs. Several recent studies have revealed that vaccinations with nanoparticles carrying peptides can induce antigen-specific immune tolerance and represent a potential approach for the treatment of autoimmune diseases [93–95]. For instance, a recent study by Clemente-Casares et al. reported that a sys-

temic therapy with nanoparticles coated with disease-specific peptides could trigger immunosuppressive immune cells, such as antigen-specific regulatory T cell type 1- (TR1-) like cells and regulatory B cells, and suppress autoantigen-loaded APCs in mouse models of T1DM, MS, and RA, which was a potential treatment for autoimmune diseases [94].

Apart from peptides from self-antigens, those from T-cell receptor (TCR) also have been explored as therapeutic vaccines to treat autoimmune diseases including rheumatic diseases, which may be mediated by their roles in modulating autoreactive T cells or activating Tregs [96–99]. Some studies have provided encouraging findings regarding the safety and the efficacy of TCR peptide-based therapeutic vaccines in patients with rheumatic diseases [96]. However, the molecular mechanisms underlying the therapeutic roles of TCR peptide-based vaccines are still not clearly defined and further studies are needed on this aspect. The advances in the technologies to assess TCR repertoire have provided much help in precisely identifying dominant TCR repertoire involving the development of rheumatic diseases, which may further facilitate the development of TCR peptide-based therapeutic vaccines for those diseases [100, 101].

3. Peptide-Based Vaccinations for Rheumatic Diseases

Numerous studies have been carried out to evaluate the feasibility of peptide-based vaccinations in treating rheumatic diseases, but most of them are related to RA and SLE and several studies focus on SjS. Therefore, the advances of peptide-based vaccinations in RA, SLE, and SjS are reviewed in detail in the following part, and the other rheumatic diseases are not referred owing to the lack of relevant studies.

3.1. RA. RA is a common rheumatic disease affecting joints which is characterized by inflammatory synovitis, progressive bone erosion, and joint destruction [102]. Improved understanding of RA pathogenesis has led to the development of several effective targeted biological treatments. Although conventional and biological antirheumatic drugs can substantially reduce disease activity and inflammation, many RA patients are still inadequately managed and suffer from unfavorable treatment outcomes [7, 102]. Therefore, to further improve the treatment outcomes of RA patients, more new therapeutic strategies are urgently needed. Peptide-based vaccination has been suggested to be a promising treatment strategy for RA.

Several key pathogenic molecules involved in the pathogenesis of RA have been identified, and targeting those molecules with passive immunotherapy have been proven to be effective in RA, such as TNF- α and IL-6. As a proinflammatory cytokine, TNF- α has an essential role in the pathogenic process of RA and is a well-validated target. Studies on therapeutic active vaccinations against pathogenic cytokines also have mainly aimed at targeting TNF- α [103–105]. Some experimental studies have explored whether active immunization with peptide-based vaccines against TNF- α could ameliorate autoimmune arthritis in animal models of RA. Capini et al. reported that active immunization with TNF- α

peptides could generate endogenous autoantibodies against TNF- α [106]. Chackerian et al. revealed that vaccination of mice with conjugated particles containing VLPs and TNF- α peptides could generate autoantibodies against TNF- α and inhibit the development of collagen-induced arthritis (CIA) [107]. Another study by Spohn et al. found that VLP-based TNF- α peptide vaccine could trigger specific antibodies and ameliorate arthritis signs without inducing reactivation of latent tuberculosis [108]. Zhang et al. designed a TNF- α epitope-scaffold immunogen using the transmembrane domain of diphtheria toxin, which could induce sustained neutralizing antibodies against TNF- α and alleviate CIA in mice [109]. Another study reported that a dual-targeting vaccine using two segments of the TNF-like domain of activator of the NF- κ B ligand (RANKL) linked to the peptide EWEFVNTPLV could induce neutralizing antibodies against TNF- α and RANKL and thus could ameliorate both bone destruction and inflammation severity by simultaneously inhibiting TNF- α and RANKL [110].

Interleukin-1 β (IL-1 β), IL-6, vascular endothelial growth factor (VEGF), and IL-23 are crucial cytokines involved in the pathogenesis of RA. Bertin-Maghit et al. reported that synthetic IL-1 β peptides could lead to autoantibodies against IL-1 β , thus inhibiting the inflammation and articular destruction in CIA mice [111]. Moreover, vaccination with IL-6 analogs could induce autoantibodies to IL-6 and protect against CIA [112]. Semerano et al. found that a peptide derived from VEGF linked to the KLH carrier protein could ameliorate inflammation and joint destruction in experimental arthritis by inducing neutralizing anti-VEGF Abs [113]. Ratsimandresy et al. found that a murine IL-23p19 peptide predicted by bioinformatics could trigger anti-IL-23 antibodies and induce protection against joint destruction and inflammation in CIA mice [114].

Apart from peptide-based vaccination against pathogenic cytokines, peptide-based tolerogenic vaccinations have been proven to be successful in the prevention and treatment of arthritis in animal models [29, 115]. Type II collagen (CII) is a well-defined autoantigen for RA and has been widely used to induce animal models of RA [116]. A study by Myers et al. revealed that an epitope peptide from CII cyanogen bromide 11 (CB11) fragment p122-147 could suppress autoimmune arthritis by inducing immune tolerance in a mouse model of CIA [117]. Another study by Ku et al. reported that vaccination with an immunodominant epitope peptide from CII CB11 p58-73 could prevent experimental arthritis in either neonatal or adult rats [118]. Several other studies further reported that administration of CII immunodominant peptides such as p184-198, p181-209, and p245-270 could suppress autoimmune response and ameliorate arthritis in CIA animal models by their tolerogenic effects [119–123]. Apart from the original CII peptides, various analog peptides of CII immunodominant peptides have also been shown to suppress autoimmune arthritis by inhibiting autoimmune T cell responses and inducing immune tolerance [124–129]. Some studies also had explored the use of vaccine delivery systems in the CII peptide-based therapeutic vaccinations for RA. Zimmerman et al. found that a Ligand Epitope Antigen Presentation System (LEAPS) therapeutic vaccine con-

taining a human CII peptide could modulate autoimmune response and reduce disease progression in the CIA mice [130]. Mikecz et al. reported that the proteoglycan (PG) immunodominant peptide PG70 attached to either DerG (DerG-PG70) or J immune cell-binding peptide (J-PG70) through LEAPS could suppress arthritis through reducing pathogenic T cell responses and promoting immunosuppressive T cells in two mouse models of RA [30].

Heat-shock proteins (HSPs) are a possible source of autoantigens from stressed cells or inflamed tissues in autoimmune diseases, and several peptides from HSPs such as HSP60, HSP65, or HSP70 have been proven to ameliorate autoimmunity in animal models of RA [131–135]. Prakken et al. reported that vaccination with HSP60 peptide containing a T cell epitope could suppress avridine-induced arthritis in rats [134]. Studies by Zonneveld-Huijssoon et al. revealed that microbial HSP60 peptide vaccine could prevent experimental arthritis by enhancing Tregs [135, 136]. A HSP70 epitope peptide B29 was found to be able to induce the protective Tregs and suppress arthritis in mice [133, 137, 138], while autologous tolDCs loaded with HSP70 B29 peptide may be a candidate therapy for RA [70]. Studies by Moudgil et al. found that pretreatment with peptides comprising mycobacterial heat-shock protein 65 (BHSP65) carboxy-terminal determinants but not the amino-terminal determinants could suppress the development of arthritis in Lewis rats [139–141]. In RA patients, a peptide derived from a heat-shock protein of bacteria (dnaJp1) administered orally significantly increased the percentage of T cells producing IL-4 and IL-10 and reduced TNF- α [131]. Several other studies also have found that some peptides derived from HSPs could inhibit autoimmune arthritis [142–144].

Antibodies against citrullinated proteins such as filaggrin, vimentin, and collagen type II have crucial roles in the pathogenesis of RA [145, 146]. Prophylactic administration of a citrullinated filaggrin peptide could reduce disease severity and incidence of arthritis in a CIA animal model [145]. Another study by Gertel et al. reported that vaccination with multiepitope peptides derived from citrullinated autoantigens could induce immune tolerance and attenuate arthritis manifestations by promoting Treg cells and inhibiting Th17 cells in an animal model of RA [147]. A further study by Gertel et al. found that a multiepitope peptide derived from citrullinated autoantigens could modulate both the expressions of key cytokines and the frequencies of T cells in peripheral blood mononuclear cells (PBMCs) from RA patients [148].

A promising immunotherapy aimed at restoring self-tolerance is the induction of antigen-specific tolerance by tolerogenic immune cells loaded with autoantigens or tolerogenic nanoparticles loaded with pathogenic peptides [149]. A phase 1 trial by Bell et al. revealed that intraarticular injection of autologous tolDCs loaded with autoantigens from autologous synovial fluid could be a safe and feasible therapy for RA patients [150]. Another phase 1 trial by Benham et al. revealed that intradermal injection of autologous modified DCs exposed to citrullinated peptides could increase the ratio of regulatory to effector T cells and reduce inflammatory cytokines in HLA risk genotype-positive RA patients [151].

Apart from peptides from autoantigens, TCR peptides also have been proposed as promising therapeutic vaccines for RA. Some studies using animal models of RA found that vaccination with TCR V beta chain peptides could prevent CIA by inhibiting pathogenic T cells [152]. Some clinical studies also have provided encouraging findings regarding the safety and the efficacy of TCR peptide-based therapeutic vaccines in RA patients [96, 153]. A placebo-controlled trial reported by Moreland et al. found that vaccination with a combination of Vbeta3, Vbeta14, and Vbeta17 TCR peptides was well tolerated and was effective in RA patients [153].

Previous studies on peptide-based vaccinations for RA have reported encouraging findings. However, most studies available now have been mainly based on animal models, while evidence from clinical studies is still limited. More studies are urgently needed to facilitate the development of an effective and safe peptide-based vaccination for RA patients. In addition, though immune tolerance induction with peptide-based vaccinations have been proven to be effective in treating RA, the underlying molecular mechanisms are still largely elusive and need to be elaborated in further studies.

3.2. SLE. SLE is a devastating and heterogeneous rheumatic disease affecting multiple organs such as the skin, hematopoietic system, and kidney [154]. Apart from those conventional drugs such as immunosuppressants and corticosteroids, the advances in targeted biological agents have substantially improved the prognosis of SLE patients [155]. However, adequate control of disease activity or achieving remission is still challenging for a large part of SLE patients, and those patients are at high risk of premature mortality [4]. Therefore, more innovative treatment strategies need to be developed to improve the prognosis of SLE patients. Some studies have explored peptide-based therapeutic vaccinations as potential therapies for SLE, some of which have uncovered promising outcomes.

Some studies have explored the feasibility of active vaccination against pathogenic cytokines such as IFN- α in the treatment of SLE. IFN- α has long proven to be a major pathogenic cytokine in the pathogenesis of SLE [156]. Anti-IFN- α drugs such as anifrolumab and sifalimumab have been shown to substantially reduce disease activity in patients with moderate-to-severe SLE [157–159]. Mathian et al. found that active immunization of human IFN- α transgenic mice with a human IFN- α kinoid (IFN-K) could induce polyclonal neutralizing antibodies against IFN- α , suggesting that IFN-K vaccination may be a promising therapy for SLE [160]. IFN-K vaccine could effectively ameliorate lupus manifestations by inducing neutralizing antibodies in both mouse lupus model and SLE patients [160–163]. Clinical trials showed that IFN-K was well tolerated and significantly reduced disease activity in SLE patients [163, 164]. Vaccination therapy by targeting pathogenic cytokines such as IL-17 has also been studied as potential treatments for SLE [161, 165, 166]. B cell-targeted therapy has been regarded a promising therapeutic approach for SLE, and anti-CD20 monoclonal antibodies such as rituximab have been proven to be effective in SLE patients. Active immunization with a CD20

mimotope peptide could induce B cell depletion and increase survival in a mouse SLE model, which offered an alternative approach for B cell depletion therapy [31].

Apart from peptide-based vaccination against pathogenic cytokines, peptide-based tolerogenic vaccinations have also been studied as a candidate treatment for SLE. Many peptide autoepitopes have been proven to be involved in the pathogenesis of SLE [167–169]. Some histone peptides such as histone H4 autoepitope peptide 16-39 (H4₁₆₋₃₉) and autoepitope peptide 71-94 (H4₇₁₋₉₄) could induce an inflammatory response, whereas others such as H2A₃₄₋₄₈ could lead to an immunosuppressive response [167, 168]. Therefore, different peptides can lead to distinct immune response during the development of SLE. A study using human PBMC cultures found that a mixture of histone autoepitope peptides could block pathogenic autoimmune response and restore immune homeostasis in lupus [170]. Treatment with H4₁₆₋₃₉ could delay the onset of severe lupus nephritis possibly by the tolerogenic effect on autoimmune Th cells and autoimmune B cells in a mouse model of lupus [167]. Other studies found that treatment with H4₇₁₋₉₄ could suppress pathogenic lupus T cells by inducing regulatory T cells [171, 172]. Several other studies also had shown that peptides derived from histone proteins could suppress murine lupus by inducing immune tolerance [173–176]. Additionally, some peptides derived from other self-antigens have also been explored as candidate therapeutic vaccines for SLE. For instance, a phosphorylated spliceosomal epitope, the P140 peptide, could repress B cell differentiation and ameliorate lupus [169, 177, 178]. Subsequent clinical studies further showed that the P140 peptide could improve the clinical and immune status of SLE patients [179–181].

Peptides from other sources such as anti-DNA mAbs have also been explored as candidate therapeutic vaccines for SLE [182, 183]. Singh et al. found that a peptide from the variable regions of heavy chains of anti-DNA mAbs could delay the onset of autoimmunity in a lupus mouse model by inducing immune tolerance [182]. Waisman et al. reported that peptides from CDRs of pathogenic anti-DNA mAbs could prevent autoantibody production and downregulate autoreactive T cell responses, representing a potential treatment for SLE [184, 185]. Several other studies further revealed that a tolerogenic peptide derived from the CDR1 of a human anti-DNA autoantibody (hCDR1) could ameliorate lupus by inducing Tregs and suppressing the activation of autoreactive cells in lupus animal models [186, 187]. Several possible mechanisms have also been proposed to explain the therapeutic role of hCDR1 in SLE, such as TGF- β -mediated suppression of autoreactive T cells and downregulation of transcription factors responsible for negative regulation of T cell activation [188, 189]. Based on the encouraging findings from experimental studies, several clinical studies were done to assess the efficacy and safety of hCDR1 (Edratide) in SLE patients, which revealed favorable outcomes in SLE patients receiving hCDR1 treatment [190–192]. Another artificial peptide pConsensus (pCons) based on the immune determinants of anti-DNA IgG sequences has also been shown to be effective in delaying disease onset in the lupus mouse model by

inducing immune tolerance and promoting Treg activity [193–197].

Though many studies had explored the possible roles of peptide-based vaccinations in treating SLE, most of them were experimental studies using animal models and few were clinical studies. The efficacy of safety of peptide-based vaccinations in SLE patients need to be explored by future clinical trials. In addition, though some pathogenic autoantibodies have been well characterized for SLE, the useful peptides for vaccination therapy of SLE are still not well defined. Future studies exploring candidate peptides for the effective vaccination therapy in SLE are recommended.

3.3. SjS. SjS is a complex and heterogeneous rheumatic disease characterized by exocrinopathy, severe fatigue, and various systemic manifestations [6]. The treatment options currently available for SjS patients are still limited especially for those with extraglandular diseases, and more studies are needed to expand the treatment options [198]. Some efforts have been made to explore the feasibility of peptide-based vaccinations for SjS in the past decade, and some have provided encouraging findings.

HSP60 and muscarinic acetylcholine 3 receptor (M3R) are important autoantigens involved in the pathogenesis of SjS [199–202]. A study by Delaleu et al. reported that vaccination with a HSP60-derived peptide (aa 437–460) could significantly reduce SjS-related histopathologic features and retain normal exocrine function in nonobese diabetic (NOD) mice [203]. Yang et al. found that a M3R peptide (aa 208–227) immunization could reduce cytokines, such as IL-17 and IFN- γ , and inhibit lymphocytic infiltration in mice [204]. An *in vitro* experiment by Sthoeger et al. revealed that the tolerogenic peptide hCDR1 could significantly reduce the expressions of IL-1 β and TNF- α but increase the expressions of TGF- β and FOXP3 in the PBMCs of SjS patients, suggesting hCDR1 as a potential candidate treatment for SjS [205]. Another study by Li et al. found that the P140 peptide generated from a spliceosomal protein could rescue MRL/lpr mice from immune infiltration and autophagy defects in the salivary glands, suggesting a candidate therapy for SjS [206].

Currently, there is no study investigating the role of peptide-based vaccination against pathogenic cytokines in the treatment of SjS. Several pathogenic cytokines have been identified in the development of SjS such as IFN- α and IL-17, and further studies are recommended to evaluate the feasibility of peptide-based vaccination against these pathogenic cytokines in treating SjS [207–209]. Moreover, studies on peptide-based tolerogenic vaccinations in the treatment of SjS are also limited, and more studies are recommended to explore them.

4. Conclusions and Perspectives

Current therapies for most rheumatic diseases are mainly aimed at ameliorating symptoms and control disease progression, and there is still a pressing need in developing more safe and cost-effective treatment strategies. Peptide-based vaccination therapy is a highly desirable and curative strategy in treating rheumatic diseases and has the potential to revo-

lutionize the therapy of rheumatic diseases. Though tremendous efforts from previous studies have been made to develop effective peptide-based vaccinations against rheumatic diseases such as RA and SLE, most studies have been done using animal models while evidence from clinical studies is still limited. Additionally, the roles of peptide-based vaccinations in other rheumatic diseases such as AS are still largely elusive and thus need to be determined by more studies in the future.

Despite encouraging findings from studies using animal models, only a few clinical trials have been done to assess their clinical benefits, and some of them have failed to replicate the promising findings from experiment studies using animal disease models. A major obstacle is the differences between animals and humans in both immune response and immune tolerance, and findings from animal models are frequently not applicable to humans. A precise identification of those pathogenic antigens and key epitopes which exert roles in both animal models and humans may help to facilitate the studies of peptide-based vaccines. Additionally, disease heterogeneity is a well-defined characteristic of rheumatic diseases, and the immunodominant pathogenic epitopes are different across patients with distinct disease stages or clinical characteristics, which can limit the therapeutic efficacy of vaccinations targeting a small part of epitopes. Neoepitopes originating from epitope spreading or modified epitopes can further increase disease heterogeneity [65]. Therefore, personalized peptide vaccinations may be a more adequate approach for developing effective vaccination therapy against rheumatic diseases, in which peptides for targeted vaccinations are specifically selected for each individual patient. Finally, an unignored obstacle is the lack of both effective and safe adjuvants for the use of peptide-based vaccinations in clinical trials. Advances in vaccine design technology such as the promising nanoparticle-carried vaccines may help to overcome this limit [94, 210, 211].

The precise identification of immunodominant epitopes or neoepitopes from pathogenic cytokines or autoantigens is critically important for the successful development of peptide-based vaccinations in treating rheumatic diseases. Recent advances in high-throughput technology, vaccinomics, and bioinformatics have helped us in identifying key immunodominant epitopes from pathogenic cytokines and essential epitope peptides from autoantigens as promising targets for the peptide-based vaccinations [65, 212]. The proper implementation of computational prediction tools of bioinformatics may facilitate the development of more innovative and effective peptide-based vaccines for rheumatic disease and also may promote the translation from preclinical studies to clinical trials. Besides, the pathogenesises of most rheumatic diseases are still not clearly defined, and dominant self-antigens involved in disease development have not yet been identified. Further studies are still urgently needed to expand our understanding of the pathogenesises of rheumatic diseases, which may uncover new therapeutic targets or dominant antigens and pave new avenues for peptide-based vaccinations for the treatment of those diseases [213].

A careful screening of epitope peptides is a critical prerequisite for the efficacy and safety of peptide-based vaccination therapy in autoimmune diseases including rheumatic

diseases [214, 215]. During the development of rheumatic diseases, epitope specificity exists in the pathogenic roles of antigens or cytokines, and different epitope peptides thus can exert obviously distinct roles in modulating immune response [216, 217]. Some epitope peptides can precipitate but not inhibit disease progression. For most rheumatic diseases, an antigen epitope able to induce immunologic tolerance is still largely elusive and it is a major challenge in developing peptide-based tolerogenic vaccinations for rheumatic diseases.

With the complex autoimmune networks, diverse autoantigens, and distinct autoreactive T cells usually exist in patients with rheumatic diseases such as SLE, SjS, and RA. Multiple autoantigens contribute to the pathogenesis of these rheumatic diseases and targeting those autoantigens separately may only have limited therapeutic potential. Therefore, treatment with a complex of epitope peptides from multiple autoantigens may increase the possibility of successful immune tolerance induction [147, 218]. Similarly, since multiple cytokines are coinstantaneously involved in the development or progression of autoimmunity, treatment with a complex of peptides from two or more different cytokines may have the potential to provide a more profound effect by concomitantly inhibiting those cytokines, which need to be evaluated in further studies.

Peptide-based vaccinations in rheumatic diseases are still at an early stage, and both the efficacy and safety of peptide-based vaccinations in patients with rheumatic diseases need to be validated in clinical trials. Besides, the optimal timing, dosing, and route of vaccinations also need to be addressed before the initiation of its clinical use. Moreover, the role of prophylactic peptide-based vaccination in preventing or delaying the onset of rheumatic diseases among high-risk individuals is also of great interest and needs to be elucidated in future studies.

Conflicts of Interest

We declare that we have no conflicts of interest.

Acknowledgment

This work was supported by grants from the National Natural Science Foundation of China (Grant Nos. 81971536 and U1605223). We thank the authors of those references for their excellent work.

References

- [1] F. Goldblatt and S. G. O'Neill, "Clinical aspects of autoimmune rheumatic diseases," *Lancet*, vol. 382, no. 9894, pp. 797–808, 2013.
- [2] A. Tran-Duy, M. Ghiti Moghadam, M. A. H. Oude Voshaar et al., "An economic evaluation of stopping versus continuing tumor necrosis factor inhibitor treatment in rheumatoid arthritis patients with disease remission or low disease activity: results from a pragmatic open-label trial," *Arthritis & Rheumatology*, vol. 70, no. 10, pp. 1557–1564, 2018.
- [3] M. R. W. Barber and A. E. Clarke, "Socioeconomic consequences of systemic lupus erythematosus," *Current Opinion in Rheumatology*, vol. 29, no. 5, pp. 480–485, 2017.
- [4] L. Durcan, T. O'Dwyer, and M. Petri, "Management strategies and future directions for systemic lupus erythematosus in adults," *Lancet*, vol. 393, no. 10188, pp. 2332–2343, 2019.
- [5] D. Aletaha and J. S. Smolen, "Diagnosis and management of rheumatoid arthritis: a review," *JAMA*, vol. 320, no. 13, pp. 1360–1372, 2018.
- [6] X. Mariette and L. A. Criswell, "Primary Sjögren's syndrome," *New England Journal of Medicine*, vol. 378, no. 10, pp. 931–939, 2018.
- [7] G. R. Burmester and J. E. Pope, "Novel treatment strategies in rheumatoid arthritis," *Lancet*, vol. 389, no. 10086, pp. 2338–2348, 2017.
- [8] A. S. Schmid and D. Neri, "Advances in antibody engineering for rheumatic diseases," *Nature Reviews Rheumatology*, vol. 15, no. 4, pp. 197–207, 2019.
- [9] A. I. Rutherford, E. Patarata, S. Subesinghe, K. L. Hyrich, and J. B. Galloway, "Opportunistic infections in rheumatoid arthritis patients exposed to biologic therapy: results from the British Society for Rheumatology Biologics Register for Rheumatoid Arthritis," *Rheumatology*, vol. 57, no. 6, pp. 997–1001, 2018.
- [10] P. Sarzi-Puttini, A. Ceribelli, D. Marotto, A. Batticciotto, and F. Atzeni, "Systemic rheumatic diseases: from biological agents to small molecules," *Autoimmunity Reviews*, vol. 18, no. 6, pp. 583–592, 2019.
- [11] N. Rabinovich, P. McInnes, D. Klein, and B. Hall, "Vaccine technologies: view to the future," *Science*, vol. 265, no. 5177, pp. 1401–1404, 1994.
- [12] W. C. Koff, D. R. Burton, P. R. Johnson et al., "Accelerating next-generation vaccine development for global disease prevention," *Science*, vol. 340, no. 6136, article 1232910, 2013.
- [13] S. U. Patil and W. G. Shreffler, "Novel vaccines: technology and development," *Journal of Allergy and Clinical Immunology*, vol. 143, no. 3, pp. 844–851, 2019.
- [14] D. Avigan and J. Rosenblatt, "Vaccine therapy in hematologic malignancies," *Blood*, vol. 131, no. 24, pp. 2640–2650, 2018.
- [15] Z. Hu, P. A. Ott, and C. J. Wu, "Towards personalized, tumour-specific, therapeutic vaccines for cancer," *Nature Reviews Immunology*, vol. 18, no. 3, pp. 168–182, 2018.
- [16] L. H. Butterfield, "Cancer vaccines," *BMJ*, vol. 350, no. apr22 14, p. h988, 2015.
- [17] E. Alspach, D. M. Lussier, A. P. Miceli et al., "MHC-II neoantigens shape tumour immunity and response to immunotherapy," *Nature*, vol. 574, no. 7780, pp. 696–701, 2019.
- [18] B. J. Hos, E. Tondini, S. I. van Kasteren, and F. Ossendorp, "Approaches to improve chemically defined synthetic peptide vaccines," *Frontiers in Immunology*, vol. 9, p. 884, 2018.
- [19] M. Skwarczynski and I. Toth, "Peptide-based synthetic vaccines," *Chemical Science*, vol. 7, no. 2, pp. 842–854, 2016.
- [20] M. Calvo Tardon, M. Allard, V. Dutoit, P. Y. Dietrich, and P. R. Walker, "Peptides as cancer vaccines," *Current Opinion in Pharmacology*, vol. 47, pp. 20–26, 2019.
- [21] P. Reche, D. R. Flower, M. Fridkis-Hareli, and Y. Hoshino, "Peptide-based immunotherapeutics and vaccines 2017," *Journal of Immunology Research*, vol. 2018, Article ID 4568239, 2 pages, 2018.

- [22] H. Khong and W. W. Overwijk, "Adjuvants for peptide-based cancer vaccines," *Journal for ImmunoTherapy of Cancer*, vol. 4, no. 1, 2016.
- [23] P. A. Ott, Z. Hu, D. B. Keskin et al., "An immunogenic personal neoantigen vaccine for patients with melanoma," *Nature*, vol. 547, no. 7662, pp. 217–221, 2017.
- [24] U. Sahin, E. Derhovanesian, M. Miller et al., "Personalized RNA mutanome vaccines mobilize poly-specific therapeutic immunity against cancer," *Nature*, vol. 547, no. 7662, pp. 222–226, 2017.
- [25] E. L. Smith and M. Peakman, "Peptide immunotherapy for type 1 diabetes-clinical advances," *Frontiers in Immunology*, vol. 9, p. 392, 2018.
- [26] S. F. G. Zorzella-Pezavento, F. Chiuso-Minicucci, T. G. D. França et al., "pVAXhsp65 vaccination primes for high IL-10 production and decreases experimental encephalomyelitis severity," *Journal of Immunology Research*, vol. 2017, Article ID 6257958, 11 pages, 2017.
- [27] the Type 1 Diabetes TrialNet Study Group, C. A. Beam, C. MacCallum et al., "GAD vaccine reduces insulin loss in recently diagnosed type 1 diabetes: findings from a Bayesian meta-analysis," *Diabetologia*, vol. 60, no. 1, pp. 43–49, 2017.
- [28] N. Schall, N. Page, C. Macri, O. Chaloin, J. P. Briand, and S. Muller, "Peptide-based approaches to treat lupus and other autoimmune diseases," *Journal of Autoimmunity*, vol. 39, no. 3, pp. 143–153, 2012.
- [29] K. S. Rosenthal, K. Mikecz, H. L. Steiner III et al., "Rheumatoid arthritis vaccine therapies: perspectives and lessons from therapeutic ligand epitope antigen presentation system vaccines for models of rheumatoid arthritis," *Expert Rev Vaccines*, vol. 14, no. 6, pp. 891–908, 2015.
- [30] K. Mikecz, T. T. Glant, A. Markovics et al., "An epitope-specific DerG-PG70 LEAPS vaccine modulates T cell responses and suppresses arthritis progression in two related murine models of rheumatoid arthritis," *Vaccine*, vol. 35, no. 32, pp. 4048–4056, 2017.
- [31] E. Favoino, M. Prete, A. Marzullo, E. Millo, Y. Shoenfeld, and F. Perosa, "CD20-mimotope peptide active immunotherapy in systemic lupus erythematosus and a reappraisal of vaccination strategies in rheumatic diseases," *Clinical Reviews in Allergy and Immunology*, vol. 52, no. 2, pp. 217–233, 2017.
- [32] W. van Eden, "Vaccination against autoimmune diseases moves closer to the clinic," *Human Vaccines & Immunotherapeutics*, vol. 16, no. 2, pp. 228–232, 2020.
- [33] D. A. Horwitz, T. M. Fahmy, C. A. Piccirillo, and A. la Cava, "Rebalancing immune homeostasis to treat autoimmune diseases," *Trends in Immunology*, vol. 40, no. 10, pp. 888–908, 2019.
- [34] R. Valenta, R. Campana, M. Focke-Tejkl, and V. Niederberger, "Vaccine development for allergen-specific immunotherapy based on recombinant allergens and synthetic allergen peptides: lessons from the past and novel mechanisms of action for the future," *Journal of Allergy and Clinical Immunology*, vol. 137, no. 2, pp. 351–357, 2016.
- [35] S. Hofmann, A. Mead, A. Malinovskis, N. R. Hardwick, and B. A. Guinn, "Analogue peptides for the immunotherapy of human acute myeloid leukemia," *Cancer Immunology, Immunotherapy*, vol. 64, no. 11, pp. 1357–1367, 2015.
- [36] M. A. Rahat, "Targeting angiogenesis with peptide vaccines," *Frontiers in Immunology*, vol. 10, p. 1924, 2019.
- [37] T. Kumai, A. Fan, Y. Harabuchi, and E. Celis, "Cancer immunotherapy: moving forward with peptide T cell vaccines," *Current Opinion in Immunology*, vol. 47, pp. 57–63, 2017.
- [38] U. Klausen, S. Holmberg, M. O. Holmström et al., "Novel strategies for peptide-based vaccines in hematological malignancies," *Frontiers in Immunology*, vol. 9, p. 2264, 2018.
- [39] D. Zagury, H. Le Buanec, B. Bizzini, A. Burny, G. Lewis, and R. C. Gallo, "Active versus passive anti-cytokine antibody therapy against cytokine-associated chronic diseases," *Cytokine and Growth Factor Reviews*, vol. 14, no. 2, pp. 123–137, 2003.
- [40] G. M. Bartelds, C. L. Krieckaert, M. T. Nurmohamed et al., "Development of antidrug antibodies against adalimumab and association with disease activity and treatment failure during long-term follow-up," *JAMA*, vol. 305, no. 14, pp. 1460–1468, 2011.
- [41] F. Atzeni, P. Sarzi-Puttini, M. Sebastiani et al., "Rate of serious infections in spondyloarthritis patients treated with anti-tumour necrosis factor drugs: a survey from the Italian registry GISEA," *Clinical and Experimental Rheumatology*, vol. 37, no. 4, pp. 649–655, 2019.
- [42] J. Foerster and M. Bachman, "Beyond passive immunization: toward a nanoparticle-based IL-17 vaccine as first in class of future immune treatments," *Nanomedicine*, vol. 10, no. 8, pp. 1361–1369, 2015.
- [43] L. Semerano, E. Assier, and M. C. Boissier, "Anti-cytokine vaccination: a new biotherapy of autoimmunity?," *Autoimmunity Reviews*, vol. 11, no. 11, pp. 785–786, 2012.
- [44] D. Zagury, A. Burny, and R. C. Gallo, "Toward a new generation of vaccines: the anti-cytokine therapeutic vaccines," *Proceedings of the National Academy of Sciences of the United States of America*, vol. 98, no. 14, pp. 8024–8029, 2001.
- [45] A. Fettelschoss-Gabriel, V. Fettelschoss, F. Thoms et al., "Treating insect-bite hypersensitivity in horses with active vaccination against IL-5," *Journal of Allergy and Clinical Immunology*, vol. 142, no. 4, pp. 1194–1205.e3, 2018.
- [46] E. Assier, L. Semerano, E. Duvallet et al., "Modulation of anti-tumor necrosis factor alpha (TNF- α) antibody secretion in mice immunized with TNF- α kinoid," *Clinical and Vaccine Immunology*, vol. 19, no. 5, pp. 699–703, 2012.
- [47] T. Jia, Y. Pan, J. Li, and L. Wang, "Strategies for active TNF- α vaccination in rheumatoid arthritis treatment," *Vaccine*, vol. 31, no. 38, pp. 4063–4068, 2013.
- [48] P. Durez, P. Vandepapeliere, P. Miranda et al., "Therapeutic vaccination with TNF-Kinoid in TNF antagonist-resistant rheumatoid arthritis: a phase II randomized, controlled clinical trial," *PLoS One*, vol. 9, no. 12, article e113465, 2014.
- [49] N. Belmellat, L. Semerano, N. Segueni et al., "Tumor necrosis factor-alpha targeting can protect against arthritis with low sensitization to infection," *Frontiers in Immunology*, vol. 8, p. 1533, 2017.
- [50] A. Jegerlehner, A. Tissot, F. Lechner et al., "A molecular assembly system that renders antigens of choice highly repetitive for induction of protective B cell responses," *Vaccine*, vol. 20, no. 25–26, pp. 3104–3112, 2002.
- [51] M. F. Bachmann and G. T. Jennings, "Vaccine delivery: a matter of size, geometry, kinetics and molecular patterns," *Nature Reviews Immunology*, vol. 10, no. 11, pp. 787–796, 2010.
- [52] A. Bavoso, A. Ostuni, J. de Vendel et al., "Aldehyde modification and alum coadjuvancy enhance anti-TNF- α

- autovaccination and mitigate arthritis in rat," *Journal of Peptide Science*, vol. 21, no. 5, pp. 400–407, 2015.
- [53] J. T. Ruiz, L. Lujan, M. Blank, and Y. Shoenfeld, "Adjuvants- and vaccines-induced autoimmunity: animal models," *Immunologic Research*, vol. 65, no. 1, pp. 55–65, 2017.
- [54] G. S. Firestein and I. B. McInnes, "Immunopathogenesis of rheumatoid arthritis," *Immunity*, vol. 46, no. 2, pp. 183–196, 2017.
- [55] A. Rosen and L. Casciola-Rosen, "Autoantigens as partners in initiation and propagation of autoimmune rheumatic diseases," *Annual Review of Immunology*, vol. 34, no. 1, pp. 395–420, 2016.
- [56] S. Albani, E. C. Koffeman, and B. Prakken, "Induction of immune tolerance in the treatment of rheumatoid arthritis," *Nature Reviews Rheumatology*, vol. 7, no. 5, pp. 272–281, 2011.
- [57] E. M. Delemarre, S. T. A. Roord, T. van den Broek et al., "Brief report: autologous stem cell transplantation restores immune tolerance in experimental arthritis by renewal and modulation of the T_H17 cell compartment," *Arthritis & Rheumatology*, vol. 66, no. 2, pp. 350–356, 2014.
- [58] J. He, R. Zhang, M. Shao et al., "Efficacy and safety of low-dose IL-2 in the treatment of systemic lupus erythematosus: a randomised, double-blind, placebo-controlled trial," *Annals of the Rheumatic Diseases*, vol. 79, no. 1, pp. 141–149, 2019.
- [59] R. Spiering, B. Margry, C. Keijzer et al., "DEC205+ dendritic cell-targeted tolerogenic vaccination promotes immune tolerance in experimental autoimmune arthritis," *Journal of Immunology*, vol. 194, no. 10, pp. 4804–4813, 2015.
- [60] W. van Eden, M. A. A. Jansen, I. Ludwig, P. van Kooten, R. van der Zee, and F. Broere, "The enigma of heat shock proteins in immune tolerance," *Frontiers in Immunology*, vol. 8, p. 1599, 2017.
- [61] W. van Eden, "Immune tolerance therapies for autoimmune diseases based on heat shock protein T-cell epitopes," *Philosophical Transactions of the Royal Society of London. Series B: Biological Sciences*, vol. 373, no. 1738, 2017.
- [62] M. Larche, "Peptide immunotherapy," *Immunology and Allergy Clinics of North America*, vol. 26, no. 2, pp. 321–332, 2006.
- [63] T. J. Briner, M. C. Kuo, K. M. Keating, B. L. Rogers, and J. L. Greenstein, "Peripheral T-cell tolerance induced in naive and primed mice by subcutaneous injection of peptides from the major cat allergen Fel d 1," *Proceedings of the National Academy of Sciences of the United States of America*, vol. 90, no. 16, pp. 7608–7612, 1993.
- [64] J. P. Clayton, G. M. Gammon, D. G. Ando, D. H. Kono, L. Hood, and E. E. Sercarz, "Peptide-specific prevention of experimental allergic encephalomyelitis. Neonatal tolerance induced to the dominant T cell determinant of myelin basic protein," *Journal of Experimental Medicine*, vol. 169, no. 5, pp. 1681–1691, 1989.
- [65] J. Pozsgay, Z. Szekanecz, and G. Sarmay, "Antigen-specific immunotherapies in rheumatic diseases," *Nature Reviews Rheumatology*, vol. 13, no. 9, pp. 525–537, 2017.
- [66] I. Raz, D. Elias, A. Avron, M. Tamir, M. Metzger, and I. R. Cohen, " β -cell function in new-onset type 1 diabetes and immunomodulation with a heat-shock protein peptide (Dia-Pep277): a randomised, double-blind, phase II trial," *Lancet*, vol. 358, no. 9295, pp. 1749–1753, 2001.
- [67] M. Alhadj Ali, Y. F. Liu, S. Arif et al., "Metabolic and immune effects of immunotherapy with proinsulin peptide in human new-onset type 1 diabetes," *Science Translational Medicine*, vol. 9, no. 402, p. eaaf7779, 2017.
- [68] L. Lu, A. Kaliyaperumal, D. T. Boumpas, and S. K. Datta, "Major peptide autoepitopes for nucleosome-specific T cells of human lupus," *Journal of Clinical Investigation*, vol. 104, no. 3, pp. 345–355, 1999.
- [69] C. Rims, H. Uchtenhagen, M. J. Kaplan et al., "Citruinated aggrecan epitopes as targets of autoreactive CD4+ T cells in patients with rheumatoid arthritis," *Arthritis & Rheumatology*, vol. 71, no. 4, pp. 518–528, 2019.
- [70] W. van Eden, M. A. A. Jansen, I. S. Ludwig et al., "Heat shock proteins can be surrogate autoantigens for induction of antigen specific therapeutic tolerance in rheumatoid arthritis," *Frontiers in Immunology*, vol. 10, p. 279, 2019.
- [71] G. Riemekasten, A. Kawald, C. Weiß et al., "Strong acceleration of murine lupus by injection of the SmD183-119 peptide," *Arthritis and Rheumatism*, vol. 44, no. 10, pp. 2435–2445, 2001.
- [72] A. R. Oany, T. Pervin, M. Mia et al., "Vaccinomics approach for designing potential peptide vaccine by targeting Shigella spp. serine protease autotransporter subfamily protein SigA," *Journal of Immunology Research*, vol. 2017, Article ID 6412353, 14 pages, 2017.
- [73] J. Alonso-Padilla, E. M. Lafuente, and P. A. Reche, "Computer-aided design of an epitope-based vaccine against Epstein-Barr virus," *Journal of Immunology Research*, vol. 2017, Article ID 9363750, 15 pages, 2017.
- [74] J. L. Sanchez-Trincado, M. Gomez-Perosanz, and P. A. Reche, "Fundamentals and methods for T- and B-cell epitope prediction," *Journal of Immunology Research*, vol. 2017, Article ID 2680160, 14 pages, 2017.
- [75] U. K. Adhikari, M. Tayebi, and M. M. Rahman, "Immunoinformatics approach for epitope-based peptide vaccine design and active site prediction against polyprotein of emerging Oropouche virus," *Journal of Immunology Research*, vol. 2018, Article ID 6718083, 22 pages, 2018.
- [76] B. Tang, J. Zhou, J. E. Park et al., "T cell receptor signaling induced by an analog peptide of type II collagen requires activation of Syk," *Clinical Immunology*, vol. 133, no. 1, pp. 145–153, 2009.
- [77] E. Mozes and A. Sharabi, "A novel tolerogenic peptide, hCDR1, for the specific treatment of systemic lupus erythematosus," *Autoimmunity Reviews*, vol. 10, no. 1, pp. 22–26, 2010.
- [78] E. Eilat, H. Zinger, A. Nyska, and E. Mozes, "Prevention of systemic lupus erythematosus-like disease in (NZBxNZW)F1 mice by treating with CDR1- and CDR3-based peptides of a pathogenic autoantibody," *Journal of Clinical Immunology*, vol. 20, no. 4, pp. 268–278, 2000.
- [79] Z. M. Stoeber, A. Sharabi, M. Dayan et al., "The tolerogenic peptide hCDR1 downregulates pathogenic cytokines and apoptosis and upregulates immunosuppressive molecules and regulatory T cells in peripheral blood mononuclear cells of lupus patients," *Human Immunology*, vol. 70, no. 3, pp. 139–145, 2009.
- [80] J. Zhao, R. Li, J. He, J. Shi, L. Long, and Z. Li, "Mucosal administration of an altered CII263-272 peptide inhibits collagen-induced arthritis by suppression of Th1/Th17 cells and expansion of regulatory T cells," *Rheumatology International*, vol. 29, no. 1, pp. 9–16, 2008.

- [81] I. Kochetkova, T. Trunkle, G. Callis, and D. W. Pascual, "Vaccination without autoantigen protects against collagen II-induced arthritis via immune deviation and regulatory T cells," *Journal of Immunology*, vol. 181, no. 4, pp. 2741–2752, 2008.
- [82] M. R. Ehlers, "Who let the dogs out? The ever-present threat of autoreactive T cells," *Science Immunology*, vol. 3, no. 20, 2018.
- [83] W. Yu, N. Jiang, P. J. R. Ebert et al., "Clonal Deletion Prunes but Does Not Eliminate Self-Specific $\alpha\beta$ CD8⁺ T Lymphocytes," *Immunity*, vol. 42, no. 5, pp. 929–941, 2015.
- [84] S. Culina, A. I. Lalanne, G. Afonso et al., "Islet-reactive CD8(+) T cell frequencies in the pancreas, but not in blood, distinguish type 1 diabetic patients from healthy donors," *Science Immunology*, vol. 3, no. 20, 2018.
- [85] S. W. Scally, J. Petersen, S. C. Law et al., "A molecular basis for the association of the HLA-DRB1 locus, citrullination, and rheumatoid arthritis," *Journal of Experimental Medicine*, vol. 210, no. 12, pp. 2569–2582, 2013.
- [86] C. Ohnmacht, A. Pullner, S. B. S. King et al., "Constitutive ablation of dendritic cells breaks self-tolerance of CD4 T cells and results in spontaneous fatal autoimmunity," *Journal of Experimental Medicine*, vol. 206, no. 3, pp. 549–559, 2009.
- [87] Y. Xia, S. Jiang, S. Weng, X. Lv, H. Cheng, and C. Fang, "Antigen-specific immature dendritic cell vaccine ameliorates anti-dsDNA antibody-induced renal damage in a mouse model," *Rheumatology*, vol. 50, no. 12, pp. 2187–2196, 2011.
- [88] R. A. Harry, A. E. Anderson, J. D. Isaacs, and C. M. U. Hilkens, "Generation and characterisation of therapeutic tolerogenic dendritic cells for rheumatoid arthritis," *Annals of the Rheumatic Diseases*, vol. 69, no. 11, pp. 2042–2050, 2010.
- [89] W. van Eden, M. A. A. Jansen, A. C. M. de Wolf, I. S. Ludwig, P. Leufkens, and F. Broere, "The immunomodulatory potential of tolDCs loaded with heat shock proteins," *Frontiers in Immunology*, vol. 8, p. 1690, 2017.
- [90] N. Giannoukakis, B. Phillips, D. Finegold, J. Harnaha, and M. Trucco, "Phase I (safety) study of autologous tolerogenic dendritic cells in type 1 diabetic patients," *Diabetes Care*, vol. 34, no. 9, pp. 2026–2032, 2011.
- [91] D. P. Funda, J. Golias, T. Hudcovic, H. Kozakova, R. Spisek, and L. Palova-Jelinkova, "Antigen loading (e.g. glutamic acid decarboxylase 65) of tolerogenic DCs (tolDCs) reduces their capacity to prevent diabetes in the non-obese diabetes (NOD)-severe combined immunodeficiency model of adoptive cotransfer of diabetes as well as in NOD mice," *Frontiers in Immunology*, vol. 9, p. 290, 2018.
- [92] M. Negahdaripour, N. Golkar, N. Hajighahramani, S. Kianpour, N. Nezafat, and Y. Ghasemi, "Harnessing self-assembled peptide nanoparticles in epitope vaccine design," *Biotechnology Advances*, vol. 35, no. 5, pp. 575–596, 2017.
- [93] R. A. Maldonado, R. A. LaMothe, J. D. Ferrari et al., "Polymeric synthetic nanoparticles for the induction of antigen-specific immunological tolerance," *Proceedings of the National Academy of Sciences of the United States of America*, vol. 112, no. 2, pp. E156–E165, 2015.
- [94] X. Clemente-Casares, J. Blanco, P. Ambalavanan et al., "Expanding antigen-specific regulatory networks to treat autoimmunity," *Nature*, vol. 530, no. 7591, pp. 434–440, 2016.
- [95] D. R. Getts, A. J. Martin, D. P. McCarthy et al., "Microparticles bearing encephalitogenic peptides induce T-cell tolerance and ameliorate experimental autoimmune encephalomyelitis," *Nature Biotechnology*, vol. 30, no. 12, pp. 1217–1224, 2012.
- [96] L. W. Moreland, L. W. Heck, W. J. Koopman et al., "V α 17 T-cell receptor peptide Vaccine," *Annals of the New York Academy of Sciences*, vol. 756, pp. 211–214, 1995.
- [97] M. Howell, S. Winters, T. Olee, H. Powell, D. Carlo, and S. Brostoff, "Vaccination against experimental allergic encephalomyelitis with T cell receptor peptides," *Science*, vol. 246, no. 4930, pp. 668–670, 1989.
- [98] A. A. Vandenbark, G. Hashim, and H. Offner, "Immunization with a synthetic T-cell receptor V-region peptide protects against experimental autoimmune encephalomyelitis," *Nature*, vol. 341, no. 6242, pp. 541–544, 1989.
- [99] H. Offner, G. Hashim, and A. Vandenbark, "T cell receptor peptide therapy triggers autoregulation of experimental encephalomyelitis," *Science*, vol. 251, no. 4992, pp. 430–432, 1991.
- [100] X. Liu, W. Zhang, M. Zhao et al., "T cell receptor β repertoires as novel diagnostic markers for systemic lupus erythematosus and rheumatoid arthritis," *Annals of the Rheumatic Diseases*, vol. 78, no. 8, pp. 1070–1078, 2019.
- [101] D. R. Thapa, R. Tonikian, C. Sun et al., "Longitudinal analysis of peripheral blood T cell receptor diversity in patients with systemic lupus erythematosus by next-generation sequencing," *Arthritis Research & Therapy*, vol. 17, no. 1, 2015.
- [102] J. S. Smolen, D. Aletaha, and I. B. McInnes, "Rheumatoid arthritis," *Lancet*, vol. 388, no. 10055, pp. 2023–2038, 2016.
- [103] I. Dalum, D. M. Butler, M. R. Jensen et al., "Therapeutic antibodies elicited by immunization against TNF- α ," *Nature Biotechnology*, vol. 17, no. 7, pp. 666–669, 1999.
- [104] H. Le Buanec, L. Delavallee, N. Bessis et al., "TNF α kinoid vaccination-induced neutralizing antibodies to TNF α protect mice from autologous TNF α -driven chronic and acute inflammation," *Proceedings of the National Academy of Sciences of the United States of America*, vol. 103, no. 51, pp. 19442–19447, 2006.
- [105] L. Delavallee, H. le Buanec, N. Bessis et al., "Early and long-lasting protection from arthritis in tumour necrosis factor α (TNF α) transgenic mice vaccinated against TNF α ," *Annals of the Rheumatic Diseases*, vol. 67, no. 9, pp. 1332–1338, 2007.
- [106] C. J. Capini, S. M. Bertin-Maghit, N. Bessis et al., "Active immunization against murine TNF α peptides in mice: generation of endogenous antibodies cross-reacting with the native cytokine and in vivo protection," *Vaccine*, vol. 22, no. 23–24, pp. 3144–3153, 2004.
- [107] B. Chackerian, D. R. Lowy, and J. T. Schiller, "Conjugation of a self-antigen to papillomavirus-like particles allows for efficient induction of protective autoantibodies," *Journal of Clinical Investigation*, vol. 108, no. 3, pp. 415–423, 2001.
- [108] G. Spohn, R. Guler, P. Johansen et al., "A virus-like particle-based vaccine selectively targeting soluble TNF- α protects from arthritis without inducing reactivation of latent tuberculosis," *Journal of Immunology*, vol. 178, no. 11, pp. 7450–7457, 2007.
- [109] L. Zhang, J. Wang, A. Xu et al., "A rationally designed TNF- α epitope-scaffold immunogen induces sustained antibody response and alleviates collagen-induced arthritis in mice," *PLoS One*, vol. 11, no. 9, article e0163080, 2016.
- [110] H. Yuan, H. Qian, S. Liu et al., "Therapeutic role of a vaccine targeting RANKL and TNF- α on collagen-induced arthritis," *Biomaterials*, vol. 33, no. 32, pp. 8177–8185, 2012.

- [111] S. Bertinmaghit, C. Capini, N. Bessis et al., "Improvement of collagen-induced arthritis by active immunization against murine IL-1 β peptides designed by molecular modelling," *Vaccine*, vol. 23, no. 33, pp. 4228–4235, 2005.
- [112] P. Galle, L. Jensen, C. Andersson et al., "Vaccination with IL-6 analogues induces autoantibodies to IL-6 and influences experimentally induced inflammation," *International Immunopharmacology*, vol. 7, no. 13, pp. 1704–1713, 2007.
- [113] L. Semerano, E. Duvallet, N. Belmellat et al., "Targeting VEGF-A with a vaccine decreases inflammation and joint destruction in experimental arthritis," *Angiogenesis*, vol. 19, no. 1, pp. 39–52, 2016.
- [114] R. A. Ratsimandresy, E. Duvallet, E. Assier et al., "Active immunization against IL-23p19 improves experimental arthritis," *Vaccine*, vol. 29, no. 50, pp. 9329–9336, 2011.
- [115] S. R. Satpute, M. Durai, and K. D. Moudgil, "Antigen-specific tolerogenic and immunomodulatory strategies for the treatment of autoimmune arthritis," *Seminars in Arthritis and Rheumatism*, vol. 38, no. 3, pp. 195–207, 2008.
- [116] K. Terato, K. A. Hasty, M. A. Cremer, J. M. Stuart, A. S. Townes, and A. H. Kang, "Collagen-induced arthritis in mice. Localization of an arthritogenic determinant to a fragment of the type II collagen molecule," *Journal of Experimental Medicine*, vol. 162, no. 2, pp. 637–646, 1985.
- [117] L. K. Myers, J. M. Stuart, J. M. Seyer, and A. H. Kang, "Identification of an immunosuppressive epitope of type II collagen that confers protection against collagen-induced arthritis," *The Journal of Experimental Medicine*, vol. 170, no. 6, pp. 1999–2010, 1989.
- [118] G. Ku, M. Kronenberg, D. J. Peacock et al., "Prevention of experimental autoimmune arthritis with a peptide fragment of type II collagen," *European Journal of Immunology*, vol. 23, no. 3, pp. 591–599, 1993.
- [119] P. Zhu, X. Y. Li, H. K. Wang et al., "Oral administration of type-II collagen peptide 250-270 suppresses specific cellular and humoral immune response in collagen-induced arthritis," *Clinical Immunology*, vol. 122, no. 1, pp. 75–84, 2007.
- [120] N. A. Staines, N. Harper, F. J. Ward, V. Malmstrom, R. Holmdahl, and S. Bansal, "Mucosal tolerance and suppression of collagen-induced arthritis (CIA) induced by nasal inhalation of synthetic peptide 184-198 of bovine type II collagen (CII) expressing a dominant T cell epitope," *Clinical and Experimental Immunology*, vol. 103, no. 3, pp. 368–375, 1996.
- [121] L. K. Myers, S. W. Cooper, K. Terato, J. M. Seyer, J. M. Stuart, and A. H. Kang, "Identification and Characterization of a Tolerogenic T Cell Determinant within Residues 181-209 of Chick Type II Collagen," *Clinical Immunology and Immunopathology*, vol. 75, no. 1, pp. 33–38, 1995.
- [122] A. Honda, A. Ametani, T. Matsumoto et al., "Vaccination with an immunodominant peptide of bovine type II collagen induces an anti-TCR response, and modulates the onset and severity of collagen-induced arthritis," *International Immunology*, vol. 16, no. 5, pp. 737–745, 2004.
- [123] A. Hasselberg, K. Schon, A. Tarkowski, and N. Lycke, "Role of CTA1R7K-COL-DD as a novel therapeutic mucosal tolerance-inducing vector for treatment of collagen-induced arthritis," *Arthritis and Rheumatism*, vol. 60, no. 6, pp. 1672–1682, 2009.
- [124] L. K. Myers, Y. Sakurai, B. Tang et al., "Peptide-induced suppression of collagen-induced arthritis in HLA-DR1 transgenic mice," *Arthritis and Rheumatism*, vol. 46, no. 12, pp. 3369–3377, 2002.
- [125] L. K. Myers, B. Tang, D. D. Brand, E. F. Rosloniec, J. M. Stuart, and A. H. Kang, "Efficacy of modified recombinant type II collagen in modulating autoimmune arthritis," *Arthritis and Rheumatism*, vol. 50, no. 9, pp. 3004–3011, 2004.
- [126] L. K. Myers, E. F. Rosloniec, J. M. Seyer, J. M. Stuart, and A. H. Kang, "A synthetic peptide analogue of a determinant of type II collagen prevents the onset of collagen-induced arthritis," *Journal of Immunology*, vol. 150, no. 10, pp. 4652–4658, 1993.
- [127] Z. Q. Yao, R. Li, and Z. G. Li, "A triple altered collagen II peptide with consecutive substitutions of TCR contacting residues inhibits collagen-induced arthritis," *Annals of the Rheumatic Diseases*, vol. 66, no. 3, pp. 423–424, 2007.
- [128] Y. Sakurai, D. D. Brand, B. Tang et al., "Analog peptides of type II collagen can suppress arthritis in HLA-DR4 (DRB1*0401) transgenic mice," *Arthritis Research & Therapy*, vol. 8, no. 5, p. R150, 2006.
- [129] L. K. Myers, D. L. Cullins, D. D. Brand, S. Kleinau, J. M. Stuart, and A. H. Kang, "T cells stimulated with an analog peptide of type II collagen require the Fc receptor γ -chain to secrete interleukin-4 and suppress autoimmune arthritis in mice," *Arthritis and Rheumatism*, vol. 63, no. 9, pp. 2661–2670, 2011.
- [130] D. H. Zimmerman, P. Taylor, A. Bendele et al., "CEL-2000: A therapeutic vaccine for rheumatoid arthritis arrests disease development and alters serum cytokine/chemokine patterns in the bovine collagen type II induced arthritis in the DBA mouse model," *International Immunopharmacology*, vol. 10, no. 4, pp. 412–421, 2010.
- [131] B. J. Prakken, R. Samodal, T. D. le et al., "Epitope-specific immunotherapy induces immune deviation of proinflammatory T cells in rheumatoid arthritis," *Proceedings of the National Academy of Sciences of the United States of America*, vol. 101, no. 12, pp. 4228–4233, 2004.
- [132] E. C. Koffeman, M. Genovese, D. Amox et al., "Epitope-specific immunotherapy of rheumatoid arthritis: clinical responsiveness occurs with immune deviation and relies on the expression of a cluster of molecules associated with T cell tolerance in a double-blind, placebo-controlled, pilot phase II trial," *Arthritis and Rheumatism*, vol. 60, no. 11, pp. 3207–3216, 2009.
- [133] M. J. C. van Herwijnen, L. Wieten, R. van der Zee et al., "Regulatory T cells that recognize a ubiquitous stress-inducible self-antigen are long-lived suppressors of autoimmune arthritis," *Proceedings of the National Academy of Sciences of the United States of America*, vol. 109, no. 35, pp. 14134–14139, 2012.
- [134] B. J. Prakken, R. van der Zee, S. M. Anderton, P. J. S. van Kooten, W. Kuis, and W. van Eden, "Peptide-induced nasal tolerance for a mycobacterial heat shock protein 60 T cell epitope in rats suppresses both adjuvant arthritis and nonmicrobially induced experimental arthritis," *Proceedings of the National Academy of Sciences*, vol. 94, no. 7, pp. 3284–3289, 1997.
- [135] E. Zonneveld-Huijssoon, F. van Wijk, S. Roord et al., "TLR9 agonist CpG enhances protective nasal HSP60 peptide vaccine efficacy in experimental autoimmune arthritis," *Annals of the Rheumatic Diseases*, vol. 71, no. 10, pp. 1706–1715, 2012.
- [136] E. Zonneveld-Huijssoon, S. T. A. Roord, W. de Jager et al., "Bystander suppression of experimental arthritis by nasal administration of a heat shock protein peptide," *Annals of the Rheumatic Diseases*, vol. 70, no. 12, pp. 2199–2206, 2011.

- [137] C. de Wolf, R. van der Zee, I. den Braber et al., "An arthritis-suppressive and Treg cell-inducing CD4+ T cell epitope is functional in the context of HLA-restricted T cell responses," *Arthritis & Rheumatology*, vol. 68, no. 3, pp. 639–647, 2016.
- [138] M. A. A. Jansen, M. J. C. van Herwijnen, P. J. S. van Kooten et al., "Generation of the first TCR transgenic mouse with CD4(+) T cells recognizing an anti-inflammatory regulatory T cell-inducing Hsp70 peptide," *Frontiers in Immunology*, vol. 7, p. 90, 2016.
- [139] K. D. Moudgil, T. T. Chang, H. Eradat et al., "Diversification of T cell responses to carboxy-terminal determinants within the 65-kD heat-shock protein is involved in regulation of autoimmune arthritis," *Journal of Experimental Medicine*, vol. 185, no. 7, pp. 1307–1316, 1997.
- [140] M. Durai, M. N. Huang, and K. D. Moudgil, "Self heat-shock protein 65-mediated regulation of autoimmune arthritis," *Journal of Autoimmunity*, vol. 33, no. 3-4, pp. 208–213, 2009.
- [141] M. Durai, R. S. Gupta, and K. D. Moudgil, "The T cells specific for the carboxyl-terminal determinants of self (rat) heat-shock protein 65 escape tolerance induction and are involved in regulation of autoimmune arthritis," *Journal of Immunology*, vol. 172, no. 5, pp. 2795–2802, 2004.
- [142] J. W. Leavenworth, X. Tang, H. J. Kim, X. Wang, and H. Cantor, "Amelioration of arthritis through mobilization of peptide-specific CD8+ regulatory T cells," *Journal of Clinical Investigation*, vol. 123, no. 3, pp. 1382–1389, 2013.
- [143] X. L. Shi, L. P. Wang, X. Feng et al., "Inhibition of adjuvant-induced arthritis by nasal administration of novel synthetic peptides from heat shock protein 65," *BMC Musculoskeletal Disorders*, vol. 15, no. 1, 2014.
- [144] M. J. C. van Herwijnen, R. van der Zee, W. van Eden, and F. Broere, "In vivo induction of functionally suppressive induced regulatory T cells from CD4+CD25- T cells using an Hsp70 peptide," *PLoS One*, vol. 10, no. 6, article e0128373, 2015.
- [145] K. A. Kuhn, L. Kulik, B. Tomooka et al., "Antibodies against citrullinated proteins enhance tissue injury in experimental autoimmune arthritis," *Journal of Clinical Investigation*, vol. 116, no. 4, pp. 961–973, 2006.
- [146] L. A. Trouw, E. M. Haisma, E. W. N. Levarht et al., "Anticyclic citrullinated peptide antibodies from rheumatoid arthritis patients activate complement via both the classical and alternative pathways," *Arthritis and Rheumatism*, vol. 60, no. 7, pp. 1923–1931, 2009.
- [147] S. Gertel, G. Serre, Y. Shoenfeld, and H. Amital, "Immune tolerance induction with multi-epitope peptide derived from citrullinated autoantigens attenuates arthritis manifestations in adjuvant arthritis rats," *Journal of Immunology*, vol. 194, no. 12, pp. 5674–5680, 2015.
- [148] S. Gertel, G. Karmon, S. Vainer et al., "Immunomodulation of RA Patients' PBMC with a Multi-epitope Peptide Derived from Citrullinated Autoantigens," *Mediators of Inflammation*, vol. 2017, Article ID 3916519, 9 pages, 2017.
- [149] I. B. McInnes and G. Schett, "Pathogenetic insights from the treatment of rheumatoid arthritis," *Lancet*, vol. 389, no. 10086, pp. 2328–2337, 2017.
- [150] G. M. Bell, A. E. Anderson, J. Diboll et al., "Autologous tolerogenic dendritic cells for rheumatoid and inflammatory arthritis," *Annals of the Rheumatic Diseases*, vol. 76, no. 1, pp. 227–234, 2016.
- [151] H. Benham, H. J. Nel, S. C. Law et al., "Citrullinated peptide dendritic cell immunotherapy in HLA risk genotype-positive rheumatoid arthritis patients," *Science Translational Medicine*, vol. 7, no. 290, 2015.
- [152] T. M. Haqqi, X. M. Qu, D. Anthony, J. Ma, and M. S. Sy, "Immunization with T cell receptor V beta chain peptides deletes pathogenic T cells and prevents the induction of collagen-induced arthritis in mice," *Journal of Clinical Investigation*, vol. 97, no. 12, pp. 2849–2858, 1996.
- [153] L. W. Moreland, E. E. Morgan, T. C. Adamson et al., "T cell receptor peptide vaccination in rheumatoid arthritis: A placebo-controlled trial using a combination of V β 3, V β 14, and V β 17 Peptides," *Arthritis and Rheumatism*, vol. 41, no. 11, pp. 1919–1929, 1998.
- [154] T. Dorner and R. Furie, "Novel paradigms in systemic lupus erythematosus," *Lancet*, vol. 393, no. 10188, pp. 2344–2358, 2019.
- [155] G. Murphy, L. Lisnevskaja, and D. Isenberg, "Systemic lupus erythematosus and other autoimmune rheumatic diseases: challenges to treatment," *Lancet*, vol. 382, no. 9894, pp. 809–818, 2013.
- [156] N. H. Chang, T. T. Li, J. J. Kim et al., "Interferon- α induces altered transitional B cell signaling and function in Systemic Lupus Erythematosus," *Journal of Autoimmunity*, vol. 58, pp. 100–110, 2015.
- [157] R. Furie, M. Khamashta, J. T. Merrill et al., "Anifrolumab, an Anti-Interferon- α receptor monoclonal antibody, in moderate-to-severe systemic lupus erythematosus," *Arthritis & Rheumatology*, vol. 69, no. 2, pp. 376–386, 2017.
- [158] M. Khamashta, J. T. Merrill, V. P. Werth et al., "Sifalimumab, an anti-interferon- α monoclonal antibody, in moderate to severe systemic lupus erythematosus: a randomised, double-blind, placebo-controlled study," *Annals of the Rheumatic Diseases*, vol. 75, no. 11, pp. 1909–1916, 2016.
- [159] K. C. Kalunian, J. T. Merrill, R. Maciuga et al., "A Phase II study of the efficacy and safety of rontalizumab (rhuMAB interferon- α) in patients with systemic lupus erythematosus (ROSE)," *Annals of the Rheumatic Diseases*, vol. 75, no. 1, pp. 196–202, 2015.
- [160] A. Mathian, Z. Amoura, E. Adam et al., "Active immunisation of human interferon α transgenic mice with a human interferon α Kinoid induces antibodies that neutralise interferon α in sera from patients with systemic lupus erythematosus," *Annals of the Rheumatic Diseases*, vol. 70, no. 6, pp. 1138–1143, 2011.
- [161] D. Zagury, H. le Buanec, A. Mathian et al., "IFN α kinoid vaccine-induced neutralizing antibodies prevent clinical manifestations in a lupus flare murine model," *Proceedings of the National Academy of Sciences of the United States of America*, vol. 106, no. 13, pp. 5294–5299, 2009.
- [162] J. Ducreux, F. A. Houssiau, P. Vandepapelière et al., "Interferon α kinoid induces neutralizing anti-interferon α antibodies that decrease the expression of interferon-induced and B cell activation associated transcripts: analysis of extended follow-up data from the interferon α kinoid phase I/II study," *Rheumatology*, vol. 55, no. 10, pp. 1901–1905, 2016.
- [163] B. R. Lauwerys, E. Hachulla, F. Spertini et al., "Down-regulation of interferon signature in systemic lupus erythematosus patients by active immunization with interferon α -kinoid," *Arthritis and Rheumatism*, vol. 65, no. 2, pp. 447–456, 2013.

- [164] S. J. Przylecki, "Uricase and its action: part I. Preparation," *Biochemical Journal*, vol. 22, no. 4, pp. 1026–1034, 1928.
- [165] K. Handono, M. Z. Pratama, D. K. Sari et al., "Effect of active immunization with IL-17A on B cell function and infection risk in pristane-induced lupus model," *International Journal of Rheumatic Diseases*, vol. 21, no. 6, pp. 1277–1286, 2018.
- [166] F. Chasset and L. Arnaud, "Targeting interferons and their pathways in systemic lupus erythematosus," *Autoimmunity Reviews*, vol. 17, no. 1, pp. 44–52, 2018.
- [167] A. Kaliyaperumal, M. A. Michaels, and S. K. Datta, "Antigen-specific therapy of murine lupus nephritis using nucleosomal peptides: tolerance spreading impairs pathogenic function of autoimmune T and B cells," *Journal of Immunology*, vol. 162, no. 10, pp. 5775–5783, 1999.
- [168] G. Riemekasten, C. Weiss, S. Schneider et al., "T cell reactivity against the SmD1(83-119) C terminal peptide in patients with systemic lupus erythematosus," *Annals of the Rheumatic Diseases*, vol. 61, no. 9, pp. 779–785, 2002.
- [169] F. Monneaux, J. M. Lozano, M. E. Patarroyo, J. P. Briand, and S. Muller, "T cell recognition and therapeutic effect of a phosphorylated synthetic peptide of the 70K snRNP protein administered in MR/lpr mice," *European Journal of Immunology*, vol. 33, no. 2, pp. 287–296, 2003.
- [170] L. Zhang, A. M. Bertucci, R. Ramsey-Goldman, E. R. Harsha-Strong, R. K. Burt, and S. K. Datta, "Major pathogenic steps in human lupus can be effectively suppressed by nucleosomal histone peptide epitope-induced regulatory immunity," *Clinical Immunology*, vol. 149, no. 3, pp. 365–378, 2013.
- [171] H. K. Kang, M. A. Michaels, B. R. Berner, and S. K. Datta, "Very low-dose tolerance with nucleosomal peptides controls lupus and induces potent regulatory T cell subsets," *Journal of Immunology*, vol. 174, no. 6, pp. 3247–3255, 2005.
- [172] H. K. Kang, M. Liu, and S. K. Datta, "Low-dose peptide tolerance therapy of lupus generates plasmacytoid dendritic cells that cause expansion of autoantigen-specific regulatory T cells and contraction of inflammatory Th17 cells," *Journal of Immunology*, vol. 178, no. 12, pp. 7849–7858, 2007.
- [173] H. Y. Wu, F. J. Ward, and N. A. Staines, "Histone peptide-induced nasal tolerance: suppression of murine lupus," *Journal of Immunology*, vol. 169, no. 2, pp. 1126–1134, 2002.
- [174] H. Y. Wu and N. A. Staines, "A deficiency of CD4+CD25+ T cells permits the development of spontaneous lupus-like disease in mice, and can be reversed by induction of mucosal tolerance to histone peptide autoantigen," *Lupus*, vol. 13, no. 3, pp. 192–200, 2004.
- [175] E. Shapira, E. Proscura, B. Brodsky, and U. Wormser, "Novel peptides as potential treatment of systemic lupus erythematosus," *Lupus*, vol. 20, no. 5, pp. 463–472, 2011.
- [176] H. K. Kang, M. Y. Chiang, M. Liu, D. Ecklund, and S. K. Datta, "The histone peptide H4 71-94 alone is more effective than a cocktail of peptide epitopes in controlling lupus: immunoregulatory mechanisms," *Journal of Clinical Immunology*, vol. 31, no. 3, pp. 379–394, 2011.
- [177] M. Wilhelm, F. Wang, N. Schall et al., "Lupus regulator peptide P140 represses B cell differentiation by reducing HLA class II molecule overexpression," *Arthritis & Rheumatology*, vol. 70, no. 7, pp. 1077–1088, 2018.
- [178] N. Page, F. Gros, N. Schall, J. P. Briand, and S. Muller, "A therapeutic peptide in lupus alters autophagic processes and stability of MHCII molecules in MRL/lpr B cells," *Autophagy*, vol. 7, no. 5, pp. 539–540, 2011.
- [179] S. Muller, F. Monneaux, N. Schall et al., "Spliceosomal peptide P140 for immunotherapy of systemic lupus erythematosus: results of an early phase II clinical trial," *Arthritis and Rheumatism*, vol. 58, no. 12, pp. 3873–3883, 2008.
- [180] R. Zimmer, H. R. Scherbarth, O. L. Rillo, J. J. Gomez-Reino, and S. Muller, "Lupuzor/P140 peptide in patients with systemic lupus erythematosus: a randomised, double-blind, placebo-controlled phase IIb clinical trial," *Annals of the Rheumatic Diseases*, vol. 72, no. 11, pp. 1830–1835, 2013.
- [181] N. Schall and S. Muller, "Resetting the autoreactive immune system with a therapeutic peptide in lupus," *Lupus*, vol. 24, no. 4–5, pp. 412–418, 2015.
- [182] R. R. Singh, F. M. Ebling, E. E. Sercarz, and B. H. Hahn, "Immune tolerance to autoantibody-derived peptides delays development of autoimmunity in murine lupus," *Journal of Clinical Investigation*, vol. 96, no. 6, pp. 2990–2996, 1995.
- [183] B. H. Hahn, R. R. Singh, W. K. Wong, B. P. Tsao, K. Bulpitt, and F. M. Ebling, "Treatment with a consensus peptide based on amino acid sequences in autoantibodies prevents T cell activation by autoantigens and delays disease onset in murine lupus," *Arthritis and Rheumatism*, vol. 44, no. 2, pp. 432–441, 2001.
- [184] A. Waisman, P. J. Ruiz, E. Israeli et al., "Modulation of murine systemic lupus erythematosus with peptides based on complementarity determining regions of a pathogenic anti-DNA monoclonal antibody," *Proceedings of the National Academy of Sciences of the United States of America*, vol. 94, no. 9, pp. 4620–4625, 1997.
- [185] Z. M. Stoeber, M. Dayan, A. Tcherniack et al., "Modulation of autoreactive responses of peripheral blood lymphocytes of patients with systemic lupus erythematosus by peptides based on human and murine anti-DNA autoantibodies," *Clinical and Experimental Immunology*, vol. 131, no. 2, pp. 385–392, 2003.
- [186] A. Sharabi, H. Zinger, M. Zborowsky, Z. M. Stoeber, and E. Mozes, "A peptide based on the complementarity-determining region 1 of an autoantibody ameliorates lupus by up-regulating CD4+CD25+ cells and TGF-beta," *Proceedings of the National Academy of Sciences of the United States of America*, vol. 103, no. 23, pp. 8810–8815, 2006.
- [187] Z. Stoeber, H. Zinger, A. Sharabi, I. Asher, and E. Mozes, "The tolerogenic peptide, hCDR1, down-regulates the expression of Interferon- α in murine and human systemic lupus erythematosus," *PLoS One*, vol. 8, no. 3, article e60394, 2013.
- [188] U. Sela, N. Mauermann, R. Hershkoviz et al., "The inhibition of autoreactive T cell functions by a peptide based on the CDR1 of an anti-DNA autoantibody is via TGF- β -mediated suppression of LFA-1 and CD44 expression and function," *Journal of Immunology*, vol. 175, no. 11, pp. 7255–7263, 2005.
- [189] U. Sela, M. Dayan, R. Hershkoviz, O. Lider, and E. Mozes, "A peptide that ameliorates lupus up-regulates the diminished expression of early growth response factors 2 and 3," *Journal of Immunology*, vol. 180, no. 3, pp. 1584–1591, 2008.
- [190] Z. M. Stoeber, A. Sharabi, Y. Molad et al., "Treatment of lupus patients with a tolerogenic peptide, hCDR1 (Edratide): immunomodulation of gene expression," *Journal of Autoimmunity*, vol. 33, no. 1, pp. 77–82, 2009.
- [191] M. B. Urowitz, D. A. Isenberg, and D. J. Wallace, "Safety and efficacy of hCDR1 (Edratide) in patients with active systemic lupus erythematosus: results of phase II study," *Lupus Science & Medicine*, vol. 2, no. 1, article e000104, 2015.

- [192] S. Lapter, A. Marom, A. Meshorer et al., "Amelioration of brain pathology and behavioral dysfunction in mice with lupus following treatment with a tolerogenic peptide," *Arthritis and Rheumatism*, vol. 60, no. 12, pp. 3744–3754, 2009.
- [193] B. H. Hahn, R. P. Singh, A. La Cava, and F. M. Ebling, "Tolerogenic treatment of lupus mice with consensus peptide induces Foxp3-expressing, apoptosis-resistant, TGF β -secreting CD8+ T cell suppressors," *Journal of Immunology*, vol. 175, no. 11, pp. 7728–7737, 2005.
- [194] R. P. Singh, A. La Cava, and B. H. Hahn, "pConsensus peptide induces tolerogenic CD8+ T cells in lupus-prone (NZB x NZW)F1 mice by differentially regulating Foxp3 and PD1 molecules," *Journal of Immunology*, vol. 180, no. 4, pp. 2069–2080, 2008.
- [195] R. P. Singh, A. La Cava, M. Wong, F. Ebling, and B. H. Hahn, "CD8+ T cell-mediated suppression of autoimmunity in a murine lupus model of peptide-induced immune tolerance depends on Foxp3 expression," *Journal of Immunology*, vol. 178, no. 12, pp. 7649–7657, 2007.
- [196] B. H. Hahn, M. Anderson, E. le, and A. L. Cava, "Anti-DNA Ig peptides promote Treg cell activity in systemic lupus erythematosus patients," *Arthritis and Rheumatism*, vol. 58, no. 8, pp. 2488–2497, 2008.
- [197] B. J. Skaggs, E. V. Lourenco, and B. H. Hahn, "Oral administration of different forms of a tolerogenic peptide to define the preparations and doses that delay anti-DNA antibody production and nephritis and prolong survival in SLE-prone mice," *Lupus*, vol. 20, no. 9, pp. 912–920, 2011.
- [198] R. I. Fox, C. M. Fox, J. E. Gottenberg, and T. Dorner, "Treatment of Sjögren's syndrome: current therapy and future directions," *Rheumatology*, 2019, <https://www.ncbi.nlm.nih.gov/pubmed/31034046>.
- [199] P. Aragona, G. Magazzu, G. Macchia et al., "Presence of antibodies against *Helicobacter pylori* and its heat-shock protein 60 in the serum of patients with Sjogren's syndrome," *Journal of Rheumatology*, vol. 26, no. 6, pp. 1306–1311, 1999.
- [200] H. de Jong, W. de Jager, M. Wenting-van Wijk et al., "Increased immune reactivity towards human hsp60 in patients with primary Sjögren's syndrome is associated with increased cytokine levels and glandular inflammation," *Clinical and Experimental Rheumatology*, vol. 30, no. 4, pp. 594–595, 2012.
- [201] E. Namkoong, S. W. Lee, N. Kim, Y. Choi, and K. Park, "Effect of anti-muscarinic autoantibodies on leukocyte function in Sjogren's syndrome," *Molecular Immunology*, vol. 90, pp. 136–142, 2017.
- [202] M. Iizuka, E. Wakamatsu, H. Tsuboi et al., "Pathogenic role of immune response to M3 muscarinic acetylcholine receptor in Sjogren's syndrome-like sialoadenitis," *Journal of Autoimmunity*, vol. 35, no. 4, pp. 383–389, 2010.
- [203] N. Delaleu, A. C. Madureira, H. Immervoll, and R. Jonsson, "Inhibition of experimental Sjögren's syndrome through immunization with HSP60 and its peptide amino acids 437–460," *Arthritis and Rheumatism*, vol. 58, no. 8, pp. 2318–2328, 2008.
- [204] L. Yang, J. Ju, W. Zhang et al., "Effects of Muscarinic Acetylcholine 3 Receptor208–227 Peptide Immunization on Autoimmune Response in Nonobese Diabetic Mice," *Clinical and Developmental Immunology*, vol. 2013, Article ID 485213, 10 pages, 2013.
- [205] Z. Sthoeger, A. Sharabi, I. Asher et al., "The tolerogenic peptide hCDR1 immunomodulates cytokine and regulatory molecule gene expression in blood mononuclear cells of primary Sjogren's syndrome patients," *Clinical Immunology*, vol. 192, pp. 85–91, 2018.
- [206] B. Li, F. Wang, N. Schall, and S. Muller, "Rescue of autophagy and lysosome defects in salivary glands of MRL/lpr mice by a therapeutic phosphopeptide," *Journal of Autoimmunity*, vol. 90, pp. 132–145, 2018.
- [207] O. Kimoto, J. Sawada, K. Shimoyama et al., "Activation of the interferon pathway in peripheral blood of patients with Sjogren's syndrome," *Journal of Rheumatology*, vol. 38, no. 2, pp. 310–316, 2011.
- [208] N. Roescher, P. P. Tak, and G. G. Illei, "Cytokines in Sjögren's syndrome: potential therapeutic targets," *Annals of the Rheumatic Diseases*, vol. 69, no. 6, pp. 945–948, 2010.
- [209] M. Sisto, L. Lorusso, R. Tamma, G. Ingravallo, D. Ribatti, and S. Lisi, "Interleukin-17 and -22 synergy linking inflammation and EMT-dependent fibrosis in Sjögren's syndrome," *Clinical and Experimental Immunology*, vol. 198, no. 2, pp. 261–272, 2019.
- [210] S. Singha, K. Shao, K. K. Ellestad, Y. Yang, and P. Santamaria, "Nanoparticles for immune stimulation against infection, cancer, and autoimmunity," *ACS Nano*, vol. 12, no. 11, pp. 10621–10635, 2018.
- [211] T. K. Kishimoto and R. A. Maldonado, "Nanoparticles for the induction of antigen-specific immunological tolerance," *Frontiers in Immunology*, vol. 9, p. 230, 2018.
- [212] S. Verma, A. Sajid, Y. Singh, and P. Shukla, "Computational tools for modern vaccine development," *Human Vaccines & Immunotherapeutics*, pp. 1–13, 2019, <https://www.ncbi.nlm.nih.gov/pubmed/31545127>.
- [213] L. T. Donlin, S. H. Park, E. Giannopoulou et al., "Insights into rheumatic diseases from next-generation sequencing," *Nature Reviews Rheumatology*, vol. 15, no. 6, pp. 327–339, 2019.
- [214] C. Daniel, B. Weigmann, R. Bronson, and H. von Boehmer, "Prevention of type 1 diabetes in mice by tolerogenic vaccination with a strong agonist insulin mimetope," *Journal of Experimental Medicine*, vol. 208, no. 7, pp. 1501–1510, 2011.
- [215] M. L. Bergman, T. Lopes-Carvalho, A. C. Martins, F. A. Grieco, D. L. Eizirik, and J. Demengeot, "Tolerogenic insulin peptide therapy precipitates type 1 diabetes," *Journal of Experimental Medicine*, vol. 214, no. 7, pp. 2153–2156, 2017.
- [216] G. Moroncini, A. Grieco, G. Nacci et al., "Epitope specificity determines pathogenicity and detectability of anti-platelet-derived growth factor receptor α autoantibodies in systemic sclerosis," *Arthritis & Rheumatology*, vol. 67, no. 7, pp. 1891–1903, 2015.
- [217] A. J. Roth, J. D. Ooi, J. J. Hess et al., "Epitope specificity determines pathogenicity and detectability in ANCA-associated vasculitis," *Journal of Clinical Investigation*, vol. 123, no. 4, pp. 1773–1783, 2013.
- [218] C. E. Smith and S. D. Miller, "Multi-peptide coupled-cell tolerance ameliorates ongoing relapsing EAE associated with multiple pathogenic autoreactivities," *Journal of Autoimmunity*, vol. 27, no. 4, pp. 218–231, 2006.

Research Article

A Multiple Antigen Peptide Vaccine Containing CD4⁺ T Cell Epitopes Enhances Humoral Immunity against *Trichinella spiralis* Infection in Mice

Yuan Gu ¹, Ximeng Sun ¹, Jingjing Huang ¹, Bin Zhan ², and Xiping Zhu ¹

¹Department of Medical Microbiology and Parasitology, School of Basic Medical Sciences, Capital Medical University, Beijing 100069, China

²Department of Pediatrics, Section of Tropical Medicine, Baylor College of Medicine, Houston, Texas 77030, USA

Correspondence should be addressed to Xiping Zhu; zhuxiping@ccmu.edu.cn

Received 27 June 2019; Revised 6 October 2019; Accepted 7 November 2019; Published 8 January 2020

Guest Editor: Yoshihiko Hoshino

Copyright © 2020 Yuan Gu et al. This is an open access article distributed under the Creative Commons Attribution License, which permits unrestricted use, distribution, and reproduction in any medium, provided the original work is properly cited.

Multiepitope peptide vaccine has some advantages over traditional recombinant protein vaccine due to its easy and fast production and possible inclusion of multiple protective epitopes of pathogens. However, it is usually poorly immunogenic and needs to conjugate to a large carrier protein. Peptides conjugated to a central lysine core to form multiple antigen peptides (MAPs) will increase the immunogenicity of peptide vaccine. In this study, we constructed a MAP consisting of CD4⁺ T cell and B cell epitopes of paramyosin (Pmy) of *Trichinella spiralis* (Ts-Pmy), which has been proved to be a good vaccine candidate in our previous work. The immunogenicity and induced protective immunity of MAP against *Trichinella spiralis* (*T. spiralis*) infection were evaluated in mice. We demonstrated that mice immunized with MAP containing CD4⁺ T cell and B cell epitopes (MAP-TB) induced significantly higher protection against the challenge of *T. spiralis* larvae (35.5% muscle larva reduction) compared to the MAP containing B cell epitope alone (MAP-B) with a 12.4% muscle larva reduction. The better protection induced by immunization of MAP-TB was correlated with boosted antibody titers (both IgG1 and IgG2a) and mixed Th1/Th2 cytokine production secreted by the splenocytes of immunized mice. Further flow cytometry analysis of lymphocytes in spleens and draining lymph nodes demonstrated that mice immunized with MAP-TB specifically enhanced the generation of T follicular helper (Tfh) cells and germinal center (GC) B cells, while inhibiting follicular regulatory CD4⁺ T (Tfr) cells and regulatory T (Treg) cells. Immunofluorescence staining of spleen sections also confirmed that MAP-TB vaccination enhanced the formation of GCs. Our results suggest that CD4⁺ T cell epitope of Ts-Pmy is crucial in vaccine component for inducing better protection against *T. spiralis* infection.

1. Introduction

Trichinellosis is a worldwide food-borne zoonosis spread between animals and people and mainly caused by the infection of *Trichinella spiralis* [1]. People are infected through eating raw or undercooked meat containing infective larvae, mostly from pigs or wild boars [2]. In China, the contaminated pork remains the predominant source of trichinellosis in humans. From 2005 to 2009, 15 outbreaks of human trichinellosis, with 1387 cases and 4 deaths, were reported in three provinces or autonomous regions of Southwestern China; 12 of them (85.71%) were caused by eating the raw

or undercooked pork [3]. A pork survey reported that the overall prevalence of *T. spiralis* infection in pigs was 0.61% (5/823) in Henan Province of China, in which 0.91% (5/550) of pigs were infected in Nanyang city alone [4]. It has been estimated that more than 40 million people are at risk of *Trichinella* infection in China [5]. In industrialized countries, although commercially produced pork under controlled management now accounts for about half of the world's pork production, the demand for free-range pork by consumers, especially in Europe and North America, is increasing. In Eastern Europe and Argentina, where traditional free-range backyard-raised pigs are often involved

with the feeding of food waste, the infected domestic pork is still blamed on many outbreaks of trichinellosis [6]. Because of the varying degrees of outdoor exposure in free-range systems, there is concern that such exposure will increase the risk of spreading *T. spiralis* from wild animal reservoirs to human beings [6]. It has been reported that rats living on pig farms play an important role in maintaining or spreading this parasite to other animals [2]. Thus, interrupting parasite transmission via vaccination of livestock with a potent and effective vaccine is a practical approach to prevent human trichinellosis.

In the past 30 years, many efforts have been dedicated to develop vaccine against *T. spiralis* infection with the purpose of reducing worm fecundity or decreasing muscle larval and adult worm burdens [1]. The vaccine candidates include excretory-secretory (ES) antigens [7], recombinant proteins [8, 9], and DNA vaccines [10], inducing different levels of partial protective immunity in animal models. However, as a tissue-dwelling helminth, it is difficult to develop an effective vaccine which induces sterile immunity because *T. spiralis* has a complex life cycle, diverse stage-specific antigens, and immune-evasion strategies [11, 12]. Subunit peptide vaccine based on multiple protective epitopes may overcome these problems and thus provides a novel approach to develop vaccines against infectious diseases such as trichinellosis [13].

In our previous study, a promising vaccine candidate, paramyosin (Pmy) of *T. spiralis* (*Ts*-Pmy), has exhibited partially protective immunity against *T. spiralis* infection in mice [14]. A protective B epitope of *Ts*-Pmy, YX1, has been characterized by screening a phage display peptide library with a protective monoclonal antibody (mAb) named as 7E2 [15]. In order to enhance host humoral immunity which plays an important role in the expulsion of *T. spiralis* [16], two potent CD4⁺ T cell epitopes of *Ts*-Pmy identified previously [17] were fused to the protective B epitope of *Ts*-Pmy (YX1) to construct a multiple antigen peptide (MAP-TB) in this study. We have observed that mice immunized with this fused MAP (MAP-TB) based on T/B epitopes of *Ts*-Pmy induced potent protection against *T. spiralis* infection which is associated with enhanced humoral immune responses.

2. Materials and Methods

2.1. Ethics Statement. This study was performed in accordance with the National Institutes of Health Guidelines for the Care and Use of Experimental Animals. All animal experimental procedures were reviewed and approved by the Institutional Animal Care and Use Committee (IACUC) of Capital Medical University (approval number: AEEI-2015-149).

2.2. Mice and Parasites. Six- to eight-week-old female BALB/c (H-2^d) mice were obtained from the Laboratory Animal Services Center of Capital Medical University (Beijing, China) and raised under specific pathogen-free standard conditions. Each experimental group consisted of ten mice. *T. spiralis* (ISS 533) strain used in this study was maintained in female ICR mice, and the muscle larvae were

TABLE 1: Amino acid sequences and positions of CD4⁺ T cell epitopes and B cell epitope of *Ts*-Pmy.

Epitope	Position in <i>Ts</i> -Pmy	Amino acid sequence
T2 (P2)	528-542	QFEIDRLAAALADAE
T5 (P5)	610-624	AIAQRKLSALSAELE
B (YX1)	88-107	EAAEGTTDAQIDANRKRESE

recovered from the muscle of infected mice using a modified pepsin-hydrochloric acid digestion method as described by Gamble et al. [18].

2.3. Synthesis of MAP. MAP-TB and MAP-B constructed in this study are four-branched MAPs containing either two CD4⁺ T cell epitopes (T2 and T5) fused with a B cell epitope (MAP-TB) or only B cell epitope (MAP-B). The T-B peptides are linked at their C terminus to the lysine core of the MAP. Two different CD4⁺ T cell epitopes, T2 and T5, representing the CD4⁺ T cell epitopes P2 and P5 identified in our previous studies [17, 19], were chosen for constructing the MAP-TB (Table 1, Figures 1(a) and 1(b)). B represents the B cell epitope originally designated as YX1, recognized by a protective mAb which conferred partial protection against *T. spiralis* infection by passive transfer [15]. The MAPs were synthesized by Aviva Systems Biology Corporation (China). The synthesis of MAPs utilized a solid-phase synthesis using 9-fluorenylmethoxycarbonyl (FMOC) as a protecting group. The synthesized MAPs were purified by high-performance liquid chromatography (HPLC), then lyophilized and stored desiccated at -80°C before use. The MAPs were also identified by MASS spectrometry, and the purity of MAPs was over 90%. The lyophilized MAPs were dissolved in PBS at 5 mg/ml as stock solutions which were stored at -40°C until use. The working concentration was 0.6 mg/ml in PBS.

2.4. Immunization Regimen. To evaluate the immune response induced by the MAP-TB and MAP-B, ten female BALB/c mice were subcutaneously immunized on the back. The MAPs were emulsified with Freund's adjuvant (Sigma-Aldrich, Germany) using complete adjuvant for the initial dose and incomplete adjuvant for the following two booster inoculations at an interval of two weeks. 30 μg of MAP-TB or MAP-B (50 μl) was emulsified with the same volume of adjuvant for a single dose. Another 10 mice were subcutaneously injected with 50 μl PBS emulsified with the same volume of the corresponding adjuvant as the control. One week after the final boost, five mice from each group were sacrificed for collecting sera, spleens, and inguinal lymph nodes (ILNs) to evaluate the induced immune responses. The rest 5 mice were challenged with 400 infective muscle larvae (ML) of *T. spiralis* for evaluating the protection as described below. A representation of experimental design is shown in Figure 2.

2.5. Antibody Responses. Anti-B cell epitope-specific antibodies induced by MAP immunization were measured by ELISA. Briefly, the plate was coated with 10 μg/well of B

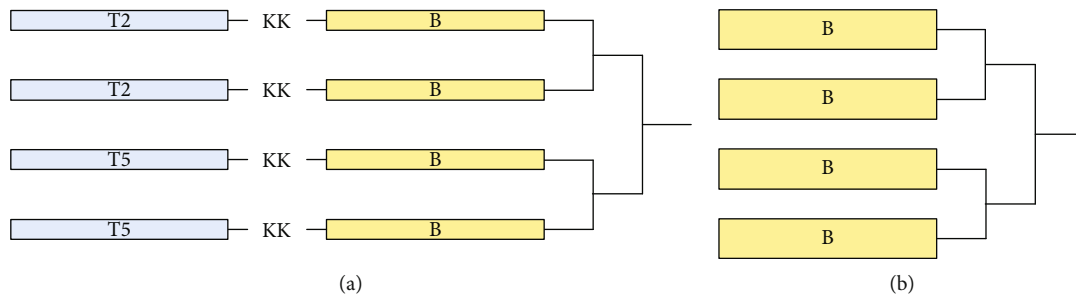


FIGURE 1: Schematic representation of the construction of MAP-TB (a) and MAP-B (b) used for immunization. In MAP-TB, B cell epitope is colinearly synthesized to T epitope, with a bi-lysine (KK) as a spacer.

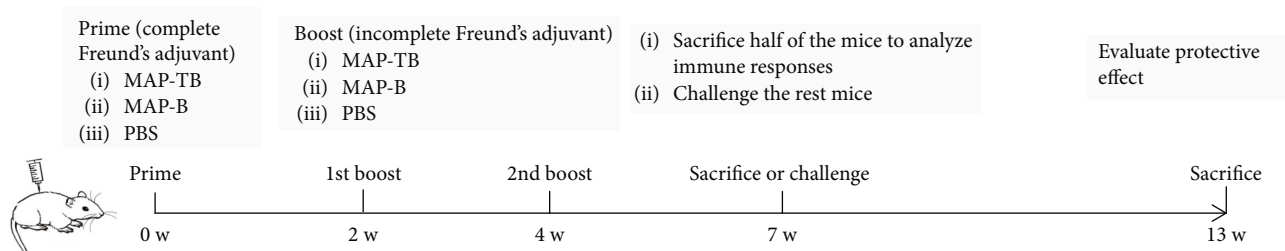


FIGURE 2: Schematic representation of experimental scheme. Three groups of mice (MAP-TB, MAP-B, and PBS) were immunized three times with Freund's adjuvant and challenged with 400 infective ML of *T. spiralis* to evaluate the protection induced by the MAPs.

cell epitope peptide YX1 in coating buffer overnight at 4°C. After blocking, serial dilutions of sera (0 w, 2 w, 4 w, 7 w, and 13 w) were added at 37°C for 30 min followed with the HRP-conjugated goat anti-mouse IgG (1:1000 dilution). The titers of each group were expressed as the geometric mean of the dilution. For IgG subclass detection, the sera were diluted at 1:2000 and 1:5000, then incubated with Biotin-conjugated Rat Anti-Mouse IgG1 or IgG2a (BD Biosciences, USA) followed by Streptavidin-HRP (BD Biosciences, USA). The color was developed with tetramethylbenzidine substrate (TMB, BD Biosciences, USA) and read at 450 nm.

2.6. Cytokine Assay. One week after the final immunization, mice were sacrificed and splenocytes were separated aseptically using mouse lymphocyte separation medium (Dakewe Biotech, China). After being centrifuged, the spleen cells were resuspended and adjusted to 1×10^7 cells/ml in complete RPMI-1640 supplemented with 10% FBS, penicillin (100 U/ml), and streptomycin (100 µg/ml). For *in vitro* stimulation, a total of 1×10^6 splenocytes were incubated with mixed peptides (2.5 µg/ml T2 and T5 individually) in 200 µl of complete RPMI-1640 for 48 h at 37°C in a humidified atmosphere containing 5% CO₂. Splenocytes stimulated simultaneously with ConA (Sigma-Aldrich, USA; 5 µg/ml) were served as positive controls. The cytokines IFN-γ, IL-2, IL-4, IL-5, and IL-6 were detected using the corresponding ELISA kit (BioLegend, USA), according to the manufacturer's instructions.

2.7. Flow Cytometric Analysis. Spleens and ILNs of mice were harvested on day 7 after the final immunization. The

lymphocytes were collected and analyzed by flow cytometry. The frequencies of CXCR5⁺PD-1⁺CD3⁺CD4⁺ Tfh cells (in spleens), CXCR5⁺PD-1^{high}CD3⁺CD4⁺ Tfh cells (in ILNs), and CD25⁺FoxP3⁺CD3⁺CD4⁺ Treg cells (in spleens) presented within the total CD4⁺ T cells; the frequencies of GL7⁺Fas⁺B220⁺ germinal center (GC) B cells presented within the total B220⁺ B cells; and the frequencies of CXCR5⁺FoxP3⁺CD3⁺CD4⁺ Tfr cells presented within the CD4⁺ T cells (in spleens and ILNs) were detected. Dead cells were excluded by viability dye staining, and duplicates were excluded by FSC/A and FSC/W gating analysis. Cells were analyzed by a BD LSRFortessa™ Flow Cytometry (BD Biosciences, USA). Data were acquired and analyzed by BD FACSDIVA™ version 8.0.2 (BD Biosciences, USA).

For surface staining, splenocytes were blocked with anti-CD16/CD32 mAb (Clone: 93, BD Pharmingen™, USA) and stained with the following antibodies: anti-CD3e-Percp-Cyanine5.5 (Clone: 145-2C11, eBioscience, USA), anti-CD4-FITC (Clone: RM4-5, eBioscience, USA), anti-PD-1-PE (Clone: J43, eBioscience, USA), and anti-CXCR5-APC (Clone: SPRCL5, eBioscience, USA) for Tfh cell analysis; with anti-GL7-FITC (Clone: GL7, BD Pharmingen™, USA), anti-Fas-PE (Clone: Jo2, BD Pharmingen™, USA), and anti-B220-PerCP-Cy5.5 (Clone: RA3-6B2, BD Pharmingen™, USA) mAb for GC B cell analysis. For viability dye staining, Fixable Viability Dye eFluor™ 450 (eBioscience, USA) was added with surface staining antibodies.

For intracellularly staining (Treg/Tfr), the splenocytes were blocked with anti-CD16/CD32 mAb (Clone: 93, BD Pharmingen™, USA), stained with anti-CD3e-Percp-Cyanine5.5, anti-CD4-FITC and anti-CXCR5-APC, or anti-

CD25-APC (Clone: PC61.5, eBioscience, USA), then fixed with FoxP3 Fixation/Permeabilization working solution (eBioscience, USA) and permeabilized with Permeabilization Buffer (eBioscience, USA). After that, the cells were intracellularly stained with anti-FoxP3-PE (Clone: FJK-16s, eBioscience, USA).

2.8. Immunofluorescence Assay. The spleens from BALB/c mice were separated one week after the final immunization and embedded in Optimal Cutting Temperature (OCT) Compound (SAKURA, USA). The tissues were frozen at -80°C before sectioning ($8\ \mu\text{m}$) on a Cryostat (Leica, Germany). After being fixed in cold acetone and blocked with 1% BSA in PBS at room temperature for 1 h, the sections were incubated with Biotinylated Peanut Agglutinin (PNA, 1:100 dilution, VECTOR, USA) at 4°C overnight. DyLight™ 488 Streptavidin (1:100 dilution, BioLegend, USA) was used as the secondary antibody at room temperature for 1 h. At last, Alexa Fluor® 647-conjugated anti-mouse CD45R (1:150 dilution, Clone RA3-6B2, BioLegend, USA) was incubated at room temperature for 1 h. The sections were scanned under a Panoramic SCAN instrument (3DHISTECH, Hungary). For quantification the area of GCs, spleen sections of three mice from each group were analyzed by ImageJ software.

2.9. Challenge Experiment. One week after the third immunization, the remaining five mice of each group were challenged orally with 400 *T. spiralis*-infective ML. Six weeks after the infection, the larvae from the muscle of each infected mouse were collected and counted. The reduction rate of ML burden was calculated based on the recovered larvae per gram (LPG) muscle from the mice immunized with MAP-TB or MAP-B versus those from the PBS control group. Specifically, it was calculated as follows: worm burden reduction rate (%) = $(1 - \text{mean number of LPG in vaccinated mice} / \text{mean number of LPG in control mice}) \times 100\%$. Three independent experiments were carried out.

2.10. Statistical Analysis. Statistical analyses were performed with One-way ANOVA using SPSS for Windows, version 17.0. All data are expressed as the mean value + standard deviations (SD) or the mean value \pm SD. P value < 0.05 were considered statistically significant.

3. Results

3.1. Mice Immunized with MAP-TB Vaccine Produced Significant Higher Antibody Responses. BALB/c mice were immunized with MAP-TB and MAP-B for three times, and the sera were collected on 0 w, 2 w, 4 w, 7 w, and 13 w. B cell epitope peptide YX1 was used as a coating antigen, and the antibody titers against YX1 were measured by ELISA. Anti-YX1 IgG titers in five mice immunized with MAP-TB were greatly elevated after the first immunization and significantly higher than those in mice immunized with MAP-B or PBS (Figure 3(a), $P < 0.01$). The IgG antibody subclass was determined at a 1:2000 dilution (Figure 3(b)) and 1:5000 (Figure 3(c)) and revealed that MAP-TB induced both IgG1 and IgG2a responses, with IgG1 being predominant. However, MAP-B contains only B epitope and immunization

of MAP-B induced a Th2 polarization direction which showed mainly IgG1 and impaired production of IgG2a.

3.2. MAP-TB Vaccination Induced a Mixed Th1 and Th2 Cytokine Response in Mice. The cytokines IFN- γ , IL-2, IL-4, IL-5, and IL-6 secreted by splenocytes of immunized mice upon stimulation of mixed peptides T2 and T5 *in vitro* were detected by corresponding specific ELISA. The levels of the typical Th1 cytokines (IFN- γ and IL-2), Th2 cytokines (IL-4 and IL-5), and IL-6 in the culture supernatants of splenocytes upon stimulation were significantly elevated in mice immunized with MAP-TB as compared with mice immunized with MAP-B or PBS (Figure 4). However, there was no significant elevation of all cytokine responses in mice immunized with MAP-B compared with the PBS control group. These results indicated that MAP-TB vaccination induced a mixed Th1 and Th2 cytokine response in mice.

3.3. MAP-TB Vaccination Enhanced Expansion of Tfh Cells and Germinal Center B Cells. The production of high-affinity antibodies relies on the complex interaction of B cells with Tfh cells in the GC reaction. Seven days after the final immunization, lymphocytes of spleens and ILNs were harvested and analyzed by flow cytometry to determine the frequencies of CXCR5 $^{+}$ PD-1 $^{+}$ CD3 $^{+}$ CD4 $^{+}$ Tfh cells (in spleens), CXCR5 $^{+}$ PD-1 $^{\text{high}}$ CD3 $^{+}$ CD4 $^{+}$ Tfh cells (in ILNs), GL7 $^{+}$ Fas $^{+}$ B220 $^{+}$ GC B cells (in spleens), CXCR5 $^{+}$ FoxP3 $^{+}$ CD3 $^{+}$ CD4 $^{+}$ Tfr cells [20] (in spleens and ILNs), and CD25 $^{+}$ FoxP3 $^{+}$ CD3 $^{+}$ CD4 $^{+}$ Treg cells (in spleens). Representative dot plots of flow cytometric analysis are shown in Figure 5. It has been proved that CXCR5 $^{+}$ PD-1 $^{\text{high}}$ CD3 $^{+}$ CD4 $^{+}$ T cells residing in lymph node GC represent a specific Tfh subset that correlate with B cell maturation and IgG production [21]. The frequencies of Tfh cells within total CD4 $^{+}$ T cells of spleens and ILNs and GC B cells within total B220 $^{+}$ B cells of spleens increased in mice immunized with MAP-TB compared with the MAP-B or PBS group (Figures 5(a) and 5(b)). Consistently, the frequencies of Tfr cells within CD4 $^{+}$ T cells of spleens and ILNs and the frequencies of Treg cells within the CD4 $^{+}$ T cells of spleens decreased significantly in mice immunized with MAP-TB compared with the other two groups (Figures 5(c) and 5(d)).

The formation of GCs through vaccination could be confirmed by PNA staining [22]. MAP-TB vaccination greatly enhanced the formation of GCs in the spleens of mice compared to the MAP-B or PBS group confirmed by immunofluorescence staining (Figure 6).

3.4. Partially Protective Immunity Elicited by MAP-TB Immunization. Challenge experiments demonstrated that mice immunized with MAP-TB induced 35.5% ML reduction compared to the PBS control group ($P < 0.01$), which was also significantly higher than MAP-B immunization (12.4% ML reduction, $P < 0.05$). However, there was no significant difference in the ML burden between the MAP-B and PBS groups (Table 2). These results indicated that MAP-TB immunization elicited partial protection against *T. spiralis* infection, whereas MAP-B immunization did not induce significant protection ($P < 0.01$).

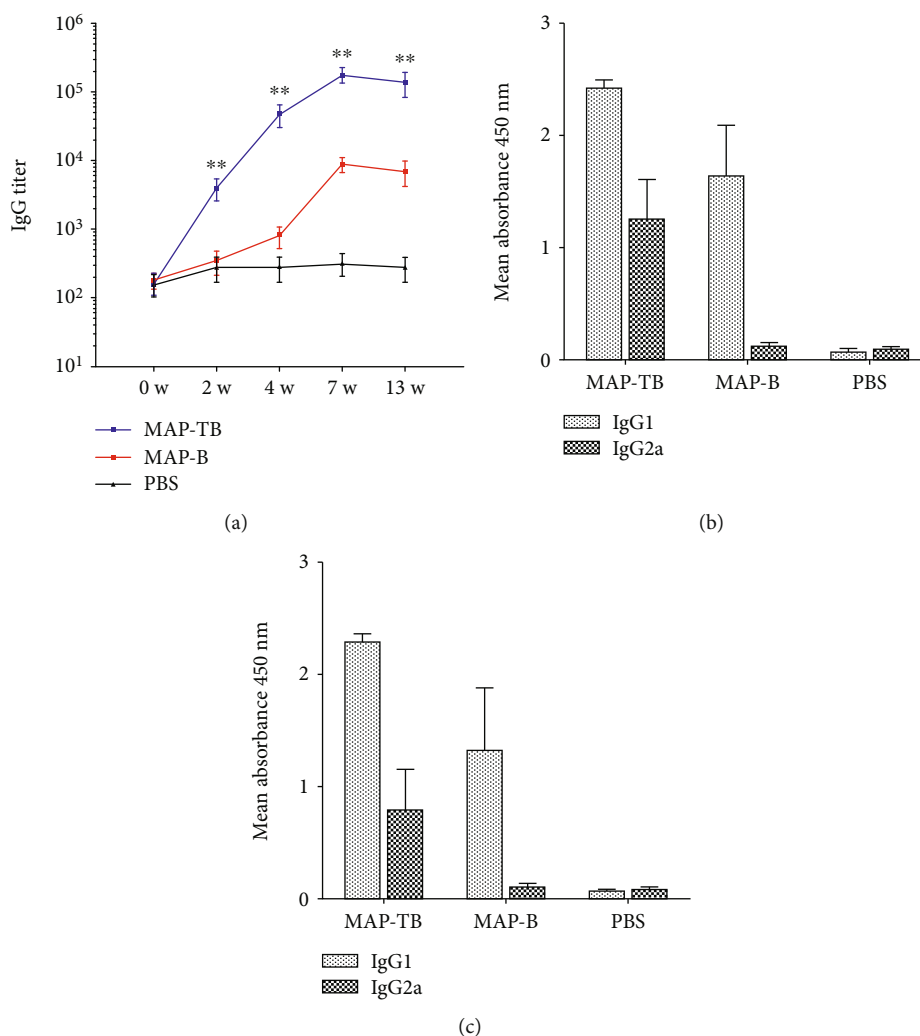


FIGURE 3: Serological antibody responses induced by immunization of MAP-TB or MAP-B measured by ELISA. (a) Specific IgG titers against B cell epitope peptide YX1 in the sera of mice immunized with MAP-TB or MAP-B on 0 w, 2 w, 4 w, 7 w, and 13 w. The total IgG is shown as the geometric mean titer of five mice within the group. ** indicates that anti-YX1 IgG titers in five mice immunized with MAP-TB were greatly elevated after the first immunization and were significantly higher than those in mice immunized with MAP-B or PBS ($P < 0.01$). (b, c) The OD₄₅₀ of subtype IgG1 and IgG2a responses in the sera of mice immunized with MAP-TB, MAP-B, or PBS at a dilution of 1:2,000 (b) and 1:5,000 (c). The values are shown as the mean + SD. The data was shown as one representative experiment out of three.

4. Discussion

During the past decades, researchers have been devoted to developing vaccines against trichinellosis utilizing different vaccine platforms, such as crude worm antigens, recombinant proteins, and DNA vaccines. As *T. spiralis* cannot be cultured *in vitro*, it is difficult to obtain a large amount of parasite antigens. In recent years, researchers have focused on recombinant proteins and DNA vaccines. For example, recombinant fructose-1,6-bisphosphate aldolase [23], serine protease [24], DNase II enzyme [25], and enolase [26] from *T. spiralis* exhibited muscle larva reductions range from 17.7% to 62.1%. Different DNA vaccines showed muscle larva reductions from 15.8% to 71.84% after *T. spiralis* larval challenge [10, 26, 27]. A few researches have been done on peptide vaccines against trichinellosis. It was first reported in 1995 that a 40-mer synthetic peptide vaccine induced a

64.3% adult worm reduction in subcutaneously immunized mice [28]. Seven years later, the same research group reported that intranasal administration of a 30-mer peptide antigen with cholera toxin B female significantly reduced worm fecundity (33.3%) compared to the controls [29]. Another research group reported that immunization of mice with an attenuated *Salmonella* strain displaying a 30-mer peptide using the ShdA autotransporter induced significantly adult worm reduction (61.83%) against *T. spiralis* infection [30]. All of the above mentioned peptides are from the *T. spiralis* gp43 antigen, which has been proved to be a highly immunodominant protein.

In our previous study, *Ts-Pmy* has been proved to be a good vaccine candidate antigen which induced significant protection in immunized mice against the challenge of *T. spiralis*-infective larvae [14]. However, as a big protein consisting of 885 amino acids with a predicted molecular

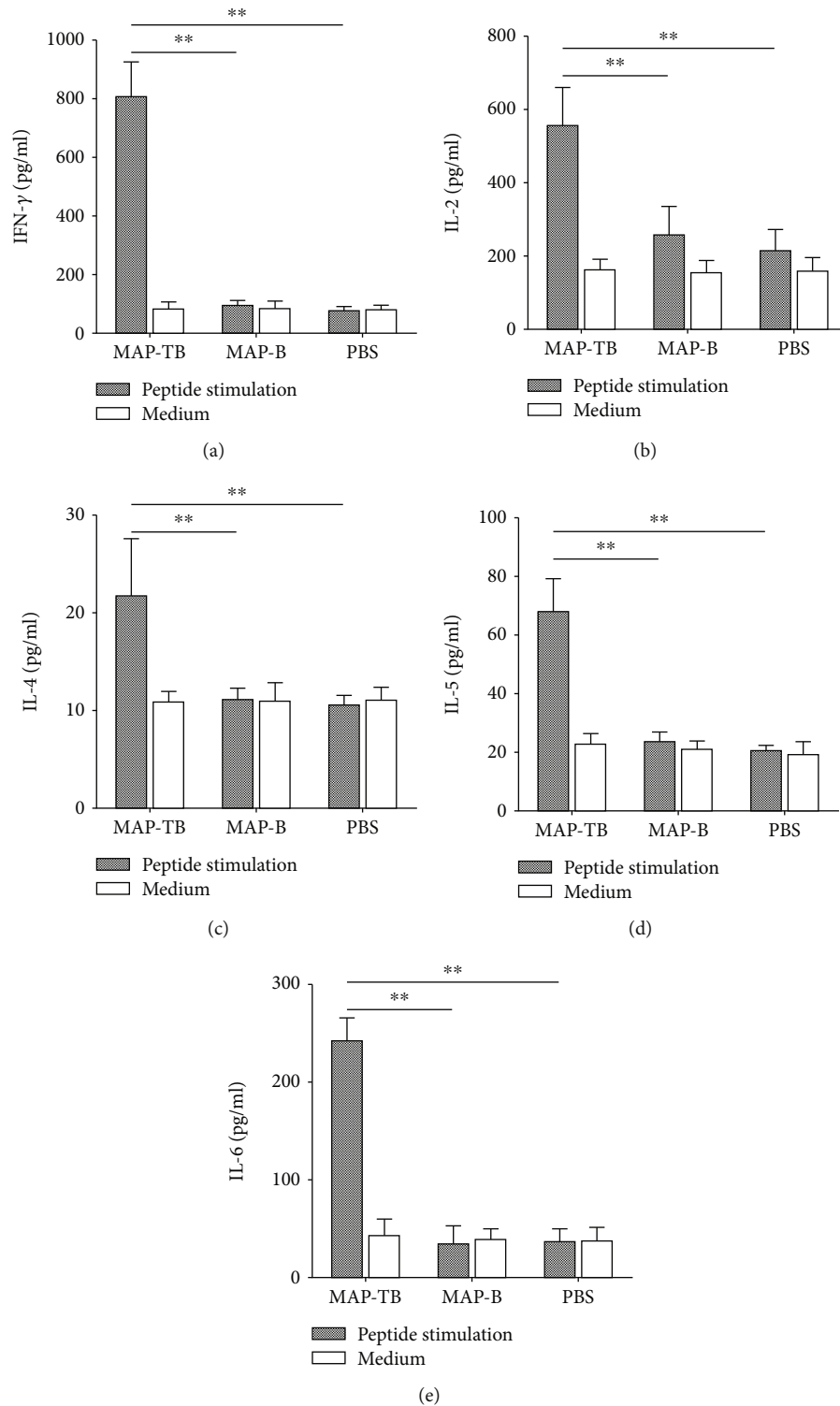


FIGURE 4: Cytokines secreted by splenocytes from immunized mice upon stimulation of mixed peptides T2 and T5 *in vitro*. Splenocytes secreted IFN- γ (a), IL-2 (b), IL-4 (c), IL-5 (d), and IL-6 (e) were detected by ELISA seven days after the final immunization. Splenocytes of each sample were stimulated simultaneously with ConA ($5 \mu\text{g/ml}$) as positive controls. All cytokines were greatly elevated upon stimulation with ConA, and the highest levels were observed as follows: IFN- γ —1280 pg/ml; IL-2—640 pg/ml; IL-4—60 pg/ml; IL-5—125 pg/ml; and IL-6—857 pg/ml (data not shown in the figure). The results are shown as the mean + SD (one representative experiment out of three). ** $P < 0.01$ ($n = 5$).

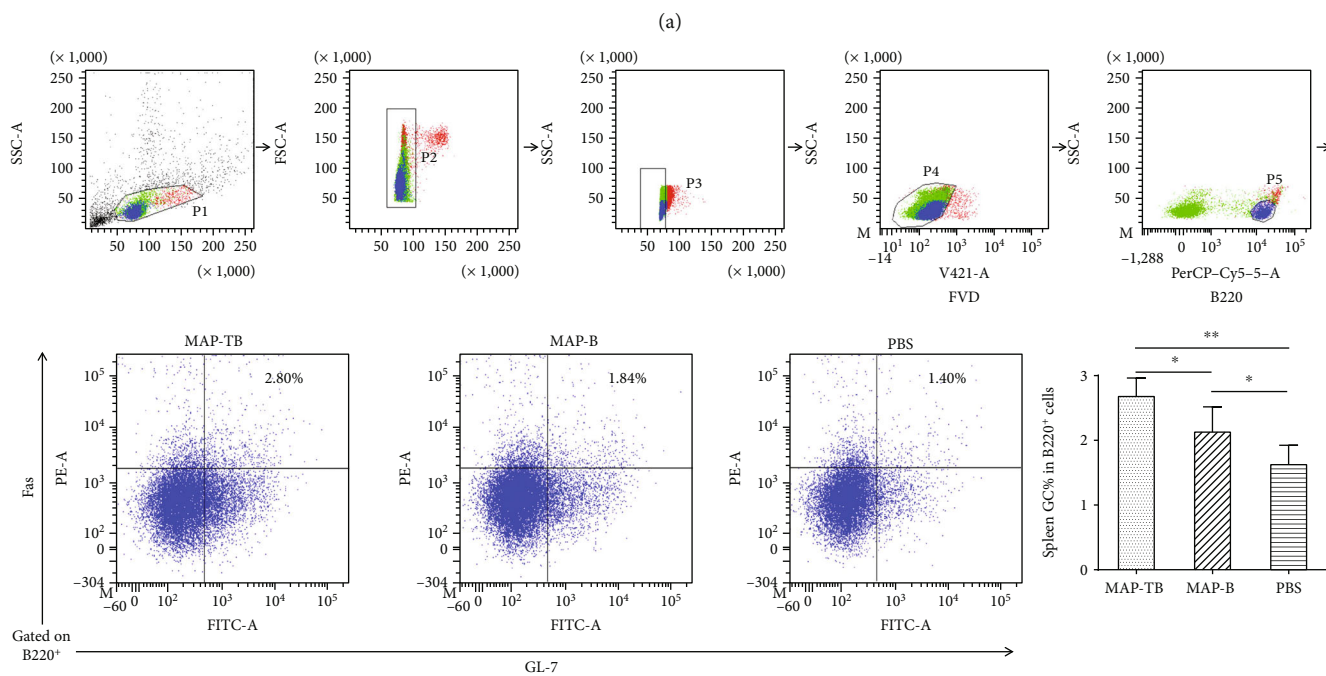
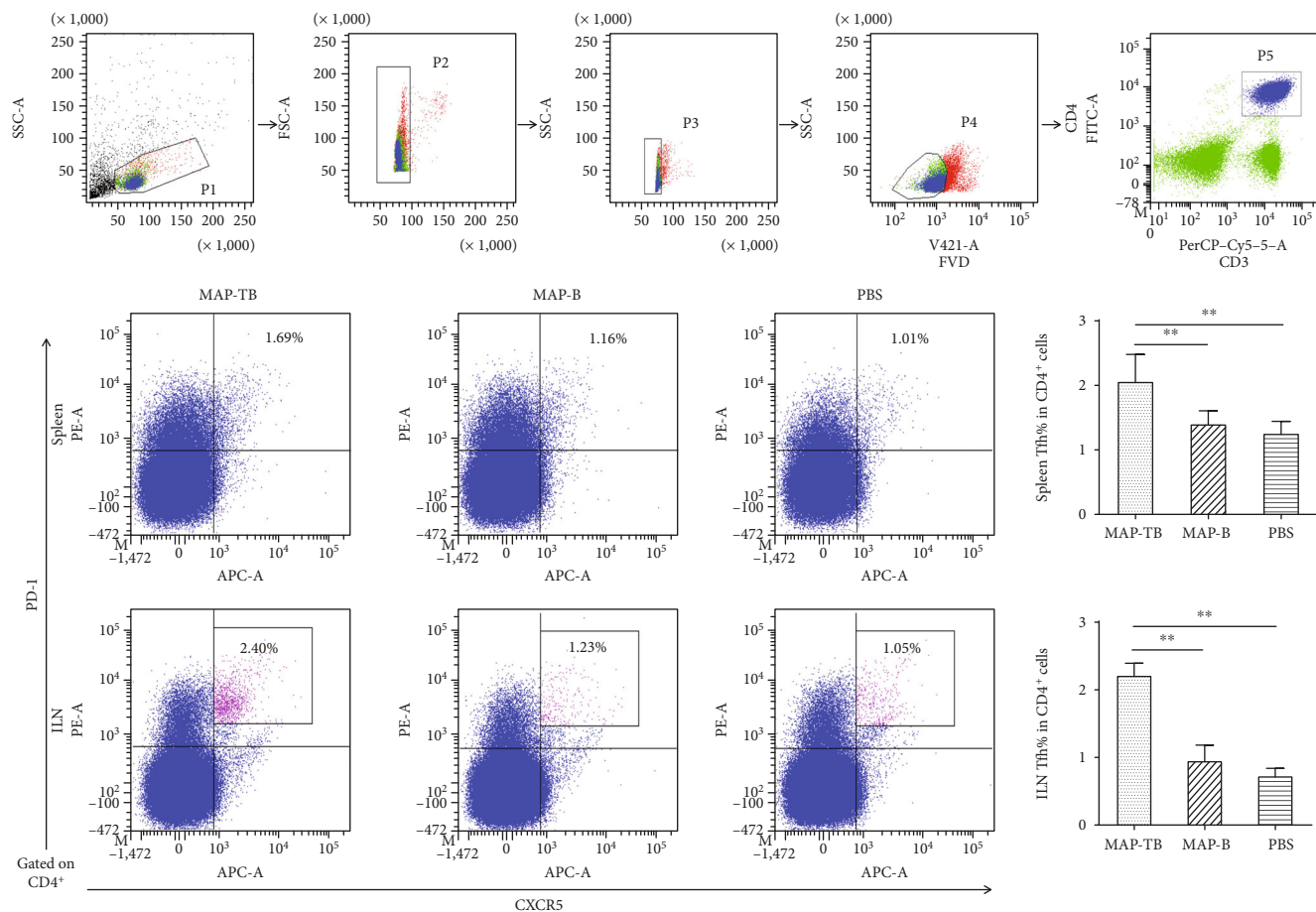


FIGURE 5: Continued.

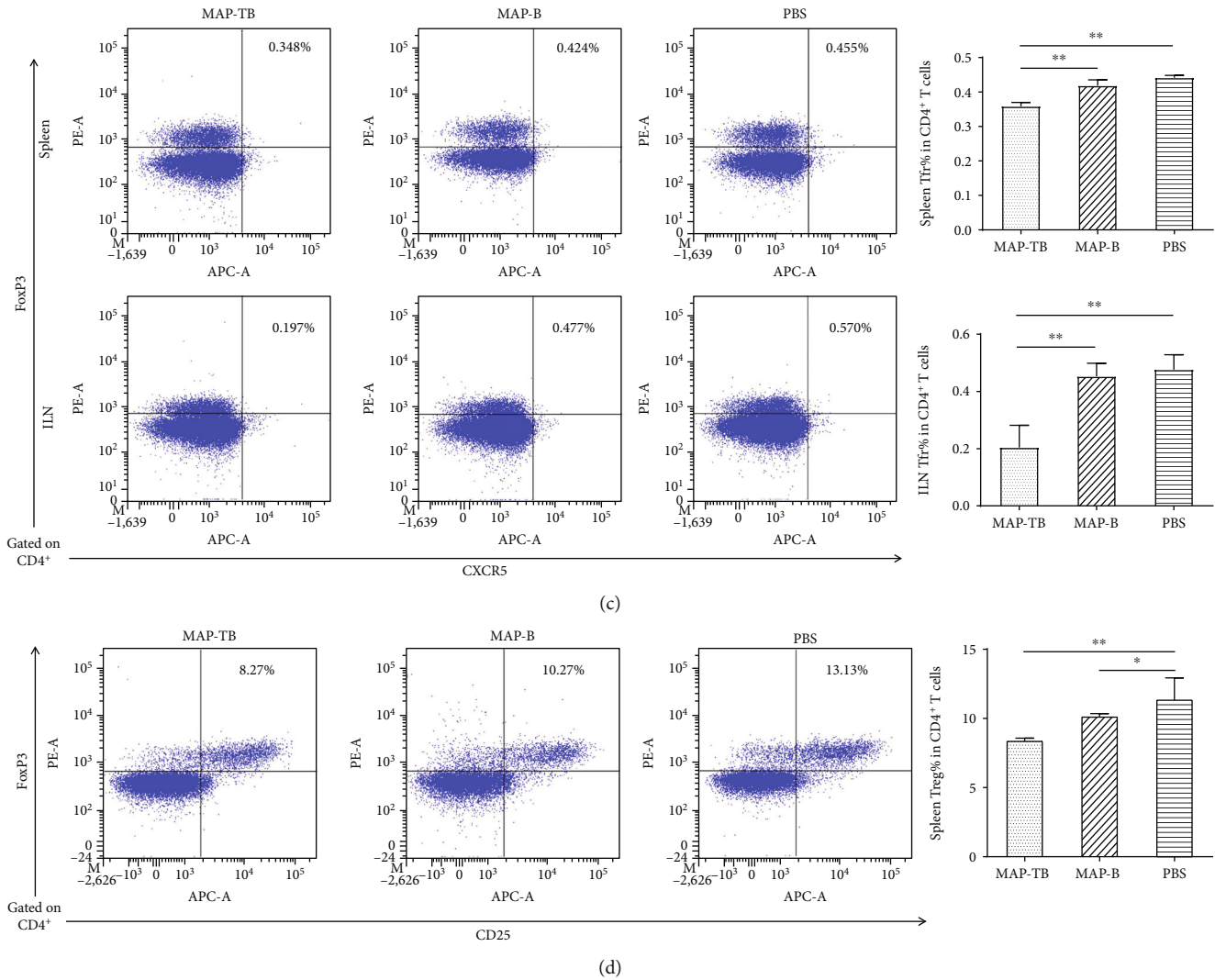


FIGURE 5: Tfh cells, GC B cells, Tfr cells, and Treg cells in the splenocytes and ILN lymphocytes of immunized mice were determined by flow cytometric analysis seven days after the final immunization. MAP-TB vaccination enhanced expansion of Tfh cells and GC B cells, while decreasing the frequencies of Tfr cells and Treg cells compared with the MAP-B or PBS group. For Tfh, Tfr, and Treg analysis, CD3⁺CD4⁺ T cells were gated and the gating strategies are shown in (a). (a) Representative dot plots of Tfh cells gated on CD4⁺ T cells of spleens and ILNs. Percentages in the upper right quadrant indicated the frequencies of CXCR5⁺PD-1⁺CD3⁺CD4⁺ Tfh cells within total CD4⁺ T cells. (b) Representative dot plots of GC B cells gated on B220⁺ B cells of the spleens. Percentages in the upper right quadrant indicated the frequencies of GC B cells within total B220⁺ B cells. (c) Representative dot plots of Tfr cells gated on CD4⁺ T cells of the spleens and ILNs. Percentages in the upper right quadrant indicated the frequencies of CXCR5⁺FoxP3⁺CD3⁺CD4⁺ cells within the CD4⁺ T cells of the spleens and ILNs. (d) Representative dot plots of Treg cells gated on CD4⁺ T cells of the spleens. Percentages in the upper right quadrant indicated the frequencies of CD25⁺FoxP3⁺CD3⁺CD4⁺ cells within the total CD4⁺ T cells of the spleens. The graphs are shown as the mean + SD (one representative experiment out of three). ***P* < 0.01; **P* < 0.05 (*n* = 5).

mass of 102 kDa, it is difficult to be expressed as a soluble recombinant protein in a prokaryotic expression system. Even in the eukaryotic expression system, only a small portion of protein could be expressed as soluble protein, which prevents its scale-up production as a recombinant protein vaccine. In addition to the difficulties in the yield of full-length recombinant protein, the complexity of the whole protein antigen may cause undesired detrimental side effects [31]. In recent years, peptide production becomes easily reproducible, fast, and cost-effective due to the advances in the peptide synthesis. In addition, chemical synthesis could

remove the concerns associated with the biological contamination of the expression system antigens in the recombinant protein production. Peptide vaccines also have some other advantages, such as being water soluble and having high stability under simple storage conditions (generally does not require “cold chain”) [32]. Due to these advantages, peptide-based vaccines are now playing an important role in the development of cancer and infective disease vaccine [13, 33]. Some clinical trials for peptide-based vaccines have been successfully tested as potential candidates for cancer therapeutic in recent years [33].

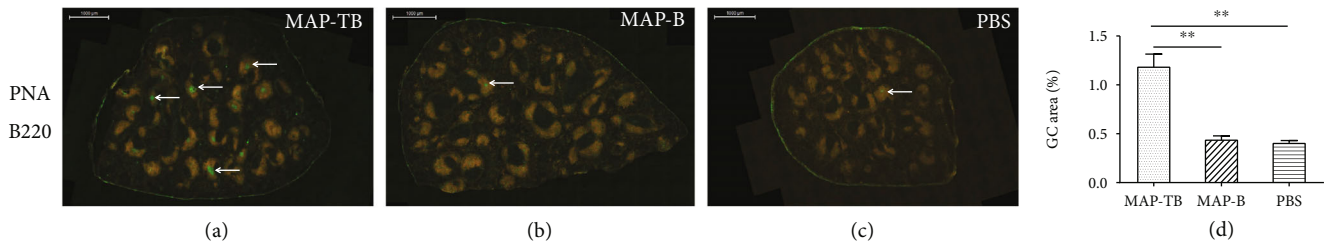


FIGURE 6: MAP-TB vaccination enhanced the formation of GCs in the spleen sections of immunized mice stained by PNA (green) and B220 (orange). The scale bar represents 1000 μm . The areas of GCs were normalized by section area, and spleen sections of three mice from each group were analyzed by ImageJ software (d).

TABLE 2: Protection elicited by MAP immunization against challenge with 400 *T. spiralis* ML in mice.

Experiment	MAP-TB	MAP-B (Mean LPG \pm SD/ML burden reduction)	PBS
1st	3799 \pm 565/35.5% ^{ab}	5156 \pm 543/12.4%	5886 \pm 1101/-
2nd	4024 \pm 637/37.2% ^{ab}	5469 \pm 701/14.6%	6403 \pm 1261/-
3rd	4105 \pm 583/33.0% ^{ab}	5444 \pm 620/11.1%	6124 \pm 1086/-

Three independent challenge experiments were carried out to evaluate the protection induced by MAP constructs. ^a $P < 0.01$ compared with PBS control group; ^b $P < 0.05$ compared with MAP-B group ($n = 5$).

However, peptide vaccine also has some disadvantages, such as poor immunogenicity and the need to conjugate to a large carrier protein (e.g., KLH and BSA). To increase the immunogenicity of a peptide-based vaccine, a new strategy of multiple antigenic peptides (MAPs) becomes a popular alternative. MAPs are peptides that are artificially branched by utilizing a lysine-based central backbone to which multiple peptide chains could be conjugated. The branched peptides sometimes can greatly increase their immunological responses because of the high molar ratio of peptide antigen to the core molecule and the high molecular weight which make them more immunogenic without the need of conjugation to a carrier protein [32, 34–36]. MAP vaccines have been studied in several infectious diseases, such as lymphatic filariasis [37], *Plasmodium falciparum* (*P. falciparum*) [38], *Yersinia pestis* [39], and HIV [40]. Clinical studies have been carried out in MAP vaccine against *P. falciparum* sporozoites [41]. In lymphatic filariasis, thioredoxin-transglutaminase MAP conferred a significantly higher protection of 63.04% than the whole protein cocktail vaccine did (55.8%) in jird models [37]. In *P. falciparum*, anti-MAP-1 (circumsporozoite protein-based) antibodies blocked the invasion of HepG2 liver cells by *P. falciparum* sporozoites (highest, 95.16% in HLA-A2 C57BL/6; lowest, 11.21% in BALB/c) [38]. This study revealed that the immune response induced by MAP was generally MHC dependent. It highlights the prospect of MAP constructs that may generate highly effective antimalarial responses in populations of genetically diverse HLA types.

Among peptide vaccines, epitope-composed one has some other unique advantages and becomes a good choice for vaccine development. This type of vaccine allows us to focus on the epitopes that possess strong immunogenicity and could induce robust protective immune effects in immu-

nized animals. Identification and correct selection of these epitopes are a crucial step in the design of an epitope-based peptide vaccine. The immunogenic epitopes on the protein of interest should be identified either by epitope prediction algorithms using bioinformatics tool [42] or by screening with antibodies [43]. These epitopes should be tested and confirmed for their ability to induce strong, long-lasting humoral (B cell or Th2 epitopes) and/or cellular immunity (CTL or Th1 epitopes) against the target pathogen [32, 42]. In this study, we constructed a MAP based on T/B cell epitope of *Ts*-Pmy and evaluated its immunogenicity and the induced protective immunity compared to the B cell epitope-conjugated MAP.

Previous studies showed that Th2 immune response was important in protective immunity against *T. spiralis* infection [16]. Therefore, Th2 epitopes should be an essential part of a vaccine against *T. spiralis* infection. During the initiation of immune response, the major histocompatibility complex-(MHC-) II combined with processed antigen epitope in antigen presenting cells trigger the activation of T helper cells which further activate cellular immunity and/or humoral immunity. In our previous work, based on the BALB/c mouse model, H-2^d-restricted CD4⁺ T cell epitopes (I-A^d and I-E^d) of *Ts*-Pmy were predicted using the SYFPEITHI database. The epitope peptides could stimulate splenocytes of r*Ts*-Pmy-immunized mice to secrete the Th2 cytokines IL-4 and IL-5. It has been further verified that these epitopes were immunodominant Th2 epitopes of *Ts*-Pmy by experiments *in vitro* and *in vivo* [17]. In the experiments of identifying and characterizing of CD4⁺ T cell epitopes, stimulation of splenocytes from mice immunized with r*Ts*-Pmy produced the highest IL-5 by peptide T5, while T2 stimulated the highest production of Th2 cytokine IL-4, as compared to the other T cell epitopes. T5 also stimulated splenocytes of

mice immunized with T5 to produce the highest IL-4 among all the candidate CD4⁺ T cell epitopes [17]. According to these results, T5 and T2 were selected as the CD4⁺ T cell epitopes to construct MAP in this study. In addition, a protective B epitope of *Ts-Pmy*, YX1, located between 88 and 107 amino acids of *Ts-Pmy*, has been identified by the recognition of a mAb 7E2 which passively transferred the protection against *T. spiralis* infection in naïve mice [15]. To evaluate whether Th2 epitopes could coordinate B cell epitope to produce the better protection against *T. spiralis* infection compared with B cell epitope alone, two types of MAP including MAP-TB and MAP-B were constructed. MAP-TB combines two Th2 epitopes and one B cell epitope while MAP-B contains only B cell epitope (Figure 1). The induced immune responses and protective effects against *T. spiralis* infection by immunization with these two MAP vaccines were further evaluated and compared.

Our previous study showed that a recombinant multi-epitope protein (rMEP) combined four CD4⁺ T cell epitopes and one B cell epitope produced a 55.4% of muscle larval reduction [19]. In this study, we demonstrated that mice immunized with MAP-TB induced significantly higher protection against the challenge of *T. spiralis*-infective larvae (35.5% ML reduction) compared to the MAP-B which induced only 12.4% ML reduction. MAP-TB did not induce comparable protection as that induced by rMEP possibly due to the less protective epitopes included in the construct of MAP-TB. Due to technical limitations of MAP synthesis, only two of four CD4⁺ T cell epitopes and one B cell epitope were constructed in MAPs in this study. The nonsterilizing immunity or low protection is a dilemma not only for vaccine development against *Trichinella* infection but also for all other helminth infections. For example, one of the most well-researched helminth diseases, schistosomiasis, the bar to achieve protective efficacy in humans was set at a consistent induction of 40% protection or better by the World Health Organization (WHO), and although this is a modest goal, it is yet to be reached with the six most promising schistosomiasis vaccine candidates (Sm28GST, IrV5, Sm14, paramyosin, TPI, and Sm23) [44, 45]. Vaccine against hookworm with less than 30% reduction in worm burden was also tested in clinical trials [46, 47]. The low protection induced by single vaccine immunization for helminth infection may be caused by the complexity of the life cycle, diversity of stage-specific antigens, immune-evasion strategies, and the modulatory effect of host responses [48]. Indeed, the pathology of parasites is directly related to the number of worms harbored by the host. Instead, the major benefit of a vaccine would be the reduction in worm burden with a concomitant reduction in morbidity, especially for the helminthic parasites, which induce nonsterilizing immunity in the host [49].

In this study, MAP-TB induced robust humoral immune response with higher IgG titers than MAP-B did. IgG subtype examination showed that MAP-TB immunization induced both IgG1 and IgG2a (with IgG1 predominant), while MAP-B mainly induced IgG1, indicating MAP-TB stimulated both Th1 and Th2 responses. The cytokine profiles secreted by the splenocytes also showed that MAP-TB immunization induced not only Th2 cytokines (IL-4 and

IL-5) but also Th1 cytokines (IFN- γ and IL-2). Th1 cytokine response was also elevated, and it was speculated that the epitopes were short peptides and they might be cross-presented by the dendritic cells.

Further flow cytometry analysis of the lymphocytes in the spleens and draining lymph nodes demonstrated that mice immunized with MAP-TB specifically enhanced the generation of Tfh cells and GC B cells and inhibited Tfr/Treg cells. Immunofluorescence staining of spleen sections also confirmed that MAP-TB vaccination enhanced the formation of GCs. All results indicated that MAP containing Th2 and B cell epitopes of *Ts-Pmy* induced better protection than MAP with B cell epitope alone, which associates with enhanced humoral immune responses, augmentation of Tfh and GC B cells, and inhibition of Tfr and Treg cells. It also indicated that B cell epitope alone could not induce strong humoral immune response, which is associated with decreased generation of Tfh and GC B cells.

Tfh cells are the unique CD4⁺ T follicular helper cells that provide cognate help to B cells to induce high-affinity antibody production in GCs [50]. Tfh cells depend on CXCR5 to localize in the follicular regions of lymphoid organs and maintain stable contact with antigen-primed B cells [51]. GCs support intense B cell clonal expansion, somatic hypermutation, selection of high-affinity B cells, and class switching of immunoglobulin genes. The products of the GC reaction are memory B cells and long-lived plasma cells that secrete high-affinity antibodies [22]. Mounting evidence suggests a strong correlation between the frequencies of Tfh cells and antigen-specific antibody responses, and more importantly, it was further proved in the human immune system [52]. Except for the inducement of Tfh proliferation, MAP-TB immunization also induced an elevation of IL-6 which has been shown to be an important regulator for the differentiation of Tfh cells [53]. It was reported that IL-6 played a pivotal role in shaping the acquired immune response by promoting the differentiation of B cells into immunoglobulin producing plasma cells and increasing the gamma globulin level in serum [54]. In addition, IL-6 is also an essential cytokine that transmits defense signals from a pathogen invasion or tissue damage site to stimulate acute phase reactions, immune responses, hematopoiesis, and various internal organs to prepare for host defense [55].

As a strong association of Tfh cells with multiple systemic and mucosal antibody responses was testified in many studies, many explorations of vaccine strategies have been made to enhance the generation of Tfh cells through the modulation of vaccine regimens. For example, an oil-in-water adjuvant, MF59, has been shown to promote GC B cell differentiation and Tfh induction [56]. Other vaccine strategies, such as incorporating DNA priming and protein boosting [57] or nanoparticle vaccines [58], have showed to expand Tfh cell populations and promote GC development, leading to enhanced humoral immunity. Antigen dose also has a positive impact on the induced frequencies of Tfh cells and subsequent serologic responses [59]. Given the importance of innate immune signals in shaping adaptive immune responses [60], a particular innate immune pathway with Tfh cell-skewing ability, such as TLR8, has

been identified for the rational design of Tfh cell-targeted vaccine adjuvants [61]. In our future studies, efforts will be targeted to trigger stronger antigen-specific Tfh responses induced by the peptide vaccines.

T follicular regulatory (Tfr) cells are a specialized subset of effector Treg cells that inhibit antibody production [62]. Successful humoral immunity is a delicate balance between stimulatory Tfh cells and inhibitory Tfr cells and not simply a result of the total number of Tfh cells [63]. Tfh and Tfr cells tightly control the size and output of the GC reaction and thus make them key targets to manipulate the vaccine design. Increasing Tfh cell formation and/or function or reducing the suppression exerted by Tfr cells in GC may be a rational strategy to improve vaccine response and efficacy [64]. Our study showed the increased frequencies of Tfh and the decreased frequencies of Tfr in the spleens and ILNs correlated with the expansion of antibody responses, which is consistent with previous studies [63, 65].

Treg cells are considered negative regulators of immune response which could suppress the activation, proliferation, and effector functions (such as cytokines production) of natural killer (NK) and NKT cells, B cells, CD4⁺ and CD8⁺ T cells, and antigen-presenting cells, *in vitro* and *in vivo* [66]. As a survival strategy of helminthic parasites, chronic helminth infection stimulates Tregs to produce regulatory and anti-inflammatory cytokines that reduce host immune responses to the invading worms [67]. Many helminth infections, such as *Heligmosomoides polygyrus* [68], *Schistosoma japonicum* [69], *Schistosoma mansoni* [70], and *Brugia malayi* [71], are known to stimulate an increased number of Tregs. Recently, our research group has found that Treg cells were significantly induced at the intestinal stage (6 days post infection) and newborn larva migration stage (15 days post infection) during the early *T. spiralis* infection [72]. In our study, we identified that immunization with MAP-TB decreased Treg ($P = 0.052$) and Tfr cells and stimulated Tfh and GC B cells in dLNs and spleens of immunized mice compared to MAP-B alone, indicating the addition of T-epitope in MAP-B could offset the immune inhibition induced by helminth infection and boost humoral immune response to vaccine antigen. This may also partly explain the protective effects induced by the immunization of MAP-TB and MAP-B.

In the current study, we found that peptide vaccine MAP-TB comprising CD4⁺ T cell epitopes could induce better protection against *T. spiralis* infection, which was associated with enhanced humoral immune response, compared to the MAP-B and PBS groups. The results from this study indicate that B-epitope alone is not efficient to induce robust humoral immune response. It is necessary to combine CD4⁺ T cell epitopes to construct an epitope-based peptide vaccine in order to induce better protection against *T. spiralis* infection. Similar studies on infective diseases also showed that potent CD4⁺ T cell epitope is a key vaccine component to elicit robust immune responses [73, 74]. As a multivalent antigen peptide vaccine could not only better cover the diversity of natural pathogen antigen and may even target several life stages of the pathogen but also better match the genetic variability of the host immune system [32], there-

fore, it is a promising strategy for developing vaccine against multicellular helminth infections such as *T. spiralis*. In our future study, including more protective epitopes (both T and B cell epitopes) in MAP constructs would be a practical way to improve protection.

Abbreviations

ES:	Excretory-secretory
GC:	Germinal center
HPLC:	High-performance liquid chromatography
ILN:	Inguinal lymph nodes
LPG:	Larvae per gram
mAb:	Monoclonal antibody
MAP:	Multiple antigen peptide
MHC:	Major histocompatibility complex
ML:	Muscle larvae
NK:	Natural killer
OCT:	Optimal cutting temperature
Pmy:	Paramyosin
PNA:	Peanut agglutinin
Tfh cell:	T follicular helper cell
Tfr cell:	T follicular regulatory cell
TMB:	Tetramethylbenzidine
Treg cell:	Regulatory T cell
Ts-Pmy:	Paramyosin of <i>Trichinella spiralis</i>

Data Availability

The data used to support the findings of this study are available within the article, or from the authors upon reasonable request.

Conflicts of Interest

The authors declare that they have no conflicts of interest.

Authors' Contributions

Yuan Gu designed and performed the experiments. Ximeng Sun and Jingjing Huang carried out the animal experiments. The manuscript was written by Yuan Gu and Bin Zhan. Xiping Zhu participated in the study design. All authors read and approved the final version of the paper.

Acknowledgments

This study was conducted with financial assistance from the National Natural Science Foundation of China (NSFC, 81572015).

References

- [1] N. Zhang, W. Li, and B. Fu, "Vaccines against *Trichinella spiralis*: progress, challenges and future prospects," *Transboundary and Emerging Diseases*, vol. 65, no. 6, pp. 1447–1458, 2018.
- [2] E. Bilska-Zajac, M. Rozycki, E. Antolak et al., "Occurrence of *Trichinella* spp. in rats on pig farms," *Annals of Agricultural and Environmental Medicine*, vol. 25, no. 4, article 99555, pp. 698–700, 2018.

- [3] J. Cui and Z. Q. Wang, "An epidemiological overview of swine trichinellosis in China," *Veterinary Journal*, vol. 190, no. 3, pp. 323–328, 2011.
- [4] P. Jiang, X. Zhang, L. A. Wang et al., "Survey of *Trichinella* infection from domestic pigs in the historical endemic areas of Henan province, Central China," *Parasitology Research*, vol. 115, no. 12, pp. 4707–4709, 2016.
- [5] X. Bai, X. Hu, X. Liu, B. Tang, and M. Liu, "Current research of trichinellosis in China," *Frontiers in Microbiology*, vol. 8, article 1472, 2017.
- [6] K. D. Murrell, "The dynamics of *Trichinella spiralis* epidemiology: out to pasture?," *Veterinary Parasitology*, vol. 231, pp. 92–96, 2016.
- [7] F. S. Quan, T. Matsumoto, J. B. Lee et al., "Immunization with *Trichinella spiralis* Korean isolate larval excretory-secretory antigen induces protection and lymphocyte subset changes in rats," *Immunological Investigations*, vol. 33, no. 1, pp. 15–26, 2004.
- [8] K. Bi, J. Yang, L. Wang, Y. Gu, B. Zhan, and X. Zhu, "Partially protective immunity induced by a 20 kDa protein secreted by *Trichinella spiralis* stichocytes," *PLoS One*, vol. 10, no. 8, article e136189, 2015.
- [9] Y. Y. Song, Y. Zhang, H. N. Ren et al., "Characterization of a serine protease inhibitor from *Trichinella spiralis* and its participation in larval invasion of host's intestinal epithelial cells," *Parasites & Vectors*, vol. 11, no. 1, p. 499, 2018.
- [10] J. F. Li, K. X. Guo, X. Qi et al., "Protective immunity against *Trichinella spiralis* in mice elicited by oral vaccination with attenuated *Salmonella*-delivered TsSP1.2 DNA," *Veterinary Research*, vol. 49, no. 1, p. 87, 2018.
- [11] R. Sun, X. Zhao, Z. Wang et al., "*Trichinella spiralis* paramyosin binds human complement C1q and inhibits classical complement activation," *PLOS Neglected Tropical Diseases*, vol. 9, no. 12, article e4310, 2015.
- [12] L. Zhao, S. Shao, Y. Chen et al., "*Trichinella spiralis* calreticulin binds human complement C1q as an immune evasion strategy," *Frontiers in Immunology*, vol. 8, p. 636, 2017.
- [13] Y. Li, K. Zheng, Y. Tan et al., "A recombinant multi-epitope peptide vaccine based on MOMP and CPSIT_p6 protein protects against *Chlamydia psittaci* lung infection," *Applied Microbiology and Biotechnology*, vol. 103, no. 2, pp. 941–952, 2019.
- [14] J. Yang, Y. Gu, Y. Yang et al., "*Trichinella spiralis*: immune response and protective immunity elicited by recombinant paramyosin formulated with different adjuvants," *Experimental Parasitology*, vol. 124, no. 4, pp. 403–408, 2010.
- [15] J. Wei, Y. Gu, J. Yang et al., "Identification and characterization of protective epitope of *Trichinella spiralis* paramyosin," *Vaccine*, vol. 29, no. 17, pp. 3162–3168, 2011.
- [16] P. Angkasekwinai, W. Sodthawon, S. Jeerawattanawart, A. Hansakon, K. Pattanapanyasat, and Y. H. Wang, "ILC2s activated by IL-25 promote antigen-specific Th2 and Th9 functions that contribute to the control of *Trichinella spiralis* infection," *PLoS One*, vol. 12, no. 9, article e184684, 2017.
- [17] Y. Gu, J. Huang, X. Wang et al., "Identification and characterization of CD4⁺ T cell epitopes present in *Trichinella spiralis* paramyosin," *Veterinary Parasitology*, vol. 231, article S0304401716302308, pp. 59–62, 2016.
- [18] H. R. Gamble, A. S. Bessonov, K. Cuperlovic et al., "International commission on Trichinellosis: recommendations on methods for the control of *Trichinella* in domestic and wild animals intended for human consumption," *Veterinary Parasitology*, vol. 93, no. 3–4, pp. 393–408, 2000.
- [19] Y. Gu, X. Sun, B. Li, J. Huang, B. Zhan, and X. Zhu, "Vaccination with a paramyosin-based multi-epitope vaccine elicits significant protective immunity against *Trichinella spiralis* infection in mice," *Frontiers in Microbiology*, vol. 8, article 1475, 2017.
- [20] M. Vaeth, G. Muller, D. Stauss et al., "Follicular regulatory T cells control humoral autoimmunity via NFAT2-regulated CXCR5 expression," *The Journal of Experimental Medicine*, vol. 211, no. 3, pp. 545–561, 2014.
- [21] H. Xu, X. Wang, A. A. Lackner, and R. S. Veazey, "PD-1^{HIGH} follicular CD4 T helper cell subsets residing in lymph node germinal centers correlate with B cell maturation and IgG production in rhesus macaques," *Frontiers in Immunology*, vol. 5, p. 85, 2014.
- [22] G. D. Victora and M. C. Nussenzweig, "Germinal centers," *Annual Review of Immunology*, vol. 30, pp. 429–457, 2012.
- [23] Y. Yang, X. Bai, C. Li et al., "Molecular characterization of fructose-1, 6-bisphosphate aldolase from *Trichinella spiralis* and its potential in inducing immune protection," *Frontiers in Cellular and Infection Microbiology*, vol. 9, p. 122, 2019.
- [24] G. G. Sun, J. J. Lei, H. N. Ren et al., "Intranasal immunization with recombinant *Trichinella spiralis* serine protease elicits protective immunity in BALB/c mice," *Experimental Parasitology*, vol. 201, pp. 1–10, 2019.
- [25] X. Qi, X. Yue, Y. Han et al., "Characterization of two *Trichinella spiralis* adult-specific DNase II and their capacity to induce protective immunity," *Frontiers in Microbiology*, vol. 9, article 2504, 2018.
- [26] X. Zhang, L. Xu, X. Song, X. Li, and R. Yan, "Molecular cloning of enolase from *Trichinella spiralis* and the protective immunity in mice," *Acta Parasitologica*, vol. 63, no. 2, pp. 252–260, 2018.
- [27] L. Wang, X. Wang, K. Bi et al., "Oral vaccination with attenuated *Salmonella typhimurium*-delivered TsPmy DNA vaccine elicits protective immunity against *Trichinella spiralis* in BALB/c mice," *PLOS Neglected Tropical Diseases*, vol. 10, no. 9, article e4952, 2016.
- [28] K. Robinson, T. Bellaby, W. C. Chan, and D. Wakelin, "High levels of protection induced by a 40-mer synthetic peptide vaccine against the intestinal nematode parasite *Trichinella spiralis*," *Immunology*, vol. 86, no. 4, pp. 495–498, 1995.
- [29] C. McGuire, W. C. Chan, and D. Wakelin, "Nasal immunization with homogenate and peptide antigens induces protective immunity against *Trichinella spiralis*," *Infection and Immunity*, vol. 70, no. 12, pp. 7149–7152, 2002.
- [30] E. N. Pompa-Mera, L. Yopez-Mulia, A. Ocana-Mondragon, E. A. García-Zepeda, G. Ortega-Pierres, and C. R. González-Bonilla, "*Trichinella spiralis*: Intranasal immunization with attenuated *Salmonella enterica* Carrying a gp43 antigen-derived 30mer epitope elicits protection in BALB/c mice," *Experimental Parasitology*, vol. 129, no. 4, article S0014489411002645, pp. 393–401, 2011.
- [31] A. Sette and J. Fikes, "Epitope-based vaccines: an update on epitope identification, vaccine design and delivery," *Current Opinion in Immunology*, vol. 15, no. 4, pp. 461–470, 2003.
- [32] M. Skwarczynski and I. Toth, "Peptide-based synthetic vaccines," *Chemical Science*, vol. 7, no. 2, pp. 842–854, 2016.
- [33] T. Bekaii-Saab, R. Wesolowski, D. H. Ahn et al., "Phase I immunotherapy trial with two chimeric HER-2 B-cell peptide

- vaccines emulsified in Montanide ISA 720VG and nor-MDP adjuvant in Patients with advanced solid tumors,” *Clinical Cancer Research*, vol. 25, no. 12, pp. 3495–3507, 2019.
- [34] J. P. Tam, “Synthetic peptide vaccine design: synthesis and properties of a high-density multiple antigenic peptide system,” *Proceedings of the National Academy of Sciences of the United States of America*, vol. 85, no. 15, pp. 5409–5413, 1988.
- [35] C. A. Moreno, R. Rodriguez, G. A. Oliveira et al., “Preclinical evaluation of a synthetic *Plasmodium falciparum* MAP malaria vaccine in Aotus monkeys and mice,” *Vaccine*, vol. 18, no. 1-2, pp. 89–99, 1999.
- [36] H. Tallima, M. Montash, P. Veprek, J. Velek, J. Jezek, and R. el Ridi, “Differences in immunogenicity and vaccine potential of peptides from *Schistosoma mansoni* glyceraldehyde 3-phosphate dehydrogenase,” *Vaccine*, vol. 21, no. 23, pp. 3290–3300, 2003.
- [37] C. Immanuel, A. Ramanathan, M. Balasubramaniyan et al., “Immunoprophylaxis of multi-antigen peptide (MAP) vaccine for human lymphatic filariasis,” *Immunologic Research*, vol. 65, no. 3, pp. 729–738, 2017.
- [38] B. Mahajan, J. A. Berzofsky, R. A. Boykins et al., “Multiple antigen peptide vaccines against *Plasmodium falciparum* malaria,” *Infection and Immunity*, vol. 78, no. 11, pp. 4613–4624, 2010.
- [39] R. K. Shreewastav, R. Ali, J. B. Uppada, and D. N. Rao, “Cell-mediated immune response to epitopic MAP (multiple antigen peptide) construct of LcrV antigen of *Yersinia pestis* in murine model,” *Cellular Immunology*, vol. 278, no. 1-2, pp. 55–62, 2012.
- [40] B. Sahay, A. M. Aranyos, M. Mishra et al., “Immunogenicity and efficacy of a novel multi-antigenic peptide vaccine based on cross-reactivity between feline and human immunodeficiency viruses,” *Viruses*, vol. 11, no. 2, p. 136, 2019.
- [41] R. Edelman, S. S. Wasserman, J. G. Kublin et al., “Immediate-type hypersensitivity and other clinical reactions in volunteers immunized with a synthetic multi-antigen peptide vaccine (PfCS-MAP1NYU) against *Plasmodium falciparum* sporozoites,” *Vaccine*, vol. 21, no. 3-4, pp. 269–280, 2002.
- [42] A. Scholzen, G. Richard, L. Moise et al., “Promiscuous *Coxiella burnetii* CD4 epitope clusters associated with human recall responses are candidates for a novel T-cell targeted multi-epitope Q fever vaccine,” *Frontiers in Immunology*, vol. 10, p. 207, 2019.
- [43] J. Ma, Y. Wei, L. Zhang et al., “Identification of a novel linear B-cell epitope as a vaccine candidate in the N2N3 subdomain of *Staphylococcus aureus* fibronectin-binding protein A,” *Journal of Medical Microbiology*, vol. 67, no. 3, pp. 423–431, 2018.
- [44] D. P. Mcmanus and A. Loukas, “Current status of vaccines for schistosomiasis,” *Clinical Microbiology Reviews*, vol. 21, no. 1, pp. 225–242, 2008.
- [45] R. Stephenson, H. You, D. P. Mcmanus, and I. Toth, “Schistosome vaccine adjuvants in preclinical and clinical research,” *Vaccines*, vol. 2, no. 3, pp. 654–685, 2014.
- [46] J. Bethony, A. Loukas, M. Smout et al., “Antibodies against a secreted protein from hookworm larvae reduce the intensity of hookworm infection in humans and vaccinated laboratory animals,” *The FASEB Journal*, vol. 19, no. 12, pp. 1743–1745, 2005.
- [47] J. M. Bethony, G. Simon, D. J. Diemert et al., “Randomized, placebo-controlled, double-blind trial of the Na-ASP-2 hookworm vaccine in unexposed adults,” *Vaccine*, vol. 26, no. 19, pp. 2408–2417, 2008.
- [48] G. Ortega-Pierres, A. Vaquero-Vera, R. Fonseca-Linan, R. M. Bermúdez-Cruz, and R. Argüello-García, “Induction of protection in murine experimental models against *Trichinella spiralis*: an up-to-date review,” *Journal of Helminthology*, vol. 89, no. 5, pp. 526–539, 2015.
- [49] A. Loukas, J. Bethony, S. Brooker, and P. Hotez, “Hookworm vaccines: past, present, and future,” *The Lancet Infectious Diseases*, vol. 6, no. 11, pp. 733–741, 2006.
- [50] Z. Shulman, A. D. Gitlin, S. Targ et al., “T follicular helper cell dynamics in germinal centers,” *Science*, vol. 341, no. 6146, pp. 673–677, 2013.
- [51] N. Fazilleau, L. Mark, L. J. McHeyzer-Williams, and M. G. McHeyzer-Williams, “Follicular helper T cells: lineage and location,” *Immunity*, vol. 30, no. 3, pp. 324–335, 2009.
- [52] A. Aljurayyan, S. Puksuriwong, M. Ahmed et al., “Activation and induction of antigen-specific T follicular helper cells play a critical role in live-attenuated influenza vaccine-induced human mucosal anti-influenza antibody response,” *Journal of Virology*, vol. 92, no. 11, 2018.
- [53] J. A. Harker, G. M. Lewis, L. Mack, and E. I. Zuniga, “Late interleukin-6 escalates T follicular helper cell responses and controls a chronic viral infection,” *Science*, vol. 334, no. 6057, pp. 825–829, 2011.
- [54] M. Narazaki and T. Kishimoto, “The two-faced cytokine IL-6 in host defense and diseases,” *International Journal of Molecular Sciences*, vol. 19, no. 11, p. 3528, 2018.
- [55] T. Kishimoto, “IL-6: from its discovery to clinical applications,” *International Immunology*, vol. 22, no. 5, pp. 347–352, 2010.
- [56] G. B. Mastelic, C. S. Eberhardt, F. Auderset et al., “MF59 mediates its B cell adjuvanticity by promoting T follicular helper cells and thus germinal center responses in adult and early life,” *The Journal of Immunology*, vol. 194, no. 10, pp. 4836–4845, 2015.
- [57] K. Hollister, Y. Chen, S. Wang et al., “The role of follicular helper T cells and the germinal center in HIV-1 gp120 DNA prime and gp120 protein boost vaccination,” *Human Vaccines & Immunotherapeutics*, vol. 10, no. 7, pp. 1985–1992, 2014.
- [58] J. J. Moon, H. Suh, A. V. Li, C. F. Ockenhouse, A. Yadava, and D. J. Irvine, “Enhancing humoral responses to a malaria antigen with nanoparticle vaccines that expand T_{fh} cells and promote germinal center induction,” *Proceedings of the National Academy of Sciences of the United States of America*, vol. 109, no. 4, pp. 1080–1085, 2012.
- [59] M. A. Pilkinton, K. J. Nicholas, C. M. Warren et al., “Greater activation of peripheral T follicular helper cells following high dose influenza vaccine in older adults forecasts seroconversion,” *Vaccine*, vol. 35, no. 2, pp. 329–336, 2017.
- [60] A. Iwasaki and R. Medzhitov, “Control of adaptive immunity by the innate immune system,” *Nature Immunology*, vol. 16, no. 4, pp. 343–353, 2015.
- [61] M. Ugolini, J. Gerhard, S. Burkert et al., “Recognition of microbial viability via TLR8 drives T_{FH} cell differentiation and vaccine responses,” *Nature Immunology*, vol. 19, no. 4, pp. 386–396, 2018.
- [62] M. A. Linterman, W. Pierson, S. K. Lee et al., “Foxp3⁺ follicular regulatory T cells control the germinal center response,” *Nature Medicine*, vol. 17, no. 8, pp. 975–982, 2011.
- [63] P. T. Sage, C. L. Tan, G. J. Freeman, M. Haigis, and A. H. Sharpe, “Defective TFH cell function and increased TFR cells

- contribute to defective antibody production in aging,” *Cell Reports*, vol. 12, no. 2, pp. 163–171, 2015.
- [64] M. A. Linterman and D. L. Hill, “Can follicular helper T cells be targeted to improve vaccine efficacy?,” *F1000Research*, vol. 5, p. 88, 2016.
- [65] D. Amodio, N. Cotugno, G. Macchiarulo et al., “Quantitative multiplexed imaging analysis reveals a strong association between immunogen-specific B cell responses and tonsillar germinal center immune dynamics in children after influenza vaccination,” *Journal of Immunology*, vol. 200, no. 2, pp. 538–550, 2018.
- [66] S. Sakaguchi, T. Yamaguchi, T. Nomura, and M. Ono, “Regulatory T cells and immune tolerance,” *Cell*, vol. 133, no. 5, pp. 775–787, 2008.
- [67] N. Ilic, A. Gruden-Movsesijan, and L. Sofronic-Milosavljevic, “*Trichinella spiralis*: shaping the immune response,” *Immunologic Research*, vol. 52, no. 1-2, pp. 111–119, 2012.
- [68] C. A. Finney, M. D. Taylor, M. S. Wilson, and R. M. Maizels, “Expansion and activation of CD4⁺CD25⁺ regulatory T cells in *Heligmosomoides polygyrus* infection,” *European Journal of Immunology*, vol. 37, no. 7, pp. 1874–1886, 2007.
- [69] X. Wen, L. He, Y. Chi et al., “Dynamics of Th17 cells and their role in *Schistosoma japonicum* infection in C57BL/6 mice,” *PLoS Neglected Tropical Diseases*, vol. 5, no. 11, article e1399, 2011.
- [70] M. Baumgart, F. Tompkins, J. Leng, and M. Hesse, “Naturally occurring CD4⁺Foxp3⁺ regulatory T cells are an essential, IL-10-independent part of the immunoregulatory network in *Schistosoma mansoni* egg-induced inflammation,” *Journal of Immunology*, vol. 176, no. 9, pp. 5374–5387, 2006.
- [71] H. J. Mcorley, Y. M. Marcus, J. Murray, M. D. Taylor, and R. M. Maizels, “Expansion of Foxp3⁺ regulatory T cells in mice infected with the filarial parasite *Brugia malayi*,” *The Journal of Immunology*, vol. 181, no. 9, pp. 6456–6466, 2008.
- [72] X.-M. Sun, K. Guo, C.-Y. Hao, B. Zhan, J.-J. Huang, and X. Zhu, “*Trichinella spiralis* excretory–secretory products stimulate host regulatory T cell differentiation through activating dendritic cells,” *Cells*, vol. 8, no. 11, p. 1404, 2019.
- [73] R. A. Holanda, J. E. Munoz, L. S. Dias et al., “Recombinant vaccines of a CD4⁺ T-cell epitope promote efficient control of *Paracoccidioides brasiliensis* burden by restraining primary organ infection,” *PLOS Neglected Tropical Diseases*, vol. 11, no. 9, article e5927, 2017.
- [74] M. Hassert, K. J. Wolf, K. E. Schwetye, R. DiPaolo, J. D. Brien, and A. K. Pinto, “CD4⁺T cells mediate protection against Zika associated severe disease in a mouse model of infection,” *PLoS Pathogens*, vol. 14, no. 9, article e1007237, 2018.

Research Article

Preliminary Evaluation of the Safety and Immunogenicity of an Antimalarial Vaccine Candidate Modified Peptide (IMPIPS) Mixture in a Murine Model

Jennifer Lambraño,^{1,2} Hernando Curtidor,¹ Catalina Avendaño ,³ Diana Díaz-Arévalo ,^{1,4} Leonardo Roa ,³ Magnolia Vanegas,¹ Manuel E. Patarroyo,^{1,5} and Manuel A. Patarroyo ^{1,4}

¹Fundación Instituto de Inmunología de Colombia (FIDIC), Bogotá, Colombia

²Master's Programme in Biochemistry, Medical School, Universidad Nacional de Colombia, Bogotá, Colombia

³Faculty of Animal Science, Universidad de Ciencias Aplicadas y Ambientales (U.D.C.A), Bogotá, Colombia

⁴School of Medicine and Health Sciences, Universidad del Rosario, Bogotá, Colombia

⁵Pathology Department, Medical School, Universidad Nacional de Colombia, Bogotá, Colombia

Correspondence should be addressed to Manuel A. Patarroyo; mapatarr.fidic@gmail.com

Received 3 October 2019; Accepted 3 December 2019; Published 30 December 2019

Academic Editor: Pedro A. Reche

Copyright © 2019 Jennifer Lambraño et al. This is an open access article distributed under the Creative Commons Attribution License, which permits unrestricted use, distribution, and reproduction in any medium, provided the original work is properly cited.

Malaria continues being a high-impact disease regarding public health worldwide; the WHO report for malaria in 2018 estimated that ~219 million cases occurred in 2017, mostly caused by the parasite *Plasmodium falciparum*. The disease cost the lives of more than 400,000 people, mainly in Africa. In spite of great efforts aimed at developing better prevention (i.e., a highly effective vaccine), diagnosis, and treatment methods for malaria, no efficient solution to this disease has been advanced to date. The Fundación Instituto de Inmunología de Colombia (FIDIC) has been developing studies aimed at furthering the search for vaccine candidates for controlling *P. falciparum* malaria. However, vaccine development involves safety and immunogenicity studies regarding their formulation in animal models before proceeding to clinical studies. The present work has thus been aimed at evaluating the safety and immunogenicity of a mixture of 23 chemically synthesised, modified peptides (immune protection-inducing protein structure (IMPIPS)) derived from different *P. falciparum* proteins. Single and repeat dose assays were thus used with male and female BALB/c mice which were immunised with the IMPIPS mixture. It was found that single and repeat dose immunisation with the IMPIPS mixture was safe, both locally and systemically. It was observed that the antibodies so stimulated recognised the parasite's native proteins and inhibited merozoite invasion of red blood cells *in vitro* when evaluating the humoral immune response induced by the IMPIPS mixture. Such results suggested that the IMPIPS peptide mixture could be a safe candidate to be tested during the next stage involved in developing an antimalarial vaccine, evaluating local safety, immunogenicity, and protection in a nonhuman primate model.

1. Introduction

Malaria represents one of the greatest public health problems worldwide. According to the World Health Organization (WHO), ~219 million new malaria-related cases occurred in 2017 accompanied by ~435,000 deaths. The African continent was the most affected region in the world (92% of cases and 93% of deaths) [1]. The *Global Technical Strategy for Malaria 2016-2030* (WHO) has suggested reducing malarial

incidence and mortality by at least 90% and eliminating it in at least 35 countries by 2030 through prevention, diagnosis, and treatment strategies [2].

No significant progress has been observed to date regarding the reduction of cases of malaria worldwide despite the differing strategies used for combating this disease (using insecticide-impregnated mosquito nets for controlling the vector, chemoprophylaxis, and case management) [1, 2]. The most recurrent problem is concerned with the increase

in strains which are resistant to antimalarial drugs and insecticide-resistant mosquitoes; this has necessitated the development and combined use of new control and prevention methods, especially a vaccine having high protection capability as time elapses [1, 3].

The Fundación Instituto de Inmunología de Colombia (FIDIC) has thoroughly demonstrated the feasibility of a chemically synthesised, multistage, multiantigen, minimum subunit-based (~20 amino acid-long peptide) vaccine by following a completely functional approach [4, 5]. This has led to ascertaining that peptides derived from the main proteins participating in merozoite (Mrz) invasion of RBCs [6] specifically bind to human RBCs and that sporozoites (Spz) invading hepatic cells [7, 8] bind to the HepG2 hepatocellular carcinoma cell line [9–12].

Immunogenicity and protection assays in *Aotus* monkeys have shown that high activity binding peptides (HABPs) [12] having a conserved sequence (cHABP) have not induced an immune response, suggesting that despite the importance of their biological role, they are immunologically silent [4, 5]. By contrast, HABPs having a variable sequence (vHABPs) have induced a nonprotective immune response (or only a short-term one) [4, 13], an immune evasion mechanism for these sequences (smokescreens distracting the immune response) [14–16]. However, when some cHABP residues [17, 18] have been replaced by amino acids (aa) having similar mass and volume, but different polarity, modified analogues (mHABPs) have been seen to induce a protective immune response in *Aotus* monkeys against experimental challenge [5, 13, 19–22].

Nuclear magnetic resonance (NMR) and *in silico* structural binding studies have shown that mHABPs having polyproline II (PPII) helix structures [23, 24] can bind to HLA-DR β 1* molecules covering most MHC-II allele variants [21, 25, 26] and have greater interaction with the T cell receptor (TCR). This would suggest the stable formation of the MHC-II-mHABP-TCR trimer complex and thus the capability for inducing a protective immune response [27–31]. Protection-inducing mHABPs have thus been called *Pf* immune protection-inducing protein structures (IMPIPS) in view of their close structure-protection relationship [32, 33].

This study thus used a murine model for evaluating the immunogenicity, local toxicity, and systemic toxicity [34–38] of a mixture of 23 IMPIPS. These were derived from the main *P. falciparum* Spz (circumsporozoite protein 1 (CSP-1), thrombospondin-related anonymous protein (TRAP), sporozoite threonine and asparagine-rich protein (STARP), sporozoite microneme proteins essential for cell traversal (SPECT-1 and SPECT-2), cell-traversal protein for ookinetes and sporozoites (CelTOS), and sporozoite invasion-associated protein 1 and 2 (SIAP-1 and SIAP-2)) [9, 11, 39, 40], as well as Mrz proteins (apical membrane antigen-1 (AMA-1), erythrocyte-binding protein 175 (EBA-175), erythrocyte-binding protein 140 (EBA-140), serine repeat antigen (SERA-5), merozoite surface protein-1 (MSP-1), and histidine-rich protein II (HRP-II)) [10, 39, 40]. Previous studies testing these peptides individually have shown that the antibodies induced were able to recognise the original

template protein when expressed as a recombinant (Supplementary Table 1).

2. Materials and Methods

2.1. Peptide Synthesis and Purification. Twenty-three polymer peptides (Table 1) were modified following previously reported principles [32, 33, 40, 41] to render them immunogenic and then synthesised using solid-phase multiple peptide synthesis following the tert-butyloxycarbonyl (t-Boc) synthesis strategy described by Merrifield [42] and modified by Houghten [43]. All peptides were derived from fully conserved and functionally relevant regions of the corresponding proteins. Such a Merck-Hitachi L-6200 A chromatograph (Merck) fitted with a UV-VIS L-4250 210 nm wavelength detector was used for determining synthesised peptide purity by high-performance reversed-phase liquid chromatography. A Microflex mass spectrometer (Bruker Daltonics) was then used for characterising them by matrix-assisted laser desorption/ionisation-time of flight (MALDI-TOF).

2.2. Animals. Forty BALB/c mice (20 males and 20 females) were used for evaluating the formulation's safety and immunogenicity. The mice were aged 5 to 6 weeks when they were immunised, according to WHO recommendations [37]. The mice were acquired from the Universidad Nacional de Colombia's Faculty of Animal Science's Biotherium.

2.2.1. Single Dose Local Tolerance. This assay enabled determining possible inflammatory reactions at the different treatments' inoculation sites [37]; this involved using 18 BALB/c mice (9 males and 9 females), following the protocols established by the regulatory authorities [34–37]. The animals were randomly assigned to 3 groups (Table 2), each consisting of 3 males and 3 females, in line with the principles of reduction and refinement [44].

The animals were immunised by subcutaneous (SC) route at the base of the tail with 100 μ L of the formulation. The animals were observed twice a day after they had been immunised for detecting changes in their behaviour, signs of disease, or toxicity. The injection site and the tissue around it were examined 1, 3, 24, 48, and 72 hours after immunisation to ascertain the presence of erythema, oedema, eschar, and necrosis; the parameters described by Cox were used for evaluating their degree [45]. The animals were anaesthetised with ketamine (80–120 mg/kg) and xylazine (5–16 mg/kg) by intraperitoneal (IP) route on the third day and sacrificed by cervical dislocation.

2.2.2. Repeat Doses. Twenty-two BALB/c 5- to 6-week-old mice (11 males and 11 females) were randomly distributed into three groups for evaluating possible toxic reactions produced by repeat inoculations (SC) of the *Pf*-IMPIPS peptide mixture (30 μ g in total). Toxicity due to repeat doses can occur as a result of repeat administration of a product over a specific period [35–37] (Table 3).

The animals were immunised 4 times with a 14-day interval as the amount of doses in an animal model must be equal to or greater than the amount of doses for clinical assays [37],

TABLE 1: List of peptides (IMPIPS) included in the mixture.

mHABP	Sequence	Protein	Theoretical mass (kDa)	Mass (<i>m/z</i>)
32958	CGGNGNGQGLNMNPPNFVNDENAGC	CSP	2,436.8	2,436.9
25608	CGKNSFSLGENPNANPGC	CSP	1,809.3	1,807.1
24312	CGDLGHVNGRDTMNNIVDENKYGC	TRAP	2,715.4	2,713.3
24242	CGVWDEWSPVSTAVGMGTRSRLKGC	TRAP	2,568.8	2,567.3
24250	CGKSLDIERKMADPQAQDNNGC	TRAP	2,393.8	2,392.2
24254	CGGAATPYSGEPSPFDEVLGEEGC	TRAP	2,372.9	2,373.2
24320	CGVIKHMRFHADYQAPFLGGGYGC	STARP	2,628.8	2,626.0
38150	CGTDLILKALGKLQNTNKGK	SPECT	2,090.9	2,089.3
38890	CGSDYTKALAAEAKVSYWVGIGC	SPECT-2	2,435.1	2,436.2
38128	CGKLTPISDSFDSDDTKESYDKGC	SPECT-2	2,612.3	2,611.7
38976	CGVDTTIWSGVNNLSHVALDGGC	SPECT-2	2,316.0	2,316.3
38880	CGETAVGALQADEIWNNTGTC	CELTOS	2,212.9	2,213.9
38162	CGKTQGHSHLRRKNGVKHPVYGC	SIAP-1	2,726.6	2,729.2
38884	CGGLHYSTDSQPNDISFGELGC	SIAP-2	2,411.0	2,411.3
13486	CGMIKASFDPTGAFKSPRYKSHGC	AMA-1	2,589.6	2,588.8
37206	CGNDKLYFDEYWKVIKKDGC	EBA-175	2,425.2	2,405.3
24292	CGLTNQINIDQEFNLMKHGFHGC	EBA-175	2,734.4	2,732.0
22690	CGNNIPSRYNLYDKMLDLDC	EBA-175	2,405.2	2,402.2
36620	CGLKNKETTKDYDMFQKIDSFLGC	EBA-140	2,785.6	2,781.7
22796	CGDNILVKMFKVIENNDKSELIGC	SERA	2,683.6	2,681.7
23426	CGKKVQNLTGDDTADLATNIVGGC	SERA	2,394.0	2,395.4
10014	CGEVLYHVPLAGVYRSLKKQLEGC	MSP-1	2,663.5	2,662.9
24230	CGSAFDDNLTAANAMGLILNKRGC	HRP-2	2,456.4	2,453.4

m/z: mass-to-charge ratio.

TABLE 2: Single dose: distribution of the groups of mice according to treatment.

	Treatment	Size
Group 1	Physiological saline solution (PSS) (control)	3M+3F
Group 2	IMPIPS mixture (30 μ g in total)+PSS (1 : 1)	3M+3F
Group 3	IMPIPS mixture (30 μ g in total)+Freund's adjuvant* (1 : 1)	3M+3F

*The immunisation was made with complete Freund's adjuvant.

TABLE 3: Repeat doses: distribution of the groups of mice according to treatment.

	Treatment	Size
Group 1	Physiological saline solution (PSS) (control)	3M+3F
Group 2	IMPIPS mixture+PSS (1 : 1)	4M+4F
Group 3	IMPIPS mixture+Freund's adjuvant* (1 : 1)	4M+4F

*The first immunisation was made with complete Freund's adjuvant and those thereafter with Freund's incomplete adjuvant.

and it would be expected that the amount of doses administered would not exceed two in clinical assays (Figure 1).

Each group was immunised with 100 μ L of the formulation on days 0, 14, 28, and 42; the formulation was administered by SC route at the base the tail. The immunisation sites were examined 1, 3, and 24 h after each injection looking for signs of erythema, oedema, eschar, and necrosis.

The animals were observed twice per day for evidence of any adverse reaction to the injection or the presence of disease, and a weekly physical examination was made for monitoring every animal's overall state of health. Their weight and food consumption were also monitored before beginning the immunisation protocol and after immunisation on days 0, 3, and 7 and every week thereafter until day 70.

Mouse body temperature was measured with an infrared thermometer (Benetech GM320) before and after each immunisation (0, 4, and 24 h) at five different sites on their abdomens. The average of five readings was recorded [46].

Blood samples were taken from the facial vein before immunisation and on days 1, 3, 40, 43, and 70 following the first immunisation to rule out acute and chronic alterations and in case of any abnormal findings. These samples were used for evaluating blood urea nitrogen (BUN), creatinine (CRE), haematocrit (HCT), red blood cell (RBC) count, white blood cell (WBC) count, and total plasma protein

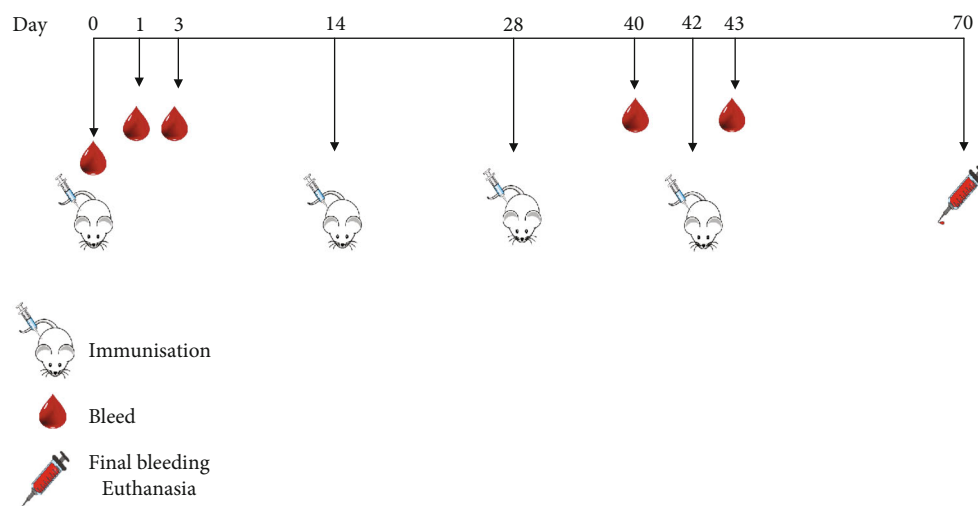


FIGURE 1: Immunisation scheme for evaluating local tolerance and systemic toxicity due to repeat doses in mice.

(TPP) levels. The animals were anaesthetised with ketamine (80-120 mg/kg) and xylazine (5-16 mg/kg) on day 70 by IP route and sacrificed by cervical dislocation [47].

The mice were necropsied, and kidney, heart, duodenum, spleen, and liver samples were taken for histological study to evaluate possible damage. The samples were kept in 10% formaldehyde and processed and analysed at the Universidad de Ciencias Aplicadas y Ambientales (U.D.C.A) pathology laboratory.

2.3. Immunogenicity

2.3.1. Indirect Immunofluorescence Assay (IFA). The indirect immunofluorescence assay (IFA) was used for evaluating an antibody's ability to recognise the parasite's native proteins, according to a previously reported methodology [48]. Briefly, RBC infected with mature schizont-stage parasites were taken from a *P. falciparum* FCB2 strain continuous culture synchronised with 5% sorbitol, at 5% to 7% parasitaemia. The RBCs were washed three times with phosphate-buffered saline (PBS) (7.2 to 7.4 pH) and spun at 1,200 g for 5 min. The pellet was suspended in filtered PBS until reaching 1% final dilution, 20 μ L/well of this suspension was seeded on 8-well slides and left to settle for 20 minutes, and the supernatant was collected. The slides were left to dry at room temperature (RT); they were then blocked with 30 μ L/well PBS-1% skimmed milk for 10 min at (RT), washed once with PBS (7.2 to 7.4 pH) for 5 min, and left to dry.

Then, in duplicate, 2.5 μ L/well serum from the final bleeding was seeded on 8-well slides at 1:20 dilution in PBS. The slides were incubated in a moist chamber for 30 min, washed with PBS (7.2 to 7.4 pH) six times for 5 min each wash, and left to dry. This was followed by placing 10 μ L/well fluorescein isothiocyanate- (FITC-) labelled anti-mouse IgG (Vector Laboratories, Inc.) in each well at 1:20 dilution in PBS as well as 1:80 4 μ L/well Evans blue to reduce background and increase contrast in the imaging/reading. The slides were incubated in a moist chamber in the dark for 30 min, washed, and left to dry. The slides were observed

with a fluorescence microscope (Olympus B51) at 1,000x magnification. The assay was made by pooling all the sera from each group due to the low serum volume available. Serum from a *P. berghei*-infected mouse was used as the positive control. The immunofluorescence signal was analysed semiquantitatively in the photographs already taken as follows: (+++) corresponds to the maximum fluorescence (positive control), (0+) to the negative control, (++) to IMPIPS plus adjuvant, and (+) to IMPIPS plus PSS.

2.3.2. Invasion Inhibition Assay. The *P. falciparum* FCB-2 strain (parasite ring stage) culture, previously synchronised with 5% sorbitol, 1-8 h postinvasion, was used for determining the ability of serum from the mice immunised with the IMPIPS mixture to inhibit Mrz invasion of erythrocytes [49]. A 384-well plate [50] seeded with 1.7 μ L/well parasite culture (2% haematocrit and 0.1% parasitaemia) was incubated with 10 μ L/well of serum from the final bleeding which had been inactivated (preimmune and postimmune) at 20%, 10%, 5%, and 2.5% concentrations (%v/v). Each well's final volume was 50 μ L, which was completed with RPMI 1640 media (Gibco); each sample was analysed in duplicate. The plate was incubated at 37°C for 48 h in a 5% O₂, 5% CO₂, and 90% N₂ atmosphere. Parasitised RBCs (pRBCs) and sera from control group mice (day 0) were used as the negative control, whilst human RBCs with chloroquine (150 nM) were used as the positive control for the invasion inhibition assay. Parasite culture supplemented with healthy human plasma was used as the culture control. The plate was spun at 1,800 rpm after 48 h incubation, and the culture supernatants were removed; the cells were then labelled with 1X 50 μ L SYBR Green (1:10,000) (Invitrogen) for 30 min in the dark. Cell suspensions were washed three times with PBS and analysed by flow cytometry (FACS-Canto II, Becton Dickinson). FlowJo 7.5 (Tree Star, Inc.) was used for analysing the data [51]. The assay was made by pooling all the sera from each group due to the low serum volume available.

2.4. Statistical Analysis. GraphPad Prism 7 software was used for statistically analysing the data for each group of animals (minimum and maximum values, the mean and standard deviation (SD)). The Shapiro-Wilk test of normality was used for comparing the groups of animals according to treatment; ANOVA was then used for analysing normally distributed data, whilst nonnormally distributed data was analysed by the Tukey or Kruskal-Wallis multiple comparison test and Dunn's multiple comparison test. Differences were considered statistically significant at $p < 0.05$. Stata software's linear regression model was used for statistically analysing histopathological results, using Pearson's X^2 test, for determining whether the IMPIPS mixture was toxic for the organs and tissues analysed here.

2.5. Ethical Statements. The mice were maintained according to the bioethical regulations laid down in Colombian Law 84/1989 [52], Colombian Ministry of Health resolution 8430/1993 [53], and the *Guide for the Care and Use of Laboratory Animals* of the National Institutes of Health [54]. Regulations stipulated by the American Veterinary Medical Association's (AVMA) Panel on Euthanasia (2013) were also considered [47]. All the animals were fed on Rodent Diet 5010 (LabDiet) and provided with water *ad libitum*. The Universidad de Ciencias Aplicadas y Ambientales (U.D.C.A) ethics committee, regulated by Agreement 285/2008, Chapter VII, endorsed this research.

3. Results

3.1. Local Tolerance: Single Dose in Mice. No deaths occurred in any of the groups being studied for this assay. None of the animals (females or males) in the different groups treated and evaluated 1, 3, 24, 48, and 72 h postimmunisation had lesions at the inoculation site, compared to the control group (not immunised).

3.2. Local and Systemic Tolerance: Repeat Doses in Mice. There were no deaths in any of the groups of animals when evaluating local toxicity due to repeat doses of the IMPIPS mixture. No local adverse reactions were observed (postimmunisation), such as erythema, oedema, eschar, or necrosis, at the inoculation site in any of the groups.

3.2.1. Physiological Parameters. The Shapiro-Wilk test of normality confirmed a normal distribution for male and female weight values. Average weight gain according to the means for each experimental group and the SD (mean \pm SD) obtained for each treatment for male mice immunised with PSS, IMPIPS+PSS, and MPIPS+adjuvant was 25.32 ± 2.56 g, 25.04 ± 3.06 g, and 23.34 ± 3.38 g, respectively, whilst for the females immunised with just PSS, IMPIPS+PSS, and IMPIPS+adjuvant, this was 19.70 ± 1.99 g, 19.23 ± 2.39 g, and 19.38 ± 3.01 , respectively (Supplementary Figure 1). Statistical analysis revealed no significant differences between the groups ($p > 0.05$).

Mean weekly consumption of food by the males immunised with PSS, IMPIPS+PSS, and MPIPS+adjuvant was 30.69 ± 1.43 g, 30.2 ± 1.25 g, and 30.97 ± 2.99 g, respectively, compared to the females immunised with PSS, IMPIPS+

PSS, and MPIPS+adjuvant (24.05 ± 1.25 g, 24.88 ± 1.20 g, and 25.27 ± 1.72 g, respectively) (Supplementary Figure 1). Statistical analysis did not reveal any significant differences between the groups ($p > 0.05$).

The temperature of male mice immunised with PSS, IMPIPS+adjuvant, and IMPIPS+PSS ranged from 30.72°C to 32.27°C , 29.56°C to 32.63°C , and 30.57°C to 32.23°C , respectively, during the study, whilst for females immunised with PSS, IMPIPS+adjuvant, and IMPIPS+PSS, it ranged from 31.05°C to 37.57°C , 29.62°C to 33.91°C , and 31.2°C to 33.35°C , respectively (Supplementary Figure 1). Overall, temperatures remained between the minimum and maximum ranges of the control group.

3.2.2. Haematological Parameters. The haematic picture evaluated parameters related to erythrocytes (erythrocyte count (RBC), haematocrit (HCT), haemoglobin (Hb), and total plasma proteins (TPP)) and leukocytes (leukocyte (WBC) count) for determining possible alterations caused by the formulation. The reference values for analysing each biochemical parameter were determined by mean control \pm SD; no significant differences ($p > 0.05$) were observed regarding either erythrocytes or leukocytes. Complete blood cell count (CBC) values came within the stated parameters, except for day 3 when control group females had a slight reduction in haematocrit and haemoglobin, possibly due to previous bleedings. By contrast, an increase in leukocytes was observed in control group males; this increase could have been caused by stress due to the bleeding.

Renal function was evaluated by measuring BUN and CRE. ANOVA analysis identified no statistically significant differences between the different treatments when comparing values between the groups or when comparing control group values (saline solution) to those for the other study groups ($p > 0.05$) (Figure 2). The reference values for analysing each biochemical parameter were determined from the means for the controls \pm SD (Figure 2).

3.2.3. Histopathology. Microcirculatory changes related to slight and moderate vascular congestion were observed in the myocardium in 2/4 females immunised with the IMPIPS+adjuvant formulation; there was no evidence of congestion in the other animals from the same group or from the other groups ($p > 0.05$). No microcirculatory changes were seen in any of the immunised animals, such as oedema and/or haemorrhage, inflammatory infiltrate, structural changes, or binucleation (Figure 3).

Slight congestion was observed in the kidneys of at least one animal from every group. These changes occurred more in females than in males, since a lesion was found in just one male compared to 6 females (2 from each group) in which congestion was observed. No microcirculatory changes such as oedema and haemorrhage, inflammatory infiltrate, structural changes, or binucleations were observed in any of the study groups (Figure 4).

No macroscopic or microscopic alterations were observed when analysing the duodenum, though 50% of the mice immunised with IMPIPS+adjuvant had mixed inflammatory infiltrate in the mesentery (Figure 5). Likewise, follicular

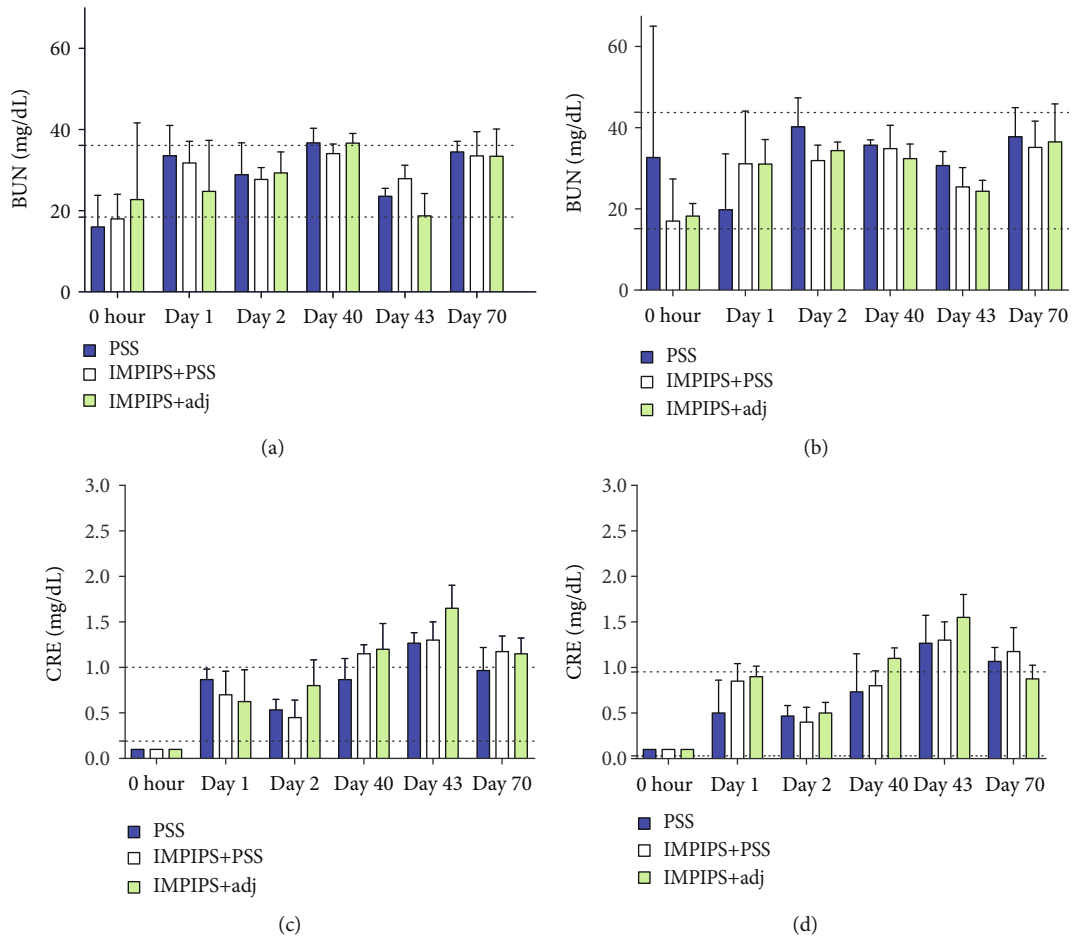


FIGURE 2: Means for the biochemical parameters: blood urea nitrogen (BUN) and creatinine (CRE). BUN and CRE values are shown for females (a and c) and males (b and d), according to time elapsed and group immunised. The horizontal dotted lines indicate the reference values.

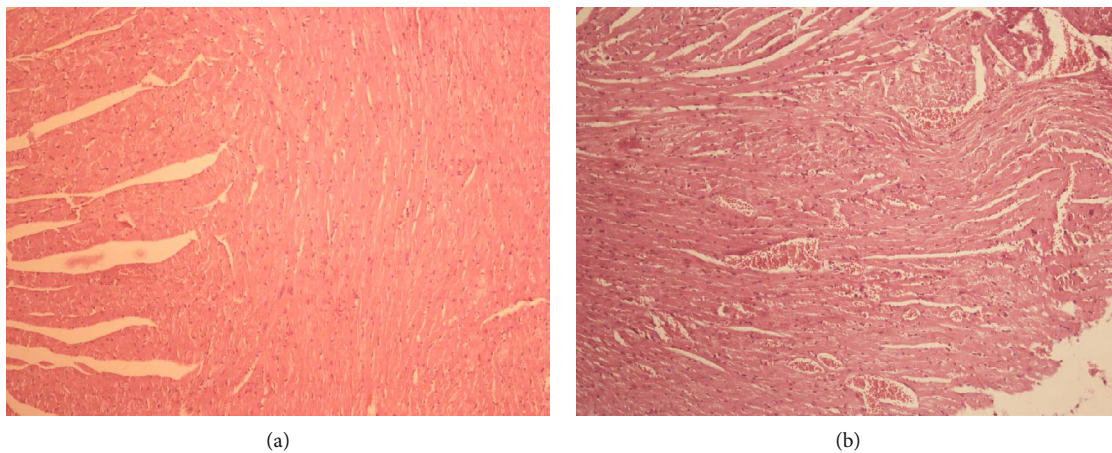


FIGURE 3: Histological section of the myocardium on day 70, stained with haematoxylin-eosin: (a) histology for the normal myocardium in a mouse treated with physiological saline solution (100x); (b) section of the myocardium from a mouse belonging to the group immunised with IMPIPS+adjuvant; microcirculatory changes related to moderate vascular congestion were observed (100x).

hyperplasia was observed in 100% of the mice immunised with IMPIPS+adjuvant when analysing lymphoid tissue, 50% being slight and 50% moderate. 37.5% of the mice

immunised with IMPIPS+PSS had this reaction to a slight degree and 25% to a moderate degree. Two (33.3%) control group mice had slight follicular hyperplasia (Figure 6). A

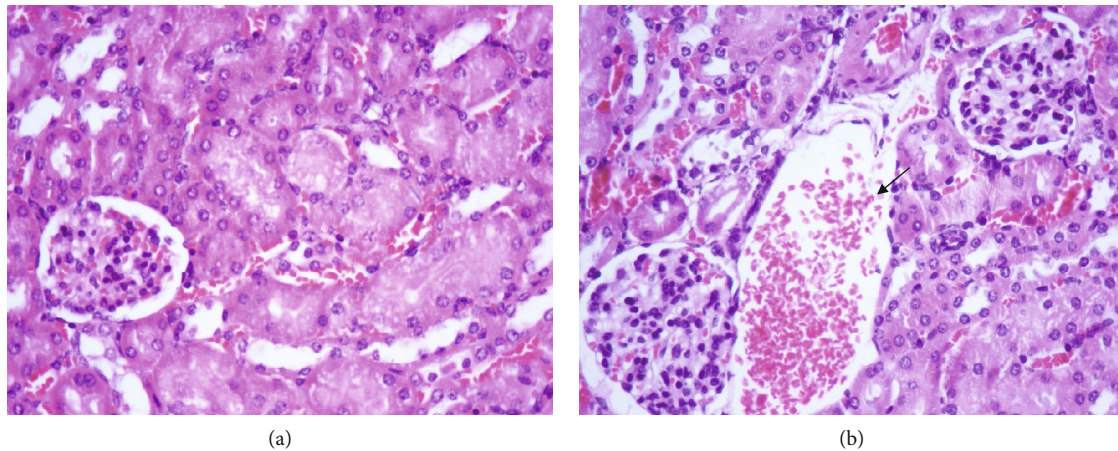


FIGURE 4: Histological section of the kidney on day 70, stained with haematoxylin-eosin: (a) histology for the normal kidney in a mouse treated with physiological saline solution (400x); (b) section of the kidney from a mouse from the group immunised with IMPIPS +adjuvant had microcirculatory changes regarding slight congestion (arrow) (400x).

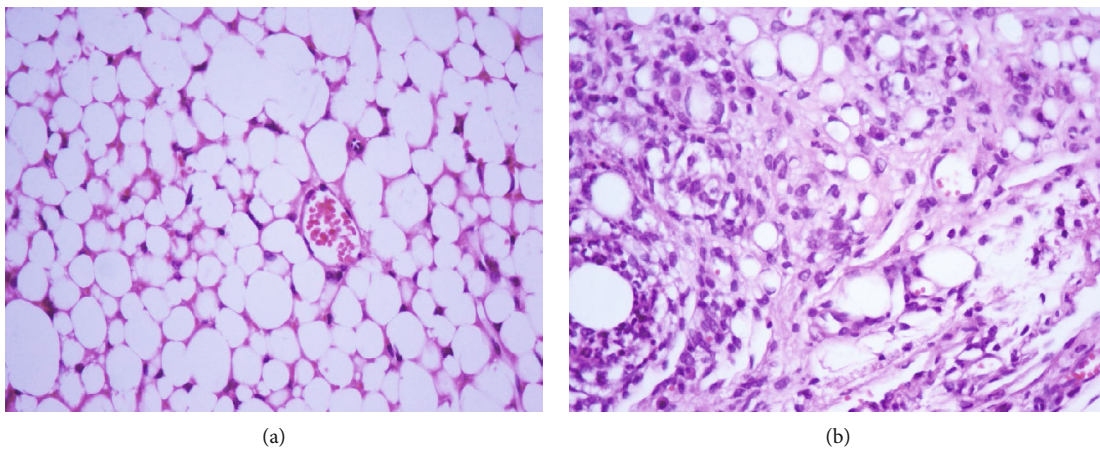


FIGURE 5: Histological section of the mouse mesentery on day 70, stained with haematoxylin-eosin: (a) histology for the normal mesentery of a mouse treated with saline solution (400x); (b) mesentery having mixed inflammatory infiltrate from a mouse treated with IMPIPS+adjuvant (400x).

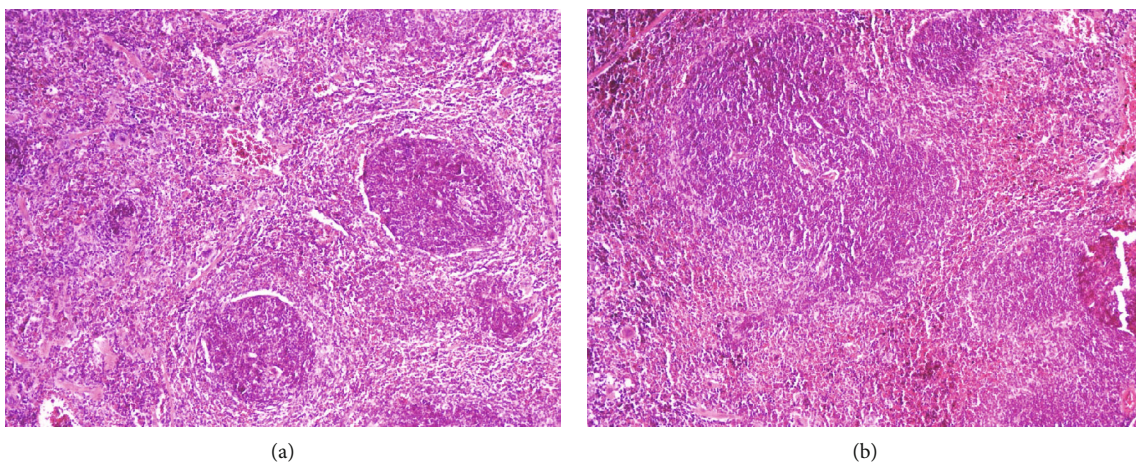


FIGURE 6: Histological section of mouse lymphoid tissue on day 70, stained with haematoxylin-eosin: (a) histology of mouse normal lymphoid tissue treated with saline solution (100x); (b) lymphoid tissue from a mouse treated with IMPIPS+adjuvant having nodular hyperplasia (100x).

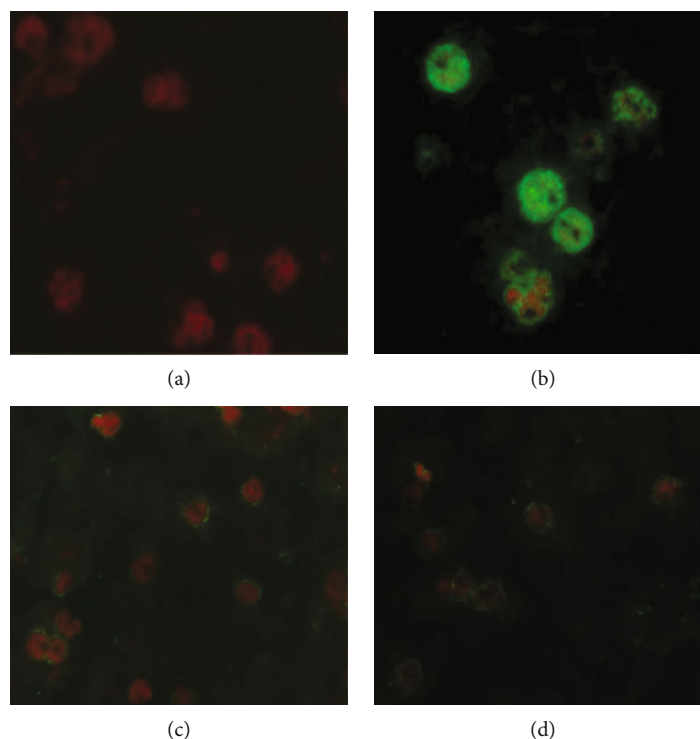


FIGURE 7: Immunofluorescence assay with mouse anti-IMPPIPS antibodies in *Plasmodium falciparum*-infected erythrocytes (FCB2 strain). Results were analysed semiquantitatively according to fluorescence intensity from null (0+) to maximum fluorescence (+++). (a) PBS (negative control) (0+). (b) Serum from a *P. berghei*-infected mouse (positive control) (+++). (c) Serum from the group of mice immunised with IMPPIPS plus adjuvant (++). (d) Serum from the group immunised with IMPPIPS plus PSS (+). Each study was done in duplicate. Mouse serum and the FITC-labelled anti-mouse IgG (green fluorescence) were used at 1:20 dilution. The samples were analysed with a fluorescence microscope (Olympus B51) with an immersion objective (1,000x).

scale was generated to semiquantify follicular hyperplasia according to the number of nodules using a magnification of 400x (Supplementary Table 2).

3.3. Immunogenicity

3.3.1. Determining Anti-IMPPIPS Serum Ability to Recognise *P. falciparum*-Infected RBC by IFA. An indirect immunofluorescence assay was used for determining anti-IMPPIPS serum ability to recognise pRBC. The serum from mice immunised with IMPPIPS+adjuvant as well as that from those immunised with IMPPIPS+PSS was able to recognise pRBC (Figure 7). Considering that some *P. berghei* proteins share high identity with their *P. falciparum* counterparts, such as enolase [55], the higher fluorescence intensity observed in the positive control might be due to the higher number of proteins being recognised versus just the six blood-stage proteins being recognised from animals immunised with the peptide mixture.

3.3.2. Determining Anti-IMPPIPS Antibodies' Merozoite Invasion Inhibition Capability. The functional role of antibodies stimulated by immunisation with IMPPIPS was determined by an *in vitro* invasion inhibition assay. The serum from animals immunised with the IMPPIPS peptide mixture+PSS was able to inhibit invasion, maximum values being 61.84% for males and 68.34% for females. Likewise,

the serum from the animals immunised with the IMPPIPS peptide mixture+adjuvant had 67.62% maximum invasion inhibition values for males and 70.82% for females. It was found that inhibition was concentration dependent ($p < 0.05$). No statistical difference was observed between inhibition percentages for the females compared to those for the males ($p > 0.05$) (Figure 8). Sera surpassing 70% were considered strong inhibitors, whilst those ranging from 50% to 69% were considered medium-high inhibitors. Those having 30% to 49% were considered medium-low inhibitors, those from 10%-29% are low inhibitors, and those $< 9\%$ were considered negative.

4. Discussion

Toxicological studies of the formulation to be used in clinical studies are of the utmost importance when developing vaccines as they provide information about possible adverse effects which might arise due to the formulation, either at the inoculation site or in the different organs and tissues of subjects being vaccinated [37, 38]. This study thus evaluated the safety and immunogenicity of a mixture of 23 modified peptides derived from 8 Spz proteins (CSP-1, TRAP, STARP, SPECT-1 and SPECT-2, CelTOS, and SIAP-1 and SIAP-2) and 6 Mrz proteins (AMA-1, EBA-175, EBA-140, SERA-5, MSP-1, and HRP-II) [9–11] in a murine model as a synthetic antimalarial vaccine candidate.

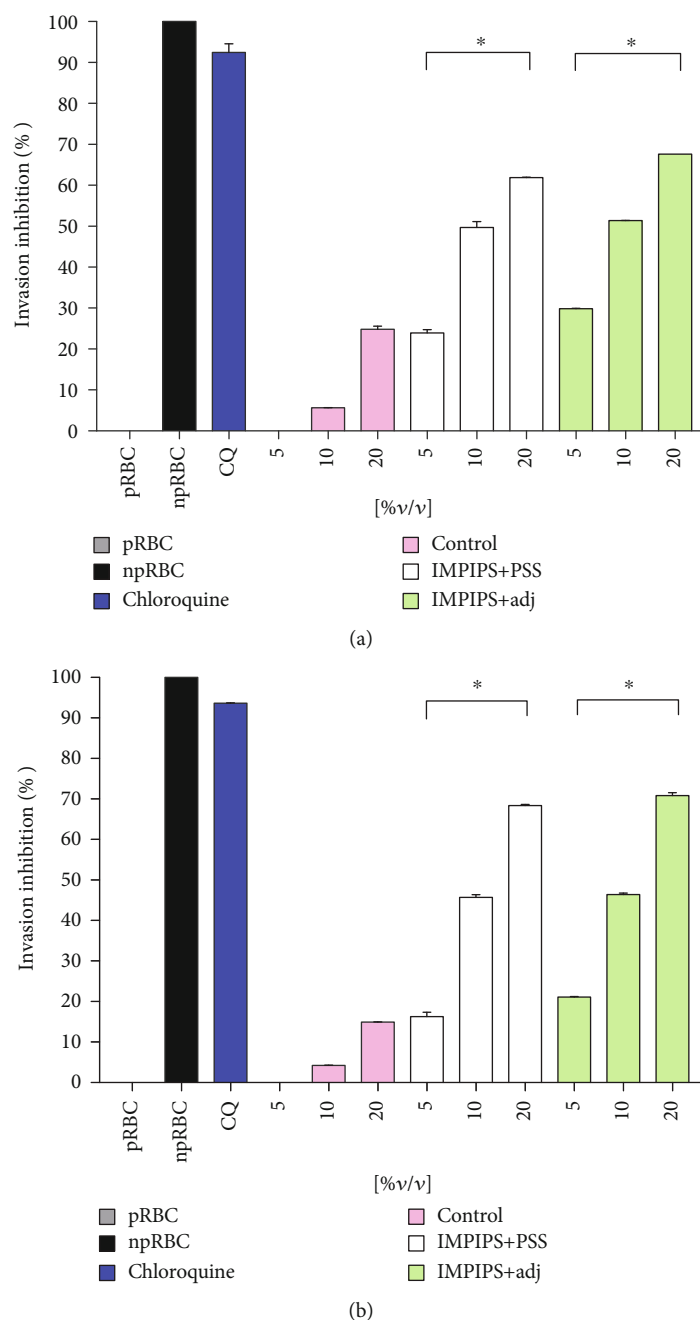


FIGURE 8: Percentage invasion inhibition of anti-IMPIPS serum. (a) Males. (b) Females. The assay was done in duplicate in three different experiments. Different serum concentrations were used (5, 10, and 20%v/v); pRBC (C-), npRBC (C+), and chloroquine (C+) were used as controls of the test. Control group mice (day 0) were used as the positive control of invasion (pink). Significance was determined at $*p < 0.05$.

The single dose local tolerance study was aimed at evaluating the site exposed to the formulation 72 h postimmunisation; no adverse reactions such as erythema, oedema, eschar, or necrosis were observed in the mice immunised with the IMPIPS mixture+PSS or in those immunised with IMPIPS+adjuvant. This suggested that the IMPIPS mixture did not produce local toxic effects due to single dose SC immunisation. The foregoing led to continuing local and systemic tolerance studies regarding repeat doses (4 immunisations) where SC immunisation also did not produce adverse effects such as erythema, oedema, eschar, or necrosis at the administration

site, suggesting that repeat IMPIPS doses did not produce irritation or toxicity at the immunisation site.

Male and female mice immunised with the IMPIPS peptide mixture+PSS or IMPIPS+adjuvant gained weight and increased their weekly food consumption, and their body temperature was within established parameters (i.e., regarding the formulation's systemic effects) [56], thereby supporting the idea that the IMPIPS mixture did not affect physiology.

Blood chemistry analysis showed that creatinine values did not exceed the parameters compared to control values

during the first bleeding. Creatinine values on day 40 exceeded the parameters; however, they became reduced by day 70, coming within normal parameters for the males. Such transitory increase could have been due to stress or dehydration since, unlike other mammals, mice excrete creatinine in their urine. Once the situation had become resolved, creatinine returned to its normal values [56]. BUN values came within normal parameters. Since no other damage was observed on day 70, the histological study of the kidneys verified that an increase in creatinine was due to prerenal causes and not to renal damage.

Regarding histological analysis, the microcirculatory changes in the myocardium compatible with congestion did not arise from administering the IMPIPS peptide mixture, since control group animals also had this pathology. Such changes could mainly have been due to the hypovolemic shock caused by the final bleeding; this would have occurred because haemorrhagic shock affects tissue perfusion [57].

Mixed inflammatory infiltrate was observed in the histological study of the mesentery; this description refers to localised accumulations of mononuclear and polymorphonuclear cells, indicating the presence of a foreign body in acute phase, i.e., causing the antigenic stimulus to continue. This finding in the animals immunised with IMPIPS+adjuvant and not in those immunised with IMPIPS+PPS or in the control group indicated that the antigen continued being active. This could have been caused by the formation of a deposit at the injection site due to the adjuvant's mechanism of action (doses 2, 3, and 4 of the formulation were administered by IP route) [58].

The nodular hyperplasia observed in animals' lymphoid tissue is mainly due to normal lymphoid nodule inflammation in response to an antigen. Such response in this case was triggered by the immunisation; such reaction is also known as reactive lymphoid hyperplasia [59] which, as expected, was much stronger in the animals immunised with the formulation containing IMPIPS+adjuvant.

FIDIC's previous studies have shown that individual immunisation of IMPIPS in *Aotus* monkeys has stimulated the production of antibodies which have been able to recognise parasite proteins in their native form and induce a protective immune response, determined by the total absence of parasites in the blood following experimental challenge [30, 32, 33]. The present study highlighted the fact that serum from male and female mice immunised with the IMPIPS mixture+adjuvant or IMPIPS+PSS recognised the parasite in the Mrz stage. This indicated that although the peptides had been modified for their presentation by human MHC-II [27, 29, 31], the mixture was capable of inducing an immune response against the native proteins from which they were derived, even in a murine model, thereby reinforcing the idea of using IMPIPS in an antimalarial vaccine [60]. Such response was seen in the immunofluorescence and invasion inhibition assays.

5. Conclusions

Local tolerance and systemic safety tests regarding single and repeat doses in this study showed no toxicity induced by the

IMPIPS mixture in a murine model 70 days after the first immunisation, reaffirming that peptide-based vaccines can represent a safe option. The IMPIPS mixture was immunogenic in a murine model, even when the peptides were designed for human MHC-II. Such results suggested that the IMPIPS mixture is safe and thus further immunogenicity and protection assays in a nonhuman primate model such as the *Aotus* spp. monkey but delivered with adjuvants authorised for human use are recommended.

Data Availability

The data used to support the findings of this study are included within the article.

Conflicts of Interest

The authors declare that there is no conflict of interest regarding the publication of this paper.

Acknowledgments

We would like to thank Jason Garry for translating this manuscript. This work was financed by COLCIENCIAS call for projects 725/2015, the Fundación Instituto de Inmunología de Colombia (FIDIC), and the Universidad de Ciencias Aplicadas y Ambientales (U.D.C.A.).

Supplementary Materials

Supplementary Figure 1: physiological parameters for male and female mice: weight, weekly consumption of food, and body temperature values. Dotted lines show upper and lower normal values. Supplementary Table 1: publications referencing peptides included in the present study, in which the antibodies raised recognise the corresponding protein expressed as a recombinant. Supplementary Table 2: semiquantitative scale of follicular hyperplasia using a 400x magnification. (*Supplementary Materials*)

References

- [1] World Health Organization (WHO), *World Malaria Report 2018*, Geneva, 2018.
- [2] World Health Organization (WHO), *Global Technical Strategy for Malaria 2016-2030*, 2015.
- [3] D. Menard and A. Dondorp, "Antimalarial drug resistance: a threat to malaria elimination," *Cold Spring Harbor Perspectives in Medicine*, vol. 7, no. 7, article a025619, 2017.
- [4] M. E. Patarroyo and M. A. Patarroyo, "Emerging rules for subunit-based multiantigenic, multistage chemically synthesized vaccines," *Accounts of Chemical Research*, vol. 41, no. 3, pp. 377–386, 2008.
- [5] M. E. Patarroyo, A. Bermudez, and M. A. Patarroyo, "Structural and immunological principles leading to chemically synthesized, multiantigenic, multistage, minimal subunit-based vaccine development," *Chemical Reviews*, vol. 111, no. 5, pp. 3459–3507, 2011.
- [6] Z. Bozdech, M. Llinás, B. L. Pulliam, E. D. Wong, J. Zhu, and J. L. DeRisi, "The transcriptome of the intraerythrocytic

- developmental cycle of *Plasmodium falciparum*,” *PLoS Biology*, vol. 1, no. 1, p. E5, 2003.
- [7] K. Kaiser, K. Matuschewski, N. Camargo, J. Ross, and S. H. Kappe, “Differential transcriptome profiling identifies Plasmodium genes encoding pre-erythrocytic stage-specific proteins,” *Molecular Microbiology*, vol. 51, no. 5, pp. 1221–1232, 2004.
 - [8] E. Lasonder, C. J. Janse, G. J. van Gemert et al., “Proteomic profiling of *Plasmodium* sporozoite maturation identifies new proteins essential for parasite development and infectivity,” *PLoS Pathogens*, vol. 4, no. 10, article e1000195, 2008.
 - [9] J. E. Garcia, A. Puentes, and M. E. Patarroyo, “Developmental biology of sporozoite-host interactions in *Plasmodium falciparum* malaria: implications for vaccine design,” *Clinical Microbiology Reviews*, vol. 19, no. 4, pp. 686–707, 2006.
 - [10] L. E. Rodriguez, H. Curtidor, M. Urquiza, G. Cifuentes, C. Reyes, and M. E. Patarroyo, “Intimate molecular interactions of *P. falciparum* merozoite proteins involved in invasion of red blood cells and their implications for vaccine design,” *Chemical Reviews*, vol. 108, no. 9, pp. 3656–3705, 2008.
 - [11] H. Curtidor, M. Vanegas, M. P. Alba, and M. E. Patarroyo, “Functional, immunological and three-dimensional analysis of chemically synthesised sporozoite peptides as components of a fully-effective antimalarial vaccine,” *Current Medicinal Chemistry*, vol. 18, no. 29, pp. 4470–4502, 2011.
 - [12] M. Urquiza, L. E. Rodriguez, J. E. Suarez et al., “Identification of *Plasmodium falciparum* MSP-1 peptides able to bind to human red blood cells,” *Parasite Immunology*, vol. 18, no. 10, pp. 515–526, 1996.
 - [13] F. Espejo, M. Cubillos, L. M. Salazar et al., “Structure, immunogenicity, and protectivity relationship for the 1585 malarial peptide and its substitution analogues,” *Angewandte Chemie, International Edition*, vol. 40, no. 24, pp. 4654–4657, 2001.
 - [14] S. Casares and T. L. Richie, “Immune evasion by malaria parasites: a challenge for vaccine development,” *Current Opinion in Immunology*, vol. 21, no. 3, pp. 321–330, 2009.
 - [15] H. Hisaeda, K. Yasutomo, and K. Himeno, “Malaria: immune evasion by parasites,” *The International Journal of Biochemistry & Cell Biology*, vol. 37, no. 4, pp. 700–706, 2005.
 - [16] M. Hommel, “Antigenic variation in malaria parasites,” *Immunology Today*, vol. 6, no. 1, pp. 28–33, 1985.
 - [17] H. Curtidor, M. Urquiza, J. E. Suarez et al., “*Plasmodium falciparum* acid basic repeat antigen (ABRA) peptides: erythrocyte binding and biological activity,” *Vaccine*, vol. 19, no. 31, pp. 4496–4504, 2001.
 - [18] M. Ocampo, M. Urquiza, F. Guzmán et al., “Two MSA 2 peptides that bind to human red blood cells are relevant to *Plasmodium falciparum* merozoite invasion,” *The Journal of Peptide Research*, vol. 55, no. 3, pp. 216–223, 2000.
 - [19] G. Cifuentes, A. Bermudez, R. Rodriguez, M. Patarroyo, and M. E. Patarroyo, “Shifting the polarity of some critical residues in malarial peptides binding to host cells is a key factor in breaking conserved antigens code of silence,” *Medicinal Chemistry*, vol. 4, no. 3, pp. 278–292, 2008.
 - [20] F. Guzman, K. Jaramillo, L. M. Salazar, A. Torres, A. Rivera, and M. E. Patarroyo, “1H-NMR structures of the *Plasmodium falciparum* 1758 erythrocyte binding peptide analogues and protection against malaria,” *Life Sciences*, vol. 71, no. 23, pp. 2773–2785, 2002.
 - [21] L. M. Salazar, M. P. Alba, H. Curtidor et al., “Changing ABRA protein peptide to fit into the HLA-DR β 1*0301 molecule renders it protection-inducing,” *Biochemical and Biophysical Research Communications*, vol. 322, no. 1, pp. 119–125, 2004.
 - [22] M. E. Patarroyo, G. Cifuentes, A. Bermúdez, and M. A. Patarroyo, “Strategies for developing multi-epitope, subunit-based, chemically synthesized anti-malarial vaccines,” *Journal of Cellular and Molecular Medicine*, vol. 12, no. 5B, pp. 1915–1935, 2008.
 - [23] A. Bermudez, M. P. Alba, M. Vanegas, M. A. Patarroyo, and M. E. Patarroyo, “Specific β -turns precede PPIIL structures binding to allele-specific HLA-DR β 1* PBRs in fully-protective malaria vaccine components,” *Frontiers in Chemistry*, vol. 6, p. 106, 2018.
 - [24] C. Reyes, A. Moreno-Vranich, and M. E. Patarroyo, “The role of pi-interactions and hydrogen bonds in fully protective synthetic malaria vaccine development,” *Biochemical and Biophysical Research Communications*, vol. 484, no. 3, pp. 501–507, 2017.
 - [25] A. Bermúdez, M. P. Alba, M. Vanegas, and M. E. Patarroyo, “3D structure determination of STARP peptides implicated in *P. falciparum* invasion of hepatic cells,” *Vaccine*, vol. 28, no. 31, pp. 4989–4996, 2010.
 - [26] M. P. Alba, L. M. Salazar, L. E. Vargas, M. Trujillo, Y. Lopez, and M. E. Patarroyo, “Modifying RESA protein peptide 6671 to fit into HLA-DR β 1* pockets induces protection against malaria,” *Biochemical and Biophysical Research Communications*, vol. 315, no. 4, pp. 1154–1164, 2004.
 - [27] M. E. Patarroyo, G. Cifuentes, C. Piraján, A. Moreno-Vranich, and M. Vanegas, “Atomic evidence that modification of H-bonds established with amino acids critical for host-cell binding induces sterile immunity against malaria,” *Biochemical and Biophysical Research Communications*, vol. 394, no. 3, pp. 529–535, 2010.
 - [28] M. E. Patarroyo, A. Bermudez, and M. P. Alba, “The high immunogenicity induced by modified sporozoites’ malarial peptides depends on their phi (ϕ) and psi (ψ) angles,” *Biochemical and Biophysical Research Communications*, vol. 429, no. 1-2, pp. 81–86, 2012.
 - [29] M. E. Patarroyo, H. Almonacid, and A. Moreno-Vranich, “The role of amino acid electron-donor/acceptor atoms in host-cell binding peptides is associated with their 3D structure and HLA-binding capacity in sterile malarial immunity induction,” *Biochemical and Biophysical Research Communications*, vol. 417, no. 3, pp. 938–944, 2012.
 - [30] A. Bermúdez, D. Calderon, A. Moreno-Vranich et al., “*Gauche*+ side-chain orientation as a key factor in the search for an immunogenic peptide mixture leading to a complete fully protective vaccine,” *Vaccine*, vol. 32, no. 18, pp. 2117–2126, 2014.
 - [31] M. E. Patarroyo, A. Moreno-Vranich, and A. Bermúdez, “Phi (Φ) and psi (Ψ) angles involved in malarial peptide bonds determine sterile protective immunity,” *Biochemical and Biophysical Research Communications*, vol. 429, no. 1-2, pp. 75–80, 2012.
 - [32] M. E. Patarroyo, A. Bermúdez, M. P. Alba et al., “IMPIPS: the immune protection-inducing protein structure concept in the search for steric-electron and topochemical principles for complete fully-protective chemically synthesised vaccine development,” *PLoS One*, vol. 10, no. 4, article e0123249, 2015.
 - [33] M. E. Patarroyo, M. A. Patarroyo, L. Pabón, H. Curtidor, and L. A. Poloche, “Immune protection-inducing protein structures (IMPIPS) against malaria: the weapons needed for beating Odysseus,” *Vaccine*, vol. 33, no. 52, pp. 7525–7537, 2015.

- [34] International Conference on Harmonisation (ICH), "ICH S6 (R1) Preclinical safety evaluation of biotechnology-derived pharmaceuticals," vol. 6, 2011.
- [35] European Medicines Agency (EMA), "Guideline on repeated dose toxicity," vol. 99, 2010.
- [36] European Agency for the Evaluation of Medicinal Products (EMA), *Note for guidance on non-clinical local tolerance testing of medicinal products*, London, 2001.
- [37] World Health Organization (WHO), *Annex 1 WHO guidelines on nonclinical evaluation of vaccines*, 2005.
- [38] World Health Organization (WHO), *Handbook: Good Laboratory Practice (GLP): Quality Practices for Regulated Non-clinical Research and Development*, 2nd edition, 2009.
- [39] M. Patarroyo, M. P. Alba, R. Rojas-Luna, A. Bermudez, and J. Aza-Conde, "Functionally relevant proteins in *Plasmodium falciparum* host cell invasion," *Immunotherapy*, vol. 9, no. 2, pp. 131–155, 2017.
- [40] M. E. Patarroyo, G. Arévalo-Pinzón, C. Reyes, A. Moreno-Vranich, and M. A. Patarroyo, "Malaria parasite survival depends on conserved binding peptides' critical biological functions," *Current Issues in Molecular Biology*, vol. 18, pp. 57–78, 2016.
- [41] H. Curtidor, C. Reyes, A. Bermúdez, M. Vanegas, Y. Varela, and M. Patarroyo, "Conserved binding regions provide the clue for peptide-based vaccine development: a chemical perspective," *Molecules*, vol. 22, no. 12, article 2199, 2017.
- [42] R. B. Merrifield, "Solid phase peptide synthesis. I. The synthesis of a tetrapeptide," *Journal of the American Chemical Society*, vol. 85, no. 14, pp. 2149–2154, 1963.
- [43] R. A. Houghten, "General method for the rapid solid-phase synthesis of large numbers of peptides: specificity of antigen-antibody interaction at the level of individual amino acids," *Proceedings of the National Academy of Sciences*, vol. 82, no. 15, pp. 5131–5135, 1985.
- [44] European Medicines Agency, *Guideline on the principles of regulatory acceptance of 3Rs (replacement, reduction, refinement) testing approaches*, 2016.
- [45] S. Cox, "Irritation and local tissue tolerance studies in pharmaceutical safety assessment," in *Preclinical Development Handbook: Toxicology*, S. Cox, Ed., pp. 233–268, John Wiley & Sons, 2008.
- [46] T. W. Adamson, D. Diaz-Arevalo, T. M. Gonzalez, X. Liu, and M. Kalkum, "Hypothermic endpoint for an intranasal invasive pulmonary aspergillosis mouse model," *Comparative Medicine*, vol. 63, no. 6, pp. 477–481, 2013.
- [47] American Veterinary Medical Association (AVMA), *AVMA guidelines for the euthanasia of animals*, 2013.
- [48] L. E. Rodriguez, R. Vera, J. Valbuena et al., "Characterisation of *Plasmodium falciparum* RESA-like protein peptides that bind specifically to erythrocytes and inhibit invasion," *Biological Chemistry*, vol. 388, no. 1, pp. 15–24, 2007.
- [49] C. Lambros and J. P. Vanderberg, "Synch stages in culture of *Plasmodium falciparum*," *The Journal of Parasitology*, vol. 65, pp. 418–420, 2012.
- [50] E. Duncan and E. Bergmenn-Litner, "Miniaturized growth inhibition assay to assess the anti-blood stage activity of antibodies," in *Malaria Vaccines Methods*, A. Vaughan, Ed., pp. 153–166, Springer, 2015.
- [51] A. Bei and M. Duraisingh, "Measuring *Plasmodium falciparum* erythrocyte invasion phenotypes using flow cytometry," in *Malaria Vaccines Methods*, A. Vaughan, Ed., pp. 167–186, Springer, 2015.
- [52] Congreso Nacional de Colombia, *Ley 84 de 1989*, Congreso de Colombia, Colombia, 1989.
- [53] Ministerio de Salud de Colombia, *Resolución Número 8430 de 1993*, Colombia, 1993.
- [54] National Research Council of the National Academies, *Guide for the Care and Use of Laboratory Animals*, Eighth edition, , 2011.
- [55] S. Dutta, A. Tewari, C. Balaji et al., "Strain-transcending neutralization of malaria parasite by antibodies against *Plasmodium falciparum* enolase," *Malaria Journal*, vol. 17, no. 1, p. 304, 2018.
- [56] M. T. Whary, N. Baumgarth, J. G. Fox, and S. W. Barthold, "Biology and diseases of mice," in *Laboratory animal medicine 2*, J. G. Fox, L. C. Anderson, G. M. Otto, K. R. Pritchett-Corning, and M. T. Whary, Eds., pp. 43–149, Elsevier, 2015.
- [57] N. T. Veith, T. Histing, M. D. Menger, T. Pohlemann, and T. Tschernig, "Helping prometheus: liver protection in acute hemorrhagic shock," *Annals of Translational Medicine*, vol. 5, no. 10, p. 206, 2017.
- [58] S. Awate, L. A. Babiuk, and G. Mutwiri, "Mechanisms of action of adjuvants," *Frontiers in Immunology*, vol. 4, p. 114, 2013.
- [59] P. J. Haley, "The lymphoid system: a review of species differences," *Journal of Toxicologic Pathology*, vol. 30, no. 2, pp. 111–123, 2017.
- [60] M. E. Patarroyo, M. P. Alba, C. Reyes, R. Rojas-Luna, and M. A. Patarroyo, "The Malaria Parasite's Achilles' Heel: Functionally-relevant Invasion Structures," *Current Issues in Molecular Biology*, vol. 18, pp. 11–20, 2016.

Research Article

A Novel Adjuvant “Sublancin” Enhances Immune Response in Specific Pathogen-Free Broiler Chickens Inoculated with Newcastle Disease Vaccine

Yangke Liu,^{1,2,3} Jiang Zhang,^{3,4} Shuai Wang,¹ Yong Guo,³ Tao He,^{2,3} and Rui Zhou^{1,5,6} 

¹State Key Laboratory of Agricultural Microbiology, College of Veterinary Medicine, Huazhong Agricultural University, Wuhan, China

²Linzhou Sinagri Yingtai Biopeptide Co., Ltd, Linzhou, China

³Key Laboratory of Feed Antibiotics Replacement Technology, Ministry of Agriculture and Rural Affairs, Linzhou, China

⁴National Feed Engineering Technology Research Center, Beijing, China

⁵Cooperative Innovation Center of Sustainable Pig Production, Wuhan, China

⁶International Research Center for Animal Diseases (MOST), Wuhan, China

Correspondence should be addressed to Rui Zhou; rzhou@mail.hzau.edu.cn

Received 17 September 2019; Accepted 18 October 2019; Published 1 December 2019

Guest Editor: Masha Fridkis-Hareli

Copyright © 2019 Yangke Liu et al. This is an open access article distributed under the Creative Commons Attribution License, which permits unrestricted use, distribution, and reproduction in any medium, provided the original work is properly cited.

Sublancin is a glycosylated antimicrobial peptide produced by *Bacillus subtilis* 168 possessing antibacterial and immunomodulatory activities. This study was aimed at investigating the effects of sublancin on immune functions and serum antibody titer in specific pathogen-free (SPF) broiler chickens vaccinated with Newcastle disease (ND) vaccine. For this purpose, 3 experiments were performed. Experiment 1: SPF broiler chicks (14 days old) were randomly allotted to 1 of 7 groups including a blank control (BC), vaccine control (VC), and 5 (3-7) vaccinated and sublancin supplemented at 5, 15, 30, 45, and 60 mg activity/L of water, respectively. Vaccinated groups (2-7) were vaccinated with ND vaccine by intranasal and intraocular routes at the 14th day. On 7, 14, 21, and 28 days post vaccination (dpv), the blood samples were collected for the determination of serum hemagglutination inhibition (HI) antibody titer. Experiment 2: SPF broiler chicks were divided into 1 of 3 groups, i.e., blank control (BC), vaccine control (VC), and sublancin treatment (ST). On 7, 14, and 21 dpv, the blood samples were collected for measuring HI antibody titer by micromethod. Experiment 3: the design of this experiment was the same as that of experiment 2. On 7 and 21 dpv, pinocytosis of peritoneal macrophages, B lymphocyte proliferation assay, measurement of CD4⁺ and CD8⁺ T cells, and serum cytokine quantitation were carried out. It was noted that sublancin promoted B lymphocyte proliferation, increased the proportion of CD8⁺ T lymphocyte subpopulations, and enhanced the antibody titer in broiler chickens. In addition, it was also observed that sublancin has the potential to induce the secretion of IFN- γ , IL-10, and IL-4. In conclusion, these findings suggested that sublancin could promote both humoral and cellular immune responses and has the potential to be a promising vaccine adjuvant.

1. Introduction

Infectious diseases, especially viral diseases, remain one of the most critical challenges in poultry industry partly due to the genetic variation of viruses or the inferior quality of the vaccines. It is widely recognized that the application of vaccines coupled with immunopotentiator could improve the efficacy of vaccination [1]. However, commonly used

adjuvants, e.g., aluminum and oil emulsion, are reported to produce some side effects, such as carcinogenesis, strong local stimulation, or failure to enhance immunogenicity of weak antigens [2]. Hence, the development of a new type of adjuvant with low toxicity and high efficiency could be of great significance and of immediate practical value in safeguarding the health-associated risk factors in the poultry industry.

Antimicrobial peptides (AMPs) are various naturally occurring molecules which provide immediate and nonspecific defense against invading pathogens [3]. A number of studies pointed out that AMPs participate in the modulation of the immune response [4, 5]. These immunopotentiating properties of AMPs make them a suitable candidate for the adjuvant design. Sublancin is a 37-amino acid AMP isolated from *Bacillus subtilis* 168 with high stability [6]. In our previous studies, we noted that sublancin alleviated *Clostridium perfringens*-induced necrotic enteritis in broilers mainly by alleviating the inflammatory response [7]. Importantly, we also found that sublancin possess the ability to activate macrophages, thereby protecting mice from cyclophosphamide-induced immunosuppression [8]. In addition, intragastric administration of sublancin induced a mixed immune response of Th1 and Th2 in ovalbumin-immunized mice [9]. These reports elucidated that sublancin could be a promising immunomodulator.

However, the immunomodulatory effects of sublancin on SPF broiler chickens remain poorly understood. Additionally, whether sublancin can improve the immune response of ND vaccine in SPF broilers is yet to be known. Although AMPs can improve the cellular and humoral immunity in animals [4], whether sublancin exhibits similar effects in SPF chickens remains to be investigated. Therefore, the present study evaluated the effects of sublancin on immune response for inducing humoral and cellular immunity against ND vaccine in SPF broilers.

2. Material and Methods

All experiments involving animals were approved by the China Agricultural University Institutional Animal Care and Use Committee (ID: SKLAB-B-2010-003).

2.1. Preparation of Sublancin. Sublancin was produced in our laboratory using a highly efficient expression system involving *Bacillus subtilis* 800 as described previously [10]. The amino acid sequence of sublancin was determined as GLGKAQCAALWLQCASGGTIGCGGGAVALCQNYRQFCR, and the peptide purity was >99.6% as determined by high-performance liquid chromatography. Sublancin was produced as lyophilized powder and stored at -20°C until further use.

2.2. Animals. Fourteen-day-old SPF broiler chicks were obtained from the Quality Control Department of Beijing Merial Vital Laboratory Animal Technology Co., Ltd. (Beijing, China) and were housed under standard conditions of temperature ($22\text{--}26^{\circ}\text{C}$), relative humidity (40–65%), and light intensity (150–300 lux). The broilers were fed with Co^{60} -irradiated sterile nutritious feed in Complete Feed (Beijing Keao Feed Co., Ltd, Beijing, China) while clean and fresh water was made available *ad libitum*.

2.3. Experimental Design

2.3.1. Experiment 1. Ninety-one, 14-day-old SPF broiler chicks were randomly allotted to 1 of 7 groups with 13 chicks in each treatment. The treatments included a blank control

(BC), vaccine control (VC), and 5 sublancin treatments in which sublancin was supplemented at 5, 15, 30, 45, and 60 mg activity/L of water, respectively. Briefly, soluble sublancin powder was mixed in 1-L drinking barrel located in each group at the rate of 5, 15, 30, 45, and 60 mg activity/L of water. Fresh sublancin was administered daily throughout the experiment. When the barrel containing sublancin was emptied, purified water without treatment was added to the barrel for the remainder of the day. The broilers in the BC and VC treatments had access to purified water without sublancin treatment all day. All the broilers except the BC group were vaccinated with LaSota ND vaccine by intranasal and intraocular routes at the 14th day. On 7, 14, 21, and 28 dpv, the blood samples were collected from the brachial vein for the determination of serum HI antibody titer by micromethod.

2.3.2. Experiment 2. Thirty, 14-day-old SPF broiler chicks were divided into 1 of 3 groups with 10 chicks in each group. The experimental treatments were similar to Exp. 1 except only one sublancin treatment was used in this experiment. In the ST group, birds were provided purified water mixed with sublancin at 30 mg activity/L of water and vaccinated with ND vaccine as in experiment 1. On 7, 14, and 21 dpv, the blood samples from the brachial vein were collected for the determination of HI antibody titer by micromethod.

2.3.3. Experiment 3. Thirty-six, 14-day-old SPF broiler chicks were randomly allocated to 1 of 3 groups with 12 chicks in each group. The design of this experiment was the same as that of experiment 2. On 7 and 21 dpv, 6 chickens per group were selected randomly for the determination of pinocytosis of peritoneal macrophages, B lymphocyte proliferation assay, measurement of CD4^{+} and CD8^{+} T cells, and serum cytokine quantitation.

2.4. Serum HI Antibody Assay. Blood samples (0.5 mL per chick) were collected from the brachial vein, put into 2 mL Eppendorf tubes, and allowed to clot at 37°C for 2 h. Serum was separated by centrifugation at 3000 rpm for 15 min for the determination of HI antibody. Serum HI antibody assay was performed as previously described [11]. The geometric mean titer was presented as reciprocal \log_2 values of the highest dilution that displayed HI.

2.5. Determination of Pinocytosis of Peritoneal Macrophages. Peritoneal cells were harvested by peritoneal lavage with 20 mL RPMI-1640 (Gibco) medium. The cell-rich lavage fluid was aspirated and centrifuged at 1500 rpm for 15 min. The pellet was resuspended at 1×10^6 cells/mL in RPMI-1640 medium supplemented with 10% fetal bovine serum (FBS) and 100 units/mL penicillin/streptomycin (Life Technologies) and seeded in 96-well plates at $100 \mu\text{L}/\text{well}$. Cells were purified by adherence to culture plates for 3 h. Thereafter, the culture medium was discarded and $100 \mu\text{L}/\text{well}$ of 0.075% neutral red was added and incubated for 1 h. After washing with PBS for 3 times, $200 \mu\text{L}$ of lysis solution (alcohol:acetic acid, 1:1 v/v) was added into each well and maintained at 37°C for 10 min. The absorbance was

measured at 570 nm by a microplate reader (IMARK type, Bio-Rad, USA).

2.6. Proliferation Assay of B Lymphocyte. Blood samples from the heart were collected and then carefully layered on the surface of the lymphocyte separation medium. After centrifugation at 1500 rpm for 15 min, a white cloud-like lymphocyte band was collected and washed twice with RPMI-1640 medium. The cell pellet was resuspended at 1×10^6 cells/mL with RPMI-1640 medium and seeded in 96-well plates at 80 μ L per well, then another 20 μ L LPS (10 μ g/mL) was added. The plates were incubated at 37°C in a humidified atmosphere with 5% CO₂. After 44 h, 20 μ L of MTT (5 μ g/mL) was added into each well. The plates were reincubated for 4 h and then centrifuged at 1500 rpm for 10 min. The supernatant was removed carefully, and 100 μ L of DMSO was added into each well. The absorbance at 450 nm was measured by a microplate auto reader as the index of B lymphocyte proliferation.

2.7. Measurement of CD4⁺ and CD8⁺ T Cells. Cellular populations in the peripheral blood from the broilers were analyzed using flow cytometry. The lymphocytes were stained with CD3-PE, CD4-FITC, and CD8-SPRD at 4°C for 30 min and then analyzed by flow cytometry (Gallios, Beckman Coulter, Brea, CA, USA). The antibodies were purchased from Southern Biotech.

2.8. Serum Cytokine Quantitation. Blood samples from the brachial vein were allowed to clot at 37°C for 2 h and subsequently centrifuged at 3000 rpm for 15 min to separate the serum. The concentrations of INF- γ , IL-2, IL-4, and IL-10 in serum were measured using commercially available chicken Enzyme-Linked Immunosorbent Assay (ELISA) kits (Cusabio Biotech Company, Wuhan, China).

2.9. Statistical Analysis. All the data were analyzed by ANOVA using SPSS Version 20.0 (SPSS Inc., Chicago, IL). Statistical differences among treatments were determined using Duncan's Multiple Range Test. Results are presented as means \pm SD. P value < 0.05 was considered significant.

3. Results

3.1. Experiment 1

3.1.1. The Dynamic Changes of Antibody Titer. The dynamic changes of antibody titer in experiment 1 are presented in Figure 1. On 21 dpv, the sublancin treatments with 30 and 60 mg activity/L of water significantly increased ($P < 0.05$) the antibody titer compared with the VC group. A numerical increase in antibody titer was observed in the 5 sublancin treatments compared with the VC group on 7, 14, and 28 dpv, although there was no statistical difference. Overall, compared with the VC group, the sublancin treatments increased the antibody titer by 1.72~40%.

3.2. Experiment 2

3.2.1. Effect of Sublancin on Serum ND Antibody Titers. Figure 2 shows the effect of sublancin on serum ND HI

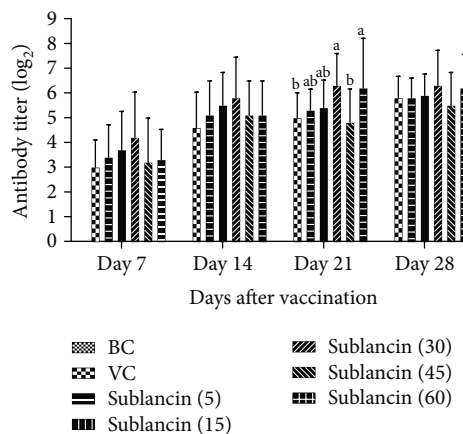


FIGURE 1: The dynamic variation of HI antibody titer in each group (\log_2) in Exp. 1. ^{a,b}Bars in the same day without the same superscripts differ significantly ($P < 0.05$).

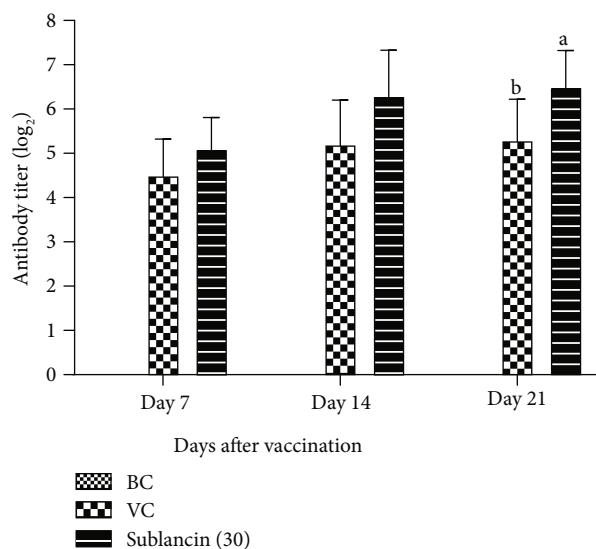


FIGURE 2: The dynamic changes of antibody titer in each group (\log_2) in Exp. 2. ^{a,b}Bars in the same day without the same superscripts differ significantly ($P < 0.05$).

antibody titers in experiment 2. In agreement with the results of experiment 1, the antibody titers in the sublancin treatment with 30 mg activity/L of water were significantly higher ($P < 0.05$) than those in the VC group on 21 dpv. On 7 and 14 dpv, the sublancin treatment with 30 mg activity/L of water resulted in a numerical increase in antibody titers by 11.76 and 21.15% compared with the VC group, although there was no statistical difference.

3.3. Experiment 3

3.3.1. Effect of Sublancin on Pinocytosis of Peritoneal Macrophages. The pinocytosis activity of broiler peritoneal macrophages was examined by the uptake of neutral red. As shown in Figure 3, the sublancin treatment with 30 mg activity/L of water had no significant effect on the pinocytosis

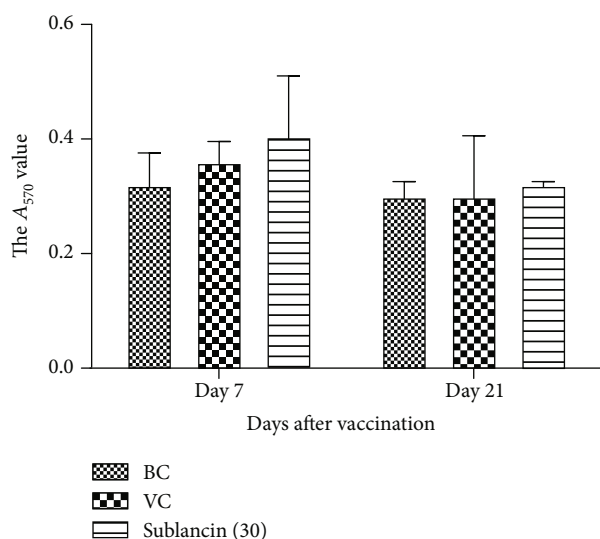


FIGURE 3: Effect of sublancin on pinocytosis of peritoneal macrophages in Exp. 3.

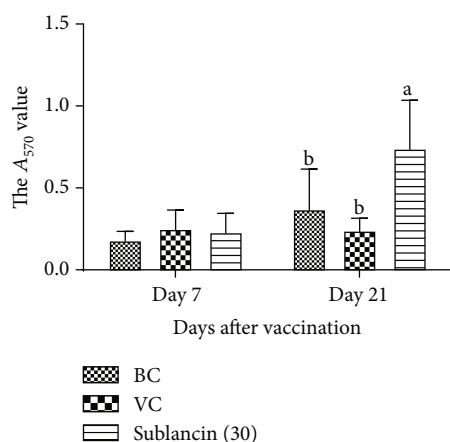


FIGURE 4: The changes of B lymphocyte proliferation in each group in Exp. 3. ^{a,b}Bars in the same day without the same superscripts differ significantly ($P < 0.05$).

activity compared with the BC and VC groups on 7 and 21 dpv.

3.3.2. The Dynamic Changes of B Lymphocyte Proliferation. The dynamic changes of the A_{450} value are presented in Figure 4. On 7 dpv, the A_{450} values did not differ among the 3 groups. However, on 21 dpv, the A_{450} values in the sublancin treatment with 30 mg activity/L of water were higher than those in the BC and VC groups ($P < 0.05$).

3.3.3. Effect of Sublancin on T Lymphocyte Subpopulations. The $CD4^+$ and $CD8^+$ subsets of T lymphocytes are primarily involved in the immune responses to specific antigenic challenges. We found that the percentage of $CD8^+$ peripheral blood lymphocytes in each group remained unchanged between the groups ($P > 0.05$) on 7 and 21 dpv. However,

the percentage of $CD4^+$ peripheral blood lymphocytes in the sublancin treatment was higher ($P < 0.05$) than that in the BC and VC groups on 7 dpv (Figure 5). Likewise, the values of $CD4^+/CD8^+$ were higher ($P < 0.05$) than those in the BC and VC groups on 21 dpv.

3.3.4. Effect of Sublancin on Cytokine Production. As shown in Figure 6, on 7 dpv, a numerical increase in serum concentrations of $INF-\gamma$ and IL-10 was observed in the sublancin treatment compared with the BC group ($P > 0.05$), although there was no statistical difference. On 21 dpv, the IL-4 concentration in the sublancin treatment also showed numerical increase when compared with that in the BC group ($P > 0.05$).

4. Discussion

Naturally occurring AMPs exhibit antibacterial properties and are also suggested to possess immune-enhancing activities [12], which make them promising adjuvant candidates for vaccine design. Ribosomally synthesized and posttranslationally modified peptides are a fast-expanding class of natural products that display a wide range of interesting biological activities. Sublancin is a member of the glycoamin family containing 2α -helices and a well-defined interhelical loop connected by an S-glucosidic linkage to Cys [13]. Mature sublancin has a molecular mass of 3879.8 Da [10]. It has previously been reported that sublancin possesses immunomodulatory properties [8, 14]. Acquired immunity comprising the humoral and cellular immunity constitutes an integral component of bird's health. Humoral immunity mediated by B lymphocytes is a crucial immune reaction against infections, thereby a change in the antibody titer reflects the state of humoral immunity in animals [15]. In our study, sublancin significantly increased the serum ND antibody titers compared with the VC group, suggesting that sublancin could promote humoral immunity.

It is well known that B cells are primarily responsible for humoral immunity, whereas T cells participate in cellular immunity. B lymphocytes mainly secrete antigens by binding the antibodies from effector B cells to eliminate antigens and participate in the humoral immune process of the body. In addition, cytokines can also be released to participate in immune regulation [16]. We noted that sublancin treatment with 30 mg activity/L of water significantly increased the proliferation of B lymphocytes, indicating that B lymphocytes were activated by sublancin. To further test the efficacy of sublancin on cellular immunity, we determined the amount of $CD4^+$ and $CD8^+$ T lymphocyte subpopulations. $CD4^+$ T lymphocytes can be activated by immunoreactive reactions with polypeptide antigens presented by major histocompatibility complex class II molecules. $CD8^+$ T lymphocytes recognize antigens presented by major histocompatibility complex class I molecules and directly kill infected or variant cells. The number and status of $CD4^+$ and $CD8^+$ T lymphocytes directly reflect the status of immunity of the body [17]. Generally, the ratio of $CD4^+/CD8^+$ T remains relatively stable, so the value and proportion of $CD4^+/CD8^+$ T lymphocyte subsets in the peripheral blood and the ability to produce cytokines can be measured in order to assess the immune status

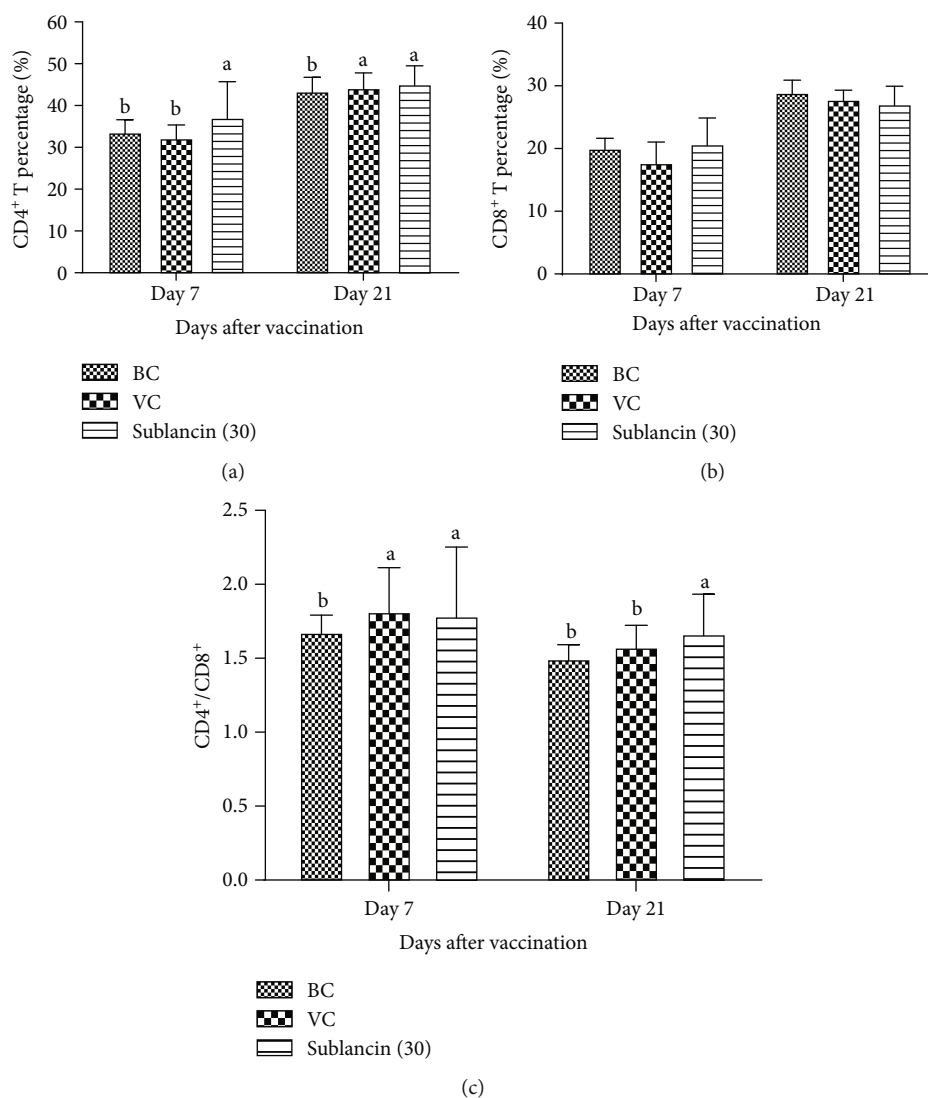


FIGURE 5: The dynamic changes of CD4⁺, CD8⁺, and CD4⁺/CD8⁺ T lymphocyte subpopulations in each group in Exp. 3. ^{a,b}Bars in the same day without the same superscripts differ significantly ($P < 0.05$).

of the body cells [18]. Our results showed that the broilers receiving sublancin at 30 mg activity/L of water had an increased value of CD4⁺ T lymphocytes on days 7 and 21 after the vaccination. The value of CD4⁺/CD8⁺ was significantly increased on days 7 and 21 after the vaccination. These results are in agreement with Xiaofei et al. [19] who reported that compound mucosal immune adjuvant can increase the percentage of CD4⁺ T and CD8⁺ T lymphocytes in chicken orally vaccinated with attenuated Newcastle disease vaccine.

Phagocytosis is one of the primary functions of macrophages, and this process is extremely crucial in excluding foreign bodies [20]. In the present study, we evaluated the phagocytic activity of macrophages by phagocytic index *via* neutral red uptake. The results showed that sublancin treatment with 30 mg activity/L of water had no significant effect on the phagocytic activity of macrophages compared with that in the BC and VC groups. These findings suggested that sublancin had no effect on the regulation of macrophages in SPF broilers. On the contrary, our previous study in mice

demonstrated that oral administration of sublancin could enhance phagocytic activity of peritoneal macrophages under normal conditions and attenuate the cyclophosphamide-induced inhibition of peritoneal macrophages phagocytic activity [8]. This discrepancy is most likely due to a species difference or physiological state of the birds.

In addition to stimulating the proliferation of immune cells, sublancin has the potential to induce the secretion of IFN- γ , IL-10, and IL-4. The Th1 cytokine IFN- γ provides protective immunity against intracellular infections by organisms including bacteria, viruses, and protozoa [21] whereas IL-10 and IL-4 participate in the Th2 immune response. In this study, sublancin was administered via oral route, thus the possibility of a loss of glycosylation, reduction of disulfides, and/or attack by endogenous proteases on this peptide during its transit through the intestine cannot be ignored. Such reactions would modify some or all characteristics of the mature sublancin. Therefore, it can be postulated that the observed effects of sublancin in the present study

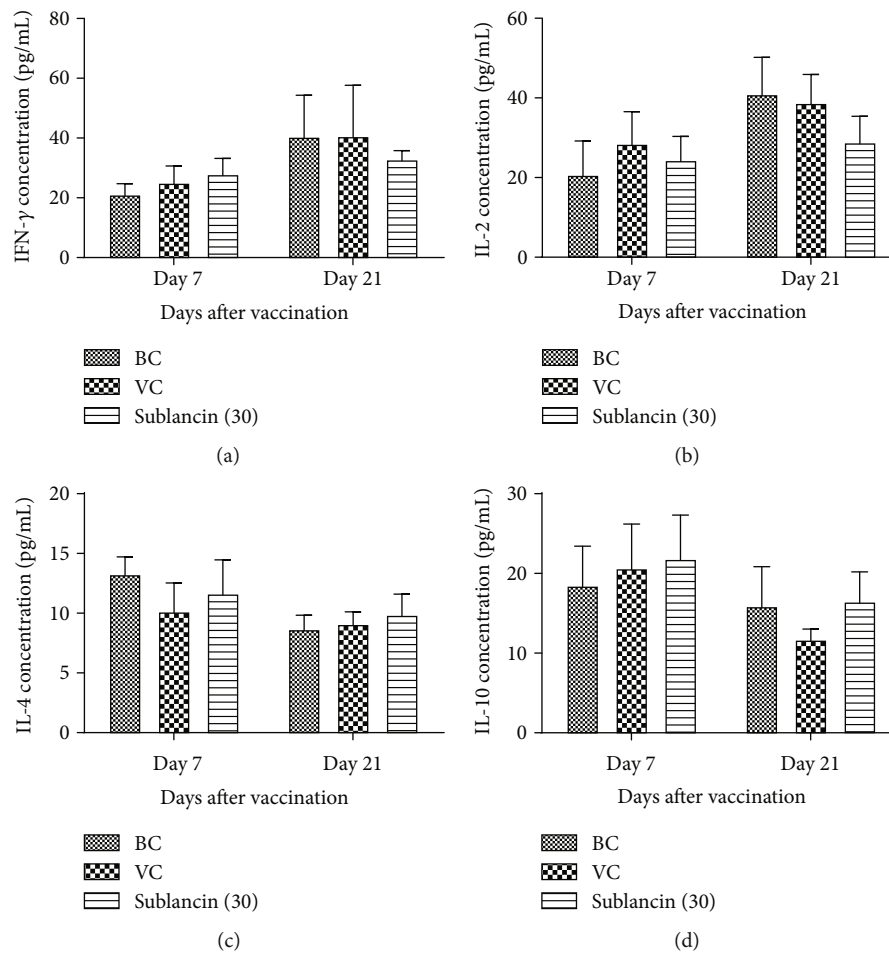


FIGURE 6: The changes of serum (a) IFN- γ , (b) IL-2, (c) IL-4, and (d) IL-10 concentrations in each group in Exp. 3.

might be due to the action of a partially modified mature sublancin or sublancin-derived peptides.

5. Conclusion

In summary, our study demonstrated that sublancin exhibited immunostimulatory properties which effectively activated B lymphocytes, increased the value of CD4⁺/CD8⁺, enhanced the ability to respond to antigens, and consequently increased the serum ND antibody titers in SPF broilers. Hence, the present study suggested that sublancin is a potential candidate to be a vaccine adjuvant.

Data Availability

The data used to support the findings of this study are available from the corresponding author upon request.

Conflicts of Interest

The authors declare that there is no conflict of interest regarding the publication of this paper.

Acknowledgments

This study was funded by the Key Research and Development Project of Henan Province of China (121100110700), the International Cooperative Projects in the National Key Research and Development Plans (2018YFE0101600), and the Hubei Province Natural Science Foundation of China for Innovative Research Groups (2016CFA015).

References

- [1] J. P. Graham, J. H. Leibler, L. B. Price et al., "The animal-human interface and infectious disease in industrial food animal production: rethinking biosecurity and biocontainment," *Public Health Reports*, vol. 123, no. 3, pp. 282–299, 2008.
- [2] L. B. Talarico, C. A. Pujol, Z. RGM et al., "The antiviral activity of sulfated polysaccharides against dengue virus is dependent on virus serotype and host cell," *Antiviral Research*, vol. 66, no. 2-3, pp. 103–110, 2005.
- [3] T. Ganz, "Defensins: antimicrobial peptides of innate immunity," *Nature Reviews Immunology*, vol. 3, no. 9, pp. 710–720, 2003.
- [4] O. N. Silva, C. de la Fuente-Núñez, E. F. Haney et al., "An anti-infective synthetic peptide with dual antimicrobial and immunomodulatory activities," *Scientific Reports*, vol. 6, no. 1, article 35465, 2016.

- [5] A. Nijnik, L. Madera, S. Ma et al., "Synthetic cationic peptide IDR-1002 provides protection against bacterial infections through chemokine induction and enhanced leukocyte recruitment," *The Journal of Immunology*, vol. 184, no. 5, pp. 2539–2550, 2010.
- [6] S. H. Paik, A. Chakicherla, and J. N. Hansen, "Identification and characterization of the structural and transporter genes for, and the chemical and biological properties of, sublancin 168, a novel lantibiotic produced by *Bacillus subtilis* 168," *The Journal of Biological Chemistry*, vol. 273, no. 36, pp. 23134–23142, 1998.
- [7] S. Wang, X. F. Zeng, Q. W. Wang et al., "The antimicrobial peptide sublancin ameliorates necrotic enteritis induced by *Clostridium perfringens* in broilers," *Journal of Animal Science*, vol. 93, no. 10, pp. 4750–4760, 2015.
- [8] S. Wang, S. Huang, Q. Ye et al., "Prevention of cyclophosphamide-induced immunosuppression in mice with the antimicrobial peptide sublancin," *Journal of Immunology Research*, vol. 2018, Article ID 4353580, 11 pages, 2018.
- [9] X. Zhang, Q. Yang, S. Wang, T. Yang, X. Zeng, and S. Qiao, "Study of antimicrobial peptide sublancin enhance acquired immunity of mice," *Chinese Journal of Animal Nutrition*, vol. 30, no. 1, pp. 236–245, 2018.
- [10] Q. Wang, X. Zeng, S. Wang et al., "The bacteriocin sublancin attenuates intestinal injury in young mice infected with *Staphylococcus aureus*," *The Anatomical Record*, vol. 297, no. 8, pp. 1454–1461, 2014.
- [11] X. Zhao, Y. Fan, D. Wang et al., "Immunological adjuvant efficacy of glycyrrhethinic acid liposome against Newcastle disease vaccine," *Vaccine*, vol. 29, no. 52, pp. 9611–9617, 2011.
- [12] S. Wang, X. Zeng, Q. Yang, and S. Qiao, "Antimicrobial peptides as potential alternatives to antibiotics in food animal industry," *International Journal of Molecular Sciences*, vol. 17, no. 5, p. 603, 2016.
- [13] C. Wu, S. Biswas, C. V. Garcia de Gonzalo, and W. A. van der Donk, "Investigations into the mechanism of action of sublancin," *ACS Infectious Diseases*, vol. 5, no. 3, pp. 454–459, 2019.
- [14] S. Wang, Q. Wang, X. Zeng et al., "Use of the antimicrobial peptide sublancin with combined antibacterial and immunomodulatory activities to protect against methicillin-resistant *Staphylococcus aureus* infection in mice," *Journal of Agricultural and Food Chemistry*, vol. 65, no. 39, pp. 8595–8605, 2017.
- [15] T. Irie, S. Watarai, and H. Kodama, "Humoral immune response of carp (*Cyprinus carpio*) induced by oral immunization with liposome-entrapped antigen," *Developmental & Comparative Immunology*, vol. 27, no. 5, pp. 413–421, 2003.
- [16] J. Q. Kou, R. Han, Y. L. Xu et al., "Differential Effects of *Naja naja atra* Venom on Immune Activity," *Evidence-Based Complementary and Alternative Medicine*, vol. 2014, Article ID 287631, 12 pages, 2014.
- [17] T. W. Phares, S. A. Stohlman, M. Hwang, B. Min, D. R. Hinton, and C. C. Bergmann, "CD4 T cells promote CD8 T cell immunity at the priming and effector site during viral encephalitis," *Journal of Virology*, vol. 86, no. 5, pp. 2416–2427, 2012.
- [18] M. Ahmed, R. Venkataraman, A. J. Logar et al., "Quantitation of immunosuppression by tacrolimus using flow cytometric analysis of interleukin-2 and interferon- γ inhibition in CD8- and CD8+ peripheral blood T cells," *Therapeutic Drug Monitoring*, vol. 23, no. 4, pp. 354–362, 2001.
- [19] X. Zhang, X. Zhang, and Q. Yang, "Effect of compound mucosal immune adjuvant on mucosal and systemic immune responses in chicken orally vaccinated with attenuated Newcastle-disease vaccine," *Vaccine*, vol. 25, no. 17, pp. 3254–3262, 2007.
- [20] M. Benoit, B. Desnues, and J. L. Mege, "Macrophage polarization in bacterial infections," *Journal of Immunology*, vol. 181, no. 6, pp. 3733–3739, 2008.
- [21] F. Malik, J. Singh, A. Khajuria et al., "A standardized root extract of *Withania somnifera* and its major constituent withanolide-a elicit humoral and cell-mediated immune responses by up regulation of Th1-dominant polarization in BALB/c mice," *Life Sciences*, vol. 80, no. 16, pp. 1525–1538, 2007.

Research Article

Immunoinformatics Approach for Multiepitope Vaccine Prediction from H, M, F, and N Proteins of Peste des Petits Ruminants Virus

Bothina B. M. Gaafar,¹ Sumaia A. Ali ^{1,2} Khoubieb Ali Abd-elrahman,³ and Yassir A. Almofti ¹

¹Department of Molecular Biology and Bioinformatics, College of Veterinary Medicine, University of Bahri, Khartoum, Sudan

²Department of Veterinary Medicine and Surgery, College of Veterinary Medicine, Sudan University of Science and Technology, Sudan

³Department of Pharmaceutical Technology, College of Pharmacy, University of Medical Science and Technology (UMST), Khartoum, Sudan

Correspondence should be addressed to Yassir A. Almofti; yamofti99@gmail.com

Received 30 April 2019; Accepted 2 August 2019; Published 30 October 2019

Guest Editor: Masha Fridkis-Hareli

Copyright © 2019 Bothina B. M. Gaafar et al. This is an open access article distributed under the Creative Commons Attribution License, which permits unrestricted use, distribution, and reproduction in any medium, provided the original work is properly cited.

Background. Small ruminant morbillivirus or peste des petits ruminants virus (PPRV) is an acute and highly contagious viral disease of goats, sheep, and other livestock. This study aimed at predicting an effective multiepitope vaccine against PPRV from the immunogenic proteins haemagglutinin (H), matrix (M), fusion (F), and nucleoprotein (N) using immunoinformatics tools. **Materials and Methods.** The sequences of the immunogenic proteins were retrieved from GenBank of the National Center for Biotechnology Information (NCBI). BioEdit software was used to align each protein from the retrieved sequences for conservancy. Immune Epitope Database (IEDB) analysis resources were used to predict B and T cell epitopes. For B cells, the criteria for electing epitopes depend on the epitope linearity, surface accessibility, and antigenicity. **Results.** Nine epitopes from the H protein, eight epitopes from the M protein, and ten epitopes from each of the F and N proteins were predicted as linear epitopes. The surface accessibility method proposed seven surface epitopes from each of the H and F proteins in addition to six and four epitopes from the M and N proteins, respectively. For antigenicity, only two epitopes $_{142}PPERV_{146}$ and $_{63}DPLSP_{67}$ were predicted as antigenic from H and M, respectively. For T cells, MHC-I binding prediction tools showed multiple epitopes that interacted strongly with BoLA alleles. For instance, the epitope $_{45}MFLSLIGLL_{53}$ from the H protein interacted with four BoLA alleles, while $_{276}FKKILCYPL_{284}$ predicted from the M protein interacted with two alleles. Although F and N proteins demonstrated no favorable interaction with B cells, they strongly interacted with T cells. For instance, $_{358}STKSCARTL_{366}$ from the F protein interacted with five alleles, followed by $_{340}SQNALYPMS_{348}$ and $_{442}IDLGPAISL_{450}$ that interacted with three alleles each. The epitopes from the N protein displayed strong interaction with BoLA alleles such as $_{490}RSAEALFRL_{498}$ that interacted with five alleles, followed by two epitopes $_{2}ATLLKSLAL_{10}$ and $_{304}QLGGEVAPY_{312}$ that interacted with four alleles each. In addition to that, four epitopes $_{3}TLLKSLALF_{11}$, $_{356}YFDPA YFRL_{364}$, $_{360}AYFRLGQEM_{368}$, and $_{412}PRQAQVSFL_{420}$ interacted with three alleles each. **Conclusion.** Fourteen epitopes were predicted as promising vaccine candidates against PPRV from four immunogenic proteins. These epitopes should be validated experimentally through in vitro and in vivo studies.

1. Introduction

Small ruminant morbillivirus (previously called peste des petits ruminants virus (PPRV)) is one of the most damaging

ruminant diseases. It is among the priority diseases indicated in the FAO-OIE Global Framework for the Progressive Control of Transboundary Animal Diseases (GF-TADs) in the 5-year Action Plan [1, 2]. PPRV is one of the top ten diseases in

sheep and goats that are having a high impact on the poor rural small ruminant farmers [3]. The disease is considered an acute and highly contagious viral disease with a high morbidity and mortality rate in small ruminants, such as goats and sheep and related wild animals [4, 5]. The disease is characterized by high fever, depression, anorexia, ocular and nasal discharge, pneumonia, necrosis and ulceration of mucous membranes, and inflammation of the gastrointestinal tract leading to severe diarrhea [6, 7]. It causes high death rates in goats and sheep up to 100% and 90%, respectively. However, sheep can be subclinically infected and play a major role in the silent spread of PPRV over large distances and across borders [1]. The disease is widely distributed in Africa, on the Arabian Peninsula, and in the Middle East and Asia [5, 8, 9]. Morbilliviruses are rapidly inactivated at environmental temperature by solar radiation and desiccation. This indicated that the transmission occurred by direct contact with infected animals or their excretions. Transmission of PPRV occurs primarily by droplet infection but may also occur by ingestion of contaminated feed or water [6].

PPRV is an enveloped single strand of negative sense RNA virus, belonging to the genus *Morbivirus*, in the family *Paramyxoviridae* which is closely related to *rinderpest virus* (RPV), *canine distemper virus* (CDV), and *measles virus* (MeV) [5, 10, 11]. The genome of morbilliviruses is organized into six transcriptional units encoding six structural proteins. These structural proteins include the nucleoprotein (N protein), matrix protein (M protein), polymerase or large protein (L protein), phosphoprotein (P protein), and two envelope glycoproteins, the haemagglutinin protein (H protein) and the fusion protein (F protein) [12–14]. The N protein played an important role in the viral life cycle, interacting with both viral and cellular proteins. It also interacted with the viral RNA to form the nucleocapsid structures seen in both the virions and infected cells [13]. The viral L and P proteins interact with the nucleocapsids to form the functional transcription/replication unit of the virion [13]. The C-termini of morbillivirus N proteins also interacted with cellular regulatory proteins such as heat shock protein Hsp72, interferon regulator factor- (IRF-) 3, and a novel cell surface receptor (genetically engineered receptor) [13]. The F protein facilitated the virus penetration of the host cell membrane. This protein is also critical for the induction of an effective protective immune response [15]. The M protein of paramyxoviruses forms an inner coat to the viral envelope and thus serves as a bridge between the surface viral glycoproteins and the ribonucleoprotein core. By virtue of its position, M appeared to play a central role in viral assembly by formation of new virions which were liberated from the infected cell by budding [16, 17]. Interaction of the PPRV H and F proteins with the host plasma membrane led to viral entry by binding of the H protein to receptors [17]. Generally, the protective cell-mediated and humoral immune responses against morbilliviruses are directed mainly against H, F, M, and N proteins. Moreover, PPRV is genetically grouped into four distinct lineages (I, II, III, and IV) based on the analysis of the fusion (F) gene. This classification of PPRV into lineages has broadened the

understanding of the molecular epidemiology and worldwide movement of PPR viruses [7, 18–20].

Vaccination is the main tool for controlling and eradicating the PPR virus [12]. Despite the fact that live attenuated vaccines have been widely used to protect small ruminants against circulating PPRV [1, 3, 7], the continuous spread of PPR disease indicated two possible hypotheses. The first is the emergence of new PPRV strains with new genetic makeup and greater fitness in the face of vaccine-elicited protection. The second is the lapses in regulatory control that ultimately lead to movement of diseased/infected individuals across the region/state/country without proper monitoring and surveillance [1].

The advances made in the field of immunoinformatics tools coinciding with the knowledge on the host immune response lead to new disciplines in vaccine design against diseases via computer in silico epitope predictions. The epitope-driven vaccine is a new concept that is being successfully applied in multiple studies, particularly to the development of vaccines targeting conserved epitopes in variable or rapidly mutating pathogens [21–23]. The identification of specific epitopes derived from infectious disease has significantly advanced the development of peptide-based vaccines. Peptides elicited more desirable manipulation of immune response through the use of the B cell epitopes. These epitopes mainly induce antibody production from B cells and cellular response and cytokine secretion from T cells. The approach regarding the molecular basis of antigen recognition and HLA binding motifs to host class I and class II MHC proteins is highly supported by the immunoinformatics which aids in designing epitope-based vaccine motifs that serve as therapeutic candidates for many infectious diseases [24].

The main objective of this study was to analyze multiple immunogenic proteins from the PPR genome for designing a safe multiepitope vaccine using immunoinformatics tools present in the Immune Epitope Database (IEDB). These proteins include haemagglutinin protein (H), matrix protein (M), fusion protein (F), and nucleoprotein (N) sequences of PPRV strains reported in the (NCBI) database.

2. Materials and Methods

2.1. Sequence Retrieval. Four immunogenic protein sequences of PPRV (updated August 2018) were retrieved from GenBank of the National Center for Biotechnology Information (NCBI) (<http://www.ncbi.nlm.nih.gov/protein>) in Oct. 2018. These included 82 sequences from the haemagglutinin protein (H protein), 67 sequences from the matrix protein (M protein), 94 sequences from the fusion protein (F protein), and 80 sequences from the nucleoprotein (N protein). All sequences were retrieved in FASTA format. The retrieved sequences, their accession numbers, and geographical locations are listed in Tables 1–4.

2.2. Phylogenetic Evolution. A phylogenetic tree of the retrieved sequences of each immunogenic protein was constructed using MEGA7.0.26 (7170509) software [25].

TABLE 1: Retrieved strains of the H protein of PPRV with their date of collection, accession numbers, and geographical regions.

No.	Accession number	Country	Year	No.	Accession number	Country	Year	No.	Accession number	Country	Year
1	AEH25644	China	2011	29	ATSI17278	Sierra Leone	2017	57	ASN64042	China	2017
2	ABY71271	China	2008	30	AMX28327	India	2017	58	ASN64036	China	2017
3	AAS68031	India	2009	31	AMX28319	India	2017	59	ASN64030	China	2017
4	ABX75304	Cote d'Ivoire	2008	32	AMX28311	India	2017	60	ASN64024	China	2017
5	ABX75312	Nigeria	2008	33	ANS54233	Liberia	2016	61	ASN64018	China	2017
6	ADM32488	India	2012	34	AKT04315	Benin	2016	62	ASN64012	China	2017
7	AEX61013	India	2012	35	AKT04307	Benin	2016	63	ASN64006	China	2017
8	ASY05923	Georgia	2017	36	AKR81281	India	2015	64	ASN64000	China	2017
9	ARB50221	China	2017	37	AKT04323	Cote d'Ivoire	2015	65	ASN63994	China	2017
10	ANS59483	India	2016	38	AJT59441	Senegal	2015	66	ASN63988	China	2017
11	AKQ09544	India	2015	39	AID07002	Ghana	2015	67	ASN63982	China	2017
12	AIL54036	UAE	2014	40	AIN40492	Kenya	2014	68	ASN63976	China	2017
13	AIL54028	Oman	2014	41	AHG50444	India	2014	69	ASN63970	China	2017
14	AIL54020	Uganda	2014	42	ACQ44671	China	2011	70	ASN63964	China	2017
15	AIL53996	Ethiopia	2014	43	ABY61988	India	2008	71	ASN63867	China	2017
16	AIL54012	India	2014	44	ABY61986	India	2008	72	ASN63861	China	2017
17	AIL54004	Ethiopia	2014	45	CAH61258	Turkey	2005	73	ASN63855	China	2017
18	CAD54790	India	2004	46	ANG60369	Nigeria	2016	74	ASN63849	China	2017
19	AHA58209	Iraq	2018	47	ANG60361	Nigeria	2016	75	ART66998	Algeria	2017
20	ARP51875	Mongolia	2018	48	AJE30413	China	2015	76	ALM55670	China	2016
21	AOO35467	China	2018	49	AJE30404	China	2015	77	ALA65398	China	2015
22	AIL29370	Turkey	2014	50	AUP34040	Nigeria	2018	78	AKN58853	China	2015
23	AGG09146	Morocco	2014	51	ASN64078	China	2015	79	AJA39814	China	2015
24	ADN03213	India	2013	52	ASN64072	China	2017	80	AIK97759	China	2014
25	ACN62119	India	2015	53	ASN64066	China	2017	81	AIK19904	Senegal	2014
26	CAJ01700	Nigeria	2005	54	ASN64060	China	2017	82	ADX95995	Nigeria	2011
27	YP_133827	Turkey	2018	55	ASN64054	China	2017				
28	AUO30190	Bangladesh	2018	56	ASN64048	China	2017				

TABLE 2: Retrieved strains of the matrix protein of PPRV with their date of collection, accession numbers, and geographical regions.

No.	Accession number	Country	Year	No.	Accession number	Country	Year	No.	Accession number	Country	Year
1	YP_133825	Turkey	2018	24	APX56396	Mali	2013	47	AIL54018	Uganda	2014
2	ANS54231	Liberia	2016	25	APX56395	Senegal	2015	48	AIL54010	India	2014
3	AKT04313	Benin	2016	26	APX56394	Comoros	2005	49	AIL53994	Ethiopia	2014
4	AKT04305	Benin	2016	27	APX56393	Mali	2018	50	AIL54002	Ethiopia	2014
5	AMX28325	India	2017	28	APX56392	Mali	2018	51	AGO28147	India	2013
6	AMX28317	India	2017	29	APX56391	Mali	2018	47	AIL54018	Uganda	2014
7	ANS59481	India	2016	30	APX56390	Algeria	2018	52	AGG09144	Morocco	2013
8	AKR81279	India	2015	31	APX56389	Guinea	2018	53	AEH25642	China	2011
9	CAJ01698	Nigeria	2005	32	APX56388	Mauritania	2018	54	ACQ44669	China	2011
10	ADN03215	India	2015	33	APX56387	Senegal	2018	55	ABY61987	India	2008
11	ADN03212	India	2012	34	APX56386	Senegal	2018	56	ABY61985	India	2008
12	ADM32486	India	2012	35	AUO30188	Bangladesh	2018	57	CAH61256	Turkey	2005
13	ACN62117	India	2012	36	ATS17276	Sierra Leone	2017	58	AOO35465	China	2016
14	AEX61011	India	2012	37	ASY05921	Georgia	2017	59	ABX75310	Nigeria	2008
15	AWD71674	Pakistan	2018	38	ARP51873	Mongolia	2017	60	ABX75302	Cote d'Ivoire	2008
16	AWD71668	Pakistan	2018	39	AKQ09542	India	2015	61	AUP34038	Nigeria	2018
17	AWD71662	Pakistan	2018	40	AKT04321	Cote d'Ivoire	2015	62	ART66996	Algeria	2017
18	AMX28309	India	2017	41	AJT59439	Senegal	2015	63	AIK19902	Senegal	2014
19	APX56401	Senegal	2018	42	AKG94167	India	2015	64	ADX95993	Nigeria	2011
20	APX56400	Senegal	2018	43	AID07000	Ghana	2015	65	AA568029	India	2009
21	APX56399	Senegal	2018	44	AIN40490	Kenya	2014	66	ANG60367	Nigeria	2016
22	APX56398	Senegal	2014	45	AIL54034	UAE	2014	67	ANG60359	Nigeria	2016
23	APX56397	Senegal	2014	46	AIL54026	Oman	2014				

TABLE 3: Retrieved strains of the fusion protein of PPRV with their date of collection, accession numbers, and geographical region.

No.	Accession number	Country	Year	No.	Accession number	Country	Year	No.	Accession number	Country	Year
1	YP_133821	Turkey	2018	28	AMQ48343	China	2016	55	AFC87747	Nigeria	2012
2	AIN40487	Kenya	2014	29	AMQ48342	China	2016	56	AFC87741	Nigeria	2012
3	AYA72170	India	2018	30	AKQ09546	India	2015	57	AFC87740	Nigeria	2012
4	AYA72169	India	2018	31	AKG94165	India	2015	58	AFC87739	Nigeria	2012
5	AYA72168	India	2018	32	AIL54030	UAE	2014	59	ABZ81035	China	2008
6	AYA72167	India	2018	33	AIL54022	Oman	2014	60	AEX61010	India	2012
7	ACN62116	India	2012	34	AIL54014	Uganda	2014	61	AEH25639	China	2011
8	ACN62115	India	2012	35	AIL53990	Ethiopia	2014	62	ACQ44667	China	2011
9	AUO30184	Bangladesh	2018	36	AIL54006	India	2014	63	CAH61252	Turkey	2005
10	AUB45018	China	2017	37	AIL53998	Ethiopia	2014	64	CAD91555	Turkey	2003
11	ATS17282	Sierra Leone	2017	38	AGJ84027	Morocco	2013	65	CAA52454	Nigeria	2005
12	ANS54228	Liberia	2016	39	AFC87764	Nigeria	2012	66	AMX28321	India	2017
13	AKT04301	Benin	2016	40	AFC87763	Nigeria	2012	67	AMX28313	India	2017
14	AKT04317	Cote d'Ivoire	2015	41	AFC87762	Nigeria	2012	68	AMX28305	India	2017
15	AJT59435	Senegal	2015	42	AFC87761	Nigeria	2012	69	ANS59477	India	2016
16	ABX75299	Cote d'Ivoire	2008	43	AFC87760	Nigeria	2012	70	AKT04309	Benin	2016
17	ABY61984	India	2008	44	AFC87759	Nigeria	2012	71	AKR81275	India	2015
18	ABX75307	Nigeria	2008	45	AFC87758	Nigeria	2012	72	AGG09141	Morocco	2013
19	ART66992	Algeria	2017	46	AFC87757	Nigeria	2012	73	ADJ05523	China	2010
20	APD77391	China	2016	47	AFC87756	Nigeria	2012	74	AAS68026	India	2009
21	ADN03214	India	2012	48	AFC87755	Nigeria	2012	75	ANG60363	Nigeria	2016
22	ADN03211	India	2012	49	AFC87754	Nigeria	2012	76	ANG60355	Nigeria	2016
23	ADM32485	India	2012	50	AFC87753	Nigeria	2012	77	AUP34034	Nigeria	2018
24	ASY05917	Georgia	2017	51	AFC87752	Nigeria	2012	78	AIK19898	Senegal	2014
25	ARP51869	India	2017	52	AFC87750	Nigeria	2012	79	ADX95989	Nigeria	2011
26	AOO35463	China	2017	53	AFC87749	Nigeria	2012	80	AID07004	Ghana	2015
27	AMQ48344	China	2016	54	AFC87748	Nigeria	2012				

TABLE 4: Retrieved strains of the nucleoprotein of PPRV with their date of collection, accession numbers, and geographical regions.

No.	Accession number	Country	Year	No.	Accession number	Country	Year	No.	Accession number	Country	Year
1	AHA58208	Iraq	2018	33	ASN63969	China	2017	65	AIL54019	Uganda	2014
2	AOO35466	China	2016	34	ASN63963	China	2017	66	AIL53995	Ethiopia	2014
3	AGJ84028	Morocco	2013	35	ASN63872	China	2017	67	AIK97758	China	2014
4	CAJ01699	Nigeria	2005	36	ASN63866	China	2017	68	AIK19903	Senegal	2014
5	AHN53450	India	2014	37	ASN63860	China	2017	69	AIL54011	India	2014
6	ADN03216	India	2012	38	ASN63854	China	2017	70	AIL54003	Ethiopia	2014
7	ADM32487	India	2012	39	ASN63848	China	2017	71	AHG50445	India	2014
8	ACN62118	India	2012	40	ARP51874	Mongolia	2017	72	AGP04219	Bangladesh	2013
9	AEX61012	India	2012	41	AMX28326	India	2017	73	AGG09145	Morocco	2013
10	ADX95994	Nigeria	2011	42	AMX28318	India	2017	74	AFR66765	China	2012
11	YP_133826	Turkey	2017	43	AMX28310	India	2017	75	ACV31220	India	2012
12	ATS17277	Sierra	2017	44	APD77392	China	2016	76	ACV31219	India	2012
13	ASY05922	Georgia	2017	45	ANS59482	India	2016	77	ACQ44670	China	2011
14	ASV72322	China	2017	46	AHF58487	India	2016	78	ADJ05518	China	2010
15	ASN64077	China	2017	47	ALM55669	China	2016	79	CAH61257	Turkey	2005
16	ASN64071	China	2017	48	AKT04314	Benin	2016	80	AXE28383	Israel	2018
17	ASN64065	China	2017	49	AKT04306	Benin	2016	81	AWD71675	Pakistan	2018
18	ASN64059	China	2017	50	ALA65397	China	2015	82	AWD71669	Pakistan	2018
19	ASN64053	China	2017	51	AKN58852	China	2015	83	AWD71663	Pakistan	2018
20	ASN64047	China	2017	52	AKR81280	India	2015	84	AUP34039	Nigeria	2018
21	ASN64041	China	2017	53	AKQ09543	India	2015	85	AUO30189	Bangladesh	2018
22	ASN64035	China	2017	54	AKT04322	Cote d'Ivoire	2015	86	ANG60368	Nigeria	2016
23	ASN64029	China	2017	55	AJT59440	Senegal	2015	87	ANG60360	Nigeria	2016
24	ASN64023	China	2017	56	AKG94168	India	2015	88	ANS54232	Liberia	2016
25	ASN64017	China	2017	57	AJA39813	China	2015	89	ART66997	Algeria	2017
26	ASN64011	China	2017	58	AID07001	Ghana	2015	90	ABX75303	Cote d'Ivoire	2008
27	ASN64005	China	2017	59	AJE30412	China	2015	91	ABX75311	Nigeria	2008
28	ASN63999	China	2017	60	AJE30403	China	2015	92	ABY71270	China	2008
29	ASN63993	China	2017	61	AJE30396	China	2015	93	AA568030	India	2009
30	ASN63987	China	2017	62	AIN40491	Kenya	2015	94	AEH25643	China	2011
31	ASN63981	China	2017	63	AIL54035	UAE	2014				
32	ASN63975	China	2017	64	AIL54027	Oman	2014				

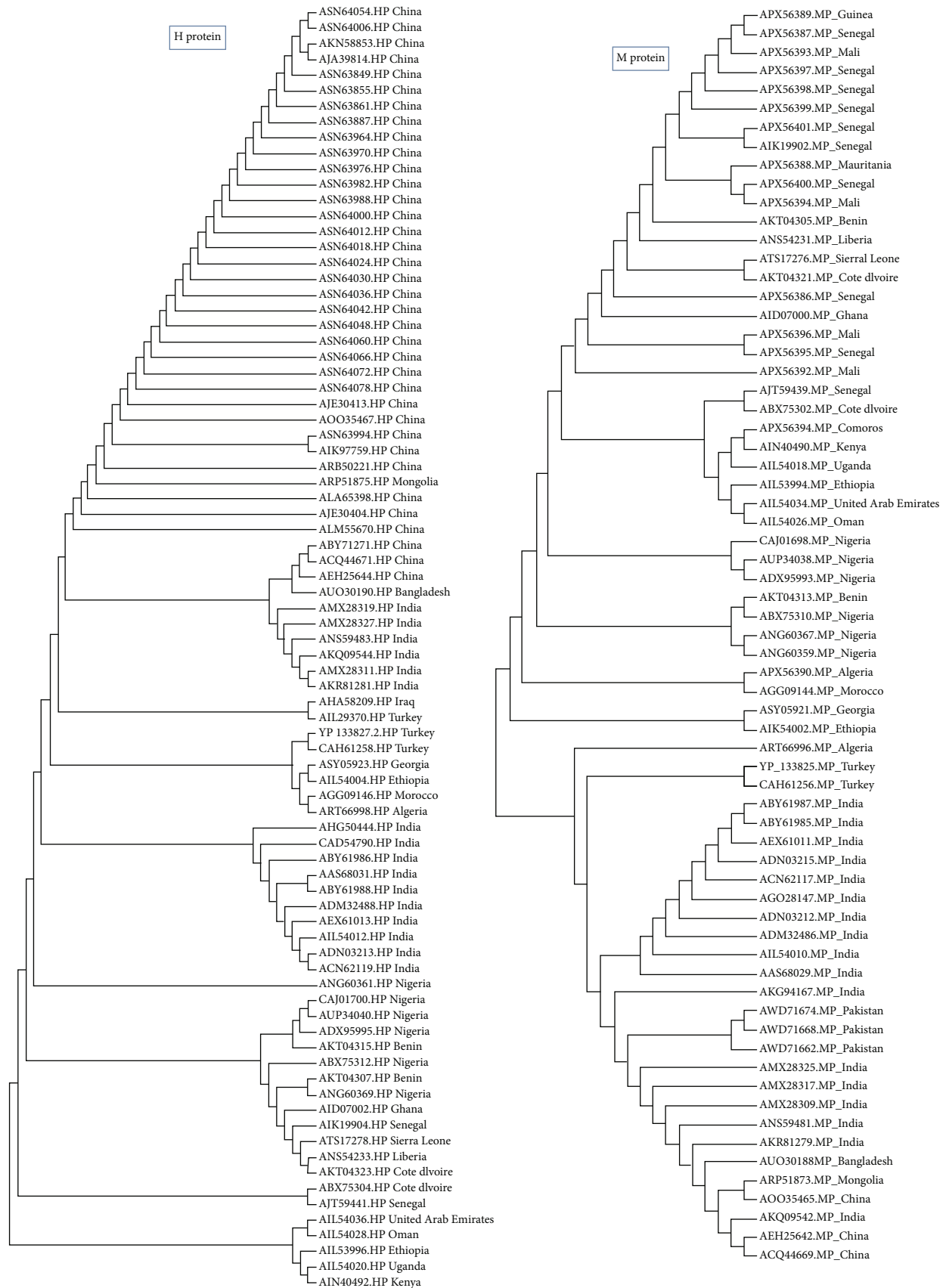


FIGURE 1: Phylogenetic tree of retrieved strains of H and M proteins. The retrieved strains demonstrated divergence in their common ancestors.

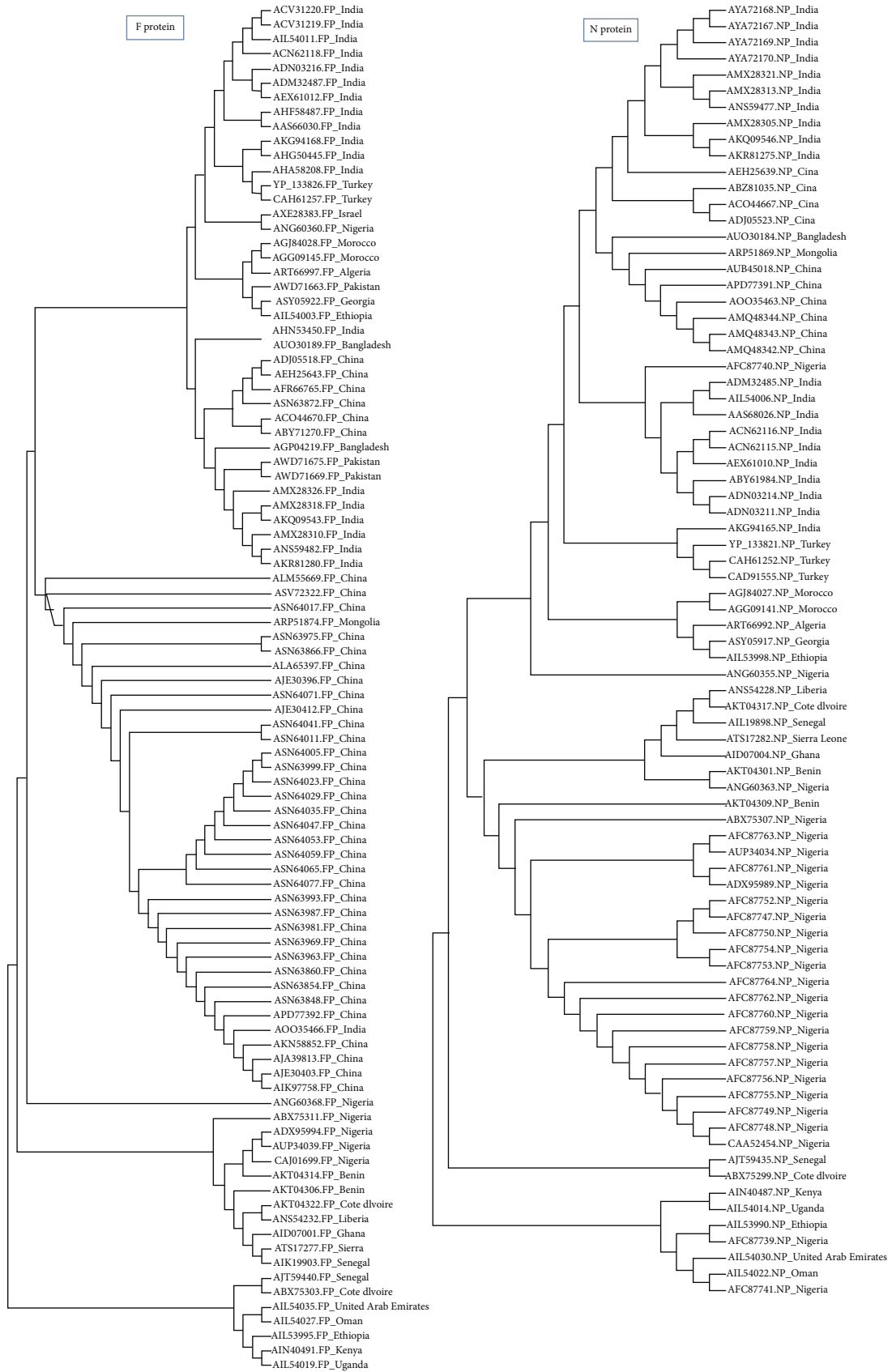


FIGURE 2: Phylogenetic tree of retrieved strains of F and N proteins. The retrieved strains demonstrated divergence in their common ancestors.

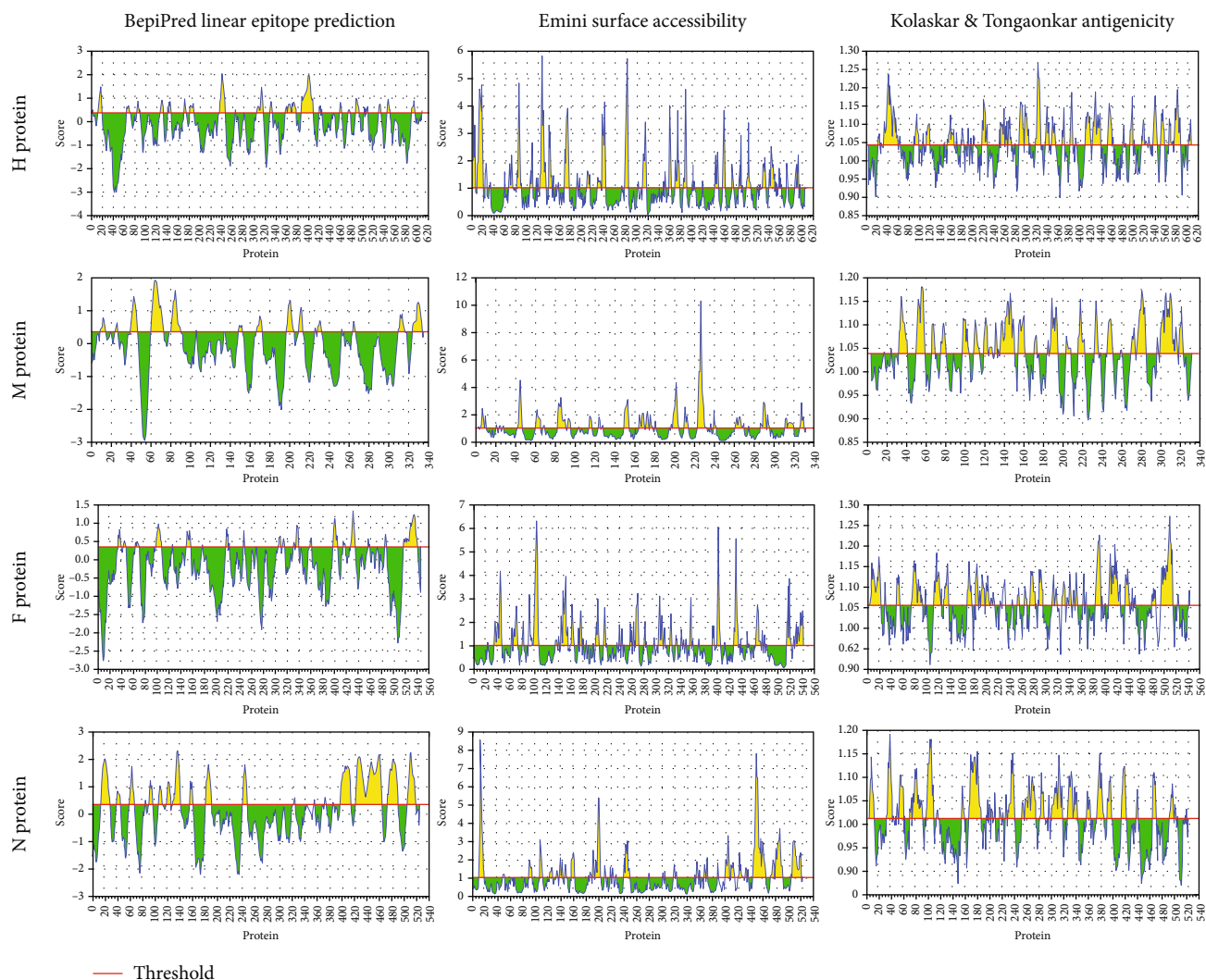


FIGURE 4: Prediction of B cell epitopes by different IEDB scales (BepiPred linear epitope prediction, Emini surface accessibility, and Kolaskar and Tongaonkar antigenicity prediction) for H, M, F, and N proteins. Regions above the threshold (red line) were proposed as a part of the B cell epitope while regions below the threshold (red line) were not.

cytotoxic T cell (CTL) epitopes that bind to the major histocompatibility complex class I alleles (MHC class I) [31]. Analysis was done using cow alleles (BoLA-D18.4, BoLA-HD6, BoLA-JSP.1, BoLA-T2a, BoLA-T2b, and BoLA-T2c). An artificial neural network (ANN) was used to predict the binding affinity [32, 33]. The peptide length for all selected epitopes was set to 9 amino acids (9mers). Percentile rank required for the peptide's binding to the specific MHC-I molecules was set in the range from 1 to 3.

2.5. Homology Modeling

2.5.1. The Three-Dimensional (3D) Structures of the Reference Sequences of PPRV.

The prediction of the three-dimensional (3D) structure of H, M, and F protein reference sequences of PPRV was performed using the RaptorX structure prediction server (<http://raptorx.uchicago.edu/StructurePrediction/predict/>) [34–36], while the N protein sequence was submitted to the SPARKS-X server (<http://sparks-lab.org/yueyang/>)

server/SPARKS-X/) [37]. The 3D structure of each protein reference sequence was later treated with Chimera software 1.8 to show the position of proposed epitopes [38].

3. Results and Discussion

The validity and benefits of peptide vaccines designed by bioinformatics tools had been verified by appreciable research [24]. The availability of the complete genome, proteome sequences, and pathogenesis of many pathogenic microorganisms contributed to the production of a vaccine through bioinformatics [24, 39]. In this study, the predicted epitopes from B and T lymphocytes would help in the development of a more effective, reliable, preventive, and therapeutic vaccine against the PPRV than the conventional methods.

3.1. Phylogenetic Evolution.

A phylogenetic tree was constructed using MEGA7.0.26 (7170509). The evolutionary divergence among each protein was analyzed. As shown in

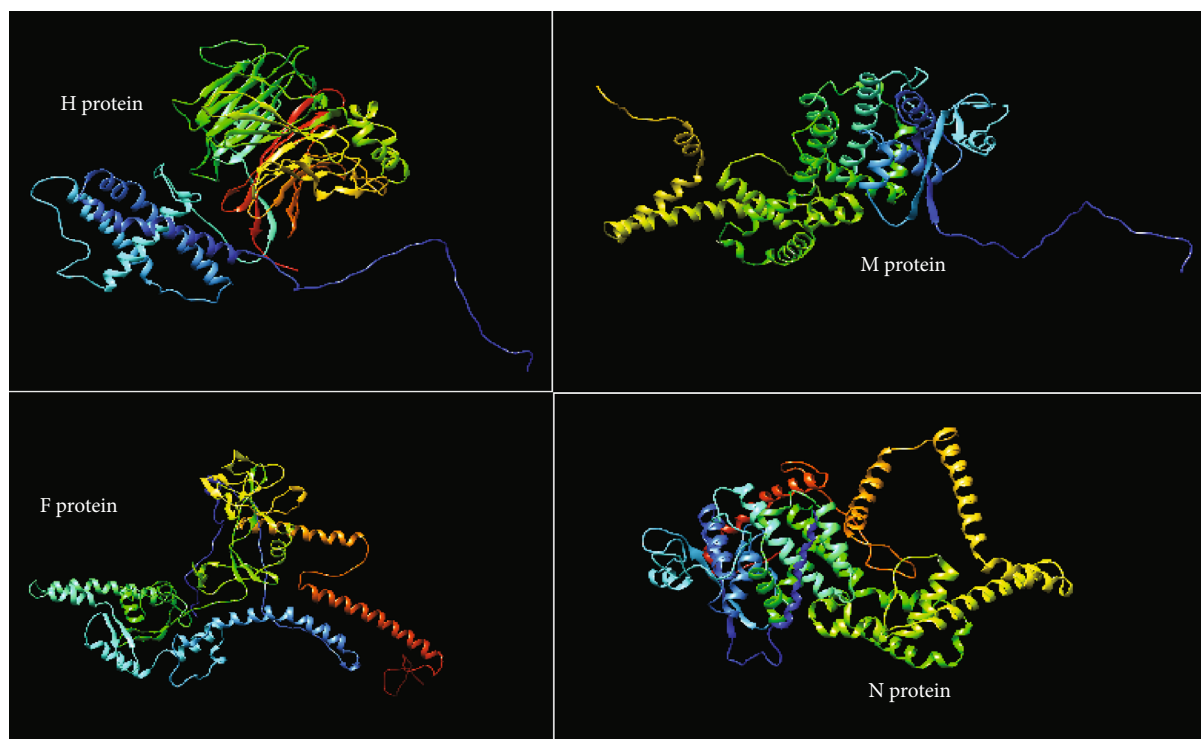


FIGURE 5: The prediction of the three-dimensional (3D) structure of H, M, and F protein reference sequences of PPRV was performed using the RaptorX structure prediction server, while the N protein sequence was submitted to the SPARKS-X server.

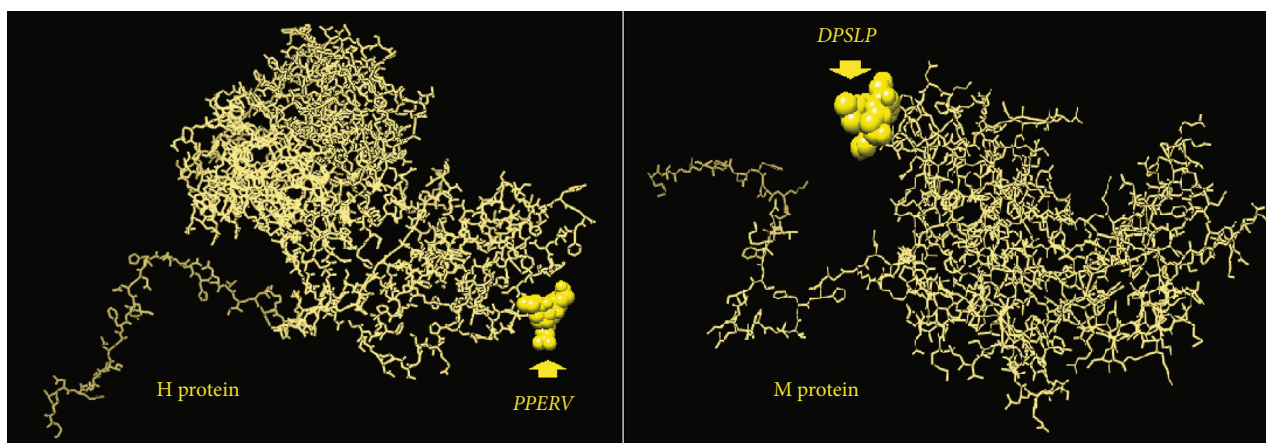


FIGURE 6: The positions of the proposed B cell epitopes in the 3D structure of the reference sequences of PPRV H and M proteins.

Figure 1, the retrieved strains of the H protein revealed that Asian strains were clustered together as well as the European and African strains. However, strains from the United Arab Emirates and Oman were closely related to African strains (namely to Ethiopian strains). With regard to the phylogeny of the M protein strains, the African strains were also clustered together, but among them, the Oman and United Arab Emirates strains were observed to be close to the Ethiopian strains same as those of the H protein. This result may indicate the transfer of the H and M strain segments between these countries. Also, some European and Turkish strains were clustered together. As shown in Figure 2, the retrieved strains of F and N proteins from the Asian strains were clustered together with molecular

divergence among them as well as the strains retrieved from the African countries. Also, the Omanis and Emiratis strains showed close relationship to the African strains. These results indicated that these strain segments were widely distributed in Africa, Asia, Europe, and the Arab region.

3.2. Sequence Alignment. Multiple sequence alignment was performed using ClustalW in BioEdit software. As shown in Figure 3, the aligned sequences of each of the four analyzed proteins (H, M, F, and N proteins) showed considerable conservancy among the retrieved strains. However, some regions exhibited differences (mutations) in some amino acids in various sequences.

TABLE 5: B cell epitope prediction from H, M, F, and N proteins; the position of peptides is according to the position of amino acids in the protein of the PPR virus.

H protein	Peptide	Start	End	Length	Emini 1.000	Kolaskar 1.041
1	PHNK	16	19	4	2.683	0.969
2	SIDHQ	83	87	5	1.169	1.03
3	PPERV [#]	142	146	5	1.904	1.047
4	TVTL	305	308	4	0.505	1.113
5	TLGG	330	333	4	0.462	0.977
6	EANWVVPSTDVRLDQ	362	376	15	1.022	1.039
7	KTRPPSFCNGTG	387	398	12	1.314	0.982
8	GPWSEGRIP	400	408	9	1.023	0.962
9	DVSR	530	533	4	1.29	1.034
M protein	Peptide	Start	End	Length	Emini 1.000	Kolaskar 1.037
1	SAWDV	10	14	5	0.533	1.044
2	GDRK	43	46	4	2.478	0.886
3	EDNDPLSP [*]	60	67	8	3.167	0.969
4	DPLSP ^{*#}	63	67	5	1.332	1.051
5	VGRT	69	72	4	0.795	1.01
6	PEEL	87	90	4	1.464	1.004
7	DNGYYS [*]	167	172	6	2.116	0.975
8	INDD	325	328	4	1.203	0.915
F protein	Peptide	Start	End	Length	Emini 1.000	Kolaskar 1.054
1	TGSA	34	37	4	0.867	0.965
2	SNQA	153	156	4	1.691	0.967
3	SLRDP	216	220	5	2.058	1.013
4	QEWYT	305	309	5	2.625	0.966
5	VFTP	331	334	4	0.643	1.112
6	GTVG	336	339	4	0.255	1.144
7	GSTKS	357	361	5	1.888	0.947
8	QDPDK	402	406	5	5.498	0.948
9	VGSREYPD	428	435	8	2.837	1.01
10	LKPDLTGTSKS	531	541	11	3.269	0.996
N protein	Peptide	Start	End	Length	Emini 1.000	Kolaskar 1.014
1	DKAPTASGSGGAI [*]	16	28	13	0.249	0.981
2	IPGDSSI	39	45	7	0.345	1.019
3	GDPDINGS	60	67	8	0.735	0.935
4	TDDPDV	92	97	6	1.569	0.992
5	STRSQS	107	112	6	2.397	0.972
6	GADLD [*]	120	124	5	0.619	0.984
7	VTAPDTAADS	182	191	10	0.594	1.02
8	RTPGNKPR	242	249	8	4.853	0.92
9	KFSA	323	326	4	0.83	1.024
10	RGTGPRQA [*]	408	415	8	1.69	0.943

^{*}Peptides revealed a higher score if they were shortened in all tools. ^{*}Epitopes that passed all the B cell prediction methods and were proposed as B cell epitopes.

3.3. Prediction of B Cell Epitopes. B cell epitope prediction methods aimed are at identifying the antigens recognized by B lymphocytes to initiate humoral immunity [24]. The important criteria for selecting a potential epitope for vaccine development are surface accessibility, hydrophobicity, flexi-

bility, and antigenicity [40]. The predicted epitopes should be located on the surface of the cells so that it is more accessible for both the humoral and the cellular immune systems. Antigenicity also is one of the important features of an antigen for vaccine development [40]. Depending on binding

TABLE 6: Position of CTL epitopes in the H protein, M protein, F protein, and N protein of PPRV that bind with high affinity with the BoLA class I alleles.

	Peptide	Start	End	Allele	Percentile rank
H protein	DLVKFISDK	113	121	BoLA-T2a	2
				BoLA-T2C	1.9
	FLRVFEIGL	251	259	BoLA-HD6	1
	GRIPAYGVI	405	413	BoLA-D18.4	2.3
				BoLA-T2b	2.1
	LLAIAGIRL	52	60	BoLA-HD6	1.5
				BoLA-T2b	2.3
	LSLIGLLAI	47	55	BoLA-T2a	2.9
	LVKFISDKI	114	122	BoLA-HD6	1.3
				BoLA-HD6	2.1
	MFLSLIGLL	45	53	BoLA-JSP.1	1.7
				BoLA-T2b	1.4
				BoLA-T2C	1.7
	VMFLSLIGL	44	52	BoLA-JSP.1	2.6
				BoLA-T2C	1.7
WCYHDCLIIY	578	586	BoLA-T2a	1.2	
WSEGRIPAY	402	410	BoLA-JSP.1	2.2	
M protein	SAWDVKGSI	10	18	BoLA-HD6	1.8
	EELLREATE	88	96	BoLA-T2b	1
	ELLREATEL	89	97	BoLA-HD6	1.3
	PQRFRRVVYM	152	160	BoLA-JSP.1	1.7
	HVGNFRRKK	220	228	BoLA-T2a	2.4
	GGIGGTSLSH	251	259	BoLA-T2a	2
	LHAQLGFKK	270	278	BoLA-T2a	1.2
	AQLGFKKIL	272	280	BoLA-T2C	2.4
	FKKILCYPL	276	284	BoLA-D18.4	1.2
				BoLA-HD6	1.3
EFRVYDDVI	316	324	BoLA-HD6	2.6	
F protein	AGVALHQSL	129	137	BoLA-T2C	1.7
	ASVLCKCYT	387	395	BoLA-T2a	1.4
	AYPTLSEIK	280	288	BoLA-T2a	2.9
				BoLA-JSP.1	2.3
	CSQNALYPM	339	347	BoLA-T2a	2.5
	DETSCVFTP	326	334	BoLA-T2b	2.7
	DLGPAISLE	443	451	BoLA-T2C	1.3
	EKLDVGTNL	451	459	BoLA-T2b	2.7
	GSTKSCART	357	365	BoLA-T2a	2.6
				BoLA-JSP.1	2.5
	GTVCSQNAL	336	344	BoLA-T2b	1.6
	GVALHQSLM	130	138	BoLA-HD6	2.1
				BoLA-HD6	2.9
	IAYPTLSEI	279	287	BoLA-JSP.1	2.3
				BoLA-D18.4	2.1
IDLGPAISL	442	450	BoLA-T2b	1.4	
			BoLA-T2C	1.2	
IQALSYALG	227	235	BoLA-T2b	2.7	
IQVGSREYP	426	434	BoLA-D18.4	2.8	
KGIKARVTY	259	267	BoLA-D18.4	1.2	

TABLE 6: Continued.

	KPDLTGTSK	532	540	BoLA-T2a	2.6
	LEKLDVGTN	450	458	BoLA-T2b	3
	LIANCASVL	382	390	BoLA-HD6	1.6
	LSKGNLIAN	377	385	BoLA-T2a	3
	LSYALGGDI	230	238	BoLA-HD6	1.8
				BoLA-JSP.1	1.2
	NALYPMSPL	342	350	BoLA-T2b	1.5
	PMSPLLQEC	346	354	BoLA-T2C	3
	RFILSKGNL	374	382	BoLA-T2b	2
	SIQALSYAL	226	234	BoLA-T2b	1
	SLMNSQAIE	136	144	BoLA-D18.4	3
				BoLA-T2C	2.5
				BoLA-D18.4	2.7
	SQNALYPMS	340	348	BoLA-HD6	1.7
				BoLA-D18.4	2.3
				BoLA-D18.4	3
				BoLA-HD6	2.7
	STKSCARTL	358	366	BoLA-JSP.1	1.6
				BoLA-T2b	2.9
				BoLA-T2C	2.7
	TGTSKSYVR	536	544	BoLA-T2a	2.9
	TKSCARTLV	359	367	BoLA-D18.4	2.3
	TLSEIKGVI	283	291	BoLA-D18.4	2.4
				BoLA-T2C	1.8
	YVATQGYLI	314	322	BoLA-HD6	2
				BoLA-T2C	2.8
				BoLA-D18.4	1.6
	ATLLKSLAL	2	10	BoLA-JSP.1	1.3
				BoLA-T2a	2.6
				BoLA-T2b	1.9
				BoLA-D18.4	2.6
	TLLKSLALF	3	11	BoLA-HD6	3
				BoLA-T2C	1.3
				BoLA-HD6	2.2
	QQLGEVAPY	304	312	BoLA-JSP.1	3
				BoLA-T2a	1.4
				BoLA-T2b	2.9
				BoLA-JSP.1	1.3
N protein	YFDPAYFRL	356	364	BoLA-T2b	2.4
				BoLA-T2C	1.5
				BoLA-HD6	1.6
	AYFRLGQEM	360	368	BoLA-JSP.1	2.1
				BoLA-T2C	2.9
				BoLA-JSP.1	1.7
	PRQAQVSFL	412	420	BoLA-T2b	2.2
				BoLA-T2C	2.6
				BoLA-D18.4	1.2
				BoLA-HD6	1.2
	RSAEALFRL	490	498	BoLA-T2a	1.9
				BoLA-T2b	2.9
				BoLA-T2C	2.7

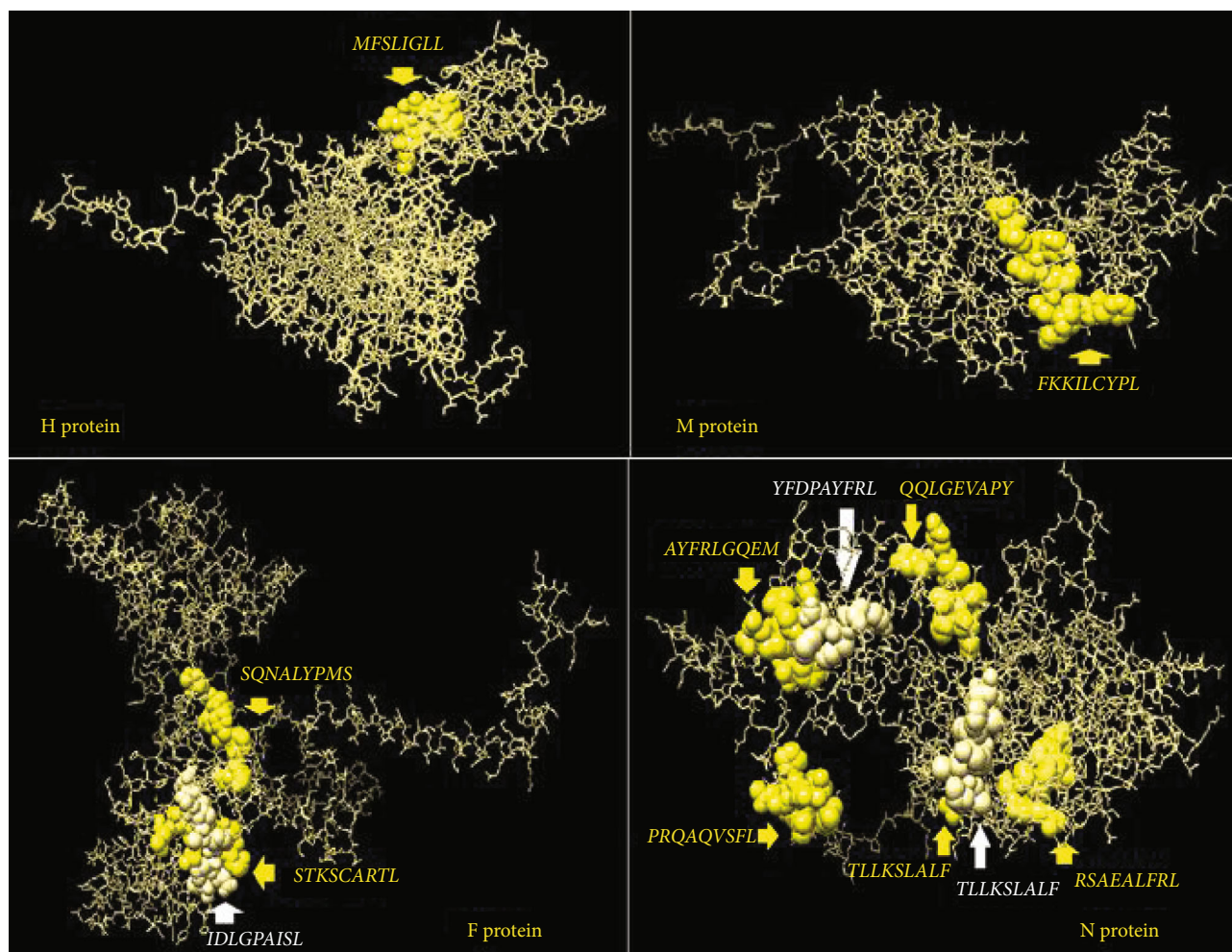


FIGURE 7: The positions of the predicted T cell epitopes in the 3D structure of the reference sequences of PPRV H, M, F, and N proteins.

affinity to B lymphocytes, the BepiPred linear epitope prediction method predicted nine linear epitopes from the H protein, eight epitopes from M proteins, and ten epitopes for each of the F and N proteins. Analysis of these linear epitopes for surface accessibility proposed seven surface epitopes from each of the H and F proteins, six epitopes from the M protein, and four epitopes from the N protein.

As shown in Figure 4, the threshold values were 0.350 and 1.000 for all epitopes predicted through the BepiPred linear epitope (conserved epitopes) and Emini prediction methods (surface accessibility), respectively. The antigenicity prediction method proposed only two epitopes for all test immunogenic proteins of PPRV. Also, Figure 4 shows that the antigenic epitopes were predicted from H, M, F, and N proteins using the Kolaskar and Tongaonkar antigenicity method under threshold values of 1.014, 1.037, 1.054, and 1.014, respectively. However, no epitopes successfully passed the threshold for the F and N proteins.

Only one epitope from each of the H and M proteins successfully overlapped all the B cell antigenic index prediction methods. Namely, these epitopes were $_{142}PPERV_{146}$ from the H protein and $_{63}DPLSP_{67}$ from the M protein. The

3D structure of the four proteins (H, M, F, and N) is shown in Figure 5. The positions of the best B cells that predicted epitopes from the H and M proteins are demonstrated in Figure 6. The overall predicted epitopes from the four proteins are illustrated in Table 5.

3.4. Prediction of CTL Epitopes That Interacted with MHC Class I (BoLA Alleles). CD8+ and CD4+ T cells have a principal role in the stimulation of immune response as well as antigen-mediated clonal expression of the B cell [14]. Unfortunately, the bovine genome project did not assemble a complete sequence of the bovine MHC-II locus [41–43]. Thus, the analysis was completed with BoLA MHC-I alleles only. Cell-mediated immunity induced by cytotoxic T lymphocytes (CTLs) is vital for the defense against viral diseases. CTLs are responsible for the immune elimination of intracellular pathogens such as viruses because these cells recognize the presented endogenous antigenic peptides by the MHC class I molecules [44].

In this study, MHC-I binding prediction methods using the IEDB database predicted different CTL epitopes that strongly interacted with various BoLA alleles. The

fusion (F) protein proposed a higher number of predicted epitopes with strong interaction with BoLA alleles. Ten epitopes were proposed based on the number of the interacted alleles. The best one was $_{358}STKSCARTL_{366}$ that associated with five alleles, followed by $_{442}IDLGPAISL_{450}$ and $_{340}SQNALYPMS_{348}$ as they linked to three alleles each. However, seven epitopes, namely, $_{339}CSQNALYPMS_{347}$, $_{336}GTVCSQNAL_{344}$, $_{279}IAYPTLSEI_{287}$, $_{230}LSYALGGDI_{238}$, $_{136}SLMNSQAIE_{144}$, $_{283}TLSEIKGVI_{291}$, and $_{314}YVATQGYLI_{322}$ were predicted to interact with two alleles.

The nucleoprotein (N) also displayed strong interaction activity with BoLA alleles. Seven epitopes were proposed with strong interaction with BoLA alleles. The top N protein epitope was $_{490}RSAEALFRL_{498}$ which was associated with five alleles, followed by two epitopes, namely, $_{2}ATLLKSLAL_{10}$, and $_{304}QQLGEVAPY_{312}$ that linked to four alleles each. In addition to that, four epitopes $_{3}TLLKSLALF_{11}$, $_{356}YFDPAYFRL_{364}$, $_{360}AYFRLGQEM_{368}$, and $_{412}PRQAQVSFL_{420}$ interacted with three bovine alleles each. Surprisingly, these two proteins (F and N) achieved promising results in CTL prediction methods, although they failed to predict any epitope carrying all the ideal traits in B cells.

The haemagglutinin (H) protein predicted five CTL epitopes, but one epitope was predicted as the best peptide, $_{45}MFLSLIGLL_{53}$, as it linked to four BoLA alleles, followed by four peptides that interacted with two alleles each. They were $_{113}DLVKFISDK_{121}$, $_{405}GRIPAYGVI_{413}$, $_{52}LLAIAGIRL_{60}$ and $_{44}VMFLSLIGL_{52}$. However, this protein showed a somewhat satisfactory result in B and T cell prediction methods. The M protein showed unsatisfactory results in CTL prediction methods different from that predicted by B cell methods. The results suggested only one epitope; $_{276}FKKILCYPL_{284}$ interacted with only two alleles. The overall epitopes that were proposed to interact with CTL alleles are illustrated in Table 6 for all proteins. The positions of the best CTL-predicted epitopes in their immunogenic protein structure are shown in Figure 7.

Vaccination is considered the most effective way of controlling PPR. The infection by morbillivirus is associated with severe immunosuppression that is characterized by a massive virus-specific immune response. Protection is mediated by cell-mediated and humoral immune responses directed mainly against particular proteins in the viral structure. These proteins included H, F, and N proteins [45–47]. It was reported that the envelope glycoproteins H and F of PPRV demonstrated a protective and neutralizing antibody response [3, 48–50]. In this study, using the immunoinformatics prediction methods, the H protein demonstrated affinity to interact with B cells that was characterized by antibody production. This result coincided with the previously published reports [3, 48–50], while the F protein failed to interact with B cells; i.e., no epitopes from the F protein had passed the threshold of the B cell prediction methods. However, this protein revealed multiple predicted epitopes that demonstrated high affinity to the alleles of CTLs. The M protein which is believed to play a very significant role in morbillivirus assembly and budding by concentrating the F, H, and N proteins at the virus-assembly site [16, 17] showed moderate affinity to B cells. One epitope

from the M protein as well as the H protein was predicted as a B cell epitope. Moreover, the M protein revealed multiple epitopes that interacted with CTLs of the cell-mediated immunity. This result indicated that the M protein besides its role in the virus assembly may also contain antigenic determinants that could be elected as vaccine candidates.

In addition to that, cell-mediated immunity plays a role in protection against the viral infection. Despite the N protein being the most frequent viral protein in PPRV, it does not induce a neutralizing antibody response in the host [50]. However, it has been found to induce a strong cell-mediated immune response, which is believed to contribute to protection. Here, in this report, the same result was obtained. The N protein demonstrated no affinity to elicit the humoral immune response. However, it showed favorable affinity to interact with a cell-mediated response. It is noteworthy that five out of seven epitopes predicted from the nucleoprotein of PPRV in this study were found to be proposed by another *in silico* study using mouse alleles and NetMHCII methods [51]. The proposed epitopes from that study were *ATLLKSLAL*, *TLLKSLALF*, *YFDPAYFRL*, *AYFRLGQEM*, and *RSALFRL*. Thus, the predictions for the different epitopes that bound to different alleles particularly from the N protein of PPRV were somewhat in agreement regardless of the alleles (cow and mouse alleles) and algorithm used (ANN, NetMHCII).

In general, epitope-based vaccines that are chemically well-characterized have become desirable candidate vaccines due to their relative ease of production and construction, chemical stability, and lack of infectious potential [52]. Many *in silico* studies have shown the value of using prediction programs to evaluate the efficiency of binding of putative epitopes to various human and animal alleles [33, 52–55].

4. Conclusion

This study focused mainly on the production of a peptide vaccine against H, M, F, and N proteins of PPRV using immunoinformatics tools. Epitopes that showed conservancy and high binding affinities to many MHC alleles are considered the best candidates for *in vitro* and *in vivo* testing. Epitopes that were predicted from B cell prediction methods like $_{142}PPERV_{146}$ and $_{305}TVTL_{308}$ from the H protein and $_{63}DPLSP_{67}$ and $_{64}PLSP_{67}$ from the M protein could act as good B cell epitopes to induce humoral immunity. While the F and N proteins failed to fulfill all B cell indexes used in this study for the prediction of promising epitopes, however, these proteins predicted epitopes that interacted with various BoLA MHC-I alleles. For instance, the best epitopes were predicted from F ($_{358}STKSCARTL_{366}$) and N ($_{490}RSAEALFRL_{498}$) proteins as they interacted with five MHC-I BoLA alleles, followed by $_{45}MFLSLIGLL_{53}$ proposed from the H protein and linked with four alleles, while the $_{276}FKKILCYPL_{284}$ epitope was predicted from the M protein linked with only two alleles. Although bioinformatics studies have been established to facilitate the peptide design, not all peptides that are predicted *in silico* are optimally immunogenic *in vivo* and it remains necessary to test the expected peptides *in vivo* to ensure that the T cell responses are elicited.

Data Availability

The [retrived strains, IEDB analysis methods] data used to support the findings of this study are included within the article.

Conflicts of Interest

The authors declare that they have no competing interests.

Acknowledgments

The authors would like to thank the staff members of the College of Veterinary Medicine, University of Bahri, Sudan, for their cooperation and support.

References

- [1] C. Schulz, C. Fast, K. Schlottau, B. Hoffmann, and M. Beer, "Neglected hosts of small ruminant morbillivirus," *Emerging Infectious Diseases*, vol. 24, no. 12, pp. 2334–2337, 2018.
- [2] FAO, O, *Global strategy for the control and eradication of PPR*, FAO and OIE, 2015.
- [3] M. Munir, "Peste des petits ruminants virus," in *Mononegaviruses of Veterinary Importance. Volume I: Pathobiology and Molecular Diagnosis*, pp. 65–98, CAB International, Oxfordshire, 2013.
- [4] A. C. Banyard, S. Parida, C. Batten, C. Oura, O. Kwiatek, and G. Libeau, "Global distribution of peste des petits ruminants virus and prospects for improved diagnosis and control," *Journal of General Virology*, vol. 91, no. 12, pp. 2885–2897, 2010.
- [5] O. Kwiatek, Y. H. Ali, I. K. Saeed et al., "Asian lineage of peste des petits ruminants virus, Africa," *Emerging Infectious Diseases*, vol. 17, no. 7, pp. 1223–1231, 2011.
- [6] O. Kwiatek, C. Minet, C. Grillet et al., "Peste des petits ruminants (PPR) outbreak in Tajikistan," *Journal of Comparative Pathology*, vol. 136, no. 2-3, pp. 111–119, 2007.
- [7] N. Kerur, M. K. Jhala, and C. G. Joshi, "Genetic characterization of Indian peste des petits ruminants virus (PPRV) by sequencing and phylogenetic analysis of fusion protein and nucleoprotein gene segments," *Research in Veterinary Science*, vol. 85, no. 1, pp. 176–183, 2008.
- [8] B. el Hag Ali and W. P. Taylor, "Isolation of peste des petits ruminants virus from the Sudan," *Research in Veterinary Science*, vol. 36, no. 1, pp. 1–4, 1984.
- [9] M. S. Shaila, D. Shamaki, M. A. Forsyth et al., "Geographic distribution and epidemiology of peste des petits ruminants viruses," *Virus Research*, vol. 43, no. 2, pp. 149–153, 1996.
- [10] T. Barrett, I. K. G. Visser, L. Mamaev, L. Goatley, M. F. van Bresse, and A. D. M. E. Osterhaus, "Dolphin and porpoise morbilliviruses are genetically distinct from phocine distemper virus," *Virology*, vol. 193, no. 2, pp. 1010–1012, 1993.
- [11] Z. Wang, J. Bao, X. Wu et al., "Peste des petits ruminants virus in Tibet, China," *Emerging Infectious Diseases*, vol. 15, no. 2, pp. 299–301, 2009.
- [12] M. Mahapatra, S. Parida, B. G. Egziabher, A. Diallo, and T. Barrett, "Sequence analysis of the phosphoprotein gene of peste des petits ruminants (PPR) virus: editing of the gene transcript," *Virus Research*, vol. 96, no. 1-2, pp. 85–98, 2003.
- [13] A. C. Banyard, R. J. Grant, C. H. Romero, and T. Barrett, "Sequence of the nucleocapsid gene and genome and antigenome promoters for an isolate of porpoise morbillivirus," *Virus Research*, vol. 132, no. 1-2, pp. 213–219, 2008.
- [14] P. Dhar, D. Muthuchelvan, A. Sanyal et al., "Sequence analysis of the haemagglutinin and fusion protein genes of peste-des-petits ruminants vaccine virus of Indian origin," *Virus Genes*, vol. 32, no. 1, pp. 71–78, 2006.
- [15] G. Berhe, C. Minet, C. le Goff et al., "Development of a dual recombinant vaccine to protect small ruminants against peste-des-petits-ruminants virus and capripoxvirus infections," *Journal of Virology*, vol. 77, no. 2, pp. 1571–1577, 2003.
- [16] A. Haffar, G. Libeau, A. Moussa, M. Cécile, and A. Diallo, "The matrix protein gene sequence analysis reveals close relationship between peste des petits ruminants virus (PPRV) and dolphin morbillivirus," *Virus Research*, vol. 64, no. 1, pp. 69–75, 1999.
- [17] G. D. Maganga, D. Verrier, R. M. Zerbinati, C. Drosten, J. F. Drexler, and E. M. Leroy, "Molecular typing of PPRV strains detected during an outbreak in sheep and goats in south-eastern Gabon in 2011," *Virology Journal*, vol. 10, no. 1, p. 82, 2013.
- [18] A. Diallo, "Control of peste des petits ruminants: classical and new generation vaccines," *Developments in Biologicals*, vol. 114, pp. 113–119, 2003.
- [19] W. G. Dundon, C. Adombi, A. Waqas et al., "Full genome sequence of a peste des petits ruminants virus (PPRV) from Ghana," *Virus Genes*, vol. 49, no. 3, pp. 497–501, 2014.
- [20] I. K. Saeed, Y. H. Ali, A. M. I. Khalafalla, and E. A. Rahman-Mahasin, "Current situation of peste des petits ruminants (PPR) in the Sudan," *Tropical Animal Health and Production*, vol. 42, no. 1, pp. 89–93, 2010.
- [21] J. M. Gershoni, A. Roitburd-Berman, D. D. Siman-Tov, N. Tarnovitski Freund, and Y. Weiss, "Epitope mapping: the first step in developing epitope-based vaccines," *BioDrugs*, vol. 21, no. 3, pp. 145–156, 2007.
- [22] S. Iurescia, D. Fioretti, V. M. Fazio, and M. Rinaldi, "Epitope-driven DNA vaccine design employing immunoinformatics against B-cell lymphoma: a biotech's challenge," *Biotechnology Advances*, vol. 30, no. 1, pp. 372–383, 2012.
- [23] A. H. Abu haraz, K. A. Abd elrahman, M. S. Ibrahim et al., "Multi epitope peptide vaccine prediction against Sudan ebola virus using immuno-informatics approaches," *Advanced Techniques in Biology & Medicine*, vol. 5, no. 1, p. 203, 2017.
- [24] J. Zheng, X. Lin, X. Wang et al., "In silico analysis of epitope-based vaccine candidates against hepatitis B virus polymerase protein," *Viruses*, vol. 9, no. 5, p. 112, 2017.
- [25] K. Tamura, G. Stecher, D. Peterson, A. Filipski, and S. Kumar, "MEGA6: molecular evolutionary genetics analysis version 6.0," *Molecular Biology and Evolution*, vol. 30, no. 12, pp. 2725–2729, 2013.
- [26] T. Hall, "BioEdit: an important software for molecular biology," *GERF Bulletin of Biosciences*, vol. 2, no. 1, pp. 60–61, 2011.
- [27] R. Vita, J. A. Overton, J. A. Greenbaum et al., "The immune epitope database (IEDB) 3.0," *Nucleic Acids Research*, vol. 43, no. D1, pp. D405–D412, 2015.
- [28] J. Larsen, O. Lund, and M. Nielsen, "Improved method for predicting linear B-cell epitopes," *Immuno Research*, vol. 2, no. 1, p. 2, 2006.
- [29] E. A. Emini, J. V. Hughes, D. S. Perlow, and J. Boger, "Induction of hepatitis A virus-neutralizing antibody by a virus-

- specific synthetic peptide," *Journal of Virology*, vol. 55, no. 3, pp. 836–839, 1985.
- [30] A. S. Kolaskar and P. C. Tongaonkar, "A semi-empirical method for prediction of antigenic determinants on protein antigens," *FEBS Letters*, vol. 276, no. 1-2, pp. 172–174, 1990.
- [31] C. Lundegaard, O. Lund, and M. Nielsen, "Accurate approximation method for prediction of class I MHC affinities for peptides of length 8, 10 and 11 using prediction tools trained on 9mers," *Bioinformatics*, vol. 24, no. 11, pp. 1397–1398, 2008.
- [32] A. Patronov and I. Doytchinova, "T-cell epitope vaccine design by immunoinformatics," *Open Biology*, vol. 3, no. 1, article 120139, 2013.
- [33] M. Abdelbagi, T. Hassan, M. Shihabeldin et al., "Immunoinformatics prediction of peptide-based vaccine against African horse sickness virus," *Immunome Research*, vol. 13, no. 2, p. 135, 2017.
- [34] M. Källberg, H. Wang, S. Wang et al., "Template-based protein structure modeling using the RaptorX web server," *Nature Protocols*, vol. 7, no. 8, pp. 1511–1522, 2012.
- [35] J. Peng and J. Xu, "RaptorX: exploiting structure information for protein alignment by statistical inference," *Proteins: Structure, Function, and Bioinformatics*, vol. 79, Supplement 10, pp. 161–171, 2011.
- [36] J. Peng and J. Xu, "A multiple-template approach to protein threading," *Proteins: Structure, Function, and Bioinformatics*, vol. 79, no. 6, pp. 1930–1939, 2011.
- [37] Y. Yang, E. Faraggi, H. Zhao, and Y. Zhou, "Improving protein fold recognition and template-based modeling by employing probabilistic-based matching between predicted one-dimensional structural properties of query and corresponding native properties of templates," *Bioinformatics*, vol. 27, no. 15, pp. 2076–2082, 2011.
- [38] W. M. Chan, S. E. Rogers, S. M. Nash, P. G. Buning, and R. Meakin, "User's manual for Chimera grid tools, version 1.8," NASA Ames Research Center, 2003, July 2006, <http://people.nas.nasa.gov/~rogers/cgt/doc/man.html>.
- [39] S. Pahil, N. Taneja, H. R. Ansari, and G. P. S. Raghava, "In silico analysis to identify vaccine candidates common to multiple serotypes of *Shigella* and evaluation of their immunogenicity," *PLoS One*, vol. 12, no. 8, article e0180505, 2017.
- [40] P. P. Kar and A. Srivastava, "Immuno-informatics analysis to identify novel vaccine candidates and design of a multi-epitope based vaccine candidate against *Theileria* parasites," *Frontiers in Immunology*, vol. 9, article 2213, 2018.
- [41] V. Nene, N. Svitek, P. Toyé et al., "Designing bovine T cell vaccines via reverse immunology," *Ticks and Tick-borne Diseases*, vol. 3, no. 3, pp. 188–192, 2012.
- [42] B. G. Sequencing, A. Consortium, C. G. Elsik, R. L. Tellam, and K. C. Worley, "The genome sequence of taurine cattle: a window to ruminant biology and evolution," *Science*, vol. 324, pp. 522–528, 2009.
- [43] A. V. Zimin, A. L. Delcher, L. Florea et al., "A whole-genome assembly of the domestic cow, *Bos taurus*," *Genome Biology*, vol. 10, no. 4, article R42, 2009.
- [44] T. K. Sahu, A. R. Rao, P. K. Meher, B. C. Sahoo, A. Gupta, and A. Rai, "Computational prediction of MHC class I epitopes for most common viral diseases in cattle (*Bos taurus*)," *Indian Journal of Biochemistry & Biophysics*, vol. 52, no. 1, pp. 34–44, 2015.
- [45] S. Naik, G. J. Renukaradhya, M. Rajasekhar, and M. S. Shaila, "Immunogenic and protective properties of haemagglutinin protein (H) of rinderpest virus expressed by a recombinant baculovirus," *Vaccine*, vol. 15, no. 6-7, pp. 603–607, 1997.
- [46] S. Naik and M. S. Shaila, "Characterization of membrane-bound and membrane anchor-less forms of hemagglutinin glycoprotein of rinderpest virus expressed by baculovirus recombinants," *Virus Genes*, vol. 14, no. 2, pp. 95–104, 1997.
- [47] G. Sinnathamby, R. Nayak, and M. S. Shaila, "Mapping of T-helper epitopes of rinderpest virus hemagglutinin protein," *Viral Immunology*, vol. 14, no. 1, pp. 83–92, 2001.
- [48] C. H. Romero, T. Barrett, R. P. Kitching, V. M. Carn, and D. N. Black, "Protection of cattle against rinderpest and lumpy skin disease with a recombinant capripoxvirus expressing the fusion protein gene of rinderpest virus," *The Veterinary Record*, vol. 135, no. 7, pp. 152–154, 1994.
- [49] G. Sinnathamby, G. J. Renukaradhya, M. Rajasekhar, R. Nayak, and M. S. Shaila, "Immune responses in goats to recombinant hemagglutinin-neuraminidase glycoprotein of *peste des petits ruminants* virus: identification of a T cell determinant," *Vaccine*, vol. 19, no. 32, pp. 4816–4823, 2001.
- [50] A. Diallo, C. Minet, C. Le Goff et al., "The threat of peste des petits ruminants: progress in vaccine development for disease control," *Vaccine*, vol. 25, no. 30, pp. 5591–5597, 2007.
- [51] B. Baloi, "In silico epitope prediction and 3D model analysis of peste des petits ruminants virus nucleoprotein (PPRV N)," *bioRxiv*, no. article 095505, 2016.
- [52] Y.-F. Liu, C.-Y. Lin, and H.-M. Hong, "In silico design, synthesis and potency of an epitope-based vaccine against foot-and-mouth disease virus," *International Journal of Pharmacology*, vol. 13, no. 2, pp. 122–133, 2017.
- [53] S. T. Idris, S. Salih, M. Basheir et al., "In silico prediction of peptide based vaccine against fowlpox virus (FPV)," *Immunome Research*, vol. 14, no. 2, p. 154, 2018.
- [54] S. O. Abd Albagi, O. Hashim Ahmed, M. A. Gumaa, K. A. Abd elrahman, A. H. Abu Haraz, and M. A., "Immunoinformatics-peptide driven vaccine and in silico modeling for Duvenhage rabies virus glycoprotein G," *Journal of Clinical & Cellular Immunology*, vol. 8, no. 4, p. 517, 2017.
- [55] N. Prabdial-Sing, A. J. Puren, and S. M. Bowyer, "Sequence-based in silico analysis of well studied hepatitis C virus epitopes and their variants in other genotypes (particularly genotype 5a) against South African human leukocyte antigen backgrounds," *BMC Immunology*, vol. 13, no. 1, p. 67, 2012.

Research Article

Enhancement of Macrophage Function by the Antimicrobial Peptide Sublancin Protects Mice from Methicillin-Resistant *Staphylococcus aureus*

Shuai Wang,^{1,2} Qianhong Ye,¹ Ke Wang,³ Xiangfang Zeng,¹ Shuo Huang,¹ Haitao Yu,¹ Qing Ge,³ Desheng Qi,² and Shiyan Qiao¹ 

¹State Key Laboratory of Animal Nutrition, Beijing Key Laboratory of Biofeed Additives, Ministry of Agriculture Feed Industry Center, China Agricultural University, Beijing 100193, China

²Department of Animal Nutrition and Feed Science, College of Animal Science and Technology, Huazhong Agricultural University, Wuhan, Hubei 430070, China

³Key Laboratory of Medical Immunology, Ministry of Health, Department of Immunology, School of Basic Medical Sciences, Peking University Health Science Center, Beijing 100191, China

Correspondence should be addressed to Shiyan Qiao; qiaoshiyan@cau.edu.cn

Received 31 May 2019; Accepted 2 August 2019; Published 8 September 2019

Guest Editor: Pedro A. Reche

Copyright © 2019 Shuai Wang et al. This is an open access article distributed under the Creative Commons Attribution License, which permits unrestricted use, distribution, and reproduction in any medium, provided the original work is properly cited.

Methicillin-resistant *Staphylococcus aureus* (MRSA) is the major pathogen responsible for community and hospital bacterial infections. Sublancin, a glucosylated antimicrobial peptide isolated from *Bacillus subtilis* 168, possesses antibacterial infective effects. In this study, we investigated the role and anti-infection mechanism of sublancin in a mouse model of MRSA-induced sublethal infection. Sublancin could modulate innate immunity by inducing the production of IL-1 β , IL-6, TNF- α , and nitric oxide, enhancing phagocytosis and MRSA-killing activity in both RAW264.7 cells and mouse peritoneal macrophages. The enhanced macrophage function by the peptide in vitro correlated with stronger protective activity in vivo in the MRSA-invasive sublethal infection model. Macrophage activation by sublancin was found to be partly dependent on TLR4 and the NF- κ B and MAPK signaling pathways. Moreover, oral administration of sublancin increased the frequencies of CD⁴⁺ and CD⁸⁺ T cells in mesenteric lymph nodes. The protective activity of sublancin was associated with in vivo augmenting phagocytic activity of peritoneal macrophages and partly improving T cell-mediated immunity. Macrophages thus represent a potentially pivotal and novel target for future development of innate defense regulator therapeutics against *S. aureus* infection.

1. Introduction

Concurrent with the success of antibiotics for treating infections, their excessive use contributes to the emergence of antibiotic-resistant bacteria [1]. Methicillin-resistant *Staphylococcus aureus* (MRSA) is widespread and multiresistant; thus, it has challenged the effectiveness of antibiotics including β -lactams, macrolides, and quinolones, as well as vancomycin which has been accepted as the first-line option for treating infections due to MRSA [2]. Antibiotic resistance has become an increasingly serious health care problem in the world [3]. This has been aggravated by a collapse in the

number of approvals of new antibacterials in the past three decades [4].

Macrophages are professional phagocytes of the innate immune system, providing a first line of defense against infections. It has been reported that macrophages play an important role in the clearance of *S. aureus* in the infected mice [5]. Mice that have been depleted of macrophages are susceptible to MRSA infection [6]. Nevertheless, some investigators have pointed out several characteristics of MRSA that may enable it to thwart the macrophage-mediated host defense [7]. Macrophages can kill bacteria directly through phagocytosis and indirectly via releasing inflammatory

molecules and nitric oxide (NO), as well as by secreting pro-inflammatory factors, such as interleukin-6 (IL-6), IL-1 β , and tumor necrosis factor- α (TNF- α) [8, 9]. Macrophages are the first immune cells that are recruited to the infection site, and they are the main source of proinflammatory cytokines after activation [10]. Many investigators have reported that progressing macrophage dysfunction may contribute to severe sepsis [11, 12].

Antimicrobial peptides (AMPs) are important components of the innate immune defense against a wide range of invading pathogens [13, 14]. Sublancin is a 37-amino-acid AMP isolated from the Gram-positive soil bacterium *Bacillus subtilis* 168 [15]. It is not a lantibiotic but rather a very unusual S-linked glycopeptide [16]. Sublancin contains two α -helices and a well-defined interhelical loop connected by a S-glucosidic linkage to a Cys [17]. Mature sublancin has a molecular mass of 3879.8 Da [18]. In our previous studies, we showed that sublancin was protective in several in vivo infection models. Although the minimum inhibitory concentration (MIC) of sublancin was much higher than that of traditional antibiotics in vitro, it was demonstrated that sublancin was effective against *Clostridium perfringens*-induced necrotic enteritis in broilers [19]. We also found that sublancin has potential for the prevention of *S. aureus* infection in mice [18]. Moreover, sublancin was further found to protect against drug-resistant bacteria in a mouse MRSA infection model [20]. Several reports have demonstrated that AMPs were capable of activating macrophage function [13, 21]. Recently, we revealed the capability of sublancin in activating macrophages and improving the innate immunity of mice in vivo [22]. Hence, the goal of the present study was to explore the potential anti-infection mechanism of this peptide. In the present study, we investigated whether sublancin can (i) activate macrophages and the signaling pathway involved in this process, (ii) inhibit bacterial growth in a model of MRSA-infected mice and macrophages, and (iii) improve immune function in mice under healthy and MRSA-induced sublethal infection conditions.

2. Materials and Methods

2.1. Mice, Cell Lines, Peritoneal Macrophages, and Chemicals. Female BALB/c mice were used for the experiments. The murine macrophage cell line RAW264.7 was obtained from China Infrastructure of Cell Line Resource (Beijing, China) and maintained in Dulbecco's Modified Eagle's Medium (DMEM) (Gibco) containing 10% fetal bovine serum (Life Technologies). Peritoneal macrophages (P-Mac) were isolated from BALB/c mice as previously described [23]. Briefly, mice were intraperitoneally injected with 2 ml 4% thioglycolate. Three days after injection, peritoneal exudate cells were harvested by lavaging the peritoneal cavity with sterile ice-cold Hank's balanced salt solution (HBSS) (Gibco, Life Technologies). These cells were incubated for 2 h, and adherent cells were used as peritoneal macrophages. Sublancin was generated in our laboratory using a highly efficient expression system involving *Bacillus subtilis* 800 as described previously [18]. The purity of this peptide was above 99.6% as determined by high-performance liquid chromatography.

Sublancin was produced as lyophilized powder, and the endotoxin concentration of the peptide was less than 0.05 EU/mg, as detected by the E-Toxate Kit (Sigma-Aldrich). Sublancin was resuspended in endotoxin-free water (Sigma-Aldrich) and stored at -20°C. All reagents used in this study were tested for endotoxin to eliminate the interference of endotoxin contamination.

2.2. Cytokine Assays. The culture supernatants of RAW264.7 cells or mouse peritoneal macrophages treated with sublancin (25, 50, 100, or 200 μ M) for 24 h were collected for the detection of IL-1 β , IL-6, and TNF- α levels using commercially available cytometric bead arrays (BD Biosciences) according to the protocol of the manufacturer. Data were acquired with a FACSCalibur flow cytometer and analyzed with BD CBA Software (BD Biosciences).

2.3. NO Production. The nitrite accumulated in the culture medium was determined by Griess reaction. RAW264.7 cells or mouse peritoneal macrophages were treated with various concentrations of sublancin (25, 50, 100, or 200 μ M). After 24 h, culture supernatants were mixed with an equal volume of Griess reagent (1% sulfanilamide, 0.1% *N*-1-naphthylethylenediamine dihydrochloride in 2.5% phosphoric acid) and incubated at room temperature for 10 min. The absorbance was detected at 540 nm, and NO concentration was determined from a calibration curve of standard sodium nitrite concentrations against absorbance.

2.4. Quantitative Real-Time PCR. To detect the effect of sublancin on gene expression, RAW264.7 cells or mouse peritoneal macrophages (1×10^6 cells/well) were preincubated on 6-well plates and treated with sublancin (25, 50, 100, or 200 μ M) for 12 h at 37°C in an atmosphere containing 5% CO₂. Total RNA were isolated using a RNeasy Mini Kit (Qiagen, Hilden, Germany). The quality and quantity of total RNA were determined by gel electrophoresis and a NanoDrop Spectrophotometer (Implen NanoPhotometer P330, Germany). cDNA was synthesized from the extracted RNA (1 μ g) using a PrimeScript 1st Strand cDNA Synthesis Kit (Takara Bio Inc., Otsu, Japan) according to the manufacturer's protocol. Real-time PCR was performed on an Applied Biosystems 7500 Real-Time PCR System (Applied Biosystems, Singapore) with the SYBR Green PCR Master Mix (Takara Bio Inc., Otsu, Japan). The PCR system contained 5.0 μ l of SYBR Green qPCR Mix, 1.0 μ l of cDNA, 0.4 μ l of primer pairs (25 μ M forward and 25 μ M reverse), and 3.6 μ l double-distilled water in a final volume of 10 μ l. The protocols for all genes included a denaturation program (1 min at 95°C) and an amplification and quantification program repeated for 40 cycles (5 s at 95°C, 30 s at 60°C), followed by the melting curve program at 60–95°C with a heating rate of 0.1°C per second and continuous fluorescence measurement. Relative gene expression data were normalized against GAPDH and analyzed using the 2^{- $\Delta\Delta$ Ct} method [24]. Primers for the selected genes are given in Table S1.

2.5. Measurement of Phagocytic Uptake. RAW264.7 cells (1×10^6 cells/well) or mouse peritoneal macrophages were cultured in 6-well plates until 80% confluent. The cells were

treated with various concentrations of sublancin (25, 50, 100, or 200 μM) for 12 h. Thereafter, 100 μl of suspended fluorescent microspheres in PBS was added to the wells (cells to beads ratio 1:20) and the cells were incubated at 37°C for 1 h. Phagocytosis was terminated by the addition of 2 ml of ice-cold PBS, and then the cells were washed three times with cold PBS and harvested. Flow cytometric analysis was performed using a FACSCalibur flow cytometer using BD CellQuest software (BD Biosciences, San Jose, CA, USA).

2.6. Determination of Macrophage MRSA-Killing Activity. MRSA ATCC43300, obtained from the American Type Culture Collection (Manassas, VA), were grown overnight at 37°C in LB broth, washed in PBS, and adjusted to 10^7 CFU/ml in DMEM medium. RAW264.7 cells or mouse peritoneal macrophages (2×10^5 cells/well) in 24-well plates were treated with or without sublancin (25 μM) for 12 hours. After being washed with antibiotic-free DMEM medium, cells were incubated with MRSA ATCC43300 for 1 hour (20 bacteria/macrophage). After infection, nonadherent bacteria were washed away using PBS, and macrophages were incubated for 30 minutes (for phagocytosis) or 24 hours (for bacteria killing) in the presence of 10 $\mu\text{g}/\text{ml}$ lysostaphin to eliminate the remaining extracellular bacteria. Intracellular bacteria were released by lysing the macrophages in 0.1% Triton X-100, and the number was determined by plating serial dilutions of cell lysates on agar plates. The bacterial killing was expressed as percent changes in bacteria counts using the following formula: (bacterial count at 24 hours/bacterial count at 1 hour) $\times 100$.

2.7. Western Blot Analysis. The RAW264.7 cells grown in a 100 mm dish were treated with 100 μM sublancin for the indicated time periods, or sublancin (25, 50, 100, or 200 μM) for 30 min. Protein was extracted by incubating the RAW264.7 cells with ice-cold lysis buffer containing 150 mM NaCl, 1% Triton X-100, 0.5% sodium deoxycholate, 0.1% SDS, 50 mM Tris-HCl at pH 7.4, and a protease-inhibitor cocktail (Applygene, Beijing, China) for 30 min. Subsequently cell extracts were centrifuged at $12,000 \times g$ at 4°C for 10 min. Protein containing supernatant was collected and quantified using a BCA Protein Assay Kit (Pierce, Rockford, IL, USA). Fifty μg of protein samples was electrophoresed on SDS polyacrylamide gels and electrotransferred to polyvinylidene difluoride membranes (Millipore, Bedford, MA, USA). Membranes were blocked with $1 \times \text{TBST}$ containing 5% of BSA (Sigma-Aldrich, St. Louis, MO) for 2 h at room temperature. The membranes were incubated with corresponding primary antibodies (1:1000 dilution overnight at 4°C) against p-p38 (Thr180/Tyr182) (Cell Signaling Technology, Cat: 4511S), p38 (Cell Signaling Technology, Cat: 8690S), p-ERK1/2 (Thr202/Tyr204) (Cell Signaling Technology, Cat: 4370S), ERK1/2 (Cell Signaling Technology, Cat: 4695S), p-JNK (Thr183/Tyr185) (Cell Signaling Technology, Cat: 4668S), JNK (Cell Signaling Technology, Cat: 9252S), p-NF- κB (Ser536) (Cell Signaling Technology, Cat: 3033P), NF- κB (Cell Signaling Technology, Cat: 8242P), I κB - α (Cell Signaling Technology, Cat: 4812S), and GAPDH (Santa Cruz Biotechnology Inc., Cat: sc-25778). After the

washing of membranes with $1 \times \text{TBST}$, membranes were incubated with a secondary antibody (horseradish peroxidase-conjugated goat anti-rabbit IgG) (Huaxingbio Biotechnology, Beijing, China, Cat: HX2031) at a ratio of 1:10,000 dilution for 1 h at room temperature. The chemifluorescence was detected with the Western Blot Luminance Reagent (Applygene, Beijing, China) using an ImageQuant LAS 4000 mini system (GE Healthcare) and quantified using a gel-imaging system with ImageQuant TL Software (GE Healthcare).

2.8. Animal Experiments. Female BALB/c mice 4–6 weeks old were used for all studies. Mice were obtained from the HFK Bioscience Co. Ltd. (Beijing, China). All mice used in this study were housed in plastic cages under 12 h light/dark cycle and had access to food and water *ad libitum*. All the techniques for the care and handling of the animals in this study were approved by the China Agricultural University Institutional Animal Care and Use Committee (ID: SKLAB-B-2010-003).

2.8.1. Animal Experiment 1: Sublancin-Mediated Immune Modulation in Mice under Healthy Conditions. The mice were randomly divided into three groups: control, sublancin low-dose group (0.3 mg/kg or 0.6 mg/kg), and sublancin high-dose group (1.0 mg/kg or 1.2 mg/kg). Mice were given sublancin by gavage once a day for 28 days (0.3 mg/kg and 1.0 mg/kg, $n = 4/\text{group}$) or 14 days (0.6 mg/kg and 1.2 mg/kg, $n = 5/\text{group}$). The control group was orally administered with distilled water daily. Twenty-four hours after the last dose, the animals were killed and blood was withdrawn for peripheral hemogram analysis. Under an aseptic technique, a laparotomy was performed through a midline incision, and peritoneal macrophages were harvested for phagocytosis assay. The peritoneal cells and spleen were collected for culture.

2.8.2. Animal Experiment 2: In Vivo Efficacy against MRSA-Induced Sublethal Infection. To study the anti-infective role of sublancin in an experimental model of MRSA-induced sublethal infection, mice were randomly allocated to one of three groups ($n = 7$ to $9/\text{group}$): (i) untreated, (ii) sublancin low-dose group (0.3 mg/kg or 0.6 mg/kg), and (iii) sublancin high-dose group (1.0 mg/kg or 1.2 mg/kg). Mice were orally administered with sublancin at the indicated doses for 14 consecutive days, while the untreated mice were given distilled water during the same periods. Twenty-four hours after the last drug administration, all mice were given a sublethal dose of MRSA ATCC43300 (1.0×10^7 CFU/mouse) intraperitoneally. Animals were euthanized 36 and 72 hours after infection and peritoneal lavage was collected in 2 ml of cold HBSS. The staphylococcal load in the peritoneal lavage was enumerated as described previously [25]. Peritoneal macrophages were collected for red fluorescent protein- (RFP-) labeled *E. coli* (Thermo Fisher Scientific, Waltham, MA) phagocytosis assay. The mesenteric lymph nodes (MLNs) were excised for flow cytometry.

2.9. NK Cell Activity. The tumor cell line Yac-1 was obtained from the American Type Culture Collection (Rockville, MD). Splenocytes were collected from mice in animal experiment 1

and cocultured with Yac-1 cells to obtain an E:T (splenocytes:Yac-1) ratio of 75:1 in V-bottomed 96-well plates. After 4 h, cytotoxicity was determined by the lactate dehydrogenase (LDH) assay using a LDH Cytotoxicity Assay Kit (Roche, Basel, Switzerland).

2.10. Cell Culture. Single-cell suspensions from spleens of mice in animal experiment 1 were prepared passing cells through a 100 μ M strainer. The splenocytes were plated at a density of 1×10^6 /ml and stimulated with 2 μ g/ml anti-CD3 and 1 μ g/ml anti-CD28 antibodies (BD PharMingen, San Diego, CA, USA). The peritoneal macrophages from mice in animal experiment 1 were cultured in the presence of 1 μ g/ml LPS (Sigma-Aldrich, St. Louis, MO) in DMEM at a density of 1×10^6 /ml. The cells were cultured at 37°C for 24 hours before supernatant collection. Supernatants from splenocyte cultures were collected and analyzed by ELISA for INF- γ . The supernatants from peritoneal macrophage cultures were analyzed for TNF- α . All ELISA kits were purchased from eBioscience Inc. (San Diego, CA, USA).

2.11. Flow Cytometry. Cells from MLNs of mice in animal experiment 2 were stained with CD62L-PE, CD44-APC, CD4-PerCP-Cy5.5, and CD8-PE-Cy7 at 4°C for 30 minutes and then analyzed by flow cytometry (Gallios; Beckman Coulter Inc., Brea, CA, USA). The antibodies were purchased from BioLegend (San Diego, CA, USA), Beijing QuantoBio Biotechnology Co. Ltd. (Beijing, China), BD PharMingen, or eBioscience Inc.

2.12. Statistical Analysis. Data are expressed as means \pm SEM and were statistically analyzed using one-way analysis of variance followed by Tukey's post hoc test (Prism Software, version 5). *P* values < 0.05 were taken to indicate statistical significance.

3. Results

3.1. Sublancin Promoted the Secretion of Cytokines and NO from RAW264.7 Cells and Mouse Peritoneal Macrophages. Activated macrophages produce cytokines such as IL-1, IL-6, and TNF- α and also secrete cytotoxic and inflammatory molecules such as nitric oxide (NO) [26, 27]. Hence, the effect of sublancin on cytokine production by RAW264.7 cells and mouse peritoneal macrophages (P-Mac) was investigated. Untreated RAW264.7 cells secreted a basal level of TNF- α , but they secreted barely detectable amounts of IL-1 β and IL-6 (Figure S1). The addition of sublancin significantly stimulated the production of IL-1 β , IL-6, and TNF- α in a concentration-dependent manner (*P* < 0.05). To study the effect of sublancin on NO production in RAW264.7 cells, we measured the secretion of NO in the culture supernatant of RAW264.7 cells stimulated with sublancin alone. Compared to the control, the addition of sublancin resulted in a marked increase in NO production in a dose-dependent manner (*P* < 0.001; Figure S1). Similar results were observed in P-Mac.

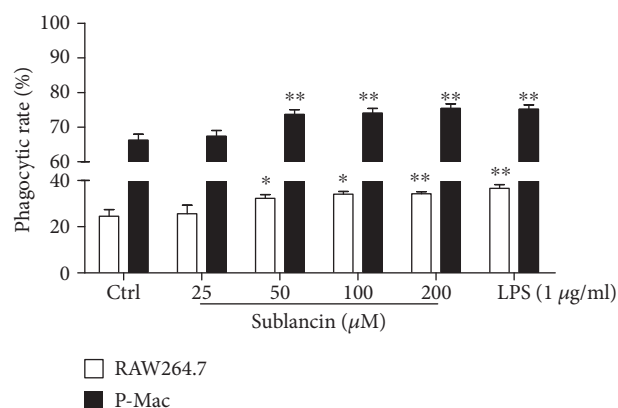


FIGURE 1: Effect of sublancin on phagocytic activity of RAW264.7 cells and mouse peritoneal macrophages (P-Mac) in vitro. RAW264.7 cells and P-Mac were treated with sublancin (0–200 μ M) or LPS (1 μ g/ml) for 12 h. Phagocytic activity of macrophage cells was assessed in terms of the population of phagocytic cells relative to the total number of cells for RAW264.7 cells and P-Mac. The values are presented as mean \pm SEM (*n* = 6). Significant differences with control cells were designated as **P* < 0.05 or ***P* < 0.01.

3.2. Sublancin Regulated mRNA Expression of Inflammatory Factors, Chemokines, and Costimulatory Molecules in RAW264.7 Cells and Peritoneal Macrophages. Due to the crucial role of inflammatory factors, chemokines, and costimulatory molecules in the activation and function of macrophages, we used quantitative RT-PCR to investigate the potentials for sublancin to regulate the expression of these mediators in RAW264.7 cells and P-Mac at the mRNA level. Consistent with the results at the protein level, a significant upregulation of IL-1 β , IL-6, TNF- α , and iNOS mRNA expression was seen in the RAW264.7 cells or P-Mac treated with sublancin (*P* < 0.05) (Figure S2). COX-2 is an important upstream regulator for prostaglandin E₂ expression. The sublancin treatments resulted in a notable increase in the mRNA expression of COX-2 compared to that of the control cells. IL-8 and monocyte chemoattractant protein-1 (MCP-1) are the primary chemokines that recruit neutrophils and monocytes, respectively. We found that sublancin increased mRNA expression of IL-8 and MCP-1 in both RAW264.7 cells and P-Mac. B7-1 and B7-2 are two classical surface markers of activated macrophages. It was found that the expression of B7-1 and B7-2 was also increased significantly in sublancin treatments, suggesting that sublancin directly induces macrophage activation.

3.3. Influence of Sublancin on Macrophage Phagocytic Activity In Vitro. Phagocytosis is one of the primary functions of macrophages, and it is specialized in excluding foreign bodies [28]. We examined the effect of sublancin on the phagocytic uptake of fluorescent microspheres in RAW264.7 cells and peritoneal macrophages using a flow cytometer. As shown in Figure 1, sublancin stimulated the phagocytic activity of RAW264.7 cells or peritoneal macrophages compared with that of the control.

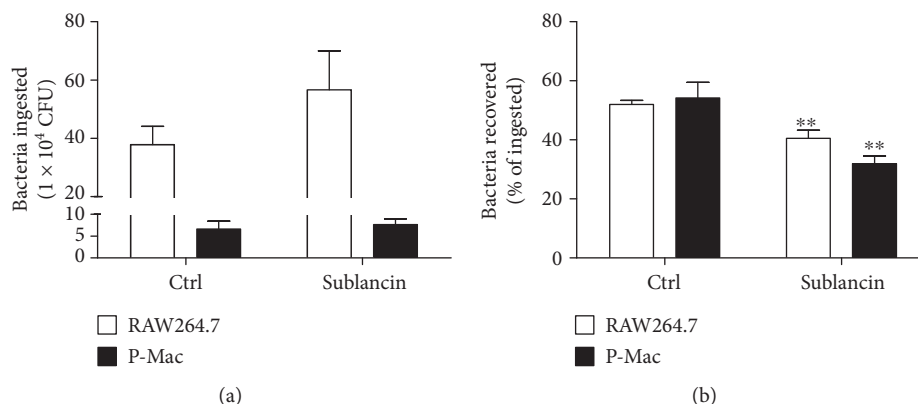


FIGURE 2: The antimicrobial peptide sublancin promoted the capacity of RAW264.7 macrophages and mouse peritoneal macrophages (P-Mac) to kill *Staphylococcus aureus* ATCC43300. RAW264.7 macrophages and P-Mac were cultured 12 hours with or without sublancin (25 μ M) and then exposed to ATCC43300 (MOI 20). Phagocytosis (a) and killing (b) of bacteria were quantified as described in Materials and Methods. Data are presented as mean \pm SEM ($n = 6$). Significant difference with control cells was designated as ** $P < 0.01$.

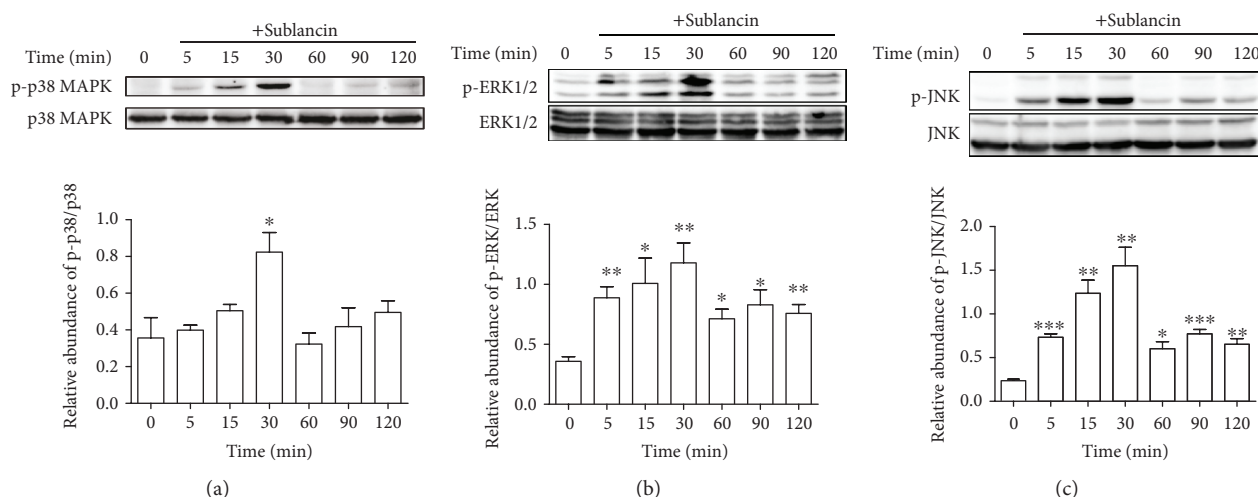


FIGURE 3: Analysis of p38, ERK, and JNK signaling pathways in RAW264.7 cells treated with sublancin for different times. RAW264.7 cells were treated with 100 μ M sublancin for the indicated times, and the phosphorylation of p38, ERK1/2, and JNK were detected by Western blot analysis. Representative immunoblots and quantitation of the phosphorylation abundance of p38 (a), ERK1/2 (b), and JNK (c). The values are presented as mean \pm SEM ($n = 3$). Significant differences with control cells were designated as * $P < 0.05$, ** $P < 0.01$, or *** $P < 0.001$.

3.4. Sublancin Enhances Bactericidal Capacity of Macrophages In Vitro. Phagocytosis is the first step of the bactericidal activity of macrophages. After 1 hour, the phagocytosis of MRSA remained unchanged in RAW264.7 cells or peritoneal macrophages preincubated with 25 μ M sublancin. Bacterial killing by macrophages was assayed after 24 hours of incubation. We observed that a marked decline in viable bacteria occurred in sublancin-treated cells (Figure 2).

3.5. Sublancin Activates RAW264.7 Cells Partly Depending on TLR4-NF- κ B/MAPK Signaling Pathways. TLR4 plays a critical role in the activation of innate immune response by recognizing specific molecular patterns. To explore whether TLR4 is involved in sublancin-induced macrophage activation, RAW264.7 cells were pretreated with a TLR4 inhibitor (TAK-242). Then, the mRNA expression of cytokines was detected using quantitative RT-PCR. As shown in

Figure S3A to S3C, with the presence of the TLR4 inhibitor, the mRNA expression of IL-1 β , IL-6, and iNOS induced by sublancin was drastically suppressed and was significantly lower than those without an inhibitor ($P < 0.001$). The results show that the immunostimulatory effect of sublancin in macrophages is exerted probably through the activation of TLR4. The stimulation of the TLR4 signaling pathway ultimately triggers the activation of the phosphorylation of MAP kinases and transcription of NF- κ B [29]. MAPKs are well-conserved protein kinases including p38 MAP kinases, extracellular signal-regulated kinase, and JNK [30–32]. Treatment with 100 μ M sublancin resulted in a significant increase in the phosphorylation of all three MAPKs (p38, ERK, and JNK) and the phosphorylation peaked 30 min after sublancin exposure (Figure 3). We also investigated the phosphorylation status of the above mediators after treatment with sublancin at different

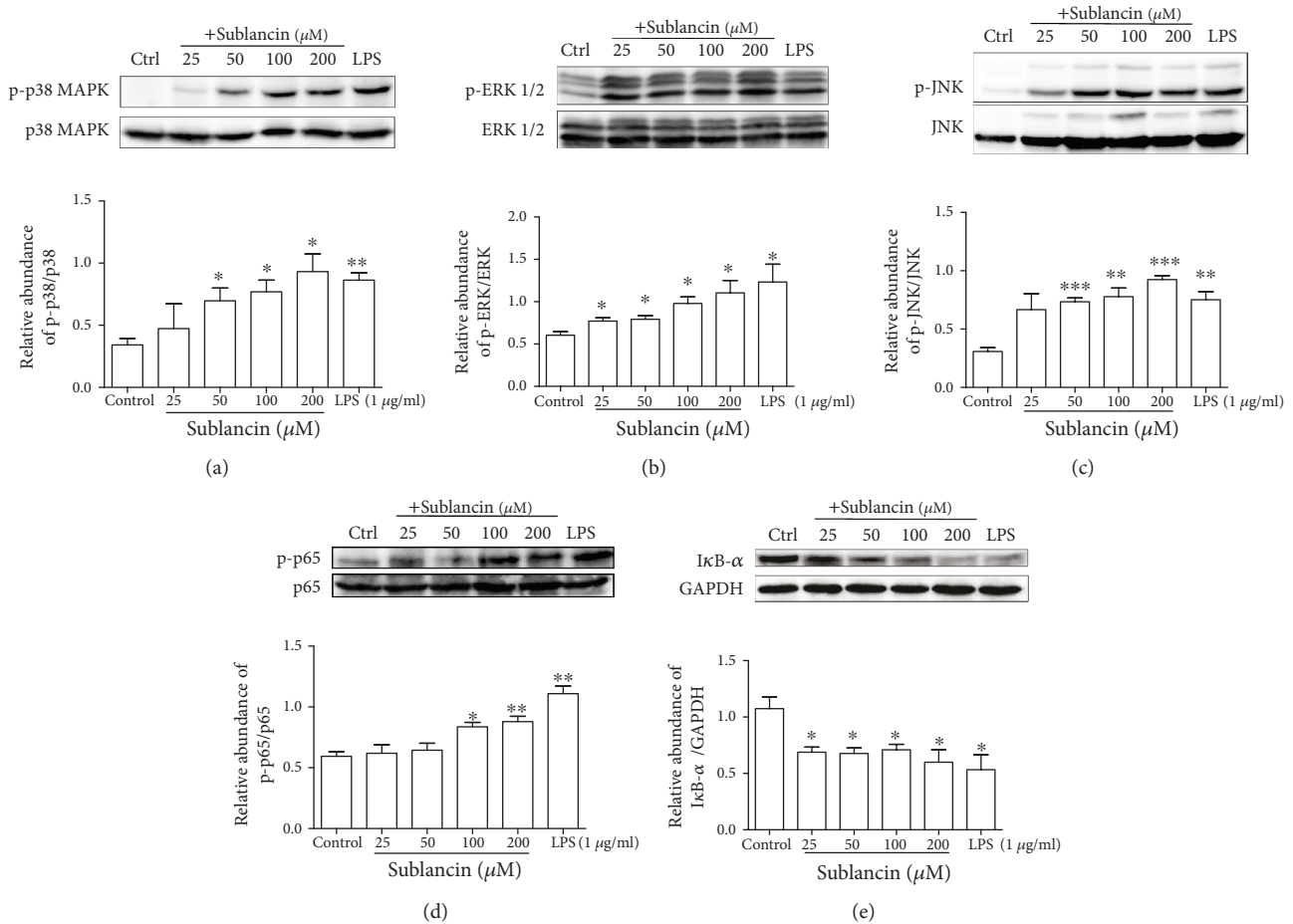


FIGURE 4: Sublancin regulates the MAPK and NF- κ B signaling pathways in macrophages. Representative Western blots for phosphorylated p38 and total p38 (a), ERK1/2 (b), JNK (c), and p65 (d) in RAW264.7 cells treated with sublancin (0-200 μ M) or LPS (1 μ g/ml) for 30 min. Relative abundance was represented as phosphorylated protein to total protein expression. (e) Western blot analysis and quantification of I κ B- α in RAW264.7 cells treated with sublancin (0-200 μ M) or LPS (1 μ g/ml) for 30 min. The values are presented as mean \pm SEM ($n = 3$). Significant differences with control cells were designated as * $P < 0.05$, ** $P < 0.01$, or *** $P < 0.001$.

concentrations for 30 min. Sublancin significantly upregulated the phosphorylation of all the three MAPKs in RAW264.7 cells in a concentration-dependent manner (Figure 4). In macrophages, NF- κ B is an important regulator of immune activation through the induction of many cytokines [33]. Sublancin stimulated the phosphorylation of NF- κ B p65, while it correspondingly decreased I κ B- α in the cytosol (Figure 4). To further confirm whether sublancin activates macrophages through MAPK and NF- κ B pathways, we used inhibitors to inhibit the initiation of signal transduction. Sublancin-induced mRNA expression of IL-1 β and IL-6 was significantly suppressed by the NF- κ B (Bay11-7082) inhibitor ($P < 0.05$) (Figures S3D, S3E). In addition, the ERK (U0126) and p38 (SB203580) inhibitors significantly exerted the inhibition of iNOS mRNA expression ($P < 0.001$) (Figure S3F). Moreover, the phosphorylation of p38 MAPK, ERK1/2, and JNK induced by sublancin was dramatically inhibited by the TLR4 inhibitor (Figure S3G). These data indicated that the activation of macrophages induced by sublancin was partly dependent on the TLR4-NF- κ B/MAPK signaling pathways.

3.6. *In Vivo Sublancin-Mediated Immune Modulation.* To evaluate the in vivo effect of sublancin, mice were orally administered with sublancin for the indicated time, and P-Mac were collected to assess phagocytosis activity and the capability of TNF- α production. Compared to the control group, the three levels of sublancin treatments (1.0 mg/kg for 28 days; 0.6 mg/kg and 1.2 mg/kg for 14 days) significantly enhanced the phagocytosis activity of P-Mac (Figures 5(a) and 5(b)), which is consistent with the data of the phagocytosis activity obtained from the in vitro study. However, no significant TNF- α promotion was found in P-Mac isolated from sublancin-treated mice (Figure 5(c)).

It has been reported that NK cells play a central role in the innate immune response to tumors and infections [34]. The sublancin treatment of 1.2 mg/kg had a tendency ($P = 0.07$) to promote NK cell activity compared with the control group (Figure 5(d)). Activated T cells (anti-CD3 and anti-CD28 stimulation for 24 hours) from the spleen were examined for IFN- γ production. As shown in Figure 5(e), spleen T cells from 1.2 mg/kg sublancin-treated mice secreted more IFN- γ than that from the control ($P < 0.05$).

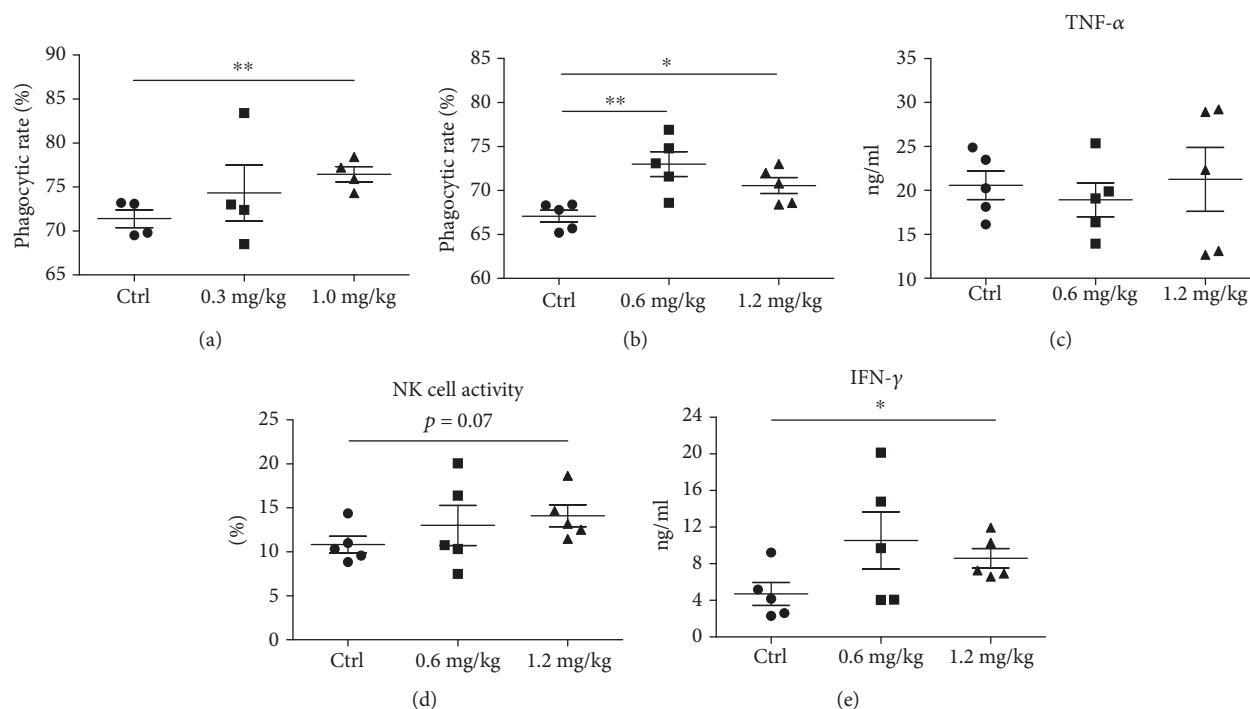


FIGURE 5: Effects of sublancin on the function of peritoneal cells and splenocytes in vivo. Sublancin enhanced the phagocytic activity of peritoneal macrophages ex vivo (a and b). Four- to six-week-old female BALB/c mice were separated into three groups: control, sublancin low-dose group (0.3 mg/kg or 0.6 mg/kg), and sublancin high-dose group (1.0 mg/kg or 1.2 mg/kg). The mice were orally administered with sublancin for 28 days (0.3 mg/kg and 1.0 mg/kg) or 14 days (0.6 mg/kg and 1.2 mg/kg). Mice in the control group were given distilled water by gavage. Peritoneal macrophages were harvested and incubated with fluorescent microspheres for the determination of phagocytic activity. (c) Comparison of TNF- α production in peritoneal macrophages stimulated with LPS (1 μ g/ml). (d) Sublancin (1.2 mg/kg) promoted a weak level of NK cell activity. Splenocytes were isolated from mice and cocultured with Yac-1 cells by a ratio (splenocytes:Yac-1) of 75:1 for 4 h. Cytotoxicity was measured by the lactate dehydrogenase assay. (e) Comparison of IFN- γ level in activated splenic T cells (2 μ g/ml anti-CD3 and 1 μ g/ml anti-CD28 antibodies). Data shown are means \pm SEM and derived from 4 to 5 mice in each group. Significant difference with the control group were designated as * $P < 0.05$ and ** $P < 0.01$.

3.7. Protection of Mice from MRSA-Induced Sublethal Infection by Sublancin. Because of the potent and promising immunomodulatory property of sublancin, this peptide was tested for its anti-infective potential. Sublancin was administered by gavage daily at the indicated doses for 14 consecutive days. Twenty-four hours after the last drug administration, mice were subjected to a sublethal dose (1.0×10^7 CFU/mouse) of MRSA ATCC43300. As shown in Figure 6, treatment with the three sublancin levels (0.6, 1.0, and 1.2 mg/kg) tended to decrease ($P < 0.1$) the number of viable bacterial counts in the peritoneal fluid 72 hours after infection. Additionally, mice treated with 1.2 mg/kg sublancin had fewer ($P < 0.05$) viable bacterial counts in the peritoneal lavage than the control mice 36 hours after infection.

Macrophages have been shown to phagocytose and directly kill bacteria. Therefore, P-Mac were collected 36 and 72 hours after infection for the RFP-labeled *Escherichia coli* phagocytosis assay. Compared with the control group, the sublancin (1.0 mg/kg) treatment stimulated the phagocytic activity of P-Mac (Figure 6(c)), which may account for the decreased number of viable bacterial counts in the peritoneal lavage. As T cells, especially CD4⁺ and CD8⁺ subsets of T cells, play a critical role in the immune responses to specific

antigenic challenges, the changes of T cells in MLNs were examined. Compared with control mice, mice treated with 1.0 mg/kg sublancin displayed a dramatic increase in the frequency of CD4⁺ and CD8⁺ T cells, with a corresponding increase in the frequency of naïve CD4⁺ T cells and memory CD8⁺ T cells (Figure 7). This difference was reflected by an increased total number of CD8⁺ T cells and naïve CD4⁺ T cells, as well as an increased number of memory CD8⁺ T cells and naïve CD4⁺ T cells (Figure 7). Similarly, mice treated with 1.2 mg/kg sublancin showed increased frequencies of CD4⁺ ($P < 0.05$) and CD8⁺ ($P = 0.06$) T cells 36 hours after infection (Figure 8). The frequencies of activated CD4⁺, naïve CD4⁺, and naïve CD8⁺ T cells were significantly increased in MLNs of 0.6 mg/kg and 1.2 mg/kg sublancin-treated mice ($P < 0.05$) (Figure 8). However, no differences in T cell frequency or cell number were observed in MLNs 72 hours after infection among the different treatments (Figure S4).

4. Discussion

Antimicrobial peptides provide immediate, effective, and nonspecific defenses against infections through direct bactericidal activity or through indirect modulation of the host defense system by enhancing immune-responsive cells [35].

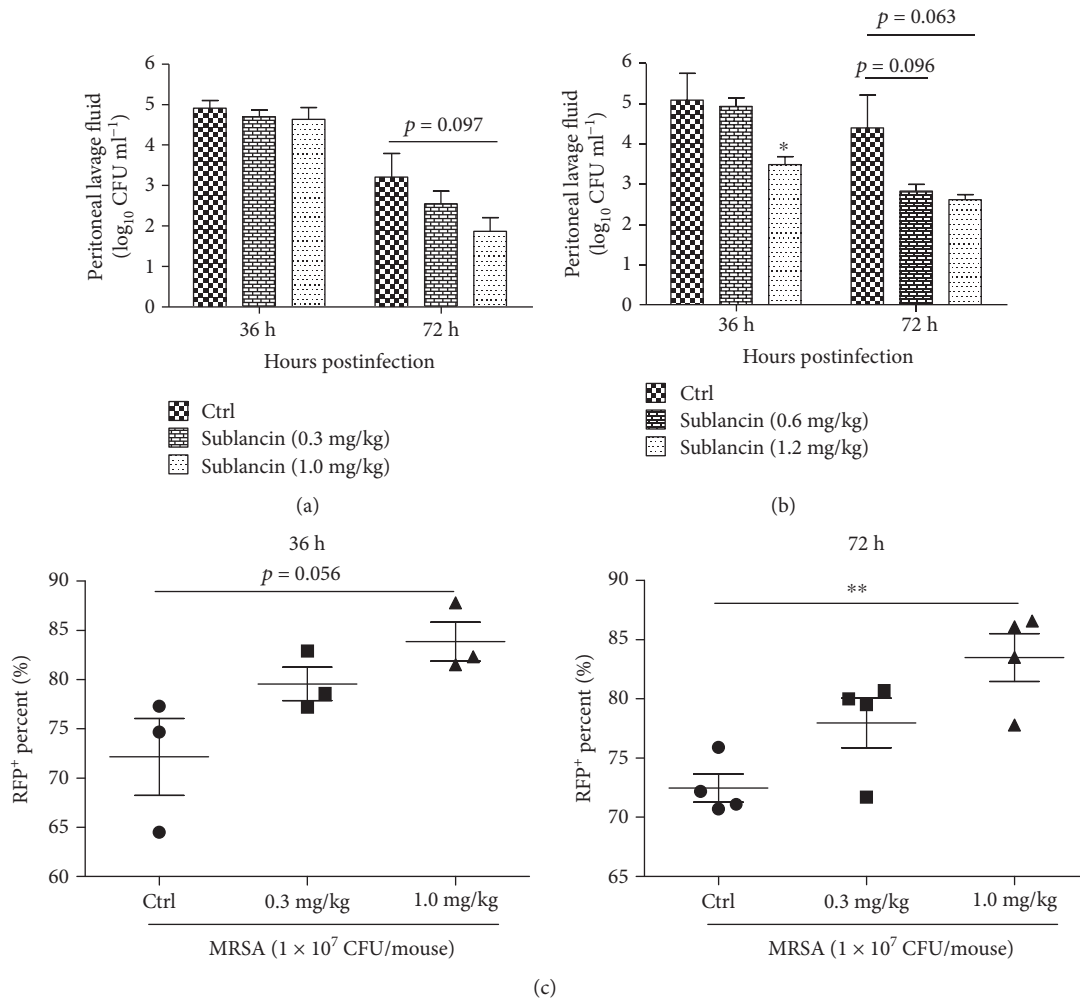


FIGURE 6: Efficacy of sublancin in the MRSA-induced sublethal infection model. (a) Mice were orally administered with sublancin at 0.3 mg/kg or 1.0 mg/kg once a day for 14 consecutive days before intraperitoneal inoculation of MRSA ATCC43300. The staphylococcal load in the peritoneal lavage was enumerated at 36 and 72 h of infection. (b) Sublancin (0.6 mg/kg or 1.2 mg/kg) was administered by gavage daily for 14 days before infection. Mice were analyzed for bacterial counts in the peritoneal lavage at 36 and 72 h of infection. (c) Peritoneal macrophages were collected 36 and 72 hours after infection for red fluorescent protein- (RFP-) labeled *Escherichia coli* phagocytosis assay. Data shown are means \pm SEM and derived from 3 to 4 mice in each group. Significant differences with the control group were designated as * $P < 0.05$ and ** $P < 0.01$.

Sublancin, produced by *Bacillus subtilis* 168, has been studied extensively for its antibacterial mechanisms [36, 37]. Following our previous studies of the anti-infective efficacy of sublancin in several *in vivo* infection models [18, 19], we examined its role and anti-infection mechanism in a mouse model of MRSA-induced sublethal infection.

Macrophage activation is the key event in innate immunity for host defense against bacterial infections, and many immunomodulatory agents activate immune responses primarily by the activation of macrophages [38, 39]. Activated macrophages are considered to be associated with the generation of IL-1 β , IL-6, TNF- α , and NO. Upon stimulation by AMPs, different immune cells have been demonstrated to produce cytokines or chemokines. For example, human neutrophil peptides 1 and 3 were found to stimulate the production of IL-1, IL-4, IL-6, and TNF- α in monocytes [40] and MCP-1 in lung epithelial cells [41]. In addition, the AMP LL-37 was shown to increase the release of IL-8 in airway epi-

thelial cells [42]. Here, we show that sublancin stimulated both the protein and mRNA levels of IL-1 β , IL-6, TNF- α , and NO in RAW264.7 cells and mouse peritoneal macrophages. Consistently, the mRNA expression of chemokines (such as IL-8 and MCP-1) and costimulatory molecules (B7-1 and B7-2) was also increased by sublancin in RAW264.7 cells and mouse peritoneal macrophages. These observations suggest that sublancin could directly enhance the activation of macrophages.

A critical finding in this study was that sublancin significantly enhanced the phagocytic activity of a macrophage against MRSA both *in vitro* and *in vivo*. Wan et al. in 2014 reported that LL-37 elevated bacterial phagocytosis by human macrophages [43]. Furthermore, it has also been demonstrated that human neutrophil peptides 1–3 enhance bacterial phagocytosis by macrophages [44]. Consistent with the above notions, we found that sublancin can simulate the phagocytosis of fluorescent microspheres in RAW264.7 cells

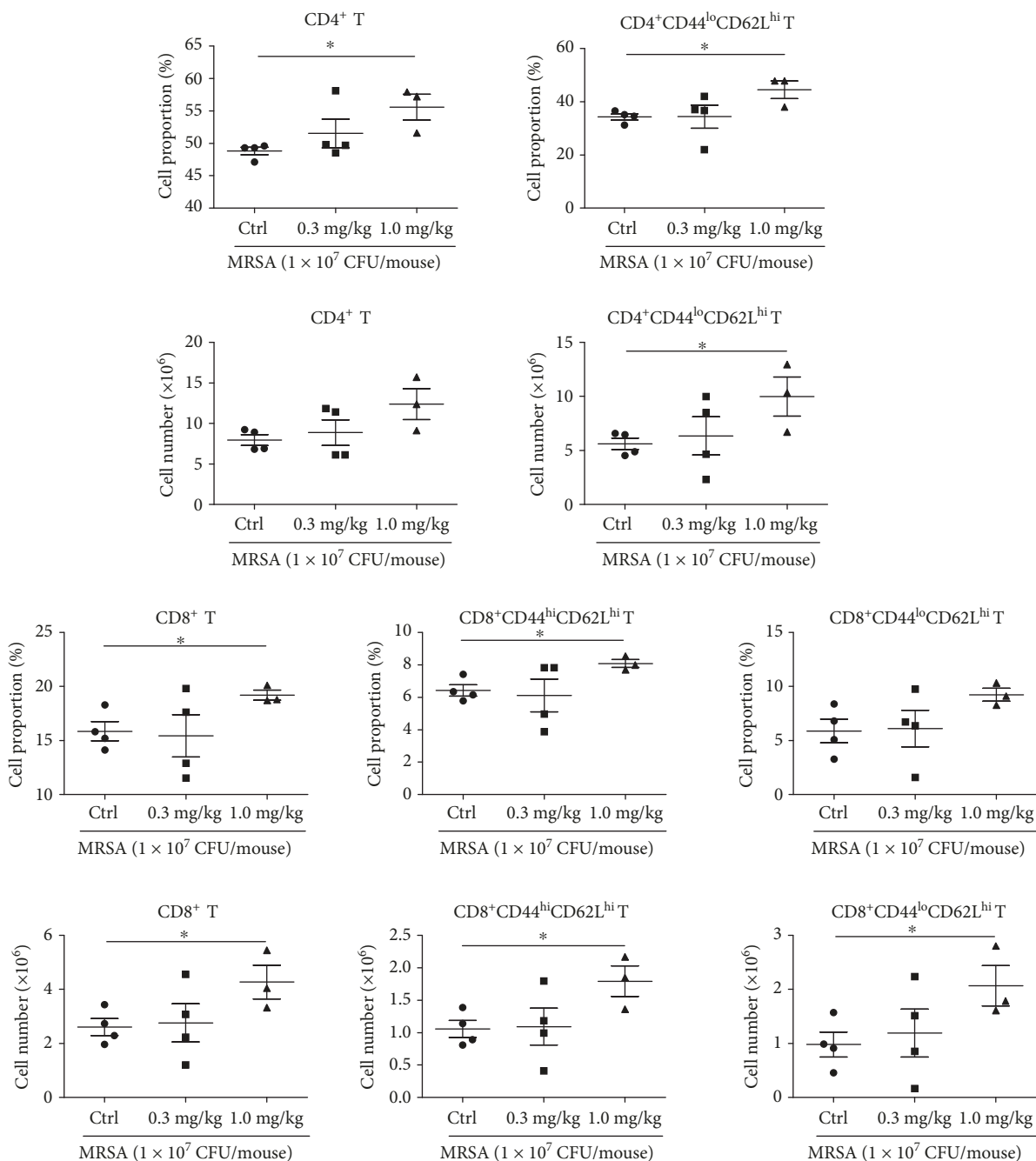


FIGURE 7: Effects of sublancin on the immune cell subset in the mesenteric lymph nodes (MLNs) of MRSA-challenged mice. Mice were orally administered with sublancin (0.3 mg/kg or 1.0 mg/kg) for 14 consecutive days before infection. Phenotypic analysis of single-cell suspensions collected from the MLNs (the MLNs were excised from the mice 36 hours after infection). The phenotype of CD4⁺ and CD8⁺ T cells was further characterized by the expression of CD44 and CD62L, cell surface receptors which are differentially expressed on memory (CD44^{hi}CD62L^{hi}) and naïve (CD44^{lo}CD62L^{hi}) T cell populations.

and peritoneal macrophages. Next, the effect of sublancin on the phagocytic activity was determined using mouse peritoneal macrophages *ex vivo*. In healthy or MRSA-challenged mice, the oral administration of sublancin enhanced the phagocytic activity of peritoneal macrophages. Mice pretreated with sublancin before the MRSA infection acquired a potent antibacterial activity. It was found that sublancin tended to decrease the bacterial burden in the peritoneal

cavity. Our previous research has shown that monocytes/macrophages are pivotal for the protective effect of sublancin [20]. Therefore, we further tested whether sublancin could enhance macrophage function by the augmentation of the bacterial clearance. In the present study, we found that the preincubation of macrophages with sublancin promoted the MRSA-killing activity in macrophages. We speculate that the sublancin-enhanced microbicidal activity of

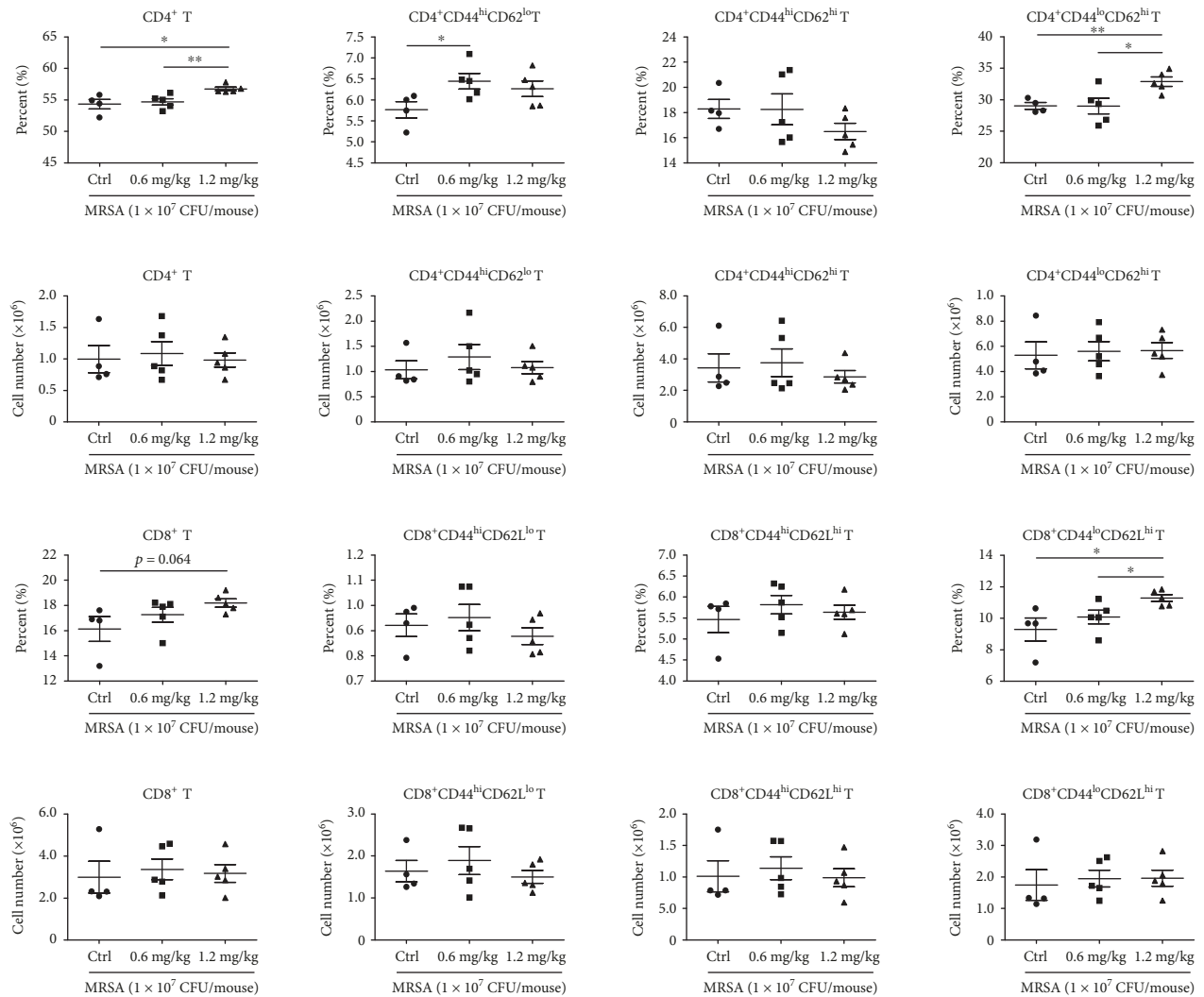


FIGURE 8: The alteration of various immune cell percentages and cell numbers in the MLNs of MRSA-challenged mice. Mice were orally administered with sublanicin (0.6 mg/kg or 1.2 mg/kg) for 14 consecutive days before infection. Phenotypic analysis of single-cell suspensions collected from the MLNs (the MLNs were excised from the mice 36 hours after infection). The phenotype of CD4⁺ and CD8⁺ T cells was further characterized by the expression of CD44 and CD62L, cell surface receptors which are differentially expressed on activated (CD44^{hi}CD62L^{lo}), memory (CD44^{hi}CD62L^{hi}), and naïve (CD44^{lo}CD62L^{hi}) T cell populations.

macrophages may be due to the activation of macrophages induced by sublanicin. Further studies are clearly warranted to elucidate the property of sublanicin in facilitating bacterial clearance by macrophages.

Increasing evidence has demonstrated that signaling via TLRs leads to the production of a mass of proinflammatory mediators including cytokines (such as IL-1, IL-6, and TNF- α) and NO [45]. TLR4 is known to stimulate the innate immune response through recognizing specific molecular patterns. In the study presented here, sublanicin-upregulated mRNA expression of IL-1 β , IL-6, TNF- α , and iNOS was drastically suppressed by the TLR4 inhibitor (TAK-242), suggesting that sublanicin activates macrophages probably via the TLR4 signaling pathway. It is well known that NF- κ B and MAPKs are involved in regulating cytokine release via the phosphorylation of transcription factors [46, 47]. We found that sublanicin induced the phosphorylation of the three MAPKs (p38 MAPK, ERK1/2, and JNK) in

RAW264.7 macrophages. In addition, both NF- κ B p65 and I κ B- α were responsive to sublanicin stimulation by enhancing the phosphorylation of NF- κ B p65 and the I κ B- α degradation, indicating that NF- κ B and MAPK signaling pathways were responsible for sublanicin-induced macrophage activation. Furthermore, sublanicin-induced mRNA expression of iNOS was significantly inhibited by ERK (U0126) and p38 (SB203580) inhibitors. The NF- κ B (Bay11-7082) inhibitor also decreased the mRNA expression of IL-1 β and IL-6 in RAW264.7 macrophages stimulated with sublanicin. These observations highlight the prominent role for the ERK1/2, p38, and NF- κ B pathways in the sublanicin-induced macrophage activation. Additionally, sublanicin-upregulated phosphorylation of p38 MAPK, ERK1/2, and JNK was obviously depressed by the TLR4 (TAK-242) inhibitor, further confirming that sublanicin acts directly on macrophages partly depending on TLR4 signaling pathways.

The results obtained from the *in vitro* assays prompted us to explore the *in vivo* immunomodulatory properties of sublancin in mice. Firstly, the peripheral hemogram analysis from mice that were treated with sublancin (0.3 mg/kg and 1.0 mg/kg) for 28 days showed no disturbances in the blood parameters (data not shown), implying that sublancin did not cause apparent toxicity *in vivo*. IFN- γ has been recognized as the pivotal cytokine of Th1-polarized immunity [48]. In the study presented here, sublancin enhanced the ability of spleen T cells to secrete IFN- γ , indicating that sublancin slightly triggered the Th1 immunity response. No promotion was observed in the TNF- α production of P-Mac isolated from sublancin-treated mice, which indicates that sublancin will not trigger an extensive inflammatory response under healthy conditions.

Importantly, treatment with sublancin protected mice from sublethal infection induced by MRSA ATCC43300. This protection was demonstrated as a significantly accelerated clearance of bacteria and was mediated partly by enhanced macrophage function. Additionally, emerging evidence also shows that T cell-mediated immunity is crucial to protect against *S. aureus* infection [49]. In the study presented here, sublancin stimulated a dramatic increase in the frequencies of CD4⁺ and CD8⁺ T cells in MLNs 36 h postinfection. It is considered that the retention of naïve CD4⁺ and CD8⁺ T cells reflects a better immune response [50, 51]. In addition, it was also reported that cellular memory responses are also critical for the antistaphylococcal immunity [52]. In the study presented here, sublancin increased the frequencies of naïve CD4⁺ and CD8⁺ T cells, as well as memory CD8⁺ T cells in MLNs at 36 hours after infection. However, there was no significant difference in T cell frequency in MLNs among the different treatments at 72 hours after infection. These findings imply that sublancin could improve T cell-mediated immunity in an early infection phase. In the present *in vivo* study, sublancin was given by oral administration. During the transit of this peptide through the gastrointestinal tract of mice, reduction of disulfides, loss of glycosylation, and/or attack of the peptide by endogenous proteases may modify some characteristics of mature sublancin. Accordingly, it could happen that the observed effects of sublancin in this study may be due to the action of sublancin-derived peptides or a partially modified mature sublancin.

In summary, sublancin might enhance not only T cell-mediated immunity but also macrophage function. Our results suggest that sublancin is an excellent alternative to counter the MRSA infections and is worthy of further investigation to successfully translate sublancin to the clinic.

Data Availability

The data used to support the findings of this study are available from the corresponding author upon request.

Conflicts of Interest

The authors declare that they have no conflict of interests.

Acknowledgments

This work was supported by the Natural Science Foundation of Hubei Province (2018CFB125), the National Key Research and Development Program of China (2016YFD0501308), and the Special Fund for Agroscientific Research in the Public Interest (201403047).

Supplementary Materials

Table S1: sequence of the primers used for quantitative PCR. Figure S1: effect of sublancin on the production of cytokines (A to C) and nitric oxide (D) from RAW264.7 cells and mouse peritoneal macrophages (P-Mac). RAW264.7 cells and P-Mac were treated with sublancin (0-200 μ M) or LPS (1 μ g/ml) for 24 h. The data are expressed as mean \pm SEM ($n = 6$). Significant differences with control cells were designated as * $P < 0.05$, ** $P < 0.01$, or *** $P < 0.001$. Figure S2: the mRNA expression of inflammatory factors (A to E), chemokines (F and G), and costimulatory molecules (H and I) in RAW264.7 cells and mouse peritoneal macrophages (P-Mac) treated with sublancin. RAW264.7 cells and P-Mac were treated with sublancin (0-200 μ M) or LPS (1 μ g/ml) for 12 h. The expression of target genes was detected by real-time PCR. GAPDH was used as an internal standard for normalization. The values are presented as mean \pm SEM ($n = 6$). Significant differences with control cells were designated as * $P < 0.05$, ** $P < 0.01$, or *** $P < 0.001$. Figure S3: sublancin activated RAW264.7 cells through TLR4 signaling pathways. (A-C) Sublancin-mediated mRNA expression of cytokines via TLR4. RAW264.7 cells were pretreated for 3 h at 37°C with the TLR4 inhibitor TAK-242 (20 μ g/ml) before stimulation with sublancin (100 μ M) for 12 h. LPS was used as a positive control. The cell pellet was used to determine the mRNA expression of target genes by real-time PCR. Data are presented as mean \pm SEM ($n = 4$). Compared with the sublancin-treated cells, statistical significance is shown with *** $P < 0.001$. Compared with the LPS-treated cells, statistical significance is shown with ### $P < 0.001$. (D-F) Sublancin-mediated mRNA expression of cytokines depends on ERK1/2, p38, and NF- κ B activation. RAW264.7 cells were pretreated for 30 min with the ERK1/2 inhibitor U0126 (10 μ M) or the p38 inhibitor SB203580 (20 μ M) or pretreated for 1 h with the NF- κ B inhibitor Bay11-7082 (5 μ M) or the JNK inhibitor SP600125 (20 μ M) and then stimulated with sublancin (100 μ M). After 12 h of incubation, the cell pellet was used to determine the mRNA expression of target genes by real-time PCR. Data are expressed as mean \pm SEM ($n = 4$). Significant differences with the sublancin-treated cells were designated as * $P < 0.05$, ** $P < 0.01$, or *** $P < 0.001$. (G) Sublancin induced the phosphorylation of p38, ERK1/2, and JNK through TLR4. RAW264.7 cells were pretreated for 3 h with the TLR4 inhibitor TAK-242 (20 μ g/ml) before exposure to sublancin (100 μ M) for 30 min. Whole protein was extracted, and then phosphorylated p38, ERK1/2, and JNK were analyzed by Western blot. The figure shown is representative of three independent experiments. Figure S4: no difference in T cell frequency or cell number was observed in MLNs 72 hours after infection among the different treatments. Mice

were orally administered with sublancin (0.6 mg/kg or 1.2 mg/kg) for 14 consecutive days before infection. Phenotypic analysis of single-cell suspensions collected from the MLNs (the MLNs were excised from the mice 72 hours after infection). The phenotype of CD4⁺ and CD8⁺ T cells was further characterized by the expression of CD44 and CD62L, cell surface receptors which are differentially expressed on activated (CD44^{hi}CD62L^{lo}), memory (CD44^{hi}CD62L^{hi}), and naïve (CD44^{lo}CD62L^{hi}) T cell populations. (*Supplementary Materials*)

References

- [1] T. P. Van Boeckel, C. Brower, M. Gilbert et al., "Global trends in antimicrobial use in food animals," *Proceedings of the National Academy of Sciences of the United States of America*, vol. 112, no. 18, pp. 5649–5654, 2015.
- [2] F. D. Lowy, "Antimicrobial resistance: the example of *Staphylococcus aureus*," *The Journal of Clinical Investigation*, vol. 111, no. 9, pp. 1265–1273, 2003.
- [3] R. H. Deurenberg and E. E. Stobberingh, "The evolution of *Staphylococcus aureus*," *Infection, Genetics and Evolution*, vol. 8, no. 6, pp. 747–763, 2008.
- [4] B. Spellberg, J. H. Powers, E. P. Brass, L. G. Miller, and J. E. Edwards, "Trends in antimicrobial drug development: implications for the future," *Clinical Infectious Diseases*, vol. 38, no. 9, pp. 1279–1286, 2004.
- [5] J. Y. Ahn, J. Y. Song, Y. S. Yun, G. Jeong, and I. S. Choi, "Protection of *Staphylococcus aureus*-infected septic mice by suppression of early acute inflammation and enhanced antimicrobial activity by ginsan," *FEMS Immunology & Medical Microbiology*, vol. 46, no. 2, pp. 187–197, 2006.
- [6] Y. Nakamura, Y. Aramaki, and T. Kakiuchi, "A mouse model for postoperative fatal enteritis due to *Staphylococcus* infection," *The Journal of Surgical Research*, vol. 96, no. 1, pp. 35–43, 2001.
- [7] T. J. Foster, "Immune evasion by *Staphylococci*," *Nature Reviews Microbiology*, vol. 3, no. 12, pp. 948–958, 2005.
- [8] M. Carini, G. Aldini, M. Orioli, A. Piccoli, G. Rossoni, and R. Maffei Facino, "Nitric oxide release and distribution following oral and intraperitoneal administration of nitroaspirin (NCX 4016) in the rat," *Life Sciences*, vol. 74, no. 26, pp. 3291–3305, 2004.
- [9] F. Balkwill, "Tumour necrosis factor and cancer," *Nature Reviews Cancer*, vol. 9, no. 5, pp. 361–371, 2009.
- [10] N. Fujiwara and K. Kobayashi, "Macrophages in inflammation," *Current Drug Target -Inflammation & Allergy*, vol. 4, no. 3, pp. 281–286, 2005.
- [11] A. Ayala and I. H. Chaudry, "Immune dysfunction in murine polymicrobial sepsis," *Shock*, vol. 6, Supplement, pp. S27–S38, 1996.
- [12] C. Munoz, J. Carlet, C. Fitting, B. Misset, J. P. Bleriot, and J. M. Cavaillon, "Dysregulation of in vitro cytokine production by monocytes during sepsis," *The Journal of Clinical Investigation*, vol. 88, no. 5, pp. 1747–1754, 1991.
- [13] R. E. W. Hancock and M. G. Scott, "The role of antimicrobial peptides in animal defenses," *Proceedings of the National Academy of Sciences of the United States of America*, vol. 97, no. 16, pp. 8856–8861, 2000.
- [14] H. N. Huang, C. Y. Pan, V. Rajanbabu, Y. L. Chan, C. J. Wu, and J. Y. Chen, "Modulation of immune responses by the antimicrobial peptide, epinecidin (Epi)-1, and establishment of an Epi-1-based inactivated vaccine," *Biomaterials*, vol. 32, no. 14, pp. 3627–3636, 2011.
- [15] S. H. Paik, A. Chakicherla, and J. N. Hansen, "Identification and characterization of the structural and transporter genes for, and the chemical and biological properties of, sublancin 168, a novel lantibiotic produced by *Bacillus subtilis* 168," *The Journal of Biological Chemistry*, vol. 273, no. 36, pp. 23134–23142, 1998.
- [16] S. Biswas, C. V. Garcia de Gonzalo, L. M. Repka, and W. A. van der Donk, "Structure-activity relationships of the S-linked glycocon sublancin," *ACS Chemical Biology*, vol. 12, no. 12, pp. 2965–2969, 2017.
- [17] C. Wu, S. Biswas, C. V. Garcia de Gonzalo, and W. A. van der Donk, "Investigations into the mechanism of action of sublancin," *ACS Infectious Diseases*, vol. 5, no. 3, pp. 454–459, 2019.
- [18] Q. Wang, X. Zeng, S. Wang et al., "The bacteriocin sublancin attenuates intestinal injury in young mice infected with *Staphylococcus aureus*," *The Anatomical Record*, vol. 297, no. 8, pp. 1454–1461, 2014.
- [19] S. Wang, X. F. Zeng, Q. W. Wang et al., "The antimicrobial peptide sublancin ameliorates necrotic enteritis induced by *Clostridium perfringens* in broilers," *Journal of Animal Science*, vol. 93, no. 10, pp. 4750–4760, 2015.
- [20] S. Wang, Q. Wang, X. Zeng et al., "Use of the antimicrobial peptide sublancin with combined antibacterial and immunomodulatory activities to protect against methicillin-resistant *Staphylococcus aureus* infection in mice," *Journal of Agricultural and Food Chemistry*, vol. 65, no. 39, pp. 8595–8605, 2017.
- [21] M. Velasco, M. J. Diaz-Guerra, P. Diaz-Achirica, D. Andreu, L. Rivas, and L. Bosca, "Macrophage triggering with cecropin A and melittin-derived peptides induces type II nitric oxide synthase expression," *Journal of Immunology*, vol. 158, no. 9, pp. 4437–4443, 1997.
- [22] S. Wang, S. Huang, Q. Ye et al., "Prevention of cyclophosphamide-induced immunosuppression in mice with the antimicrobial peptide sublancin," *Journal of Immunology Research*, vol. 2018, Article ID 4353580, 11 pages, 2018.
- [23] A. B. N. Putra, H. Morishige, S. Nishimoto et al., "Effect of collagens from jellyfish and bovine Achilles tendon on the activity of J774.1 and mouse peritoneal macrophage cells," *Journal of Functional Foods*, vol. 4, no. 2, pp. 504–512, 2012.
- [24] K. J. Livak and T. D. Schmittgen, "Analysis of relative gene expression data using real-time quantitative PCR and the 2^{-ΔΔCT} method," *Methods*, vol. 25, no. 4, pp. 402–408, 2001.
- [25] S.-A. Li, W.-H. Lee, and Y. Zhang, "Efficacy of OH-CATH30 and Its Analogs against Drug-Resistant Bacteria In Vitro and in Mouse Models," *Antimicrobial Agents and Chemotherapy*, vol. 56, no. 6, pp. 3309–3317, 2012.
- [26] P. J. Duerksen-Hughes, D. B. Day, S. M. Laster, N. A. Zachariades, L. Aquino, and L. R. Gooding, "Both tumor necrosis factor and nitric oxide participate in lysis of simian virus 40-transformed cells by activated macrophages," *The Journal of Immunology*, vol. 149, no. 6, pp. 2114–2122, 1992.
- [27] C. F. Nathan, "Secretory products of macrophages," *The Journal of Clinical Investigation*, vol. 79, no. 2, pp. 319–326, 1987.
- [28] M. Benoit, B. Desnues, and J. L. Mege, "Macrophage polarization in bacterial infections," *Journal of Immunology*, vol. 181, no. 6, pp. 3733–3739, 2008.

- [29] B. W. Jones, T. K. Means, K. A. Heldwein et al., "Different Toll-like receptor agonists induce distinct macrophage responses," *Journal of Leukocyte Biology*, vol. 69, no. 6, pp. 1036–1044, 2001.
- [30] C. R. Weston and R. J. Davis, "The JNK signal transduction pathway," *Current Opinion in Genetics & Development*, vol. 12, no. 1, pp. 14–21, 2002.
- [31] A. R. Nebreda and A. Porras, "p38 MAP kinases: beyond the stress response," *Trends in Biochemical Sciences*, vol. 25, no. 6, pp. 257–260, 2000.
- [32] T. P. Garrington and G. L. Johnson, "Organization and regulation of mitogen-activated protein kinase signaling pathways," *Current Opinion in Cell Biology*, vol. 11, no. 2, pp. 211–218, 1999.
- [33] E. B. Kopp and S. Ghosh, "NF- κ B and rel proteins in innate immunity," *Advances in Immunology*, vol. 58, pp. 1–27, 1995.
- [34] G. Alter, J. M. Malenfant, and M. Altfeld, "CD107a as a functional marker for the identification of natural killer cell activity," *Journal of Immunological Methods*, vol. 294, no. 1–2, pp. 15–22, 2004.
- [35] O. N. Silva, C. de la Fuente-Núñez, E. F. Haney et al., "An anti-infective synthetic peptide with dual antimicrobial and immunomodulatory activities," *Scientific Reports*, vol. 6, no. 1, 2016.
- [36] T. R. H. M. Kouwen, E. N. Trip, E. L. Denham, M. J. J. B. Sibbald, J. Y. F. Dubois, and J. M. van Dijk, "The large mechanosensitive channel *MscL* determines bacterial susceptibility to the bacteriocin sublancin 168," *Antimicrobial Agents and Chemotherapy*, vol. 53, no. 11, pp. 4702–4711, 2009.
- [37] C. V. Garcia De Gonzalo, E. L. Denham, R. A. T. Mars, J. Stülke, W. A. van der Donk, and J. M. van Dijk, "The phosphoenolpyruvate:sugar phosphotransferase system is involved in sensitivity to the glucosylated bacteriocin sublancin," *Antimicrobial Agents and Chemotherapy*, vol. 59, no. 11, pp. 6844–6854, 2015.
- [38] K. Y. Lee and Y. J. Jeon, "Macrophage activation by polysaccharide isolated from *Astragalus membranaceus*," *International Immunopharmacology*, vol. 5, no. 7–8, pp. 1225–1233, 2005.
- [39] H. Gao, G. Y. Li, J. Huang et al., "Protective effects of Zhuyeqing liquor on the immune function of normal and immunosuppressed mice in vivo," *BMC Complementary and Alternative Medicine*, vol. 13, no. 1, 2013.
- [40] Y. V. Chaly, E. M. Paleolog, T. S. Kolesnikova, I. I. Tikhonov, E. V. Petratchenko, and N. N. Voitenok, "Human neutrophil α -defensin modulates cytokine production in human monocytes and adhesion molecule expression in endothelial cells," *European Cytokine Network*, vol. 11, no. 2, pp. 257–266, 2000.
- [41] H. Zhang, G. Porro, N. Orzech, B. Mullen, M. Liu, and A. S. Slutsky, "Neutrophil defensins mediate acute inflammatory response and lung dysfunction in dose-related fashion," *American Journal of Physiology-Lung Cellular and Molecular Physiology*, vol. 280, no. 5, pp. L947–L954, 2001.
- [42] G. S. Tjabringa, J. Aarbiou, D. K. Ninaber et al., "The antimicrobial peptide LL-37 activates innate immunity at the airway epithelial surface by transactivation of the epidermal growth factor receptor," *Journal of Immunology*, vol. 171, no. 12, pp. 6690–6696, 2003.
- [43] M. Wan, A. M. van der Does, X. Tang, L. Lindbom, B. Agerberth, and J. Z. Haeggstrom, "Antimicrobial peptide LL-37 promotes bacterial phagocytosis by human macrophages," *Journal of Leukocyte Biology*, vol. 95, no. 6, pp. 971–981, 2014.
- [44] O. Soehnlein, Y. Kai-Larsen, R. Frithiof et al., "Neutrophil primary granule proteins HBP and HNP1-3 boost bacterial phagocytosis by human and murine macrophages," *The Journal of Clinical Investigation*, vol. 118, no. 10, pp. 3491–3502, 2008.
- [45] S. B. Mizel, A. N. Honko, M. A. Moors, P. S. Smith, and A. P. West, "Induction of macrophage nitric oxide production by Gram-negative flagellin involves signaling via heteromeric Toll-like receptor 5/Toll-like receptor 4 complexes," *Journal of Immunology*, vol. 170, no. 12, pp. 6217–6223, 2003.
- [46] G. L. Johnson and R. Lapadat, "Mitogen-activated protein kinase pathways mediated by ERK, JNK, and p38 protein kinases," *Science*, vol. 298, no. 5600, pp. 1911–1912, 2002.
- [47] L. Ashall, C. A. Horton, D. E. Nelson et al., "Pulsatile stimulation determines timing and specificity of NF- κ B-dependent transcription," *Science*, vol. 324, no. 5924, pp. 242–246, 2009.
- [48] A. Nijnik, J. Pistolic, A. Wyatt, S. Tam, and R. E. W. Hancock, "Human cathelicidin peptide LL-37 modulates the effects of IFN- γ on APCs," *Journal of Immunology*, vol. 183, no. 9, pp. 5788–5798, 2009.
- [49] B. Spellberg and R. Daum, "Development of a vaccine against *Staphylococcus aureus*," *Seminars in Immunopathology*, vol. 34, no. 2, pp. 335–348, 2012.
- [50] N. L. La Gruta and P. G. Thomas, "Interrogating the relationship between naïve and immune antiviral T cell repertoires," *Current Opinion in Virology*, vol. 3, no. 4, pp. 447–451, 2013.
- [51] W. Tinago, E. Coghlan, A. Macken et al., "Clinical, immunological and treatment-related factors associated with normalised CD4⁺/CD8⁺ T-cell ratio: effect of naive and memory T-cell subsets," *PLoS One*, vol. 9, no. 5, p. e97011, 2014.
- [52] A. F. Brown, A. G. Murphy, S. J. Lalor et al., "Memory Th1 cells are protective in invasive *Staphylococcus aureus* infection," *PLOS Pathogens*, vol. 11, no. 11, 2015.